A design rule to include the effect of leaning columns in steel frame stability

Broeks, Wim M.

Award date:
2021

A DESIGN RULE TO INCLUDE THE EFFECT OF LEANING COLUMNS IN STEEL FRAME STABILITY

GRADUATION REPORT
29-1-2021
TU/e Eindhoven

Broeks, W.M.
E-mail: w.m.broeks@student.tue.nl
wm.broeks@hotmail.com
Identity number: 1262947

Graduation Committee: H.H. Snijder (TU/e)
Graduation Committee: P. Teeuwen (Witteveen & Bos)
Graduation Committee: D. Leonetti (TU/e)
Graduation Committee: H. Hofmeyer (TU/e)

ACKNOWLEDGMENTS

This graduation report has been written to graduate for the degree of Master of Science at Eindhoven University of Technology (TU/e), program Architecture, Building, and Planning (ABP), Structural Design.

I would like to thank the members of my graduation committee, prof. ir. H.H. (Bert) Snijder, dr. ir. P.A. (Paul) Teeuwen, dr. ir. D. (Davide) Leonetti, and dr. ir. H. (Herm) Hofmeyer for their extensive supervision of this research, and the amount of time spent to accomplish this. The knowledge shared in the graduation meetings helped to finish this graduation project. Furthermore, I would like to thank prof. ir. H.H. (Bert) Snijder again for initiating this research.

Lastly, I would like to thank my family, friends, and girlfriend for their moral support.

W. (Wim) Broeks

Eindhoven, January 2021

SUMMARY

The stability of a steel structure is often ensured by one part of a frame, the so-called stabilizing frame. When the steel structure deforms in the lateral direction and the other parts of the steel structure are hinged connected to the stabilizing frame, the vertical loads on the columns that are not part of the stabilizing frame introduce additional lateral loads on the stabilizing frame due to leaning. This phenomenon is called the leaning column effect, or in Dutch 'aanpendelende belasting'. To ensure the resistance of the stabilizing frame, these additional leaning column loads have to be taken into account by the design rules. Back in the days, the NEN series were in force. In the code NEN 6771, the effect of the leaning column is included in the load side of the design rule by an equivalent total force F_{tot}. However, the background for this design rule is unknown. Nowadays, the Eurocode (EC) series are in force and ensure the structural safety of all structures. In the EC EN 1993-1-1, it appears that this leaning column effect is not included in the design rule.

The aim of this graduation project is to numerically verify the design rule of the NEN 6771, where they included the leaning column effect in the load side of the design rule, and rewrite the design rule of the EN 1993-1-1 to also include the leaning column effect. First, the design rule of the EN 1993-1-1 is rewritten with the same content as the NEN 6771, but the same format as the current EN 1993-1-1 design rule. After that, the ultimate resistance loads obtained with the various design rules will be compared with the ultimate loads determined with various analyses with the Finite Element Method (FEM). As a starting point of the research, the most simplistic form of a stabilizing frame with a leaning column was taken, as illustrated in Figure 1.

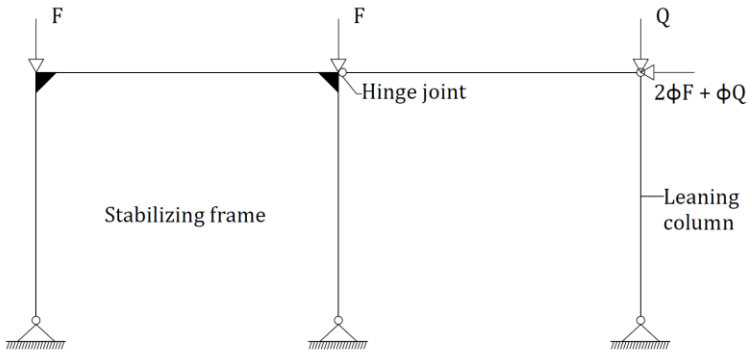

Figure 1: Frame configuration with a stabilizing frame and a leaning column

The Finite Element (FE) Model has to reflect reality in the best way. To achieve this, a study has been performed to create the most realistic model and in the end, this model is translated into an actual model including the leaning column effect. The analysis that should determine the ultimate load that the frame can carry also should reflect reality in the best way. Therefore various analysis methods were studied and performed by the FE-Model. To validate the accuracy of the way of modeling and the analysis methods, a validation study was performed for a sway frame without a leaning column.

After validating the model, the various analyses are performed again for a frame including the leaning column effect and this is processed in a case study. The numerical results of the various analyses are compared to the ultimate resistance load according to the codes, to see whether the codes cover the actual structural resistance of a frame including a leaning column. It was found that using the buckling length in the design rules determined with the nomogram in the Dutch National Annex NB.NA (the method that is most used in practice) gave results that were way off from the most realistic results, namely the buckling length determined with the FE-model. For

that reason, literature is studied where the leaning column effect was included in the buckling length. This gave promising results since all the results were safe and close to the most realistic approach.

To check whether the results were safe for all cases, a large range of leaning column problems was studied in a parametric study. The frame in Figure 1 was extended with a larger leaning column load and a larger horizontal load to increase the range of the leaning column problems. Figure 1 is also shortened to a frame without a leaning column for validation reasons. These new frame configurations are analyzed with variable parameters C and $\bar{\lambda}$, where C is the stiffness ratio and $\bar{\lambda}$ the slenderness ratio. Combining all the frame configurations and variable parameters resulted in 105 different frames that are analyzed, where 30 configurations were without a leaning column and 75 were with a leaning column.

For the 75 frames with leaning columns, it has been found that both the NEN 6771 and the current EN 1993-1-1 design rules do not give safe results when the slenderness ratio of the frames is increasing. This has led to the use of the most accurate method where the leaning column effect is included in the buckling length, namely the Yura approach. The Yura approach is called after the author J.A. Yura and makes use of simple equilibrium combined with the Euler buckling equation. For all considered frame configurations the Yura approach gives safe results, it is very accurate, and besides that, very practical to use.

TABLE OF CONTENTS

NOMENCLATURE

LIST OF ABBRAVIATIONS

AF	= Applied Force
DR	= Design-Resistance
EC	= EuroCode
FE	= Finite-Element
FEM	= Finite-Element-Method
GMNIA	= Geometrical and Material Non-linear Analysis with Imperfections
LA	= Linear elastic Analysis
LBA	= Linear elastic Bifurcation Analysis
LPF	= Load Proportionality Factor
LTB	= Lateral Torsional Buckling
NEN	= NEderlandse Norm
NMD	= Normalized Matrix of Displacements
RF	= Reaction Force
U.C.	= Unity Check

LIST OF SYMBOLS

$\textit{"symbol"}_{x,y,z}$	= direction indication for each symbol, X-, Y- or Z-direction
α	= imperfection factor, which depends on the type of the cross-section, the thickness, the yield strength, and the buckling plane
α_{cr}	= amplification factor by which the design loads would have to be increased to cause elastic instability
$\alpha_{GMNIA,i}$	= load proportionality factor, where $_{GMNIA,i}$ stand for the corresponding GMNIA
α_h	= reduction factor for height h applicable to columns
α_k	= imperfection factor, in NEN 6771 format
α_m	= reduction factor for the number of columns in a row
$\alpha_{ult,k}$	= minimum load amplifier of the design loads to reach the characteristic resistance of the most critical cross-section.
β	= modified length factor to increase the length of the structure to obtain the critical buckling length
$\beta_{nomogram}$	= modified length factor that does not take into account leaning column load, determined with the nomogram
β_{Yura}	= modified length factor that takes into account the leaning column load, determined with the Yura approach
γ_1	= partial material factor
δ	= (bow) deflection at the middle of the member
Δ	= lateral side-sway deformation of the frame
η_{cr}	= shape of the elastic critical buckling mode
η_{init}	= amplitude of the elastic critical buckling mode
θ_i	= angle
$\bar{\lambda}$	= relative slenderness ratio
λ_0	= plateau value for the buckling curve (0.2)
λ_e	= slenderness of a member where the Euler buckling stress is equal to $f_{y,d}$ in NEN 6771 format
λ_n	= value that represents the nomogram of the Dutch National Annex NB.NA
λ_{rel}	= relative slenderness ratio in NEN 6771 format
$\lambda_{y,z}$	= slenderness of a member relating to buckling of the relevant axis, in NEN 6771 format
μ	= correction factor to take the boundary condition at the other end of the supporting beam into account
ν	= Poisson's ratio in the elastic stage
ϕ	= slope of the structure due to global initial sway imperfection
ϕ_0	= basic value for global initial sway imperfection
χ	= buckling reduction factor
a	= leverarm
A	= area of the cross-section
A_j	= imperfection amplitude for each buckling mode
b	= width
b_1	= width of the stabilizing frame
b_2	= width of the leaning beam that connects the leaning column to the stabilizing frame
C	= stiffness ratio
C_i	= flexibility parameter, where i indicates A or B (the two member ends of the considered column)

C_m	= equivalent uniform moment factor
e_0	= initial bow imperfection of the column also called the Ayrton-Perry format
$e_{0,\delta}$	= bow imperfection, including additional deflection due to 2nd order behavior
E	= modulus of elasticity
$EI\left\|\eta_{cr}^{"}\right\|_{max}$	= maximum bending moment due to η_{cr} at the critical cross-section
$EI_{Q=10}$	= bending stiffness (EI) increased with a factor of 10 to prevent the wrong failure mode
f_u	= ultimate strength
f_y	= yield strength
$f_{y,d}$	= design value of the yield strength
$f_{y,d,Q=10}$	= design value of the yield strength increased with a factor of 10 to prevent the wrong failure mode
F	= applied vertical load
F_{cr}	= critical Euler buckling load
F_{lean}	= additional vertical design load that the stabilizing column has to carry
F_{shayan}	= statistically determined single factor
F_{tot}	= total vertical design load that the stabilizing column has to carry
F_{ult}	= ultimate load that the frame can carry
$F_{ult,GMNIA,i}$	= ultimate load that the frame can carry obtained with FEM, where GMNIA,i stands for the corresponding GMNIA
G_i	= flexibility parameter in American stand format, where i indicates A or B (the two member ends of the considered column)
h	= height of the structure
H	= applied horizontal load
i_i	= Surface momentum regarding the corresponding axis, in NEN 6771 format
I_i	= moment of inertia, where i indicates the axis direction
I_{bm}	= moment of inertia of the beam
I_{cln}	= moment of inertia of the column
k	= interaction factor depending on the relevant instability and plasticity phenomena
k_1	= reduction factor for columns longer than 5 m, in NEN 6771 format
k_2	= factor that takes into account the number of columns to be supported under compression or compression and bending, in NEN 6771 format
K	= modified length factor in American standard format
K_{exact}	= exact modified length factor in American standard format
K_n	= modified length factor that takes into account the leaning column load, in American standard format
K_o	= modified length factor that does take into account the leaning column load, in American standard format
L	= length of the member
L_{bm}	= length of the beam
L_{cln}	= length of the column
L_{cr}	= critical buckling length
m	= number of columns in a row
M	= bending moment
M_{el}	= elastic bending moment resistance of the cross-section
M_{Ed}	= design value of the maximum bending moment along the member
$M_{0,Ed}$	= design value of the first-order bending moment
$M_{II,Ed}$	= design value of the 2nd order bending moment
$M_{Ed,max}^{II}$	= maximum design value of the 2nd order bending moment
M_{pl}	= plastic bending moment resistance of the cross-section
M_{Rd}	= design value of the elastic or plastic moment resistance of the column, depending on the cross-section class
M_{Rk}	= characteristic moment resistance of the cross-section
$M_{u,d}$	= design value of the bending moment resistance of the column in NEN 6771 format
n	= amplification factor in NEN 6771 format
n_s	= highest number of floors of the frame, in NEN 6771 format
$N_{c,u,d}$	= design value of the normal force resistance of the column in NEN 6771 format
N_{Ed}	= design value of the axial load
N_{pl}	= plastic resistance to normal force of the cross-section
N_{Rd}	= design value of the plastic load resistance of the column cross-section
N_{Rk}	= characteristic resistance to normal force of the cross-section
N_{ult}	= ultimate design resistance load
$N_{ult,DR,i,j}$	= ultimate design resistance load, where i stands for the corresponding design code and j for the corresponding method for determining L_{cr}
P	= distance from the central point of the arc to the chord length
P-Δ	= 2nd order behavior of the total structure

P-δ	= 2nd order behavior of a single member along the length
P_j	= proportion factor of each buckling mode
Q	= applied leaning column load
r	= radius of the arc of the buckling shape
W_i	= section modulus where i stands for elastic or plastic
U	= lateral displacement obtained from Abaqus
x	= distance from the central point of the arc to the actual sway imperfection along L_{cr}
y	= distance from the central point of the arc to the actual sway imperfection perpendicular to the L_{cr} direction

1 INTRODUCTION

1.1 MOTIVATION AND PROBLEM DEFINITION

1.1.1 The leaning column effect

In design rules, the stability of a column is often considered as a function of an individual column. However, the stability of a column is actually a function of all of the columns in the story and therefore a system problem, not only an individual member problem [1]. The so-called 2nd order effects will introduce additional loads on an individual member induced by other members. The 2nd order effects of a structure can be sub-divided into a P-Δ and P-δ effect. P-Δ refers to the 2nd order behavior of the total structure, and P-δ refers to the 2nd order behavior of a single member along the length. This is illustrated in Figure 2, where it can be seen that P-Δ concerns the lateral deflection of the frame and P-δ the deflection of the member. P-Δ effects require an accurate determination of the buckling modes and the corresponding buckling lengths.

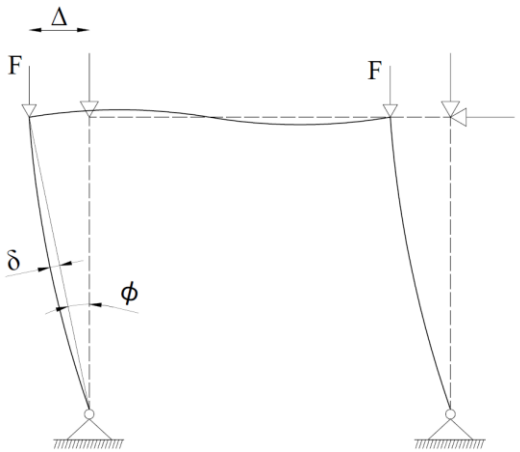

Figure 2: P-Δ and P-δ effect for a sway frame [2]

The above can be translated into a frame with a leaning column. Consider an unbraced sway frame with pin-ended supported columns as shown in Figure 3. The stabilizing frame takes care of the stability of the leaning column, so the leaning column does not participate in the lateral resistance of the structure. When considering the P-Δ effects for the frame of Figure 3, one can see that in the deformed situation, a horizontal force due to leaning will act on the frame coming from the leaning column, illustrated in Figure 4. The stabilizing frame also has to stabilize the leaning column, resulting in a greater 2nd order effect.

Section 1.1.2.1 will show that the NEN 6771 tried to consider the leaning column effect in a system problem, where they consider additional loads on the stabilizing columns. These additional loads represent the loads from the leaning column effect. In Section 1.1.2.2 it will be seen that the leaning column effect is not present in the Eurocode series, since the EN 1993-1-1 considers the criterium as an individual problem.

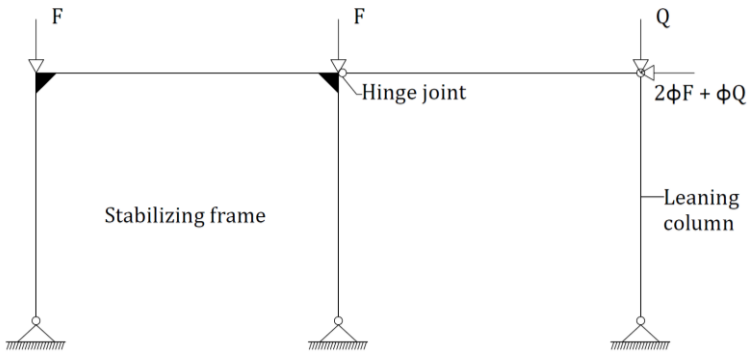

Figure 3: Frame configuration with a stabilizing frame and a leaning column

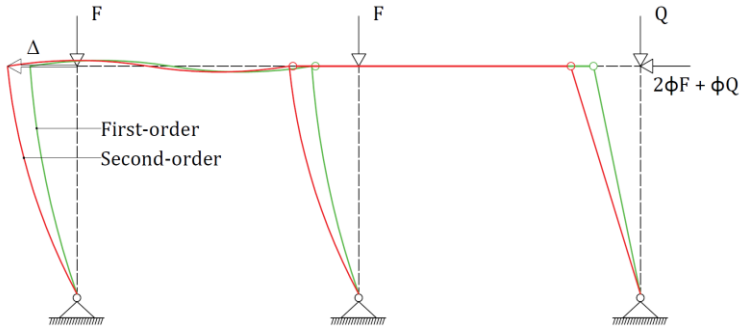

Figure 4: P-Δ effect for a sway frame with a leaning column

1.1.2 Design rules according to the codes

1.1.2.1 Design rules for member stability according to the NEN 6771

In the early days, the NEN 6770 and NEN 6771 provided design rules for steel structures in The Netherlands. Design rules about the stability of columns loaded in compression and bending could be found in both standards, but the NEN 6771 offers the clearest design rules. The assessment criteria for a column loaded in compression and bending is given as the following:

$$\frac{N_{c;s;d}}{N_{c;u;d}} + \frac{n}{n-1} \cdot \frac{F_{tot;s;d} \cdot e^* + M_{equ;s;d}}{M_{u;d}} \leq 1 \qquad (1)$$

For comparison reasons, equation (1), the design rule of the NEN 6771, is given with the abbreviations used by the EN 1993-1-1, given as the following:

$$\frac{N_{Ed}}{N_{Rd}} + \frac{\alpha_{cr}}{\alpha_{cr}-1} \cdot \frac{F_{tot} \cdot e_0 + M_{Ed}}{M_{Rd}} \leq 1 \qquad (2)$$

Where:

N_{Ed} = design value of the axial load ($N_{c;s;d}$ in NEN 6771 format);

N_{Rd} = design value of the plastic load resistance of the column cross-section ($N_{c;u;d}$ in NEN 6771 format);

α_{cr} = amplification factor by which the design loads would have to be increased to cause elastic instability (n in NEN 6771 format);

F_{tot} = total vertical load on one considered column, including a part of the vertical load on the leaning column(s) ($F_{tot;s;d}$ in NEN 6771 format);

e_0 = initial bow imperfection of the column, δ in Figure 2 (e^* in NEN 6771 format);

M_{Ed} = design value of the maximum bending moment along the member ($M_{equ;s;d}$ in NEN 6771 format);

M_{Rd} = design value of the elastic or plastic moment resistance of the column, depending on the cross-section class ($M_{u;d}$ in NEN 6771 format).

Where e_0 in equation (2) follows from the Ayrton-Perry format and is given in equation (3):

$$e_0 = \alpha_k(\lambda_{rel} - \lambda_0) \cdot \frac{W}{A} \tag{3}$$

The derivation of equation (3) will be given in section 1.1.2.2 based on the EN 1993-1-1, but in this section, the values from the NEN 6771 regarding equation (3) will be discussed without further explanation. Value λ_{rel} in equation (3) is the relative slenderness given by $\lambda_{rel} = \lambda_y/\lambda_e$, where $\lambda_y = L_{cr}/i_y$ and $\lambda_e = \pi \cdot \sqrt{E/f_y}$, where $i_y = \sqrt{I/A}$. Values E and f_y are the Young's modulus and yield strength of the material respectively. Values A and I are the area and the moment of inertia of the cross-section respectively. The critical buckling length (L_{cr}) can be determined from the Euler buckling load equation:

$$F_{cr} = \frac{\pi^2 EI}{(\beta \cdot L)^2} = \frac{\pi^2 EI}{L_{cr}^2} \tag{4}$$

Equation (2) is a design rule for a column under compression and bending in a two-dimensional frame. Since it is a two-dimensional case, lateral- and flexural torsional buckling are not considered. Equation part N_{Ed}/N_{Rd} represents the plastic member resistance unity-check due to normal force in the column, without considering buckling. The amplification factor $\alpha_{cr}/(\alpha_{cr} - 1)$ takes into account the second-order effects, where $\alpha_{cr} = F_{cr}/N_{Ed}$, where F_{cr} is the elastic critical Euler buckling load as given by equation (4). Criterium $(F_{tot} \cdot e_0 + M_{Ed})/M_{Rd}$ represents the ratio between the elastic or plastic bending moment resistance of the column and the acting bending moments due to imperfections, the leaning column effect, and the loads on the column.

The last part of the equation, the bending moment criterium, and second-order effects can be explained by considering a single column and the corresponding P-δ effect, as illustrated in Figure 5. The column in Figure 5 shows an imperfect column loaded in compression by vertical load F. In the loaded state, the first-order bending moment at equilibrium is equal to $M_{0,Ed} = F \cdot e_0$, where value e_0 is given as the Ayrton Perry format, which describes the real behavior of a column, including buckling. However, due to deflection e_0, an additional non-linear lateral deflection '$e_{0,\delta}$' will occur and the bending moment at equilibrium will increase to $M_{II,Ed} = F(e_0 + e_{0,\delta})$. This is called the second-order effect and can also be derived from multiplying the first-order bending moment with the amplification factor, leading to $M_{II,Ed} = M_{0,Ed} \cdot \frac{\alpha_{cr}}{\alpha_{cr}-1}$. Combining these equations leads to equation (5):

$$F \cdot (e_0 + e_{0,\delta}) = F \cdot e_0 \cdot \left(\frac{\alpha_{cr}}{\alpha_{cr} - 1}\right) \; with \; \alpha_{cr} = \frac{F_{cr}}{N_{Ed}} \tag{5}$$

The second term of equation (5) contains a big part of the last term of equation (2), meaning that it takes into account the second-order effects as just described.

As discussed in section 1.1.1, the P-Δ effect should also be considered to include the leaning column effect. In the NEN 6771, the effect of the leaning column is included in the load side of the equation, namely the value F_{tot}. The NEN 6771 offers solutions on how to include the effect of the leaning column in F_{tot}, and these solutions that are based on equilibrium are dependent on the mechanical scheme of the frame. Figure 6 shows how the NEN 6771 considers the total vertical load (F_{tot}) for the unbraced sway frame in Figure 3. In this case, the vertical load Q from the leaning

column is divided over the stabilizing columns of the frame, resulting in 3/2 N_{Ed} per stabilizing column. However, the background of the accuracy of this design rule is unknown.

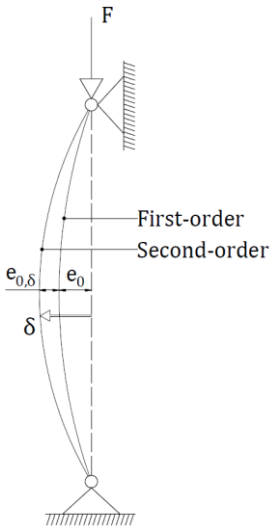

Figure 5: P-δ effect due to vertical loading on an imperfect column

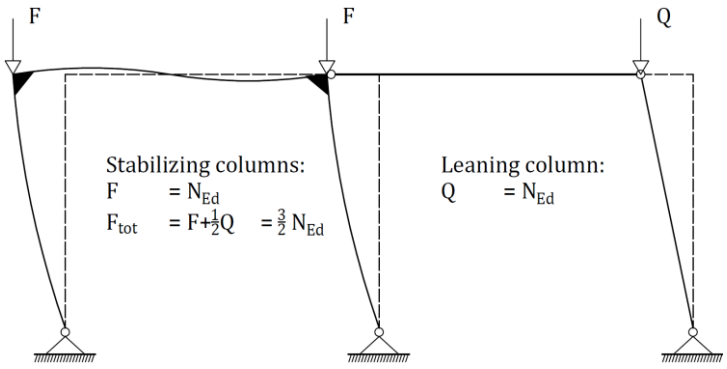

Figure 6: Derivation of F_{tot} for an unbraced sway frame [3]

1.1.2.2 Design rules for member stability according to the Eurocode

In 2012, the Eurocode (EC) was adopted in The Netherlands as a replacement for the NEN standards. The Eurocode is a European standard to assess the structural performance and safety of all possible building structures. The EC EN 1993-1-1 is the basic part containing the design rules for steel structures. The design rule for columns loaded in compression and bending according to the EN 1993-1-1 is given as the following:

$$\frac{N_{Ed}}{\chi_y \cdot N_{Rd}} + k_{yy}\frac{M_{y,Ed} + \Delta M_{y,Ed}}{\chi_{LT} \cdot M_{y,Rd}} + k_{yz}\frac{M_{z,Ed} + \Delta M_{z,Ed}}{\chi_{LT} \cdot M_{z,Rd}} \leq 1 \qquad (6)$$

Equation (6) is the three-dimensional design rule for columns loaded in the Y-direction. In this research, only a two-dimensional case will be considered en therefor equation (6) will be reduced to:

$$\frac{N_{Ed}}{\chi \cdot N_{Rd}} + k\frac{M_{Ed} + \Delta M}{\chi_{LT} M_{Rd}} \leq 1 \qquad (7)$$

Where:

N_{Ed} = design value of the axial load;

N_{Rd} = design value of the plastic load resistance of the column cross-section;
χ = buckling reduction factor;
k = interaction factors depending on the relevant instability and plasticity phenomena [2];
M_{Ed} = design value of the maximum bending moment along the member;
ΔM = bending moments due to the shift of the center of gravity in case of local buckling
M_{Rd} = design value of the elastic or plastic moment resistance of the column, depending on the cross-section class.
χ_{LT} = Lateral torsional buckling reduction factor;

Since local buckling and any out-of-plane behavior is not of interest, values χ_{LT} and ΔM *in* equation (7) can be left out. Lateral torsional buckling reduction factor χ_{LT} is left out because a two-dimensional case is considered and any out-of-plane (lateral torsional buckling) deformations in the FE-model will not be allowed. The reason for letting out bending moment ΔM is that profile classes 1, 2, and 3 will not be considered to omit local buckling. According to Table 3 of Annex A, this leads to ΔM=0. This will reduce equation (7) to:

$$\frac{N_{Ed}}{\chi \cdot N_{Rd}} + k\frac{M_{Ed}}{M_{Rd}} \leq 1 \qquad (8)$$

Equation (8) is valid for a column under compression and bending in a two-dimensional frame. In this case of this research, the lateral-torsional buckling reduction factor is left out, since any out-of-plane deformations in the Finite Element Model (FE-Model) will not be allowed. The term $N_{Ed}/\chi \cdot N_{Rd}$ presents the member resistance criteria due to normal force in the column, including buckling, where N_{Rd} is given by $N_{Rd} = A \cdot f_y/\gamma_1$, and where γ_1 is the partial resistance factor. For the second term the difference between equation (2) from the NEN 6771, and equation (8) from the EN 1993-1-1, can be spotted in value k.

The value k represents the interaction factor that depends on the relevant instability and plasticity phenomena [2]. The value of k can be derived from two different methods. Back in the days when the EN 1993-1-1 was written, two different teams of researchers treated the field of beam-columns. This has led to two different methods that are both included in the EN 1993-1-1 as Annex A (method 1) and Annex B (method 2). Both methods consider the most complex behavior of a member subjected to compression and biaxial bending, including all possible interactions and non-linear effects [4]. Boissonade et al. [4] state that in method 1 all the influences of material and geometrical nonlinearities and interactions between loading components are reflected by separate factors. Boissonade et al. [4] also state that, in contrast, method 2 uses a reduced number of such factors as a result of the globalization of several effects and calibration of the latter based on extensive numerical solutions. For further background information about the design rule of the Eurocode see chapter 2 of appendix A.

Annex B (method 2) of the Eurocode is used to make a comparison with the content of the NEN 6771. Interaction factor k will be derived for method 2 in the theoretical form. The starting point of the derivation is given in equation (9), which is the criterium for a column loaded in compression and bending [4]:

$$\frac{N_{Ed}}{N_{Rk}} + \frac{1}{1-\frac{N_{Ed}}{F_{cr}}} \cdot \frac{C_m \cdot M_{Ed} + N_{Ed} \cdot e_0}{M_{Rk}} \leq 1 \qquad (9)$$

Equation (9) makes use of a different notation of the amplification factor. The first step of the derivation is the expression for a column under compression and bending. Basically, equation (9) is the same as equation (2) from the NEN 6771. The only difference in equation (9) is the factor

C_m, $N_{Rk,}$ and M_{Rk}. Values N_{Rk} and M_{Rk} are the characteristic axial resistance and the characteristic bending-moment resistance respectively, given by $N_{Rk} = A \cdot f_y$ and $M_{Rk} = W \cdot f_y$. Factor C_m is the equivalent uniform moment factor depending on the corresponding bending moment diagram. The factor C_m is a standard value that can be obtained from the EN 1993-1-1, which indicates where the maximum bending moment can be found along the beam. This is explained in Figure 7, where the maximum bending moments $M_{0,Ed} = F \cdot e_0$ and $M = F \cdot a$ are not acting on the same location of the column. With the factor C_m from the EN 1993-1-1 the maximum acting bending moment on the column, $M_{Ed,max}^{II} = C_m \cdot M$ can be found.

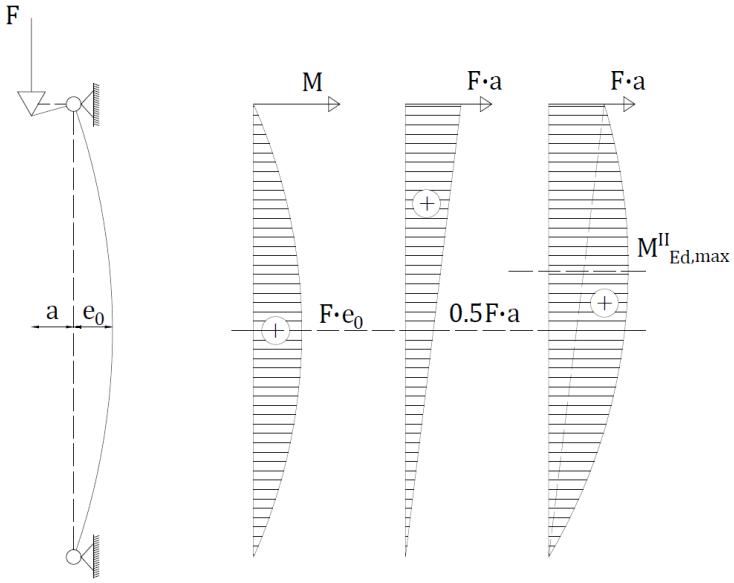

Figure 7: Column with an imperfection loaded on compression and bending, where $M_{Ed,max}$ shifts [5]

Until now, imperfection e_0 had no value. To proceed with the derivation of method 2, this value of imperfection e_0 needs to be included. Therefore e_0 will be numerically derived. This will be done by considering a column only loaded in compression. With the characteristic resistance values considered, the following condition for this column should be met:

$$\frac{N_{Ed}}{N_{Rk}} + \frac{1}{1 - \frac{N_{Ed}}{F_{cr}}} \cdot \frac{N_{Ed} \cdot e_0}{M_{Rk}} \leq 1 \tag{10}$$

When the axial compression force increases until collapse, N_{Ed} will be equal to $\chi \cdot N_{Rk}$. Substituting this in (10) gives:

$$\frac{\chi \cdot N_{Rk}}{N_{Rk}} + \frac{1}{1 - \frac{\chi \cdot N_{Rk}}{F_{cr}}} \cdot \frac{\chi \cdot N_{Rk} \cdot e_0}{M_{Rk}} = 1 \tag{11}$$

Solving e_0 from equation (11) gives:

$$e_0 = \frac{1 - \chi}{\chi} \cdot \frac{1}{1 - \frac{\chi \cdot N_{Rk}}{F_{cr}}} \cdot \frac{M_{Rk}}{N_{Rk}} \tag{12}$$

For class 1, 2, and 3 the relative slenderness is given by $\bar{\lambda} = \sqrt{N_{Rk}/F_{cr}}$. Substituting $\bar{\lambda}$ in (12) gives the following value for e_0:

$$e_0 = \left(\frac{1}{\chi} - 1\right)\left(1 - \chi \cdot \bar{\lambda}^2\right)\frac{M_{Rk}}{N_{Rk}} \tag{13}$$

Equation (13) is written in the Ayrton-Perry format and gives a value for e_0. When proceeding with the derivation of interaction factor k for method 2, equation (13) should be substituted in (9), leading to the following:

$$\frac{N_{Ed}}{N_{Rk}} + \frac{1}{1 - \frac{N_{Ed}}{F_{cr}}} \cdot \frac{C_m \cdot M_{Ed}}{M_{Rk}} + \frac{1}{1 - \frac{N_{Ed}}{F_{cr}}} \cdot \frac{N_{Ed}}{N_{Rk}}\left(\frac{1}{\chi} - 1\right)\left(1 - \chi \cdot \bar{\lambda}^2\right) \leq 1 \tag{14}$$

Multiplying (14) with $1 - N_{Ed}/F_{cr}$ gives:

$$\left(1 - \frac{N_{Ed}}{F_{cr}}\right)\frac{N_{Ed}}{N_{Rk}} + \frac{N_{Ed}}{N_{Rk}}\left(\frac{1}{\chi} - 1\right)\left(1 - \chi \cdot \bar{\lambda}^2\right) \leq \left(1 - \frac{N_{Ed}}{F_{cr}}\right) - \frac{C_m \cdot M_{Ed}}{M_{Rk}} \tag{15}$$

Substituting $\bar{\lambda} = \sqrt{N_{Rk}/F_{cr}}$ in (15) gives:

$$\left(1 - \frac{N_{Ed}}{N_{Rk}} \cdot \bar{\lambda}^2\right)\frac{N_{Ed}}{N_{Rk}} + \frac{N_{Ed}}{N_{Rk}}\left(\frac{1}{\chi} - 1\right)\left(1 - \chi \cdot \bar{\lambda}^2\right) \leq \left(1 - \frac{N_{Ed}}{N_{Rk}} \cdot \bar{\lambda}^2\right) - \frac{C_m \cdot M_{Ed}}{M_{Rk}} \tag{16}$$

Equation (16) can be rewritten to:

$$\frac{N_{Ed}}{N_{Rk}} - \frac{N_{Ed}^2}{N_{Rk}^2} \cdot \bar{\lambda}^2 + \frac{N_{Ed}}{\chi \cdot N_{Rk}} - \frac{N_{Ed}}{N_{Rk}} \cdot \bar{\lambda}^2 - \frac{N_{Ed}}{N_{Rk}} + \frac{N_{Ed}}{N_{Rk}} \cdot \chi\bar{\lambda}^2 - 1 + \frac{N_{Ed}}{N_{Rk}}\bar{\lambda}^2 \leq -\frac{C_m \cdot M_{Ed}}{M_{Rk}} \tag{17}$$

Now some terms in equation (17) cancel each other out and give:

$$-\frac{N_{Ed}^2}{N_{Rk}^2}\bar{\lambda}^2 + \frac{N_{Ed}}{\chi \cdot N_{Rk}} + \frac{N_{Ed}}{N_{Rk}}\chi \cdot \bar{\lambda}^2 - 1 \leq -\frac{C_m \cdot M_{Ed}}{M_{Rk}} \tag{18}$$

Equation (18) can be rewritten to:

$$\left(-1 + \frac{N_{Ed}}{\chi \cdot N_{Rk}}\right)\left(1 - \frac{N_{Ed}}{N_{Rk}} \cdot \chi \cdot \bar{\lambda}^2\right) \leq -\frac{C_m \cdot M_{Ed}}{M_{Rk}} \tag{19}$$

Now the following should be assumed:

$$\frac{1}{k} = \left(1 - \frac{N_{Ed}}{N_{Rk}} \cdot \chi \cdot \bar{\lambda}^2\right) \tag{20}$$

Substituting (20) in (19) gives:

$$\left(-1 + \frac{N_{Ed}}{\chi \cdot N_{Rk}}\right)\frac{1}{k} + \frac{C_m \cdot M_{Ed}}{M_{Rk}} \leq 0 \tag{21}$$

Multiplying (21) with k gives:

$$\frac{N_{Ed}}{\chi \cdot N_{Rk}} + k\frac{C_m \cdot M_{Ed}}{M_{Rk}} \leq 1 \; where \; k = \frac{1}{1 - \frac{N_{Ed}}{N_{Rk}}\chi \cdot \bar{\lambda}^2} \tag{22}$$

Combining k in equation (22) with $\bar{\lambda}^2 = N_{Rk}/F_{cr}$ gives:

$$\frac{N_{Ed}}{\chi \cdot N_{Rk}} + k\frac{C_m \cdot M_{Ed}}{M_{Rk}} \leq 1 \; where \; k = \frac{1}{1 - \frac{\chi \cdot N_{Ed}}{F_{cr}}} \tag{23}$$

When considering cross-section classes 1 and 2, yielding of the full cross-section of the member is allowed. For a cross-section of class 3, the extreme compression fiber can reach its yield strength, but local buckling is liable to prevent the development of the plastic moment resistance [6]. For cross-section classes 1 and 2 this leads to the values $N_{Rk} = N_{pl}$ and $M_{Rk} = M_{pl}$, where N_{pl} and M_{pl} are the plastic axial resistance and the plastic bending-moment resistance respectively. For cross-section class 3 this leads to $N_{Rk} = N_{pl}$ and $M_{Rk} = M_{el}$, where M_{el} is the elastic bending-moment resistance. Substituting these values in equation (23) gives:

$$\frac{N_{Ed}}{\chi \cdot N_{pl}} + k\frac{C_m \cdot M_{Ed}}{M_{el}} \leq 1 \; where \; k = \frac{1}{1 - \frac{\chi \cdot N_{Ed}}{F_{cr}}} \tag{24}$$

Substituting $N_{pl} = \frac{N_{Rk}}{\gamma_1} = \frac{f_y \cdot A}{\gamma_1} = N_{Rd}$ and $M_{el} = \frac{M_{Rk}}{\gamma_1} = \frac{f_y \cdot W_{el}}{\gamma_1} = M_{Rd}$, where W is the elastic section modulus of the cross-section, in (24) gives:

$$\frac{N_{Ed}}{\chi \cdot N_{Rd}} + k\frac{C_m \cdot M_{Ed}}{M_{Rd}} \leq 1 \; where \; k = \frac{1}{1 - \frac{\chi \cdot N_{Ed}}{F_{cr}}} \tag{25}$$

The interaction factor k in equation (25) is the theoretical value for method 2 of the EN 1993-1-1. Equation (25) is based on a linear cross-section interaction formulae, while in practice the elastic-plastic behavior for a member under compression and bending is way more complex [5]. This has led to numerical simulations to derive interaction factor k as presented in the EN 1993-1-1. The basis for this formulation is the additional format for the Ayrton-Perry format and is given as $\left(\frac{1}{\chi} - 1\right)\left(1 - \chi \cdot \bar{\lambda}^2\right) = \eta\chi = \alpha\chi(\bar{\lambda} - 0.2)$. Tables in the EN 1993-1-1 provide solutions for the interaction factor k, which are based on this value. For a two-dimensional case, a member with profile class 1 or 2, and buckling about the strong axis, this has led to equation (26), which is the final format in the EN 1993-1-1:

$$\frac{N_{Ed}}{\chi \cdot N_{Rd}} + k\frac{M}{M_{Rd}} \leq 1 \text{ where } k = C_m\left(1 + (\bar{\lambda} - 0.2) \cdot \frac{N}{\chi \cdot N_{Rd}}\right) \leq C_m\left(1 + 0.8 \cdot \frac{N}{\chi \cdot N_{Rd}}\right) \tag{26}$$

From equation (9) it can be seen that the starting point of the format of the EN 1993-1-1 design rule is the same as equation (2) from the NEN 6771 and already taking into account second-order effects. However, from equation (10) to (25) it can be seen that the Eurocode does not explicitly take into account the effect of the leaning column. Both design rules provide design rules for columns loaded in compression and bending but differ in presentation and content. The design rules in the Eurocode makes it hard for authorities to clearly check, what value for the leaning column effect an engineer has accounted for, or to see it has been taken into account at all.

1.2 RESEARCH OBJECTIVE

The research goal is to numerically verify the design rule of the NEN 6771 for the 'leaning column effect' and validate and rewrite the design rule of the EC EN1993-1-1 for a more clear presentation and content in the form of an explicit expression that describes the part of the leaning column effect.

1.3 RESEARCH APPROACH

The numerical verification of the design rules will be done by comparing the ultimate load that the frame can carry to the ultimate resistance load. The ultimate load that the frame can carry will be determined with a geometrical and material non-linear analysis with imperfections (GMNIA) in software Abaqus that reflects reality in the best way possible, resulting in $F_{ult,GMNIA}$. The ultimate resistance load will be determined by increasing load N_{Ed} until the design rule reaches unity and compared to $F_{ult,GMNIA}$.. An example for the NEN 6771 is illustrated in Figure 8, where equating the design rule of the NEN 6771 to unity results in the ultimate resistance load, given as $N_{ult,DR,NEN}$.

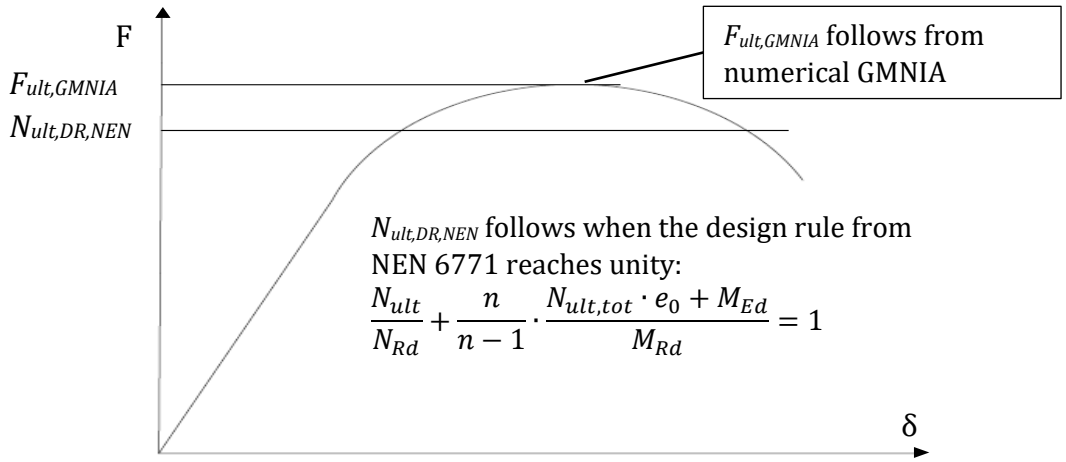

Figure 8: Force-displacement graph where the GMNIA and NEN 6771 will be compared

The design rule of the EN 1993-1-1 will be validated in the same way. The ultimate resistance load $N_{ult,DR,EC}$ will be found after increasing N_{Ed} until unity is reached. This is given by:

$$\frac{N_{ult}}{\chi \cdot N_{Rd}} + k\frac{M_{Ed}}{M_{Rd}} = 1 \qquad (27)$$

The design rule of the EN 1993-1-1 will be rewritten with the approach of the NEN 6771, to include the leaning column effect in the load side of the equation, but in the same format as the current EN 1993-1-1 design rule, to make the contribution of the 'leaning column effect' more clear in the EC. When validating the modified design rule of the EN 1993-1-1 ($N_{ult,DR,modEC}$), this should result in the same ultimate resistance load as the NEN 6771.

As a starting point of the research, the frame in Figure 3 will be considered, because it is expected that this configuration has the most impact of the leaning column effect. An FE-Model that can be compared with Figure 3 will be created that reflect reality. To achieve this, a study will be performed about how to create the most realistic model. The analysis method that should determine the ultimate load also should reflect reality. Therefore various analysis methods will be studied. To validate the accuracy of the model, a validation study will be performed over a sway frame without a leaning column, where the results of the literature and the FE-model will be compared. After that, the FE-Model can be used to carry out the analysis and determine $F_{ult,GMNIA}$.

Various schematizations of the frame with a leaning column and variable parameters will be considered. These various schematizations are discussed in section 1.4. The parameters that will be adjusted are the slenderness ratio and the stiffness ratio. The stiffness ratio is defined by $C = \frac{I_{cln}/L_{cln}}{I_{bm}/L_{bm}}$, where I_{cln} and I_{bm} are the second moment of inertia of the column and beam respectively, and where L_{cln} and L_{bm} are the lengths of the column and beam respectively. The stiffness ratio will be pinned on values 1, 1.5, and 2. In ratio C only L_{bm} will be a variable parameter, meaning that for a frame with the same cross-section for column and beam, the length times x1.5 and x2 already lead to stiffness ratios 1.5 and 2. However, theoretically, this ratio difference can also indicate different cross-sections (I_i) between column and beam, which can lead to less stiff structures. The slenderness ratio is defined by $\bar{\lambda} = \sqrt{N_{Rk}/F_{cr}}$, where $F_{cr} = \frac{\pi^2 EI}{L_{cr}^2}$ as given in equation (4) and $N_{Rk} = A \cdot f_y$. For obtaining different slenderness ratios, different cross-sections of the column are used. This makes that the cross-section properties in the equations will be variable, which are *A* and *EI*. The smaller the cross-section are over the height, the bigger the slenderness ratio is. Please note that the cross-section of the column also will be used for the beam.

This research focuses on rolled steel cross-sections of classes 1, 2, and 3. The fact that the cross-section is rolled influences the residual stress pattern, which will be used to model the imperfections of the frame. The EN 1993-1-1 classifies steel cross-sections in different classes, namely cross-section classes 1, 2, 3, and 4. Here classes 1 and 2 can develop their full plastic moment resistance and class 3 only its elastic moment resistance. Class 4 only can develop an elastic moment resistance over an effective area, since it is subjected to the effects of local buckling. Since the effect of local buckling does not influence the leaning column effect it is not of interest, and therefore cross-sections of class 4 will not be considered in this research. The leaning column effect is most vulnerable for side-sway modes, and therefore lateral-torsional buckling (LTB) will also not be considered in this research. The reason is that the leaning column effect has the most influence in a two-dimensional case and any out-of-plane deformations in the FE-Model will not be allowed.

This research also will consider different ways of determining the buckling length. The use of FE-software allows the determination of a more accurate value of the buckling length. However, in practice different methods will be used, for example, the nomogram equation, resulting in a higher (unsafer) ultimate load. In the progress, there will be looked for the most accurate way to determine L_{cr} that includes the leaning column effect.

1.4 RESEARCH SCOPE

In this research, a large range of frames will be studied that are the most vulnerable for the leaning column effect. These frame configurations are shown in Figure 9. Frame A is a sway frame with only a small vertical leaning column load and a small horizontal load due to imperfections. Frame A-V is the extended version of A with an increased vertical leaning column load (Q) of x10, where V stands for an increased Vertical load. To avoid that buckling of the leaning column is the governing failure mode, the leaning column is strengthened and stiffened with $10f_{y,d,}$ and $10EI$. Frame A-H is also an extended version of A but now with an increased Horizontal load. The horizontal load (H) is based on the grid dimensions of the frame, just as in practice, meaning that the increased horizontal load will not be the same for every frame. Frame A-VH combines the increased horizontal and vertical load. These four frame configurations are all vulnerable to side-sway deformations. For that reason also a stiffer frame configuration is considered, namely frame B. Frame B is a sway frame, but with clamped column ends which reduces the lateral side-sway deformations. The frame is performed with only a small Q and H. To validate the correctness of

the various GMNIA, also frame configurations without a leaning column will be performed, as shown in Figure 10.

All the results for the frames above will be plotted along the slenderness ratio $\bar{\lambda}$ from section 1.3. The frame configurations and the corresponding parameters cover a large range of $\bar{\lambda}$ and will be discussed more in-depth in chapter 7.

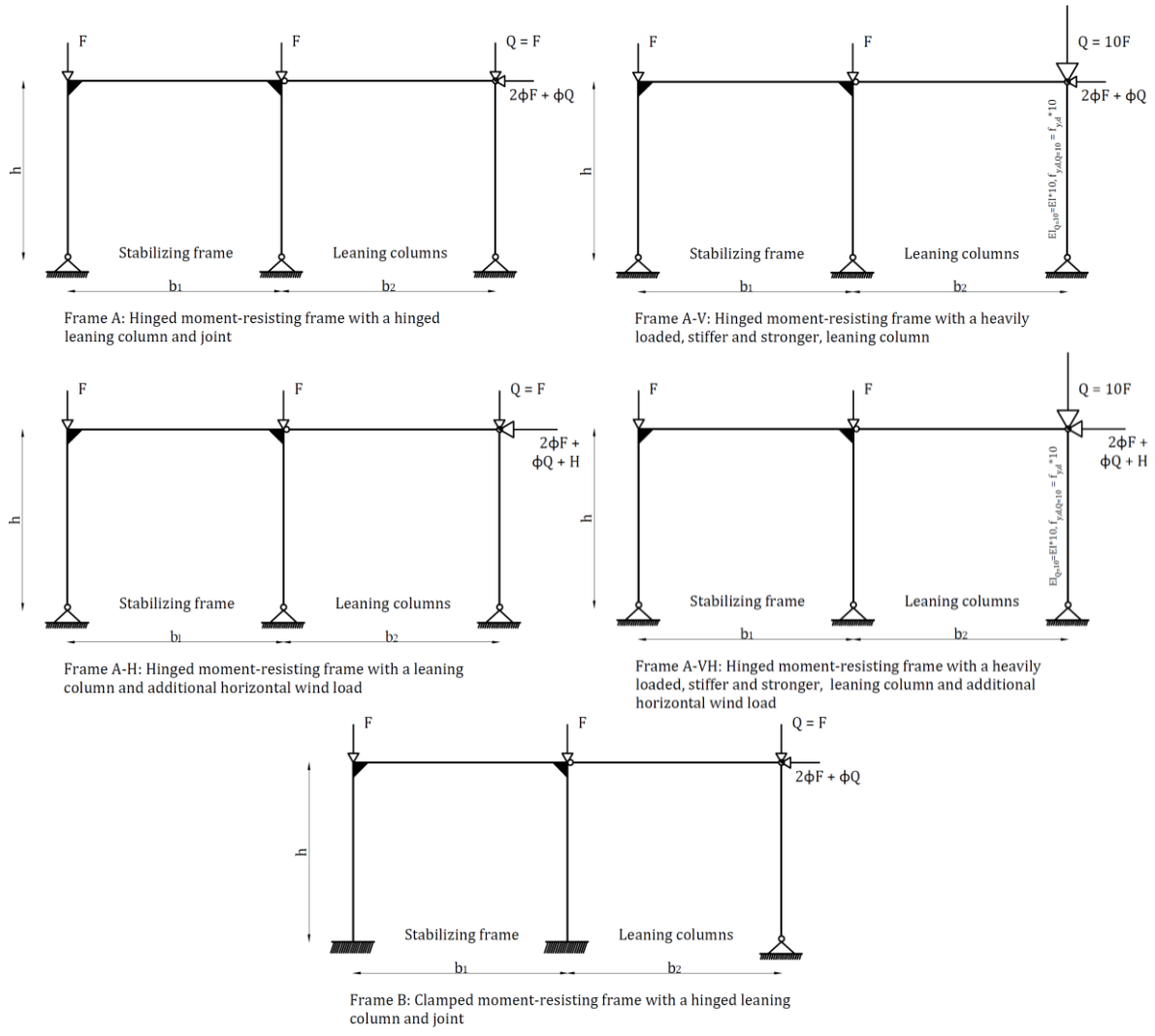

Figure 9: The frame configurations that present the research scope for the leaning column problem

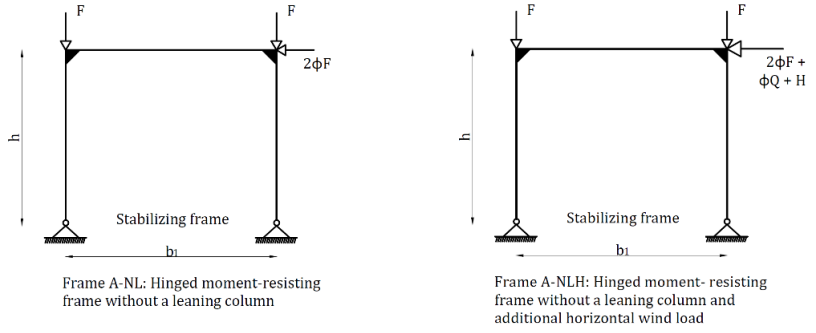

Figure 10: Frame configurations without the leaning column effect to validate the analyses

2 MODIFIED DESIGN RULE EN 1993-1-1

The modified design rule for the EN 1993-1-1, where the leaning column effect is included in the load side of the equation similar to the NEN 6771, can be developed right from the start and will be elaborated on in this chapter. The modified design rule will include the leaning column effect similarly to the NEN 6771. The final format of the modified design rule will be similar to the EN 1993-1-1. In chapter 6, the modified design rule will be used as one of the three ways to determine the ultimate design load. The other two ways are the actual NEN 6771 and EN 1993-1-1 design rules as described in section 1.1.2.

2.1 DEVELOPMENT MODIFIED DESIGN RULE EN 1993-1-1

From section 1.1.2.1 and 1.1.2.2 the two following practical assessment criteria for a column loaded in compression and bending are found (equation (2) and (9) respectively):

Starting point EN 1993-1-1:

$$\frac{N_{Ed}}{N_{Rk}} + \frac{1}{1 - \frac{N_{Ed}}{F_{cr}}} \cdot \frac{C_m \cdot M_{Ed} + N_{Ed} \cdot e_0}{M_{Rk}} \leq 1 \tag{28}$$

NEN 6771:

$$\frac{N_{Ed}}{N_{Rd}} + \frac{\alpha_{cr}}{\alpha_{cr} - 1} \cdot \frac{F_{tot} \cdot e_0 + M_{Ed}}{M_{Rd}} \leq 1 \tag{29}$$

By implementing the principle of value F_{tot} from equation (28) in equation (29), the leaning column effect can be included in the equation of the EN 1993-1-1. According to Figure 6, F_{tot} is 3/2 of load F. In the current design rule of the EN 1993-1-1 1F is already assessed by the design rule, meaning that $1/2$ of F is not. By splitting F_{tot} to F and F_{lean} = ½ F, the leaning column effect can be included in the modified design rule and the current format of the EN 1993-1-1 can be kept. The principle of F_{lean} is shown in Figure 11, which should lead to the same result as the NEN 6771.

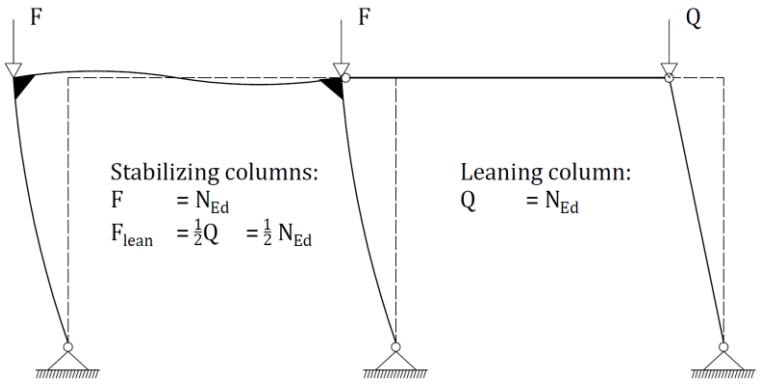

Figure 11: Derivation of F_{lean} for an unbraced sway frame

The derivation for Annex B method 2, as given in section 1.1.2.2, is elaborated again with starting point equation (30):

$$\frac{N_{Ed}}{N_{Rk}} + \frac{1}{1 - \frac{N_{Ed}}{F_{cr}}} \cdot \frac{C_m \cdot M_{Ed} + N_{Ed} \cdot e_0 + F_{lean} \cdot e_0}{M_{Rk}} \leq 1 \tag{30}$$

Value e_0 is again taken as the Ayrton-Perry format:

$$e_0 = \left(\frac{1}{\chi} - 1\right)\left(1 - \chi \cdot \bar{\lambda}^2\right)\frac{M_{Rk}}{N_{Rk}} \tag{31}$$

Substituting (31) in 30) gives:

$$\begin{aligned}\frac{N_{Ed}}{N_{Rk}} + \frac{1}{1 - \frac{N_{Ed}}{F_{cr}}} \cdot \frac{C_m \cdot M_{Ed}}{M_{Rk}} + \frac{1}{1 - \frac{N_{Ed}}{F_{cr}}} \cdot \frac{N_{Ed}}{N_{Rk}}\left(\frac{1}{\chi} - 1\right)\left(1 - \chi \cdot \bar{\lambda}^2\right) \\ + \frac{1}{1 - \frac{N_{Ed}}{F_{cr}}} \cdot \frac{F_{lean}}{N_{Rk}}\left(\frac{1}{\chi} - 1\right)\left(1 - \chi \cdot \bar{\lambda}^2\right) \leq 1\end{aligned} \tag{32}$$

Multiplying (32) with $1 - N_{Ed}/F_{cr}$ gives:

$$\begin{aligned}\left(1 - \frac{N_{Ed}}{F_{cr}}\right)\frac{N_{Ed}}{N_{Rk}} + \frac{N_{Ed}}{N_{Rk}}\left(\frac{1}{\chi} - 1\right)\left(1 - \chi \cdot \bar{\lambda}^2\right) + \frac{F_{lean}}{N_{Rk}}\left(\frac{1}{\chi} - 1\right)\left(1 - \chi \cdot \bar{\lambda}^2\right) \\ \leq \left(1 - \frac{N_{Ed}}{F_{cr}}\right) - \frac{C_m \cdot M_{Ed}}{M_{Rk}}\end{aligned} \tag{33}$$

Substituting $\bar{\lambda} = \sqrt{N_{Rk}/F_{cr}}$ in (33) gives:

$$\begin{aligned}\left(1 - \frac{N_{Ed}}{N_{Rk}} \cdot \bar{\lambda}^2\right)\frac{N_{Ed}}{N_{Rk}} + \frac{N_{Ed}}{N_{Rk}}\left(\frac{1}{\chi} - 1\right)\left(1 - \chi \cdot \bar{\lambda}^2\right) + \frac{F_{lean}}{N_{Rk}}\left(\frac{1}{\chi} - 1\right)\left(1 - \chi \cdot \bar{\lambda}^2\right) \\ \leq \left(1 - \frac{N_{Ed}}{N_{Rk}} \cdot \bar{\lambda}^2\right) - \frac{C_m \cdot M_{Ed}}{M_{Rk}}\end{aligned} \tag{34}$$

Equation (34) can be rewritten to:

$$\begin{aligned}\frac{N_{Ed}}{N_{Rk}} - \frac{N_{Ed}^2}{N_{Rk}^2} \cdot \bar{\lambda}^2 + \frac{N_{Ed}}{\chi \cdot N_{Rk}} - \frac{N_{Ed}}{N_{Rk}} \cdot \bar{\lambda}^2 - \frac{N_{Ed}}{N_{Rk}} + \frac{N_{Ed}}{N_{Rk}} \cdot \chi\bar{\lambda}^2 + \frac{F_{lean}}{\chi \cdot N_{Rk}} - \frac{F_{lean}}{N_{Rk}} \cdot \bar{\lambda}^2 \\ - \frac{F_{lean}}{N_{Rk}} + \frac{F_{lean}}{N_{Rk}} \cdot \chi\bar{\lambda}^2 - 1 + \frac{N_{Ed}}{N_{Rk}} \cdot \bar{\lambda}^2 \leq -\frac{C_m \cdot M_{Ed}}{M_{Rk}}\end{aligned} \tag{35}$$

In this case, some of the values with N_{Ed} in equation (35) cancel each other out, but the values with F_{lean} in the equation do not. Therefore, only a part of the equation (35) can be rewritten to:

$$\begin{aligned}-\frac{N_{Ed}^2}{N_{Rk}^2}\bar{\lambda}^2 + \frac{N_{Ed}}{\chi \cdot N_{Rk}} + \frac{N_{Ed}}{N_{Rk}}\chi \cdot \bar{\lambda}^2 + \frac{F_{lean}}{\chi \cdot N_{Rk}} - \frac{F_{lean}}{N_{Rk}} \cdot \bar{\lambda}^2 - \frac{F_{lean}}{N_{Rk}} + \frac{F_{lean}}{N_{Rk}} \cdot \chi\bar{\lambda}^2 \\ -1 \leq -\frac{C_m \cdot M_{Ed}}{M_{Rk}}\end{aligned} \tag{36}$$

Then equation (36) can be rewritten to:

$$\left(-1 + \frac{N_{Ed}}{\chi \cdot N_{Rk}}\right)\left(1 - \frac{N_{Ed}}{N_{Rk}} \cdot \chi \cdot \bar{\lambda}^2\right) + \left(\bar{\lambda}^2 - \frac{1}{\chi}\right)(\chi - 1)\frac{F_{lean}}{N_{Rk}} \leq -\frac{C_m \cdot M_{Ed}}{M_{Rk}} \tag{37}$$

Now the following should be assumed:

$$\frac{1}{k} = \left(1 - \frac{N_{Ed}}{N_{Rk}} \cdot \chi \cdot \bar{\lambda}^2\right) \tag{38}$$

Substituting (38) in (37) gives:

$$\left(-1 + \frac{N_{Ed}}{\chi \cdot N_{Rk}}\right)\frac{1}{k} + \left(\bar{\lambda}^2 - \frac{1}{\chi}\right)(\chi - 1)\frac{F_{lean}}{N_{Rk}} + \frac{C_m \cdot M_{Ed}}{M_{Rk}} \leq 0 \tag{39}$$

Multiplying (39) with k gives:

$$\frac{N_{Ed}}{\chi \cdot N_{Rk}} + k\left(\bar{\lambda}^2 - \frac{1}{\chi}\right)(\chi - 1)\frac{F_{lean}}{N_{Rk}} + k\frac{C_m \cdot M_{Ed}}{M_{Rk}} \leq 1 \; where \; k = \frac{1}{1 - \frac{N_{Ed}}{N_{Rk}}\chi \cdot \bar{\lambda}^2} \tag{40}$$

Combining k in equation (40) with $\bar{\lambda}^2 = N_{Rk}/F_{cr}$ gives:

$$\frac{N_{Ed}}{\chi \cdot N_{Rk}} + k\left(\bar{\lambda}^2 - \frac{1}{\chi}\right)(\chi - 1)\frac{F_{lean}}{N_{Rk}} + k\frac{C_m \cdot M_{Ed}}{M_{Rk}} \leq 1 \; where \; k = \frac{1}{1 - \frac{\chi \cdot N_{Ed}}{F_{cr}}} \tag{41}$$

As described in section 1.1.2.2, the values for cross-section classes 1 and 2 leads to the values $N_{Rk} = N_{pl}$ and $M_{Rk} = M_{pl}$, where N_{pl} and M_{pl} are the plastic axial resistance and the plastic bending-moment resistance respectively. For cross-section class 3 this leads to $N_{Rk} = N_{pl}$ and $M_{Rk} = M_{el}$, where M_{el} is the elastic bending-moment resistance. Substituting these values in equation (41) gives:

$$\frac{N_{Ed}}{\chi \cdot N_{pl}} + k\left(\bar{\lambda}^2 - \frac{1}{\chi}\right)(\chi - 1)\frac{F_{lean}}{N_{pl}} + k\frac{C_m \cdot M_{Ed}}{M_{el}} \leq 1 \; where \; k = \frac{1}{1 - \frac{\chi \cdot N_{Ed}}{F_{cr}}} \tag{42}$$

Substituting $N_{pl} = \frac{N_{Rk}}{\gamma_1} = \frac{f_y \cdot A}{\gamma_1} = N_{Rd}$ and $M_{el} = \frac{M_{Rk}}{\gamma_1} = \frac{f_y \cdot W_{el}}{\gamma_1} = M_{Rd}$ in (42) gives:

$$\frac{N_{Ed}}{\chi \cdot N_{Rd}} + k\left(\bar{\lambda}^2 - \frac{1}{\chi}\right)(\chi - 1)\frac{F_{lean}}{N_{Rd}} + k\frac{C_m \cdot M_{Ed}}{M_{Rd}} \leq 1 \; where \; k = \frac{1}{1 - \frac{\chi \cdot N_{Ed}}{F_{cr}}} \tag{43}$$

Where equation (43) is based on a linear cross-section interaction formula and interaction factor k is the theoretical value for method 2 of the EN 1993-1-1. Equation (43) is the format of the modified design rule of the Eurocode and gives the same result as equation (2) from the NEN 6771.

3 STRUCTURAL STABILITY OF FRAMES

To compare the design rules with real structural behavior, the FE analyses should provide sufficient accuracy regarding the structural stability of the frame. This chapter will discuss the types of analysis that have to be considered to study such a frame including the leaning column effect. Non-linearities, or also called imperfections, play a role in the accuracy of the analyses and also will be discussed in this chapter. At the end of this chapter, the considered analyses and the corresponding imperfections that will be used will be listed and discussed.

3.1 ANALYSIS METHODS

Structures carried out in steel are usually slender structures when compared to other materials. Instability phenomena are in most cases present, so it is necessary to verify the global stability of the structure. Due to deformations that slender structures undergo, this verification needs a 2nd order analysis. A global analysis directly accounting for all imperfections (geometrical and material) and all 2nd order effects is the most convenient one, leading to a second-order inelastic analysis. This method is commonly called a Geometrical and Material Non-linear Analysis with Imperfections, the so-called GMNIA [2]. Regarding the input that is needed to carry out the design rules and the GMNIA as will be described in section 3.3, additionally, a linear elastic analysis (LA) and linear elastic bifurcation analysis (LBA) will be performed. The following analysis methods are suitable:

- first-order elastic analysis: In this approach, small deformations without imperfections are assumed. Equilibrium is determined on the undeformed state, so not taking into account additional internal forces due to deformations of the structure. Additionally, superposition is valid and any inelastic behavior of the material is ignored according to Hooke's law, leading to a linear result [1]. This type of analysis applies to a linear elastic analysis (LA).
- elastic buckling analysis: An elastic buckling analysis determines the critical buckling load of the structure. This load can be determined from the eigenvalue of the structure or an iterative process based on the equilibrium in the deformed state. The result of this analysis is only a single value at which the structure buckles and is referred to as the Euler buckling load [1]. The Euler buckling load takes into account linear elastic behavior and small deformations without imperfections. This type of analysis applies to a linear elastic bifurcation analysis (LBA), resulting in α_{cr}.
- second-order elastoplastic analysis: This analysis combines the second-order elastic analysis with the first-order elastic-plastic analysis. This type of analysis takes non-linearity into account and the material behavior is considered as elastoplastic, leading to a realistic behavior reflecting reality. The model takes into account large deformations in such a way that it influences the state of equilibrium [1]. This type of analysis applies to a geometrical and material nonlinear analysis including imperfections (GMNIA).

Figure 12 shows the load-displacement history for the various approaches. It can be seen that the second-order inelastic analysis leads to the lowest ultimate load that the frame can carry compared to other analyses. It should be noted that structures have more than one buckling mode and therefore more than just the first buckling mode should be considered to reflect reality in the best way. Also, for the calculation of the elastic critical load, the structural model that represents the structure should adequately reproduce the elastic behavior, so including the behavior of the joints and initial stiffness.

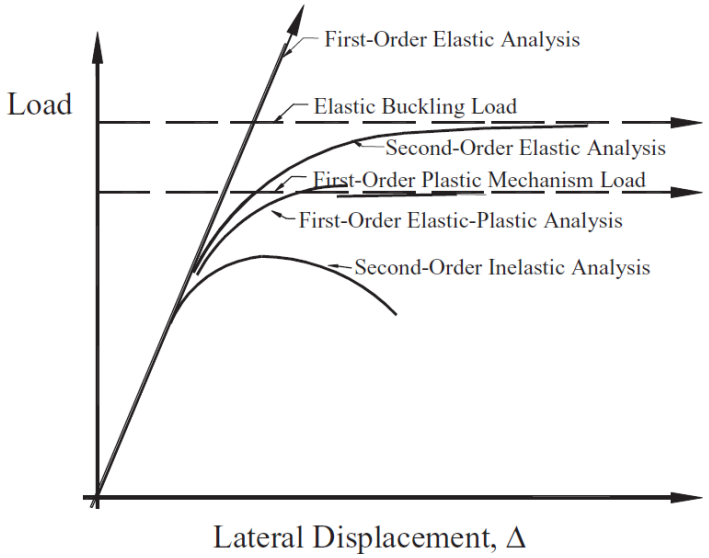

Figure 12: Load-displacement paths [1]

3.2 IMPERFECTIONS

Imperfections, as mentioned in section 1.1, are always present in steel structures, and are responsible for the additional secondary forces that will occur in the structure. There are several types of imperfections:

- Residual stresses (material imperfections);
- Eccentricities in joints (geometrical imperfections);
- Eccentricities of loads (geometrical imperfections);
- lack of verticality, lack of straightness, and lack of flatness in members (geometrical imperfections);
- imperfections leading to torsional effects;
- slip in bolt holes, and similar stiffness effects.

In this research, imperfections will be considered according to the Eurocode and the literature. In the EN 1993-1-1 clause 5.3.1(2) it is stated that in the analysis, the imperfections should be taken into account in the form of equivalent geometric imperfections. This form reflects all imperfections as discussed above. In the case of imperfections based on the literature, as many imperfections as possible will be modeled aiming for the most realistic representation of the frame. The effects of the imperfections that should be taken into account are global imperfections for frames and local imperfections for individual members. [7]

For the imperfections for global analysis of frames, the EN 1993-1-1 clause 5.3.2(1) consider the shape and direction that lead to the governing situation and effects. This makes that the assumed shape of global imperfections and local imperfections may be derived from the direction of the elastic buckling mode. These buckling modes are also dependent on the behavior of the structure. When a structure is sensitive to lateral deformations it is called “sway mode”, and when a structure is not sensitive to lateral deformations it is called “non-sway mode”. This is illustrated in Figure 13. According to the EN 1993-1-1 clause 5.3.2(3), for frames sensitive to buckling in a sway mode, it is allowed to take imperfections into account by considering an equivalent imperfection in the form of an initial sway imperfection and individual bow imperfections of the members.

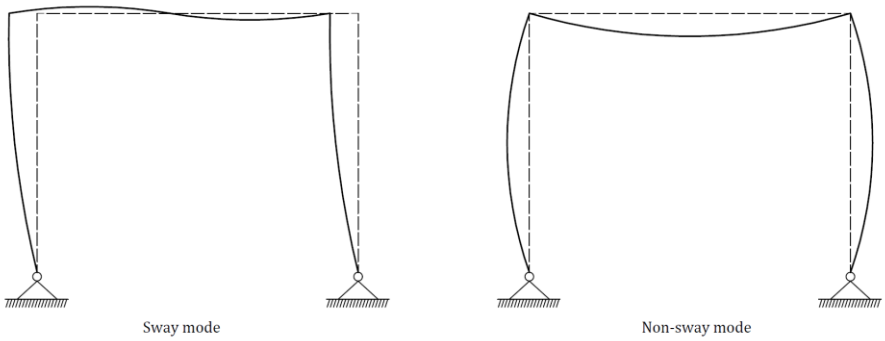

Figure 13: Sway mode frame (left) and non-sway mode frame (right) [2]

The EN 1993-1-1 allows replacing the effects of sway imperfections and local bow imperfections as described above by equivalent horizontal forces, as illustrated in Figure 14.

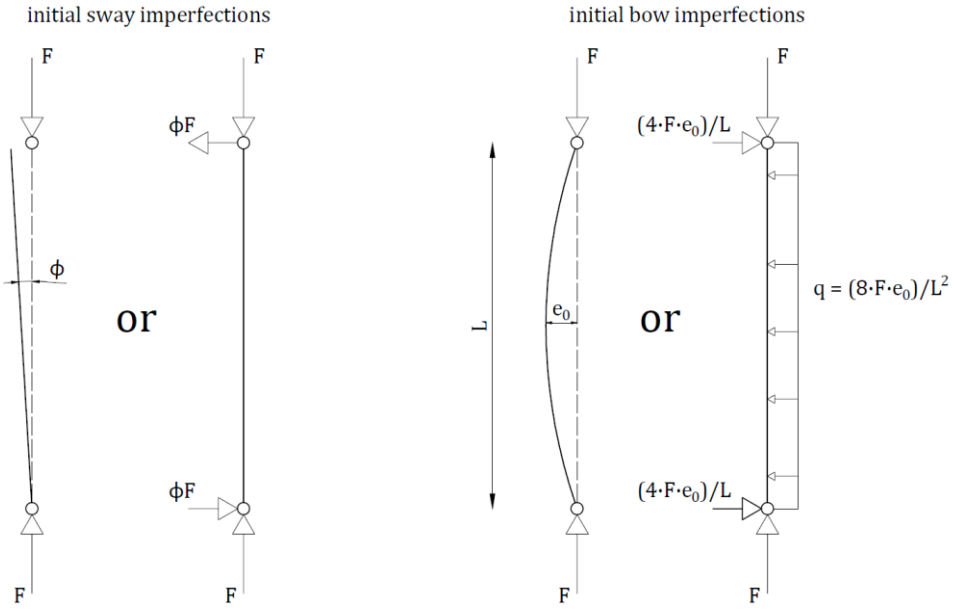

Figure 14: Replacement of initial imperfections by equivalent horizontal forces [7]

Structures are the most sensitive to imperfections like the eigenmode. It is possible to use displacement normalization, which makes use of the actual buckling modes. This technique normalizes the matrix of displacements of the buckling shape and makes it possible to plot the normalized matrix of displacements (NMD) as an imperfection on the structure. This can be performed by the Finite Element software and results in a more realistic behavior of the structure. An additional way to aim for a more realistic model is the implementation of residual stresses. Residual stresses develop due to differential cooling after hot rolling and any other kind of process involving heat and can be included in an FE-Model [2].

3.3 ANALYSIS METHODS USED AND THEIR CORRESPONDING IMPERFECTIONS

To determine the ultimate load that the frame can carry (F_{ult}), various GMNIA with different imperfections will be performed. These GMNIA's aims to accurately determine the ultimate load that the frame can carry. The inputs for the imperfections are based on the EN 1993-1-1 or the literature. To determine the magnitude of the imperfections, in most cases on the forehand an LBA and LA are needed.

3.3.1 GMNIA I according to EN 1993-1-1 Clause 5.3.2(3)

GMNIA I makes use of the equivalent sway and bow imperfections according to the EN 1993-1-1. For the derivation of the global initial sway imperfection, the EN 1993-1-1 clause 5.3.2(3a) [7] refers to Figure 15, indicating a lack of verticality of the structure. The slope ϕ of the imperfect structure is given by:

$$\phi = \phi_0 \cdot \alpha_h \cdot \alpha_m \tag{44}$$

Where ϕ_0 is the basic value of $\phi_0 = 1/200$, α_h is the reduction factor for height h applicable to columns and α_m is the reduction factor for the number of columns in a row, and follow from:

$$\alpha_h = \frac{2}{\sqrt{h}} \qquad \text{but} \qquad \frac{2}{3} \leq \alpha_h \leq 1 \qquad ; \qquad \alpha_m = \sqrt{0.5\left(1 + \frac{1}{m}\right)} \tag{45}$$

Where h is the height of the structure in meters and m is the number of columns in a row, including only those columns which carry a vertical load F not less than 50% of the average value of the column in the vertical plane considered. The lateral displacement can be found by $\Delta = \phi h$.

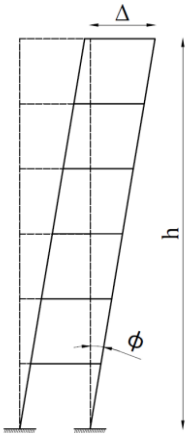

Figure 15: Equivalent sway imperfections [7]

According to EN 1993-1-1 clause 5.3.2(3b) [7], the relative initial local bow imperfections of members for flexural buckling in a bending mode are based on the numerical format of the Ayrton-Perry format, as discussed in section 1.1.2.2. Bow imperfection e_0 is given by equation (46):

$$e_0 = \alpha(\bar{\lambda} - 0.2)\frac{M_{Rk}}{N_{Rk}} \tag{46}$$

Where α is the imperfection factor for the relevant buckling curve. For the value of α see table 1 of appendix A. Value e_0 is the maximum initial lateral displacement over height L, as shown in Figure 16.

The corresponding flow chart of GMNIA I is given in Figure 17, where $\alpha_{ult,k}$ is the minimum force amplifier for the load N_{Ed} to reach the characteristic resistance N_{Rk} of the most axially stressed cross-section without taking buckling into account [7]. The imperfections are induced on the structure by equivalent forces, as illustrated in Figure 14.

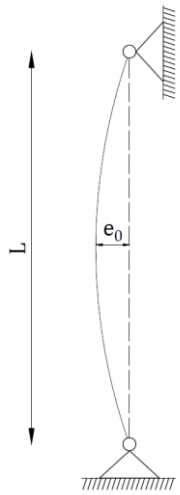

Figure 16: Maximum amplitude of the initial lateral displacement e_0

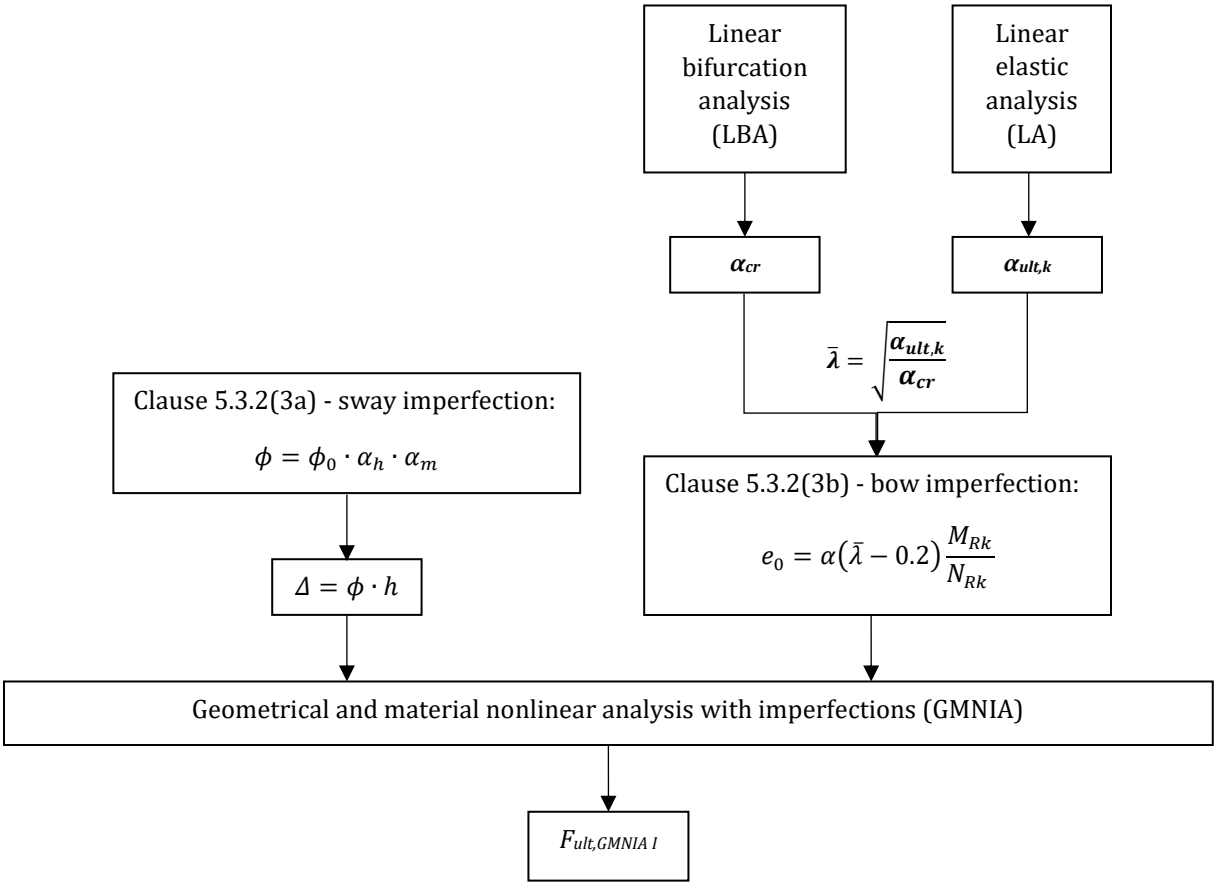

Figure 17: Flow chart of GMNIA I for obtaining $F_{ult,GMNIA\ I}$

3.3.2 GMNIA II according to EN 1993-1-1 clause 5.3.2(11)

As an alternative for clause 5.3.2(3), one can choose to derive the imperfections with clause 5.3.2(11). This will be used in GMNIA II. Clause 5.3.2(11) induces the imperfections on the structure by scaling the normalized matrix of displacements of the critical eigenmode with equivalent scaling-factor η_{init}. The solutions for clause 5.3.2(11) are given in equation (47) and (48):

$$\eta_{init} = e_0 \cdot \frac{F_{cr}}{EI\left|\eta_{cr}^{"}\right|_{max}}\eta_{cr} = \frac{e_0}{\bar{\lambda}^2} \cdot \frac{N_{Rk}}{EI\left|\eta_{cr}^{"}\right|_{max}}\eta_{cr} \quad (47)$$

$$e_0 = \alpha\left(\bar{\lambda} - 0.2\right)\frac{M_{Rk}}{N_{Rk}} \cdot \frac{1 - \frac{\chi^{\bar{\lambda}^2}}{\gamma_{M1}}}{1 - \chi^{\bar{\lambda}^2}} \; for \; \bar{\lambda} > 0.2 \quad (48)$$

Where, according to Comité Européen de Normalisation [7], the abbreviations are the following:
$EI\left|\eta_{cr}^{"}\right|_{max}$ = is the bending moment due to η_{cr} at the critical cross-section;
η_{cr} = shape of elastic critical buckling mode.

The corresponding flow chart of GMNIA II is given in Figure 18.

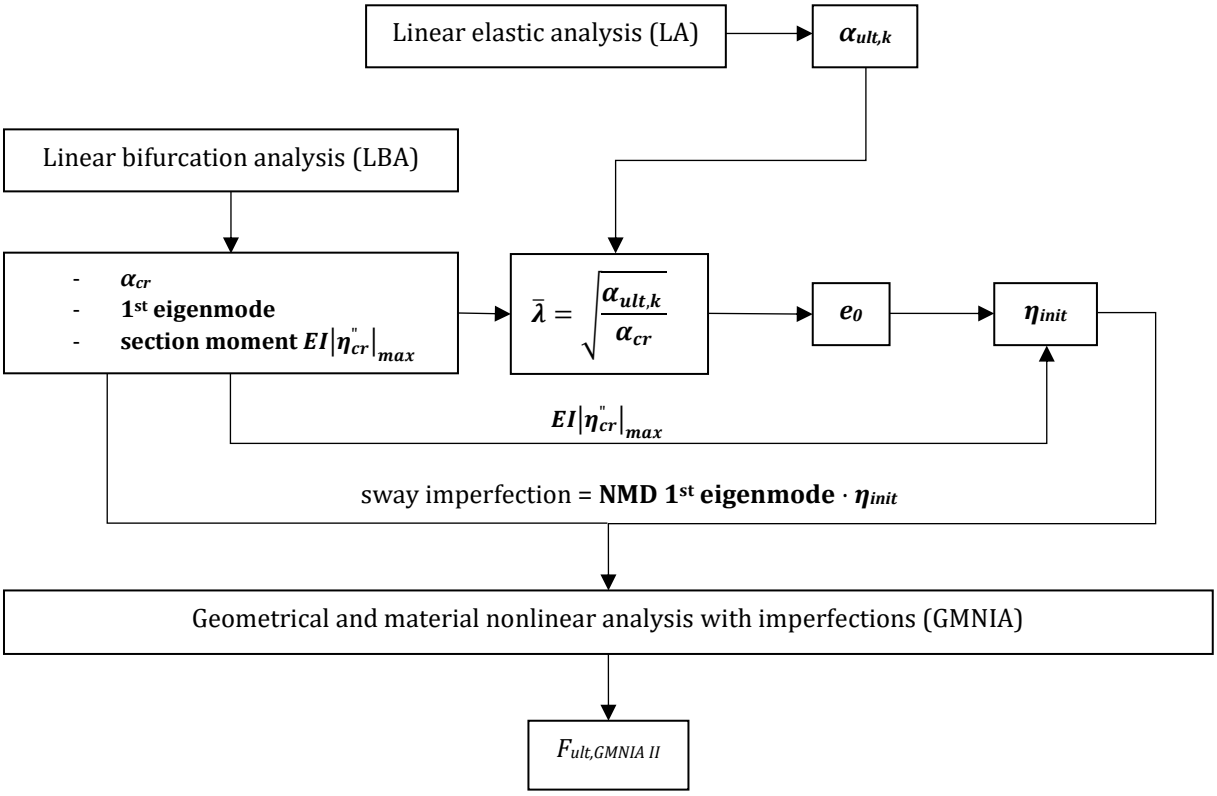

Figure 18: Flow chart of GMNIA II for obtaining $F_{ult,GMNIA\ II}$

3.3.3 GMNIA III according to Vogel et al.

GMNIA III takes into account geometrical imperfections and residual stresses from the literature, aiming for a more realistic representation of the structure. When one chooses to implement residual stresses, this has some consequences for the GMNIA analyses. The first one is the way of modeling in the software. The equivalent imperfections of the EN 1993-1-1 allow modeling with beam elements since geometrical imperfections do not need many details in the modeling. However, these beam elements do not allow the implementation of residual stresses, leading to the usage of shell elements when residual stresses are considered. These elements need a more detailed approach to modeling and will be discussed in chapter 4. Secondly, the EN 1993-1-1 does not cover the field of analysis with the implementation of residual stresses. This means that all amplitudes of imperfections that have to be included in GMNIA III have to be obtained from the literature.

The European Convention for Constructional Steelwork (ECCS) offers some basic input parameters for the analysis, focussing on the use of computer software. These parameters will lead overall to comparable results. In this research only rolled I-sections will be considered. According to the elastic-plastic analysis that was discussed by Vogel et al. [8], the residual stress pattern that has to be taken into account is shown in Figure 19, and the initial geometrical imperfection in Figure 20.

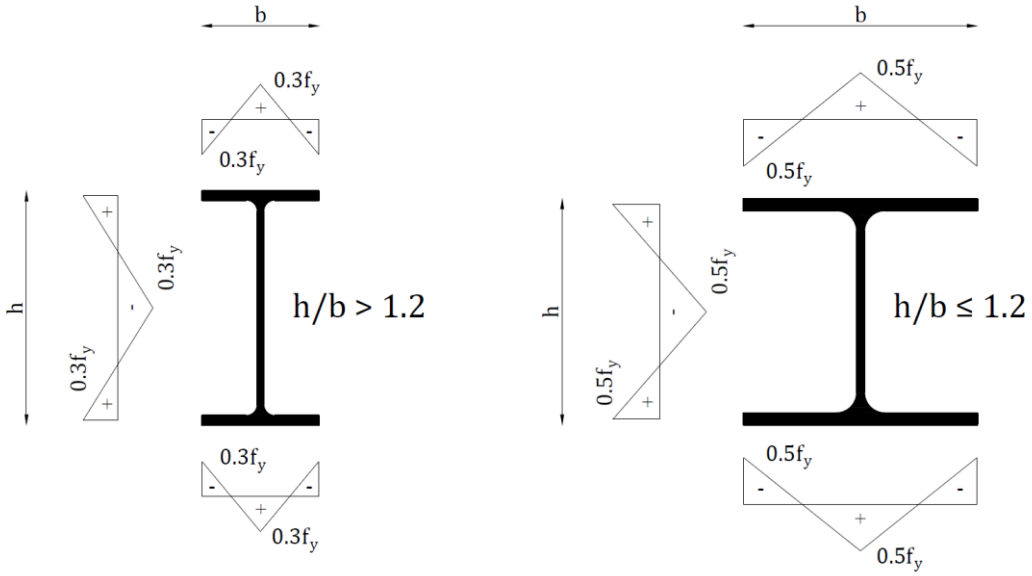

Figure 19: The magnitude of residual stresses for rolled I-shape sections according to Vogel et al. [8]

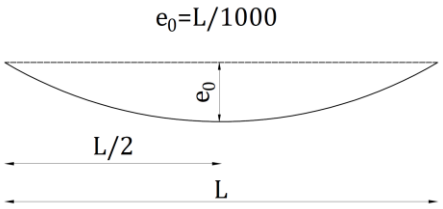

Figure 20: Geometric imperfections for the elastic-plastic analysis according to Vogel et al. [8]

Based on the initial bow imperfection in Figure 20, the sway imperfection can be sized based on the buckling length of the structure. The buckling mode of a structure follows a half-sinus wave, which is the same form as the initial bow imperfection. This means that the lateral sway deflection lays on the line of the buckling mode of the structure, which in this case is equal to $e_0 = L_{cr}/1000$. Figure 21 gives the initial sway imperfections following the corresponding buckling mode for a pin-ended connected frame (left) and a clamped-ended connected frame (right).

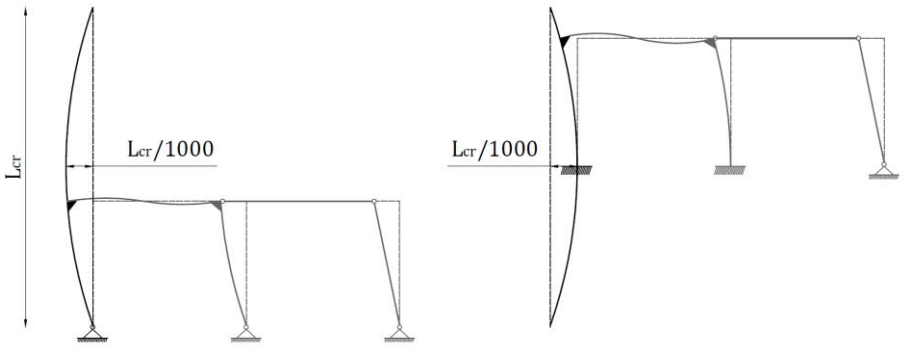

Figure 21: Sway imperfection based on $e_0 = L_{cr}/1000$ for pin-ended frame (left) and clamped-ended frame (right)

Based on equation (4), L_{cr} can be derived from equation (49):

$$L_{cr} = \pi \cdot \sqrt{\frac{EI}{\alpha_{cr} \cdot N_{Ed}}} \tag{49}$$

Where $\alpha_{cr} \cdot N_{Ed}$ represents the critical load F_{cr}. Figure 21 shows that the actual lateral displacement of the frame is not at the height of $L_{cr}/1000$. This is only the case when $L_{cr} = 2L$. To obtain the value at the correct height, geometrical corrections have to be taken. An example of such a geometrical correction is shown in Figure 22.

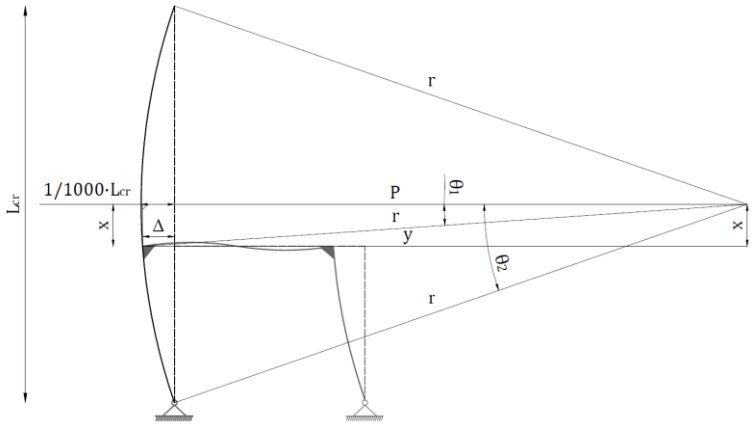

Figure 22: Geometrical correction for the sway imperfection based on Vogel et al. [8]

For GMNIA III the initial geometrical sway imperfections also will be induced on the structure by the normalized matrix displacement of the critical eigenmode obtained by the LBA. The corresponding flow chart is given in Figure 23.

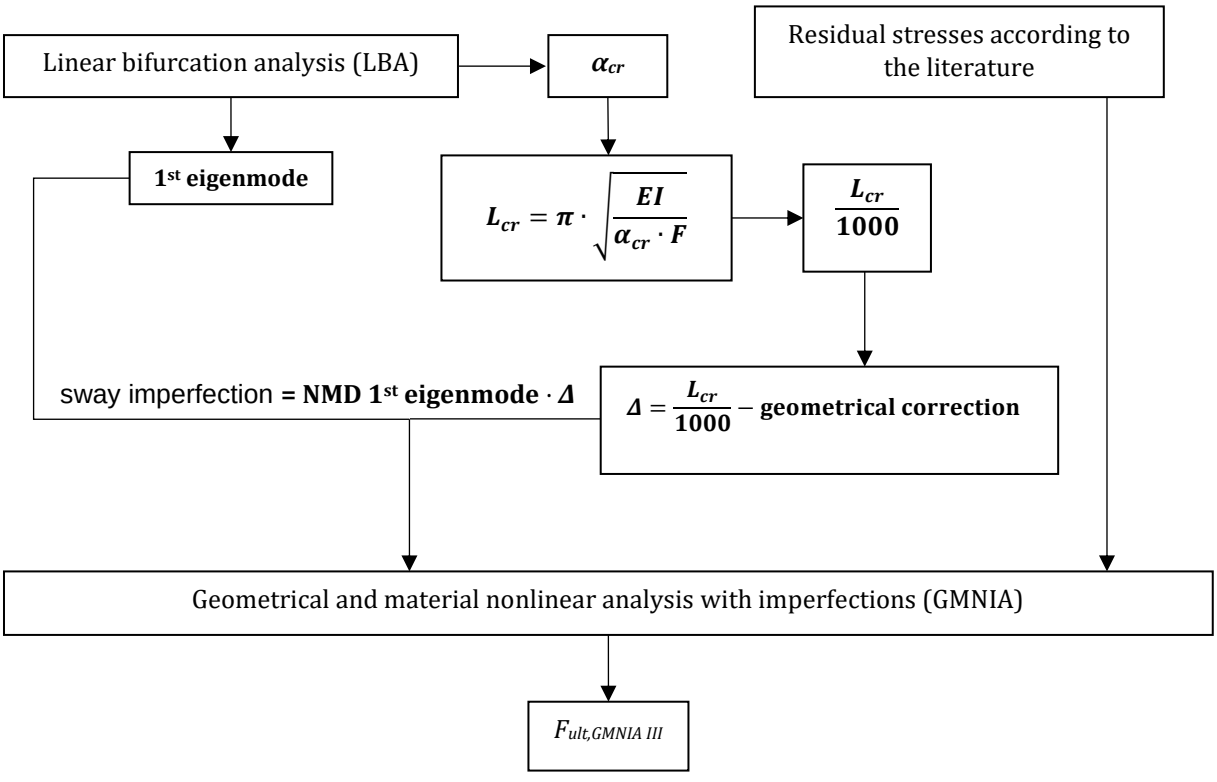

Figure 23: Flow chart of GMNIA III for obtaining $F_{ult,GMNIA\ III}$

3.3.4 GMNIA IV according to Shayan et al. and Vogel et al.

As stated before, sway and bow imperfections are the initial geometrical imperfections that should be taken into account to cover all influences of the geometrical imperfections or even the material imperfections in the case of the EN 1993-1-1. These initial geometrical imperfections should be implemented in such a way that the worst-case scenario will be obtained which will lead to the ultimate load. However, Shayan et al. [9] state that the worst-case scenario of imperfections may be overly conservative, and that also in a lot of cases it is not clear on forehand what will be the worst-case scenario. For that reason, Shayan et al. [9] researched analyses for steel structural systems and developed a rational method of modeling initial geometric imperfections. With statistical data for initial geometric imperfection, they extended the scaling of elastic buckling mode (EBM). Normally, an EBM is based on the first eigenmode of the structure, which should represent the most critical imperfection geometry (GMNIA II and GMNIA III). However, as a result of plastic deformations, the final failure mode of the frame may be different from the critical elastic buckling mode [9]. In the EBM-method developed by Shayan et al. [9], they consider the initial geometric imperfection as a linear superposition of several scaled buckling modes. From statistical data from other literature, Shayan et al. [9] developed scaling factors for each bucking mode that are presented in Table 1. With one equation, one can calculate the imperfection amplitude for each buckling mode (A_j) that can be implemented in the FE-model. For sway modes the solution is given by equation (50):

$$A_j = P_j \cdot F_{shayan} \cdot h \tag{50}$$

Where P_j is the proportion of each mode, F_{shayan} a single factor, and h the height of the frame. Table 1 offers scaling factors up to ten different buckling modes. However, Shayan et al. [9] show that for unbraced frames, 3 modes already give sufficient accuracy to determine the correct initial geometric imperfection.

Table 1: Proportion of each mode to model initial geometric imperfections for unbraced frames [9]

Number of modes	P_1	P_2	P_3	P_4	P_5	P_6	P_7	P_8	P_9	P_{10}	F_{shayan}
1	1										0.001228
2	0.782	0.218									0.001566
3	0.623	0.161	0.216								0.001838
4	0.522	0.121	0.178	0.178							0.002147
5	0.441	0.103	0.155	0.155	0.143						0.002504
6	0.386	0.090	0.138	0.138	0.120	0.128					0.002817
7	0.350	0.079	0.127	0.127	0.109	0.113	0.098				0.00309
8	0.316	0.071	0.110	0.110	0.103	0.104	0.091	0.093			0.003413
9	0.283	0.064	0.099	0.099	0.091	0.091	0.085	0.089	0.099		0.003782
10	0.266	0.060	0.089	0.089	0.084	0.082	0.077	0.083	0.090	0.077	0.004030

The residual stresses are induced in the same way on the structure as GMNIA III (section 3.3.3). The corresponding flow chart for GMNIA IV is given in Figure 24.

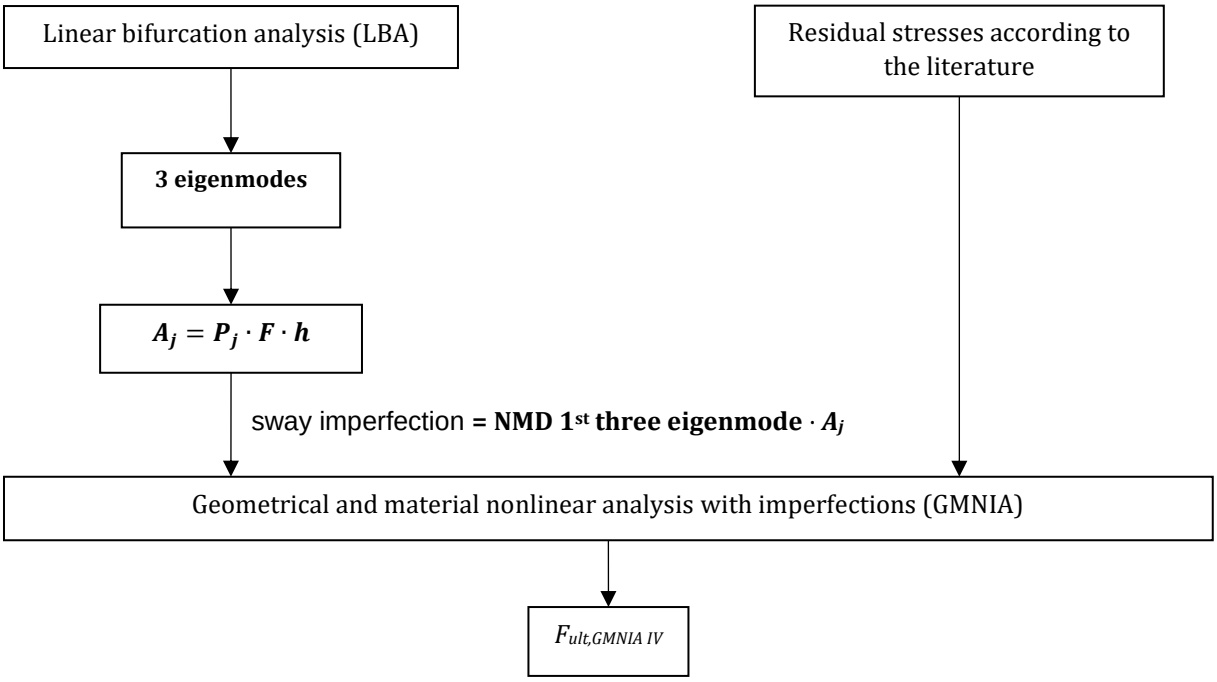

Figure 24: Flow chart of GMNIA IV for obtaining $F_{ult,GMNIA\ IV}$

4 FINITE ELEMENT MODEL

In this chapter, the Finite Element Model that will be used to carry out the various analyses will be discussed. The LBA and GMNIA for a frame as discussed in section 3.1 can both be performed with beam elements and shell elements. The difference between the type of elements is that beam elements only offer the ability to create a model based on the centerline of the cross-section, where a shell element can model the frame more accurately. This allows shell elements to model the flanges and web separately, which allows the implementation of residual stresses. Beam elements offer a more general approach with less detailed information regarding the frame but are still be able to apply sway and bow imperfections, which is prescribed by the EN 1993-1-1. As discussed before the sway and bow imperfections of the EN 1993-1-1 are equivalent imperfections where residual stresses are taken into account. This means that modeling residual stresses with shell elements reflects 'reality' better. According to Taris [10], modeling with shell elements has the following advantages:

- supports can be placed exactly at the desired location;
- connections between columns and beams can be modeled like real connections;
- local buckling can occur (when relevant).

In this chapter, the FE-Model with shell elements will be extensively discussed to ensure the accuracy of the model. In the end, a comparison will be made between beam and shell elements to verify the global correctness of the shell element model.

4.1 ELEMENT TYPE

For shell elements, Abaqus offers three different calculation methods that are based on two different theories. The first theory is the Kirchhoff theory, which is suitable for thin plates and shells in a small deflection situation. The Kirchhoff theory assumes that the straight lines perpendicular to the mid-surface remain linear after deformation and will stay perpendicular to the mid-surface. Therefore the elongation influence along the mid-surface deflection may be neglected [11]. The theory also makes use of the kinematic assumption that the deformation of the element does not lead to a change of thickness in the element. The second theory is the Mindlin theory, which, instead of the Kirchhoff theory, includes shear deformation and rotary inertia effects. This is achieved by the fact that the normal straight line to the mid-surface remains straight but not necessarily perpendicular to the mid-surface after deformation. This leads to including shear deformation and rotary inertia effects in the calculation. This theory is interesting for thick elements. For both theories, Abaqus offers a separate calculation method, but also offers the ability to combine the theory. This calculation method is called the general-purpose and uses thick shell theory as the shell thickness increases and uses Kirchhoff thin shell theory as the thickness decreases [12]. Abaqus assumes a shell to be thin when the thickness-to-span ratio is smaller than 1/15. For the frame dimensions considered this leads to the Kirchhoffs theory. These elements are also called S4-elements in Abaqus, where the 4 indicates the number of nodes per element.

4.2 RELEVANT ANALYSE METHODS OF ABAQUS

4.2.1 Static, general

For a LA, the static, general step of Abaqus will be used. The static, general step is a linear or nonlinear analysis, which ignores time-dependent material effects and neglects inertia effects. It makes use of the Newton Raphson method and ends when the structure is unstable. [13]

4.2.2 Static, Riks

The static Riks analysis determines the behavior of the structure after instability and continues where the Newton Raphson fails. When the load is scaled by a single scalar parameter, the Riks method can provide solutions regardless of whether the response is stable or unstable. The single scaled load is used as an unknown and instead, the arc length is used as a measure along with the result. This makes the Riks method suitable for limit load problems since the complete load-displacement path is obtained, where the ultimate load that the frame can carry be obtained from.

4.2.3 Linear perturbation buckling

In a linear perturbation buckling analysis, Abaqus determine the eigenvalue for which the model stiffness matrix becomes singular. This results in the eigenvalue where the structure reaches the Euler buckling load referred to as α_{cr}. This analysis method will be used for LBA. [14]

4.3 SHELL ELEMENT MODEL

4.3.1 Parts of the frame

The model is shown in Figure 27, which is a three-dimensional view of (all) the frames in the research-scope as discussed in section 1.4 (Figure 9), with variable conditions. There are several ways to model the complete frame, but in the end, the most realistic one should be used. To achieve this, the model is divided into different parts (columns, beams, and stiffeners), where the dimensions of these parts are based on the probable factory dimensions. The assumption is made that the columns will be manufactured till the top of the frame, where the beams will be placed between the columns. This principle is indicated by the arrows in Figure 25 and Figure 26. To achieve the most realistic joint, stiffeners will be added to the joint, which can also be seen in Figure 25 and Figure 26. The stiffener placed in the leaning column is placed to prevent local buckling in the model, in reality, this stiffener will not be there.

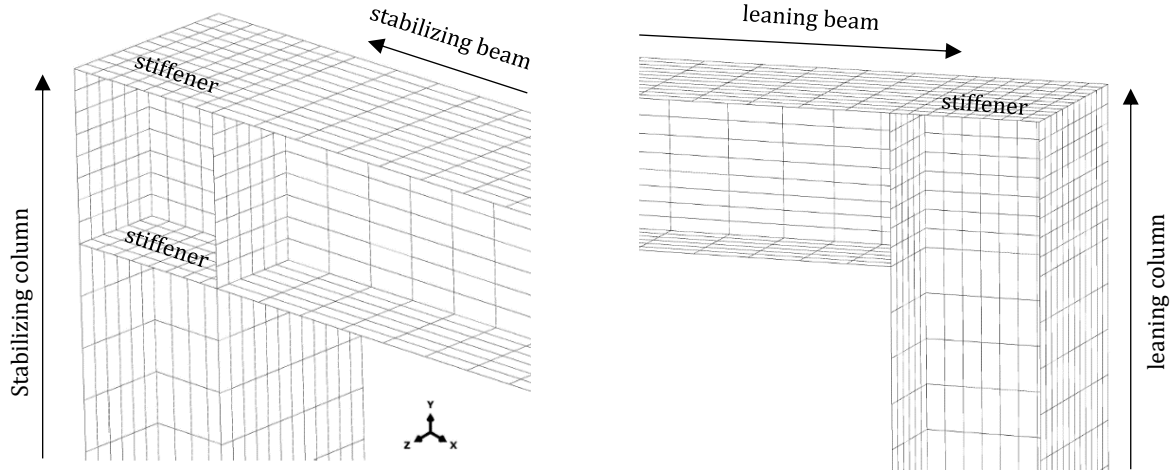

Figure 25: Column-beam joint for the stabilizing frame (left) and leaning column (right) in the FE-model

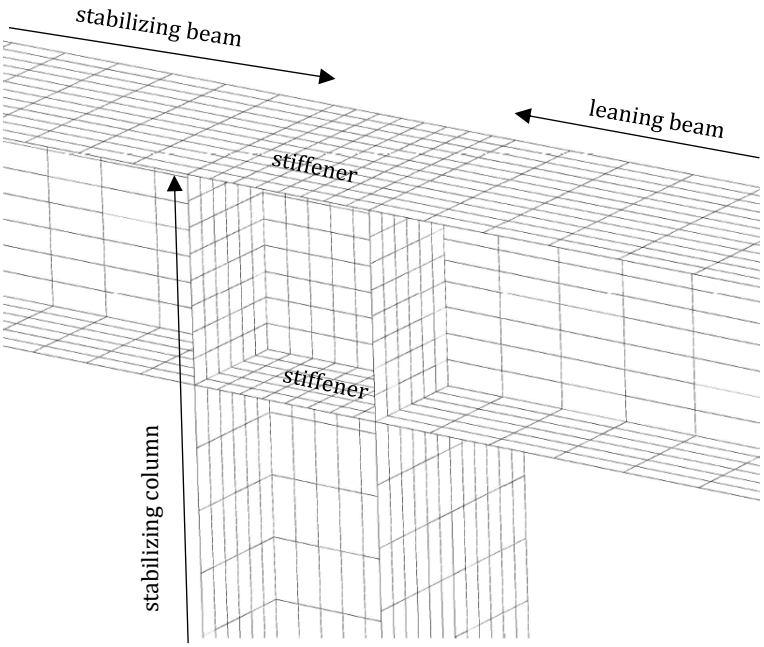

Figure 26: Beam-column-beam joint in the FE-model

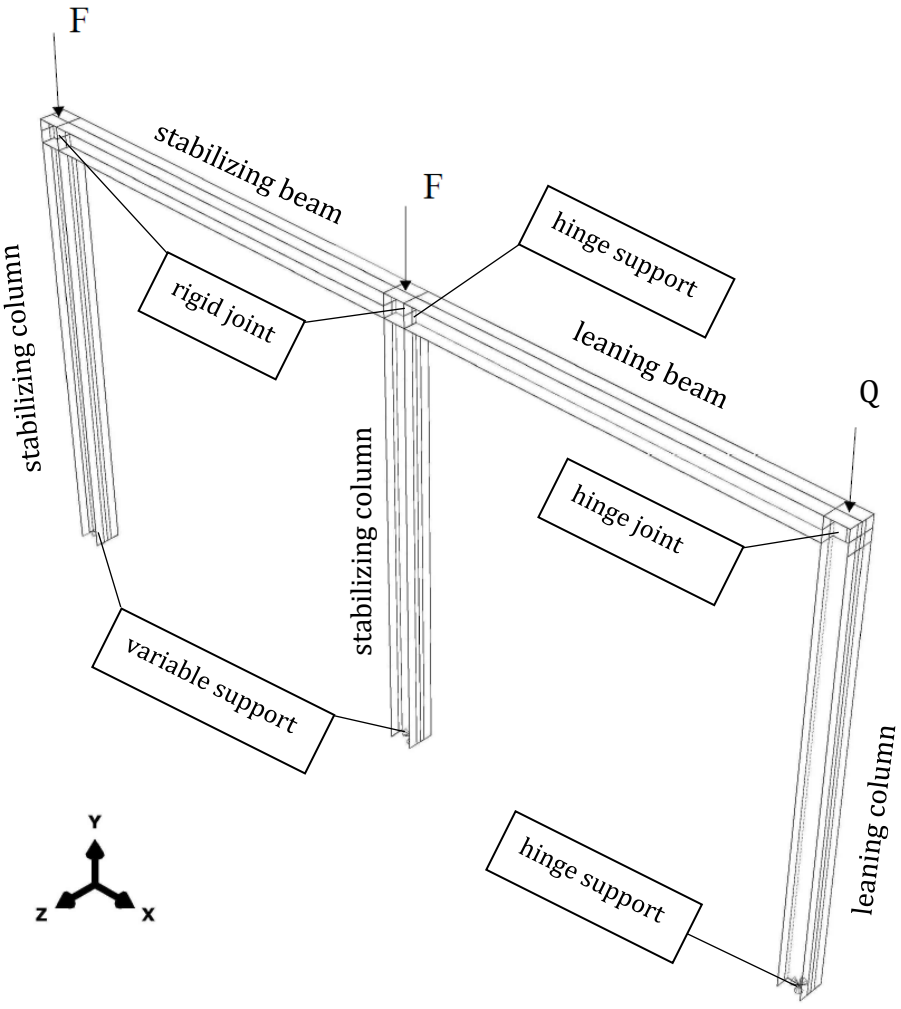

Figure 27: Variable FE-Model corresponding to the different mechanical schematizations as shown in section 1.4

4.3.2 Interaction of parts

4.3.2.1 General

The members of the frame in the FE-model, also called parts, will be assembled to create the actual model of the structure. To connect the parts and make them work together, interactions between the parts have to be implemented in the model. To simulate the correct structural behavior, different types of interaction will be used. In this research, the coupling and tie constraint is used. The coupling constraint couples the behavior and movement of a collection of nodes to one reference point. As experienced by Taris [10], supports or loads on one node of the shell element can lead to local buckling. The coupling constraint can avoid this structural behavior since it will let the cross-section behave as a whole while transferring the load to the support on one node and applying the load on one node. The option will also be used for situations where a perfectly hinged joint is desired. The coupling can act as an endplate, transferring the forces to one node. This node can be used as a perfect hinge. For the coupling type, the kinematic coupling type is used. The kinematic coupling type constrains the behavior and movement of the selected nodes to the rigid body of the reference node, where the degrees of freedom can be applied with respect to the local coordinate system of Abaqus [15].

The coupling constraint as just discussed only couples nodes of one particular part together per coupling. With the tie constraint, the surfaces and/or nodes of different parts can be tied together. Each node in the slave surface (second set of nodes or surfaces) will follow the master surface (first set of nodes or surfaces) by having the same values for its degrees of freedom to the closest master surface. By default the tie constraint accounts for shell element thickness, meaning that the actual top or bottom surface is considered while tying the closest surfaces. The rotation of the degrees of freedom from the slave surface is by default constrained to the master surface, leading to a rigid connection. When a hinge connection is desired, a constraint ratio can be specified, allowing the node to rotate.

4.3.2.2 Perfect hinge for leaning column connection

To obtain a leaning-column situation that can be compared with a two-dimensional mechanical scheme, the leaning frame should be connected to the stabilizing frame as a perfect hinge. To obtain a perfect hinge the end-nodes of the beam should be coupled to the center-node of the cross-section, as shown on the left in Figure 28. This gives the same principle as a head plate connected to the beam. The center-node should be tied to the column. This interaction between beam and column should happen at the same location as the center-node of the beam, therefore the node in the top-flange of the column should be selected. This is illustrated on the right of Figure 28, where can be seen that an area of the top-flange of the column is connected to the center-node of the beam. By default Abaqus only constrains the nodes that connect, meaning that only the node at the center-node of the beam is connected to the beam, which should be the case.

When plotting the deformations of a frame one can see that the actual deformations indicate that the joint is a perfect hinge. This can be seen in Figure 29, where the gap indicates that only the center-node is connected.

4.3.2.3 Rigid connection for stabilizing frame joint

With only a tie constraint, a rigid connection between the stabilizing- beam and column can be created. Figure 30 shows that all intersections between the column and beam (left) and stiffeners and column (right) are tied together to create a rigid connection. Note that for the column-beam intersection only the intersecting nodes are connected.

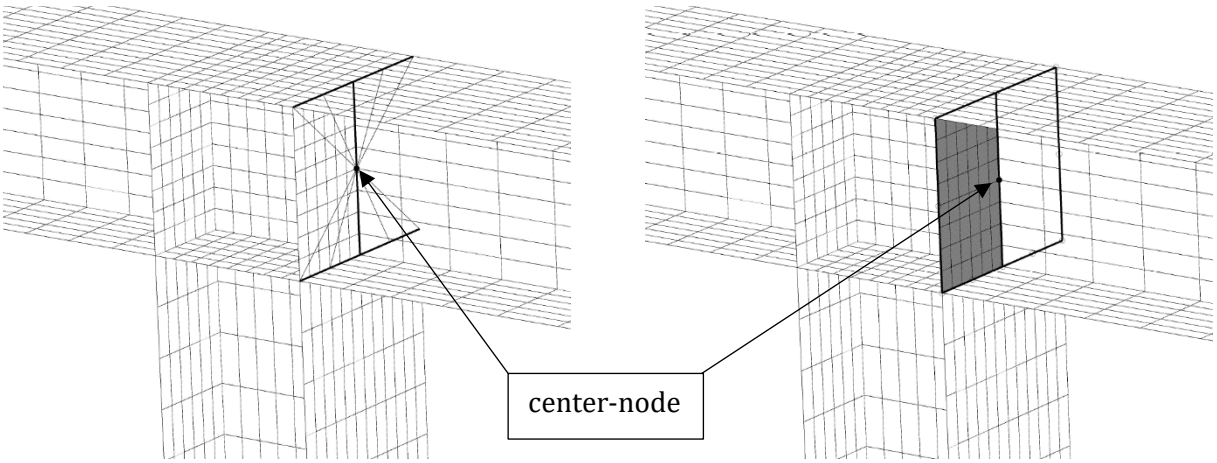

Figure 28: Coupling constraint (left) and tie constraint to one node (right) to create a hinge connection

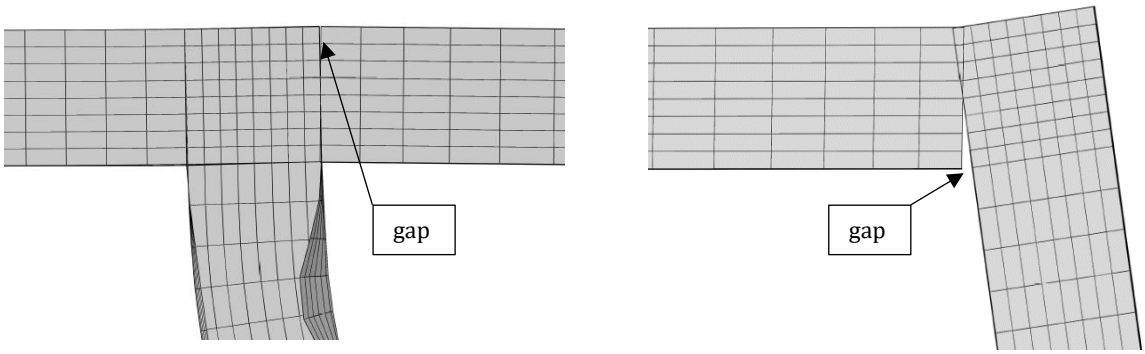

Figure 29: Deformed structure which indicates that the hinged joint act as a perfect hinge

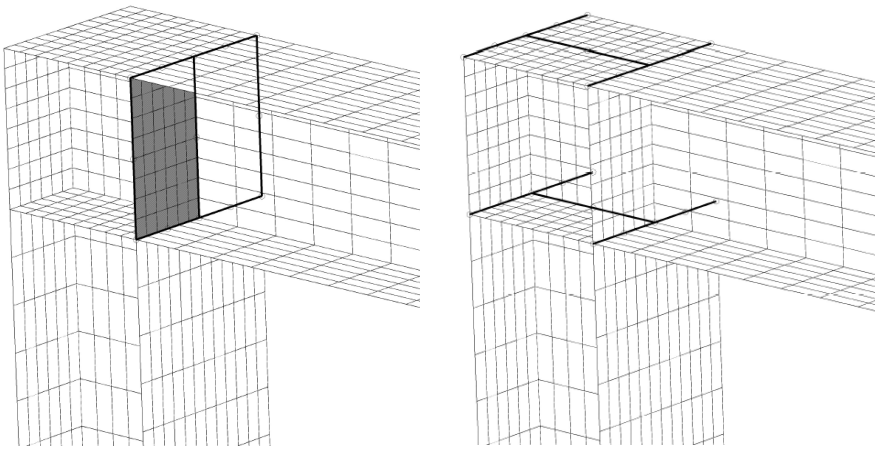

Figure 30: Tie constraints between column-beam (left) and stiffeners-column (right) to create a rigid joint

4.3.2.4 Applied conditions

Boundary conditions and load conditions should be applied to the centerline of the structure, otherwise, the model can not be compared with a two-dimensional mechanical scheme. To accomplish this, the conditions will be applied at one particular node, comparable with the perfect hinge at the leaning beam connection as just discussed above. When considering this way of modeling, measures should be taken, otherwise, the stresses that will occur at the particular node

will lead to local buckling of the web. For the top of the column, this means that the applied load will lead to local buckling in the middle of the web. To avoid this, the nodes of the web in the joint are coupled to one particular node, where the load will be applied. Due to this coupling, the load is spread over the nodes of the web in the joint. This is shown on the left of Figure 31. Additionally, this way of modeling also induces a stiff joint, corresponding to the mechanical scheme. To avoid local buckling at the bottom of the column due to the boundary condition, the nodes of the cross-section are coupled to one particular node at the center of the cross-section. This is shown on the right of Figure 31.

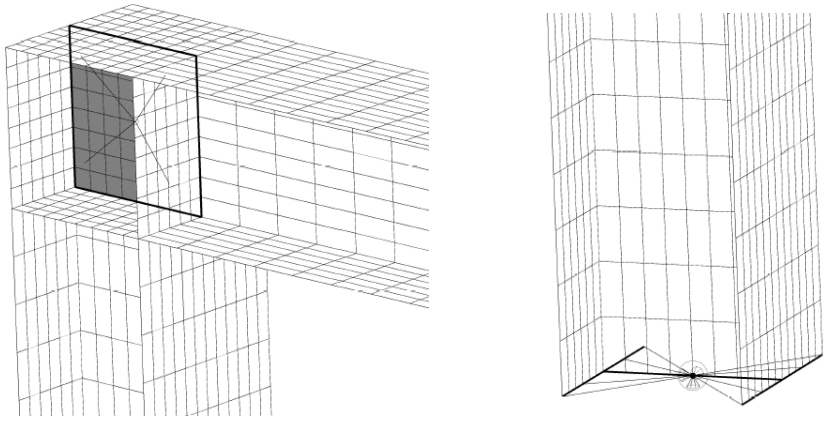

Figure 31: Coupling of nodes to apply the load conditions (left) and the boundary conditions (right)

4.3.2.5 Imperfections

Section 3.2 (Figure 14) showed that equivalent bow imperfections (GMNIA I) can be induced on the structure by an equivalent line load. Since Abaqus does not give the ability to apply line loads on shell elements, the use of coupling nodes will be used again. By coupling nodes over the height of the structure to one particular reference node, a point load equivalent to the sum of the line load can be applied at this reference node to induce the bow imperfection, as shown in Figure 32. The nodes that should be coupled are the web-flange intersection nodes at one side of the cross-section so that the load goes directly into the web. If nodes on the flanges are coupled and loaded, the flanges will deform, which is not desired.

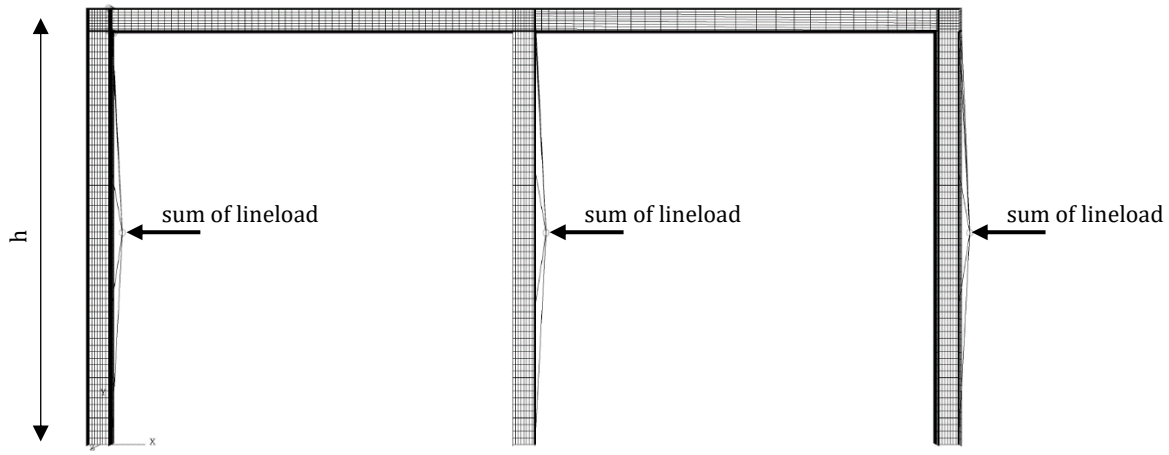

Figure 32: Bow imperfection induced by equivalent point-load

4.3.3 Supports

It is stated that out-of-plane deformations will be prevented in this research. Therefore only an in-plane GMNIA will be performed. To prevent out-of-plane deformation, all nodes of the webs for

the beam and columns need to be fully laterally supported. Only the webs must be constrained out-of-plane, so transverse strain can occur freely [10]. For hinge connected frames the simulation of the column must allow the rotation of the cross-section of the member to obtain the correct buckling mode. This can be achieved with the use of a single column point fixation at the bottom of the column, as discussed in section 4.3.2. Both boundary conditions are shown in Figure 33.

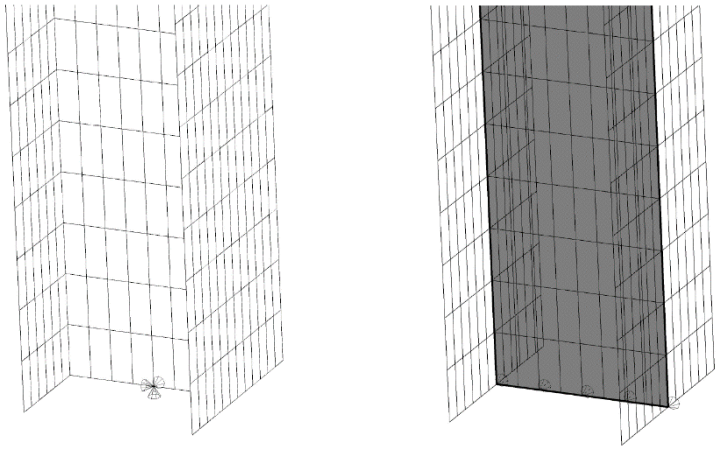

Figure 33: Boundary conditions in X and Y direction (left) and Z direction (right)

4.3.4 Cross-section

A I- or H-section in shell-elements is an assembly of two flanges and a web, all rectangular. But when we look at the hot-rolling manufacturing process of an I- and H-section, this process induces a root radius in the corners of the web on the flanges due to the shape of the press. A complication of modeling shell-elements is that this root radius cannot be modeled. This results in cross-sections that differ somewhat from reality. However, since this research is about the stability of a frame structure, and not focused on a cross-section specific case, the root radius will not be modeled. In the literature has been found that Taris [10] created an overlap between the web and the flanges in the cross-section to compromise the area of the cross-section in the FE-Model compared to the actual cross-section. However, this method has not been proven to be correct and therefore a model without overlap is used in the FE-model, meaning that it differs from the actual cross-section. Figure 34 illustrates the differences between the cross-sections when considering a HEA 300.

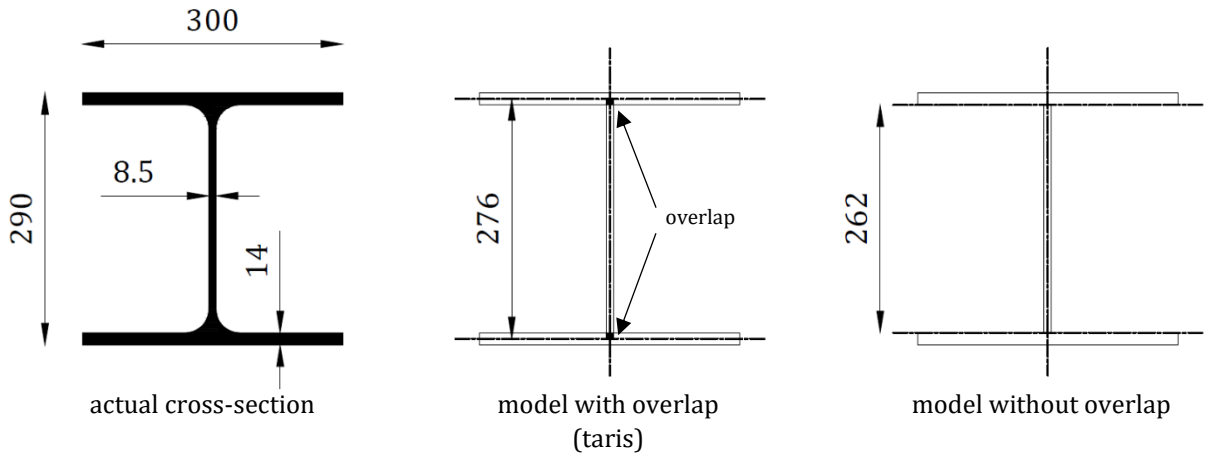

Figure 34: Actual HEA300 cross-section (left), HEA300 FE-model with overlap according to Taris (middle), and HEA300 FE-model without overlap

4.3.5 Mesh

The mesh is responsible for the accuracy of the results that are obtained from the FE-model. When a mesh has incorrect element shapes regarding the structure or the mesh is too coarse, it can lead to unreliable and unsafe results. In the validation- and case study (chapter 5 and 6) the size of the mesh will be studied to assess what the influence of the mesh-density is on the results. Based on the mesh size, the residual stress pattern is averaged over the mesh elements.

4.4 COMPARISON

The shell model that is used to carry out the case study in chapter 6 is in the process of modeling verified and compared to a beam model. This is considered to verify the outcome of the beam element model and the shell element model. For the beam elements, the Euler-Bernoulli theory is used, which results in B23 elements. From Figure 35 it can be seen that the differences between the model are minimal, with a maximum difference of the ultimate load of 2%. The analysis method for both models is a GMNIA, performed with the Static, Riks step. From Figure 35 it can be seen that the difference between behavior after instability is again minimal, where the shell elements have a larger range. Note that the results of this graph are intermediate and are only for verifying the different element models.

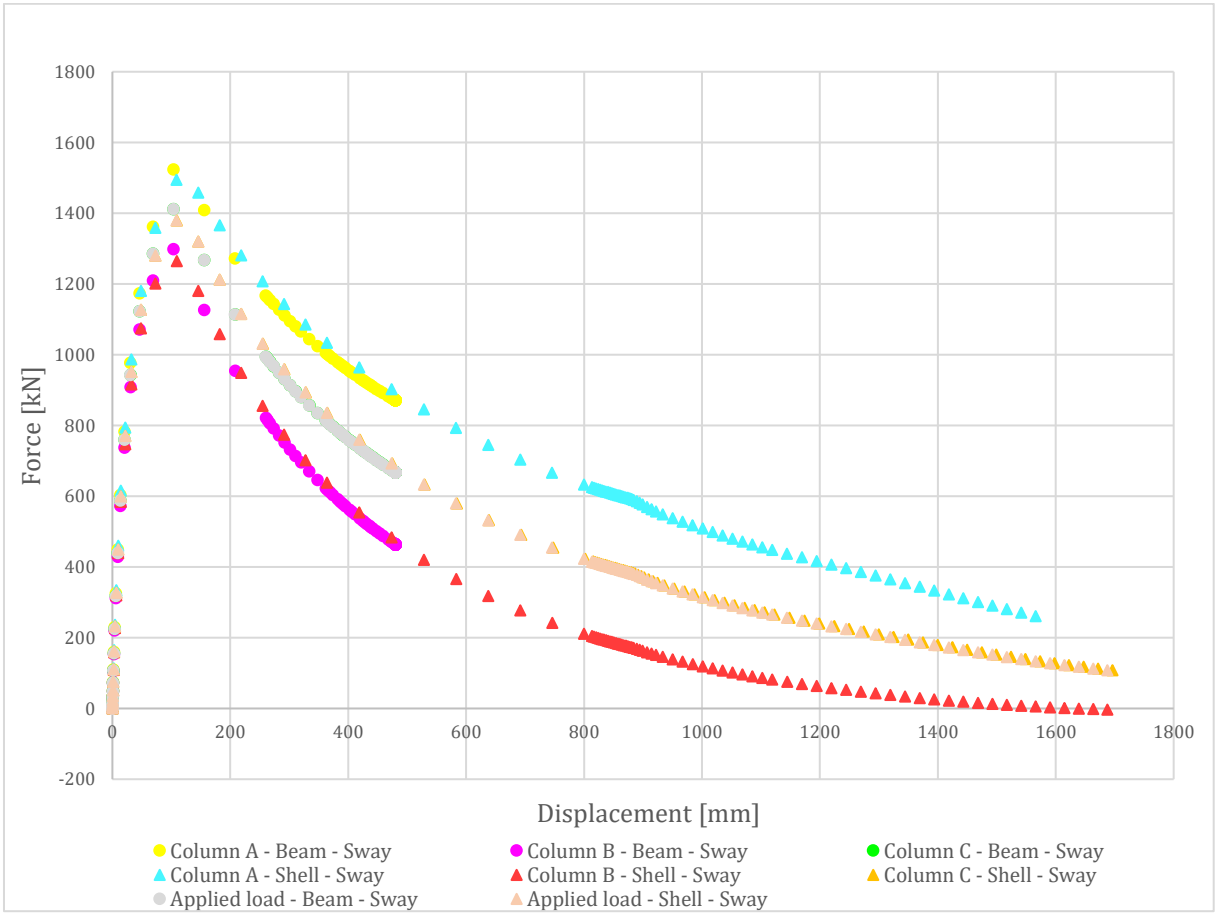

Figure 35: Comparison shell and beam elements with sway imperfections

5 VALIDATION STUDY SWAY FRAME

5.1 INTRODUCTION

In section 4.4 already a small validation is elaborated to validate the chosen elements. In this chapter, a complete validation study will be elaborated over a case from the literature. This validation case will be modeled with the methods as described in chapter 4 and analyzed with the various analysis methods as described in section 3.3. The aim is to validate the correctness and accuracy of the Finite Element Method (FEM) calculations. The literature that is used is a study from Taris [10], where an unbraced laterally supported steel sway-frame is modeled and compared to other literature, aiming to validate the scope of the general method of Eurocode 1993-1-1. The sway-frame that is used is a simple stabilizing structure consisting of two columns and a beam, where the top of the columns and the end of the beam are rigidly connected and the bottom of the column is pin-ended. At half of the column and each quarter of the beam, the frame is restricted in the Z-direction (out-of-plane). The frame is loaded with a vertical uniformly distributed load along the beam and horizontal point load in X-direction (in-plane) at the center of the left column-beam joint. The dimensions of the frame and the cross-sections are shown in Figure 36. The material is an elastic-perfectly plastic material with a yield-strength of 275 N/mm^2, considered with an engineering stress-strain diagram.

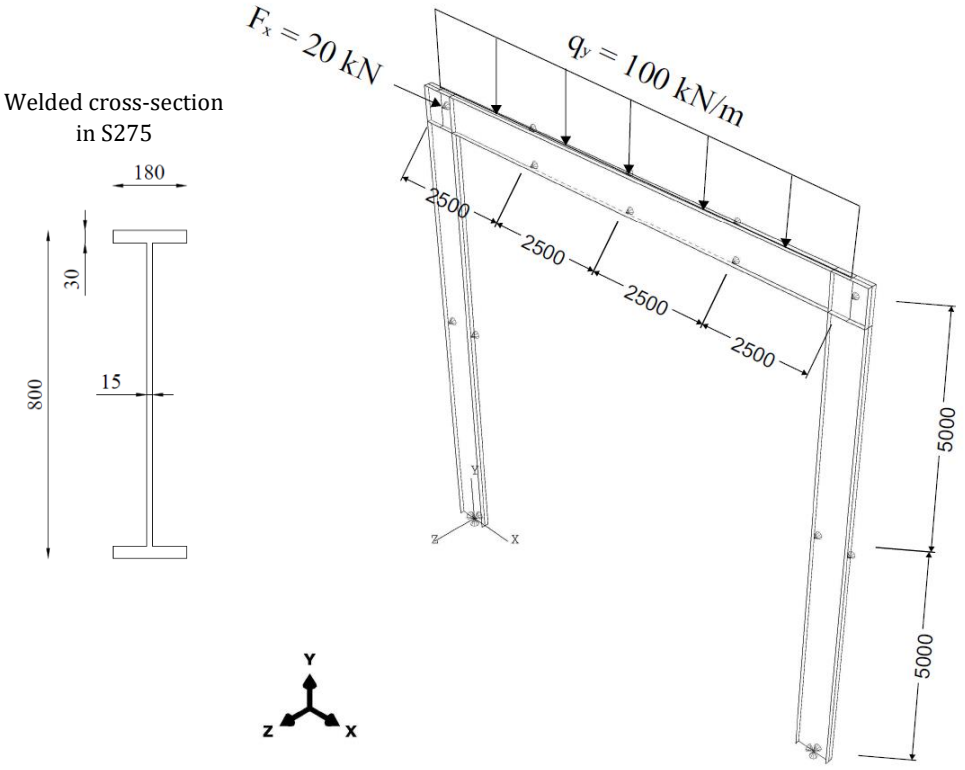

Figure 36: Three-dimensional illustration of the dimensions of the considered frame

5.2 ANALYSIS METHODS AND IMPERFECTIONS

The frame in this validation study is not fully restricted in the out-of-plane direction, but only at various nodes. This allows deformation and buckling in the weak axis of the frame and therefore also out-of-plane imperfections are taken into account in this chapter. The magnitudes of the imperfections will be as described in section 3.3. However, to make the results of the FEM calculations comparable with the work of Taris [10], the imperfections for the various analyses

are also based on the imperfections of Taris. Taris only used sway-imperfections in his study and therefore GMNIA I is only performed with an equivalent sway imperfection. Analysis method GMNIA II is performed three times, where the imperfections for the first one (GMNIA II) is based on section 3.3.2, and for the other two analyses (GMNIA IIa and GMNIA IIb) the imperfections are derived as Taris [10]. Table 2 shows the imperfections and their magnitudes that are used in the validation study. Analysis method GMNIA IV is not used by Taris and makes it that GMNIA II and GMNIA IV give unique results and are not directly comparable with Taris.

Table 2: Imperfections that are used in the various analyses in the validation study

ANALYSES	IMPERFECTIONS		RESIDUAL STRESSES
	In-plane	Out-of-plane	
LBA	-	-	-
GMNIA I	In-plane sway imperfection according to EN 1993-1-1 Clause 5.3.2(3) induced with equivalent forces	-	NO
GMNIA II	In-plane sway imperfection according to EN 1993-1-1 Clause 5.3.2(3) induced with equivalent forces	First out-of-plane eigenmode sized according to EN 1993-1-1 Clause 5.3.2(11) (η_{init}) induced with the normalized matrix of displacements	NO
GMNIA IIa	In-plane sway imperfection according to EN 1993-1-1 Clause 5.3.2(3) induced with equivalent forces	First out-of-plane eigenmode sized according to EN 1993-1-1 Clause 5.3.2(3) induced with the normalized matrix of displacements	NO
GMNIA IIb	In-plane sway imperfection according to EN 1993-1-1 Clause 5.3.2(3) induced with equivalent forces	First out-of-plane eigenmode sized as sway imperfection according to NEN 6771 induced with the normalized matrix of displacements	NO
GMNIA III	In-plane sway imperfection sized as $L_{cr}/1000$ induced with equivalent forces	First out-of-plane eigenmode sized as $L_{cr}/1000$ induced with the normalized matrix of displacements -	YES
GMNIA IV	First in-plane eigenmode sized as $A = P \cdot F \cdot h$ induced with the normalized matrix of displacements -	First three out-of-plane eigenmodes sized as $A_j = P_j \cdot F \cdot h$ induced with the normalized matrix of displacements -	YES

5.3 MESH REFINEMENT STUDY AND THE CORRESPONDING RESIDUAL STRESSES

Taris [10] made use of shell281 elements in Ansys. These elements are an eight-node element with six degrees of freedom at each node and are suitable for thin to moderately-thick shell elements. As described in section 4.1, the elements that are used for this validation study are a four-node S4 shell-element in Abaqus. To ensure the accuracy of the FE-model, the mesh-size that is needed for the four-node S4 elements is studied with a mesh-refinement study. The mesh-refinement study is performed for an elastic problem and a plastic problem. The reason for that is that since the considered frame is an instability problem, the deformation is hard to compare. The elastic problem is studied with an LBA, where the critical force amplifier α_{cr} is compared for the different mesh-sizes. For the plastic problem, an in-plane GMNIA (GMNIA I) is performed and the reaction force (RF) in kN and the load proportionality factor (LPF) at the ultimate load are compared. In Table 3 and Table 4, the results of the mesh-refinement study are shown. In both

studies, the mesh size of Taris is taken as a starting point (most coarse mesh). Both mesh-refinement studies result in a reliable mesh-size of 48.125x48.125x45 (axbxc), which is the mesh-size that will be used for this validation study. This mesh size is labeled as a coarse mesh and will be used for all analyses, except GMNIA IIIb. For GMNIA IIIb the finest mesh will be used. The mesh size direction of the coding a, b and c are shown in Figure 37.

Table 3: Results for the elastic mesh-refinement study for the validation study

axbxc	Number of elements [-]	Rel. mesh density $\frac{X}{385x192.5x45}$ [-]	Critical force amplifier (α_{cr}) [-]	CPU time [s]	% Error $\frac{24.063x24.063x22.5 - X}{24.063x24.063x22.}$ (%)
24.063x24.063x22.5	65468	61.1	2.6004	520.1	0.00%
48.125x48.125x45	**16240**	**15.15**	**2.6057**	**118.6**	**-0.2%**
192.5x96.25x45	2832	2.64	2.6798	14.2	-3.05%
385x192.5x45	1072	1	2.8163	6.2	-8.30%

Table 4: Results for the plastic mesh-refinement study for the validation study

axbxc	Rel. mesh density $\frac{X}{385x192.5x45}$ [-]	Reaction force (RF) [kN]	Load proportionality factor (LPF) [-]	CPU time [s]	% Error $\frac{6.25x6.25x6.25 - X}{6.25x6.25x6.25}$ RF (%)	LPF (%)
24.063x24.063x22.5	61.1	1145.1	2.5100	4689.2	0.00%	0.00%
48.125x48.125x45	**15.15**	**1148.7**	**2.5192**	**1032.5**	**-0.32%**	**-0.37%**
192.5x96.25x45	2.64	1160.2	2.5415	171.7	-1.32%	-1.26%
385x192.5x45	1	1173.0	2.5665	76.8	-2.44%	-2.25%

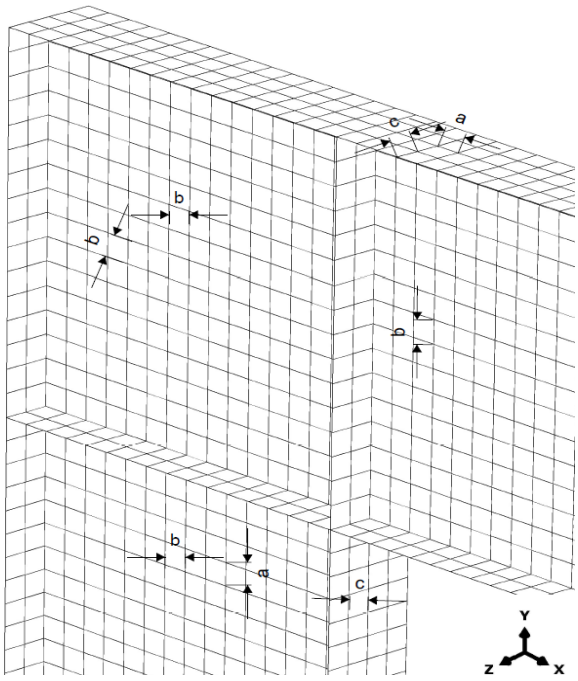

Figure 37: Mesh-size coding illustrated on the left column-beam joint

Analysis methods GMNIA III (a and b) and GMNIA IV include residual stresses that will be applied to each mesh element in FEM. The pattern of the residual stresses is dependent on the mesh size. Figure 38 shows the residual stress patterns for the actual profile, the coarse mesh, and the fine mesh for welded cross-sections. According to Table 3 and Table 4, the eight-node S8 elements that Taris used, allowed him to use a more coarse mesh than the S4 element used in this research. For comparison reasons, the mesh that will be used for the S4 elements will follow the same coarse mesh pattern as Taris [10], as shown in Figure 38. To see the influence of the results, also the finest mesh pattern is used (labeled as fine mesh) to come closer to the actual residual stress pattern.

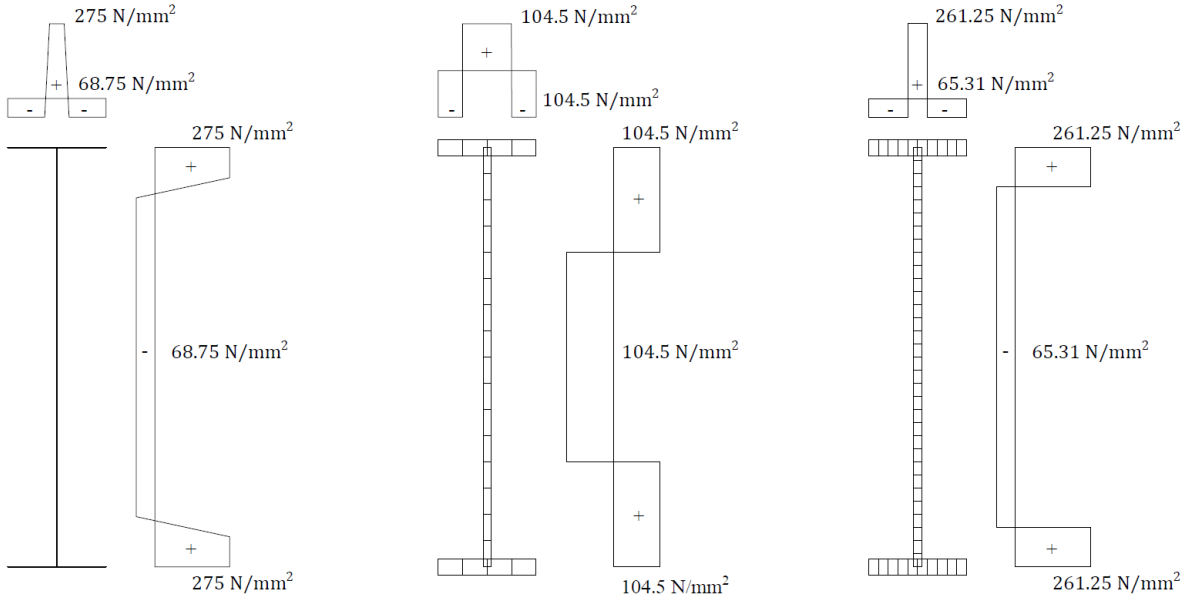

Figure 38: Residual stress pattern for the actual profile (left), coarse mesh (middle), and fine mesh (right)

5.4 NUMERICAL RESULTS OF THE VARIOUS ANALYSES - VALIDATION STUDY

5.4.1 LBA

The LBA is performed for different purposes. The first purpose is to obtain α_{cr}, which can be compared to other LPF but also be used to determine L_{cr}. The other purpose is to determine the input for the other various analyses. The first input is the normalized matrix of displacements for the governing critical eigenmode (in-plane and out-of-plane) and the second input is the bending moment at the critical cross-section due to the governing critical eigenmode ($EI|\eta''_{cr}|_{max}$ in GMNIA II).

The critical eigenmode results in a load factor of $\alpha_{cr,z}$ =2.61, as shown on the left in Figure 39. It appears that the first eigenmode is also the critical eigenmode for out-of-plane buckling, which results in the normalized matrix of displacements as shown on the left of Figure 39. The first in-plane buckling mode is found at eigenmode 23 with a load factor of $\alpha_{cr,x}$ =14.56, shown on the right of the figure. The corresponding $EI|\eta''_{cr}|_{max}$ at the critical cross-section is $EI|\eta''_{cr}|_{max} = 1.382 \cdot 10^6$, as shown in Figure 40.

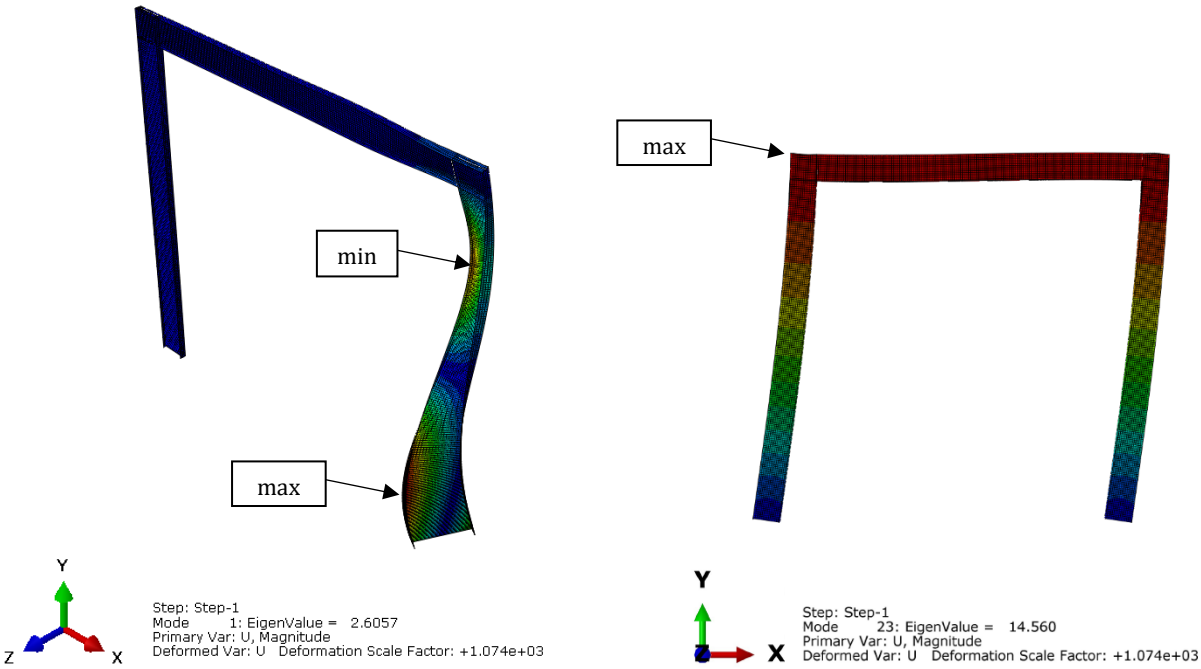

Figure 39: First out-of-plane eigenmode (left) and in-plane eigenmode (right)

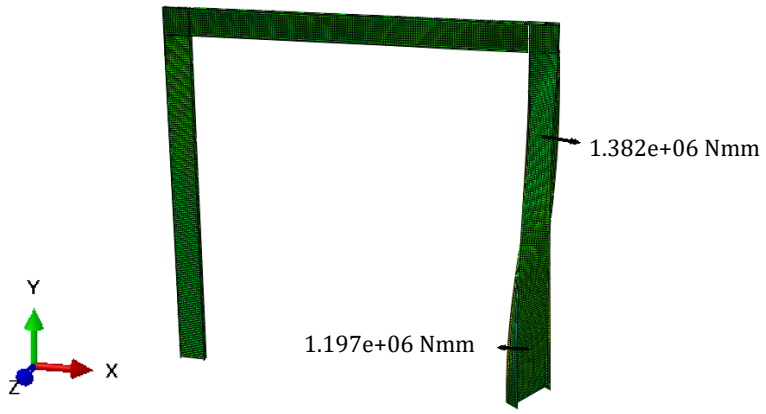

Figure 40: Resultant of section-moment $EI|\eta''_{cr}|_{max}$ plotted on the deformed state

5.4.2 GMNIA I according to EN 1993-1-1 clause 5.3.2(3) (in-plane)

For GMNIA I, only a sway imperfection according to EN 1993-1-1 clause 5.3.2(3) is used, and is given as the following:

$$\phi_0 = 1/200$$

$$\alpha_h = \frac{2}{\sqrt{h}} = \frac{2}{\sqrt{10}} = 0.632, \text{where } 0.632 \leq \frac{2}{3} \rightarrow = \frac{2}{3}$$

$$\alpha_m = \sqrt{0.5\left(1 + \frac{1}{m}\right)} = \sqrt{0.5\left(1 + \frac{1}{2}\right)} = 0.886$$

$$\phi = \phi_0 \cdot \alpha_h \cdot \alpha_m = \frac{1}{200} \cdot \frac{2}{3} \cdot 0.866 = 2.89 \cdot 10^{-3}$$

$$\Delta_x = 2.89 \cdot 10^{-3} \cdot 10000 = 28.9 \text{ mm}$$

The in-plane sway imperfection Δ_x is induced on the structure as an equivalent force as shown in Figure 14. This in-plane GMNIA results in an LPF of $\alpha_{GMNIA\ I}$ =2.52. The load-displacement path

corresponding to this LPF is shown in Figure 41, where each dot is a converged equilibrium state. The displacement taken is the lateral displacement in the X-direction at the left top node. The result of the LBA is also shown in Figure 41.

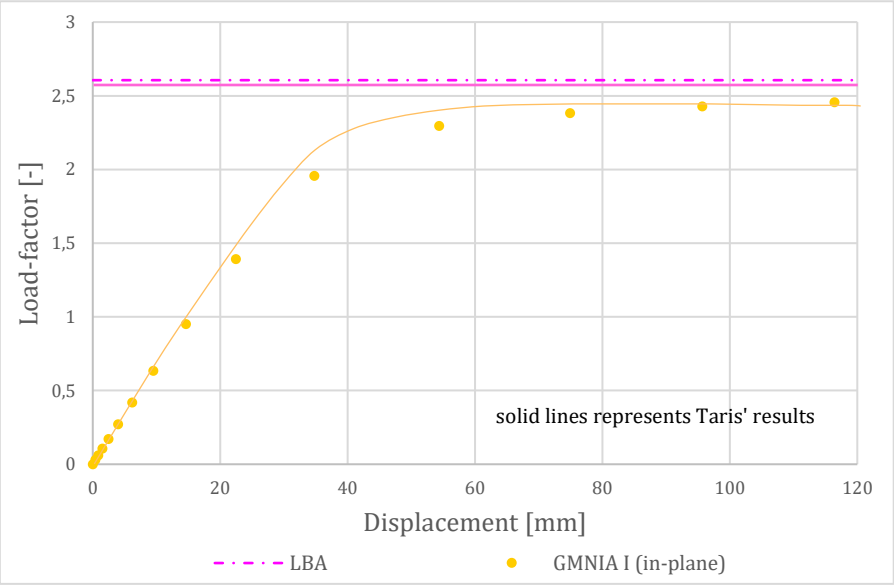

Figure 41: Load displacement diagram for GMNIA I, including the buckling load from the LBA

5.4.3 GMNIA II according to EN 1993-1-1 clause 5.3.2(11)

For GMNIA II, the same in-plane imperfection is taken as GMNIA I, namely the equivalent sway imperfection of the EN 1993-1-1 clause 5.3.2(3). This results in:

$\Delta_x = 28.9$ mm

For the out-of-plane imperfection, the normalized matrix of displacements of the first out-of-plane eigenmode as shown in Figure 39 is used, sized according to the EN 1993-1-1 clause 5.3.2(11). In Taris [10] can be found that for the section modulus the plastic section modulus $W_{z,pl}$ is used. However, this does not match with the cross-section class to the corresponding geometry of the cross-section. Since this chapter is only a validation study about the FE-Model and not the actual calculation, $W_{z,pl}$ is also used in this study. The scale-factor of the imperfection is determined by the following:

$W_{z,pl} = 2 \cdot \left(740 \cdot 7.5 \cdot 3.75 + 2 \cdot (90 \cdot 30 \cdot 45)\right) = 527625 \text{ mm}^3$

$M_{Rk,z} = f_{y,d} \cdot W_{z,pl} = 275 \cdot 527625 \ = 145.1 \cdot 10^6 \text{ Nmm}$

$N_{Rk} = \ f_{y,d} \cdot A = 275 \cdot 21900 = 6022.5 \cdot 10^3 \text{ N}$

$F_{cr,z} = 520000 \cdot 2.61 = 1355 \cdot 10^3 \text{ N (LBA)}$

$$\bar{\lambda} = \sqrt{\frac{\alpha_{ult,k}}{\alpha_{cr,z}}} = \sqrt{\frac{N_{Rk}}{F_{cr,z}}} = \sqrt{\frac{6022.5 \cdot 10^3}{1355 \cdot 10^3}} = 2.11\ [-]$$

$\alpha = 0.49$, according to table 1 in appendix A

$\phi = 0.5\left[1 + \alpha\left(\bar{\lambda} - 0.2\right) + \bar{\lambda}^2\right] = 0.5[1 + 0.49 \cdot (2.11 - 0.2) + 2.11^2] = 3.19\ [-]$

$$\chi = \frac{1}{\phi + \sqrt{\phi^2 - \bar{\lambda}^2}} = \frac{1}{3.19 + \sqrt{3.19^2 - 2.11^2}} = 0.18\ [-]$$

$$e_0 = \alpha(\bar{\lambda} - 0.2)\frac{M_{Rk,z}}{N_{Rk}} \cdot \frac{1 - \frac{\chi^{\bar{\lambda}^2}}{\gamma_{M1}}}{1 - \chi^{\bar{\lambda}^2}} = 0.49 \cdot (2.11 - 0.2)\frac{145.1 \cdot 10^6}{6022.5 \cdot 10^3} \cdot \frac{1 - \frac{0.18^{2.11^2}}{1}}{1 - 0.18^{2.11^2}} = 22.53\ \text{mm}$$

$$EI\left|\eta_{cr}^{"}\right|_{max} = 1.382 \cdot 10^6\ \text{Nmm}$$

$$\eta_{init} = e_0 \cdot \frac{F_{cr,z}}{EI\left|\eta_{cr}^{"}\right|_{max}}\eta_{cr} = 22.53 \cdot \frac{1355 \cdot 10^3}{1.382 \cdot 10^6} = 22.09\ \text{mm}$$

The in-plane sway imperfection Δ_x is induced on the structure as an equivalent force. Value η_{init} is the magnitude to scale the normalized matrix of displacements. This GMNIA results in an LPF of $\alpha_{GMNIA\ II}$=1.65. GMNIA II is the Analysis method where the normalized matrix of displacements is sized by a value determined according to EN 1993-1-1 clause 5.3.2(11). In the study of Taris, the analysis method as GMNIA II is used, but not the specific value determined according to EN 1993-1-1 clause 5.3.2(11). For that reason, the result of section 5.4.3 can not be compared directly to the result of Taris. In the upcoming sections, 5.4.4 and 5.4.5 the same determination is used but now with magnitudes as Taris, which makes them comparable to the results of Taris.

5.4.4 GMNIA IIa according to EN 1993-1-1 clause 5.3.2(3)

For GMNIA IIa, the same in-plane imperfection is taken as GMNIA I, namely the equivalent sway imperfection of the EN 1993-1-1 clause 5.3.2(3). This results in:

$$\Delta_x = 28.9\ \text{mm}$$

The critical out-of-plane eigenmode that is obtained from the LBA (left of Figure 39) is somewhat shaped like a bow imperfection. According to EN 1993-1-1 clause 5.3.2(3), the bow imperfection for cross-section with buckling curve C can be shaped as $L_{cr}/150$, which gives the following:

$$L_{cr,z} = \pi \cdot \sqrt{\frac{E \cdot I_z}{\alpha_{cr,z} \cdot N_{Ed}}} = \pi \cdot \sqrt{\frac{210000 \cdot 293.68 \cdot 10^5}{2.6057 \cdot 520000}} = 6702\ \text{mm}$$

$$e_{0,z} = \frac{L_{cr,z}}{150} = \frac{6702}{150} = 44.68\ \text{mm}$$

The in-plane sway imperfection Δ_x is induced on the structure as an equivalent force. Value $e_{0,z}$ is the magnitude factor to scale the normalized matrix of displacements of the first out-of-plane eigenmode. This GMNIA results in an LPF of $\alpha_{GMNIA\ IIa}$=1.48

5.4.5 GMNIA IIb according to NEN 6771

For GMNIA IIb, the same in-plane imperfection is taken as GMNIA I, namely the equivalent sway imperfection of the EN 1993-1-1 clause 5.3.2(3). This results in:

$$\Delta_x = 28.9\ \text{mm}$$

As discussed in section 5.4.4, the critical out-of-plane eigenmode that is obtained from the LBA is somewhat shaped like a bow imperfection. According to NEN 6771, the bow imperfection can be shaped with the magnitude of the following equation:

$$e_{0,z} = \alpha_k \cdot \left(\lambda_{z,rel} - \lambda_0\right) \cdot \frac{M_{z,u,d}}{N_{c,u,d}}$$

$$L_{cr,z} = \pi \cdot \sqrt{\frac{E \cdot I_z}{\alpha_{cr,z} \cdot N_{Ed}}} = \pi \cdot \sqrt{\frac{210000 \cdot 293.68 \cdot 10\text{^}5}{2.6057 \cdot 520000}} = 6702 \text{ mm}$$

$$I_z = \frac{1}{12} \cdot 740 \cdot 15^3 + 2 \cdot \left(\frac{1}{12} \cdot 30 \cdot 180^3\right) = 293.68 \cdot 10^5 \text{ mm}^4$$

$$i_z = \sqrt{\frac{I_z}{A}} = \sqrt{\frac{293.68 \cdot 10^5}{21900}} = 36.62 \text{ mm}$$

$$\lambda_e = \pi \cdot \sqrt{\frac{E}{f_{y,d}}} = \pi \cdot \sqrt{\frac{210000}{275}} = 86.81$$

$$\lambda_z = \frac{L_{cr,z}}{i_z} = \frac{6702}{36.62} = 183.03$$

$$\lambda_{z,rel} = \frac{\lambda_z}{\lambda_e} = \frac{183.03}{86.81} = 2.11$$

$$W_{z,pl} = 2 \cdot \left(740 \cdot 7.5 \cdot 3.75 + 2 \cdot (90 \cdot 30 \cdot 45)\right) = 527625 \text{ mm}^3$$

$$M_{z,u,d} = f_{y,d} \cdot W_{z,pl} = 275 \cdot 527625 \ = 145.1 \cdot 10^6 \text{ Nmm}$$

$$N_{c,u,d} = f_{y,d} \cdot A = 275 \cdot 21900 = 6022.5 \cdot 10^3 \text{ N}$$

$\alpha_k = 0.49$, according to table 25 of the NEN 6770

$\lambda_0 = 0.20$, according to table 25 of the NEN 6770

$$e_{0,z} = 0.49 \cdot (2.11 - 0.2) \cdot \frac{145.1 \cdot 10^6}{6022.5 \cdot 10^3} = 22.53 \text{ mm}$$

The in-plane sway imperfection Δ_x is induced on the structure as an equivalent force. Value $e_{0,z}$ is the magnitude to scale the normalized matrix of displacements of the first out-of-plane eigenmode. This GMNIA results in an LPF of $\alpha_{GMNIA\ IIb}$=1.64. In the graph in Figure 42, it can be seen that the use of the Ayrton-Perry format (equation (46)) in GMNIA II and GMNIA IIb results in an evenly ultimate LPF. From this figure, it also can be seen that the use of $L_{cr,z}/150$ results in a lower ultimate LPF, somewhat more conservative.

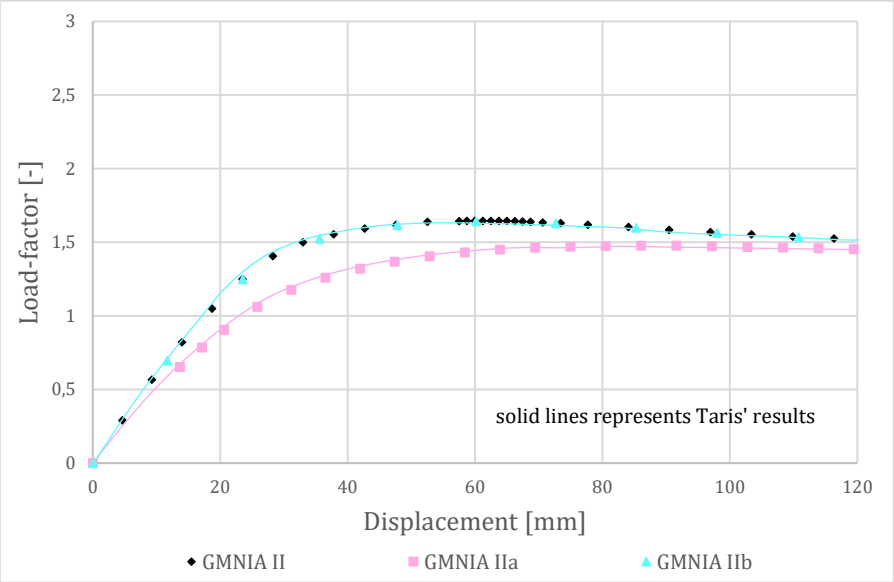

Figure 42: Load displacement diagram for GMNIA II, GMNIA IIa, and GMNIA IIb

5.4.6 GMNIA III according to Vogel et al.

For GMNIA III, the magnitude of the imperfections is derived according to Vogel et al. [8], as described in section 3.3.3. The residual stress pattern that is plotted on the structure is shown in section 5.3. The determination of the magnitude of the in- and out-of-plane imperfection to scale the normalized matrix of displacements is the following:

In-plane:

$$I_y = \frac{1}{12} \cdot 15 \cdot 740^3 + 2 \cdot \left(\frac{1}{12} \cdot 180 \cdot 30^3 + 30 \cdot 180 \cdot 385^2 \right) = 21081.7 \cdot 10^5 \text{ mm}^4$$

$$L_{cr,x} = \pi \cdot \sqrt{\frac{E \cdot I_y}{\alpha_{cr,x} \cdot N_{Ed}}} = \pi \cdot \sqrt{\frac{210000 \cdot 2108170000}{14.560 \cdot 520000}} = 24023 \text{ mm}$$

$$\frac{L_{cr,x}}{1000} = \frac{24023}{1000} = 24.02 \text{ mm}$$

The formula $L_{cr,x}/1000$ gives the sway imperfection at the middle of the buckling length. In the case of the in-plane imperfection, the middle of the buckling length does not match with the height of the frame. To obtain the in-plane imperfection at the height of the frame, a geometrical correction has to be used, as described in section 3.3.2. The geometrical correction can be derived by the following:

$$P = r - 24.02$$

$$r^2 = P^2 + \left(\frac{24023}{2} \right)^2$$

$$(P + 24.02)^2 = P^2 + \left(\frac{24023}{2} \right)^2$$

$$P^2 + 48.04P + 577.11 = P^2 + \left(\frac{24023}{2} \right)^2$$

$$P = 3002882 \text{ mm}$$

$$r = 2002906 \text{ mm}$$

$$x = \frac{24023}{2} - 10000 = 2011.6 \text{ mm}$$

$$y = \sqrt{2002906^2 - 2011.6^2} = 3002905$$

$\Delta_x = 3002905 - 3002882 = 23.35$ mm (without rounding off)

Value Δ_x is the magnitude to scale the normalized matrix of displacements of the first in-plane eigenmode.

Out-of-plane:

$$e_{0,z} = \frac{L_{cr,z}}{1000} = \frac{6702}{1000} = 6.70 \text{ mm}$$

Value $e_{0,z}$ is the magnitude to scale the normalized matrix of displacements of the first out-of-plane eigenmode. The value does not have to be corrected since it is at the middle of the buckling length.

This GMNIA results in an LPF of $\alpha_{GMNIA\ IIIa}$ =1.82 (coarse) for the coarse mesh and $\alpha_{GMNIA\ IIIb}$ = 1.99 (fine) for the fine mesh. For both analyses, the load-displacement path is plotted in Figure 43. It can be seen that the analysis with a finer mesh leads to a higher ultimate LPF, which is unlogic and can not be described. This will be further discussed in section 5.5.

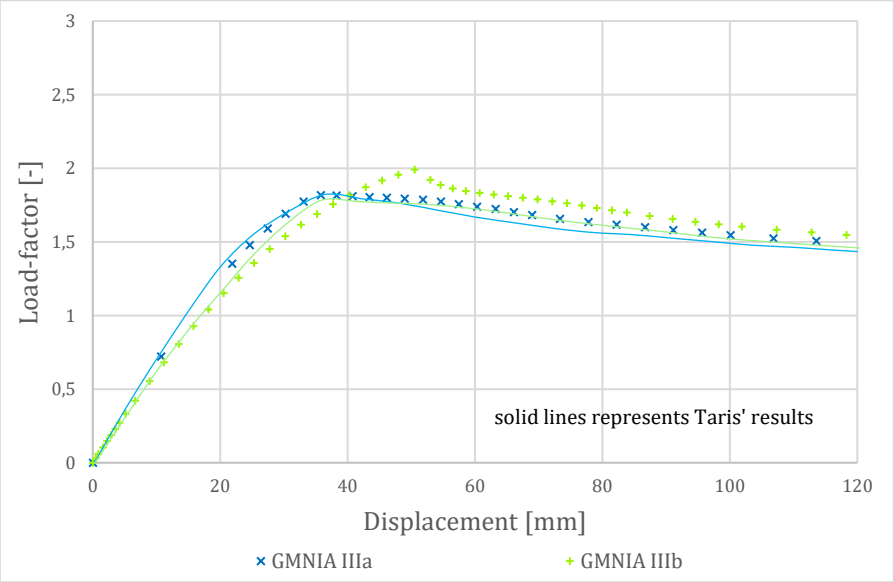

Figure 43: Load displacement diagram for GMNIA IIIa and GMNIA IIIb

5.4.7 GMNIA IV according to Shayan et al. and Vogel et al.

Analysis method GMNIA IV makes use of imperfections based on various eigenmodes with scale factors according to Shayan et al. [9], and residual stresses according to Vogel et al. [8], as described in section 3.3.4. For the in-plane imperfection, only the first eigenmode is used, since this eigenmode was the only in-plane buckling shape obtained. This eigenmode shape is the top illustration in Figure 44. The three eigenmodes that are taken for the out-of-plane direction are the first three out-of-plane eigenmodes, namely mode 1, mode 3, and mode 8 (bottom illustrations in Figure 44).

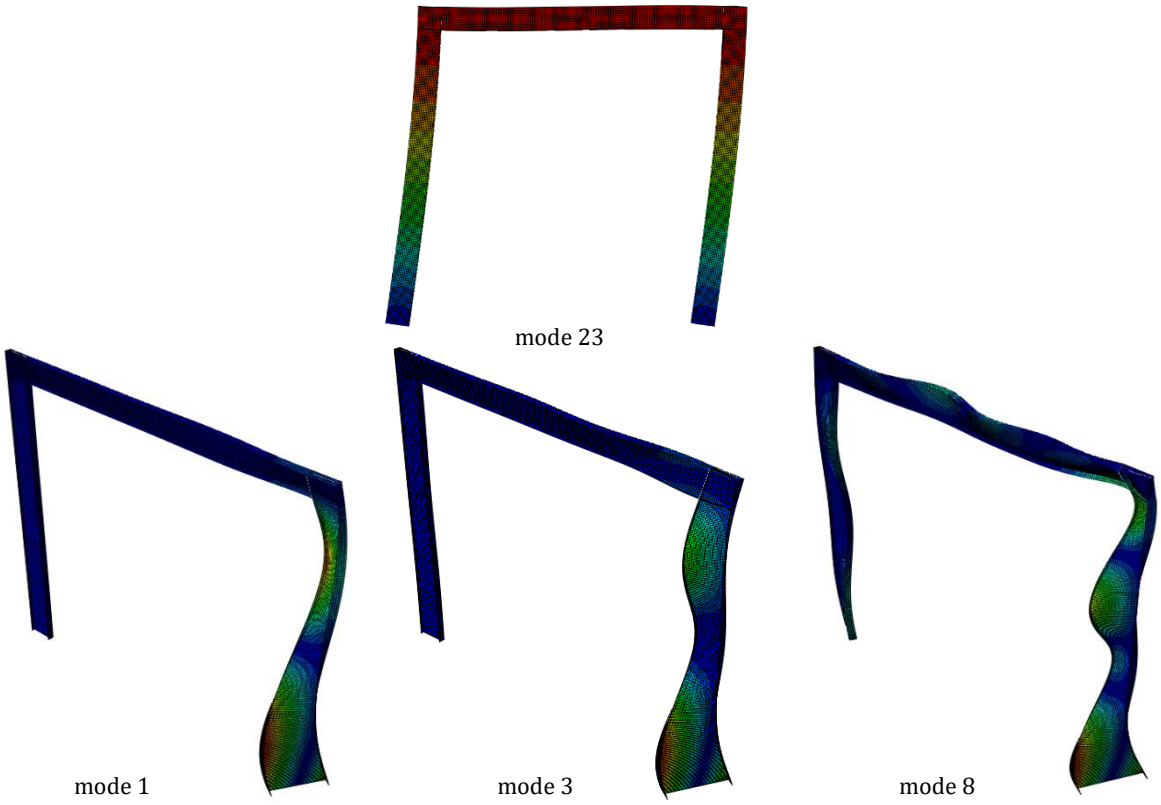

Figure 44: The first in-plane eigenmode (top) and the first three out-of-plane eigenmodes (bottom) where the normalized matrix of displacements will be scaled as imperfection in GMNIA IV

The magnitude of the in- and out-of-plane normalized matrix of displacements are based on Table 1 and given as the following:

In-plane:

$P_{1,x} = 1$ according to Table 1
$F_{shayan} = 0.001228$ according to Table 1
$h = 10000$ mm
$A_{1,x} = P_{1,x} \cdot F_{shayan} \cdot h = 1 \cdot 0.001228 \cdot 10000 = 12.28$

Out-of-plane:

$P_{1,z} = 0{,}623$ according to Table 1
$P_{2,z} = 0{,}161$ according to Table 1
$P_{3,z} = 0.216$ according to Table 1
$F_{shayan} = 0.001838$ according to Table 1
$h = 10000$ mm

$A_{1,z} = P_{1,z} \cdot F_{shayan} \cdot h = 0.623 \cdot 0.001838 \cdot 10000 = 11.4$
$A_{2,z} = P_{2,z} \cdot F_{shayan} \cdot h = 0.161 \cdot 0.001838 \cdot 10000 = 2.96$
$A_{3,z} = P_{3,z} \cdot F_{shayan} \cdot h = 0.216 \cdot 0.001838 \cdot 10000 = 3.97$

Value $A_{1,x}$ is the magnitude to scale the normalized matrix of displacements of the first in-plane eigenmode, mode 23. Values $A_{1,z}$, $A_{2,z}$, and $A_{3,z}$ are the magnitude to scale the normalized matrix of displacements of the three first out-of-plane eigenmode, modes 1, 3, and 8 respectively. This GMNIA results in an LPF of $\alpha_{GMNIA\ IV}$=1.73. The load-displacement path is plotted in Figure 45.

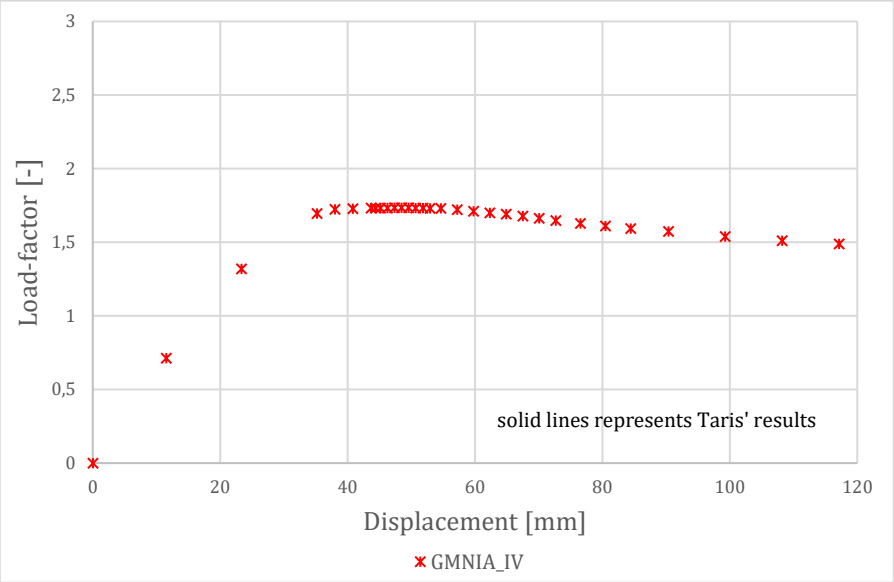

Figure 45: Load displacement diagram for GMNIA IV

5.5 COMPARISON OF RESULTS

In this paragraph, the results of the validation study and the results of Taris will be compared. Note that this paragraph is only to validate the FEM calculations performed with the FE-model as described in chapter 4, and not to determine which analysis method is the closest to reality since this is already been done by Taris [10]. Determination of the most valid analysis method will be done in chapter 6 for a case including the leaning column effect.

Overall it can be stated that the possible difference between the results of the validation study and Taris for all analysis methods can be explained by the different way of modeling the cross-section, as can be seen in Figure 34. The difference between the models with and without overlap in the cross-section has led to a different moment of inertia and area, resulting in (minimal) differences in magnitudes of the imperfections. These differences are shown in Table 5.

Table 5: Differences for the properties and magnitudes of the imperfections

	Taris	Author's validation study
Cross-section:	A = 22350 $I_y = 217231 \cdot 10^4$ mm^4 $I_z = 2938 \cdot 10^4$ mm^4	A = 21900 $I_y = 210817 \cdot 10^4$ mm^4 $I_z = 2936 \cdot 10^4$ mm^4
Imperfection:	GMNIA I: In-plane = 28,9 mm GMNIA IIa: In-plane = 28,9 mm Out-of-plane = 45.1 mm GMNIA IIb: In-plane = 28,9 mm Out-of-plane = 22.8 mm GMNIA IIIa and IIIb: In-plane = 23,5 mm Out-of-plane = 6.76 mm	GMNIA I: In-plane = 28,9 mm GMNIA IIa: In-plane = 28,9 mm Out-of-plane = 44.68 mm GMNIA IIb: In-plane = 28,9 mm Out-of-plane = 22.53 mm GMNIA IIIa and IIIb: In-plane = 23,35 mm Out-of-plane = 6.7 mm

The results of the ultimate LPF for the various analyses are given in Table 6 and Figure 46. Here can be seen that the differences are minimal, except for GMNIA IIIb. The minimal differences for the majority of the analyses can be explained by the difference in cross-section properties as explained above, and the fact that the in-plane imperfection is induced by equivalent forces, instead of the normalized matrix of displacements, as Taris did. The larger difference for GMNIA IIIb is harder to explain. When we compare IIIa (coarse mesh) and IIIb (fine mesh) it is expected that the finer mesh will result in a lower ultimate LPF, but instead, the value is 10% higher. Figure 43 shows that the load-displacement path for GMNIA IIIa and GMNIA IIIb of Taris (solid line with ditto color) leaps down, where the load-displacement path for GMNIA IIIb in this study leaps up. The reason for that is unknown.

As discussed before, GMNIA II and GMNIA IV are unique results and can not be compared to the results of Taris to validate the model. Nevertheless, the results of Table 6 indicate that GMNIA II and GMNIA IV give similar results.

Table 6: Comparison of the various analyses

	Ultimate LPF							
	LBA	GMNIA I	GMNIA II	GMNIA IIa	GMNIA IIb	GMNIA IIIa	GMNIA IIIb	GMNIA IV
Taris	2.56	2.44	-	1.47	1.63	1.81	1.78	-
Author	2.61	2.52	1.65	1.48	1.64	1.82	1.99	1.73
Difference $\frac{T-X}{T}$	1.69%	3.07%	-	0.44%	0.66%	0.38%	10.60%	-

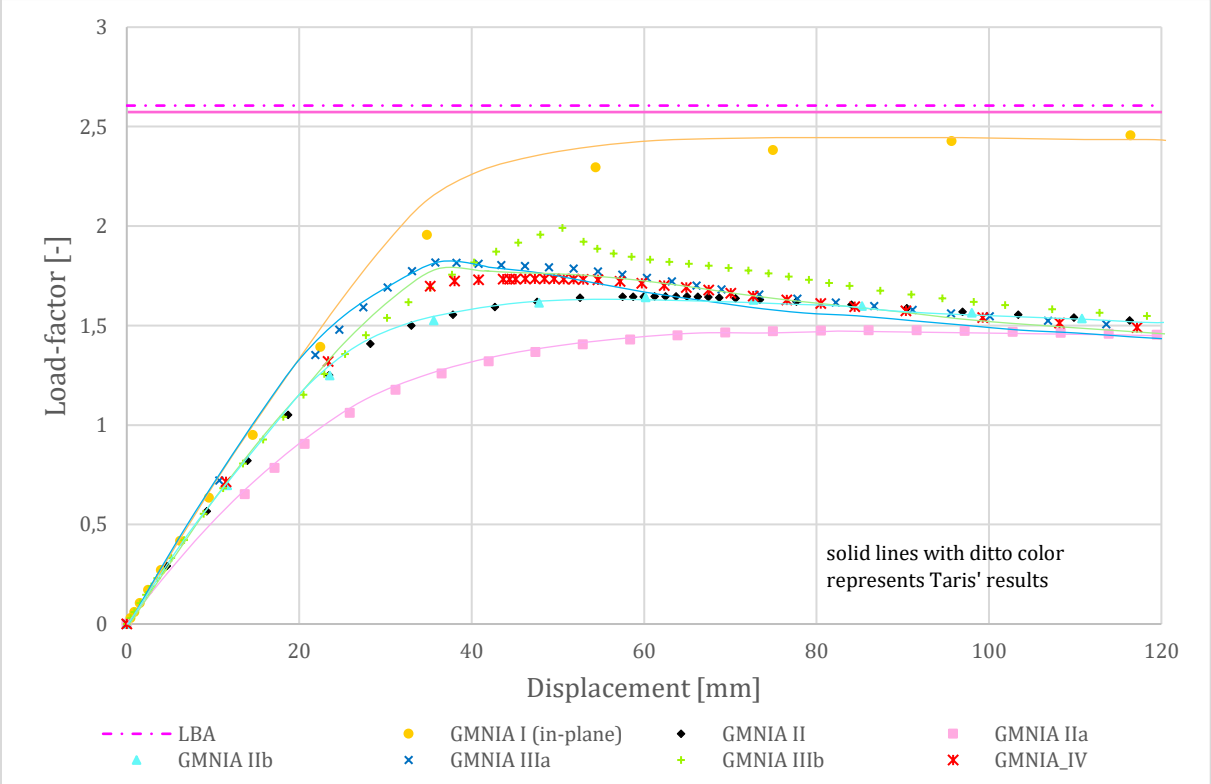

Figure 46: Load-displacement diagram with the results of all the analyses

6 CASE STUDY SWAY FRAME INCLUDING LEANING COLUMN

6.1 INTRODUCTION

The next step is to perform the various analyses once again, but now for a frame including the leaning column effect. This will be elaborated in this chapter. In section 6.5, the ultimate resistance load of the frame will be determined according to the design rules of the NEN 6771 and the EN 1993-1-1. The goal of this chapter is to determine which of these various analyses reflect reality in the best way for a frame including the leaning column effect and how this reflects the design codes.

The frame that will be studied is an unbraced fully lateral supported steel sway frame with a leaning column. The leaning column effect is included by adding a beam and column, where the beam is (and must be) pin-ended connected to the stabilizing frame, as shown in Figure 3. The fully lateral support condition is met by preventing the displacement of the webs of all members in the Z-direction, as discussed in section 4.3.3. The frame is loaded with a vertical point load F applied at the top of every column. The dimensions of the frame and the cross-sections are shown in Figure 47. The mechanical scheme that is used in this case study represents the execution of the frame that is the most vulnerable for the leaning column effect, shown in Figure 48.

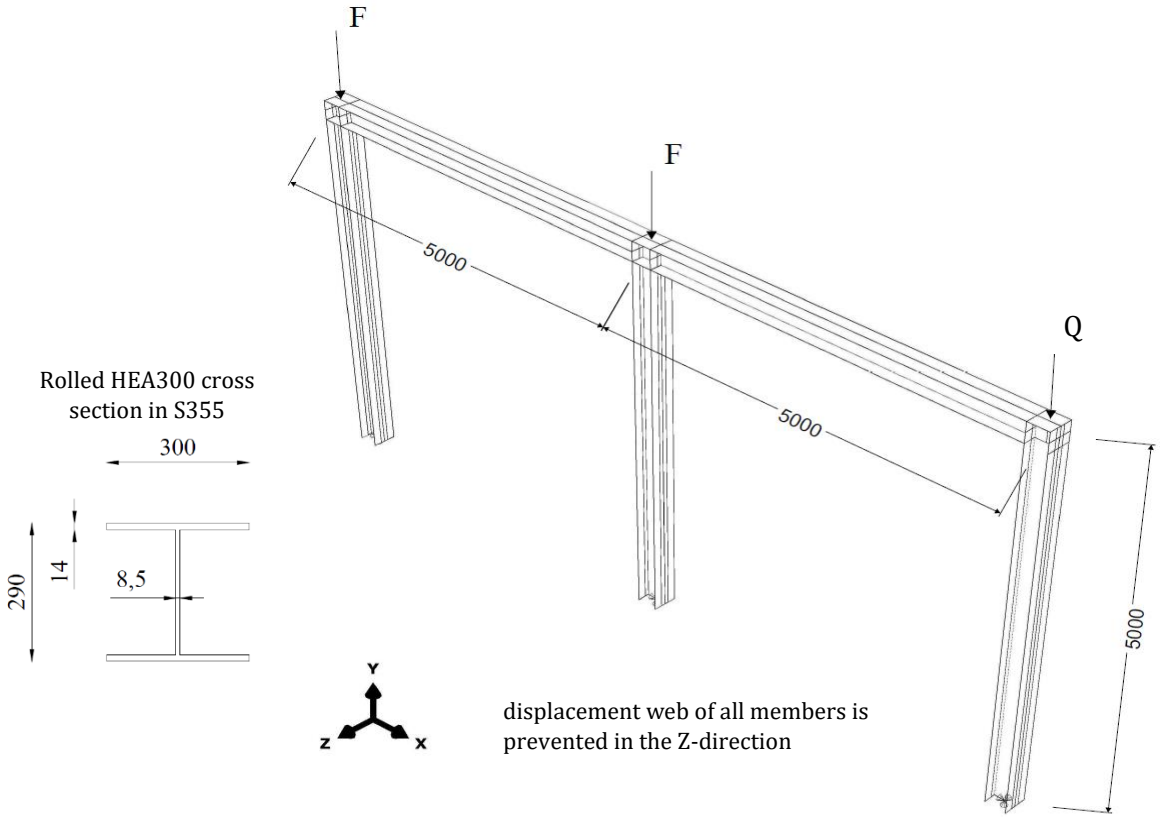

Figure 47: Three-dimensional illustration of the frame including the leaning column effect

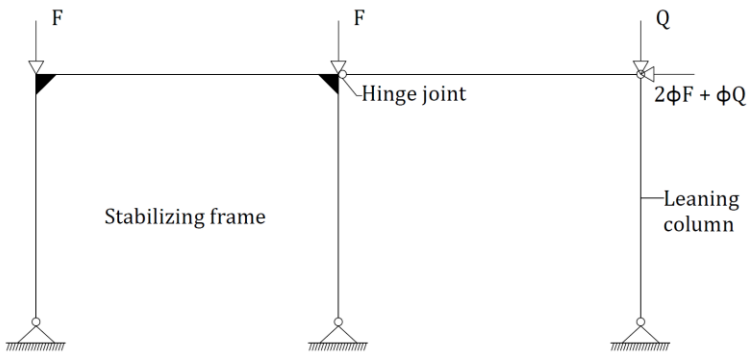

Figure 48: Mechanical scheme for the leaning column problem considered in the case study

In contrast to chapter 5, elastic-plastic material properties are used with linear strain hardening to reflect reality even more. True stress-strain behavior, can not be used due to a lack of material test data. The material that is used has a yield-strength of 355 N/mm² and an ultimate tensile strength of 490 N/mm². It turned out that the results are not affected by the linear strain hardening, since the problem that is considered is an instability problem.

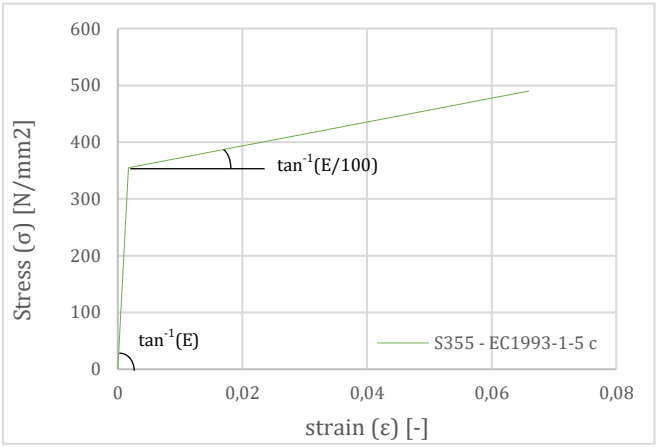

Figure 49: Engineering stress-strain diagram for elastic-plastic material with linear strain-hardening behavior for steel quality S355 according to EN 1993-1-5

6.2 ANALYSIS METHOD AND IMPERFECTIONS

The structure in this case study is fully restricted in the out-of-plane direction and only included in-plane imperfections. The imperfections are shaped and sized according to section 3.3. Table 7 shows how the imperfections are determined and how it is induced on the frame.

Table 7: Imperfections that are used in the various analyses in the case study

ANALYSES	IMPERFECTIONS	RESIDUAL STRESSES
LBA	-	-
GMNIA I	Sway imperfection according to EN 1993-1-1 Clause 5.3.2(3) induced with equivalent forces	NO
GMNIA II	First eigenmode sized according to EN 1993-1-1 Clause 5.3.2(11) (η_{init}) induced with the normalized matrix of displacements	NO
GMNIA III	First eigenmode sized as $L_{cr}/1000$ induced with the normalized matrix of displacements	YES
GMNIA IV	First three eigenmodes sized as $A_j = P_j \cdot F \cdot h$ induced with the normalized matrix of displacements	YES

6.3 MESH REFINEMENT STUDY AND THE CORRESPONDING RESIDUAL STRESSES

In section 5.3 only a smaller mesh refinement study is elaborated. The reason for that is that the results of chapter 5 are only for validation purposes, and not for obtaining actual results regarding this research. For the case study including the leaning column, the mesh is even more important. The mesh size used in the model is determinative of the results that will be obtained from the FE-Model. With a mesh-refinement study, the mesh is found where the result-difference is found acceptable compared to the finest mesh. Also regarding residual stresses, the mesh size plays an important role. A finer mesh is needed to precisely model the configuration of the residual stresses as discussed in section 3.3.3. The model should be modeled in such a way that the mesh size is adjustable in the region of the intersection of the beam with the column.

Also for the case study, the mesh is studied with an elastic LBA and a plastic GMNIA, since the deformation of the frame is hard to compare. It turned out that the starting mesh (314x145x50) already gave reasonable results. This allowed smaller divide steps to obtain reasonable results and therefore different combinations of mesh sizes are studied, resulting in various mesh element shapes. The results of the mesh refinement study are shown in Table 8 and Table 9. The mesh refinement study resulted in a mesh of 78.5x32.75x25, with only 0.11%, 0.33, and 0.42% differences compared to the finest mesh. The mesh size direction of the coding a, b and c are shown in Figure 50.

Table 8: Results for the elastic mesh-refinement study for the case study

axbxc	Number of elements [-]	Rel. mesh density $\frac{X}{50x145x314}$ [-]	Critical force amplifier (α_{cr}) [-]	CPU time [s]	% Error $\frac{26.2x22.2x25 - X}{26.2x22.2x25}$ (%)
26.2x22.2x25	22370	23.01	1.7877	440.3	0.00%
39.25x32.75x25	16286	16.75	1.7882	262.5	-0.03%
78.5x32.75x25	**8536**	**8.78**	**1.7897**	**98.8**	**-0.11%**
78.5x65.5x25	7248	7.46	1.7903	84.8	-0.15%
52.33x49.12x50	7058	7.26	1.7947	102.3	-0.39%
157x32.75x25	4692	4.83	1.7926	24.0	-0.27%
78.5x65.5x50	4128	4.25	1.796	42.7	-0.46%
157x65.5x25	3832	3.94	1.7932	21.0	-0.31%
157x65.5x50	2176	2.39	1.7984	12.4	-0.60%
314x65.5x50	1216	1.25	1.804	6.9	-0.91%
314x145x50	972	1	1.8074	5.6	-1.10%

Table 9: Results for the plastic mesh-refinement study for the case study

axbxc	Rel. mesh density $\frac{X}{50x145x314}$	Reaction force (RF)	Applied force (AF)	CPU time	% Error $\frac{6.25x6.25x6.25 - X}{6.25x6.25x6.25}$	
	[-]	[kN]	[kN]	[s]	RF (%)	AF (%)
26.2x22.2x25	23.01	1440.2	1324.2	2038.8	0.00%	0.00%
39.25x32.75x25	16.75	1441.3	1325.6	1180.0	-0.08%	-0.11%
78.5x32.75x25	**8.78**	**1444.5**	**1329.7**	**611.8**	**-0.30%**	**-0.42%**
78.5x65.5x25	7.46	1444.8	1329.1	507.3	-0.32%	-0.37%
52.33x49.12x50	7.26	1427.8	1309.1	483.8	0.86%	1.14%
157x32.75x25	4.83	1450.0	1336.5	340.1	-0.68%	-0.93%
78.5x65.5x50	4.25	1431.5	1312.1	283.1	0.60%	0.92%
157x65.5x25	3.94	1449.6	1335.0	276.6	-0.66%	-0.81%
157x65.5x50	2.39	1442.7	1315.9	155.9	-0.17%	0.63%
314x65.5x50	1.25	1457.9	1328.2	94.2	-1.23%	-0.31%
314x145x50	1	1453.5	1325.9	74.6	-0.92%	-0.13%

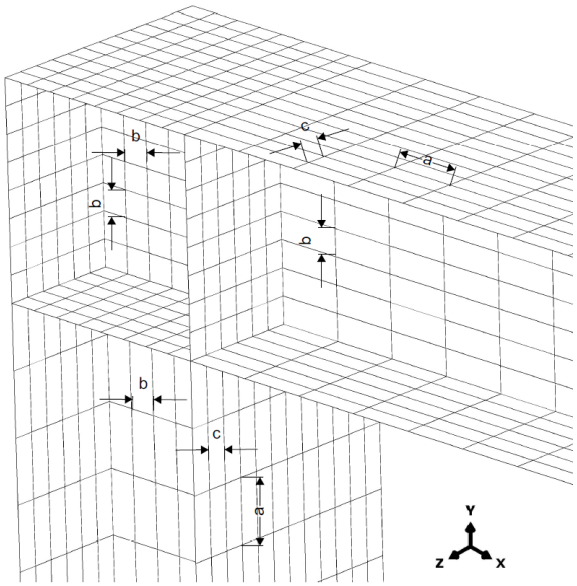

Figure 50: Mesh-size coding illustrated on the left column-beam joint of the leaning column problem

In the case study, HEA300 cross-sections are used for the members of the frame. The HEA300 cross-section is fabricated with a hot-rolling process. Residual stresses develop due to differential cooling after hot rolling. Figure 51 shows on the left the actual residual stress for a HEA300. The patterns for the FE-model are based on the mesh size 78.5x32.75x25 and will be used in analysis methods GMNIA III and GMNIA IV. The corresponding residual stress pattern is shown on the right of Figure 51. In contrast to chapter 5, there is no distinction made between the coarse or fine mesh and therefore only one mesh size is used for residual stresses.

Vogel et al. [8] do not advise how to deal with residual stresses for material that differ from the S235 steel quality. It is expected that the residual stresses for S355 are lower than $0.5f_y$. In the process, calculations were processed with $0.375f_y$, to see the influence of lower residual stresses. It turned out that the results only differ 1-2% and for that reason, the rule of $0.5f_y$ will be maintained.

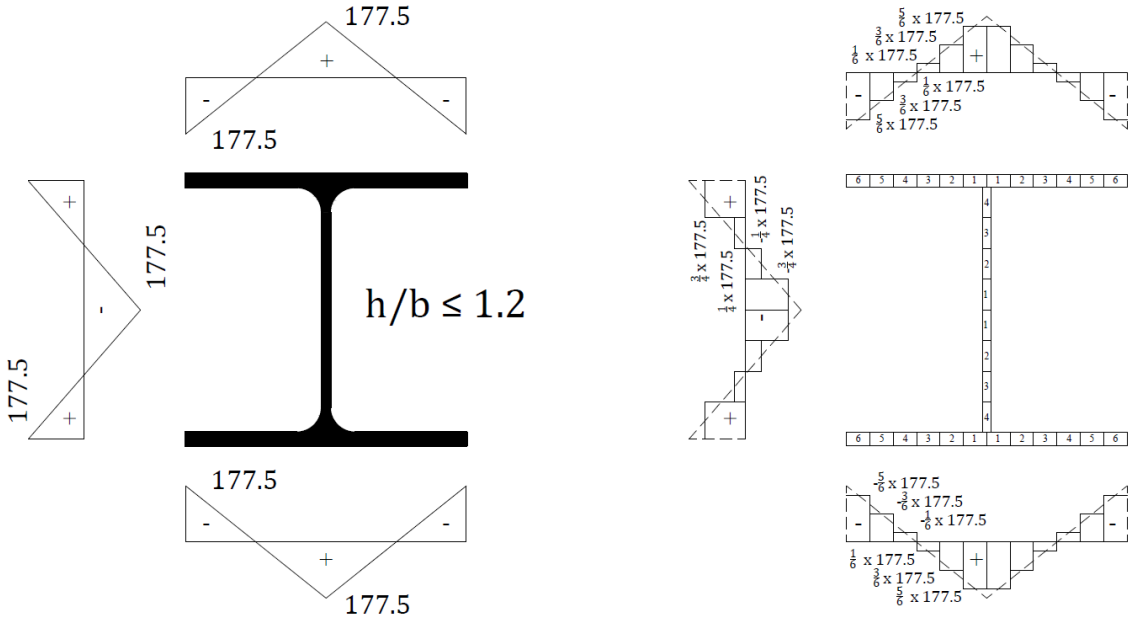

Figure 51: Residual stress pattern for the actual cross-section (left), and the FE-model mesh (right)

6.4 NUMERICAL RESULTS OF THE VARIOUS ANALYSES

6.4.1 LBA

As mentioned before, the study of this chapter only takes in-plane displacements into account. This is achieved by a model that is laterally supported at the webs in the Z-direction. This results in only in-plane eigenmodes, where the first eigenmode is the critical sway-mode eigenmode. The frame as shown in Figure 47 is loaded with F=Q=1000 kN. The critical eigenmode for the frame is shown in Figure 52. The critical eigenmode results in a load factor of α_{cr} =1.7898, also shown in Figure 52. This results in an ultimate load of $F_{ult,LBA} = F_{cr}$ = 1789.8 kN. The corresponding section moment at the critical cross-section is $EI|\eta''_{cr}|_{max} = 2.575 \cdot 10^6$ Nmm, where the critical cross-section is located on the column directly under the lower stiffener and is shown in Figure 53. Due to explicitly modeling shell elements with the real connections, the length of the elements will decrease compared to the beam elements. This is because the columns and connections are separately modeled when using shell elements, resulting in a somewhat lower $EI|\eta''_{cr}|_{max}$. However, in the progress, it has been experienced that this difference does not influence the results.

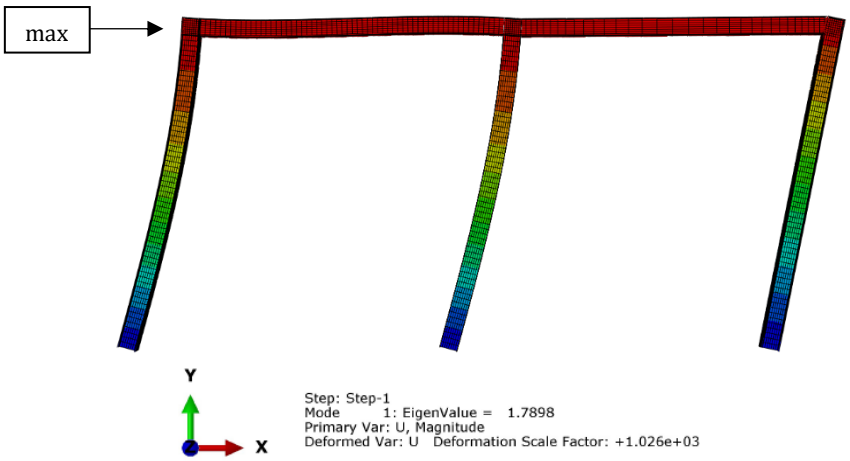

Figure 52: Critical eigenmode for a frame with a leaning column

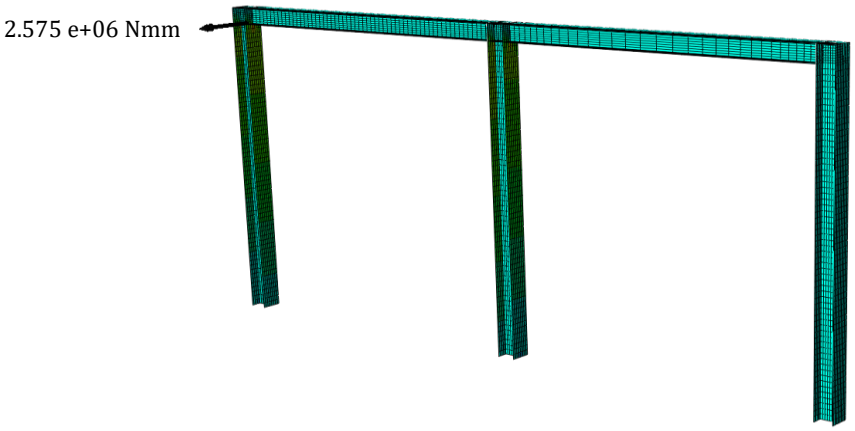

Figure 53: Resultant of section-moment $EI\left|\eta''_{cr}\right|_{max}$ for the eigenmode of Figure 52, plotted on the undeformed state

6.4.2 GMNIA I according to EN 1993-1-1 Clause 5.3.2(3)

The buckling shape found in Figure 52 follows a sway mode, where each column additionally deforms with a bow imperfection. For that reason both sway- and bow imperfections of the EN 1993-1-1 Clause 5.3.2(3) are induced on the frame, and are determined as the following:

Sway imperfection:

$$\phi_0 = 1/200$$

$$\alpha_h = \frac{2}{\sqrt{h}} = \frac{2}{\sqrt{5}} = 0.894, \text{where } \frac{2}{3} \leq 0.894 \leq 1$$

$$\alpha_m = \sqrt{0.5\left(1+\frac{1}{m}\right)} = \sqrt{0.5\left(1+\frac{1}{3}\right)} = 0.816$$

$$\phi = \phi_0 \cdot \alpha_h \cdot \alpha_m = \frac{1}{200} \cdot 0.894 \cdot 0.816 = 3.647 \cdot 10^{-3}$$

$$\Delta = 3.647 \cdot 10^{-3} \cdot 5000 = 18.3 \text{ mm}$$

Bow imperfection:
A HEA300 profile in S355 gives a section classification of 3 for outstand flanges loaded in compression, so the elastic section modulus has to be used.

$$I = \frac{1}{12} \cdot 8.5 \cdot 262^3 + 2 \cdot \left(\frac{1}{12} \cdot 300 \cdot 14^3 + 14 \cdot 300 \cdot 138^2\right) = 1728.5 \cdot 10^5 \text{ mm}^4$$

$$W_{el} = \frac{17285 \cdot 10^4}{145} = 119.2 \cdot 10^4 \text{ mm}^3$$

$$M_{Rk} = f_y \cdot W_{el} = 355 \cdot 119.2 \cdot 10^4 = 423.2 \cdot 10^6 \text{ Nmm}$$

$$N_{Rk} = f_y \cdot A = 355 \cdot 10627 = 3772.6 \cdot 10^3 \text{ N}$$

$$F_{cr} = 1789.8 \cdot 10^3 = 1789.8 \cdot 10^3 \text{ N}$$

$$\bar{\lambda} = \sqrt{\frac{\alpha_{ult,k}}{\alpha_{cr}}} = \sqrt{\frac{N_{Rk}}{F_{cr}}} = \sqrt{\frac{3772.6 \cdot 10^3}{1789.8 \cdot 10^3}} = 1.45$$

$\alpha = 0.34$ according to table 1 in appendix A

$$e_0 = \alpha(\bar{\lambda} - 0.2)\frac{M_{Rk}}{N_{Rk}} = 0.34 \cdot (1.45 - 0.2)\frac{423.2 \cdot 10^6}{3772.6 \cdot 10^3} = 47.7 \text{ mm}$$

The Sway imperfection Δ and bow imperfection e_0 are induced on the structure as an equivalent force as shown in Figure 14. This GMNIA results in an ultimate load of $F_{ult,GMNIA\ I}$ = 1338.3 kN. The load-displacement path corresponding to this analysis is shown in Figure 54, where each dot is a converged equilibrium state. The displacement taken is the lateral displacement at the left top node. The figure also includes the F_{cr} obtained from the LBA.

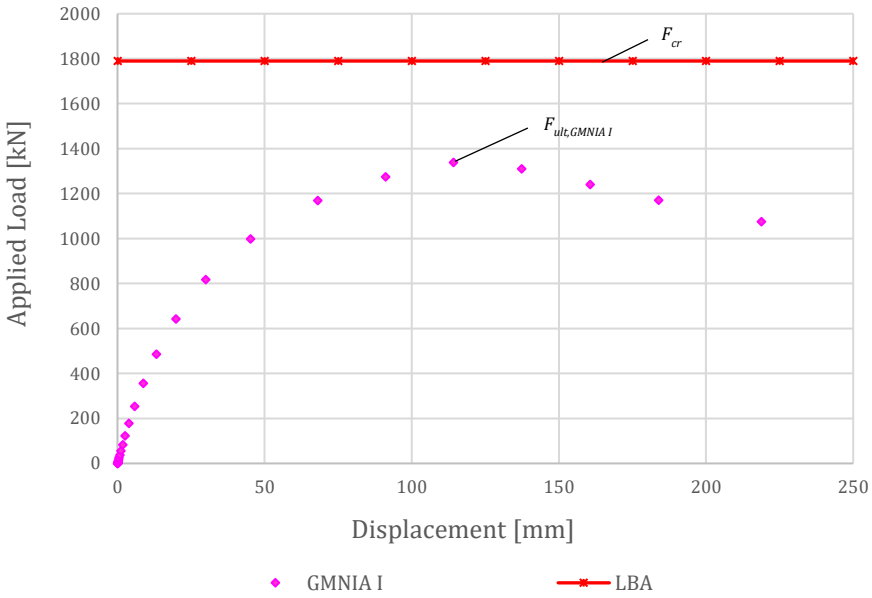

Figure 54: Load displacement diagram for GMNIA I, including the buckling load from the LBA

6.4.3 GMNIA II according to EN 1993-1-1 clause 5.3.2(11)

The imperfection for GMNIA II is induced with a scale-factor (η_{init}) to size the normalized matrix of displacements of the critical eigenmode. The scale-factor is determined as the following:

$M_{Rk} = 423.2 \cdot 10^6$ Nmm according to section 6.4.2

$N_{Rk} = 3772.6 \cdot 10^3$ N according to section 6.4.2

$\bar{\lambda} = 1.45$ according to section 6.4.2

$\alpha = 0.34$ according to section 6.4.2

$$\phi = 0.5\left[1 + \alpha(\bar{\lambda} - 0.2) + \bar{\lambda}^2\right] = 0.5[1 + 0.34 \cdot (1.45 - 0.2) + 1.45^2] = 1.766$$

$$\chi = \frac{1}{\phi + \sqrt{\phi^2 - \bar{\lambda}^2}} = \frac{1}{1.766 + \sqrt{1.766^2 - \overline{1.45^2}}} = 0.36$$

$$e_0 = \alpha(\bar{\lambda} - 0.2)\frac{M_{Rk}}{N_{Rk}} \cdot \frac{1 - \frac{\chi^{\bar{\lambda}^2}}{\gamma_{M1}}}{1 - \chi^{\bar{\lambda}^2}} = 0.34 \cdot (1.45 - 0.2)\frac{423.2 \cdot 10^6}{3772.6 \cdot 10^3} \cdot \frac{1 - \frac{0.36^{1.45^2}}{1}}{1 - 0.36^{1.45^2}} = 47.7 \text{ mm}$$

$EI\left|\eta''_{cr}\right|_{max} = 2.575 \cdot 10^6$ according to Figure 53

$$\eta_{init} = e_0 \cdot \frac{F_{cr}}{EI\left|\eta''_{cr}\right|_{max}} \eta_{cr} = 47.7 \cdot \frac{1789.8 \cdot 10^3}{2.575 \cdot 10^6} = 33.2\ [-]$$

The magnitude of the scale-factor η_{init}, which is used to size the normalized matrix of displacements of the critical eigenmode, is $\eta_{init} = 33.2$. This GMNIA results in an ultimate load of $F_{ult,GMNIA\ II}$ = 1507.0 kN. The load-displacement path corresponding to this analysis is shown in Figure 55, where each dot is a converged equilibrium state. The displacement taken is the lateral displacement at the left top node.

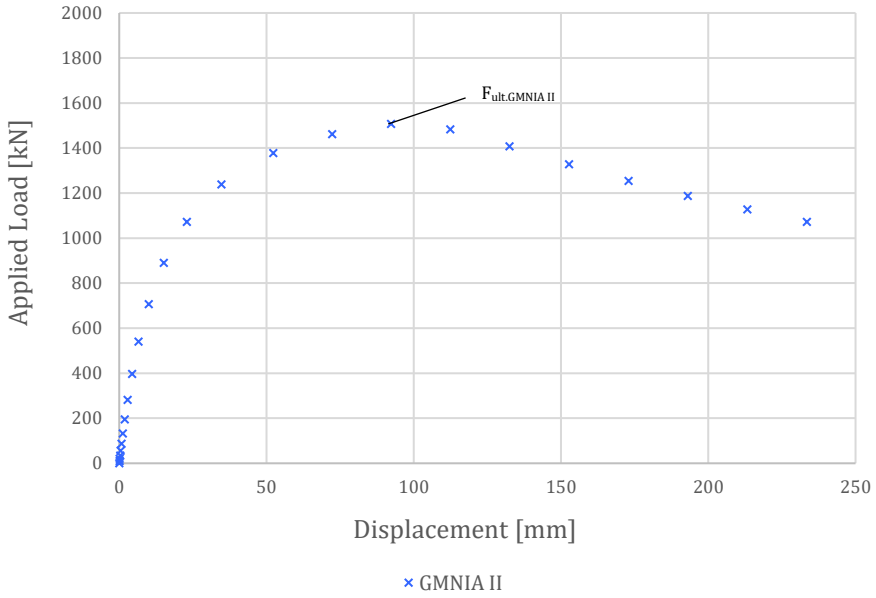

Figure 55: Load displacement diagram for GMNIA II

6.4.4 GMNIA III according to Vogel et al.

For GMNIA III, the magnitude of the imperfections is derived according to Vogel et al. [8], as described in section 3.3.3. The residual stress pattern that is plotted on the structure is shown in section 6.3. The determination of the magnitude of the imperfection to scale the normalized matrix of displacements for the critical eigenmode is the following:

$N_{Ed} = 1000 \cdot 10^3$ N

$I = 1728.5 \cdot 10^5$ mm^4 according to section 6.4.2

$\alpha_{cr} =$ 1.7898 according to Figure 52

$$L_{cr} = \pi \cdot \sqrt{\frac{E \cdot I}{\alpha_{cr} \cdot N_{Ed}}} = \pi \cdot \sqrt{\frac{210000 \cdot 1.7285 \cdot 10^8}{1.7898 \cdot 1000000}} = 14148 \text{ mm}$$

$$\frac{L_{cr}}{1000} = \frac{14148}{1000} = 14.15 \text{ mm}$$

The formula $L_{cr}/1000$ gives the sway imperfection at the middle of the buckling length. The middle of the buckling length, however, does not match with the height of the frame. To obtain the imperfection at the height of the frame, a geometrical correction has to be performed, as described in section 3.3.3. The geometrical correction can be derived by the following:

$P = r - 14.15$

$$r^2 = P^2 + \left(\frac{14148}{2}\right)^2$$

$$(P + 14.15)^2 = P^2 + \left(\frac{14148}{2}\right)^2$$

$P^2 + 28.3P + 200.2 = P^2 + \left(\frac{14148}{2}\right)^2$, gives $P = 1768459.8$ mm

$r = 1768474$ mm

$x = \frac{14148}{2} - 5000 = 2073.9$ mm

$y = \sqrt{1768474 - 2073.9^2} = 1768472.7$ mm

$\Delta = 1768472.7 - 1768459.8 = 12.93$ mm (without rounding off)

Value $\Delta = 12.93$ is the magnitude to scale the normalized matrix of displacements of the critical eigenmode. This GMNIA results in an ultimate load of $F_{ult,GMNIA\ III}$ = 1604.9 kN. The load-displacement path corresponding to this analysis is shown in Figure 56, where each dot is a converged equilibrium state. The displacement taken is the lateral displacement at the left top node.

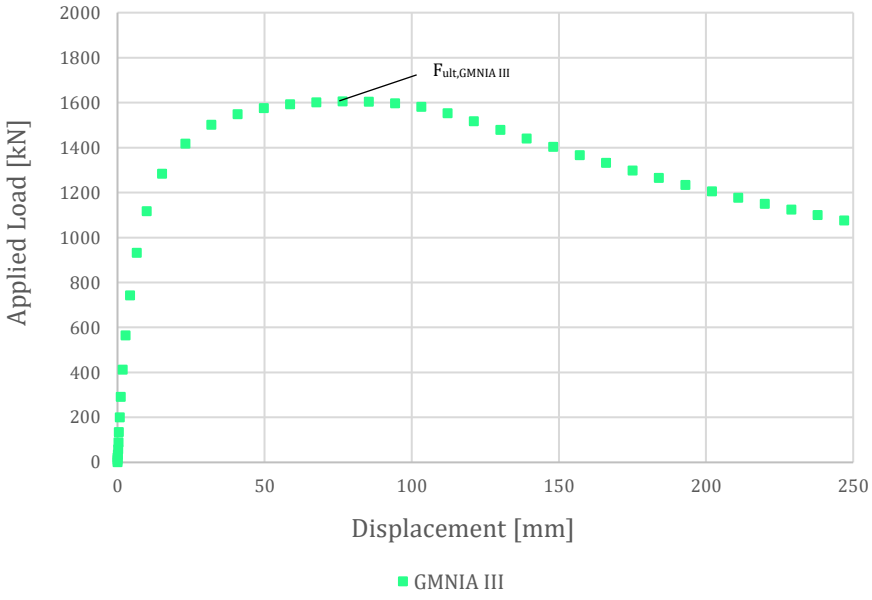

Figure 56: Load displacement diagram for GMNIA III

6.4.5 GMNIA IV according to Shayan et al. and Vogel et al.

Analysis method GMNIA IV makes use of imperfections based on various eigenmodes with scale-factors according to Shayan et al. [9], and residual stresses according to Vogel et al. [8], as described in section 3.3.4. This section also described that the use of three eigenmodes already gives valid results. However, since we are studying a leaning column problem, all the three eigenmodes should be side-sway eigenmode. It has been experienced in the process that otherwise not the lowest ultimate load that the frame can carry is found. For the frame considered in this case-study, only two eigenmodes have this side-sway eigenmode, mode 1 and mode 64, and are shown in Figure 57. The side-sway eigenmodes deform in the opposite direction. This will be corrected in the imperfection amplitude factor.

The magnitude of the normalized matrix of displacements are based on Table 1 and given as the following:

$P_1 = 0.782$ according to Table 1

$P_2 = 0.218$ according to Table 1

$F_{shayan} = 0.001566$ according to Table 1

$h = 5000$ mm

$A_1 = -(P_1 \cdot F_{shayan} \cdot h) = -(0.782 \cdot 0.001566 \cdot 5000) = -6.12$

$A_2 = P_2 \cdot F_{shayan} \cdot h = 0.218 \cdot 0.001566 \cdot 5000 = 1.71$

Values A_1 and A_2 are the magnitudes to scale the normalized matrix of displacements of the two eigenmodes, modes 1 and 64 respectively. This GMNIA results in an ultimate load of $F_{ult,GMNIA\ IV}$ = 1671.9 kN. The load-displacement path corresponding to this analysis is shown in Figure 58, where each dot is a converged equilibrium state. The displacement taken is the lateral displacement at the left top node.

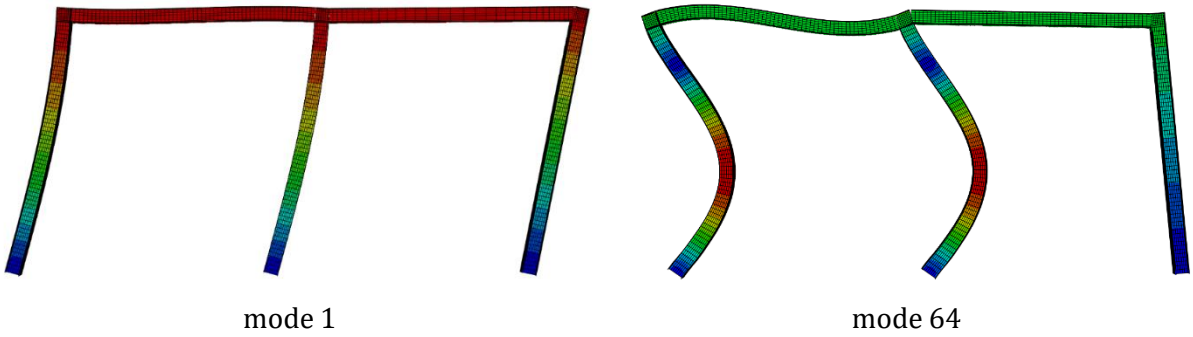

Figure 57: The first two side-sway eigenmodes for the normalized matrix of displacements that are used on the structure in GMNIA IV

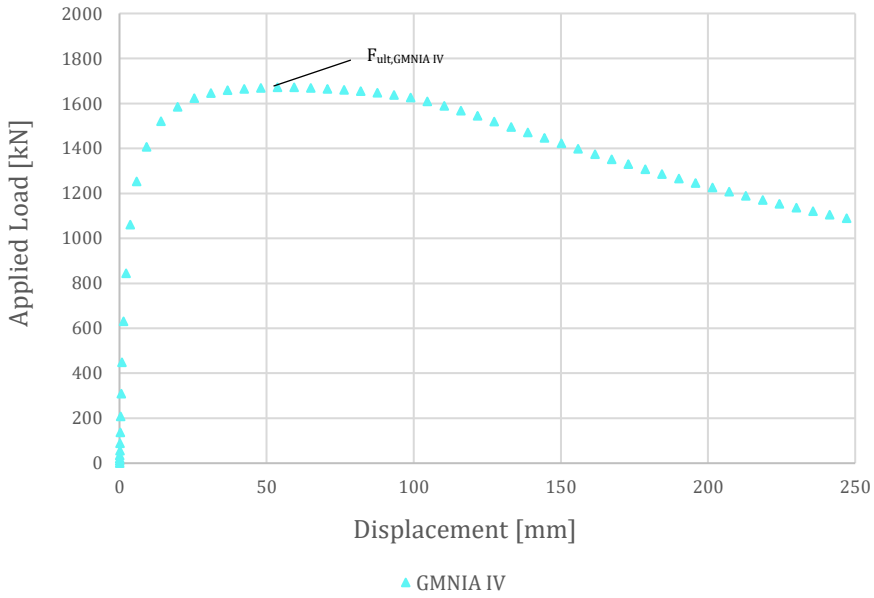

Figure 58: Load displacement diagram for GMNIA IV

6.5 ULTIMATE RESISTANCE LOADS ACCORDING TO THE CODES

6.5.1 NEN 6771

The assessment criteria for a column loaded in compression and bending according to the NEN 6771 is given by equation (2) in section 1.1.2.1 and is the following:

$$\frac{N_{Ed}}{N_{Rd}} + \frac{\alpha_{cr}}{\alpha_{cr} - 1} \cdot \frac{F_{tot} \cdot e_0 + M_{Ed}}{M_{Rd}} \leq 1$$

To determine the ultimate resistance load, the axial load N_{Ed} in the equation above should be increased until unity is reached. This will result in $F_{ult,DR,NEN}$, where the elaboration of $F_{ult,DR,NEN}$ is given below:

$\alpha_{cr} = 1.7898$, according to section 6.4.1.

To determine L_{cr}, α_{cr} is used from the LBA from section 6.4.1. This is the method that reflects reality in the best way. Section 6.7 will discuss the influence of this choice.

$$L_{cr} = \pi \cdot \sqrt{\frac{E \cdot I}{\alpha_{cr} \cdot N_{Ed}}} = \pi \cdot \sqrt{\frac{210000 \cdot 1.7285 \cdot 10^8}{1.7898 \cdot 1000 \cdot 10^3}} = 14148 \text{ mm}$$

$$i = \sqrt{\frac{I}{A}} = \sqrt{\frac{1.7285 \cdot 10^8}{10627}} = 127.53 \text{ mm}$$

$$\lambda_e = \pi \cdot \sqrt{\frac{E}{f_{y,d}}} = \pi \cdot \sqrt{\frac{210000}{355}} = 76.41$$

$$\lambda = \frac{L_{cr}}{i} = \frac{14148}{127.53} = 110.93$$

$$\lambda_{rel} = \frac{\lambda}{\lambda_e} = \frac{111.61}{76.41} = 1.45$$

$$M_{Rd} = \frac{f_{y,d} \cdot W_{el}}{\gamma_0} = \frac{355 \cdot 1.192 \cdot 10^6}{1} = 423.2 \cdot 10^6 \text{ Nmm}$$

$$N_{Rd} = \frac{f_{y,d} \cdot A}{\gamma_0} = \frac{355 \cdot 10627}{1} = 3772.6 \cdot 10^3 \text{ N}$$

$\alpha_k = 0.34$, according to table 25 of the NEN 6770

$\lambda_0 = 0.20$, according to table 25 of the NEN 6770

$$e_0 = \alpha_k \cdot (\lambda_{rel} - \lambda_0) \cdot \frac{M_{Rd}}{N_{Rd}} = 0.34 \cdot (1.45 - 0.2) \cdot \frac{423.2 \cdot 10^6}{3772.6 \cdot 10^3} = 47.7 \text{ mm}$$

$$\alpha_{cr} = \frac{F_{cr}}{N_{Ed}} = \frac{1789.8 \cdot 10^3}{N_{ult}}$$

$$\phi_0 = \frac{1}{250}, n_s = 1, n_k = 3$$

$$k_1 = \sqrt{0.2 + \frac{1}{n_s}}, \text{but } \leq 1 \text{ gives } \sqrt{0.2 + \frac{1}{1}} = 1.095 = 1$$

$$k_2 = \sqrt{0.5 + \frac{1}{n_s}}, \text{but } \leq 1 \text{ gives } \sqrt{0.5 + \frac{1}{3}} = 0.913$$

$$\phi = \phi_0 \cdot k_1 \cdot k_2 = \frac{1}{250} \cdot 1 \cdot 0.913 = 3.647 \cdot 10^{-3}$$

$$\phi N_{Ed} = \phi N_{ult} = 3.647 \cdot 10^{-3} \cdot \mathrm{N_{ult}}$$

To make the results comparable, the Eurocode series is leading. The bending moment factor is taken according to the Eurocode (0.9) instead of the NEN 6771 (0.85):

$$M = 0.9 \cdot M_{Ed} = 0.9 \cdot \frac{3 \cdot \phi F \cdot h}{2} = \frac{3 \cdot \phi F_{ult} \cdot h}{2} = 0.9 \cdot \frac{3 \cdot 3.647 \cdot 10^{-3} \cdot N_{ult} \cdot 5000}{2}$$

According to Figure 6, F_{tot} is equal to $F_{tot} = \frac{3}{2} N_{Ed}$, resulting in $F_{tot,ult} = \frac{3}{2} F_{ult}$

$$\frac{N_{ult}}{3772.6 \cdot 10^3} + \frac{\frac{1789.8 \cdot 10^3}{N_{ult}}}{\frac{1789.8 \cdot 10^3}{N_{ult}} - 1} \cdot \frac{\frac{3}{2} F_{ult} \cdot 47.7 + 0.9 \cdot \frac{3 \cdot 3.647 \cdot 10^{-3} \cdot N_{ult} \cdot 5000}{2}}{423.2 \cdot 10^6} = 1$$

Solving the equation above results in an ultimate resistance load of:

$N_{ult,DR,NEN,LBA} = 1131.6$ kN

It should be noted that the leaning column effect now is taken into account twice. First with α_{cr}, since the leaning column is modeled, and later with F_{tot}.

6.5.2 EN 1993-1-1

The assessment criteria for a column loaded in compression and bending according to the EN 1993-1-1 is given by equation (25) in section 1.1.2.2 and is the following:

$$\frac{N_{Ed}}{\chi \cdot N_{Rd}} + k \frac{C_m \cdot M_{Ed}}{M_{Rd}} \leq 1 \; where \; k = \frac{1}{1 - \frac{\chi \cdot N_{Ed}}{F_{cr}}}$$

To determine the ultimate resistance load, $\mathrm{N_{Ed}}$ in the equation above should be increased until unity is reached. This will result in $F_{ult,DR,EC}$, where the elaboration of $F_{ult,DR,EC}$ is given below. To determine L_{cr}, α_{cr} is used from the LBA from chapter 6.4.1.

$F_{cr} = 1789.8 \cdot 10^3$ N, according to section 6.4.2

$\bar{\lambda} = 1.45$, according to section 6.4.2

$\Phi = 1.766$, according to section 6.4.3

$\chi = 0.36$, according to section 6.4.3

$N_{Rk} = 3772.6 \cdot 10^3$ N according to section 6.4.2

$$N_{Rd} = \frac{N_{Rk}}{\gamma_0} = \frac{3772.6 \cdot 10^3}{1} = 3772.6 \cdot 10^3 \text{ N}$$

$M_{Rk} = 423.2 \cdot 10^6$ Nmm according to section 6.4.2

$$M_{Rd} = \frac{M_{Rk}}{\gamma_0} = \frac{423.2 \cdot 10^6}{1} = 423.2 \cdot 10^6 \text{ Nmm}$$

$\phi = 3.647 \cdot 10^{-3}$ according to section 6.4.2

$C_m = 0.9$ according to table 7 in appendix A

$$\phi N_{Ed} = \phi N_{ult} = 3.647 \cdot 10^{-3} \cdot N_{ult}$$

$$C_m \cdot M_{Ed} = 0.9 \cdot \frac{3 \cdot \phi F \cdot h}{2} = \frac{3 \cdot \phi N_{ult} \cdot h}{2} = 0.9 \cdot \frac{3 \cdot 3.647 \cdot 10^{-3} \cdot N_{ult} \cdot 5000}{2}$$

$$k = \frac{1}{1 - \frac{\chi \cdot N_{Ed}}{F_{cr}}} = \frac{1}{1 - \frac{0.36 \cdot N_{ult}}{1789.8 \cdot 10^3}}$$

$$\frac{N_{ult}}{0.357 \cdot 3772.6 \cdot 10^3} + \frac{1}{1 - \frac{0.36 \cdot N_{ult}}{1789.8 \cdot 10^3}} \cdot \frac{0.9 \cdot \frac{3 \cdot 3.647 \cdot 10^{-3} \cdot N_{ult} \cdot 5000}{2}}{423.2 \cdot 10^6} = 1$$

Solving the equation above results in an ultimate resistance load of:

$N_{ult,DR,EC,LBA} = 1230.6$ kN

6.5.3 Modified EC1991-1-1

In the following derivation, the leaning column effect is included in the assessment criteria for a column loaded in compression and bending according to the EN 1993-1-1, as derived in section 2.1. The equation is given by equation (43) and is the following:

$$\frac{N_{Ed}}{\chi \cdot N_{Rd}} + k\left(\bar{\lambda}^2 - \frac{1}{\chi}\right)(\chi - 1)\frac{F_{lean}}{N_{Rd}} + k\frac{C_m \cdot M_{Ed}}{M_{Rd}} \leq 1 \; where \; k = \frac{1}{1 - \frac{\chi \cdot N_{Ed}}{F_{cr}}}$$

To determine the ultimate resistance load, N_{Ed} in the equation above should be increased until unity is reached. This will result in $N_{ult,DR,modEC}$, where the elaboration of $N_{ult,DR,modEC}$ is given below:

To determine L_{cr}, α_{cr} is used from the LBA from chapter 6.4.1.

$F_{cr} = 1789.8 \cdot 10^3$ N, according to section 6.4.2

$\bar{\lambda} = 1.45$, according to section 6.4.2

$\Phi = 1.766$, according to section 6.4.3

$\chi = 0.36$, according to section 6.4.3

$\phi = 3.647 \cdot 10^{-3}$ according to section 6.4.2

$C_m = 0.9$ according to table 7 in appendix A

$$\phi N_{Ed} = \phi F_{ult} = 3.647 \cdot 10^{-3} \cdot F_{ult}$$

$N_{Rd} = 3772.6 \cdot 10^3$ N, according to section 6.5.2

$M_{Rd} = 423.2 \cdot 10^6$ Nmm, according to section 6.5.2

$C_m \cdot M_{Ed} = \frac{3 \cdot 3.647 \cdot 10^{-3} \cdot F_{ult} \cdot 5000}{2}$ according to section 6.5.2

$k = \frac{1}{1 - \frac{0.36 \cdot F_{ult}}{1789.8 \cdot 10^3}}$ according to section 6.5.2

$$\frac{F_{ult}}{0.357 \cdot 3772.6 \cdot 10^3} + \frac{1}{1 - \frac{0.36 \cdot F_{ult}}{1789.8 \cdot 10^3}} \cdot \left(1.46^2 - \frac{1}{0.357}\right)(0.357 - 1)\frac{F_{lean}}{3772.6 \cdot 10^3} + \frac{1}{1 - \frac{0.36 \cdot F_{ult}}{1789.8 \cdot 10^3}} \cdot \frac{0.9 \cdot \frac{3 \cdot 3.647 \cdot 10^{-3} \cdot F_{ult} \cdot 5000}{2}}{423.2 \cdot 10^6} = 1$$

According to Figure 11, F_{lean} is equal to $F_{lean} = \frac{1}{2}Q = \frac{1}{2}F$, resulting in $F_{lean,ult} = \frac{1}{2}F_{ult}$

$$\frac{F_{ult}}{0.357 \cdot 3772.6 \cdot 10^3} + \frac{1}{1 - \frac{0.36 \cdot F_{ult}}{1789.8 \cdot 10^3}} \cdot \left(1.46^2 - \frac{1}{0.357}\right)(0.357 - 1)\frac{\frac{1}{2}F_{ult}}{3772.6 \cdot 10^3} + \frac{1}{1 - \frac{0.36 \cdot F_{ult}}{1789.8 \cdot 10^3}} \cdot \frac{0.9 \cdot \frac{3 \cdot 3.647 \cdot 10^{-3} \cdot F_{ult} \cdot 5000}{2}}{423.2 \cdot 10^6} = 1$$

Solving the equation above results in an ultimate resistance load of:

$N_{ult,DR,modEC,LBA} = 1131.6$ kN, which is the same ultimate resistance load as the NEN 6771 (section 6.5.1). It should be noted that also for the modified EN 1993-1-1 equation, the leaning column effect is taken into account twice. First with α_{cr}, since the leaning column is modeled, and later with F_{lean}.

6.6 COMPARISON OF THE RESULTS

6.6.1 Differences and similarities

In this research, no actual tests are performed, meaning that the results cannot be compared to the actual real behavior of the structure. However, the GMNIA with residual stresses, GMNIA III and GMNIA IV, are assumed to be the closest to reality. These GMNIA's have the most realistic shape and magnitudes of the imperfections implemented and on top of that, they also have the residual stresses modeled. Ultimate loads $F_{ult,GMNIA\ III}$, and $F_{ult,GMNIA\ IV}$ are very close and only differ -4.1% of each other. This small difference strengthens the fact that the GMNIA III and GMNIA IV are close to reality since they both find (almost) the same result. This difference is also confirmed by the statement of Shayan et al. [9], which is that the use of only the first critical eigenmode (which is the case for GMNIA III) leads to conservative results. This confirmation is also the reason that from now all values that will be compared to the GMNIA, will be compared to GMNIA IV.

The difference with the ultimate load $F_{ult,GMNIA\ II}$ (-9.85%) can be described by the fact that the imperfections of the EN 1993-1-1 include equivalent material imperfections (residual stresses, etc.) which should cover all cases, and therefore GMNIA II is conservative. For the same reason GMNIA I is even more conservative since the bow and sway imperfections that are both included uses equivalent imperfections. This leads to a conservative $F_{ult,GMNIA\ I}$, which differ -19.95%. All the

load-displacement paths are shown in Figure 59, and the differences in ultimate loads are given in Table 10.

When we compare the ultimate loads obtained by the various analyses to the ultimate resistance loads obtained by the codes, it can be seen that the results of the EN 1993-1-1 lie under the results of the various analyses. The large (positive) differences as given in Table 11 indicate that the EN 1993-1-1 design rules are conservative and therefore safe for this frame. In Figure 59 and Table 10 also the ultimate resistance load for the NEN 6771 and modified EN 1993-1 is shown. Here it can be seen that the modified EN 1993-1-1 design rule from section 2.1 gives the same result as the NEN 6771. However, as already mentioned in section 6.5.1 and 6.5.3, the ultimate resistance loads of the NEN 6771 and the modified EN 1993-1-1 takes into account the leaning column effect twice, since the leaning column effect is also considered in the LBA and is for that reason a useless result. But since $N_{ult,NEN,LBA}$, and $N_{ult,modEC,LBA}$ are the most realistic value of the ultimate resistance load obtained by the NEN 6771 and the modified EN 1993-1-1 respectively they are still shown.

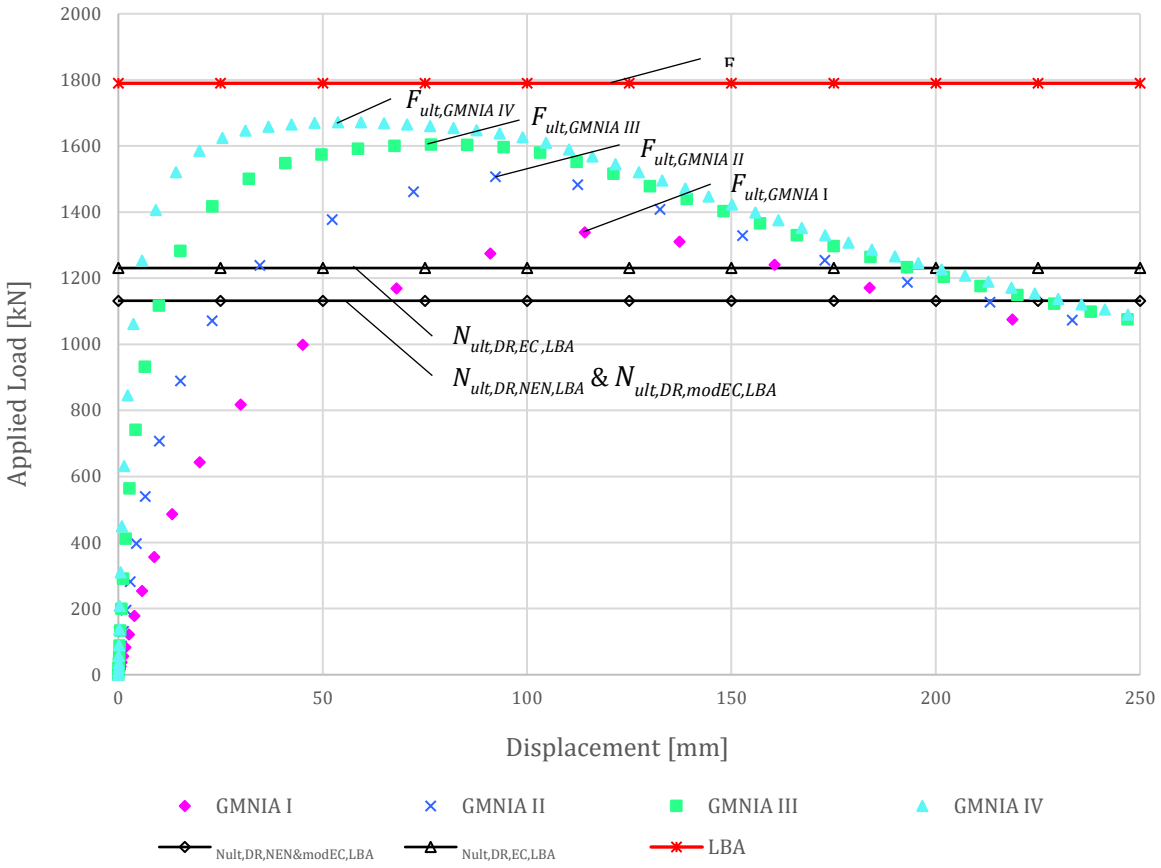

Figure 59: The load-displacement paths for all analyses including the ultimate resistance loads

Table 10: Differences ultimate (design-resistance) loads compared to the model closest to reality (GMNIA IV)

	Ultimate load (F_{ult}) in kN					
	$N_{ult,DR,NEN,LBA}$ & $N_{ult,DR,modEC,LBA}$	$N_{ult,DR,EC,LBA}$	$F_{ult,GMNIA\ I}$	$F_{ult,GMNIA\ II}$	$F_{ult,GMNIA\ III}$	$F_{ult,GMNIA\ IV}$
Result	1131.6 kN	1230.6 kN	1338.3 kN	1507.0 kN	1604.6 kN	1671.9 kN
Difference $\frac{X-GMNIA\ IV}{GMNIA\ IV}$	-32.31 %	-26.38 %	-19.95 %	-9.85 %	-4.06 %	0.00%

Table 11: Differences between the ultimate resistance loads compared to the ultimate loads

	Ultimate load (F_{ult}) in kN					
	$N_{ult,DR,NEN,LBA}$ & $N_{ult,DR,modEC,LBA}$	$N_{ult,DR,EC,LBA}$	$F_{ult,GMNIA\ I}$	$F_{ult,GMNIA\ II}$	$F_{ult,GMNIA\ III}$	$F_{ult,GMNIA\ IV}$
Result	1131.6 kN	1230.6 kN	1338.3 kN	1507.0 kN	1604.6 kN	1671.9 kN
Difference $\frac{X-EC}{EC}$	-8.04 %	0.00 %	8.75 %	22.46 %	30.39 %	35.86 %

The deformation when the ultimate load is reached of the various analyses are given in Figure 60 and as can be seen, they follow the buckling shape as obtained by the LBA. The deformations at the ultimate loads confirm that the frame that is considered fails due to an instability problem by 2nd order behavior.

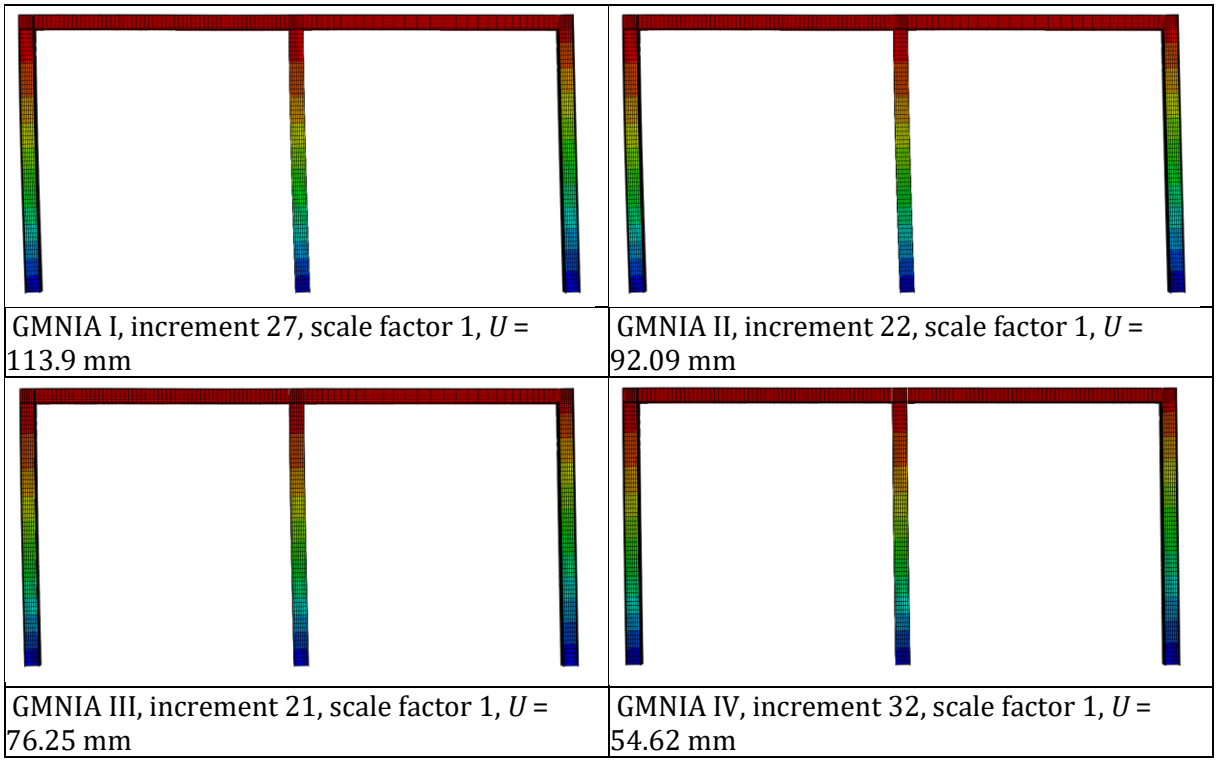

GMNIA I, increment 27, scale factor 1, U = 113.9 mm

GMNIA II, increment 22, scale factor 1, U = 92.09 mm

GMNIA III, increment 21, scale factor 1, U = 76.25 mm

GMNIA IV, increment 32, scale factor 1, U = 54.62 mm

Figure 60: Deformed state of the various analyses when the ultimate load is reached

6.7 INFLUENCE OF THE BUCKLING LENGTH DETERMINATION METHOD

In practice, it is more obvious that a structural engineer will determine L_{cr} differently than creating an extensive FE-model, as done in previous sections. In this paragraph, the influence of different ways of determining the buckling length is studied. Chapter 1 in appendix A gives more background information about the considered options.

Also, since in the previous sections the buckling length from the LBA is used, it means that in the case of the NEN 6771, the leaning column effect is taken into account twice, as already described in 6.6.1. In this paragraph, only combinations of inputs will be used that will lead to only taking into account the leaning column effect once (or not at all in case of the EC in combination with the nomogram). This will also be mentioned in the upcoming sections.

6.7.1.1 L_{cr} according to the nomogram in the Dutch National Annex of the EN 1993-1-1

A common way to determine L_{cr} for a frame is the use of the nomogram from the Dutch National Annex of the EN 1993-1-1 (NB.NA). The nomogram gives the result as the effective length factor $\beta_{nomogram}=L_{cr}/L=\pi/\lambda_n$, where λ_n can be derived with equation (51):

$$C_A \cdot C_B \cdot \lambda_n^2 \cdot \sin(\lambda_n) = (C_A + C_B) \cdot \lambda_n \cdot \cos(\lambda_n) + \sin(\lambda_n), for\ 0 \leq \lambda_n \leq \pi \qquad (51)$$

Where A and B refer to the ends of the column and where:

$$C_i = \frac{\sum \frac{I_{cln}}{L_{cln}}}{\sum \mu \frac{I_{bm}}{L_{bm}}} \qquad (52)$$

The equation is solved in the following way:

$C_A = \infty$, since the bottom of the frame, is pinned

$\mu = 6$, since the other end of the beam, is rigidly connected to one or more columns which are also loaded in compression.

$I_{cln} = I_{bm} = 1728.5 \cdot 10^5$ mm^4 according to 6.4.2

L_{cln} and L_{bm} are both 5000 mm according to Figure 47.

$$C_B = \frac{\sum \frac{I_{cln}}{L_{cln}}}{\sum \mu \frac{I_{bm}}{L_{bm}}} = \frac{\frac{1728.5 \cdot 10^5}{5000}}{6 \cdot \frac{1728.5 \cdot 10^5}{5000}} = 0.167$$

$\infty \cdot 0.167 \cdot \lambda_n^2 \cdot \sin(\lambda_n) = (\infty + 0.167) \cdot \lambda_n \cdot \cos(\lambda_n) + \sin(\lambda_n)$, solving gives $\lambda_n = 1.35$

$$\beta_{nomogram} = \frac{\pi}{\lambda_n} = 2.3279$$

$L_{cr} = 2.3279 \cdot 5000 = 11639$ mm

When we carry out again the equations for the ultimate resistance load as given in section 6.5 with $L_{cr} = 11639$ mm as input, the following ultimate resistance loads are obtained:

$N_{ult,DR,NEN,nomogram} = 1447.6$ kN
$N_{ult,DR,EC,nomogram} = 1580.6$ kN
$N_{ult,DR,modEC,nomogram} = 1447.6$ kN

Please note that in the case of $N_{ult,DR,EC,nomogram}$ no leaning column effect is considered, and that the results are the magnitude of the ultimate resistance load that will be found in practice by engineers. The new results are plotted in the load-displacement graph, shown in Figure 61.

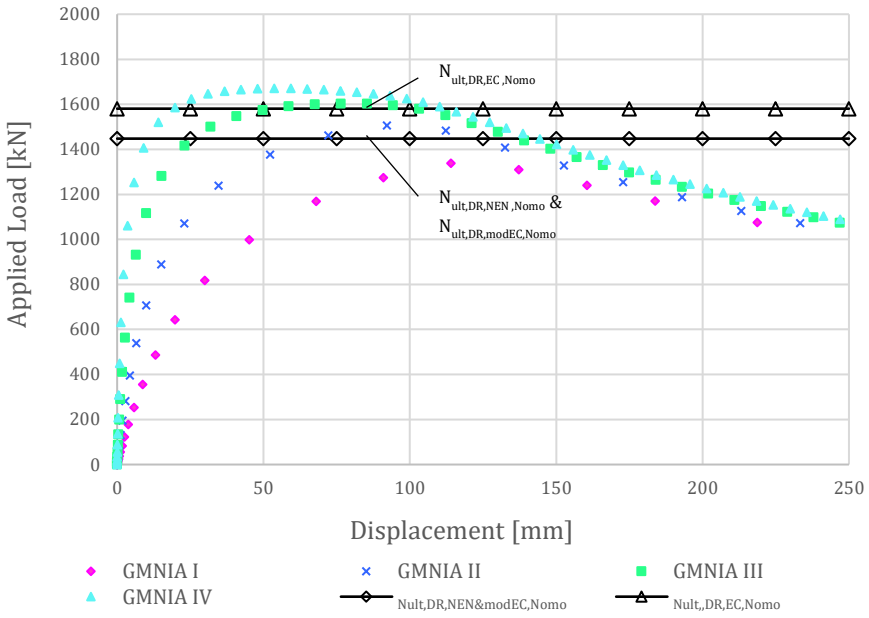

Figure 61: The load-displacement paths for all analyses including the ultimate resistance, where L_{cr} is determined with the nomogram

The result of 11639 mm (nomogram) can be described by the fact that the leaning column effect is not included in the nomogram. When an LBA is performed for a frame without a leaning column, a load factor α_{cr} of 2.6010 is found. This value and the corresponding buckling shape is shown in Figure 62. When this α_{cr} is used in the Euler buckling equation, the following L_{cr} is found:

$$L_{cr} = \pi \cdot \sqrt{\frac{E \cdot I}{\alpha_{cr} \cdot N_{Ed}}} = \pi \cdot \sqrt{\frac{210000 \cdot 1.7285 \cdot 10^8}{2.6010 \cdot 1000 \cdot 10^3}} = 11736 \text{ mm}$$

When we carry out again the design rules for the ultimate resistance loads as given in section 6.5 with $L_{cr} = 11736$ mm as input, results are found that only differ +/- 1 % from the results obtained with the nomogram. Therefore it is stated that these results are the same.

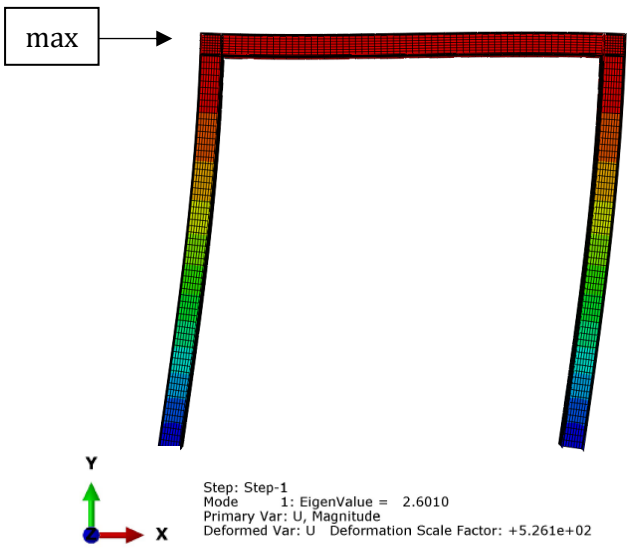

Figure 62: LBA without leaning column with a corresponding $\alpha_{cr} = 2.6010$

6.7.1.2 L_{cr} according to extended American nomogram by L.F. Geschwindner [1]

The American codes for structural safety, LRFD, and AISC [16] specifications make also use of a nomogram to determine the buckling length. The nomogram results in a factor *K* that has to be multiplied with the height of the column, which is the same proceeder as the Eurocode with β. The American equation is given in equation (53):

$$F_{cr} = \frac{(\pi^2 EI)}{(K_{exact} \cdot L)^2} \tag{53}$$

Here can be seen that equation (53) is the same equation as (4), and that gives that $K_{exact} = \beta$. The value of K_{exact} can be derived with the following equation:

$$\frac{G_A G_B (\pi/K)^2 - 36}{6(G_A + G_B)} = \frac{\pi/K}{tan\ (\pi/K)} \tag{54}$$

Where A and B refer to the ends of the column and where:

$$G_i = \frac{\sum I_{cln}/L_{cln}}{\sum I_{bm}/L_{bm}} \tag{55}$$

The nomogram equation without the leaning column effect is solved in the following way:

$G_A = \infty$, since the bottom of the frame is pinned

$I_{cln} = I_{bm} = 1728.5 \cdot 10^5$ mm^4 according to 6.4.2

L_{cln} and L_{bm} are both 5000 mm according to Figure 47.

$$G_B = \frac{\sum \frac{I_{cln}}{L_{cln}}}{\sum \frac{I_{bm}}{L_{bm}}} = \frac{\frac{1728.5 \cdot 10^5}{5000}}{\frac{1728.5 \cdot 10^5}{5000}} = 1$$

$$\frac{\infty \cdot 1 \cdot (\pi/K)^2 - 36}{6 \cdot (\infty + 1)} = \frac{\pi/K}{\tan\ (\pi/K)}, \text{ solving gives } K = 2.3279$$

$L_{cr} = 2.3279 \cdot 5000 = 11639$ mm

The result that is obtained, namely $L_{cr} = 11639$ mm, is the same result as the nomogram from the Dutch National Annex (section 6.7.1.1). However, American researcher L.F. Geschwindner [1] extended equation (54) to include the leaning column effect. Any steps for extending equation (54) are unknown, but Geschwindner [1] came up with the following equation to include the leaning column in the American nomogram:

$$\frac{G_A G_B (\pi/K)^2 - 36}{6(G_A + G_B)}\left(1 + \frac{Q}{F}\right) - \frac{\pi/K}{\tan(\pi/K)}\left(1 + \frac{Q}{F}\right) + \frac{6 \tan\left(\frac{\pi}{2K}\right)}{(G_A + G_B)\left(\frac{\pi}{2K}\right)}\left(\frac{Q}{F}\right) + \left(\frac{Q}{F}\right) = 0 \tag{56}$$

The extended nomogram equation is solved in the following way:

$G_A = \infty$, according to the above

$$G_B = \frac{\sum \frac{I_{cln}}{L_{cln}}}{\sum \frac{I_{bm}}{L_{bm}}} = \frac{\frac{1728.5 \cdot 10^5}{5000}}{2 \cdot \frac{1728.5 \cdot 10^5}{5000}} = 0.5, \text{since now the leaning column is included}$$

$$\frac{\infty \cdot 0.5 \cdot (\pi/K)^2 - 36}{6 \cdot (\infty + 0.5)} \cdot \left(1 + \frac{1}{2}\right) - \frac{\pi/K}{\tan(\pi/K)} \cdot \left(1 + \frac{1}{2}\right) + \frac{6 \tan\left(\frac{\pi}{2K}\right)}{(\infty + 0.5)\left(\frac{\pi}{2K}\right)} \cdot \frac{1}{2} + \frac{1}{2} = 0$$

Solving the above gives the effective length factor $K_{exact} = 2.59$, which gives $L_{cr} = 2.59 \cdot 5000 = 12971$ mm. When we carry out again the equations for the ultimate resistance load as given in section 6.5 with $L_{cr} = 12971$ mm as input, the following ultimate resistance load is obtained:

$N_{ult,DR,EC,L.F.G} = 1383.8$ kN

In this case, only the EN 1993-1-1 design rule is considered since the leaning column effect is now already taken into account in L_{cr}. The new ultimate resistance load is shown in Figure 63.

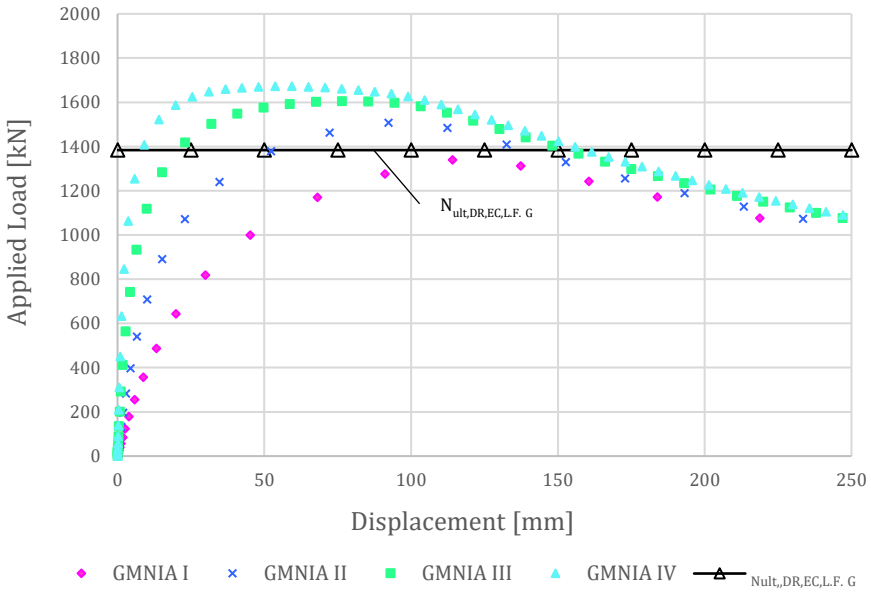

Figure 63: Ultimate resistance load where L_{cr} is determined with the equation from Geschwindner

6.7.1.3 L_{cr} according to the Yura approach (equilibrium)

J.A. Yura invented a method to include the leaning column effect in the buckling length. The approach makes use of simple equilibrium combined with the Euler buckling equation. Consider the leaning column situation in a deformed frame as shown in Figure 64. For equilibrium of the leaning column CD, load Q must be balanced with a horizontal force with a magnitude of $Q\Delta/L$. When this horizontal force is applied in point B to reach equilibrium, one can see that in the deformed state the bending moment in point A will increase with $L \cdot (Q \cdot \Delta)/L$, resulting in a bending moment of $\Delta F + \Delta Q$. This indicates that column AB is loaded by $F+Q$. The solutions for the leaning column load F_{tot} in the NEN 6771 are determined in the same way. However, where the NEN 6771 used this load in the load side of the design rule, Yura used the equilibrium approach to rewrite the Euler buckling equation. This has led to a factor based on the ratio between the sum of the load and the applied load on the stabilizing frame. [1]

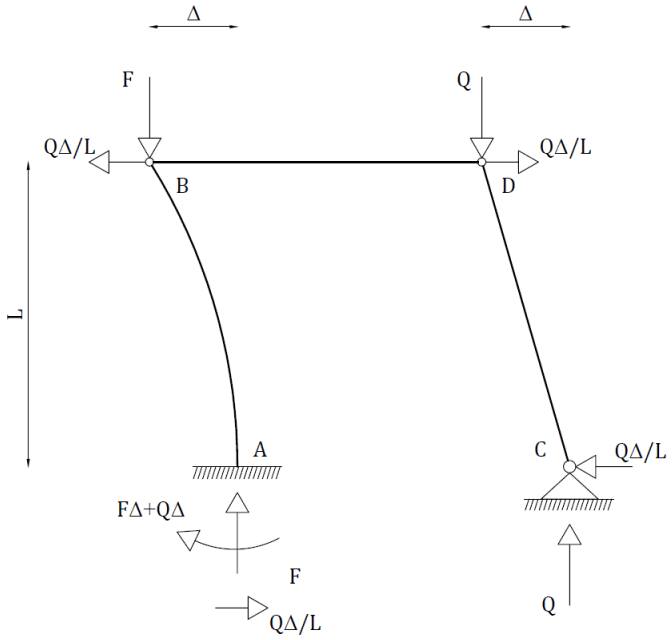

Figure 64: Equilibrium forces in stabilizing column (A-B) and leaning column (C-D) for Yura approach

To derive this factor, we will start with the American notation of the Euler buckling solution for a case with a leaning column load, given in equation (57):

$$F + Q = \frac{\pi^2 EI}{K_o^2 L^2} \tag{57}$$

Where K_o is the modified effective length factor which does not account for the leaning column. To include the leaning column effect in the effective length factor, equation (57) can be rewritten as the following:

$$F = \frac{\pi^2 EI}{K_n^2 L^2} \tag{58}$$

Where K_n in equation (58) is the modified effective length factor which does account for the leaning column effect. Loads F and Q in equation (57) and (58) needs to be replaced with the sum of loads F and Q (ΣF and ΣQ) in case of a frame with more than one leaning column and more than one restraining column. According to Geschwindner [1], it should be noted that this approach maintains the assumption that all restraining columns in a story buckle in a sway mode simultaneously. Solving $\frac{K_n^2}{K_o^2} = \frac{\Sigma F + \Sigma Q}{\Sigma F}$ gives:

$$K_n = K_o \sqrt{\frac{\sum F + \sum Q}{\sum F}} \tag{59}$$

Factors K_o and K_n are American notations for the modified effective length factor, where K_n takes into account the leaning column load, and K_o does not. In the Eurocode the notation for the modified effective length factor is β, and in the case of the nomogram, it does not take into account the leaning column load. This is already experienced in section 6.7.1.1. and for that reason, we now call $K_o = \beta_{nomogram}$, where $\beta_{nomogram}$ is the modified effective length factor obtained from section 6.7.1.1. Substituting the above in (59) gives:

$$\beta_{Yura} = \beta_{nomogram} \cdot \sqrt{\frac{\sum F + \sum Q}{\sum F}} \tag{60}$$

Applying equation (60) for the frame gives:

$\beta_{nomogram} =$ 2.3279, according to section 6.7.1.1.

$$\frac{\sum F + \sum Q}{\sum F} = \frac{2+1}{2} = \frac{3}{2}$$

$$\beta_{Yura} = 2.3279 \cdot \sqrt{\frac{3}{2}} = 2.85$$

Solving the above gives the effective length factor $\beta_{Yura} = 2.85$, gives $L_{cr} = 2.85 \cdot 5000 =$ 14255 mm. When we carry out again the equations for the ultimate resistance load as given in section 6.5 with $L_{cr} =$ 14255 mm as input, the following ultimate resistance loads are obtained:

$N_{ult,DR,EC,Yura} =$ 1217.6 kN

Once again only the EN 1993-1-1 design rule is considered since the leaning column effect is already taken into account in L_{cr}. The new ultimate resistance load is shown in Figure 65.

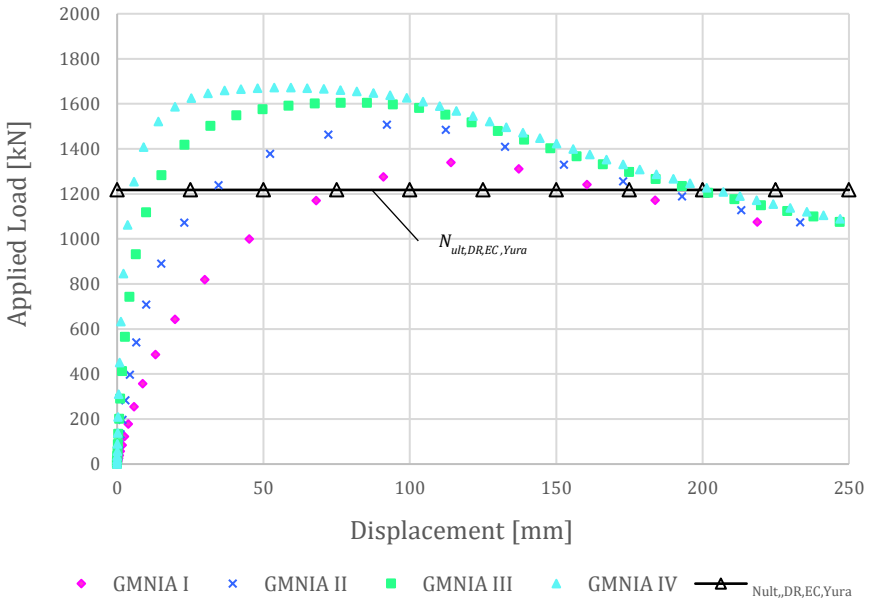

Figure 65: Ultimate resistance load where L_{cr} is determined with the Yura approach

6.7.1.4 Comparison

In section 6.7.1.1, the ultimate resistance loads are determined which in practice would be found by the engineers. It can be seen that $N_{ult,DR,i,nomogram}$ are way higher than $N_{ult,DR,i,LBA}$. These higher results lead to less conservative results. Table 12 shows that the difference for $N_{ult,DR,NEN,nomogram}$ and $N_{ult,DR,EC,nomogram}$ are 27.93% and 28.44% respectively compared to the results obtained with the LBA. If we compare $N_{ult,DR,NEN,nomogram}$ to the various analyses, it still covers the ultimate loads of GMNIA II, III, and IV, as can be seen in Table 13, where the positive percentages indicate that the design-resistance load covers that type of analysis. Section 6.6.1 explained that the results of GMNIA III and GMNIA IV are assumed as closest to reality and that GMNIA I and GMNIA II give

somewhat conservative results. This means that the results of the NEN 6771 are safe due to the bigger margin compared to GMNIA III and GMNIA IV. When we compare $N_{ult,DR,EC,nomogram}$ to the various analyses, the result is almost equal to GMNIA III and GMNIA IV, namely 1.52% and 5.78% respectively (Table 13). This indicates that the results of the EN 1993-1-1 for this frame is safe, but with a small margin.

When the extended American nomogram equation of Geschwindner [1] is considered (section 6.7.1.2) it results in a lower, and more realistic, ultimate resistance load compared to $N_{ult,DR,EC,nomogram}$. This leads to more conservative results, where $N_{ult,DR,EC,l.F.\ G}$ has a margin of 15.96% and 20.82% from GMNIA III and GMNIA IV respectively (Table 13). But when we compare the results to the most realistic one, $N_{ult,DR,EC,l.F.\ G}$ still differ 12.45% from $N_{ult,DR,EC,LBA}$ (Table 12).

The Yura approach makes use of the same equilibrium consideration as the solutions for F_{tot} in the NEN 6771. But instead of using the equilibrium approach in the load side of the equation, Yura used it in the derivations of L_{cr}. This different approach leads to different but more accurate results (6.7.1.3). With the use of the Yura approach, $N_{ult,DR,EC,Yura}$ has a margin of 31.78% and 37.31% from GMNIA III and GMNIA IV respectively (Table 13), which is almost the same as the results obtained with the LBA. The high accuracy of the Yura approach is also confirmed by the fact that $N_{ult,DR,EC,Yura}$ only differ -1.06% from $N_{ult,DR,EC,LBA}$ (Table 12).

Since the ultimate resistance loads of the NEN 6771 and the modified EN 1993-1-1 takes into account the leaning column effect twice, the result is considered useless. For that reason, this result in Table 12 has a strikethrough.

Table 12: Results of the various ultimate resistance loads and compared to the most realistic input, where the strikethrough indicates a useless result due to taking the leaning column effect into account twice

	Ultimate DR load (N_{ult}) in kN		Error compared to LBA in %	
	$N_{ult,DR,NEN}$ & $N_{ult,DR,modEC}$	$N_{ult,DR,EC}$	% $N_{ult,DR,NEN}$ & $N_{ult,DR,modEC}$	% $N_{ult,DR,EC}$
LBA with leaning column	~~1131.6 kN~~	1230.6 kN	-	0.00 %
Nomogram	1446.6 kN	1580.6 kN	27.93 %	28.44 %
Geschwindner	-	1383.8 kN	-	12.45 %
Yura	-	1217.6 kN	-	-1.06 %

Table 13: Differences between the ultimate loads (horizontal) and the ultimate resistance loads (vertical)

Difference $\frac{F_{ult}-N_{ult}}{N_{ult}}$		Ultimate load (F_{ult}) in kN			
		$F_{ult,GMNIA\ I}$	$F_{ult,GMNIA\ II}$	$F_{ult,GMNIA\ III}$	$F_{ult,GMNIA\ IV}$
Ultimate DR load (N_{ult}) in kN		1338.3 kN	1507.0 kN	1604.6 kN	1671.9 kN
$N_{ult,DR,EC,LBA}$	1230.6 kN	8.75%	22.46%	30.39%	35.86%
$N_{ult,DR,NEN,nomogram}$ & $N_{ult,DR,modEC,nomogram}$	1446.6 kN	-7.55%	4.10%	10.85%	15.48%
$N_{ult,DR,EC,nomogram}$	1580.6 kN	-15.33%	-4.66%	1.52%	5.78%
$N_{ult,DR,EC,L.F.\ G.}$	1383.8 kN	-3.29%	8.90%	15.96%	20.82%
$N_{ult,DR,EC,Yura}$	1217.6 kN	9.91%	23.77%	31.78%	37.31%

6.8 CONCLUSIONS

GMNIA III and GMNIA IV were on the forehand assumed to reflect reality in the best way due to realistic modeling of imperfection shapes and realistic residual stresses. The difference between GMNIA III and GMNIA IV is confirmed by the statement of Shayan et al. [9], which is that the use of only the first critical eigenmode (which is the case for GMNIA III) leads to conservative results. The results of GMNIA I and GMNIA II are conservative due to the equivalent imperfections that are present in the design rules for imperfections of the EN 1993-1-1 Clause 5.3.2(3) and 5.3.2(11). Due to the above, GMNIA IV will be used as the ultimate load that the frame can carry.

The modified EC1991-1-1 design rule gives the same result as the NEN 6771, as intended. The combination of the NEN 6771 (and modified EN 1993-1-1) and the nomogram is not considered anymore since this takes into account the leaning column effect twice. With the most realistic way of determining L_{cr}, the LBA with the leaning column, the ultimate resistance load from the current EN 1993-1-1 cover the ultimate load obtained with GMNIA IV with a high conservatism margin (35.9%). This means that the leaning column effect is taken into account in the LBA. However, in practice, a more common way of determining L_{cr} is used, namely the nomogram in the Dutch National Annex of the EN 1993-1-1, where the leaning column effect is not present in the buckling length (equation (49)). When the nomogram is combined with the NEN 6771 (and modified EN 1993-1-1) and the current EN 1993-1-1 design rule, higher ultimate resistance loads are found, roughly 28% higher than the LBA. When these ultimate resistance loads are compared to the ultimate load obtained with GMNIA IV, conservatism margins of 15.48% (NEN&modEN) and 5.78% (current EN) are found. This means that the design rules combined with the nomogram lead to safe results, but only with a small conservatism margin, where the margins decreased almost 20% compared to the LBA.

The decrease of 20% suggests that there can be a lot gained with including the leaning column effect in the buckling length. In the literature, there have been searched for practical methods to include the leaning column in the buckling length. This has led to two methods, the extended American nomogram equation of Geschwindner and the equilibrium approach of Yura. The current EN 1993-1-1 design rule in combination with the extended nomogram equation of Geschwindner lowers the ultimate resistance load but still differs 12.5% with the LBA, meaning that the approach is not accurate. The Yura approach in combination with the EN 1993-1-1, however, gives results that are close to the LBA, with only a difference of -1.06%. The use of the Yura approach leads to a conservatism margin of 37.31%, which is almost the same margin obtained with the LBA.

All these conservatism margins as discussed above can be grouped into three different types and translated into three unity check graphs. The three different types are:

- The results where the leaning column effect is included in the load-side of the design rule equation (NEN 6771 & modified EN 1993-1-1 in combination with the nomogram)
- The results where the leaning column effect is not included (EN 1993-1-1 in combination with the nomogram)
- The results where the leaning column effect is included in the buckling length (EN 1993-1-1 in combination with the LBA, Geschwinderner, and Yura)

The unity checks are obtained by dividing the ultimate resistance loads ($N_{ult,i,j}$) with the ultimate load that the frame can carry according to GMNIA IV ($F_{ult,GMNIA\ IV}$), so are presenting the ratio between N_{ult} and F_{ult}. The unity check graphs are shown in Figure 66 and Figure 67, where the determination of the values is shown in the graph. These graphs visualize the conservatism margin whether they are safe or unsafe, where higher unity checks lead to lower conservatism margins. For the frame considered in this chapter, the margins are all on the safe side.

As already discussed before, the modified EC1991-1-1 design rule gives the same result as the NEN 6771. This means that converting the NEN 6771 into a modified EN 1993-1-1 equation, and therefore a clearer presentation of the leaning column effect, is possible.

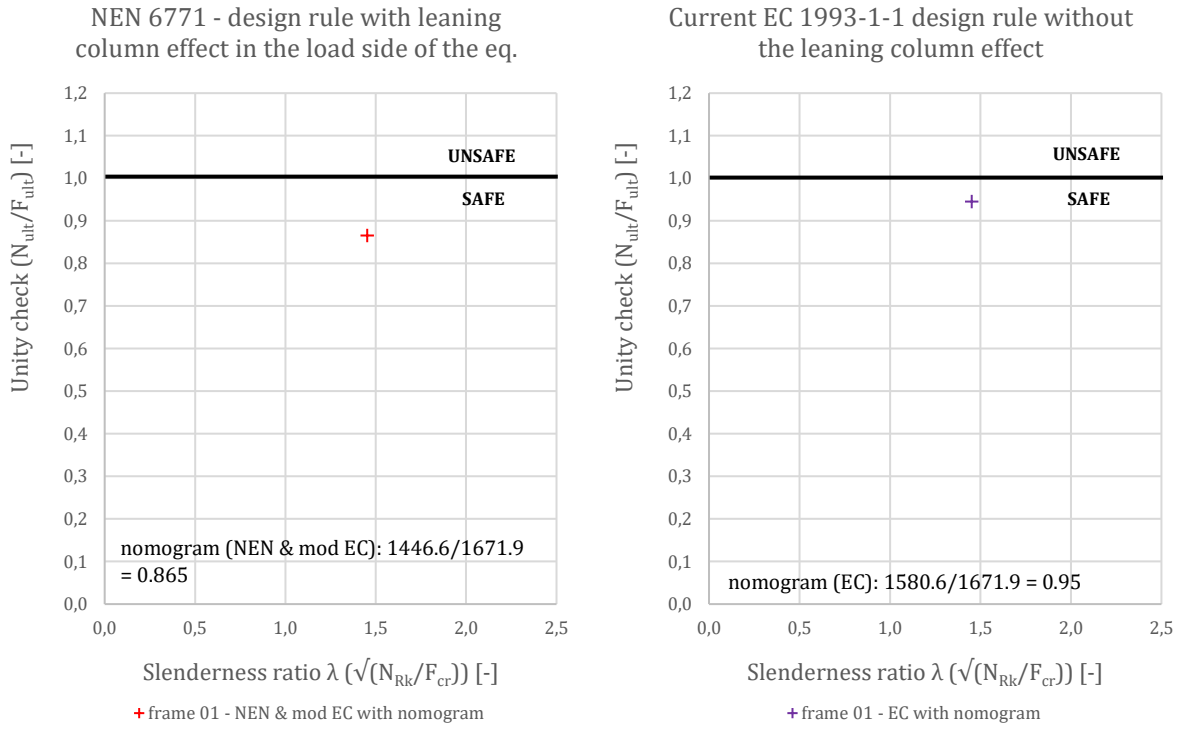

Figure 66: Unity check graphs for the NEN 6771& mod EN 1993-1-1 (left) and current EN 1993-1-1 (right)

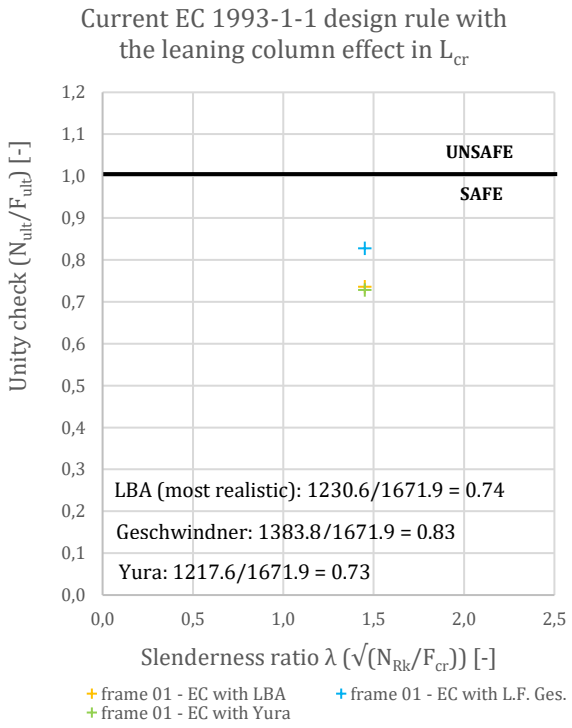

Figure 67: Unity check graph for the EN 1993-1-1 in combination with the LBA and Yura

7 PARAMETRIC STUDY

7.1 INTRODUCTION

In chapter 6, a case study is elaborated for one sway frame that is sensitive to the leaning column effect, loaded with only a small leaning column load and a horizontal load due to imperfections of the columns. In this chapter, the frame configuration will be analyzed with different dimensions. These parameters will be discussed in section 7.2. This is to study the leaning column effect for a range of simple cases that are the most vulnerable for the leaning column effect, but only with small leaning column and horizontal loads. The frame configurations as already described in the research scope (section 1.4) will also be studied. Each frame configuration will be analyzed fifteen times. These different parameters and frame configurations aim to cover a large range of leaning column problems. In the upcoming sections, a more in-depth description will be given for each frame configuration and the corresponding parameters. The parametric study has yet to prove whether all those margins as discussed in section 6.8 are safe for all cases.

In sections 7.2 and 7.3 the various parameters and frame configurations will be discussed. The input for and from these sections is given in appendix B. The most important inputs from appendix B will be given in table format per frame. In these tables, the abbreviations will be used as already used in the previous chapters. Value Δ is the imperfection magnitude to scale the normalized matrix of displacements of the first out-of-plane eigenmode in GMNIA III, values A_1, A_2, and A_3 are the imperfection magnitudes to scale the normalized matrix of displacements of the first three eigenmodes for GMNIA IV. For GMNIA IV, up to three eigenmodes will be used, as discussed in section 3.3.4. However, section 6.4.5 already showed that not for all cases three side-sway eigenmodes will be found, while only side-sway eigenmodes are desired to obtain the ultimate load that the frame can carry. In the upcoming frame configurations a variation of 1, 2, or 3 critical eigenmodes for GMNIA IV are used, depending on the stiffness of the total frame. When $A_3 = 0$ or $A_3 = A_2 = 0$ it indicates that only 2 or 1 eigenmodes respectively are used. Section 7.4 shows the results of the parametric study in table format. Behind the results of the ultimate design resistance loads goes a large calculation sheet, which is given in appendix C. The scripts that are used to carry out the parametric study in Abaqus are given in appendix D.

In this chapter, the results with the extended nomogram equation of Geschwindner are not considered anymore, due to the lack of accuracy.

7.2 PARAMETERS

As mentioned before, various frame configurations will be analyzed with various parameters, all aiming to cover a large range of leaning column problems. The various parameters that will be considered are based on different stiffness and slenderness ratios. It is expected that how higher the slenderness and stiffness ratio, how higher the influence of the leaning column effect. The stiffness ratio is defined by $C = \frac{I_{cln}/L_{cln}}{I_{bm}/L_{bm}}$, where I_{cln} and I_{bm} are the second moment of inertia of the column and beam respectively, and where L_{cln} and L_{bm} are the lengths of the column and beam respectively. The stiffness ratio will be pinned on values 1, 1.5, and 2. In ratio C only L_{bm} will be variable, meaning that for a frame with the same cross-section for column and beam, the length times x1.5 and x2 already lead to stiffness ratios 1.5 and 2. However, theoretically, this ratio difference can also indicate different cross-sections (I_i) between column and beam, which can lead to less stiff structures.

The slenderness ratio is defined by $\bar{\lambda} = \sqrt{\frac{N_{Rk}}{F_{cr}}}$, where $F_{cr} = \frac{\pi^2 EI}{L_{cr}^2}$ as given in equation (4) and $N_{Rk} = A \cdot f_y$. For obtaining different slenderness ratios, the frame is performed with a different cross-section of the column. This gives that the cross-section properties in the equations will be variable, which are *A* and *EI*. The smaller the cross-section over the height, the bigger the slenderness ratio. Please note that the same cross-section is used for the beam.

The L_{cr} of a structure depends on the stiffness of a structure, so depends on ratio C. This means that the frames with a different C also have a slightly different $\bar{\lambda}$. For determining $\bar{\lambda}$, the most realistic parameters will be used, and that is the α_{cr} from the LBA. Value α_{cr} from the LBA includes the leaning column effect and this leads to a higher slenderness ratio. These higher slenderness ratios will be used to plot all the results. In practice these slenderness ratios $\bar{\lambda}$ will not be found due to the lack of the leaning column effect in the nomogram.

The frame that is elaborated in chapter 6 is again considered in the parametric study and performed with 1.5x and 2x the width. The other twelve frames are based on a height and width of 3000 mm. The corresponding cross-sections and ratios are given in Table 14.

Table 14: Visualization of the frames that are obtained with the variable parameters

	b=5000, C=1	*b*=7500, C=1.5	*b*=10000, C=2
HEA300 $\bar{\lambda}$ varies	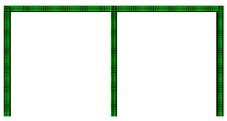	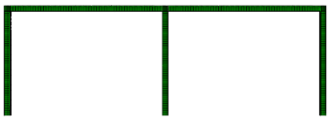	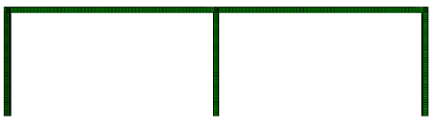
	b=3000, C=1	*b*=4500, C=1.5	*b*=6000, C=2
HEA120 $\bar{\lambda}$ varies			
HEA160 $\bar{\lambda}$ varies	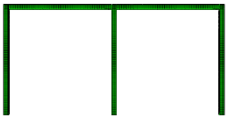	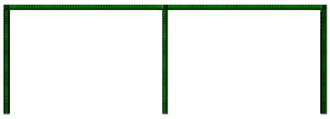	
HEA220 $\bar{\lambda}$ varies	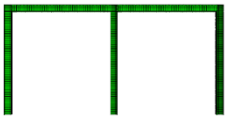	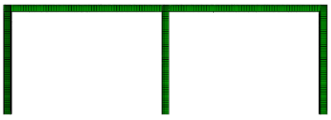	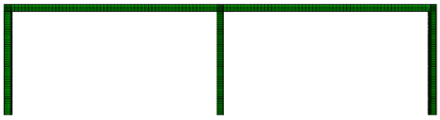
HEA280 $\bar{\lambda}$ varies	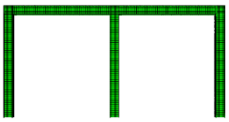		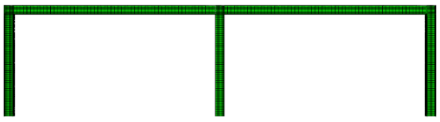

7.3 FRAME CONFIGURATION

7.3.1 Frame A

The first frame configuration that is elaborated is already explained in section 6.1 and shortly introduced in section 7.1. It is a sway frame that is sensitive to the leaning column effect, loaded with a vertical leaning column load $Q = F$, and a horizontal load of $2\phi F + \phi Q$, as shown in Figure 68, where ϕ (equation 44) is the slope of the structure due to imperfections.

Table 15 gives the corresponding parameters and input-values when combining the various fifteen frames from section 7.2 with frame configuration A. The parameters and input-values in the table are the most interesting regarding F_{ult} and N_{ult}. The determination of the values for frame

01 is already explained in detail in sections 6.4 and 6.5. The slenderness ratio varies from 0.96 to 2.56. For all corresponding values see appendix B.

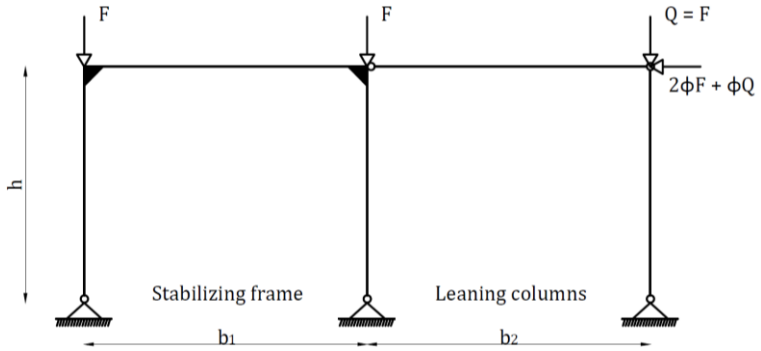

Figure 68: Frame A – Pin-ended moment-resisting frame with a hinged leaning column

Table 15: Input values for frame A to carry out GMNIA III and GMNIA IV

	H-section	h	b_1=b_2	F	Q	H	φ	λ	C	α_{cr}	$L_{cr,LBA}$	$L_{cr,nomogram}$	$L_{cr,Yura}$	Δ	A_1	A_2	A_3
	[-]	[mm]	[mm]	[kN]	[kN]	[kN]	[-]	[-]	[-]	[-]	[mm]	[mm]	[mm]	[mm]	[-]	[-]	[-]
frame 01	HEA300	5000	5000	1000	1000	0	3.65E-03	1.45	1	1.79	14148	11639	14255	12.93	-6.12	1.71	0
frame 02	HEA300	5000	7500	1000	1000	0	3.65E-03	1.55	1.5	1.58	15073	12421	15213	13.37	-6.12	1.71	0
frame 03	HEA300	5000	10000	1000	1000	0	3.65E-03	1.64	2	1.40	15991	13173	16133	13.75	-6.12	1.71	0
frame A1	HEA120	3000	3000	1000	1000	0	4.08E-03	2.25	1	0.17	8432	6984	8553	7.73	-3.44	0.89	1.19
frame A2	HEA120	3000	4500	1000	1000	0	4.08E-03	2.41	1.5	0.15	9014	7453	9128	8.01	-3.44	0.89	1.19
frame A3	HEA120	3000	6000	1000	1000	0	4.08E-03	2.56	2	0.13	9576	7904	9680	8.24	-3.44	0.89	1.19
frame A4	HEA160	3000	3000	1000	1000	0	4.08E-03	1.68	1	0.46	8458	6984	8553	7.74	-3.67	1.02	0
frame A5	HEA160	3000	4500	1000	1000	0	4.08E-03	1.80	1.5	0.41	9027	7453	9128	8.01	-3.67	1.02	0
frame A6	HEA160	3000	6000	1000	1000	0	4.08E-03	1.91	2	0.36	9583	7904	9680	8.24	-3.67	1.02	0
frame A7	HEA220	3000	3000	1000	1000	0	4.08E-03	1.22	1	1.47	8546	6984	8553	7.79	-3.68	0	0
frame A8	HEA220	3000	4500	1000	1000	0	4.08E-03	1.30	1.5	1.30	9083	7453	9128	8.04	-3.68	0	0
frame A9	HEA220	3000	6000	1000	1000	0	4.08E-03	1.37	2	1.16	9624	7904	9680	8.26	-3.68	0	0
frame A10	HEA280	3000	3000	1000	1000	0	4.08E-03	0.96	1	3.58	8673	6984	8553	7.85	-3.68	0	0
frame A11	HEA280	3000	4500	1000	1000	0	4.08E-03	1.01	1.5	3.21	9167	7453	9128	8.07	-3.68	0	0
frame A12	HEA280	3000	6000	1000	1000	0	4.08E-03	1.07	2	2.87	9687	7904	9680	8.28	-3.68	0	0

7.3.2 Frame A-NL

Frame A-NL is a sway frame without the leaning column. This frame configuration is performed to see whether the conservatism margin between the design rules and GMNIA IV is comparable to the other frame configurations, so for validation reasons. This means that the leaning column load is reduced to 0, so Q = 0, leading to a horizontal load of $2\phi F$, as shown in Figure 69. The most interesting inputs for frame A-NL are given in Table 16. The slenderness ratio varies from 0.79 to 2.11 and differs slightly from frame A due to the absence of the leaning column effect. For all corresponding values see appendix B.

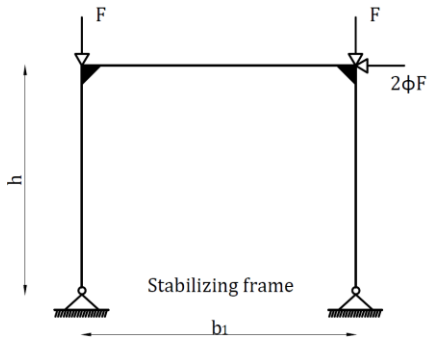

Figure 69: Frame A-NL – pin-ended moment-resisting frame without a leaning column

Table 16: Input values for frame A-NL to carry out GMNIA III and GMNIA IV

	H-section	h	b_1=b_2	F	Q	H	φ	λ	C	α_{cr}	$L_{cr,LBA}$	$L_{cr,nomogram}$	$L_{cr,Yura}$	Δ	A_1	A_2	A_3
	[-]	[mm]	[mm]	[kN]	[kN]	[kN]	[-]	[-]	[-]	[-]	[mm]	[mm]	[mm]	[mm]	[-]	[-]	[-]
frame 01-NL	HEA300	5000	5000	1000	0	0	3.65E-03	1.20	1	2.60	11736	11639	11639	11.48	5.73	1.48	1.99
frame 02-NL	HEA300	5000	7500	1000	0	0	3.65E-03	1.28	1.5	2.31	12456	12421	12421	11.97	5.73	1.48	1.99
frame 03-NL	HEA300	5000	10000	1000	0	0	3.65E-03	1.35	2	2.06	13178	13173	13173	12.41	5.73	1.48	1.99
frame A1-NL	HEA120	3000	3000	1000	0	0	4.08E-03	1.87	1	0.25	6996	6984	6984	6.85	3.44	0.89	1.19
frame A2-NL	HEA120	3000	4500	1000	0	0	4.08E-03	1.99	1.5	0.22	7449	7453	7453	7.17	3.44	0.89	1.19
frame A3-NL	HEA120	3000	6000	1000	0	0	4.08E-03	2.11	2	0.19	7892	7904	7904	7.44	3.44	0.89	1.19
frame A4-NL	HEA160	3000	3000	1000	0	0	4.08E-03	1.40	1	0.67	7017	6984	6984	6.87	3.44	0.89	1.19
frame A5-NL	HEA160	3000	4500	1000	0	0	4.08E-03	1.48	1.5	0.59	7460	7453	7453	7.17	3.44	0.89	1.19
frame A6-NL	HEA160	3000	6000	1000	0	0	4.08E-03	1.57	2	0.53	7898	7904	7904	7.44	3.44	0.89	1.19
frame A7-NL	HEA220	3000	3000	1000	0	0	4.08E-03	1.01	1	2.14	7087	6984	6984	6.92	3.44	0.89	1.19
frame A8-NL	HEA220	3000	4500	1000	0	0	4.08E-03	1.07	1.5	1.91	7505	7453	7453	7.20	3.44	0.89	1.19
frame A9-NL	HEA220	3000	6000	1000	0	0	4.08E-03	1.13	2	1.71	7930	7904	7904	7.46	3.44	0.89	1.19
frame A10-NL	HEA280	3000	3000	1000	0	0	4.08E-03	0.79	1	5.21	7188	6984	6984	6.99	3.67	1.02	0
frame A11-NL	HEA280	3000	4500	1000	0	0	4.08E-03	0.84	1.5	4.70	7572	7453	7453	7.25	3.67	1.02	0
frame A12-NL	HEA280	3000	6000	1000	0	0	4.08E-03	0.88	2	4.23	7981	7904	7904	7.49	3.67	1.02	0

7.3.3 Frame A-V

Frame A-V is similar to frame A, but now with an increased leaning column load of a factor x10. This is performed to study the same frame as frame A, but now with an increased leaning column load, and therefore also higher slenderness ratio. The frame configuration is shown in Figure 70. The leaning column load is increased to $10F$, so $Q = 10F$, where the $10F$ has to represent a row of ten leaning columns. The horizontal load is again $2\phi F + \phi Q$. To avoid that the buckling of the leaning column is the governing failure mode, the leaning column is strengthened and stiffened with $10f_{y,d,}$ and $10EI$. The most interesting inputs for frame A-V are given in Table 17. The slenderness ratio varies from 1.88 to 5.05, which is a large increase compared to frame A, and therefore covers a larger range of leaning column problems. For all corresponding values see appendix B.

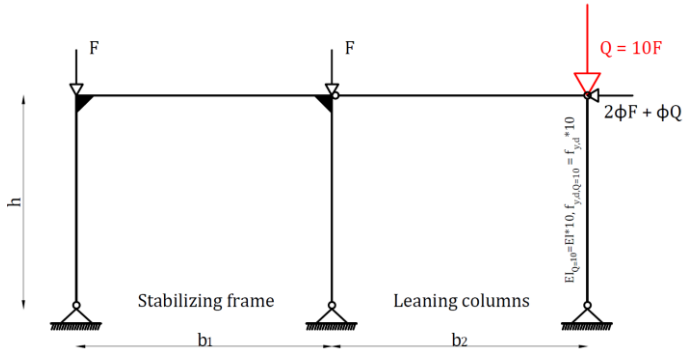

Figure 70: Frame A-V – pin-ended moment-resisting frame with a heavily loaded, stiffer, and stronger, leaning column

Table 17: Input values for frame A-V to carry out GMNIA III and GMNIA IV

	H-section	h	$b_1=b_2$	F	Q	H	φ	λ	C	α_{cr}	$L_{cr,LBA}$	$L_{cr,nomogram}$	$L_{cr,Yura}$	Δ	A_1	A_2	A_3
	[-]	[mm]	[mm]	[kN]	[kN]	[kN]	[-]	[-]	[-]	[-]	[mm]	[mm]	[mm]	[mm]	[-]	[-]	[-]
frame 01-V	HEA300	5000	5000	1000	10000	0	3.65E-03	2.84	1	0.47	27681	11639	28511	16.39	6.12	-1.71	0
frame 02-V	HEA300	5000	7500	1000	10000	0	3.65E-03	3.04	1.5	0.41	29663	12421	30426	16.63	6.12	-1.71	0
frame 03-V	HEA300	5000	10000	1000	10000	0	3.65E-03	3.24	2	0.36	31599	13173	32267	16.84	6.12	-1.71	0
frame A1-V	HEA120	3000	3000	1000	10000	0	4.08E-03	4.40	1	0.04	16482	6984	17106	9.82	3.44	-0.89	-1.19
frame A2-V	HEA120	3000	4500	1000	10000	0	4.08E-03	4.73	1.5	0.04	17725	7453	18256	9.97	3.44	-0.89	-1.19
frame A3-V	HEA120	3000	6000	1000	10000	0	4.08E-03	5.05	2	0.03	18908	7904	19360	10.10	3.44	-0.89	-1.19
frame A4-V	HEA160	3000	3000	1000	10000	0	4.08E-03	3.29	1	0.12	16542	6984	17106	9.82	3.67	-1.02	0
frame A5-V	HEA160	3000	4500	1000	10000	0	4.08E-03	3.53	1.5	0.10	17758	7453	18256	9.97	3.67	-1.02	0
frame A6-V	HEA160	3000	6000	1000	10000	0	4.08E-03	3.77	2	0.09	18931	7904	19360	10.10	3.67	-1.02	0
frame A7-V	HEA220	3000	3000	1000	10000	0	4.08E-03	2.39	1	0.38	16734	6984	17106	9.85	3.68	0	0
frame A8-V	HEA220	3000	4500	1000	10000	0	4.08E-03	2.55	1.5	0.34	17885	7453	18256	9.99	3.68	0	0
frame A9-V	HEA220	3000	6000	1000	10000	0	4.08E-03	2.71	2	0.30	19029	7904	19360	10.11	3.68	0	0
frame A10-V	HEA280	3000	3000	1000	10000	0	4.08E-03	1.88	1	0.93	17009	6984	17106	9.88	3.68	0	0
frame A11-V	HEA280	3000	4500	1000	10000	0	4.08E-03	1.99	1.5	0.82	18074	7453	18256	10.01	3.68	0	0
frame A12-V	HEA280	3000	6000	1000	10000	0	4.08E-03	2.12	2	0.73	19179	7904	19360	10.12	3.68	0	0

7.3.4 Frame A-H, A-NLH, and A-VH

Additionally, frame A, frame A-NL, and frame A-V are extended with an additional horizontal load, to see the influence of a larger lateral displacement. This is interesting since, in the case of the design rules, the additional horizontal load only leads to a higher M_{Ed}, but in the case of the GMNIA also to larger lateral displacements, leading to a higher leaning column effect. The horizontal load H is based on a wind load of 1 kN/m², with an area of $h*b$ ($b=b_1=b_2$). This means that the horizontal load is different for some cases since the width is a variable. The additional horizontal loads are shown in red in Figure 71, Figure 72, and Figure 73. The most interesting inputs are given in Table 18, Table 19, and Table 20. Here it can be seen that the input is the same as for frame A, frame A-NL, and Frame A-V, except load H. For all corresponding values see appendix B.

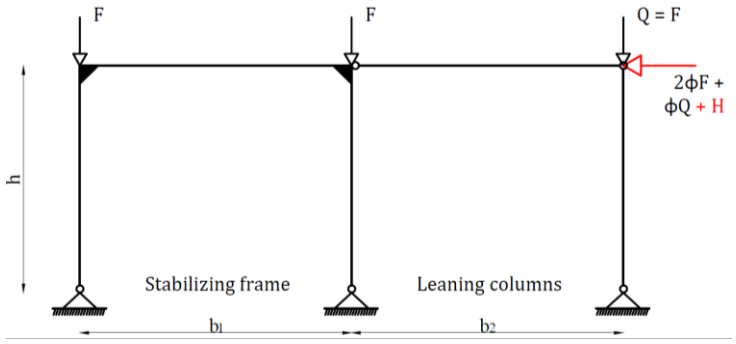

Figure 71: Frame A-H – pin-ended moment-resisting frame with a leaning column and additional horizontal wind load

Table 18: Input values for frame A-H to carry out GMNIA III and GMNIA IV

	H-section	h	$b_1=b_2$	F	Q	H	φ	λ	C	α_{cr}	$L_{cr,LBA}$	$L_{cr,nomogram}$	$L_{cr,Yura}$	Δ	A_1	A_2	A_3
	[-]	[mm]	[mm]	[kN]	[kN]	[kN]	[-]	[-]	[-]	[-]	[mm]	[mm]	[mm]	[mm]	[-]	[-]	[-]
frame 01-H	HEA300	5000	5000	1000	1000	12.5	3.65E-03	1.45	1	1.79	14148	11639	14255	-12.93	-6.12	1.71	0
frame 02-H	HEA300	5000	7500	1000	1000	18.75	3.65E-03	1.55	1.5	1.58	15073	12421	15213	-13.37	-6.12	1.71	0
frame 03-H	HEA300	5000	10000	1000	1000	25	3.65E-03	1.64	2	1.40	15991	13173	16133	-13.75	-6.12	1.71	0
frame A1-H	HEA120	3000	3000	1000	1000	4.5	4.08E-03	2.25	1	0.17	8432	6984	8553	-7.73	-3.44	0.89	-1.19
frame A2-H	HEA120	3000	4500	1000	1000	6.75	4.08E-03	2.41	1.5	0.15	9014	7453	9128	-8.01	-3.44	0.89	-1.19
frame A3-H	HEA120	3000	6000	1000	1000	9	4.08E-03	2.56	2	0.13	9576	7904	9680	-8.24	-3.44	0.89	-1.19
frame A4-H	HEA160	3000	3000	1000	1000	4.5	4.08E-03	1.68	1	0.46	8458	6984	8553	-7.74	-3.67	1.02	0
frame A5-H	HEA160	3000	4500	1000	1000	6.75	4.08E-03	1.80	1.5	0.41	9027	7453	9128	-8.01	-3.67	1.02	0
frame A6-H	HEA160	3000	6000	1000	1000	9	4.08E-03	1.91	2	0.36	9583	7904	9680	-8.24	-3.67	1.02	0
frame A7-H	HEA220	3000	3000	1000	1000	4.5	4.08E-03	1.22	1	1.47	8546	6984	8553	-7.79	-3.68	0	0
frame A8-H	HEA220	3000	4500	1000	1000	6.75	4.08E-03	1.30	1.5	1.30	9083	7453	9128	-8.04	-3.68	0	0
frame A9-H	HEA220	3000	6000	1000	1000	9	4.08E-03	1.37	2	1.16	9624	7904	9680	-8.26	-3.68	0	0
frame A10-H	HEA280	3000	3000	1000	1000	4.5	4.08E-03	0.96	1	3.58	8673	6984	8553	-7.85	-3.68	0	0
frame A11-H	HEA280	3000	4500	1000	1000	6.75	4.08E-03	1.01	1.5	3.21	9167	7453	9128	-8.07	-3.68	0	0
frame A12-H	HEA280	3000	6000	1000	1000	9	4.08E-03	1.07	2	2.87	9687	7904	9680	-8.28	-3.68	0	0

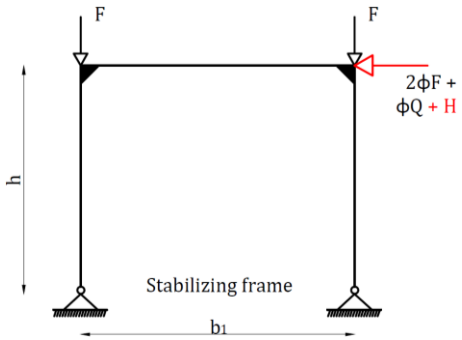

Figure 72: Frame A-NLH: pin-ended moment-resisting frame without a leaning column and with an additional horizontal wind load

Table 19: Input values for frame A-NLH to carry out GMNIA III and GMNIA IV

	H-section	h	$b_1=b_2$	F	Q	H	φ	λ	C	α_{cr}	$L_{cr,LBA}$	$L_{cr,nomogram}$	$L_{cr,Yura}$	Δ	A_1	A_2	A_3
	[-]	[mm]	[mm]	[kN]	[kN]	[kN]	[-]	[-]	[-]	[-]	[mm]	[mm]	[mm]	[mm]	[-]	[-]	[-]
frame 01-NLH	HEA300	5000	5000	1000	0	12.5	3.65E-03	1.20	1	2.60	11736	11639	11639	-11.48	-5.73	-1.48	-1.99
frame 02-NLH	HEA300	5000	7500	1000	0	18.75	3.65E-03	1.28	1.5	2.31	12456	12421	12421	-11.97	-5.73	-1.48	-1.99
frame 03-NLH	HEA300	5000	10000	1000	0	25	3.65E-03	1.35	2	2.06	13178	13173	13173	-12.41	-5.73	-1.48	-1.99
frame A1-NLH	HEA120	3000	3000	1000	0	4.5	4.08E-03	1.87	1	0.25	6996	6984	6984	-6.85	-3.44	-0.89	-1.19
frame A2-NLH	HEA120	3000	4500	1000	0	6.75	4.08E-03	1.99	1.5	0.22	7449	7453	7453	-7.17	-3.44	-0.89	-1.19
frame A3-NLH	HEA120	3000	6000	1000	0	9	4.08E-03	2.11	2	0.19	7892	7904	7904	-7.44	-3.44	-0.89	-1.19
frame A4-NLH	HEA160	3000	3000	1000	0	4.5	4.08E-03	1.40	1	0.67	7017	6984	6984	-6.87	-3.44	-0.89	-1.19
frame A5-NLH	HEA160	3000	4500	1000	0	6.75	4.08E-03	1.48	1.5	0.59	7460	7453	7453	-7.17	-3.44	-0.89	-1.19
frame A6-NLH	HEA160	3000	6000	1000	0	9	4.08E-03	1.57	2	0.53	7898	7904	7904	-7.44	-3.44	-0.89	-1.19
frame A7-NLH	HEA220	3000	3000	1000	0	4.5	4.08E-03	1.01	1	2.14	7087	6984	6984	-6.92	-3.44	-0.89	-1.19
frame A8-NLH	HEA220	3000	4500	1000	0	6.75	4.08E-03	1.07	1.5	1.91	7505	7453	7453	-7.20	-3.44	-0.89	-1.19
frame A9-NLH	HEA220	3000	6000	1000	0	9	4.08E-03	1.13	2	1.71	7930	7904	7904	-7.46	-3.44	-0.89	-1.19
frame A10-NLH	HEA280	3000	3000	1000	0	4.5	4.08E-03	0.79	1	5.21	7188	6984	6984	-6.99	-3.67	-1.02	0
frame A11-NLH	HEA280	3000	4500	1000	0	6.75	4.08E-03	0.84	1.5	4.70	7572	7453	7453	-7.25	-3.67	-1.02	0
frame A12-NLH	HEA280	3000	6000	1000	0	9	4.08E-03	0.88	2	4.23	7981	7904	7904	-7.49	-3.67	-1.02	0

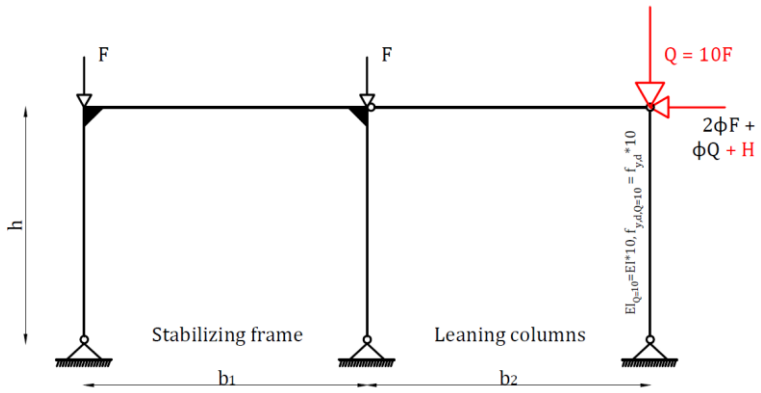

Figure 73: Frame A-VH – pin-ended moment resisting frame with a heavy loaded, stronger and stiffer, leaning column and additional horizontal wind load

Table 20: Input values for frame A-VH to carry out GMNIA III and GMNIA IV

	H-section	h	b_1=b_2	F	Q	H	φ	λ	C	α_{cr}	$L_{cr,LBA}$	$L_{cr,nomogram}$	$L_{cr,Yura}$	Δ	A_1	A_2	A_3
	[-]	[mm]	[mm]	[kN]	[kN]	[kN]	[-]	[-]	[-]	[-]	[mm]	[mm]	[mm]	[mm]	[-]	[-]	[-]
frame 01-VH	HEA300	5000	5000	1000	10000	12.5	3.65E-03	2.84	1	0.47	27681	11639	28511	-16.39	-6.12	1.71	0
frame 02-VH	HEA300	5000	7500	1000	10000	18.75	3.65E-03	3.04	1.5	0.41	29663	12421	30426	-16.63	-6.12	1.71	0
frame 03-VH	HEA300	5000	10000	1000	10000	25	3.65E-03	3.24	2	0.36	31599	13173	32267	-16.84	-6.12	1.71	0
frame A1-VH	HEA120	3000	3000	1000	10000	4.5	4.08E-03	4.40	1	0.04	16482	6984	17106	-9.82	-3.44	0.89	-1.19
frame A2-VH	HEA120	3000	4500	1000	10000	6.75	4.08E-03	4.73	1.5	0.04	17725	7453	18256	-9.97	-3.44	0.89	-1.19
frame A3-VH	HEA120	3000	6000	1000	10000	9	4.08E-03	5.05	2	0.03	18908	7904	19360	-10.10	-3.44	0.89	-1.19
frame A4-VH	HEA160	3000	3000	1000	10000	4.5	4.08E-03	3.29	1	0.12	16542	6984	17106	-9.82	-3.67	1.02	0
frame A5-VH	HEA160	3000	4500	1000	10000	6.75	4.08E-03	3.53	1.5	0.10	17758	7453	18256	-9.97	-3.67	1.02	0
frame A6-VH	HEA160	3000	6000	1000	10000	9	4.08E-03	3.77	2	0.09	18931	7904	19360	-10.10	-3.67	1.02	0
frame A7-VH	HEA220	3000	3000	1000	10000	4.5	4.08E-03	2.39	1	0.38	16734	6984	17106	-9.85	-3.68	0	0
frame A8-VH	HEA220	3000	4500	1000	10000	6.75	4.08E-03	2.55	1.5	0.34	17885	7453	18256	-9.99	-3.68	0	0
frame A9-VH	HEA220	3000	6000	1000	10000	9	4.08E-03	2.71	2	0.30	19029	7904	19360	-10.11	-3.68	0	0
frame A10-VH	HEA280	3000	3000	1000	10000	4.5	4.08E-03	1.88	1	0.93	17009	6984	17106	-9.88	-3.68	0	0
frame A11-VH	HEA280	3000	4500	1000	10000	6.75	4.08E-03	1.99	1.5	0.82	18074	7453	18256	-10.01	-3.68	0	0
frame A12-VH	HEA280	3000	6000	1000	10000	9	4.08E-03	2.12	2	0.73	19179	7904	19360	-10.12	-3.68	0	0

7.3.5 Frame B

To check what the leaning column effect does in a more stiff frame, a stiffer mechanical scheme is considered. This frame configuration is called Frame B and is shown in Figure 74, where the bottom ends of the column are clamped and marked in red. For this different mechanical scheme, the buckling length reduces, so a lower slenderness ratio will be obtained. Besides the lower slenderness ratio, this configuration did not lead to any interesting results. Therefore frame B is only performed with a small leaning column load. The parameters and input-values are given in Table 21. For all corresponding values see appendix B. The slenderness ratio varies from 0.49 to 1.24.

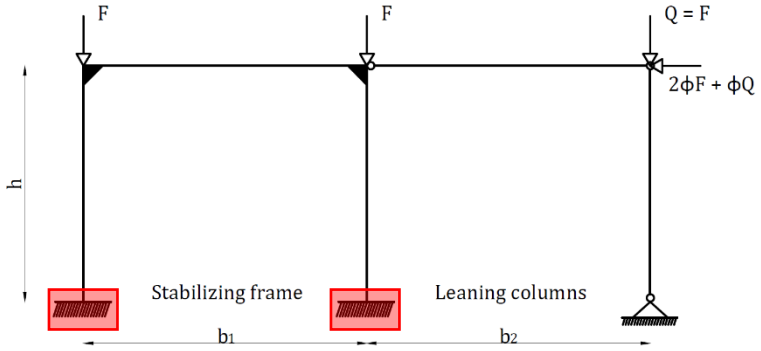

Figure 74: Clamped moment-resisting frame with a hinge-connected leaning column

Table 21: Input values for frame B to carry out GMNIA III and GMNIA IV

	H-section	h	b_1=b_2	F	Q	H	φ	λ	C	α_{cr}	$L_{cr,LBA}$	$L_{cr,nomogram}$	$L_{cr,Yura}$	Δ	A_1	A_2	A_3
	[-]	[mm]	[mm]	[kN]	[kN]	[kN]	[-]	[-]	[-]	[-]	[mm]	[mm]	[mm]	[mm]	[-]	[-]	[-]
frame B01	HEA300	5000	5000	1000	1000	0	3.65E-03	0.73	1	7.05	7131	5783	7082	5.98	-6.12	-1.71	0
frame B02	HEA300	5000	7500	1000	1000	0	3.65E-03	0.77	1.5	6.38	7491	6111	7484	6.65	-6.12	-1.71	0
frame B03	HEA300	5000	10000	1000	1000	0	3.65E-03	0.80	2	5.87	7815	6397	7834	7.20	-6.12	-1.71	0
frame B1	HEA120	3000	3000	1000	1000	0	4.08E-03	1.12	1	0.68	4200	3470	4249	3.43	-3.44	-0.89	-1.19
frame B2	HEA120	3000	4500	1000	1000	0	4.08E-03	1.18	1.5	0.61	4429	3667	4491	3.87	-3.44	-0.89	-1.19
frame B3	HEA120	3000	6000	1000	1000	0	4.08E-03	1.24	2	0.56	4629	3838	4701	4.22	-3.44	-0.89	-1.19
frame B4	HEA160	3000	3000	1000	1000	0	4.08E-03	0.84	1	1.84	4238	3470	4249	3.51	-3.44	-0.89	-1.19
frame B5	HEA160	3000	4500	1000	1000	0	4.08E-03	0.89	1.5	1.66	4461	3667	4491	3.93	-3.44	-0.89	-1.19
frame B6	HEA160	3000	6000	1000	1000	0	4.08E-03	0.93	2	1.52	4658	3838	4701	4.27	-3.44	-0.89	-1.19
frame B7	HEA220	3000	3000	1000	1000	0	4.08E-03	0.62	1	5.71	4339	3470	4249	3.70	-3.68	0	0
frame B8	HEA220	3000	4500	1000	1000	0	4.08E-03	0.65	1.5	5.20	4545	3667	4491	4.08	-3.68	0	0
frame B9	HEA220	3000	6000	1000	1000	0	4.08E-03	0.68	2	4.79	4735	3838	4701	4.40	-3.68	0	0
frame B10	HEA280	3000	3000	1000	1000	0	4.08E-03	0.49	1	13.44	4478	3470	4249	3.96	-3.68	0	0
frame B11	HEA280	3000	4500	1000	1000	0	4.08E-03	0.51	1.5	12.39	4663	3667	4491	4.28	-3.68	0	0
frame B12	HEA280	3000	6000	1000	1000	0	4.08E-03	0.53	2	11.49	4842	3838	4701	4.56	-3.68	0	0

A different mechanical scheme means also a different distribution of the internal forces. In the case of frame A, the acting critical bending moment is the height times the horizontal load divided over the two columns, as shown on the left in Figure 75. When the bottom ends of the column are clamped, as is the case for frame B, then the critical bending moment reduces due to the bending moment resistance of the bottom end. However, the value for the bending moment is harder to determine since frame B is a statically indeterminate frame with the 3rd degree. Implementing the statically indeterminate frame in the calculation, and still be able to solve for the ultimate load takes a lot of effort. For that reason, linear interpolation over the results of computer software MatrixFrame is used to calculate a boundary factor (*bf* in Figure 75) to reduce the bending moment. Value bf is obtained by applying a horizontal load of 100 kN in the computer software and then dividing the $M_{Ed,software}$ of frame B by the $M_{Ed,software}$ of frame A.

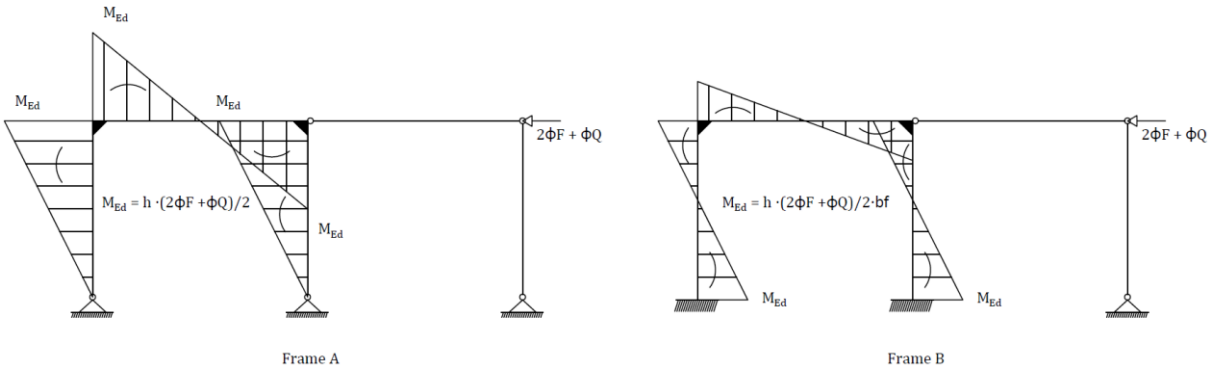

Figure 75: Bending moment diagram for the pin-ended frame (left) and clamped frame (right)

7.4 RESULTS

7.4.1 Frame A, A-NL, A-V, and B

The results are bundled for the frame configurations without and with the additional horizontal load. In this section, the results of the frame configurations without the additional horizontal load are given, which are frames A, A-NL, A-V, and B. The results of the frames are processed in the same way as explained in chapter 6, meaning that for each frame $F_{ult,i,}$ and $N_{ult,i}$ are performed as in section 6.4 and 6.5 respectively, and converted into a unity check as in section 6.8. The results for frame A, A-NL, A-V, and B are given in Table 24. For all corresponding values see appendix C.

Section 6.8 concluded that the Yura approach gives the most accurate result for frame 01 compared to the ultimate resistance load with the most realistic input (LBA). The values in Table 24 indicates that this is also the case for all other frames. For that reason, all the results with the Yura approach are compared to the most realistic approach in Table 22.

Table 22: Difference between $U.C._{EC,Yura}$ and $U.C._{EC,LBA}$ $\left(\frac{U.C._{EC,Yura}-U.C._{EC,LBA}}{U.C._{EC,LBA}}\right)$ for frames A, A-NL, A-V, and B

frame 01	-1.06%	frame 01-NL	1.01%	frame 01-V	-4.85%	frame B01	0.36%
frame 02	-1.35%	frame 02-NL	0.37%	frame 02-V	-4.27%	frame B02	0.05%
frame 03	-1.35%	frame 03-NL	0.05%	frame 03-V	-3.58%	frame B03	-0.16%
frame A1	-2.39%	frame A1-NL	0.29%	frame A1-V	-6.47%	frame B1	-1.26%
frame A2	-2.15%	frame A2-NL	-0.08%	frame A2-V	-5.22%	frame B2	-1.58%
frame A3	-1.87%	frame A3-NL	-0.24%	frame A3-V	-4.24%	frame B3	-1.83%
frame A4	-1.69%	frame A4-NL	0.67%	frame A4-V	-5.64%	frame B4	-0.18%
frame A5	-1.74%	frame A5-NL	0.14%	frame A5-V	-4.74%	frame B5	-0.51%
frame A6	-1.61%	frame A6-NL	-0.11%	frame A6-V	-3.91%	frame B6	-0.74%
frame A7	-0.10%	frame A7-NL	1.43%	frame A7-V	-3.48%	frame B7	0.79%
frame A8	-0.64%	frame A8-NL	0.73%	frame A8-V	-3.33%	frame B8	0.50%
frame A9	-0.79%	frame A9-NL	0.39%	frame A9-V	-2.86%	frame B9	0.33%
frame A10	1.20%	frame A10-NL	1.79%	frame A10-V	-0.83%	frame B10	1.27%
frame A11	0.40%	frame A11-NL	1.10%	frame A11-V	-1.50%	frame B11	0.99%
frame A12	0.08%	frame A12-NL	0.75%	frame A12-V	-1.45%	frame B12	0.84%

7.4.2 Frame A-H, A-NLH, and A-VH

In this section, the results of the frame configurations with the additional horizontal load are given, which are frames AH, A-NLH, and A-VH. The results for frame AH, A-NLH, A-VH are given in Table 25. For all corresponding values see appendix C. The difference between the Yura approach and the most realistic approach (LBA) are given in Table 23.

Table 23:Difference between $U.C._{EC,Yura}$ and $U.C._{EC,LBA}$ $\left(\frac{U.C._{EC,Yura}-U.C._{EC,LBA}}{U.C._{EC,LBA}}\right)$ for frames A-H, A-NLH and A-VH

frame 01-H	-1.05%	frame 01-VH	-4.83%	frame 01-NLH	1.00%
frame 02-H	-1.33%	frame 02-VH	-4.24%	frame 02-NLH	0.36%
frame 03-H	-1.31%	frame 03-VH	-3.55%	frame 03-NLH	0.05%
frame A1-H	-2.35%	frame A1-VH	-6.44%	frame A1-NLH	0.28%
frame A2-H	-2.09%	frame A2-VH	-5.19%	frame A2-NLH	-0.08%
frame A3-H	-1.81%	frame A3-VH	-4.21%	frame A3-NLH	-0.23%
frame A4-H	-1.66%	frame A4-VH	-5.61%	frame A4-NLH	0.66%
frame A5-H	-1.71%	frame A5-VH	-4.71%	frame A5-NLH	0.14%
frame A6-H	-1.58%	frame A6-VH	-3.88%	frame A6-NLH	-0.10%
frame A7-H	-0.10%	frame A7-VH	-3.47%	frame A7-NLH	1.43%
frame A8-H	-0.63%	frame A8-VH	-3.31%	frame A8-NLH	0.73%
frame A9-H	-0.78%	frame A9-VH	-2.84%	frame A9-NLH	0.38%
frame A10-H	1.20%	frame A10-VH	-0.83%	frame A10-NLH	1.80%
frame A11-H	0.40%	frame A11-VH	-1.49%	frame A11-NLH	1.11%
frame A12-H	0.08%	frame A12-VH	-1.44%	frame A12-NLH	0.75%

Table 24: Summary of the outputs and results for frames A, A-NL, A-V, and B

	λ	C	$F_{,ult,GMNIA\ IV}$	$N_{ult,NEN\&\ modEC,\ nomogram}$	$N_{,ult,EC,\ nomogram}$	$N_{,ult,EC,\ LBA}$	$N_{,ult,EC,\ Yura}$	U.C. NEN&modEC, nomogram	U.C. EC,nomogram	U.C. EC,LBA	U.C. EC,Yura	$F_{,ult,GMNIA\ III}$
	[-]	[-]	[kN]	[kN]	[kN]	[kN]	[kN]	[-]	[-]	[-]	[-]	[kN]
frame 01	1.45	1	1671.9	1447.6	1580.6	1230.6	1217.6	0.87	0.95	0.74	0.73	1604.6
frame 02	1.55	1.5	1503.3	1339.9	1462.1	1123.6	1108.4	0.89	0.97	0.75	0.74	1449.3
frame 03	1.64	2	1355.0	1244.4	1356.2	1028.4	1014.5	0.92	1.00	0.76	0.75	1311.5
frame A1	2.25	1	165.5	172.0	184.3	135.6	132.4	1.04	1.11	0.82	0.80	160.5
frame A2	2.41	1.5	145.8	155.6	166.3	121.0	118.4	1.07	1.14	0.83	0.81	142.0
frame A3	2.56	2	129.6	141.7	151.1	109.0	106.9	1.09	1.17	0.84	0.83	126.8
frame A4	1.68	1	441.5	409.5	444.9	338.4	332.7	0.93	1.01	0.77	0.75	425.6
frame A5	1.80	1.5	392.7	375.5	407.3	306.0	300.6	0.96	1.04	0.78	0.77	380.0
frame A6	1.91	2	351.3	346.0	374.5	278.1	273.6	0.99	1.07	0.79	0.78	342.2
frame A7	1.22	1	1334.2	1032.5	1127.6	910.5	909.6	0.77	0.85	0.68	0.68	1227.5
frame A8	1.30	1.5	1215.9	968.5	1059.5	843.9	838.5	0.80	0.87	0.69	0.69	1133.7
frame A9	1.37	2	1103.0	909.9	996.1	781.6	775.5	0.82	0.90	0.71	0.70	1041.3
frame A10	0.96	1	2572.3	1937.0	2091.4	1790.0	1811.4	0.75	0.81	0.70	0.70	2346.8
frame A11	1.01	1.5	2518.6	1852.1	2008.8	1702.0	1708.9	0.74	0.80	0.68	0.68	2278.0
frame A12	1.07	2	2434.8	1771.3	1928.2	1611.2	1612.5	0.73	0.79	0.66	0.66	2197.3
frame 01-NL	1.20	1	2318.1	1649.1	1649.1	1632.7	1649.1	0.71	0.71	0.70	0.71	2142.7
frame 02-NL	1.28	1.5	2129.1	1519.9	1519.9	1514.4	1519.9	0.71	0.71	0.71	0.71	1989.3
frame 03-NL	1.35	2	1946.8	1405.2	1405.2	1404.4	1405.2	0.72	0.72	0.72	0.72	1835.9
frame A1-NL	1.87	1	235.7	190.1	190.1	189.5	190.1	0.81	0.81	0.80	0.81	228.9
frame A2-NL	1.99	1.5	209.8	170.8	170.8	171.0	170.8	0.81	0.81	0.81	0.81	204.5
frame A3-NL	2.11	2	188.1	154.8	154.8	155.2	154.8	0.82	0.82	0.82	0.82	184.4
frame A4-NL	1.40	1	623.6	462.8	462.8	459.7	462.8	0.74	0.74	0.74	0.74	590.4
frame A5-NL	1.48	1.5	562.5	422.0	422.0	421.4	422.0	0.75	0.75	0.75	0.75	537.4
frame A6-NL	1.57	2	508.5	386.7	386.7	387.1	386.7	0.76	0.76	0.76	0.76	489.2
frame A7-NL	1.01	1	1682.9	1180.2	1180.2	1163.6	1180.2	0.70	0.70	0.69	0.70	1540.4
frame A8-NL	1.07	1.5	1606.6	1105.8	1105.8	1097.7	1105.8	0.69	0.69	0.68	0.69	1467.1
frame A9-NL	1.13	2	1519.8	1036.8	1036.8	1032.8	1036.8	0.68	0.68	0.68	0.68	1387.2
frame A10-NL	0.79	1	2686.7	2190.3	2190.3	2151.8	2190.3	0.82	0.82	0.80	0.82	2538.6
frame A11-NL	0.84	1.5	2632.3	2101.5	2101.5	2078.6	2101.5	0.80	0.80	0.79	0.80	2543.0
frame A12-NL	0.88	2	2659.4	2014.6	2014.6	1999.6	2014.6	0.76	0.76	0.75	0.76	2477.1
frame 01-V	2.84	1	462.5	746.8	1179.8	375.7	357.4	1.61	2.55	0.81	0.77	453.9
frame 02-V	3.04	1.5	404.4	699.3	1112.9	334.1	319.9	1.73	2.75	0.83	0.79	398.4
frame 03-V	3.24	2	357.4	657.5	1051.3	299.6	288.8	1.84	2.94	0.84	0.81	353.5
frame A1-V	4.40	1	44.0	96.4	146.3	38.3	35.9	2.19	3.32	0.87	0.81	43.4
frame A2-V	4.73	1.5	38.2	89.2	134.9	33.6	31.9	2.34	3.54	0.88	0.84	37.7
frame A3-V	5.05	2	33.6	83.0	124.9	29.9	28.6	2.47	3.72	0.89	0.85	33.3
frame A4-V	3.29	1	119.7	214.9	336.7	99.8	94.2	1.80	2.81	0.83	0.79	117.7
frame A5-V	3.53	1.5	104.2	200.5	315.1	88.3	84.1	1.92	3.02	0.85	0.81	102.8
frame A6-V	3.77	2	92.0	187.8	295.5	78.9	75.8	2.04	3.21	0.86	0.82	91.1
frame A7-V	2.39	1	377.3	529.9	829.3	294.5	284.3	1.40	2.20	0.78	0.75	369.7
frame A8-V	2.55	1.5	331.9	498.8	790.8	264.3	255.5	1.50	2.38	0.80	0.77	326.8
frame A9-V	2.71	2	294.3	471.3	754.5	238.4	231.6	1.60	2.56	0.81	0.79	291.3
frame A10-V	1.88	1	908.9	1022.4	1528.2	652.6	647.2	1.12	1.68	0.72	0.71	885.5
frame A11-V	1.99	1.5	810.3	970.0	1478.7	596.5	587.6	1.20	1.82	0.74	0.73	795.3
frame A12-V	2.12	2	723.3	923.2	1430.8	544.8	536.9	1.28	1.98	0.75	0.74	714.6
frame B01	0.73	1	2781.6	2633.3	2792.7	2548.7	2558.0	0.95	1.00	0.92	0.92	3031.8
frame B02	0.77	1.5	2780.1	2555.0	2720.6	2466.1	2467.3	0.92	0.98	0.89	0.89	2778.2
frame B03	0.80	2	2909.0	2487.2	2657.1	2391.9	2388.1	0.86	0.91	0.82	0.82	2790.0
frame B1	1.12	1	579.9	428.0	465.5	389.2	384.3	0.74	0.80	0.67	0.66	607.1
frame B2	1.18	1.5	555.2	405.3	441.4	364.8	359.0	0.73	0.80	0.66	0.65	567.7
frame B3	1.24	2	533.7	386.3	421.1	344.6	338.3	0.72	0.79	0.65	0.63	531.9
frame B4	0.84	1	1156.4	831.4	890.8	793.8	792.3	0.72	0.77	0.69	0.69	1173.7
frame B5	0.89	1.5	1142.3	800.8	861.2	760.2	756.3	0.70	0.75	0.67	0.66	1160.2
frame B6	0.93	2	1126.6	774.6	835.4	730.9	725.5	0.69	0.74	0.65	0.64	1139.5
frame B7	0.62	1	2014.6	1660.2	1737.8	1620.6	1633.3	0.82	0.86	0.80	0.81	2016.4
frame B8	0.65	1.5	2021.2	1621.8	1704.3	1583.0	1591.0	0.80	0.84	0.78	0.79	2014.8
frame B9	0.68	2	2022.3	1588.3	1674.6	1548.4	1553.5	0.79	0.83	0.77	0.77	2008.7
frame B10	0.49	1	2828.4	2710.2	2790.1	2648.3	2681.9	0.96	0.99	0.94	0.95	2824.4
frame B11	0.51	1.5	2828.4	2664.9	2752.5	2609.9	2635.7	0.94	0.97	0.92	0.93	2818.7
frame B12	0.53	2	2828.4	2625.3	2719.2	2573.1	2594.7	0.93	0.96	0.91	0.92	2815.8

Table 25: Summary of the outputs and results for frames A, A-NL, A-V, and B

	λ	C	$F_{,ult,GMNIA\ IV}$	$N_{ult,NEN\&\ modEC,\ nomogram}$	$N_{,ult,EC,\ nomogram}$	$N_{,ult,EC,\ LBA}$	$N_{,ult,EC,\ Yura}$	U.C. NEN&modEC, nomogram	U.C. EC,nomogram	U.C. EC,LBA	U.C. EC,Yura	$F_{,ult,GMNIA\ III}$
	[-]	[-]	[kN]	[kN]	[kN]	[kN]	[kN]	[-]	[-]	[-]	[-]	[kN]
frame 01-H	1.45	1	1457.5	1328.4	1444.4	1127.7	1115.9	0.91	0.99	0.77	0.77	1426.7
frame 02-H	1.55	1.5	1241.7	1177.0	1276.9	985.9	972.9	0.95	1.03	0.79	0.78	1222.5
frame 03-H	1.64	2	1062.8	1045.8	1131.7	864.1	852.7	0.98	1.06	0.81	0.80	1045.7
frame A1-H	2.25	1	127.6	142.7	152.3	112.8	110.2	1.12	1.19	0.88	0.86	126.2
frame A2-H	2.41	1.5	100.8	116.7	124.0	91.1	89.2	1.16	1.23	0.90	0.89	99.1
frame A3-H	2.56	2	78.8	95.3	101.0	73.7	72.3	1.21	1.28	0.93	0.92	77.1
frame A4-H	1.68	1	381.3	373.1	403.9	308.4	303.2	0.98	1.06	0.81	0.80	373.1
frame A5-H	1.80	1.5	318.8	326.4	352.2	266.1	261.6	1.02	1.10	0.83	0.82	314.0
frame A6-H	1.91	2	268.1	286.7	308.4	230.7	227.1	1.07	1.15	0.86	0.85	265.7
frame A7-H	1.22	1	1227.7	991.2	1080.1	872.4	871.5	0.81	0.88	0.71	0.71	1145.8
frame A8-H	1.30	1.5	1084.7	910.7	992.9	791.8	786.8	0.84	0.92	0.73	0.73	1024.9
frame A9-H	1.37	2	958.1	838.1	913.3	718.4	712.8	0.87	0.95	0.75	0.74	912.7
frame A10-H	0.96	1	2564.7	1893.9	2042.7	1746.6	1767.6	0.74	0.80	0.68	0.69	2346.3
frame A11-H	1.01	1.5	2414.8	1789.7	1937.9	1640.3	1646.9	0.74	0.80	0.68	0.68	2215.3
frame A12-H	1.07	2	2246.0	1691.4	1836.8	1533.6	1534.7	0.75	0.82	0.68	0.68	2071.0
frame 01-VH	2.84	1	411.3	694.4	1089.8	348.7	331.9	1.69	2.65	0.85	0.81	406.4
frame 02-VH	3.04	1.5	342.3	625.9	986.1	298.5	285.8	1.83	2.88	0.87	0.84	335.8
frame 03-VH	3.24	2	287.3	565.8	892.4	257.3	248.2	1.97	3.11	0.90	0.86	282.7
frame A1-VH	4.40	1	34.0	81.3	122.3	32.4	30.3	2.39	3.59	0.95	0.89	33.7
frame A2-VH	4.73	1.5	26.4	68.4	102.0	25.8	24.5	2.59	3.87	0.98	0.93	25.8
frame A3-VH	5.05	2	20.3	57.3	84.7	20.7	19.8	2.82	4.18	1.02	0.98	19.7
frame A4-VH	3.29	1	104.2	198.3	308.7	92.1	86.9	1.90	2.96	0.88	0.83	103.4
frame A5-VH	3.53	1.5	85.7	177.3	276.0	78.0	74.3	2.07	3.22	0.91	0.87	84.7
frame A6-VH	3.77	2	71.0	159.0	246.9	66.7	64.1	2.24	3.48	0.94	0.90	70.1
frame A7-VH	2.39	1	353.0	512.2	799.0	284.2	274.3	1.45	2.26	0.81	0.78	346.6
frame A8-VH	2.55	1.5	302.1	473.8	747.4	250.6	242.3	1.57	2.47	0.83	0.80	296.8
frame A9-VH	2.71	2	260.3	439.9	699.3	222.1	215.8	1.69	2.69	0.85	0.83	255.3
frame A10-VH	1.88	1	871.5	1003.2	1497.1	639.1	633.9	1.15	1.72	0.73	0.73	851.6
frame A11-VH	1.99	1.5	764.2	942.6	1433.2	578.3	569.7	1.23	1.88	0.76	0.75	751.9
frame A12-VH	2.12	2	671.9	888.3	1371.8	522.8	515.3	1.32	2.04	0.78	0.77	664.1
frame 01-NLH	1.20	1	2020.4	1503.3	1503.3	1488.4	1503.3	0.74	0.74	0.74	0.74	1907.4
frame 02-NLH	1.28	1.5	1750.3	1323.3	1323.3	1318.5	1323.3	0.76	0.76	0.75	0.76	1668.3
frame 03-NLH	1.35	2	1519.2	1168.5	1168.5	1167.9	1168.5	0.77	0.77	0.77	0.77	1452.3
frame A1-NLH	1.87	1	185.3	156.8	156.8	156.3	156.8	0.85	0.85	0.84	0.85	181.1
frame A2-NLH	1.99	1.5	146.0	127.2	127.2	127.3	127.2	0.87	0.87	0.87	0.87	142.1
frame A3-NLH	2.11	2	114.6	103.2	103.2	103.5	103.2	0.90	0.90	0.90	0.90	112.2
frame A4-NLH	1.40	1	535.9	419.3	419.3	416.5	419.3	0.78	0.78	0.78	0.78	517.1
frame A5-NLH	1.48	1.5	447.6	364.0	364.0	363.5	364.0	0.81	0.81	0.81	0.81	437.0
frame A6-NLH	1.57	2	388.4	317.6	317.6	317.9	317.6	0.82	0.82	0.82	0.82	377.5
frame A7-NLH	1.01	1	1556.3	1128.8	1128.8	1112.9	1128.8	0.73	0.73	0.72	0.73	1443.0
frame A8-NLH	1.07	1.5	1423.3	1034.2	1034.2	1026.7	1034.2	0.73	0.73	0.72	0.73	1327.7
frame A9-NLH	1.13	2	1287.2	948.3	948.3	944.7	948.3	0.74	0.74	0.73	0.74	1214.0
frame A10-NLH	0.79	1	2806.6	2137.8	2137.8	2099.9	2137.8	0.76	0.76	0.75	0.76	2652.5
frame A11-NLH	0.84	1.5	2739.7	2025.0	2025.0	2002.7	2025.0	0.74	0.74	0.73	0.74	2563.9
frame A12-NLH	0.88	2	2636.8	1916.1	1916.1	1901.7	1916.1	0.73	0.73	0.72	0.73	2465.9

7.5 CONCLUSIONS

7.5.1 Frame A, A-NL, A-V, and B

The results from Table 24 can be plotted into a unity check graph, where each symbol indicates a different frame configuration. First, the unity check graphs are given for the NEN 6771 & modified EN 1993-1-1 and the current EN 1993-1-1 in Figure 76, left and right respectively. It can be seen that the EN 1993-1-1 many frame configurations lie in the unsafe region. This was expected since the current EN 1993-1-1 does not take into account the leaning column effect at all. The unsafe results start at about a slenderness ratio of 1.5 and go up to a unity check of 3.7 for a slenderness ratio of 5.0. As discussed before, the NEN 6771 considered the leaning column effect in the load

side of the equation (F_{tot}). It can be stated from Figure 76 that the NEN 6771 & modified EN 1993-1-1 gives lower ultimate design resistance loads than the current EN 1993-1-1, which is (almost) safe enough for frame A and B, but in the case of frame A-V with the increased leaning column effect it gives unsafe results. Unsafe results start at about a slenderness ratio of 2 and increase somewhat linearly up to a unity check of 2.5 for a slenderness ratio of 5.0.

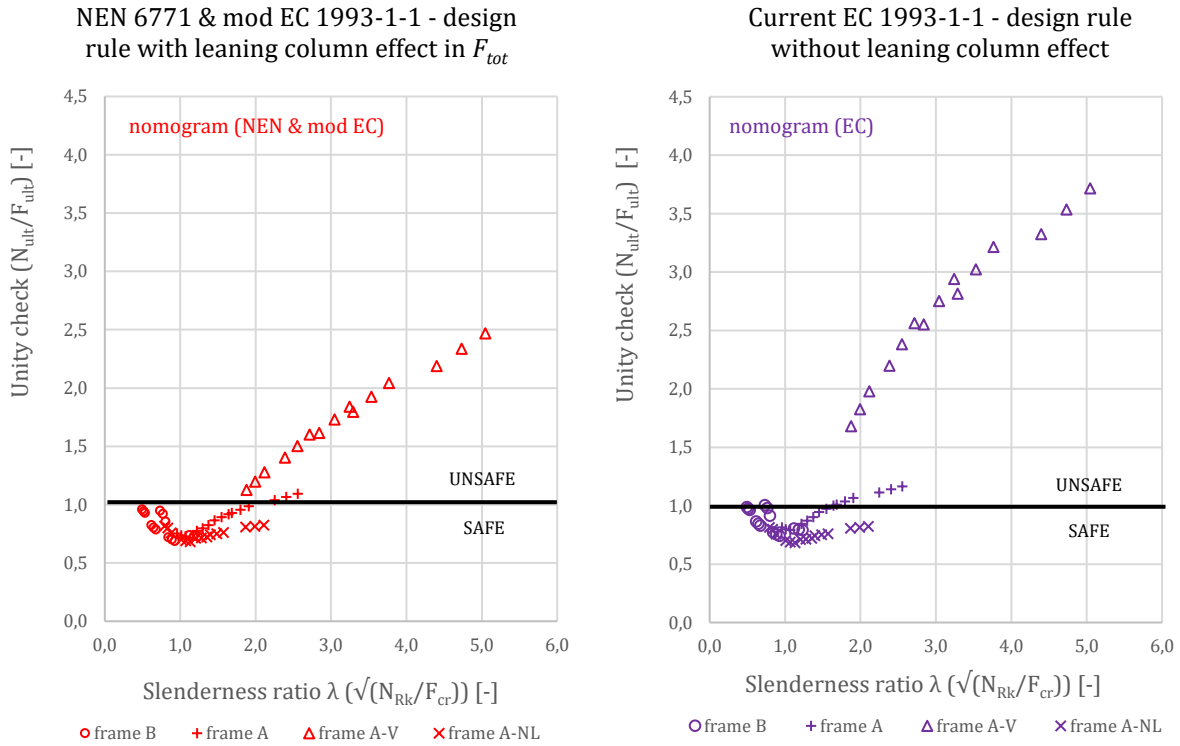

Figure 76: Unity check graphs for the NEN 6771& mod EN 1993-1-1 (left) and current EN 1993-1-1 (right) for frames A, A-NL, A-V, and B

Next, the unity check graph is given for the EN 1993-1-1 design rule where the leaning column effect is included in L_{cr} for frames A, A-NL, A-V, and B. In Figure 77 the results are shown for the EN 1993-1-1 design rule in combination with L_{cr} obtained from the LBA (most realistic) and with the Yura approach. The sentence new L_{cr} is used in the title of Figure 77 since the current nomogram does not include the leaning column effect in L_{cr}. Figure 77 shows that including the leaning column effect in L_{cr} leads to safe results for all cases. When we compare the results to Figure 76, it can be seen that all the results of the EN 1993-1-1 with the new L_{cr} are lower than the results from the NEN 6771 & modified EN 1993-1-1 and the current EN 1993-1-1 (specific values in Table 24). This means that results for the frames that are safe in the case of the NEN 6771 & modified EN 1993-1-1 and the current EN 1993-1-1 will be more conservative when considering the EN 1993-1-1 with the new L_{cr}. This increase in conservatism is different per frame configuration.

Section 6.7.1.4 showed that $N_{ult,EC,Yura}$ for frame 01 only differ -1.06% to $N_{ult,EC,LBA}$, where $N_{ult,EC,LBA}$ is performed with the most realistic input obtained from the FE-model and assumed as the most realistic design-resistance load. This means that for frame 01 the Yura approach is very accurate. When this difference is calculated for all frames, as given in Table 22, it can be seen that this is the case for all frames. The lowest difference has a value of -6.47% and the highest difference a value of 1.79%. The mean of all differences is -1.07%. The mean indicates that on average the results with Yura are lower than the most realistic one, which leads to safer results. Considering the above

gives that using the Yura approach in combination with the EN 1993-1-1 design rule give for all cases accurate and safe results.

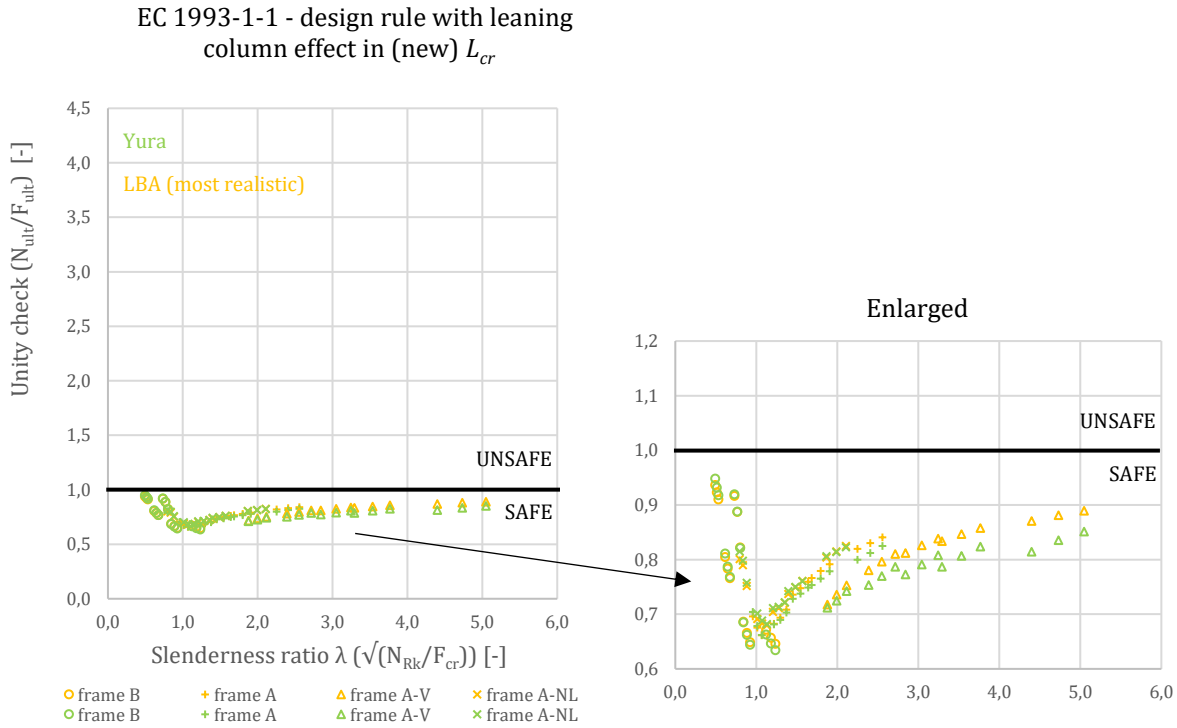

Figure 77: Unity check graph for the EN 1993-1-1 in combination with the LBA and Yura for frames A, A-NL, A-V, and B

As discussed before Frame A-NL is included to check whether the ratios between N_{ult} and F_{ult} are reliable. Due to the absence of the leaning column effect in frame A-NL, the slenderness ratio $\bar{\lambda}$ are lower than compared to frame A, as can be seen in Table 24. However, the ratios between N_{ult} and F_{ult} for frame A-NL are comparable to the ratios for frames A and B, which have a comparable slenderness ratio. This is the case for both Figure 76 and Figure 77, meaning that this validates the other results.

7.5.2 Frames A-H, A-NLH, and A-VH

As already explained in section 7.3.4, frames A-H, A-NLH, and A-VH are only extended with an additional horizontal load and this means that for the ultimate resistance loads only M_{Ed} increases in equation (2) and (6), while in the FE-model the actual additional horizontal displacement is also taken into account. When we look at the unity checks as given in Table 24 and Table 25, it can be seen that the additional horizontal load influences the results, since all the unity checks found in Table 25 are higher than in Table 24. For example, when we consider the unity checks in Table 25 for frame 01-H, they are all higher than the unity checks for frame 01 in Table 24. This means that the additional horizontal displacement is indeed not taken into account in the design rules and therefore decreases the conservatism margins.

Since section 7.5.1 already showed that the NEN 6771 & modified EN 1993-1-1 and the current EN 1993-1-1 lead to unsafe results, the results for these design rules will not be plotted in a unity check graph, since it will only show that the results are even more unsafe. In the case of the EN 1993-1-1 design rule where the leaning column effect is included in $L_{cr,}$ the decrease of the conservatism margin can result in unsafe unity checks, due to the already small margin for the slender frame configurations. When we plot the unity check graph for the EN 1993-1-1 design rule where the leaning column effect is included in L_{cr} for frames A-H, A-NLH, and A-VH (Figure 78), we can see that the conservatism margin decreased and for the most slender frame even led to an

unsafe result when considering the LBA. However, the small difference between the results with LBA and Yura as found in Table 23 (-4.21%), makes that Yura does lead to a safe result. The lowest difference in Table 23 has a value of -6.44% and the highest difference a value of 1.80%. The mean of all differences is -1.39%, which again leads to safe results.

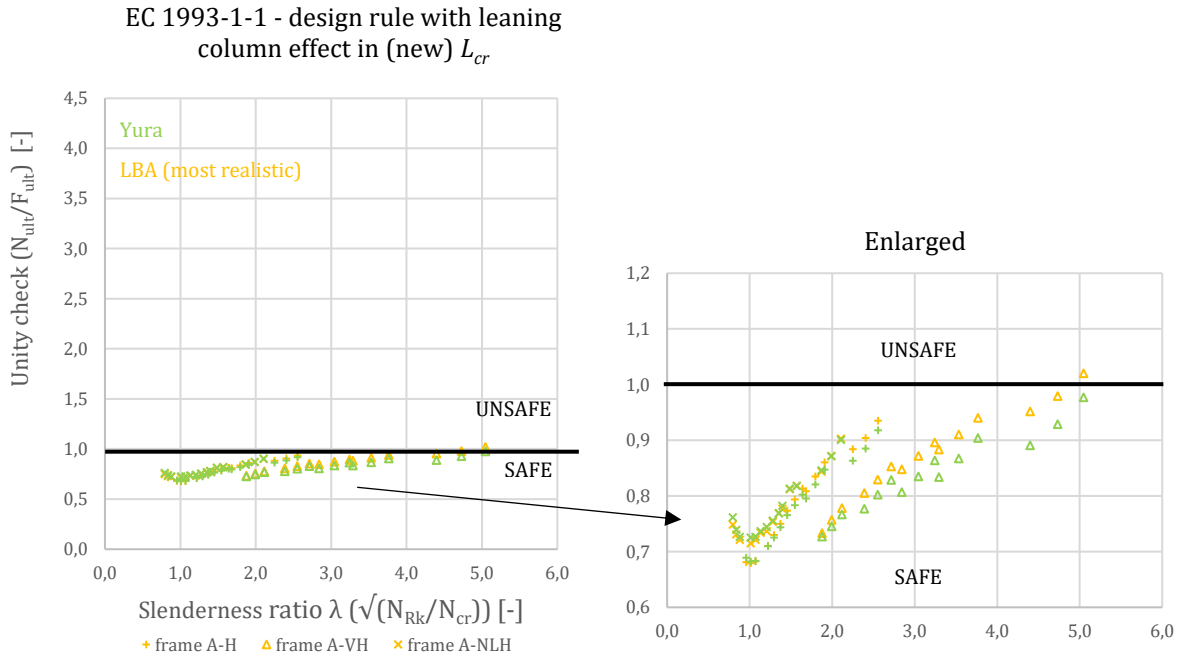

Figure 78: Unity check graph for the EN 1993-1-1 in combination with the LBA and Yura for frames A-H, A-NLH, and A-H

7.5.3 Differences between GMNIA III and GMNIA IV

As already discussed in section 6.6.1 is only GMNIA IV considered in chapter 7. The imperfections of GMNIA IV are performed according to Shayan et al. [9]. In their paper, they state that the use of only the first critical eigenmode (which is the case for GMNIA III) leads to conservative results. However, to validate GMNIA IV the differences between GMNIA IV and GMNIA III are plotted in Figure 79. The differences between GMNIA III and GMNIA IV are close to each other with a maximum difference of 10%. The difference is the largest in the region where the most conservative results lay, namely between $\bar{\lambda}$=0.5-2, meaning that this difference does not influence the end conclusion.

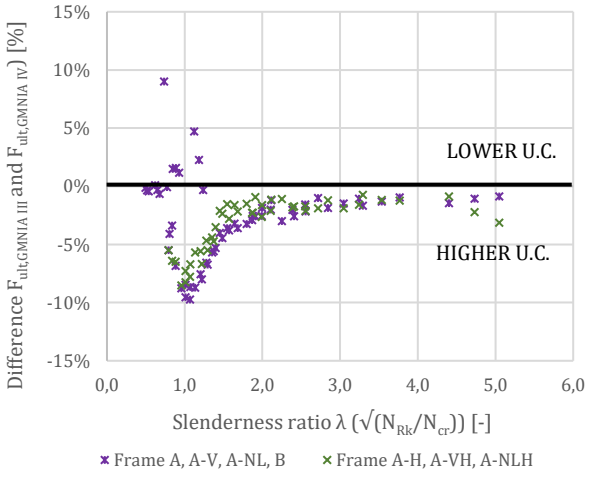

Figure 79: Differences between GMNIA III and GMNIA IV, plotted along with the slenderness ratio

8 CONCLUSIONS AND RECOMMENDATIONS

8.1 CONCLUSIONS

In The Netherlands, in the past, the NEN 6771 provided the design rules about the stability of steel columns loaded in compression and bending. It was found that the design rules of the NEN 6771 include the leaning column effect in the load side of the equation with the value F_{tot}. In 2012, the Eurocode was adopted in The Netherlands as a replacement for the NEN series. The Eurocode (EC) is a European standard to assess the structural safety of all possible building structures. The EC EN 1993-1-1 is the basic part containing the design rules for steel structures. It was found that the design rules of the EN 1993-1-1 do not include the leaning column effect at all. For that reason, the goal of this research is to numerically verify the design rule of the NEN 6771 for the leaning column effect, since the background of the NEN 6771 about the leaning column effect is unknown, and validate and rewrite the design rule of the EN 1993-1-1 for a more clear presentation and content regarding the leaning column effect.

In the process of this research, some decisions were made that did not reflect reality precisely. These decisions were about modeling the cross-section without the root radius and the high residual stresses for steel quality's higher than S235. In the process, it turned out that these decisions influence the results barely.

The research scope aimed to cover all the cases where the leaning column effect is governing and reflects a large range of leaning column problems. The parameter that is used to reflect the range is the slenderness ratio, defined by $\bar{\lambda} = \sqrt{N_{Rk}/F_{cr}}$. The frame configurations were studied extensively by carrying out various geometric and material non-linear analyses with imperfections (GMNIA) with a parametric Finite Element (FE) model and comparing them to various ultimate resistance outcomes from the design rules. This extensive study showed that some margins between GMNIA IV, the simulation closest to reality, and the design rule of the EN 1993-1-1 are unsafe. For a slenderness ratio greater than 1.5, the current EN 1993-1-1 design rule gives unsafe results. The NEN 6771 design rule, also known as the design rule where the leaning column effect is included in the load side of the equation, decreased the ultimate resistance load, but not enough. At a slenderness ratio greater than 2, the design rule of the NEN 6771 is also not safe anymore. This can be explained by the fact that the design rule considers the member problem more as a function of an individual column (P-δ effect), instead of a function of all columns in the story (P-Δ effect). The lateral deflection (Δ) that increases the bending moment is predicted inaccurately, which leads to unsafer results when the lateral deflection increases. This can be seen by the linear increase of the unity checks along with the slenderness ratio. Different behavior is spotted for frame B, the frame with the clamped column ends, which can not be explained.

Authorities asked whether it is possible to rewrite the current EN 1993-1-1 design rule since it is hard to check for what value for the leaning column effect an engineer has accounted for, or to see it has been taken into account at all. It is possible to rewrite the design rule of the NEN 6771 into EN 1993-1-1 format. When the derivation of the EN 1993-1-1 design rule is carried again from the starting point, but now including a new value F_{lean}, the following equation is obtained:

$$\frac{N_{Ed}}{\chi \cdot N_{Rd}} + k\left(\bar{\lambda}^2 - \frac{1}{\chi}\right)(\chi - 1)\frac{F_{lean}}{N_{Rd}} + k\frac{C_m \cdot M_{Ed}}{M_{Rd}} \leq 1 \; where \; k = \frac{1}{1 - \frac{\chi \cdot N_{Ed}}{F_{cr}}}$$

F_{lean} represents the additional load on the frame due to the leaning column effect, instead of the total load on the structure as F_{tot} does in the NEN 6771 design rule. The modified EN 1993-1-1 equation gives the same results as the design rule of the NEN 6771, as intended. However, the equation has no use since the results of the NEN 6771 are unsafe.

Due to the unsafe result of the NEN 6771, different ways to include the leaning column effect in the design rules are studied. Geschwindner [1] wrote a paper about several ways to include the leaning column effect in the buckling length. These approaches are studied, and the literature study showed that several of these approaches overlap. For that reason, only two approaches are extensively investigated, namely the approach of Geschwindner and Yura. The results of the approaches can be related to the results of the FE-model since the α_{cr} obtained from the LBA can be used to determine an L_{cr} that reflects reality in the best way. In the case of Geschwindner, the American nomogram equation to determine the buckling length is extended to include the leaning column effect. However, it is found that this approach is not very accurate to the results obtained with the LBA. The Yura approach is based on the equilibrium of the structure. By equating the Euler buckling equation where the leaning column effect is not taken into account to the Euler buckling equation where the leaning column effect is included, the following equation is found:

$$\beta_{Yura} = \beta_{nomogram} \cdot \sqrt{\frac{\sum F + \sum Q}{\sum F}}$$

Where β_{Yura} is the modified effective length factor which takes into account the leaning column effect and $\beta_{nomogram}$ the modified effective length factor found by the nomogram in the Dutch National Annex NB.NA, which does not take into account the leaning column effect. The research showed that the use of β_{Yura} gives similar buckling lengths as the LBA, which is assumed as most realistic, and for that reason is used in the parametric study.

For all the slenderness ratios considered in the parametric study, the current EN 1993-1-1 design rule in combination with the Yura approach gives safe results. Besides that, also the differences between the results of the Yura approach and the LBA are low. The lowest difference between the ultimate resistance loads obtained with LBA and Yura has a value of -6.47% and the highest difference a value of 1.79%. The mean of all differences is -1.07%. The negative mean indicates that on average ultimate resistance loads with Yura are lower than the most realistic one (LBA), which leads to a higher, and therefore safer, conservatism margin.

For the design rules, a higher horizontal load only increases the bending moment M_{Ed}, while in the FE-model also the actual additional horizontal displacement is taken into account. For that reason, the increase of the horizontal load influences the conservatism margins, and in the case of the most slender structure with the LBA, the conservatism margin is reduced to even a negative value, meaning that the result for this frame is unsafe with a unity check of 1.02. However, the (small) difference between Yura and LBA gives that with considering the Yura approach, the frame is safe with a unity check of 0.98.

The research shows that a modified buckling length equation is more effective than a modified EN 1993-1-1 equation for including the leaning column effect. The modified buckling length equation is easy to implement since the current way of determining β with the Dutch National Annex can be kept, and only has to be extended with the square root of the sum of the load on the total structure (∑stabilizing load F + ∑leaning column load Q) divided by the sum of the load on the stabilizing structure (∑stabilizing load F), or in other terms $\sqrt{(\sum F + \sum Q)/\sum F}$.

8.2 RECOMMENDATIONS

To apply the Yura approach in the Eurocode more research has to be done since only the most simplistic frame configuration has been studied. To ensure the correctness of the Yura approach, more complicated frame configurations should be studied and analyzed with FEM, for example, frames with more stories and more rows of attached leaning columns. In the case of frame A-V, the model should represent a stabilizing frame with a row of ten columns attached to it, without actual modeling these columns. It could be the case that when modeling the columns, the frame behaves differently. In the case of more stories, the stiffness of the joint is an important aspect, which can not be simulated by only adjusting the height of the simplistic frame configuration.

The additional horizontal wind load of 1 kN/m^2 is based on a broad assumption. It is recommended to apply a more accurate wind load for each frame height, since the slender frames are reasonable affected by the wind load. For more complicated frames this also can lead to high wind loads. When unsafe results are found related to higher wind loads in combination with the leaning column effect, it is advised to study the design rules regarding the lateral deflection of the structure. Currently, the lateral deflection is not predicted accurately. It is expected that the amplificiation factor ($\frac{\alpha_{cr}}{\alpha_{cr}-1}$) and the slope ($\phi = \phi_0 \cdot \alpha_h \cdot \alpha_m$) in the EC EN 1993-1-1 cause this.

In this research, the load is only applied to the columns. It is recommended to check the influence on the results when the beams are loaded, and failure of the beam is the first failure mode. In practice, the load is applied to the beam, instead of only on the column. This can influence the behavior of the structure.

9 BIBLIOGRAPHY

[1] L. F. Geschwindner, "A Practical Look at Frame Analysis, Stability and Leaning Columns," *Engineering Journal,* vol. Fourth Quarter, pp. 167-181, 2002.

[2] L. Simões da Silva, R. Simões and H. Gervásio, "Eurocode 3: Design of Steel Structures; Part 1-1: General rules and rules for buildings," ECCS Eurocode Design Manuals, Mem Martins, Portugal, 2010.

[3] H. Snijder, F. Bijlaard and H. Steenbergen, "Valkuilen in de TGB Staal," *Bouwen met staal 125,* pp. 19-24, juli/augustus 1995.

[4] N. Boissonnade, R. Greiner, J. Jaspart and J. Lindner, Book: Rules for Member Stability in EN 1993-1-1; Background documentation and design guidelines, Portugal: ECCS, 2006.

[5] H. Snijder and H. Steenbergen, Stabiliteit 3; Staven belast op druk en buiging, unpublished.

[6] K. Loorits, "Classification of cross sections for steel beams in different design codes," *Rakenteiden Mekaniikka, Vol 28,* vol. 28, pp. 19-33, 1995.

[7] Comité Européen de Normalisation, "Eurocode 3: Design of steel structures- Part 1-1: General rules and rules for buildings," CEN, Brussels, 2005.

[8] U. Vogel and e. al., "Ultimate Limit State Calculation of Sway Frames with Rigid Joints. Publication No 33," ECCS, Brussels, 1984.

[9] S. Shayan, K. J. R. Rasmussen and H. Zhang, "On the modelling of initial geometric imperfections of steel frames in advanced analysis," *Journal of Constructional Steel Research 98,* pp. 167-177, 2014.

[10] S. Taris, "MASTER THESIS - Stability of unbraced laterally supported steel sway-frames - applicability and scope of the general method of Eurocode 3," Technical University of Eindhoven, Eindhoven, 2009.

[11] Z. Zhuang, Z. Liu, J. Liao and B. Cheng, "Extended Finite Element Method," Elsevier Inc., Beijing, 2014.

[12] Abaqus-docs, "Choosing a shell element," Abaqus, 2012. [Online]. Available: https://abaqus-docs.mit.edu/2017/English/SIMACAEELMRefMap/simaelm-c-shellelem.htm. [Accessed 06 May 2020].

[13] Abaqus-docs, "Configuring a static, general procedure," Abaqus, 2012. [Online]. Available: https://abaqus-docs.mit.edu/2017/English/SIMACAECAERefMap/simacae-t-simconfigurestatic.htm. [Accessed 19 May 2020].

[14] Abaqus-docs, "Eigenvalue buckling prediction," Abaqus, 2012. [Online]. Available: https://abaqus-docs.mit.edu/2017/English/SIMACAEANLRefMap/simaanl-c-eigenbuckling.htm. [Accessed 07 May 2020].

[15] Abaqus-docs, "Coupling constraints," Abaqus, 2012. [Online]. Available: https://abaqus-docs.mit.edu/2017/English/SIMACAECSTRefMap/simacst-c-coupling.htm. [Accessed 07 May 2020].

[16] American Institute of Steel Construction, Inc. (AISC), "Load and Resistance Factor Design Specification for Structural Steel Buildings," AISC, Chicago, 19999.

APPENDIX A – LITERATURE AND INPUTS FOR THE DESIGN CODES

APPENDIX A:
LITERATURE AND INPUTS FOR THE DESIGN CODES

TABLE OF CONTENTS

1 VARIOUS NOMOGRAM SOLUTIONS

1.1 DUTCH ANNEX NB.NA

The NEN 6770 offers two nomographs where the solution for L_{cr} can be derived from. These nomographs are shown in Figure 1, where the left nomograph covers non-sway frames and the right nomograph sway frames. [1]

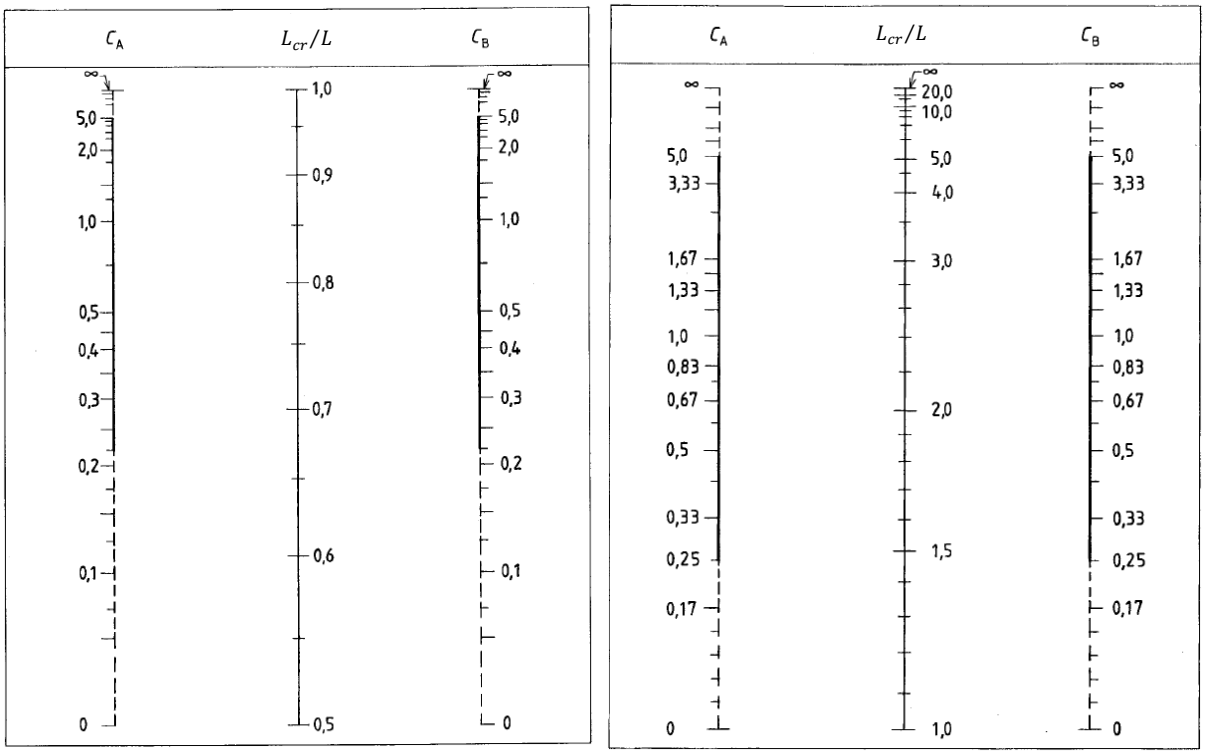

Figure 1: Nomogram for buckling length (L_{cr}) non-sway (left) and sway (right) frames

Value L_{cr} can be obtained from the nomograms by deriving flexibility parameters C_A and C_B, where the indices A and B refer to the two member-ends of the considered column. The flexibility parameters C_A and C_B can be derived with equation (28)

$$C_i = \frac{\sum \frac{I_{cln}}{L_{cln}}}{\sum \mu \frac{I_{bm}}{L_{bm}}} \quad (1)$$

Where I_{cln} and I_{bm} are the second moments of inertia of the column and the connected beam respectively, L_{cln} and L_{bm} are the length of the column and the connected beam respectively, and μ a correction factor. This correction factor μ takes the boundary condition at the other end of the supporting beam into account and is different between a non-sway and sway frames.

For non-sway frames:
μ is 2 if the other end is rigidly connected to one or more columns which are also loaded in compression;
μ is 3 if the other end is pinned;
μ is 4 if the other end is clamped.

For sway frames:
μ is 3 if the other end is pinned;
μ is 4 if the other end is clamped;
μ is 6 if the other end is rigidly connected to one or more columns which are also loaded in compression.

1.2 MODIFIED NOMOGRAPH EQUATION

Equation (2) gives the solution for the critical buckling load of the perfect column. In reality, perfectly pinned ends in a steel structure do not exist. Therefore equation (2) is extended as the following:

$$F_{cr} = \frac{(\pi^2 EI)}{(K_{exact} \cdot L_{cr})^2} \tag{2}$$

Where the K-factor is a mathematic adjustment on the capacity of the column, aiming for a better representation of reality. According to G.L. Geschwindner (2002) [2] the American codes for structural safety, LRFD, and AISC [3] specifications make use of a nomograph to determine the factor K. G.L. Geschwindner (2002) [2] states that the equation where this nomograph is based on is as follows:

$$\frac{G_A G_B (\pi/K)^2 - 36}{6(G_A + G_B)} = \frac{\pi/K}{\tan(\pi/K)} \tag{3}$$

Where A and B refer to the ends of the column and where:

$$G = \frac{\sum I_c/L_c}{\sum I_b/L_b} \tag{4}$$

To include the leaning column effect in equation (3), Figure 2 will be considered. For equilibrium of the leaning column CD, load Q must be balanced with a horizontal force with a magnitude of $Q\Delta/L$. This horizontal force must then be applied at point B to reach equilibrium.

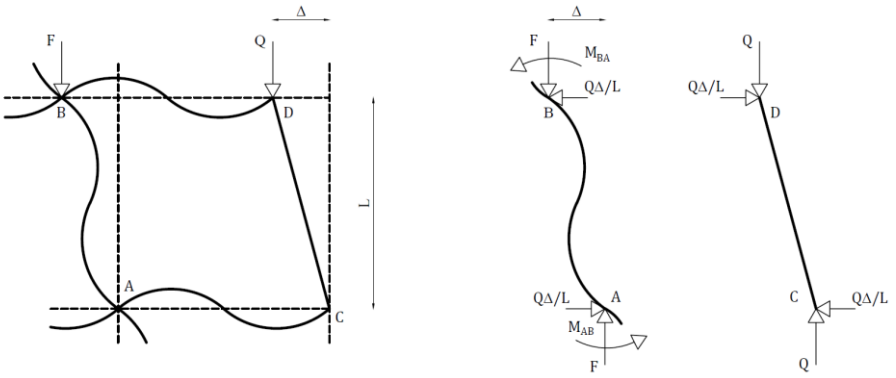

Figure 2: stabilizing column (A-B) and leaning column (C-D) [2]

Further steps for extending equation (3) are unknown, but G.L. Geschwindner (2002) [2] states the following:" *Equations of equilibrium at the joints of column AB and the sway equilibrium equation can be written for the structure in the displaced configuration. Member end moment equations are then written using the slope deflection method, incorporating the stability functions necessary to account for the influence of axial load on column AB. Combining these equations and*

setting the determinate of the coefficients equal to zero will yield the following buckling condition equation. (eq. 5)"

$$\frac{G_A G_B(\pi/K)^2 - 36}{6(G_A + G_B)}\left(1 + \frac{Q}{F}\right) - \frac{\frac{\pi}{K}}{\tan\left(\frac{\pi}{K}\right)}\left(1 + \frac{Q}{P}\right) + \frac{6\tan\left(\frac{\pi}{2K}\right)}{(G_A + G_B)\left(\frac{\pi}{2K}\right)}\left(\frac{Q}{F}\right) + \left(\frac{Q}{F}\right) = 0 \qquad (5)$$

If the load on the leaning column is zero, $Q = 0$, then equation (5) will reduce to equation (3). This suggests that equation (5) is correct.

1.3 YURA APPROACH

The Yura approach makes use of a kinematic model aiming for equilibrium. Consider the leaning column situation in a deformed frame as shown in Figure 3. Again, for an equilibrium of the leaning column CD, load Q must be balanced with a horizontal force with a magnitude of $Q\Delta/L$. When this horizontal force is applied in point B to reach equilibrium, one can see that in the deformed state the bending moment in point A will increase with $L \cdot \frac{Q \cdot \Delta}{L}$, resulting in a bending moment of $\Delta F + \Delta Q$. This indicates that column AB is loaded by F+Q. However, G.L. Geschwindner (2002) [2] states that this assumption that the buckling load equals F+Q is slightly conservative since the buckled shape due to an axial load and the deflected shape due to a lateral load differ only slightly. This approach assumes that all stabilizing columns in a story buckle a side sway mode simultaneously.

To make this approach comparable with the other approaches, the result will be rewritten to critical load formulation with factor K_o:

$$F + Q = \frac{\pi^2 EI}{K_o^2 L_{cr}^2} \qquad (6)$$

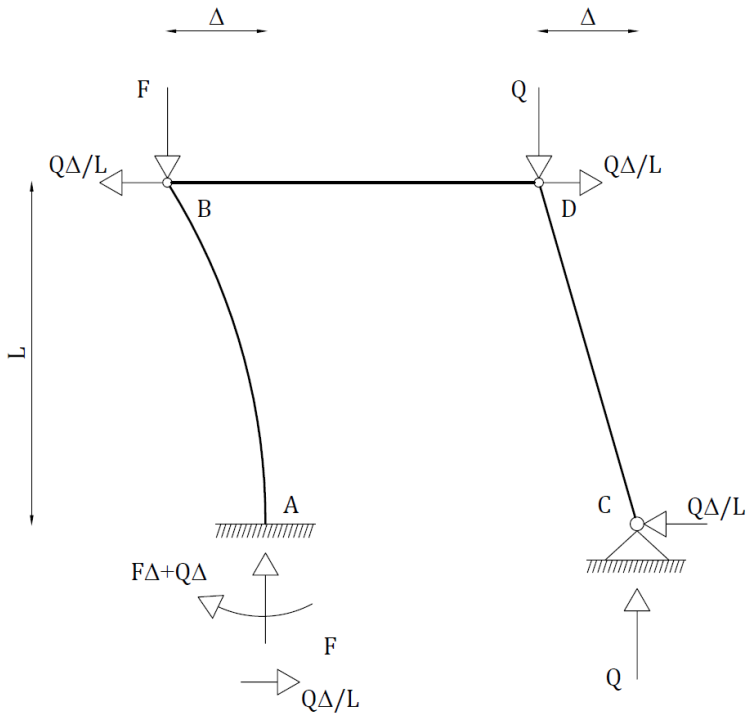

Figure 3: Equilibrium forces in stabilizing column (A-B) and leaning column (C-D) for Yura derivation

The leaning column effect is now taken into account in a new *K*-factor K_n, given as:

$$F = \frac{\pi^2 EI}{K_n^2 L_{cr}^2} \tag{7}$$

Substituting $\frac{K_n^2}{K_o^2} = \frac{F+Q}{F}$ in (6) gives:

$$K_n = K_o \sqrt{\frac{F+Q}{F}} \tag{8}$$

Where K_o and K_n are modified effective length factors

1.4 LIM & MCNAMARA APPROACH

The approach of Lim & McNamara also assumes that all stabilizing columns in a story buckle a side sway mode simultaneously. These researchers developed the sway buckling equation through the use of stability functions and an eigenvalue solution [2]. The K_n-factor is given as:

$$K_n = K_o \sqrt{1 + n \frac{F_0}{F_n}} \tag{9}$$

Where K_o and K_n are modified effective length factors, $n = \sum Q / \sum F$, F_o is the eigenvalue solution for a frame without leaning columns and F_n is the eigenvalue solution for a frame with leaning columns. G.L. Geschwindner (2002) [2] states that normal end conditions lead to $F_o/F_n = 1$. Substituting this in equation (9) results in the same equation for K_n as the Yura approach:

$$K_n = K_o \sqrt{1 + \frac{\sum Q}{\sum F}} = K_o \sqrt{\frac{F+Q}{F}} \tag{10}$$

This suggests that the approach of Lim & McNamara also indicates that the stabilizing column of Figure 3 is loaded by *F*+*Q*.

1.5 LEMESSURIER APPROACH

The previous approach determined a constant value for a story by which the nomograph value of K_o was modified. This approach takes into account the contribution to the lateral resistance of each column along with the magnitude of the load on that column [2]. This is carried out by multiplying the constant value for a story with I/F, where I is the moment of inertia of the column and *F* the load of the stabilizing column. This gives the following equation for the effective length factor K_i:

$$K_n^2 = \frac{I_i}{F_i} \pi^2 \frac{\sum F + \sum Q + \sum (C_L \cdot F)}{\sum (\beta \cdot I)} \tag{11}$$

Where:

$$\beta = \frac{6(G_A + G_B) + 36}{2(G_A + G_B) + G_A \cdot G_B + 3} \tag{12}$$

C_L = $\frac{\beta \cdot K_o^2}{\pi^2} - 1$, but is equal to 0 for leaning columns;
K_n = effective length of the column, accounting for leaning columns;
F, Q = load on stabilizing column and leaning column respectively;

$\sum F$ and $\sum Q$ represent the total load on the columns in a story. $\sum(\beta \cdot I)$ represents the sum of $\beta \cdot I$ for each column participating in lateral sway resistance [2].

1.6 AMERICAN INSTITUTE OF STEEL CONSTRUCTION

Since the equation of LeMussurier is experienced as complex, the AISC modified these equations to a more simpler format. G.L. Geschwindner (2002) [2] states that for the story-buckling model it is assumed that there is no reduction in column stiffness due to the presence of axial load, leading to $C_L = 0$, which gives $\beta = \pi^2/K_o^2$. Substituting this in (14) gives:

$$K_n = \sqrt{\frac{I}{F} \cdot \frac{\sum F + \sum Q}{\sum(I/K_o^2)}} \tag{13}$$

G.L. Geschwindner (2002) [2] states that equation (16) is the same equation as presented in the LRFD. When a structure as shown in Figure 3 is considered, this equation again reduces to equation (11). That means that also this approach indicates that the stabilizing column of Figure 3 is loaded by *F*+*Q*.

2 LITERATURE REGARDING EC 1993-1-1

In 2012, the Eurocode was adopted in The Netherlands. The Eurocode is a European standard to assess the structural performance and safety of all possible building structures. The Eurocode EC 1993-1-1 is the basic part containing the design rules for steel structures. In Clause 6.3.3(4), the EC 1993-1-1 offers a three-dimensional design rule for members in bending and axial compression. For understanding the theory and the derivation of the three-dimensional design rule, it will be studied in the next sections. Besides that, the design rules, including Annex A and Annex B, will be translated into a two-dimensional format, which makes it comparable with the design rules from the NEN 6771.

The EC 1993-1-1 classifies steel cross-sections in different classes, namely cross-section classes 1, 2, 3, and 4. Here can classes 1 and 2 develop their full plastic moment resistance and class 3 only their elastic moment resistance. Class 4 only can develop an elastic moment resistance over an effective area, since it is subjected to the effects of local buckling. Since the effect of local buckling is not of interest, cross-sections of class 4 will not be considered in the upcoming sections. This is also the case for lateral-torsional buckling (LTB) because a two-dimensional case in this graduation project will be considered and any out-of-plane deformations in the Finite Element (FE) model will not be allowed.

2.1 MEMBERS IN COMPRESSION

Members in compression present the first term of the design rules for bending and axial compression. For that reason, this behavior will be discussed separately. The design rule in the EC 1993-1-1 for members in compression is given by the following:

$$\frac{N_{Ed}}{\frac{\chi \cdot A \cdot f_y}{\gamma_1}} \tag{14}$$

Or in the more simplistic format:

$$\frac{N_{Ed}}{(\chi \cdot N_{Rd})} \tag{15}$$

Equation (15) represents the member resistance unity-check due to axial loading of the column. Value N_{Rd} represents the plastic load resistance of the member and is given by $N_{Rd} = A \cdot f_y/\gamma_1$, where A is the area of the cross-section, f_y the yield strength of the material and γ_1 is the partial material factor. The reduction factor χ for flexural buckling can be derived from the design rules for members in only compression, given as the following:

$$\chi = \frac{1}{\phi + \sqrt{\phi^2 - \bar{\lambda}^2}} \tag{16}$$

Where, for class 1, 2, and 3 cross-sections, $\bar{\lambda}$ is the relative slenderness. If $\bar{\lambda} < 0.2$, then the buckling effect may be ignored, and only cross-sectional checks apply [4]. $\bar{\lambda}$ is given by:

$$\bar{\lambda} = \sqrt{N_{Rk}/F_{cr}} \tag{17}$$

Where N_{Rk} is the characteristic axial resistance, given by $A \cdot f_y$ and F_{cr} is the elastic critical buckling load given by $F_{cr} = \pi^2 EI/L_{cr}^2$. The intermediate factor Φ is given by:

$$\Phi = 0.5\left[1 + \alpha\left(\bar{\lambda} - 0.2\right) + \bar{\lambda}^2\right] \tag{18}$$

The analytical formulation of the buckling curves was derived by Maquoi and Rondal [5]. This formulation was based on the Ayrton-Perry format.

$$\left(\frac{1}{\chi} - 1\right)\left(1 - \chi \cdot \bar{\lambda}^2\right) = \eta\chi = \alpha\chi(\bar{\lambda} - 0.2) \tag{19}$$

The value η represents the generalized initial imperfection. This value can estimate the buckling phenomenon of initial imperfections such as residual stresses, initial out-of-straightness, or eccentrically applied forces [5]. Value 0.2 in equation (18) represents the plateau in the buckling curves, where χ=1.0, as can be seen in Figure 4. Value α in equation (18) is the imperfection factor and depends on the type of the cross-section, the thickness of the plates, the yield strength, and the buckling plane [5]. The value α can be obtained from Table 1, where the relating buckling curve can be obtained from Table 2. The buckling curves are shown in Figure 4.

Table 1: Imperfection factor α from the EC 1993-1-1

BUCKLING CURVE	a_0	a	b	c	d
Imperfection factor α	0.13	0.21	0.34	0.49	0.76

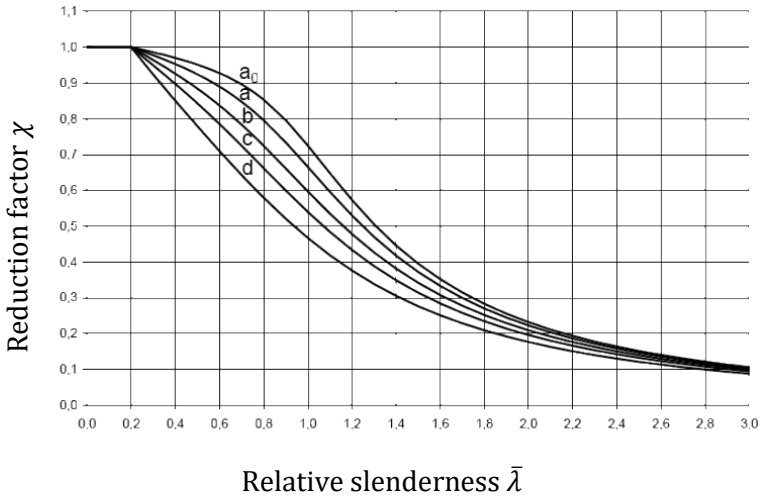

Figure 4: Buckling curves from the EC 1993-1-1 [6]

Table 2: Buckling curves for the relation cross-sections [4]

CROSS-SECTION	LIMITS	BUCKLING ABOUT AXIS	BUCKLING CURVE	
			S235 S275 S355 S420	S460
Rolled I-section 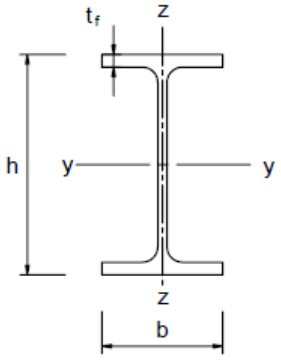	h/b > 1,2 $t_f \leq 40$ mm	y-y z-z	a b	a_0 a_0
	40 mm < $t_f \leq$ 100mm	y-y z-z	b c	a a
	h/b ≤ 1,2 $t_f \leq 100$ mm	y-y z-z	b c	a a
	t_f > 100mm	y-y z-z	d d	c c

2.2 MEMBERS IN BENDING AND AXIAL COMPRESSION

A member under bending and compression can have additional second-order moments due to second-order displacements, the so-called P-δ effect. Figure 5 shows a column with an imperfection e_0, and a column subjected to a vertical and horizontal load. The moment equilibrium leads to the theory and abbreviations that are used to obtain the design rules in the NEN 6771, with the P-δ effect taken into account. To get an insight behind the theory of the EC 1993-1-1 the same column will be considered, but now with an initial bow imperfection defined by a transverse displacement e_0, subjected to bending moment and axial compression. This is illustrated in Figure 5, which also shows the bending moment diagram due to the first-order moments and the second-order moments that result from the lateral deformation [5].

The present approach of EC3-1-1 is based on a linear-additive interaction formula, given by:

$$f\left(\frac{F}{F_u}, \frac{M_y}{M_{uy}}, \frac{M_z}{M_{uz}}\right) \leq 1.0 \qquad (20)$$

Where F, M_y, and M_z are the applied forces, and F_u, M_{uy}, and M_{uz} are the design resistances. This interaction formula treats a three-dimensional case and takes into account the instability phenomena. Luís Simões da Silva et al. [5] (2010) state that: "*The development of the design rules, and in particular those adopted by EC 1993-1-1, is quite complex, as they have to incorporate two instability modes, flexural buckling and lateral-torsional buckling (or a combination of both), different cross-sectional shapes and several shapes of bending moment diagram, among other aspects.*" In the next sections, these aspects will be discussed separately, leading to the design rules that are presented in the EC 1993-1-1.

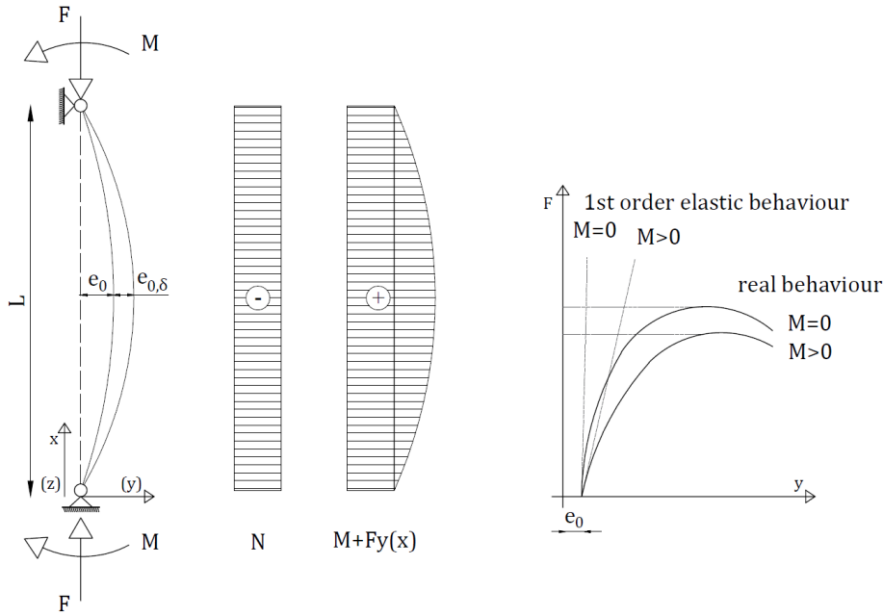

Figure 5: Behaviour of a member subjected to bending and compression [5]

2.2.1 Elastic flexural buckling

A member with an initial imperfection and loaded with axial compression N_{Ed} can be expressed by the following format: [4]

$$\frac{N_{Ed}}{N_{Rd}} + \frac{1}{1 - \frac{N_{Ed}}{F_{cr}}} \cdot \frac{N_{Ed} \cdot e_0}{M_{Rd}} \leq 1 \tag{21}$$

The equivalent geometrical imperfection e_0 is given by: [4]

$$e_0 = \frac{(1-\chi)\left(1-\chi\bar{\lambda}^2\right)}{\chi} \cdot \frac{M_{el,Rd}}{N_{pl,Rd}} \tag{22}$$

Where χ and $\bar{\lambda}$ the reduction factor for flexural buckling and the relative slenderness respectively, as given in section 2.1. $M_{el,Rd}$ and $N_{pl,Rd}$ are the elastic moment resistance and the plastic axial load resistance of the member respectively. When an additional first-order bending moment is acting on the member, equation (21) can be extended, leading to the following equation [4]:

$$\frac{N_{Ed}}{N_{Rd}} + \frac{1}{1 - \frac{N_{Ed}}{F_{cr}}} \cdot \frac{N_{Ed} \cdot e_0}{M_{Rd}} + \frac{M^{II}_{Ed,max}}{M_{Rd}} \leq 1 \tag{23}$$

Where $M_{Ed,max}^{II}$ is the maximum second-order bending moment. With different possible loading cases, it may appear that the maximum second-order bending moment, acts on a different location than the first-order bending moment or the bending moment due to imperfections. This principle is illustrated in Figure 6.

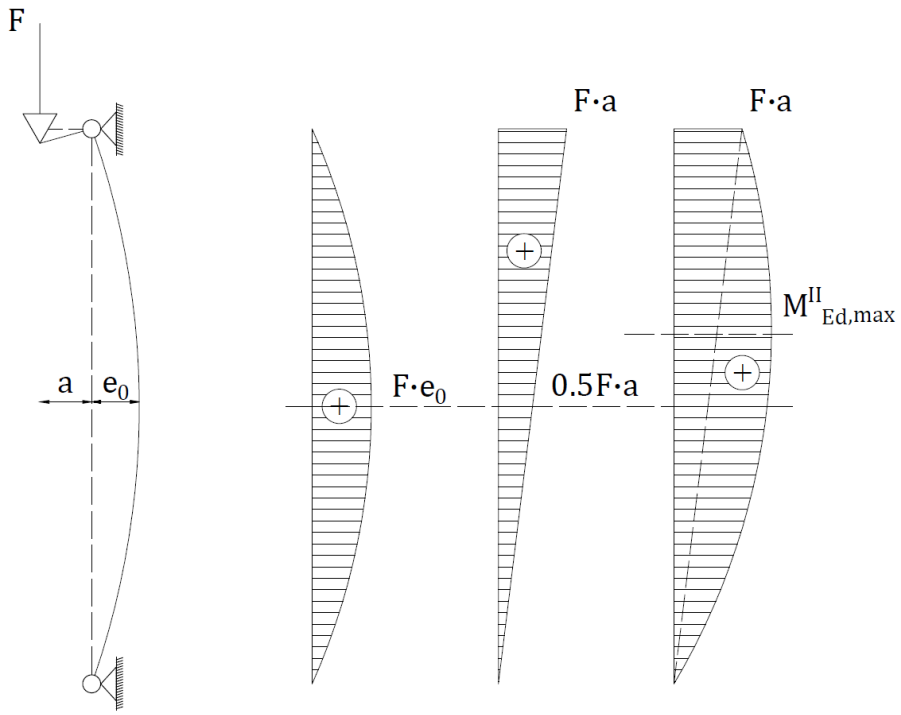

Figure 6:Column with an imperfection loaded on compression and a bending moment at one end [7]

The EC 1993-1-1 avoided the determination of the precise location of $M_{Ed,max}^{II}$, by using the so-called equivalent moment concepts. Boissonade et al. [4] (2010) describes this concept as the following: *"This consists of replacing the actual first-order bending system on the member already subjected to the same axial force by a sinusoidal first-order bending moment that produces the same implified bending moment."*. This leads to the term $C_m \cdot M_{Ed}$, where values for C_m will be discussed later. The maximum second-order bending moment $M_{Ed,max}^{II}$ can then be given as:

$$M_{Ed,max}^{II} = \frac{C_m \cdot M_{Ed}}{1 - \frac{N_{Ed}}{F_{cr}}} \tag{24}$$

With this term for the maximum second-order bending moment $M_{Ed,max}^{II}$, an elastic second-order check of the most loaded cross-section on the member can be derived from [4]:

$$\frac{N_{Ed}}{N_{Rd}} + \frac{1}{1 - \frac{N_{Ed}}{F_{cr}}} \cdot \frac{N_{Ed} \cdot e_0}{M_{Rd}} + \frac{1}{1 - \frac{N_{Ed}}{F_{cr}}} \frac{C_m \cdot M_{Ed}}{M_{Rd}} \leq 1 \tag{25}$$

The EC 1993-1-1 has chosen to rewrite this formulation, for making the classical bucking term appear separately. This is given as the following:

$$\frac{N_{Ed}}{\chi \cdot N_{Rd}} + \mu \frac{1}{1 - \frac{N_{Ed}}{F_{cr}}} \frac{C_m \cdot M_{Ed}}{M_{Rd}} \leq 1 \text{ where } \mu = \frac{1 - \frac{N_{Ed}}{F_{cr}}}{1 - \chi \cdot \frac{N_{Ed}}{F_{cr}}} \tag{26}$$

2.2.2 Elastic-plastic flexural buckling without lateral torsional buckling

Equation (26) is based on elastic second-order theory, so are only valid for class 3 cross-sections. To allow yielding along the member, equation (26) is extended, given by [5]:

$$\frac{N_{Ed}}{\chi \cdot N_{pl,Rd}} + \mu \frac{1}{1 - \frac{N_{Ed}}{N_{cr}}} \cdot \frac{C_m \cdot M_{Ed}}{C \cdot M_{pl,Rd}} \tag{27}$$

In this case, the full plastic moment resistance presents bending moment resistance. Factor C takes into account the plasticity effects in the interaction between mono-axial bending and axial force along the member [4]. This will prevent that the full plastic bending resistance is taken into account, but an intermediate elastic-plastic value, given by $C \cdot M_{pl,Rd}$. This takes care of Class 1 and 2 cross-sections, but also still the class 3 cross-section.

To make a clear presentation for the design rules for members in bending and axial compression they minimized the design rule. The final presentation format of the design rules in the EC 1993-1-1 are the following, presenting three-dimensional design rules:

$$\frac{N_{Ed}}{\frac{\chi_y \cdot N_{Rk}}{\gamma_{m1}}} + k_{yy} \frac{M_{y,Ed} + \Delta M_{y,Ed}}{\chi_{LT} \frac{M_{y,Rk}}{\gamma_{m1}}} + k_{yz} \frac{M_{z,Ed} + \Delta M_{z,Ed}}{\chi_{LT} \frac{M_{z,Rk}}{\gamma_{m1}}} \leq 1 \tag{28}$$

$$\frac{N_{Ed}}{\frac{\chi_z \cdot N_{Rk}}{\gamma_{m1}}} + k_{zy} \frac{M_{y,Ed} + \Delta M_{y,Ed}}{\chi_{LT} \frac{M_{y,Rk}}{\gamma_{m1}}} + k_{zz} \frac{M_{z,Ed} + \Delta M_{z,Ed}}{\chi_{LT} \frac{M_{z,Rk}}{\gamma_{m1}}} \leq 1 \tag{29}$$

For comparison reasons with the NEN 6771, the design rules (28) and (29) for columns loaded in compression and three-dimensional bending is rewritten into a two-dimensional case and given as the following:

$$\frac{N_{Ed}}{\chi \cdot N_{Rd}} + k \frac{M_{Ed}}{M_{Rd}} \leq 1 \tag{30}$$

Where:

N_{Ed} = design value of the load;
N_{Rd} = design value of the plastic load resistance of the column cross-section;
χ = buckling reduction factor;
k = interaction factors depending on the relevant instability and plasticity phenomena [5];
M_{Ed} = design value of the maximum bending moment along the member;
M_{Rd} = elastic or plastic moment resistance of the column, depending on the cross-section class.

Equation (30) is valid for a column under compression and bending in a two-dimensional frame. Compared to equation (28) and (29), the three-dimensional values are converted to a two-dimensional case, and the lateral-torsional buckling reduction factor χ_{LT} and the bending moments due to the shift of the center of gravity ΔM are left out. Reduction factor χ_{LT} is left out because a two-dimensional case is considered and any out-of-plane (lateral torsional buckling) deformations in the FE-model will not be allowed. The reason for letting out bending moment ΔM is that profile classes 1, 2, and 3 will not be considered. According to Table 3, obtained from the EC 1993-1-1, this leads to $\Delta M = 0$.

Table 3: Values for $F_{Rk} = f_y \cdot A_i$, $M_{Rk} = f_y \cdot W_i$ and ΔM from the EC 1993-1-1

CLASS	1	2	3	4
A_i	A	A	A	A_{eff}
W	W_{pl}	W_{pl}	W_{el}	W_{eff}
ΔM_y	0	0	0	$e_{N,yç} \cdot N_{Ed}$

The term $k\frac{M_{Ed}}{M_{Rd}}$ in equation (30) represents the member resistance unity-check due to a bending moment in the column. Value M_{Rd} is given by $M_{Rd} = W \cdot f_y/\gamma_1$, where γ_1 is the partial material factor and the section modulus W can be found in Table 3, where W_{pl} and W_{el} are the plastic and elastic section modulus respectively. Value k in equation (30) represents the interaction factors that depend on the relevant instability and plasticity phenomena [5]. The value k can be derived from two different methods. Back in the days when the EC 1993-1-1 was written, two different teams of researchers treated the field of beam-columns. This has led to two different methods that are both are included in the EC 1993-1-1 as Annex A (method 1) and Annex B (method 2). Both methods consider the most complex behavior of a member subjected to compression and biaxial bending, including all possible interactions and non-linear effects [4]. Boissonade et al. (2006) [4] state that in method 1 all the influences of material and geometrical nonlinearities and interactions between loading components are reflected by separate factors. Boissonade et al. (2006) [4] also state that, in contrast, method 2 uses a reduced number of such factors as a result of globalization of several effects and calibration of the latter based on extensive numerical solutions. Therefore it is stated that Method 1 is better in identifying and accounting for structural effects, and Method 2 is better in focusing on the direct design of standard cases [4].

In the next paragraphs, only the design rules for a two-dimensional case will be discussed, since this is only of interest, where the EC 1993-1-1 offers the design rules for three-dimensional cases. This means that only the equations for the y-y plane are considered. Both Methods from Annex A and B for the derivation of factor K will be discussed in the next paragraphs.

2.2.2.1 Method 1

For Method 1, the following derivation of interaction factor k from Annex A is given:

Table 4: Interaction factor k for Method 1 from EC 1993-1-1 Annex A

INTERACTION FACTORS	ELASTIC SECTIONAL PROPERTIES (CLASS 3 OR 4)	PLASTIC SECTIONAL PROPERTIES (CLASS 1 OR 2)
k	$C_m C_{mLT} \frac{\mu_y}{1 - \frac{N_{Ed}}{F_{cr}}}$	$C_m C_{mLT} \frac{\mu_y}{1 - \frac{N_{Ed}}{F_{cr}}} \frac{1}{C_{yy}}$

According to Method 1, a member is not susceptible to torsional deformations if $I_T \geq I_y$, or when the following condition is verified:

$$\bar{\lambda}_0 \leq 0.2\sqrt{C_1}^4 \sqrt{\left(1 - \frac{N_{Ed}}{N_{cr,z}}\right)\left(1 - \frac{N_{Ed}}{N_{cr,T}}\right)} \tag{31}$$

Since it is stated that lateral-torsional buckling is not considered, equation (31) is stated as true. This gives the following:

$$\text{If } \bar{\lambda}_0 \le 0.2\sqrt{C_1}\cdot\sqrt[4]{\left(1-\frac{N_{Ed}}{N_{cr,z}}\right)\left(1-\frac{N_{Ed}}{N_{cr,T}}\right)} \text{ then: } C_m = C_{m,0}\ ;\ \ C_{mLT} = 1.0 \tag{32}$$

According to Table 4, some additional terms for the derivation of *k* are given. The information includes the calculation of factor C_{yy}, this factor depends on the degree of plasticity in the cross-section at the collapse of the member [5].

$$\mu_y = \frac{1-\frac{N_{Ed}}{F_{cr,y}}}{1-\chi_y\frac{N_{Ed}}{F_{cr,y}}} \tag{33}$$

$$\mathrm{w_y} = \frac{\mathrm{W_{pl,y}}}{\mathrm{W_{el,y}}} \le 1.5 \tag{34}$$

$$n_{pl} = \frac{N_{Ed}}{N_{Rk}/\gamma_{M1}} \tag{35}$$

$$\alpha_{LT} = 1-\frac{I_T}{I_y} \ge 0 \tag{36}$$

$$C_{yy} = 1+(w_y-1)\left[\left(2-\frac{1.6}{w_y}C_{my}{}^2\cdot\bar{\lambda}_{max}-\frac{1.6}{w_y}C_{my}{}^2\cdot\bar{\lambda}_{max}{}^2\right)n_{pl}-b_{LT}\right] \ge \frac{W_{el,y}}{W_{pl,y}} \tag{37}$$

$$b_{LT} = 0.5a_{LT}\cdot\bar{\lambda}_0{}^2\cdot\frac{M_{y,Ed}}{\chi_{LT}\cdot M_{pl,y,Rd}}\cdot\frac{M_{z,Ed}}{M_{pl,z,Rd}} \tag{38}$$

$$\bar{\lambda}_{max} = max\,(\bar{\lambda}_y,\bar{\lambda}_z) \tag{39}$$

$\bar{\lambda}_0$ is the non-dimensional slenderness for lateral-torsional buckling due to uniform bending moment, that is, taking $\Psi_y = 1.0$ in Table 5. Based on the corresponding bending moment diagram, C_m should be derived from Table 5.

Table 5: Equivalent factors of uniform moment C_m

DIAGRAM OF MOMENTS	$C_{m,0}$
M_1 ——— ψM_1 $-1 \le \psi \le 1$	$C_{m,0} = 0.79 + 0.21\Psi_i + 0.36(\Psi_i - 0.33)\frac{N_{Ed}}{F_{cr,i}}$
M(x) M(x)	$C_{m,0} = 1+\left(\frac{\pi^2\cdot E\cdot I_i\cdot\lvert\delta_x\rvert}{L^2\cdot\lvert M_{i,Ed}(x)\rvert}-1\right)\frac{N_{Ed}}{F_{cr,i}}$ *$M_{i,Ed(x)}$ is the maximum moment $M_{y,Ed}$ or $M_{z,Ed}$ according to the first-order analyses* *$\lvert\delta_x\rvert$ is the maximum lateral deflection δ_z (due to $M_{y,Ed}$) or δ_y(due to $M_{z,Ed}$) along the member*

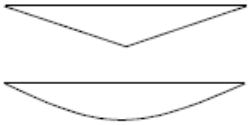	$C_{m,0} = 1 - 0.18\frac{N_{Ed}}{F_{cr,i}}$ $C_{m,0} = 1 + 0.03\frac{N_{Ed}}{F_{cr,i}}$

2.2.2.2 Method 2

Table 6 gives in the interaction factor k in members not susceptible to torsional deformations according to Method 2, Annex B. Table 7 gives the calculation of the equivalent uniform moment factors C_m.

Table 6: interaction factors k in members not susceptible to torsional deformations according to Method 2 [5]

INTERA-CTION FACTOR	TYPE OF SECTION	ELASTIC SECTIONAL PROPERTIES (CLASS 3 OR 4 SECTIONS)	PLASTIC SECTIONAL PROPERTIES (CLASS 1 OR 2 SECTIONS)
k_{yy}	I or H sections and rectangular hollow sections	$C_m\left(1 + 0.6\bar{\lambda}_y \frac{N_{Ed}}{\chi_y \cdot N_{Rk}/\gamma_{M1}}\right)$ $\leq C_m\left(1 + 0.6\frac{N_{Ed}}{\chi_y \cdot N_{Rk}/\gamma_{M1}}\right)$	$C_m\left(1 + (\bar{\lambda}_y - 0.2)\frac{N_{Ed}}{\chi_y \cdot N_{Rk}/\gamma_{M1}}\right)$ $\leq C_m\left(1 + 0.8\frac{N_{Ed}}{\chi_y \cdot N_{Rk}/\gamma_{M1}}\right)$

Table 7: Equivalent factors of uniform moment C_m

DIAGRAM OF MOMENTS	RANGE		C_m	
			UNIFORM LOADING	CONCENTRATED LOAD
	$-1 \leq \Psi \leq 1$		$0.6 + 0.4\Psi \geq 0.4$	
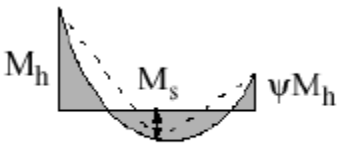 $\alpha_s = M_s/M_h$	$0 \leq \alpha_s \leq 1$	$-1 \leq \Psi \leq 1$	$0.2 + 0.8\alpha_s \geq 0.4$	$0.2 + 0.8\alpha_s \geq 0.4$
	$-1 \leq \alpha_s \leq 0$	$0 \leq \Psi \leq 1$	$0.1 - 0.8\alpha_s \geq 0.4$	$-0.8\alpha_s \geq 0.4$
		$-1 \leq \Psi \leq 0$	$0.1(1 - \Psi) - 0.8\alpha_s \geq 0.4$	$0.2(-\Psi) - 0.8\alpha_s \geq 0.4$
 $\alpha_h = M_h/M_s$	$-1 \leq \alpha_h \leq 1$	$-1 \leq \Psi \leq 1$	$0.95 + 0.05\alpha_h$	$0.90 + 0.10\alpha_h$
	$-1 \leq \alpha_h \leq 1$	$0 \leq \Psi \leq 1$	$0.95 + 0.05\alpha_h$	$0.90 + 0.10\alpha_h$
		$-1 \leq \Psi \leq 0$	$0.95 + 0.05\alpha_h(1 + 2\Psi)$	$0.90 + 0.10\alpha_h(1 + 2\Psi)$
In the calculation of α_s or α_h parameters, a hogging moment should be taken as negative and a sagging moment should be taken as positive.				
For members with sway buckling mode, the equivalent uniform moment factor should be taken as C_m =0.9				

Factors C_m and C_{mLT} should be obtained from the diagram of bending moments between the relevant braced sections, according to the following:		
Moment factor	Bending axis	Points braced in direction
C_m	y-y	z-z

For this graduation project, the statement "*For members with sway buckling mode, the equivalent uniform moment factor should be taken as C_m =0.9*" will be very important.

3 BIBLIOGRAPHY

[1] Nederlands Normalisatie-instituut, "NEN 6770 - steel structures - basic requirements and basic rules for calculation of predominantly staticaly loaded structures," Delft, 1997.

[2] L. F. Geschwindner, "A Practical Look at Frame Analysis, Stability and Leaning Columns," *Engineering Journal,* vol. Fourth Quarter, pp. 167-181, 2002.

[3] American Institute of Steel Construction, Inc. (AISC), "Load and Resistance Factor Deisng Specification for Structural Steel Buildings," AISC, Chicago, 19999.

[4] N. Boissonnade, R. Greiner, J. Jaspart and J. Lindner, Rules for Member Stability in EN 1993-1-1; Background documentation and design guidelines, Mem Martins, Portugal: ECCS, 2006.

[5] L. Simões da Silva, R. Simões and H. Gervásio, "Eurocode 3: Design of Steel Structures; Part 1-1: General rules and rules for buildings," ECCS Eurocode Design Manuals, Mem Martins, Portugal, 2010.

[6] Comité Européen de Normalisation, "Eurocode 3: Design of steel structures- Part 1-1: General rules and rules for buildings," CEN, Brussels, 2005.

[7] H. Snijder and H. Steenbergen, Stabiliteit 3; Staven belast op druk en buiging.

APPENDIX B – INPUT FEM MODEL PARAMETRIC STUDY

In the sheets below, the input is given for the parametric FE-model script. The sheets are sub-divided in:

- Frames A, A-NL, A-V, A-H, A-NLH, and A-VH
- Frame B

id	Frame properties													Section properties									
id																							
id	E	ν	F	Q	H	$f_{y,d}$	f_u	ε	h	b1	b2	m		profile 1	h1	P1h	P1b	P1w	P1tf	I_y	$W_{y,el}$	$W_{y,pl}$	A
id	N/mm²	[-]	N	N	N	N/mm²	N/mm²	%	mm	mm	mm	[-]			mm	mm	mm	mm	mm	mm⁴	mm³	mm³	mm²
01	210000	0.3	1000000	1000000	0	355	490	0.06429	5000	5000	5000	3	-	HEA300	290	262	300	8.5	14	1.7285E+08	1.1920E+06	1.3051E+06	10627
02	210000	0.3	1000000	1000000	0	355	490	0.06429	5000	7500	7500	3	-	HEA300	290	262	300	8.5	14	1.7285E+08	1.1920E+06	1.3051E+06	10627
03	210000	0.3	1000000	1000000	0	355	490	0.06429	5000	10000	10000	3	-	HEA300	290	262	300	8.5	14	1.7285E+08	1.1920E+06	1.3051E+06	10627
A1	210000	0.3	1000000	1000000	0	355	490	0.06429	3000	3000	3000	3	-	HEA120	114	98	120	5	8	5.7957E+06	1.0168E+05	1.1377E+05	2410
A2	210000	0.3	1000000	1000000	0	355	490	0.06429	3000	4500	4500	3	-	HEA120	114	98	120	5	8	5.7957E+06	1.0168E+05	1.1377E+05	2410
A3	210000	0.3	1000000	1000000	0	355	490	0.06429	3000	6000	6000	3	-	HEA120	114	98	120	5	8	5.7957E+06	1.0168E+05	1.1377E+05	2410
A4	210000	0.3	1000000	1000000	0	355	490	0.06429	3000	3000	3000	3	-	HEA160	152	134	160	6	9	1.5946E+07	2.0981E+05	2.3285E+05	3684
A5	210000	0.3	1000000	1000000	0	355	490	0.06429	3000	4500	4500	3	-	HEA160	152	134	160	6	9	1.5946E+07	2.0981E+05	2.3285E+05	3684
A6	210000	0.3	1000000	1000000	0	355	490	0.06429	3000	6000	6000	3	-	HEA160	152	134	160	6	9	1.5946E+07	2.0981E+05	2.3285E+05	3684
A7	210000	0.3	1000000	1000000	0	355	490	0.06429	3000	3000	3000	3	-	HEA220	210	188	220	7	11	5.1842E+07	4.9373E+05	5.4343E+05	6156
A8	210000	0.3	1000000	1000000	0	355	490	0.06429	3000	4500	4500	3	-	HEA220	210	188	220	7	11	5.1842E+07	4.9373E+05	5.4343E+05	6156
A9	210000	0.3	1000000	1000000	0	355	490	0.06429	3000	6000	6000	3	-	HEA220	210	188	220	7	11	5.1842E+07	4.9373E+05	5.4343E+05	6156
A10	210000	0.3	1000000	1000000	0	355	490	0.06429	3000	3000	3000	3	-	HEA280	270	244	280	8	13	1.3000E+08	9.6294E+05	1.0546E+06	9232
A11	210000	0.3	1000000	1000000	0	355	490	0.06429	3000	4500	4500	3	-	HEA280	270	244	280	8	13	1.3000E+08	9.6294E+05	1.0546E+06	9232
A12	210000	0.3	1000000	1000000	0	355	490	0.06429	3000	6000	6000	3	-	HEA280	270	244	280	8	13	1.3000E+08	9.6294E+05	1.0546E+06	9232
id																							
01-NL	210000	0.3	1000000	0	0	355	490	0.06429	5000	5000	5000	3	-	HEA300	290	262	300	8.5	14	1.7285E+08	1.1920E+06	1.3051E+06	10627
02-NL	210000	0.3	1000000	0	0	355	490	0.06429	5000	7500	7500	3	-	HEA300	290	262	300	8.5	14	1.7285E+08	1.1920E+06	1.3051E+06	10627
03-NL	210000	0.3	1000000	0	0	355	490	0.06429	5000	10000	10000	3	-	HEA300	290	262	300	8.5	14	1.7285E+08	1.1920E+06	1.3051E+06	10627
A1-NL	210000	0.3	1000000	0	0	355	490	0.06429	3000	3000	3000	3	-	HEA120	114	98	120	5	8	5.7957E+06	1.0168E+05	1.1377E+05	2410
A2-NL	210000	0.3	1000000	0	0	355	490	0.06429	3000	4500	4500	3	-	HEA120	114	98	120	5	8	5.7957E+06	1.0168E+05	1.1377E+05	2410
A3-NL	210000	0.3	1000000	0	0	355	490	0.06429	3000	6000	6000	3	-	HEA120	114	98	120	5	8	5.7957E+06	1.0168E+05	1.1377E+05	2410
A4-NL	210000	0.3	1000000	0	0	355	490	0.06429	3000	3000	3000	3	-	HEA160	152	134	160	6	9	1.5946E+07	2.0981E+05	2.3285E+05	3684
A5-NL	210000	0.3	1000000	0	0	355	490	0.06429	3000	4500	4500	3	-	HEA160	152	134	160	6	9	1.5946E+07	2.0981E+05	2.3285E+05	3684
A6-NL	210000	0.3	1000000	0	0	355	490	0.06429	3000	6000	6000	3	-	HEA160	152	134	160	6	9	1.5946E+07	2.0981E+05	2.3285E+05	3684
A7-NL	210000	0.3	1000000	0	0	355	490	0.06429	3000	3000	3000	3	-	HEA220	210	188	220	7	11	5.1842E+07	4.9373E+05	5.4343E+05	6156
A8-NL	210000	0.3	1000000	0	0	355	490	0.06429	3000	4500	4500	3	-	HEA220	210	188	220	7	11	5.1842E+07	4.9373E+05	5.4343E+05	6156
A9-NL	210000	0.3	1000000	0	0	355	490	0.06429	3000	6000	6000	3	-	HEA220	210	188	220	7	11	5.1842E+07	4.9373E+05	5.4343E+05	6156
A10-NL	210000	0.3	1000000	0	0	355	490	0.06429	3000	3000	3000	3	-	HEA280	270	244	280	8	13	1.3000E+08	9.6294E+05	1.0546E+06	9232
A11-NL	210000	0.3	1000000	0	0	355	490	0.06429	3000	4500	4500	3	-	HEA280	270	244	280	8	13	1.3000E+08	9.6294E+05	1.0546E+06	9232
A12-NL	210000	0.3	1000000	0	0	355	490	0.06429	3000	6000	6000	3	-	HEA280	270	244	280	8	13	1.3000E+08	9.6294E+05	1.0546E+06	9232
id																							
01-V	210000	0.3	1000000	10000000	0	355	490	0.06429	5000	5000	5000	3	-	HEA300	290	262	300	8.5	14	1.7285E+08	1.1920E+06	1.3051E+06	10627
02-V	210000	0.3	1000000	10000000	0	355	490	0.06429	5000	7500	7500	3	-	HEA300	290	262	300	8.5	14	1.7285E+08	1.1920E+06	1.3051E+06	10627
03-V	210000	0.3	1000000	10000000	0	355	490	0.06429	5000	10000	10000	3	-	HEA300	290	262	300	8.5	14	1.7285E+08	1.1920E+06	1.3051E+06	10627
A1-V	210000	0.3	1000000	10000000	0	355	490	0.06429	3000	3000	3000	3	-	HEA120	114	98	120	5	8	5.7957E+06	1.0168E+05	1.1377E+05	2410
A2-V	210000	0.3	1000000	10000000	0	355	490	0.06429	3000	4500	4500	3	-	HEA120	114	98	120	5	8	5.7957E+06	1.0168E+05	1.1377E+05	2410
A3-V	210000	0.3	1000000	10000000	0	355	490	0.06429	3000	6000	6000	3	-	HEA120	114	98	120	5	8	5.7957E+06	1.0168E+05	1.1377E+05	2410
A4-V	210000	0.3	1000000	10000000	0	355	490	0.06429	3000	3000	3000	3	-	HEA160	152	134	160	6	9	1.5946E+07	2.0981E+05	2.3285E+05	3684
A5-V	210000	0.3	1000000	10000000	0	355	490	0.06429	3000	4500	4500	3	-	HEA160	152	134	160	6	9	1.5946E+07	2.0981E+05	2.3285E+05	3684
A6-V	210000	0.3	1000000	10000000	0	355	490	0.06429	3000	6000	6000	3	-	HEA160	152	134	160	6	9	1.5946E+07	2.0981E+05	2.3285E+05	3684
A7-V	210000	0.3	1000000	10000000	0	355	490	0.06429	3000	3000	3000	3	-	HEA220	210	188	220	7	11	5.1842E+07	4.9373E+05	5.4343E+05	6156
A8-V	210000	0.3	1000000	10000000	0	355	490	0.06429	3000	4500	4500	3	-	HEA220	210	188	220	7	11	5.1842E+07	4.9373E+05	5.4343E+05	6156
A9-V	210000	0.3	1000000	10000000	0	355	490	0.06429	3000	6000	6000	3	-	HEA220	210	188	220	7	11	5.1842E+07	4.9373E+05	5.4343E+05	6156
A10-V	210000	0.3	1000000	10000000	0	355	490	0.06429	3000	3000	3000	3	-	HEA280	270	244	280	8	13	1.3000E+08	9.6294E+05	1.0546E+06	9232
A11-V	210000	0.3	1000000	10000000	0	355	490	0.06429	3000	4500	4500	3	-	HEA280	270	244	280	8	13	1.3000E+08	9.6294E+05	1.0546E+06	9232
A12-V	210000	0.3	1000000	10000000	0	355	490	0.06429	3000	6000	6000	3	-	HEA280	270	244	280	8	13	1.3000E+08	9.6294E+05	1.0546E+06	9232
id																							
01-H	210000	0.3	1000000	1000000	12500	355	490	0.06429	5000	5000	5000	3	-	HEA300	290	262	300	8.5	14	1.7285E+08	1.1920E+06	1.3051E+06	10627
02-H	210000	0.3	1000000	1000000	18750	355	490	0.06429	5000	7500	7500	3	-	HEA300	290	262	300	8.5	14	1.7285E+08	1.1920E+06	1.3051E+06	10627
03-H	210000	0.3	1000000	1000000	25000	355	490	0.06429	5000	10000	10000	3	-	HEA300	290	262	300	8.5	14	1.7285E+08	1.1920E+06	1.3051E+06	10627
A1-H	210000	0.3	1000000	1000000	4500	355	490	0.06429	3000	3000	3000	3	-	HEA120	114	98	120	5	8	5.7957E+06	1.0168E+05	1.1377E+05	2410
A2-H	210000	0.3	1000000	1000000	6750	355	490	0.06429	3000	4500	4500	3	-	HEA120	114	98	120	5	8	5.7957E+06	1.0168E+05	1.1377E+05	2410
A3-H	210000	0.3	1000000	1000000	9000	355	490	0.06429	3000	6000	6000	3	-	HEA120	114	98	120	5	8	5.7957E+06	1.0168E+05	1.1377E+05	2410
A4-H	210000	0.3	1000000	1000000	4500	355	490	0.06429	3000	3000	3000	3	-	HEA160	152	134	160	6	9	1.5946E+07	2.0981E+05	2.3285E+05	3684
A5-H	210000	0.3	1000000	1000000	6750	355	490	0.06429	3000	4500	4500	3	-	HEA160	152	134	160	6	9	1.5946E+07	2.0981E+05	2.3285E+05	3684
A6-H	210000	0.3	1000000	1000000	9000	355	490	0.06429	3000	6000	6000	3	-	HEA160	152	134	160	6	9	1.5946E+07	2.0981E+05	2.3285E+05	3684
A7-H	210000	0.3	1000000	1000000	4500	355	490	0.06429	3000	3000	3000	3	-	HEA220	210	188	220	7	11	5.1842E+07	4.9373E+05	5.4343E+05	6156
A8-H	210000	0.3	1000000	1000000	6750	355	490	0.06429	3000	4500	4500	3	-	HEA220	210	188	220	7	11	5.1842E+07	4.9373E+05	5.4343E+05	6156
A9-H	210000	0.3	1000000	1000000	9000	355	490	0.06429	3000	6000	6000	3	-	HEA220	210	188	220	7	11	5.1842E+07	4.9373E+05	5.4343E+05	6156
A10-H	210000	0.3	1000000	1000000	4500	355	490	0.06429	3000	3000	3000	3	-	HEA280	270	244	280	8	13	1.3000E+08	9.6294E+05	1.0546E+06	9232
A11-H	210000	0.3	1000000	1000000	6750	355	490	0.06429	3000	4500	4500	3	-	HEA280	270	244	280	8	13	1.3000E+08	9.6294E+05	1.0546E+06	9232
A12-H	210000	0.3	1000000	1000000	9000	355	490	0.06429	3000	6000	6000	3	-	HEA280	270	244	280	8	13	1.3000E+08	9.6294E+05	1.0546E+06	9232
id																							
01-VH	210000	0.3	1000000	10000000	12500	355	490	0.06429	5000	5000	5000	3	-	HEA300	290	262	300	8.5	14	1.7285E+08	1.1920E+06	1.3051E+06	10627
02-VH	210000	0.3	1000000	10000000	18750	355	490	0.06429	5000	7500	7500	3	-	HEA300	290	262	300	8.5	14	1.7285E+08	1.1920E+06	1.3051E+06	10627
03-VH	210000	0.3	1000000	10000000	25000	355	490	0.06429	5000	10000	10000	3	-	HEA300	290	262	300	8.5	14	1.7285E+08	1.1920E+06	1.3051E+06	10627
A1-VH	210000	0.3	1000000	10000000	4500	355	490	0.06429	3000	3000	3000	3	-	HEA120	114	98	120	5	8	5.7957E+06	1.0168E+05	1.1377E+05	2410
A2-VH	210000	0.3	1000000	10000000	6750	355	490	0.06429	3000	4500	4500	3	-	HEA120	114	98	120	5	8	5.7957E+06	1.0168E+05	1.1377E+05	2410
A3-VH	210000	0.3	1000000	10000000	9000	355	490	0.06429	3000	6000	6000	3	-	HEA120	114	98	120	5	8	5.7957E+06	1.0168E+05	1.1377E+05	2410
A4-VH	210000	0.3	1000000	10000000	4500	355	490	0.06429	3000	3000	3000	3	-	HEA160	152	134	160	6	9	1.5946E+07	2.0981E+05	2.3285E+05	3684
A5-VH	210000	0.3	1000000	10000000	6750	355	490	0.06429	3000	4500	4500	3	-	HEA160	152	134	160	6	9	1.5946E+07	2.0981E+05	2.3285E+05	3684
A6-VH	210000	0.3	1000000	10000000	9000	355	490	0.06429	3000	6000	6000	3	-	HEA160	152	134	160	6	9	1.5946E+07	2.0981E+05	2.3285E+05	3684
A7-VH	210000	0.3	1000000	10000000	4500	355	490	0.06429	3000	3000	3000	3	-	HEA220	210	188	220	7	11	5.1842E+07	4.9373E+05	5.4343E+05	6156
A8-VH	210000	0.3	1000000	10000000	6750	355	490	0.06429	3000	4500	4500	3	-	HEA220	210	188	220	7	11	5.1842E+07	4.9373E+05	5.4343E+05	6156
A9-VH	210000	0.3	1000000	10000000	9000	355	490	0.06429	3000	6000	6000	3	-	HEA220	210	188	220	7	11	5.1842E+07	4.9373E+05	5.4343E+05	6156
A10-VH	210000	0.3	1000000	10000000	4500	355	490	0.06429	3000	3000	3000	3	-	HEA280	270	244	280	8	13	1.3000E+08	9.6294E+05	1.0546E+06	9232
A11-VH	210000	0.3	1000000	10000000	6750	355	490	0.06429	3000	4500	4500	3	-	HEA280	270	244	280	8	13	1.3000E+08	9.6294E+05	1.0546E+06	9232
A12-VH	210000	0.3	1000000	10000000	9000	355	490	0.06429	3000	6000	6000	3	-	HEA280	270	244	280	8	13	1.3000E+08	9.6294E+05	1.0546E+06	9232
id																							
01-NLH	210000	0.3	1000000	0	12500	355	490	0.06429	5000	5000	5000	3	-	HEA300	290	262	300	8.5	14	1.7285E+08	1.1920E+06	1.3051E+06	10627
02-NLH	210000	0.3	1000000	0	18750	355	490	0.06429	5000	7500	7500	3	-	HEA300	290	262	300	8.5	14	1.7285E+08	1.1920E+06	1.3051E+06	10627
03-NLH	210000	0.3	1000000	0	25000	355	490	0.06429	5000	10000	10000	3	-	HEA300	290	262	300	8.5	14	1.7285E+08	1.1920E+06	1.3051E+06	10627
A1-NLH	210000	0.3	1000000	0	4500	355	490	0.06429	3000	3000	3000	3	-	HEA120	114	98	120	5	8	5.7957E+06	1.0168E+05	1.1377E+05	2410
A2-NLH	210000	0.3	1000000	0	6750	355	490	0.06429	3000	4500	4500	3	-	HEA120	114	98	120	5	8	5.7957E+06	1.0168E+05	1.1377E+05	2410
A3-NLH	210000	0.3	1000000	0	9000	355	490	0.06429	3000	6000	6000	3	-	HEA120	114	98	120	5	8	5.7957E+06	1.0168E+05	1.1377E+05	2410
A4-NLH	210000	0.3	1000000	0	4500	355	490	0.06429	3000	3000	3000	3	-	HEA160	152	134	160	6	9	1.5946E+07	2.0981E+05	2.3285E+05	3684
A5-NLH	210000	0.3	1000000	0	6750	355	490	0.06429	3000	4500	4500	3	-	HEA160	152	134	160	6	9	1.5946E+07	2.0981E+05	2.3285E+05	3684
A6-NLH	210000	0.3	1000000	0	9000	355	490	0.06429	3000	6000	6000	3	-	HEA160	152	134	160	6	9	1.5946E+07	2.0981E+05	2.3285E+05	3684
A7-NLH	210000	0.3	1000000	0	4500	355	490	0.06429	3000	3000	3000	3	-	HEA220	210	188	220	7	11	5.1842E+07	4.9373E+05	5.4343E+05	6156
A8-NLH	210000	0.3	1000000	0	6750	355	490	0.06429	3000	4500	4500	3	-	HEA220	210	188	220	7	11	5.1842E+07	4.9373E+05	5.4343E+05	6156
A9-NLH	210000	0.3	1000000	0	9000	355	490	0.06429	3000	6000	6000	3	-	HEA220	210	188	220	7	11	5.1842E+07	4.9373E+05	5.4343E+05	6156
A10-NLH	210000	0.3	1000000	0	4500	355	490	0.06429	3000	3000	3000	3	-	HEA280	270	244	280	8	13	1.3000E+08	9.6294E+05	1.0546E+06	9232
A11-NLH	210000	0.3	1000000	0	6750	355	490	0.06429	3000	4500	4500	3	-	HEA280	270	244	280	8	13	1.3000E+08	9.6294E+05	1.0546E+06	9232
A12-NLH	210000	0.3	1000000	0	9000	355	490	0.06429	3000	6000	6000	3	-	HEA280	270	244	280	8	13	1.3000E+08	9.6294E+05	1.0546E+06	9232
id	1	2	3	4	5	6	7	8	9	10	11	12	13	14	15	16	17	18	19	20	21	22	23

id	Section properties																				
id																					
id	section class	profile 2	h2	P2h	P2b	P2w	P2tf	I_y	$W_{y,el}$	$W_{y,pl}$	A	section class	profile 4	h4	P4h	P4b	P4w	P4tf	I_y	$W_{y,el}$	$W_{y,pl}$
id	[-]		mm	mm	mm	mm	mm	mm^4	mm^2	mm^3	mm^2	[-]		mm	mm	mm	mm	mm	mm^4	mm^2	mm^3
01	3	HEA300	290	262	300	8.5	14	1.7285E+08	1.1920E+06	1.3051E+06	10627	3	HEA300	290	262	300	8.5	14	1.7285E+08	1.1920E+06	1.3051E+06
02	3	HEA300	290	262	300	8.5	14	1.7285E+08	1.1920E+06	1.3051E+06	10627	3	HEA300	290	262	300	8.5	14	1.7285E+08	1.1920E+06	1.3051E+06
03	3	HEA300	290	262	300	8.5	14	1.7285E+08	1.1920E+06	1.3051E+06	10627	3	HEA300	290	262	300	8.5	14	1.7285E+08	1.1920E+06	1.3051E+06
A1	1	HEA120	114	98	120	5	8	5.7957E+06	1.0168E+05	1.1377E+05	2410	1	HEA120	114	98	120	5	8	5.7957E+06	1.0168E+05	1.1377E+05
A2	1	HEA120	114	98	120	5	8	5.7957E+06	1.0168E+05	1.1377E+05	2410	1	HEA120	114	98	120	5	8	5.7957E+06	1.0168E+05	1.1377E+05
A3	1	HEA120	114	98	120	5	8	5.7957E+06	1.0168E+05	1.1377E+05	2410	1	HEA120	114	98	120	5	8	5.7957E+06	1.0168E+05	1.1377E+05
A4	1	HEA160	152	134	160	6	9	1.5946E+07	2.0981E+05	2.3285E+05	3684	1	HEA160	152	134	160	6	9	1.5946E+07	2.0981E+05	2.3285E+05
A5	1	HEA160	152	134	160	6	9	1.5946E+07	2.0981E+05	2.3285E+05	3684	1	HEA160	152	134	160	6	9	1.5946E+07	2.0981E+05	2.3285E+05
A6	1	HEA160	152	134	160	6	9	1.5946E+07	2.0981E+05	2.3285E+05	3684	1	HEA160	152	134	160	6	9	1.5946E+07	2.0981E+05	2.3285E+05
A7	2	HEA220	210	188	220	7	11	5.1842E+07	4.9373E+05	5.4343E+05	6156	2	HEA220	210	188	220	7	11	5.1842E+07	4.9373E+05	5.4343E+05
A8	2	HEA220	210	188	220	7	11	5.1842E+07	4.9373E+05	5.4343E+05	6156	2	HEA220	210	188	220	7	11	5.1842E+07	4.9373E+05	5.4343E+05
A9	2	HEA220	210	188	220	7	11	5.1842E+07	4.9373E+05	5.4343E+05	6156	2	HEA220	210	188	220	7	11	5.1842E+07	4.9373E+05	5.4343E+05
A10	3	HEA280	270	244	280	8	13	1.3000E+08	9.6294E+05	1.0546E+06	9232	3	HEA280	270	244	280	8	13	1.3000E+08	9.6294E+05	1.0546E+06
A11	3	HEA280	270	244	280	8	13	1.3000E+08	9.6294E+05	1.0546E+06	9232	3	HEA280	270	244	280	8	13	1.3000E+08	9.6294E+05	1.0546E+06
A12	3	HEA280	270	244	280	8	13	1.3000E+08	9.6294E+05	1.0546E+06	9232	3	HEA280	270	244	280	8	13	1.3000E+08	9.6294E+05	1.0546E+06
id																					
01-NL	3	HEA300	290	262	300	8.5	14	1.7285E+08	1.1920E+06	1.3051E+06	10627	3	HEA300	290	262	300	8.5	14	1.7285E+08	1.1920E+06	1.3051E+06
02-NL	3	HEA300	290	262	300	8.5	14	1.7285E+08	1.1920E+06	1.3051E+06	10627	3	HEA300	290	262	300	8.5	14	1.7285E+08	1.1920E+06	1.3051E+06
03-NL	3	HEA300	290	262	300	8.5	14	1.7285E+08	1.1920E+06	1.3051E+06	10627	3	HEA300	290	262	300	8.5	14	1.7285E+08	1.1920E+06	1.3051E+06
A1-NL	1	HEA120	114	98	120	5	8	5.7957E+06	1.0168E+05	1.1377E+05	2410	1	HEA120	114	98	120	5	8	5.7957E+06	1.0168E+05	1.1377E+05
A2-NL	1	HEA120	114	98	120	5	8	5.7957E+06	1.0168E+05	1.1377E+05	2410	1	HEA120	114	98	120	5	8	5.7957E+06	1.0168E+05	1.1377E+05
A3-NL	1	HEA120	114	98	120	5	8	5.7957E+06	1.0168E+05	1.1377E+05	2410	1	HEA120	114	98	120	5	8	5.7957E+06	1.0168E+05	1.1377E+05
A4-NL	1	HEA160	152	134	160	6	9	1.5946E+07	2.0981E+05	2.3285E+05	3684	1	HEA160	152	134	160	6	9	1.5946E+07	2.0981E+05	2.3285E+05
A5-NL	1	HEA160	152	134	160	6	9	1.5946E+07	2.0981E+05	2.3285E+05	3684	1	HEA160	152	134	160	6	9	1.5946E+07	2.0981E+05	2.3285E+05
A6-NL	1	HEA160	152	134	160	6	9	1.5946E+07	2.0981E+05	2.3285E+05	3684	1	HEA160	152	134	160	6	9	1.5946E+07	2.0981E+05	2.3285E+05
A7-NL	2	HEA220	210	188	220	7	11	5.1842E+07	4.9373E+05	5.4343E+05	6156	2	HEA220	210	188	220	7	11	5.1842E+07	4.9373E+05	5.4343E+05
A8-NL	2	HEA220	210	188	220	7	11	5.1842E+07	4.9373E+05	5.4343E+05	6156	2	HEA220	210	188	220	7	11	5.1842E+07	4.9373E+05	5.4343E+05
A9-NL	2	HEA220	210	188	220	7	11	5.1842E+07	4.9373E+05	5.4343E+05	6156	2	HEA220	210	188	220	7	11	5.1842E+07	4.9373E+05	5.4343E+05
A10-NL	3	HEA280	270	244	280	8	13	1.3000E+08	9.6294E+05	1.0546E+06	9232	3	HEA280	270	244	280	8	13	1.3000E+08	9.6294E+05	1.0546E+06
A11-NL	3	HEA280	270	244	280	8	13	1.3000E+08	9.6294E+05	1.0546E+06	9232	3	HEA280	270	244	280	8	13	1.3000E+08	9.6294E+05	1.0546E+06
A12-NL	3	HEA280	270	244	280	8	13	1.3000E+08	9.6294E+05	1.0546E+06	9232	3	HEA280	270	244	280	8	13	1.3000E+08	9.6294E+05	1.0546E+06
id																					
01-V	3	HEA300	290	262	300	8.5	14	1.7285E+08	1.1920E+06	1.3051E+06	10627	3	HEA300	290	262	300	8.5	14	1.7285E+08	1.1920E+06	1.3051E+06
02-V	3	HEA300	290	262	300	8.5	14	1.7285E+08	1.1920E+06	1.3051E+06	10627	3	HEA300	290	262	300	8.5	14	1.7285E+08	1.1920E+06	1.3051E+06
03-V	3	HEA300	290	262	300	8.5	14	1.7285E+08	1.1920E+06	1.3051E+06	10627	3	HEA300	290	262	300	8.5	14	1.7285E+08	1.1920E+06	1.3051E+06
A1-V	1	HEA120	114	98	120	5	8	5.7957E+06	1.0168E+05	1.1377E+05	2410	1	HEA120	114	98	120	5	8	5.7957E+06	1.0168E+05	1.1377E+05
A2-V	1	HEA120	114	98	120	5	8	5.7957E+06	1.0168E+05	1.1377E+05	2410	1	HEA120	114	98	120	5	8	5.7957E+06	1.0168E+05	1.1377E+05
A3-V	1	HEA120	114	98	120	5	8	5.7957E+06	1.0168E+05	1.1377E+05	2410	1	HEA120	114	98	120	5	8	5.7957E+06	1.0168E+05	1.1377E+05
A4-V	1	HEA160	152	134	160	6	9	1.5946E+07	2.0981E+05	2.3285E+05	3684	1	HEA160	152	134	160	6	9	1.5946E+07	2.0981E+05	2.3285E+05
A5-V	1	HEA160	152	134	160	6	9	1.5946E+07	2.0981E+05	2.3285E+05	3684	1	HEA160	152	134	160	6	9	1.5946E+07	2.0981E+05	2.3285E+05
A6-V	1	HEA160	152	134	160	6	9	1.5946E+07	2.0981E+05	2.3285E+05	3684	1	HEA160	152	134	160	6	9	1.5946E+07	2.0981E+05	2.3285E+05
A7-V	2	HEA220	210	188	220	7	11	5.1842E+07	4.9373E+05	5.4343E+05	6156	2	HEA220	210	188	220	7	11	5.1842E+07	4.9373E+05	5.4343E+05
A8-V	2	HEA220	210	188	220	7	11	5.1842E+07	4.9373E+05	5.4343E+05	6156	2	HEA220	210	188	220	7	11	5.1842E+07	4.9373E+05	5.4343E+05
A9-V	2	HEA220	210	188	220	7	11	5.1842E+07	4.9373E+05	5.4343E+05	6156	2	HEA220	210	188	220	7	11	5.1842E+07	4.9373E+05	5.4343E+05
A10-V	3	HEA280	270	244	280	8	13	1.3000E+08	9.6294E+05	1.0546E+06	9232	3	HEA280	270	244	280	8	13	1.3000E+08	9.6294E+05	1.0546E+06
A11-V	3	HEA280	270	244	280	8	13	1.3000E+08	9.6294E+05	1.0546E+06	9232	3	HEA280	270	244	280	8	13	1.3000E+08	9.6294E+05	1.0546E+06
A12-V	3	HEA280	270	244	280	8	13	1.3000E+08	9.6294E+05	1.0546E+06	9232	3	HEA280	270	244	280	8	13	1.3000E+08	9.6294E+05	1.0546E+06
id																					
01-H	3	HEA300	290	262	300	8.5	14	1.7285E+08	1.1920E+06	1.3051E+06	10627	3	HEA300	290	262	300	8.5	14	1.7285E+08	1.1920E+06	1.3051E+06
02-H	3	HEA300	290	262	300	8.5	14	1.7285E+08	1.1920E+06	1.3051E+06	10627	3	HEA300	290	262	300	8.5	14	1.7285E+08	1.1920E+06	1.3051E+06
03-H	3	HEA300	290	262	300	8.5	14	1.7285E+08	1.1920E+06	1.3051E+06	10627	3	HEA300	290	262	300	8.5	14	1.7285E+08	1.1920E+06	1.3051E+06
A1-H	1	HEA120	114	98	120	5	8	5.7957E+06	1.0168E+05	1.1377E+05	2410	1	HEA120	114	98	120	5	8	5.7957E+06	1.0168E+05	1.1377E+05
A2-H	1	HEA120	114	98	120	5	8	5.7957E+06	1.0168E+05	1.1377E+05	2410	1	HEA120	114	98	120	5	8	5.7957E+06	1.0168E+05	1.1377E+05
A3-H	1	HEA120	114	98	120	5	8	5.7957E+06	1.0168E+05	1.1377E+05	2410	1	HEA120	114	98	120	5	8	5.7957E+06	1.0168E+05	1.1377E+05
A4-H	1	HEA160	152	134	160	6	9	1.5946E+07	2.0981E+05	2.3285E+05	3684	1	HEA160	152	134	160	6	9	1.5946E+07	2.0981E+05	2.3285E+05
A5-H	1	HEA160	152	134	160	6	9	1.5946E+07	2.0981E+05	2.3285E+05	3684	1	HEA160	152	134	160	6	9	1.5946E+07	2.0981E+05	2.3285E+05
A6-H	1	HEA160	152	134	160	6	9	1.5946E+07	2.0981E+05	2.3285E+05	3684	1	HEA160	152	134	160	6	9	1.5946E+07	2.0981E+05	2.3285E+05
A7-H	2	HEA220	210	188	220	7	11	5.1842E+07	4.9373E+05	5.4343E+05	6156	2	HEA220	210	188	220	7	11	5.1842E+07	4.9373E+05	5.4343E+05
A8-H	2	HEA220	210	188	220	7	11	5.1842E+07	4.9373E+05	5.4343E+05	6156	2	HEA220	210	188	220	7	11	5.1842E+07	4.9373E+05	5.4343E+05
A9-H	2	HEA220	210	188	220	7	11	5.1842E+07	4.9373E+05	5.4343E+05	6156	2	HEA220	210	188	220	7	11	5.1842E+07	4.9373E+05	5.4343E+05
A10-H	3	HEA280	270	244	280	8	13	1.3000E+08	9.6294E+05	1.0546E+06	9232	3	HEA280	270	244	280	8	13	1.3000E+08	9.6294E+05	1.0546E+06
A11-H	3	HEA280	270	244	280	8	13	1.3000E+08	9.6294E+05	1.0546E+06	9232	3	HEA280	270	244	280	8	13	1.3000E+08	9.6294E+05	1.0546E+06
A12-H	3	HEA280	270	244	280	8	13	1.3000E+08	9.6294E+05	1.0546E+06	9232	3	HEA280	270	244	280	8	13	1.3000E+08	9.6294E+05	1.0546E+06
id																					
01-VH	3	HEA300	290	262	300	8.5	14	1.7285E+08	1.1920E+06	1.3051E+06	10627	3	HEA300	290	262	300	8.5	14	1.7285E+08	1.1920E+06	1.3051E+06
02-VH	3	HEA300	290	262	300	8.5	14	1.7285E+08	1.1920E+06	1.3051E+06	10627	3	HEA300	290	262	300	8.5	14	1.7285E+08	1.1920E+06	1.3051E+06
03-VH	3	HEA300	290	262	300	8.5	14	1.7285E+08	1.1920E+06	1.3051E+06	10627	3	HEA300	290	262	300	8.5	14	1.7285E+08	1.1920E+06	1.3051E+06
A1-VH	1	HEA120	114	98	120	5	8	5.7957E+06	1.0168E+05	1.1377E+05	2410	1	HEA120	114	98	120	5	8	5.7957E+06	1.0168E+05	1.1377E+05
A2-VH	1	HEA120	114	98	120	5	8	5.7957E+06	1.0168E+05	1.1377E+05	2410	1	HEA120	114	98	120	5	8	5.7957E+06	1.0168E+05	1.1377E+05
A3-VH	1	HEA120	114	98	120	5	8	5.7957E+06	1.0168E+05	1.1377E+05	2410	1	HEA120	114	98	120	5	8	5.7957E+06	1.0168E+05	1.1377E+05
A4-VH	1	HEA160	152	134	160	6	9	1.5946E+07	2.0981E+05	2.3285E+05	3684	1	HEA160	152	134	160	6	9	1.5946E+07	2.0981E+05	2.3285E+05
A5-VH	1	HEA160	152	134	160	6	9	1.5946E+07	2.0981E+05	2.3285E+05	3684	1	HEA160	152	134	160	6	9	1.5946E+07	2.0981E+05	2.3285E+05
A6-VH	1	HEA160	152	134	160	6	9	1.5946E+07	2.0981E+05	2.3285E+05	3684	1	HEA160	152	134	160	6	9	1.5946E+07	2.0981E+05	2.3285E+05
A7-VH	2	HEA220	210	188	220	7	11	5.1842E+07	4.9373E+05	5.4343E+05	6156	2	HEA220	210	188	220	7	11	5.1842E+07	4.9373E+05	5.4343E+05
A8-VH	2	HEA220	210	188	220	7	11	5.1842E+07	4.9373E+05	5.4343E+05	6156	2	HEA220	210	188	220	7	11	5.1842E+07	4.9373E+05	5.4343E+05
A9-VH	2	HEA220	210	188	220	7	11	5.1842E+07	4.9373E+05	5.4343E+05	6156	2	HEA220	210	188	220	7	11	5.1842E+07	4.9373E+05	5.4343E+05
A10-VH	3	HEA280	270	244	280	8	13	1.3000E+08	9.6294E+05	1.0546E+06	9232	3	HEA280	270	244	280	8	13	1.3000E+08	9.6294E+05	1.0546E+06
A11-VH	3	HEA280	270	244	280	8	13	1.3000E+08	9.6294E+05	1.0546E+06	9232	3	HEA280	270	244	280	8	13	1.3000E+08	9.6294E+05	1.0546E+06
A12-VH	3	HEA280	270	244	280	8	13	1.3000E+08	9.6294E+05	1.0546E+06	9232	3	HEA280	270	244	280	8	13	1.3000E+08	9.6294E+05	1.0546E+06
id																					
01-NLH	3	HEA300	290	262	300	8.5	14	1.7285E+08	1.1920E+06	1.3051E+06	10627	3	HEA300	290	262	300	8.5	14	1.7285E+08	1.1920E+06	1.3051E+06
02-NLH	3	HEA300	290	262	300	8.5	14	1.7285E+08	1.1920E+06	1.3051E+06	10627	3	HEA300	290	262	300	8.5	14	1.7285E+08	1.1920E+06	1.3051E+06
03-NLH	3	HEA300	290	262	300	8.5	14	1.7285E+08	1.1920E+06	1.3051E+06	10627	3	HEA300	290	262	300	8.5	14	1.7285E+08	1.1920E+06	1.3051E+06
A1-NLH	1	HEA120	114	98	120	5	8	5.7957E+06	1.0168E+05	1.1377E+05	2410	1	HEA120	114	98	120	5	8	5.7957E+06	1.0168E+05	1.1377E+05
A2-NLH	1	HEA120	114	98	120	5	8	5.7957E+06	1.0168E+05	1.1377E+05	2410	1	HEA120	114	98	120	5	8	5.7957E+06	1.0168E+05	1.1377E+05
A3-NLH	1	HEA120	114	98	120	5	8	5.7957E+06	1.0168E+05	1.1377E+05	2410	1	HEA120	114	98	120	5	8	5.7957E+06	1.0168E+05	1.1377E+05
A4-NLH	1	HEA160	152	134	160	6	9	1.5946E+07	2.0981E+05	2.3285E+05	3684	1	HEA160	152	134	160	6	9	1.5946E+07	2.0981E+05	2.3285E+05
A5-NLH	1	HEA160	152	134	160	6	9	1.5946E+07	2.0981E+05	2.3285E+05	3684	1	HEA160	152	134	160	6	9	1.5946E+07	2.0981E+05	2.3285E+05
A6-NLH	1	HEA160	152	134	160	6	9	1.5946E+07	2.0981E+05	2.3285E+05	3684	1	HEA160	152	134	160	6	9	1.5946E+07	2.0981E+05	2.3285E+05
A7-NLH	2	HEA220	210	188	220	7	11	5.1842E+07	4.9373E+05	5.4343E+05	6156	2	HEA220	210	188	220	7	11	5.1842E+07	4.9373E+05	5.4343E+05
A8-NLH	2	HEA220	210	188	220	7	11	5.1842E+07	4.9373E+05	5.4343E+05	6156	2	HEA220	210	188	220	7	11	5.1842E+07	4.9373E+05	5.4343E+05
A9-NLH	2	HEA220	210	188	220	7	11	5.1842E+07	4.9373E+05	5.4343E+05	6156	2	HEA220	210	188	220	7	11	5.1842E+07	4.9373E+05	5.4343E+05
A10-NLH	3	HEA280	270	244	280	8	13	1.3000E+08	9.6294E+05	1.0546E+06	9232	3	HEA280	270	244	280	8	13	1.3000E+08	9.6294E+05	1.0546E+06
A11-NLH	3	HEA280	270	244	280	8	13	1.3000E+08	9.6294E+05	1.0546E+06	9232	3	HEA280	270	244	280	8	13	1.3000E+08	9.6294E+05	1.0546E+06
A12-NLH	3	HEA280	270	244	280	8	13	1.3000E+08	9.6294E+05	1.0546E+06	9232	3	HEA280	270	244	280	8	13	1.3000E+08	9.6294E+05	1.0546E+06
id	24	25	26	27	28	29	30	31	32	33	34	35	36	37	38	39	40	41	42	43	44

id	Section properties													Model							
id																					
id	A	section class	profile 5	h5	P5h	P5b	P5w	P5tf	I_y	$W_{y,el}$	$W_{y,pl}$	A	section class		joint	condition	C	ma1	mb1	mc1	rs1
id	mm^2	[-]		mm	mm	mm	mm	mm	mm^4	mm^2	mm^3	mm^2	[-]		[-]	[-]	[-]	[-]	[-]	[-]	[-]
01	10627	3	HEA300	290	262	300	8.5	14	1.7285E+08	1.1920E+06	1.3051E+06	10627	3	-	1	1	1	78.96666667	32.75	25	0.5
02	10627	3	HEA300	290	262	300	8.5	14	1.7285E+08	1.1920E+06	1.3051E+06	10627	3	-	1	1	1.5	78.96666667	32.75	25	0.5
03	10627	3	HEA300	290	262	300	8.5	14	1.7285E+08	1.1920E+06	1.3051E+06	10627	3	-	1	1	2	78.96666667	32.75	25	0.5
A1	2410	1	HEA120	114	98	120	5	8	5.7957E+06	1.0168E+05	1.1377E+05	2410	1	-	1	1	1	48.36666667	12.25	10	0.5
A2	2410	1	HEA120	114	98	120	5	8	5.7957E+06	1.0168E+05	1.1377E+05	2410	1	-	1	1	1.5	48.36666667	12.25	10	0.5
A3	2410	1	HEA120	114	98	120	5	8	5.7957E+06	1.0168E+05	1.1377E+05	2410	1	-	1	1	2	48.36666667	12.25	10	0.5
A4	3684	1	HEA160	152	134	160	6	9	1.5946E+07	2.0981E+05	2.3285E+05	3684	1	-	1	1	1	47.76666667	16.75	13.33333333	0.5
A5	3684	1	HEA160	152	134	160	6	9	1.5946E+07	2.0981E+05	2.3285E+05	3684	1	-	1	1	1.5	47.76666667	16.75	13.33333333	0.5
A6	3684	1	HEA160	152	134	160	6	9	1.5946E+07	2.0981E+05	2.3285E+05	3684	1	-	1	1	2	47.76666667	16.75	13.33333333	0.5
A7	6156	2	HEA220	210	188	220	7	11	5.1842E+07	4.9373E+05	5.4343E+05	6156	2	-	1	1	1	46.86666667	23.5	18.33333333	0.5
A8	6156	2	HEA220	210	188	220	7	11	5.1842E+07	4.9373E+05	5.4343E+05	6156	2	-	1	1	1.5	46.86666667	23.5	18.33333333	0.5
A9	6156	2	HEA220	210	188	220	7	11	5.1842E+07	4.9373E+05	5.4343E+05	6156	2	-	1	1	2	46.86666667	23.5	18.33333333	0.5
A10	9232	3	HEA280	270	244	280	8	13	1.3000E+08	9.6294E+05	1.0546E+06	9232	3	-	1	1	1	45.93333333	30.5	23.33333333	0.5
A11	9232	3	HEA280	270	244	280	8	13	1.3000E+08	9.6294E+05	1.0546E+06	9232	3	-	1	1	1.5	45.93333333	30.5	23.33333333	0.5
A12	9232	3	HEA280	270	244	280	8	13	1.3000E+08	9.6294E+05	1.0546E+06	9232	3	-	1	1	2	45.93333333	30.5	23.33333333	0.5
id																					
01-NL	10627	3	HEA300	290	262	300	8.5	14	1.7285E+08	1.1920E+06	1.3051E+06	10627	3	-	1	1	1	78.96666667	32.75	25	0.5
02-NL	10627	3	HEA300	290	262	300	8.5	14	1.7285E+08	1.1920E+06	1.3051E+06	10627	3	-	1	1	1.5	78.96666667	32.75	25	0.5
03-NL	10627	3	HEA300	290	262	300	8.5	14	1.7285E+08	1.1920E+06	1.3051E+06	10627	3	-	1	1	2	78.96666667	32.75	25	0.5
A1-NL	2410	1	HEA120	114	98	120	5	8	5.7957E+06	1.0168E+05	1.1377E+05	2410	1	-	1	1	1	48.36666667	12.25	10	0.5
A2-NL	2410	1	HEA120	114	98	120	5	8	5.7957E+06	1.0168E+05	1.1377E+05	2410	1	-	1	1	1.5	48.36666667	12.25	10	0.5
A3-NL	2410	1	HEA120	114	98	120	5	8	5.7957E+06	1.0168E+05	1.1377E+05	2410	1	-	1	1	2	48.36666667	12.25	10	0.5
A4-NL	3684	1	HEA160	152	134	160	6	9	1.5946E+07	2.0981E+05	2.3285E+05	3684	1	-	1	1	1	47.76666667	16.75	13.33333333	0.5
A5-NL	3684	1	HEA160	152	134	160	6	9	1.5946E+07	2.0981E+05	2.3285E+05	3684	1	-	1	1	1.5	47.76666667	16.75	13.33333333	0.5
A6-NL	3684	1	HEA160	152	134	160	6	9	1.5946E+07	2.0981E+05	2.3285E+05	3684	1	-	1	1	2	47.76666667	16.75	13.33333333	0.5
A7-NL	6156	2	HEA220	210	188	220	7	11	5.1842E+07	4.9373E+05	5.4343E+05	6156	2	-	1	1	1	46.86666667	23.5	18.33333333	0.5
A8-NL	6156	2	HEA220	210	188	220	7	11	5.1842E+07	4.9373E+05	5.4343E+05	6156	2	-	1	1	1.5	46.86666667	23.5	18.33333333	0.5
A9-NL	6156	2	HEA220	210	188	220	7	11	5.1842E+07	4.9373E+05	5.4343E+05	6156	2	-	1	1	2	46.86666667	23.5	18.33333333	0.5
A10-NL	9232	3	HEA280	270	244	280	8	13	1.3000E+08	9.6294E+05	1.0546E+06	9232	3	-	1	1	1	45.93333333	30.5	23.33333333	0.5
A11-NL	9232	3	HEA280	270	244	280	8	13	1.3000E+08	9.6294E+05	1.0546E+06	9232	3	-	1	1	1.5	45.93333333	30.5	23.33333333	0.5
A12-NL	9232	3	HEA280	270	244	280	8	13	1.3000E+08	9.6294E+05	1.0546E+06	9232	3	-	1	1	2	45.93333333	30.5	23.33333333	0.5
id																					
01-V	10627	3	HEA300	290	262	300	8.5	14	1.7285E+08	1.1920E+06	1.3051E+06	10627	3	-	1	1	1	78.96666667	32.75	25	0.5
02-V	10627	3	HEA300	290	262	300	8.5	14	1.7285E+08	1.1920E+06	1.3051E+06	10627	3	-	1	1	1.5	78.96666667	32.75	25	0.5
03-V	10627	3	HEA300	290	262	300	8.5	14	1.7285E+08	1.1920E+06	1.3051E+06	10627	3	-	1	1	2	78.96666667	32.75	25	0.5
A1-V	2410	1	HEA120	114	98	120	5	8	5.7957E+06	1.0168E+05	1.1377E+05	2410	1	-	1	1	1	48.36666667	12.25	10	0.5
A2-V	2410	1	HEA120	114	98	120	5	8	5.7957E+06	1.0168E+05	1.1377E+05	2410	1	-	1	1	1.5	48.36666667	12.25	10	0.5
A3-V	2410	1	HEA120	114	98	120	5	8	5.7957E+06	1.0168E+05	1.1377E+05	2410	1	-	1	1	2	48.36666667	12.25	10	0.5
A4-V	3684	1	HEA160	152	134	160	6	9	1.5946E+07	2.0981E+05	2.3285E+05	3684	1	-	1	1	1	47.76666667	16.75	13.33333333	0.5
A5-V	3684	1	HEA160	152	134	160	6	9	1.5946E+07	2.0981E+05	2.3285E+05	3684	1	-	1	1	1.5	47.76666667	16.75	13.33333333	0.5
A6-V	3684	1	HEA160	152	134	160	6	9	1.5946E+07	2.0981E+05	2.3285E+05	3684	1	-	1	1	2	47.76666667	16.75	13.33333333	0.5
A7-V	6156	2	HEA220	210	188	220	7	11	5.1842E+07	4.9373E+05	5.4343E+05	6156	2	-	1	1	1	46.86666667	23.5	18.33333333	0.5
A8-V	6156	2	HEA220	210	188	220	7	11	5.1842E+07	4.9373E+05	5.4343E+05	6156	2	-	1	1	1.5	46.86666667	23.5	18.33333333	0.5
A9-V	6156	2	HEA220	210	188	220	7	11	5.1842E+07	4.9373E+05	5.4343E+05	6156	2	-	1	1	2	46.86666667	23.5	18.33333333	0.5
A10-V	9232	3	HEA280	270	244	280	8	13	1.3000E+08	9.6294E+05	1.0546E+06	9232	3	-	1	1	1	45.93333333	30.5	23.33333333	0.5
A11-V	9232	3	HEA280	270	244	280	8	13	1.3000E+08	9.6294E+05	1.0546E+06	9232	3	-	1	1	1.5	45.93333333	30.5	23.33333333	0.5
A12-V	9232	3	HEA280	270	244	280	8	13	1.3000E+08	9.6294E+05	1.0546E+06	9232	3	-	1	1	2	45.93333333	30.5	23.33333333	0.5
id																					
01-H	10627	3	HEA300	290	262	300	8.5	14	1.7285E+08	1.1920E+06	1.3051E+06	10627	3	-	1	1	1	78.96666667	32.75	25	0.5
02-H	10627	3	HEA300	290	262	300	8.5	14	1.7285E+08	1.1920E+06	1.3051E+06	10627	3	-	1	1	1.5	78.96666667	32.75	25	0.5
03-H	10627	3	HEA300	290	262	300	8.5	14	1.7285E+08	1.1920E+06	1.3051E+06	10627	3	-	1	1	2	78.96666667	32.75	25	0.5
A1-H	2410	1	HEA120	114	98	120	5	8	5.7957E+06	1.0168E+05	1.1377E+05	2410	1	-	1	1	1	48.36666667	12.25	10	0.5
A2-H	2410	1	HEA120	114	98	120	5	8	5.7957E+06	1.0168E+05	1.1377E+05	2410	1	-	1	1	1.5	48.36666667	12.25	10	0.5
A3-H	2410	1	HEA120	114	98	120	5	8	5.7957E+06	1.0168E+05	1.1377E+05	2410	1	-	1	1	2	48.36666667	12.25	10	0.5
A4-H	3684	1	HEA160	152	134	160	6	9	1.5946E+07	2.0981E+05	2.3285E+05	3684	1	-	1	1	1	47.76666667	16.75	13.33333333	0.5
A5-H	3684	1	HEA160	152	134	160	6	9	1.5946E+07	2.0981E+05	2.3285E+05	3684	1	-	1	1	1.5	47.76666667	16.75	13.33333333	0.5
A6-H	3684	1	HEA160	152	134	160	6	9	1.5946E+07	2.0981E+05	2.3285E+05	3684	1	-	1	1	2	47.76666667	16.75	13.33333333	0.5
A7-H	6156	2	HEA220	210	188	220	7	11	5.1842E+07	4.9373E+05	5.4343E+05	6156	2	-	1	1	1	46.86666667	23.5	18.33333333	0.5
A8-H	6156	2	HEA220	210	188	220	7	11	5.1842E+07	4.9373E+05	5.4343E+05	6156	2	-	1	1	1.5	46.86666667	23.5	18.33333333	0.5
A9-H	6156	2	HEA220	210	188	220	7	11	5.1842E+07	4.9373E+05	5.4343E+05	6156	2	-	1	1	2	46.86666667	23.5	18.33333333	0.5
A10-H	9232	3	HEA280	270	244	280	8	13	1.3000E+08	9.6294E+05	1.0546E+06	9232	3	-	1	1	1	45.93333333	30.5	23.33333333	0.5
A11-H	9232	3	HEA280	270	244	280	8	13	1.3000E+08	9.6294E+05	1.0546E+06	9232	3	-	1	1	1.5	45.93333333	30.5	23.33333333	0.5
A12-H	9232	3	HEA280	270	244	280	8	13	1.3000E+08	9.6294E+05	1.0546E+06	9232	3	-	1	1	2	45.93333333	30.5	23.33333333	0.5
id																					
01-VH	10627	3	HEA300	290	262	300	8.5	14	1.7285E+08	1.1920E+06	1.3051E+06	10627	3	-	1	1	1	78.96666667	32.75	25	0.5
02-VH	10627	3	HEA300	290	262	300	8.5	14	1.7285E+08	1.1920E+06	1.3051E+06	10627	3	-	1	1	1.5	78.96666667	32.75	25	0.5
03-VH	10627	3	HEA300	290	262	300	8.5	14	1.7285E+08	1.1920E+06	1.3051E+06	10627	3	-	1	1	2	78.96666667	32.75	25	0.5
A1-VH	2410	1	HEA120	114	98	120	5	8	5.7957E+06	1.0168E+05	1.1377E+05	2410	1	-	1	1	1	48.36666667	12.25	10	0.5
A2-VH	2410	1	HEA120	114	98	120	5	8	5.7957E+06	1.0168E+05	1.1377E+05	2410	1	-	1	1	1.5	48.36666667	12.25	10	0.5
A3-VH	2410	1	HEA120	114	98	120	5	8	5.7957E+06	1.0168E+05	1.1377E+05	2410	1	-	1	1	2	48.36666667	12.25	10	0.5
A4-VH	3684	1	HEA160	152	134	160	6	9	1.5946E+07	2.0981E+05	2.3285E+05	3684	1	-	1	1	1	47.76666667	16.75	13.33333333	0.5
A5-VH	3684	1	HEA160	152	134	160	6	9	1.5946E+07	2.0981E+05	2.3285E+05	3684	1	-	1	1	1.5	47.76666667	16.75	13.33333333	0.5
A6-VH	3684	1	HEA160	152	134	160	6	9	1.5946E+07	2.0981E+05	2.3285E+05	3684	1	-	1	1	2	47.76666667	16.75	13.33333333	0.5
A7-VH	6156	2	HEA220	210	188	220	7	11	5.1842E+07	4.9373E+05	5.4343E+05	6156	2	-	1	1	1	46.86666667	23.5	18.33333333	0.5
A8-VH	6156	2	HEA220	210	188	220	7	11	5.1842E+07	4.9373E+05	5.4343E+05	6156	2	-	1	1	1.5	46.86666667	23.5	18.33333333	0.5
A9-VH	6156	2	HEA220	210	188	220	7	11	5.1842E+07	4.9373E+05	5.4343E+05	6156	2	-	1	1	2	46.86666667	23.5	18.33333333	0.5
A10-VH	9232	3	HEA280	270	244	280	8	13	1.3000E+08	9.6294E+05	1.0546E+06	9232	3	-	1	1	1	45.93333333	30.5	23.33333333	0.5
A11-VH	9232	3	HEA280	270	244	280	8	13	1.3000E+08	9.6294E+05	1.0546E+06	9232	3	-	1	1	1.5	45.93333333	30.5	23.33333333	0.5
A12-VH	9232	3	HEA280	270	244	280	8	13	1.3000E+08	9.6294E+05	1.0546E+06	9232	3	-	1	1	2	45.93333333	30.5	23.33333333	0.5
id																					
01-NLH	10627	3	HEA300	290	262	300	8.5	14	1.7285E+08	1.1920E+06	1.3051E+06	10627	3	-	1	1	1	78.96666667	32.75	25	0.5
02-NLH	10627	3	HEA300	290	262	300	8.5	14	1.7285E+08	1.1920E+06	1.3051E+06	10627	3	-	1	1	1.5	78.96666667	32.75	25	0.5
03-NLH	10627	3	HEA300	290	262	300	8.5	14	1.7285E+08	1.1920E+06	1.3051E+06	10627	3	-	1	1	2	78.96666667	32.75	25	0.5
A1-NLH	2410	1	HEA120	114	98	120	5	8	5.7957E+06	1.0168E+05	1.1377E+05	2410	1	-	1	1	1	48.36666667	12.25	10	0.5
A2-NLH	2410	1	HEA120	114	98	120	5	8	5.7957E+06	1.0168E+05	1.1377E+05	2410	1	-	1	1	1.5	48.36666667	12.25	10	0.5
A3-NLH	2410	1	HEA120	114	98	120	5	8	5.7957E+06	1.0168E+05	1.1377E+05	2410	1	-	1	1	2	48.36666667	12.25	10	0.5
A4-NLH	3684	1	HEA160	152	134	160	6	9	1.5946E+07	2.0981E+05	2.3285E+05	3684	1	-	1	1	1	47.76666667	16.75	13.33333333	0.5
A5-NLH	3684	1	HEA160	152	134	160	6	9	1.5946E+07	2.0981E+05	2.3285E+05	3684	1	-	1	1	1.5	47.76666667	16.75	13.33333333	0.5
A6-NLH	3684	1	HEA160	152	134	160	6	9	1.5946E+07	2.0981E+05	2.3285E+05	3684	1	-	1	1	2	47.76666667	16.75	13.33333333	0.5
A7-NLH	6156	2	HEA220	210	188	220	7	11	5.1842E+07	4.9373E+05	5.4343E+05	6156	2	-	1	1	1	46.86666667	23.5	18.33333333	0.5
A8-NLH	6156	2	HEA220	210	188	220	7	11	5.1842E+07	4.9373E+05	5.4343E+05	6156	2	-	1	1	1.5	46.86666667	23.5	18.33333333	0.5
A9-NLH	6156	2	HEA220	210	188	220	7	11	5.1842E+07	4.9373E+05	5.4343E+05	6156	2	-	1	1	2	46.86666667	23.5	18.33333333	0.5
A10-NLH	9232	3	HEA280	270	244	280	8	13	1.3000E+08	9.6294E+05	1.0546E+06	9232	3	-	1	1	1	45.93333333	30.5	23.33333333	0.5
A11-NLH	9232	3	HEA280	270	244	280	8	13	1.3000E+08	9.6294E+05	1.0546E+06	9232	3	-	1	1	1.5	45.93333333	30.5	23.33333333	0.5
A12-NLH	9232	3	HEA280	270	244	280	8	13	1.3000E+08	9.6294E+05	1.0546E+06	9232	3	-	1	1	2	45.93333333	30.5	23.33333333	0.5
id	45	46	47	48	49	50	51	52	53	54	55	56	57	58	59	60	61	62	63	64	65

id	Model												LBA					
id																		
id	ma2	mb2	mc2	rs2	ma4	mb4	mc4	rs4	ma5	mb5	mc5	rs5	α_{cr}	mode 1	mode 2	mode 3	F_{cr}	
id	[-]	[-]	[-]	[-]	[-]	[-]	[-]	[-]	[-]	[-]	[-]	[-]	[-]	[-]	[-]	[-]	N	
01	78.96666667	32.75	25	0.5	78.96666667	32.75	25	0.5	78.96666667	32.75	25	0.5	1.7898	1	64	335	1.79E+06	
02	120.6333333	32.75	25	0.5	78.96666667	32.75	25	0.5	120.6333333	32.75	25	0.5	1.5768	1	40	330	1.58E+06	
03	162.3	32.75	25	0.5	78.96666667	32.75	25	0.5	162.3	32.75	25	0.5	1.401	1	26	327	1.40E+06	
A1	48.36666667	12.25	10	0.5	48.36666667	12.25	10	0.5	48.36666667	12.25	10	0.5	0.16897	1	4	7	1.69E+05	
A2	73.36666667	12.25	10	0.5	48.36666667	12.25	10	0.5	73.36666667	12.25	10	0.5	0.14785	1	4	7	1.48E+05	
A3	98.36666667	12.25	10	0.5	48.36666667	12.25	10	0.5	98.36666667	12.25	10	0.5	0.13099	1	4	7	1.31E+05	
A4	47.76666667	16.75	13.33333333	0.5	47.76666667	16.75	13.33333333	0.5	47.76666667	16.75	13.33333333	0.5	0.46194	1	4	189	4.62E+05	
A5	72.76666667	16.75	13.33333333	0.5	47.76666667	16.75	13.33333333	0.5	72.76666667	16.75	13.33333333	0.5	0.4056	1	4	189	4.06E+05	
A6	97.76666667	16.75	13.33333333	0.5	47.76666667	16.75	13.33333333	0.5	97.76666667	16.75	13.33333333	0.5	0.35985	1	4	179	3.60E+05	
A7	46.86666667	23.5	18.33333333	0.5	46.86666667	23.5	18.33333333	0.5	46.86666667	23.5	18.33333333	0.5	1.4712	1	134	140	1.47E+06	
A8	71.86666667	23.5	18.33333333	0.5	46.86666667	23.5	18.33333333	0.5	71.86666667	23.5	18.33333333	0.5	1.3025	1	108	309	1.30E+06	
A9	96.86666667	23.5	18.33333333	0.5	46.86666667	23.5	18.33333333	0.5	96.86666667	23.5	18.33333333	0.5	1.1601	1	72	74	1.16E+06	
A10	45.93333333	30.5	23.33333333	0.5	45.93333333	30.5	23.33333333	0.5	45.93333333	30.5	23.33333333	0.5	3.5822	1	1	1	3.58E+06	
A11	70.93333333	30.5	23.33333333	0.5	45.93333333	30.5	23.33333333	0.5	70.93333333	30.5	23.33333333	0.5	3.2065	1	1	1	3.21E+06	
A12	95.93333333	30.5	23.33333333	0.5	45.93333333	30.5	23.33333333	0.5	95.93333333	30.5	23.33333333	0.5	2.8712	1	1	1	2.87E+06	
id																		
01-NL	78.96666667	32.75	25	0.5	78.96666667	32.75	25	0.5	78.96666667	32.75	25	0.5	2.601	1	2	43	2.60E+06	
02-NL	120.6333333	32.75	25	0.5	78.96666667	32.75	25	0.5	120.6333333	32.75	25	0.5	2.3089	1	2	35	2.31E+06	
03-NL	162.3	32.75	25	0.5	78.96666667	32.75	25	0.5	162.3	32.75	25	0.5	2.0629	1	2	19	2.06E+06	
A1-NL	48.36666667	12.25	10	0.5	48.36666667	12.25	10	0.5	48.36666667	12.25	10	0.5	0.24542	1	2	3	2.45E+05	
A2-NL	73.36666667	12.25	10	0.5	48.36666667	12.25	10	0.5	73.36666667	12.25	10	0.5	0.21647	1	2	3	2.16E+05	
A3-NL	98.36666667	12.25	10	0.5	48.36666667	12.25	10	0.5	98.36666667	12.25	10	0.5	0.19285	1	2	3	1.93E+05	
A4-NL	47.76666667	16.75	13.33333333	0.5	47.76666667	16.75	13.33333333	0.5	47.76666667	16.75	13.33333333	0.5	0.67112	1	2	3	6.71E+05	
A5-NL	72.76666667	16.75	13.33333333	0.5	47.76666667	16.75	13.33333333	0.5	72.76666667	16.75	13.33333333	0.5	0.59388	1	2	3	5.94E+05	
A6-NL	97.76666667	16.75	13.33333333	0.5	47.76666667	16.75	13.33333333	0.5	97.76666667	16.75	13.33333333	0.5	0.52982	1	2	3	5.30E+05	
A7-NL	46.86666667	23.5	18.33333333	0.5	46.86666667	23.5	18.33333333	0.5	46.86666667	23.5	18.33333333	0.5	2.1392	1	34	95	2.14E+06	
A8-NL	71.86666667	23.5	18.33333333	0.5	46.86666667	23.5	18.33333333	0.5	71.86666667	23.5	18.33333333	0.5	1.9079	1	26	75	1.91E+06	
A9-NL	96.86666667	23.5	18.33333333	0.5	46.86666667	23.5	18.33333333	0.5	96.86666667	23.5	18.33333333	0.5	1.7085	1	18	55	1.71E+06	
A10-NL	45.93333333	30.5	23.33333333	0.5	45.93333333	30.5	23.33333333	0.5	45.93333333	30.5	23.33333333	0.5	5.2148	1	136	1	5.21E+06	
A11-NL	70.93333333	30.5	23.33333333	0.5	45.93333333	30.5	23.33333333	0.5	70.93333333	30.5	23.33333333	0.5	4.6994	1	122	1	4.70E+06	
A12-NL	95.93333333	30.5	23.33333333	0.5	45.93333333	30.5	23.33333333	0.5	95.93333333	30.5	23.33333333	0.5	4.2304	1	122	1	4.23E+06	
id																		
01-V	78.96666667	32.75	25	0.5	78.96666667	32.75	25	0.5	78.96666667	32.75	25	0.5	0.46754	1	52	1	4.68E+05	
02-V	120.6333333	32.75	25	0.5	78.96666667	32.75	25	0.5	120.6333333	32.75	25	0.5	0.40714	1	37	1	4.07E+05	
03-V	162.3	32.75	25	0.5	78.96666667	32.75	25	0.5	162.3	32.75	25	0.5	0.35879	1	4	1	3.59E+05	
A1-V	48.36666667	12.25	10	0.5	48.36666667	12.25	10	0.5	48.36666667	12.25	10	0.5	0.044217	1	4	7	4.42E+04	
A2-V	73.36666667	12.25	10	0.5	48.36666667	12.25	10	0.5	73.36666667	12.25	10	0.5	0.038233	1	4	7	3.82E+04	
A3-V	98.36666667	12.25	10	0.5	48.36666667	12.25	10	0.5	98.36666667	12.25	10	0.5	0.033598	1	4	7	3.36E+04	
A4-V	47.76666667	16.75	13.33333333	0.5	47.76666667	16.75	13.33333333	0.5	47.76666667	16.75	13.33333333	0.5	0.12078	1	4	1	1.21E+05	
A5-V	72.76666667	16.75	13.33333333	0.5	47.76666667	16.75	13.33333333	0.5	72.76666667	16.75	13.33333333	0.5	0.1048	1	4	1	1.05E+05	
A6-V	97.76666667	16.75	13.33333333	0.5	47.76666667	16.75	13.33333333	0.5	97.76666667	16.75	13.33333333	0.5	0.09222	1	4	1	9.22E+04	
A7-V	46.86666667	23.5	18.33333333	0.5	46.86666667	23.5	18.33333333	0.5	46.86666667	23.5	18.33333333	0.5	0.38371	1	1	1	3.84E+05	
A8-V	71.86666667	23.5	18.33333333	0.5	46.86666667	23.5	18.33333333	0.5	71.86666667	23.5	18.33333333	0.5	0.3359	1	1	1	3.36E+05	
A9-V	96.86666667	23.5	18.33333333	0.5	46.86666667	23.5	18.33333333	0.5	96.86666667	23.5	18.33333333	0.5	0.29672	1	1	1	2.97E+05	
A10-V	45.93333333	30.5	23.33333333	0.5	45.93333333	30.5	23.33333333	0.5	45.93333333	30.5	23.33333333	0.5	0.93133	1	1	1	9.31E+05	
A11-V	70.93333333	30.5	23.33333333	0.5	45.93333333	30.5	23.33333333	0.5	70.93333333	30.5	23.33333333	0.5	0.8248	1	1	1	8.25E+05	
A12-V	95.93333333	30.5	23.33333333	0.5	45.93333333	30.5	23.33333333	0.5	95.93333333	30.5	23.33333333	0.5	0.73248	1	1	1	7.32E+05	
id																		
01-H	78.96666667	32.75	25	0.5	78.96666667	32.75	25	0.5	78.96666667	32.75	25	0.5	1.7898	1	64	335	1.79E+06	
02-H	120.6333333	32.75	25	0.5	78.96666667	32.75	25	0.5	120.6333333	32.75	25	0.5	1.5768	1	40	330	1.58E+06	
03-H	162.3	32.75	25	0.5	78.96666667	32.75	25	0.5	162.3	32.75	25	0.5	1.401	1	26	327	1.40E+06	
A1-H	48.36666667	12.25	10	0.5	48.36666667	12.25	10	0.5	48.36666667	12.25	10	0.5	0.16897	1	4	7	1.69E+05	
A2-H	73.36666667	12.25	10	0.5	48.36666667	12.25	10	0.5	73.36666667	12.25	10	0.5	0.14785	1	4	7	1.48E+05	
A3-H	98.36666667	12.25	10	0.5	48.36666667	12.25	10	0.5	98.36666667	12.25	10	0.5	0.13099	1	4	7	1.31E+05	
A4-H	47.76666667	16.75	13.33333333	0.5	47.76666667	16.75	13.33333333	0.5	47.76666667	16.75	13.33333333	0.5	0.46194	1	4	189	4.62E+05	
A5-H	72.76666667	16.75	13.33333333	0.5	47.76666667	16.75	13.33333333	0.5	72.76666667	16.75	13.33333333	0.5	0.4056	1	4	189	4.06E+05	
A6-H	97.76666667	16.75	13.33333333	0.5	47.76666667	16.75	13.33333333	0.5	97.76666667	16.75	13.33333333	0.5	0.35985	1	4	179	3.60E+05	
A7-H	46.86666667	23.5	18.33333333	0.5	46.86666667	23.5	18.33333333	0.5	46.86666667	23.5	18.33333333	0.5	1.4712	1	134	140	1.47E+06	
A8-H	71.86666667	23.5	18.33333333	0.5	46.86666667	23.5	18.33333333	0.5	71.86666667	23.5	18.33333333	0.5	1.3025	1	108	309	1.30E+06	
A9-H	96.86666667	23.5	18.33333333	0.5	46.86666667	23.5	18.33333333	0.5	96.86666667	23.5	18.33333333	0.5	1.1601	1	72	74	1.16E+06	
A10-H	45.93333333	30.5	23.33333333	0.5	45.93333333	30.5	23.33333333	0.5	45.93333333	30.5	23.33333333	0.5	3.5822	1	1	1	3.58E+06	
A11-H	70.93333333	30.5	23.33333333	0.5	45.93333333	30.5	23.33333333	0.5	70.93333333	30.5	23.33333333	0.5	3.2065	1	1	1	3.21E+06	
A12-H	95.93333333	30.5	23.33333333	0.5	45.93333333	30.5	23.33333333	0.5	95.93333333	30.5	23.33333333	0.5	2.8712	1	1	1	2.87E+06	
id																		
01-VH	78.96666667	32.75	25	0.5	78.96666667	32.75	25	0.5	78.96666667	32.75	25	0.5	0.46754	1	52	1	4.68E+05	
02-VH	120.6333333	32.75	25	0.5	78.96666667	32.75	25	0.5	120.6333333	32.75	25	0.5	0.40714	1	37	1	4.07E+05	
03-VH	162.3	32.75	25	0.5	78.96666667	32.75	25	0.5	162.3	32.75	25	0.5	0.35879	1	4	1	3.59E+05	
A1-VH	48.36666667	12.25	10	0.5	48.36666667	12.25	10	0.5	48.36666667	12.25	10	0.5	0.044217	1	4	7	4.42E+04	
A2-VH	73.36666667	12.25	10	0.5	48.36666667	12.25	10	0.5	73.36666667	12.25	10	0.5	0.038233	1	4	7	3.82E+04	
A3-VH	98.36666667	12.25	10	0.5	48.36666667	12.25	10	0.5	98.36666667	12.25	10	0.5	0.033598	1	4	7	3.36E+04	
A4-VH	47.76666667	16.75	13.33333333	0.5	47.76666667	16.75	13.33333333	0.5	47.76666667	16.75	13.33333333	0.5	0.12078	1	4	1	1.21E+05	
A5-VH	72.76666667	16.75	13.33333333	0.5	47.76666667	16.75	13.33333333	0.5	72.76666667	16.75	13.33333333	0.5	0.1048	1	4	1	1.05E+05	
A6-VH	97.76666667	16.75	13.33333333	0.5	47.76666667	16.75	13.33333333	0.5	97.76666667	16.75	13.33333333	0.5	0.09222	1	4	1	9.22E+04	
A7-VH	46.86666667	23.5	18.33333333	0.5	46.86666667	23.5	18.33333333	0.5	46.86666667	23.5	18.33333333	0.5	0.38371	1	1	1	3.84E+05	
A8-VH	71.86666667	23.5	18.33333333	0.5	46.86666667	23.5	18.33333333	0.5	71.86666667	23.5	18.33333333	0.5	0.3359	1	1	1	3.36E+05	
A9-VH	96.86666667	23.5	18.33333333	0.5	46.86666667	23.5	18.33333333	0.5	96.86666667	23.5	18.33333333	0.5	0.29672	1	1	1	2.97E+05	
A10-VH	45.93333333	30.5	23.33333333	0.5	45.93333333	30.5	23.33333333	0.5	45.93333333	30.5	23.33333333	0.5	0.93133	1	1	1	9.31E+05	
A11-VH	70.93333333	30.5	23.33333333	0.5	45.93333333	30.5	23.33333333	0.5	70.93333333	30.5	23.33333333	0.5	0.8248	1	1	1	8.25E+05	
A12-VH	95.93333333	30.5	23.33333333	0.5	45.93333333	30.5	23.33333333	0.5	95.93333333	30.5	23.33333333	0.5	0.73248	1	1	1	7.32E+05	
id																		
01-NLH	78.96666667	32.75	25	0.5	78.96666667	32.75	25	0.5	78.96666667	32.75	25	0.5	2.601	1	2	43	2.60E+06	
02-NLH	120.6333333	32.75	25	0.5	78.96666667	32.75	25	0.5	120.6333333	32.75	25	0.5	2.3089	1	2	35	2.31E+06	
03-NLH	162.3	32.75	25	0.5	78.96666667	32.75	25	0.5	162.3	32.75	25	0.5	2.0629	1	2	19	2.06E+06	
A1-NLH	48.36666667	12.25	10	0.5	48.36666667	12.25	10	0.5	48.36666667	12.25	10	0.5	0.24542	1	2	3	2.45E+05	
A2-NLH	73.36666667	12.25	10	0.5	48.36666667	12.25	10	0.5	73.36666667	12.25	10	0.5	0.21647	1	2	3	2.16E+05	
A3-NLH	98.36666667	12.25	10	0.5	48.36666667	12.25	10	0.5	98.36666667	12.25	10	0.5	0.19285	1	2	3	1.93E+05	
A4-NLH	47.76666667	16.75	13.33333333	0.5	47.76666667	16.75	13.33333333	0.5	47.76666667	16.75	13.33333333	0.5	0.67112	1	2	3	6.71E+05	
A5-NLH	72.76666667	16.75	13.33333333	0.5	47.76666667	16.75	13.33333333	0.5	72.76666667	16.75	13.33333333	0.5	0.59388	1	2	3	5.94E+05	
A6-NLH	97.76666667	16.75	13.33333333	0.5	47.76666667	16.75	13.33333333	0.5	97.76666667	16.75	13.33333333	0.5	0.52982	1	2	3	5.30E+05	
A7-NLH	46.86666667	23.5	18.33333333	0.5	46.86666667	23.5	18.33333333	0.5	46.86666667	23.5	18.33333333	0.5	2.1392	1	34	95	2.14E+06	
A8-NLH	71.86666667	23.5	18.33333333	0.5	46.86666667	23.5	18.33333333	0.5	71.86666667	23.5	18.33333333	0.5	1.9079	1	26	75	1.91E+06	
A9-NLH	96.86666667	23.5	18.33333333	0.5	46.86666667	23.5	18.33333333	0.5	96.86666667	23.5	18.33333333	0.5	1.7085	1	18	55	1.71E+06	
A10-NLH	45.93333333	30.5	23.33333333	0.5	45.93333333	30.5	23.33333333	0.5	45.93333333	30.5	23.33333333	0.5	5.2148	1	136	1	5.21E+06	
A11-NLH	70.93333333	30.5	23.33333333	0.5	45.93333333	30.5	23.33333333	0.5	70.93333333	30.5	23.33333333	0.5	4.6994	1	122	1	4.70E+06	
A12-NLH	95.93333333	30.5	23.33333333	0.5	45.93333333	30.5	23.33333333	0.5	95.93333333	30.5	23.33333333	0.5	4.2304	1	122	1	4.23E+06	
id	66	67	68	69	70	71	72	73	74	75	76	77	78	79	80	81	82	83	84

id	GMNIA III											GMNIA IV								
id						$P^2+C1*P+C2$ $=r^2-P^2$	P+(L_{cr}/1000)	Lcr/2-h	$\sqrt{(r^2-x^2)}$	y-P										
id	$L_{cr} = \pi*\sqrt{(EI/\alpha_{cr}*F)}$	L_{cr}/1000	r^2-P^2	C_1	C_2	P	r	x	y	Δ		n	P_1	P_2	P_3	F	h	A_1	A_2	A_3
id	mm	mm	mm	[-]	[-]	mm	mm	mm	mm	mm		[-]	[-]	[-]	[-]	[-]	mm	[-]	[-]	[-]
01	14147.7	14.15	50039600.6	28.30	200.16	1768459.8	1768474	2073.9	1768472.7	12.93	-	2	0.782	0.218	0	0.001566	5000	-6.12	1.71	0.00
02	15073.0	15.07	56799135.6	30.15	227.20	1884122.5	1884138	2536.5	1884135.9	13.37	-	2	0.782	0.218	0	0.001566	5000	-6.12	1.71	0.00
03	15990.8	15.99	63926393.3	31.98	255.71	1998841.6	1998858	2995.4	1998855.3	13.75	-	2	0.782	0.218	0	0.001566	5000	-6.12	1.71	0.00
A1	8431.5	8.43	17772727.9	16.86	71.09	1053938.6	1053947	1215.8	1053946.3	7.73	-	3	0.623	0.161	0.216	0.001838	3000	-3.44	0.89	1.19
A2	9013.7	9.01	20311517.4	18.03	81.25	1126703.0	1126712	1506.8	1126711.0	8.01	-	3	0.623	0.161	0.216	0.001838	3000	-3.44	0.89	1.19
A3	9576.2	9.58	22925855.7	19.15	91.70	1197019.0	1197029	1788.1	1197027.3	8.24	-	3	0.623	0.161	0.216	0.001838	3000	-3.44	0.89	1.19
A4	8458.4	8.46	17886239.0	16.92	71.54	1057298.9	1057307	1229.2	1057306.7	7.74	-	2	0.782	0.218	0	0.001566	3000	-3.67	1.02	0.00
A5	9026.8	9.03	20370732.8	18.05	81.48	1128344.2	1128353	1513.4	1128352.2	8.01	-	2	0.782	0.218	0	0.001566	3000	-3.67	1.02	0.00
A6	9583.4	9.58	22960592.6	19.17	91.84	1197925.5	1197935	1791.7	1197933.8	8.24	-	2	0.782	0.218	0	0.001566	3000	-3.67	1.02	0.00
A7	8546.0	8.55	18258692.9	17.09	73.03	1068250.5	1068259	1273.0	1068258.3	7.79	-	1	1	0	0	0.001228	3000	-3.68	0.00	0.00
A8	9082.6	9.08	20623561.6	18.17	82.49	1135324.7	1135334	1541.3	1135332.8	8.04	-	1	1	0	0	0.001228	3000	-3.68	0.00	0.00
A9	9623.9	9.62	23155063.3	19.25	92.62	1202987.9	1202998	1812.0	1202996.2	8.26	-	1	1	0	0	0.001228	3000	-3.68	0.00	0.00
A10	8672.6	8.67	18803555.4	17.35	75.21	1084072.3	1084081	1336.3	1084080.2	7.85	-	1	1	0	0	0.001228	3000	-3.68	0.00	0.00
A11	9166.6	9.17	21006735.1	18.33	84.03	1145823.0	1145832	1583.3	1145831.1	8.07	-	1	1	0	0	0.001228	3000	-3.68	0.00	0.00
A12	9687.1	9.69	23459910.9	19.37	93.84	1210881.0	1210891	1843.5	1210889.2	8.28	-	1	1	0	0	0.001228	3000	-3.68	0.00	0.00
id																				
01-NL	11736.0	11.74	34433247.6	23.47	137.73	1466990.4	1467002	868.0	1467001.9	11.48	-	3	0.623	0.161	0.216	0.001838	5000	5.73	1.48	1.99
02-NL	12456.2	12.46	38789413.6	24.91	155.16	1557022.5	1557035	1228.1	1557034.4	11.97	-	3	0.623	0.161	0.216	0.001838	5000	5.73	1.48	1.99
03-NL	13178.0	13.18	43415035.7	26.36	173.66	1647245.6	1647259	1589.0	1647258.0	12.41	-	3	0.623	0.161	0.216	0.001838	5000	5.73	1.48	1.99
A1-NL	6996.1	7.00	12236402.3	13.99	48.95	874510.7	874518	498.1	874517.6	6.85	-	3	0.623	0.161	0.216	0.001838	3000	3.44	0.89	1.19
A2-NL	7449.3	7.45	13872859.2	14.90	55.49	931153.5	931161	724.6	931160.6	7.17	-	3	0.623	0.161	0.216	0.001838	3000	3.44	0.89	1.19
A3-NL	7892.3	7.89	15571987.8	15.78	62.29	986530.0	986538	946.1	986537.4	7.44	-	3	0.623	0.161	0.216	0.001838	3000	3.44	0.89	1.19
A4-NL	7017.5	7.02	12311314.3	14.03	49.25	877183.6	877191	508.7	877190.4	6.87	-	3	0.623	0.161	0.216	0.001838	3000	3.44	0.89	1.19
A5-NL	7459.9	7.46	13912523.1	14.92	55.65	932483.6	932491	729.9	932490.8	7.17	-	3	0.623	0.161	0.216	0.001838	3000	3.44	0.89	1.19
A6-NL	7898.0	7.90	15594672.2	15.80	62.38	987248.3	987256	949.0	987255.7	7.44	-	3	0.623	0.161	0.216	0.001838	3000	3.44	0.89	1.19
A7-NL	7087.2	7.09	12557119.0	14.17	50.23	885897.1	885904	543.6	885904.0	6.92	-	3	0.623	0.161	0.216	0.001838	3000	3.44	0.89	1.19
A8-NL	7504.5	7.50	14079453.3	15.01	56.32	938061.2	938069	752.3	938068.4	7.20	-	3	0.623	0.161	0.216	0.001838	3000	3.44	0.89	1.19
A9-NL	7930.4	7.93	15722674.2	15.86	62.89	991291.7	991300	965.2	991299.2	7.46	-	3	0.623	0.161	0.216	0.001838	3000	3.44	0.89	1.19
A10-NL	7188.0	7.19	12916717.1	14.38	51.67	898492.3	898499	594.0	898499.3	6.99	-	2	0.782	0.218	0	0.001566	3000	3.67	1.02	0.00
A11-NL	7571.9	7.57	14333339.6	15.14	57.33	946481.1	946489	785.9	946488.4	7.25	-	2	0.782	0.218	0	0.001566	3000	3.67	1.02	0.00
A12-NL	7980.6	7.98	15922394.2	15.96	63.69	997567.9	997576	990.3	997575.4	7.49	-	2	0.782	0.218	0	0.001566	3000	3.67	1.02	0.00
id																				
01-V	27680.9	27.68	191557678.6	55.36	766.23	3460095.2	3460123	8840.4	3460111.6	16.39	-	2	0.782	0.218	0	0.001566	5000	6.12	-1.71	0.00
02-V	29663.2	29.66	219975627.7	59.33	879.90	3707879.0	3707909	9831.6	3707895.6	16.63	-	2	0.782	0.218	0	0.001566	5000	6.12	-1.71	0.00
03-V	31598.7	31.60	249619212.0	63.20	998.48	3949819.7	3949851	#####	3949836.6	16.84	-	2	0.782	0.218	0	0.001566	5000	6.12	-1.71	0.00
A1-V	16482.2	16.48	67915749.0	32.96	271.66	2060267.1	2060284	5241.1	2060276.9	9.82	-	3	0.623	0.161	0.216	0.001838	3000	3.44	-0.89	-1.19
A2-V	17725.3	17.73	78546841.9	35.45	314.19	2215657.5	2215675	5862.7	2215667.5	9.97	-	3	0.623	0.161	0.216	0.001838	3000	3.44	-0.89	-1.19
A3-V	18908.5	18.91	89382839.9	37.82	357.53	2363553.0	2363572	6454.2	2363563.1	10.10	-	3	0.623	0.161	0.216	0.001838	3000	3.44	-0.89	-1.19
A4-V	16541.9	16.54	68408422.2	33.08	273.63	2067726.3	2067743	5270.9	2067736.2	9.82	-	2	0.782	0.218	0	0.001566	3000	3.67	-1.02	0.00
A5-V	17758.3	17.76	78839401.0	35.52	315.36	2219780.0	2219798	5879.2	2219789.9	9.97	-	2	0.782	0.218	0	0.001566	3000	3.67	-1.02	0.00
A6-V	18930.8	18.93	89593920.1	37.86	358.38	2366342.2	2366361	6465.4	2366352.3	10.10	-	2	0.782	0.218	0	0.001566	3000	3.67	-1.02	0.00
A7-V	16734.0	16.73	70006486.5	33.47	280.03	2091738.6	2091755	5367.0	2091748.5	9.85	-	1	1	0	0	0.001228	3000	3.68	0.00	0.00
A8-V	17885.3	17.89	79970791.8	35.77	319.88	2235650.8	2235669	5942.6	2235660.8	9.99	-	1	1	0	0	0.001228	3000	3.68	0.00	0.00
A9-V	19029.5	19.03	90530429.2	38.06	362.12	2378677.5	2378697	6514.7	2378687.6	10.11	-	1	1	0	0	0.001228	3000	3.68	0.00	0.00
A10-V	17008.8	17.01	72324628.5	34.02	289.30	2126088.7	2126106	5504.4	2126098.6	9.88	-	1	1	0	0	0.001228	3000	3.68	0.00	0.00
A11-V	18073.8	18.07	81665975.1	36.15	326.66	2259221.7	2259240	6036.9	2259231.7	10.01	-	1	1	0	0	0.001228	3000	3.68	0.00	0.00
A12-V	19179.0	19.18	91958956.2	38.36	367.84	2397371.2	2397390	6589.5	2397381.3	10.12	-	1	1	0	0	0.001228	3000	3.68	0.00	0.00
id																				
01-H	14147.7	14.15	50039600.6	28.30	200.16	1768459.8	1768474	2073.9	1768472.7	-12.93	-	2	0.782	0.218	0	0.001566	5000	-6.12	1.71	0.00
02-H	15073.0	15.07	56799135.6	30.15	227.20	1884122.5	1884138	2536.5	1884135.9	-13.37	-	2	0.782	0.218	0	0.001566	5000	-6.12	1.71	0.00
03-H	15990.8	15.99	63926393.3	31.98	255.71	1998841.6	1998858	2995.4	1998855.3	-13.75	-	2	0.782	0.218	0	0.001566	5000	-6.12	1.71	0.00
A1-H	8431.5	8.43	17772727.9	16.86	71.09	1053938.6	1053947	1215.8	1053946.3	-7.73	-	3	0.623	0.161	0.216	0.001838	3000	-3.44	0.89	-1.19
A2-H	9013.7	9.01	20311517.4	18.03	81.25	1126703.0	1126712	1506.8	1126711.0	-8.01	-	3	0.623	0.161	0.216	0.001838	3000	-3.44	0.89	-1.19
A3-H	9576.2	9.58	22925855.7	19.15	91.70	1197019.0	1197029	1788.1	1197027.3	-8.24	-	3	0.623	0.161	0.216	0.001838	3000	-3.44	0.89	-1.19
A4-H	8458.4	8.46	17886239.0	16.92	71.54	1057298.9	1057307	1229.2	1057306.7	-7.74	-	2	0.782	0.218	0	0.001566	3000	-3.67	1.02	0.00
A5-H	9026.8	9.03	20370732.8	18.05	81.48	1128344.2	1128353	1513.4	1128352.2	-8.01	-	2	0.782	0.218	0	0.001566	3000	-3.67	1.02	0.00
A6-H	9583.4	9.58	22960592.6	19.17	91.84	1197925.5	1197935	1791.7	1197933.8	-8.24	-	2	0.782	0.218	0	0.001566	3000	-3.67	1.02	0.00
A7-H	8546.0	8.55	18258692.9	17.09	73.03	1068250.5	1068259	1273.0	1068258.3	-7.79	-	1	1	0	0	0.001228	3000	-3.68	0.00	0.00
A8-H	9082.6	9.08	20623561.6	18.17	82.49	1135324.7	1135334	1541.3	1135332.8	-8.04	-	1	1	0	0	0.001228	3000	-3.68	0.00	0.00
A9-H	9623.9	9.62	23155063.3	19.25	92.62	1202987.9	1202998	1812.0	1202996.2	-8.26	-	1	1	0	0	0.001228	3000	-3.68	0.00	0.00
A10-H	8672.6	8.67	18803555.4	17.35	75.21	1084072.3	1084081	1336.3	1084080.2	-7.85	-	1	1	0	0	0.001228	3000	-3.68	0.00	0.00
A11-H	9166.6	9.17	21006735.1	18.33	84.03	1145823.0	1145832	1583.3	1145831.1	-8.07	-	1	1	0	0	0.001228	3000	-3.68	0.00	0.00
A12-H	9687.1	9.69	23459910.9	19.37	93.84	1210881.0	1210891	1843.5	1210889.2	-8.28	-	1	1	0	0	0.001228	3000	-3.68	0.00	0.00
id																		0.00	0.00	0.00
01-VH	27680.9	27.68	191557678.6	55.36	766.23	3460095.2	3460123	8840.4	3460111.6	-16.39	-	2	0.782	0.218	0	0.001566	5000	-6.12	1.71	0.00
02-VH	29663.2	29.66	219975627.7	59.33	879.90	3707879.0	3707909	9831.6	3707895.6	-16.63	-	2	0.782	0.218	0	0.001566	5000	-6.12	1.71	0.00
03-VH	31598.7	31.60	249619212.0	63.20	998.48	3949819.7	3949851	#####	3949836.6	-16.84	-	2	0.782	0.218	0	0.001566	5000	-6.12	1.71	0.00
A1-VH	16482.2	16.48	67915749.0	32.96	271.66	2060267.1	2060284	5241.1	2060276.9	-9.82	-	3	0.623	0.161	0.216	0.001838	3000	-3.44	0.89	-1.19
A2-VH	17725.3	17.73	78546841.9	35.45	314.19	2215657.5	2215675	5862.7	2215667.5	-9.97	-	3	0.623	0.161	0.216	0.001838	3000	-3.44	0.89	-1.19
A3-VH	18908.5	18.91	89382839.9	37.82	357.53	2363553.0	2363572	6454.2	2363563.1	-10.10	-	3	0.623	0.161	0.216	0.001838	3000	-3.44	0.89	-1.19
A4-VH	16541.9	16.54	68408422.2	33.08	273.63	2067726.3	2067743	5270.9	2067736.2	-9.82	-	2	0.782	0.218	0	0.001566	3000	-3.67	1.02	0.00
A5-VH	17758.3	17.76	78839401.0	35.52	315.36	2219780.0	2219798	5879.2	2219789.9	-9.97	-	2	0.782	0.218	0	0.001566	3000	-3.67	1.02	0.00
A6-VH	18930.8	18.93	89593920.1	37.86	358.38	2366342.2	2366361	6465.4	2366352.3	-10.10	-	2	0.782	0.218	0	0.001566	3000	-3.67	1.02	0.00
A7-VH	16734.0	16.73	70006486.5	33.47	280.03	2091738.6	2091755	5367.0	2091748.5	-9.85	-	1	1	0	0	0.001228	3000	-3.68	0.00	0.00
A8-VH	17885.3	17.89	79970791.8	35.77	319.88	2235650.8	2235669	5942.6	2235660.8	-9.99	-	1	1	0	0	0.001228	3000	-3.68	0.00	0.00
A9-VH	19029.5	19.03	90530429.2	38.06	362.12	2378677.5	2378697	6514.7	2378687.6	-10.11	-	1	1	0	0	0.001228	3000	-3.68	0.00	0.00
A10-VH	17008.8	17.01	72324628.5	34.02	289.30	2126088.7	2126106	5504.4	2126098.6	-9.88	-	1	1	0	0	0.001228	3000	-3.68	0.00	0.00
A11-VH	18073.8	18.07	81665975.1	36.15	326.66	2259221.7	2259240	6036.9	2259231.7	-10.01	-	1	1	0	0	0.001228	3000	-3.68	0.00	0.00
A12-VH	19179.0	19.18	91958956.2	38.36	367.84	2397371.2	2397390	6589.5	2397381.3	-10.12	-	1	1	0	0	0.001228	3000	-3.68	0.00	0.00
id																				
01-NLH	11736.0	11.74	34433247.6	23.47	137.73	1466990.4	1467002	868.0	1467001.9	-11.48	-	3	0.623	0.161	0.216	0.001838	5000	-5.73	-1.48	-1.99
02-NLH	12456.2	12.46	38789413.6	24.91	155.16	1557022.5	1557035	1228.1	1557034.4	-11.97	-	3	0.623	0.161	0.216	0.001838	5000	-5.73	-1.48	-1.99
03-NLH	13178.0	13.18	43415035.7	26.36	173.66	1647245.6	1647259	1589.0	1647258.0	-12.41	-	3	0.623	0.161	0.216	0.001838	5000	-5.73	-1.48	-1.99
A1-NLH	6996.1	7.00	12236402.3	13.99	48.95	874510.7	874518	498.1	874517.6	-6.85	-	3	0.623	0.161	0.216	0.001838	3000	-3.44	-0.89	-1.19
A2-NLH	7449.3	7.45	13872859.2	14.90	55.49	931153.5	931161	724.6	931160.6	-7.17	-	3	0.623	0.161	0.216	0.001838	3000	-3.44	-0.89	-1.19
A3-NLH	7892.3	7.89	15571987.8	15.78	62.29	986530.0	986538	946.1	986537.4	-7.44	-	3	0.623	0.161	0.216	0.001838	3000	-3.44	-0.89	-1.19
A4-NLH	7017.5	7.02	12311314.3	14.03	49.25	877183.6	877191	508.7	877190.4	-6.87	-	3	0.623	0.161	0.216	0.001838	3000	-3.44	-0.89	-1.19
A5-NLH	7459.9	7.46	13912523.1	14.92	55.65	932483.6	932491	729.9	932490.8	-7.17	-	3	0.623	0.161	0.216	0.001838	3000	-3.44	-0.89	-1.19
A6-NLH	7898.0	7.90	15594672.2	15.80	62.38	987248.3	987256	949.0	987255.7	-7.44	-	3	0.623	0.161	0.216	0.001838	3000	-3.44	-0.89	-1.19
A7-NLH	7087.2	7.09	12557119.0	14.17	50.23	885897.1	885904	543.6	885904.0	-6.92	-	3	0.623	0.161	0.216	0.001838	3000	-3.44	-0.89	-1.19
A8-NLH	7504.5	7.50	14079453.3	15.01	56.32	938061.2	938069	752.3	938068.4	-7.20	-	3	0.623	0.161	0.216	0.001838	3000	-3.44	-0.89	-1.19
A9-NLH	7930.4	7.93	15722674.2	15.86	62.89	991291.7	991300	965.2	991299.2	-7.46	-	3	0.623	0.161	0.216	0.001838	3000	-3.44	-0.89	-1.19
A10-NLH	7188.0	7.19	12916717.1	14.38	51.67	898492.3	898499	594.0	898499.3	-6.99	-	2	0.782	0.218	0	0.001566	3000	-3.67	-1.02	0.00
A11-NLH	7571.9	7.57	14333339.6	15.14	57.33	946481.1	946489	785.9	946488.4	-7.25	-	2	0.782	0.218	0	0.001566	3000	-3.67	-1.02	0.00
A12-NLH	7980.6	7.98	15922394.2	15.96	63.69	997567.9	997576	990.3	997575.4	-7.49	-	2	0.782	0.218	0	0.001566	3000	-3.67	-1.02	0.00
id	109	110	111	112	113	114	115	116	117	118	119	120	121	122	123	124	125	126	127	128

id	Frame properties												Section properties										
id	E	v	F	Q	$f_{y,d}$	f_u	ε	h	b1	b2	m		profile 1	h1	P1h	P1b	P1w	P1tf	I_y	$W_{y,el}$	$W_{y,pl}$	A	section class
id	N/mm²	[-]	N	N	N/mm²	N/mm²	%	mm	mm	mm	[-]			mm	mm	mm	mm	mm	mm⁴	mm³	mm³	mm²	[-]
B01	210000	0.3	1000000	1000000	355	490	0.06429	5000	5000	5000	3	-	HEA300	290	262	300	8.5	14	1.7285E+08	1.1920E+06	1.3051E+06	10627	3
B02	210000	0.3	1000000	1000000	355	490	0.06429	5000	7500	7500	3	-	HEA300	290	262	300	8.5	14	1.7285E+08	1.1920E+06	1.3051E+06	10627	3
B03	210000	0.3	1000000	1000000	355	490	0.06429	5000	10000	10000	3	-	HEA300	290	262	300	8.5	14	1.7285E+08	1.1920E+06	1.3051E+06	10627	3
B1	210000	0.3	1000000	1000000	355	490	0.06429	3000	3000	3000	3	-	HEA120	114	98	120	5	8	5.7957E+06	1.0168E+05	1.1377E+05	2410	1
B2	210000	0.3	1000000	1000000	355	490	0.06429	3000	4500	4500	3	-	HEA120	114	98	120	5	8	5.7957E+06	1.0168E+05	1.1377E+05	2410	1
B3	210000	0.3	1000000	1000000	355	490	0.06429	3000	6000	6000	3	-	HEA120	114	98	120	5	8	5.7957E+06	1.0168E+05	1.1377E+05	2410	1
B4	210000	0.3	1000000	1000000	355	490	0.06429	3000	3000	3000	3	-	HEA160	152	134	160	6	9	1.5946E+07	2.0981E+05	2.3285E+05	3684	1
B5	210000	0.3	1000000	1000000	355	490	0.06429	3000	4500	4500	3	-	HEA160	152	134	160	6	9	1.5946E+07	2.0981E+05	2.3285E+05	3684	1
B6	210000	0.3	1000000	1000000	355	490	0.06429	3000	6000	6000	3	-	HEA160	152	134	160	6	9	1.5946E+07	2.0981E+05	2.3285E+05	3684	1
B7	210000	0.3	1000000	1000000	355	490	0.06429	3000	3000	3000	3	-	HEA220	210	188	220	7	11	5.1842E+07	4.9373E+05	5.4343E+05	6156	2
B8	210000	0.3	1000000	1000000	355	490	0.06429	3000	4500	4500	3	-	HEA220	210	188	220	7	11	5.1842E+07	4.9373E+05	5.4343E+05	6156	2
B9	210000	0.3	1000000	1000000	355	490	0.06429	3000	6000	6000	3	-	HEA220	210	188	220	7	11	5.1842E+07	4.9373E+05	5.4343E+05	6156	2
B10	210000	0.3	1000000	1000000	355	490	0.06429	3000	3000	3000	3	-	HEA280	270	244	280	8	13	1.3000E+08	9.6294E+05	1.0546E+06	9232	3
B11	210000	0.3	1000000	1000000	355	490	0.06429	3000	4500	4500	3	-	HEA280	270	244	280	8	13	1.3000E+08	9.6294E+05	1.0546E+06	9232	3
B12	210000	0.3	1000000	1000000	355	490	0.06429	3000	6000	6000	3	-	HEA280	270	244	280	8	13	1.3000E+08	9.6294E+05	1.0546E+06	9232	3
id	1	2	3	4	5	6	7	8	9	10	11	12	13	14	15	16	17	18	19	20	21	22	23

id	Section properties																						
id	profile 2	h2	P2h	P2b	P2w	P2tf	I_y	$W_{y,el}$	$W_{y,pl}$	A	section class		profile 4	h4	P4h	P4b	P4w	P4tf	I_y	$W_{y,el}$	$W_{y,pl}$	A	section class
id		mm	mm	mm	mm	mm	mm⁴	mm²	mm³	mm²	[-]			mm	mm	mm	mm	mm	mm⁴	mm²	mm³	mm²	[-]
B01	HEA300	290	262	300	8.5	14	1.7285E+08	1.1920E+06	1.3051E+06	10627	3		HEA300	290	262	300	8.5	14	1.7285E+08	1.1920E+06	1.3051E+06	10627	3
B02	HEA300	290	262	300	8.5	14	1.7285E+08	1.1920E+06	1.3051E+06	10627	3		HEA300	290	262	300	8.5	14	1.7285E+08	1.1920E+06	1.3051E+06	10627	3
B03	HEA300	290	262	300	8.5	14	1.7285E+08	1.1920E+06	1.3051E+06	10627	3		HEA300	290	262	300	8.5	14	1.7285E+08	1.1920E+06	1.3051E+06	10627	3
B1	HEA120	114	98	120	5	8	5.7957E+06	1.0168E+05	1.1377E+05	2410	1		HEA120	114	98	120	5	8	5.7957E+06	1.0168E+05	1.1377E+05	2410	1
B2	HEA120	114	98	120	5	8	5.7957E+06	1.0168E+05	1.1377E+05	2410	1		HEA120	114	98	120	5	8	5.7957E+06	1.0168E+05	1.1377E+05	2410	1
B3	HEA120	114	98	120	5	8	5.7957E+06	1.0168E+05	1.1377E+05	2410	1		HEA120	114	98	120	5	8	5.7957E+06	1.0168E+05	1.1377E+05	2410	1
B4	HEA160	152	134	160	6	9	1.5946E+07	2.0981E+05	2.3285E+05	3684	1		HEA160	152	134	160	6	9	1.5946E+07	2.0981E+05	2.3285E+05	3684	1
B5	HEA160	152	134	160	6	9	1.5946E+07	2.0981E+05	2.3285E+05	3684	1		HEA160	152	134	160	6	9	1.5946E+07	2.0981E+05	2.3285E+05	3684	1
B6	HEA160	152	134	160	6	9	1.5946E+07	2.0981E+05	2.3285E+05	3684	1		HEA160	152	134	160	6	9	1.5946E+07	2.0981E+05	2.3285E+05	3684	1
B7	HEA220	210	188	220	7	11	5.1842E+07	4.9373E+05	5.4343E+05	6156	2		HEA220	210	188	220	7	11	5.1842E+07	4.9373E+05	5.4343E+05	6156	2
B8	HEA220	210	188	220	7	11	5.1842E+07	4.9373E+05	5.4343E+05	6156	2		HEA220	210	188	220	7	11	5.1842E+07	4.9373E+05	5.4343E+05	6156	2
B9	HEA220	210	188	220	7	11	5.1842E+07	4.9373E+05	5.4343E+05	6156	2		HEA220	210	188	220	7	11	5.1842E+07	4.9373E+05	5.4343E+05	6156	2
B10	HEA280	270	244	280	8	13	1.3000E+08	9.6294E+05	1.0546E+06	9232	3		HEA280	270	244	280	8	13	1.3000E+08	9.6294E+05	1.0546E+06	9232	3
B11	HEA280	270	244	280	8	13	1.3000E+08	9.6294E+05	1.0546E+06	9232	3		HEA280	270	244	280	8	13	1.3000E+08	9.6294E+05	1.0546E+06	9232	3
B12	HEA280	270	244	280	8	13	1.3000E+08	9.6294E+05	1.0546E+06	9232	3		HEA280	270	244	280	8	13	1.3000E+08	9.6294E+05	1.0546E+06	9232	3
id	24	25	26	27	28	29	30	31	32	33	34	35	36	37	38	39	40	41	42	43	44	45	

id	Section properties												Model							
id	profile 5	h5	P5h	P5b	P5w	P5tf	I_y	$W_{y,el}$	$W_{y,pl}$	A	section class		joint	condition	C	ma1	mb1	mc1	rs1	ma2
id		mm	mm	mm	mm	mm	mm⁴	mm²	mm³	mm²	[-]		[-]	[-]	[-]	[-]	[-]	[-]	[-]	[-]
B01	HEA300	290	262	300	8.5	14	1.7285E+08	1.1920E+06	1.3051E+06	10627	3	-	1	2	1	78.96666667	32.75	25	0.5	78.96666667
B02	HEA300	290	262	300	8.5	14	1.7285E+08	1.1920E+06	1.3051E+06	10627	3	-	1	2	1.5	78.96666667	32.75	25	0.5	120.6333333
B03	HEA300	290	262	300	8.5	14	1.7285E+08	1.1920E+06	1.3051E+06	10627	3	-	1	2	2	78.96666667	32.75	25	0.5	162.3
B1	HEA120	114	98	120	5	8	5.7957E+06	1.0168E+05	1.1377E+05	2410	1	-	1	2	1	48.36666667	12.25	10	0.5	48.36666667
B2	HEA120	114	98	120	5	8	5.7957E+06	1.0168E+05	1.1377E+05	2410	1	-	1	2	1.5	48.36666667	12.25	10	0.5	73.36666667
B3	HEA120	114	98	120	5	8	5.7957E+06	1.0168E+05	1.1377E+05	2410	1	-	1	2	2	48.36666667	12.25	10	0.5	98.36666667
B4	HEA160	152	134	160	6	9	1.5946E+07	2.0981E+05	2.3285E+05	3684	1	-	1	2	1	47.76666667	16.75	13.33333333	0.5	47.76666667
B5	HEA160	152	134	160	6	9	1.5946E+07	2.0981E+05	2.3285E+05	3684	1	-	1	2	1.5	47.76666667	16.75	13.33333333	0.5	72.76666667
B6	HEA160	152	134	160	6	9	1.5946E+07	2.0981E+05	2.3285E+05	3684	1	-	1	2	2	47.76666667	16.75	13.33333333	0.5	97.76666667
B7	HEA220	210	188	220	7	11	5.1842E+07	4.9373E+05	5.4343E+05	6156	2	-	1	2	1	46.86666667	23.5	18.33333333	0.5	46.86666667
B8	HEA220	210	188	220	7	11	5.1842E+07	4.9373E+05	5.4343E+05	6156	2	-	1	2	1.5	46.86666667	23.5	18.33333333	0.5	71.86666667
B9	HEA220	210	188	220	7	11	5.1842E+07	4.9373E+05	5.4343E+05	6156	2	-	1	2	2	46.86666667	23.5	18.33333333	0.5	96.86666667
B10	HEA280	270	244	280	8	13	1.3000E+08	9.6294E+05	1.0546E+06	9232	3	-	1	2	1	45.93333333	30.5	23.33333333	0.5	45.93333333
B11	HEA280	270	244	280	8	13	1.3000E+08	9.6294E+05	1.0546E+06	9232	3	-	1	2	1.5	45.93333333	30.5	23.33333333	0.5	70.93333333
B12	HEA280	270	244	280	8	13	1.3000E+08	9.6294E+05	1.0546E+06	9232	3	-	1	2	2	45.93333333	30.5	23.33333333	0.5	95.93333333
id	46	47	48	49	50	51	52	53	54	55	56	57	58	59	60	61	62	63	64	65

id	Model												LBA					
id	mb2	mc2	rs2	ma4	mb4	mc4	rs4	ma5	mb5	mc5	rs5		α_{cr}	mode 1	mode 2	mode 3	F_{cr}	
id	[-]	[-]	[-]	[-]	[-]	[-]	[-]	[-]	[-]	[-]	[-]		[-]	[-]	[-]	[-]	N	
B01	32.75	25	0.5	78.96666667	32.75	25	0.5	78.96666667	32.75	25	0.5	-	7.0456	1	2	1	7.05E+06	-
B02	32.75	25	0.5	78.96666667	32.75	25	0.5	120.6333333	32.75	25	0.5	-	6.3849	1	2	1	6.38E+06	-
B03	32.75	25	0.5	78.96666667	32.75	25	0.5	162.3	32.75	25	0.5	-	5.8661	1	2	1	5.87E+06	-
B1	12.25	10	0.5	48.36666667	12.25	10	0.5	48.36666667	12.25	10	0.5	-	0.68102	1	5	8	6.81E+05	-
B2	12.25	10	0.5	48.36666667	12.25	10	0.5	73.36666667	12.25	10	0.5	-	0.61236	1	5	8	6.12E+05	-
B3	12.25	10	0.5	48.36666667	12.25	10	0.5	98.36666667	12.25	10	0.5	-	0.56049	1	2	3	5.60E+05	-
B4	16.75	13.33333333	0.5	47.76666667	16.75	13.33333333	0.5	47.76666667	16.75	13.33333333	0.5	-	1.8399	1	41	274	1.84E+06	-
B5	16.75	13.33333333	0.5	47.76666667	16.75	13.33333333	0.5	72.76666667	16.75	13.33333333	0.5	-	1.6609	1	4	274	1.66E+06	-
B6	16.75	13.33333333	0.5	47.76666667	16.75	13.33333333	0.5	97.76666667	16.75	13.33333333	0.5	-	1.523	1	4	272	1.52E+06	-
B7	23.5	18.33333333	0.5	46.86666667	23.5	18.33333333	0.5	46.86666667	23.5	18.33333333	0.5	-	5.7074	1	337	1	5.71E+06	-
B8	23.5	18.33333333	0.5	46.86666667	23.5	18.33333333	0.5	71.86666667	23.5	18.33333333	0.5	-	5.2013	1	337	1	5.20E+06	-
B9	23.5	18.33333333	0.5	46.86666667	23.5	18.33333333	0.5	96.86666667	23.5	18.33333333	0.5	-	4.7931	1	337	1	4.79E+06	-
B10	30.5	23.33333333	0.5	45.93333333	30.5	23.33333333	0.5	45.93333333	30.5	23.33333333	0.5	-	13.435	1	1	1	1.34E+07	-
B11	30.5	23.33333333	0.5	45.93333333	30.5	23.33333333	0.5	70.93333333	30.5	23.33333333	0.5	-	12.391	1	1	1	1.24E+07	-
B12	30.5	23.33333333	0.5	45.93333333	30.5	23.33333333	0.5	95.93333333	30.5	23.33333333	0.5	-	11.493	1	1	1	1.15E+07	-
id	66	67	68	69	70	71	72	73	74	75	76	77	78	79	80	81	82	107

id	GMNIA III											GMNIA IV								
id	$\pi*\sqrt{(EI/\alpha_{cr}*F)}$					$P^2+C_1*P+C_2=r^2-P^2$	P+(L_{cr}/1000)	L_{cr}/2-h	$\sqrt{(r^2-x^2)}$	y-P								P_i*F*h	P_i*F*h	P_i*F*h
id	L_{cr}	L_{cr}/1000	r^2-P^2	C_1	C_2	P	r	x	y	Δ		n	P_1	P_2	P_3	F	h	A_1	A_2	A_3
id	mm	mm	mm	[-]	[-]	mm	mm	mm	mm	mm		[-]	[-]	[-]	[-]	[-]	mm	[-]	[-]	[-]
B01	7130.7	7.13	12711603.99	14.26	50.85	891329.8455	891337	-1434.7	891335.8	5.98	-	2	0.782	0.218	0	0.001566	5000	-6.12	-1.71	0.00
B02	7490.5	7.49	14026981.95	14.98	56.11	936311.5713	936319	-1254.7	936318.2	6.65	-	2	0.782	0.218	0	0.001566	5000	-6.12	-1.71	0.00
B03	7814.7	7.81	15267533.30	15.63	61.07	976838.368	976846	-1092.6	976845.6	7.20	-	2	0.782	0.218	0	0.001566	5000	-6.12	-1.71	0.00
B1	4199.8	4.20	4409647.06	8.40	17.64	524976.8914	524981	-900.1	524980.3	3.43	-	3	0.623	0.161	0.216	0.001838	3000	-3.44	-0.89	-1.19
B2	4429.0	4.43	4904072.51	8.86	19.62	553626.2997	553631	-785.5	553630.2	3.87	-	3	0.623	0.161	0.216	0.001838	3000	-3.44	-0.89	-1.19
B3	4629.4	4.63	5357915.11	9.26	21.43	578676.9527	578682	-685.3	578681.2	4.22	-	3	0.623	0.161	0.216	0.001838	3000	-3.44	-0.89	-1.19
B4	4238.2	4.24	4490662.12	8.48	17.96	529777.441	529782	-880.9	529780.9	3.51	-	3	0.623	0.161	0.216	0.001838	3000	-3.44	-0.89	-1.19
B5	4460.8	4.46	4974633.77	8.92	19.90	557594.9456	557599	-769.6	557598.9	3.93	-	3	0.623	0.161	0.216	0.001838	3000	-3.44	-0.89	-1.19
B6	4658.4	4.66	5425061.87	9.32	21.70	582291.7262	582296	-670.8	582296.0	4.27	-	3	0.623	0.161	0.216	0.001838	3000	-3.44	-0.89	-1.19
B7	4338.9	4.34	4706554.47	8.68	18.83	542362.7022	542367	-830.5	542366.4	3.70	-	1	1	0	0	0.001228	3000	-3.68	0.00	0.00
B8	4545.1	4.55	5164514.44	9.09	20.66	568136.9291	568141	-727.4	568141.0	4.08	-	1	1	0	0	0.001228	3000	-3.68	0.00	0.00
B9	4734.7	4.73	5604345.61	9.47	22.42	591835.111	591840	-632.7	591839.5	4.40	-	1	1	0	0	0.001228	3000	-3.68	0.00	0.00
B10	4478.2	4.48	5013628.30	8.96	20.05	559776.0821	559781	-760.9	559780.0	3.96	-	1	1	0	0	0.001228	3000	-3.68	0.00	0.00
B11	4663.1	4.66	5436050.06	9.33	21.74	582881.129	582886	-668.5	582885.4	4.28	-	1	1	0	0	0.001228	3000	-3.68	0.00	0.00
B12	4841.8	4.84	5860793.20	9.68	23.44	605224.4581	605229	-579.1	605229.0	4.56	-	1	1	0	0	0.001228	3000	-3.68	0.00	0.00
id	108	109	110	111	112	113	114	115	116	117	118	119	120	121	122	123	124	125	126	127

APPENDIX C – INPUT AND OUTPUT FOR DESIGN RULES

In the sheets below, the in- and output of the design rules are given. The sheets are sub-divided in:

- Frames A, A-NL, A-V, A-H, A-NLH, and A-VH – NEN 6771 with nomogram
- Frames A, A-NL, A-V, A-H, A-NLH, and A-VH – Modified EN 1993-1-1 with nomogram
- Frames A, A-NL, A-V, A-H, A-NLH, and A-VH – Current EN 1993-1-1 with LBA, Yura, and Geschwindner
- Frame B – NEN 6771 with nomogram
- Frame B – Modified EN 1993-1-1 with nomogram
- Frame B – Current EN 1993-1-1 with LBA, Yura, and Geschwindner

	NEN 6771 with Nomogram														
	variable for solve function			$(EI_c/L_c)/(\mu(EI_b/L_b)$		$C_A*C_B*\lambda^2*\sin(\lambda)$	$(C_A+C_B)*\lambda*\cos(\lambda)+\sin(\lambda)$	eq1-eq2=0	π/λ (K_0)	$\pi/\lambda*h$	$\sqrt{(I/A)}$	$\pi*\sqrt{(E/f_{yd})}$	L_{cr}/i	λ/λ_e	W_i*f_{yd}
	N_{ult}	μ	C_A	C_B	λ	eq1	eq2	SOLVE FOR = 0, λ	nomogram	L_{cr}	i	λ_e	λ	λ_{rel}	M_{Rk}
	N	[-]	[-]	[-]	[-]	[-]	[-]	[-]	[-]	mm	mm	mm	mm	[-]	Nmm
01	1447584	6	1E+104	0.167	1.35	2.9615E+103	2.9615E+103	0.00	2.33	11639	127.53	76.41	91.27	1.19	423174646
02	1339919	6	1E+104	0.250	1.26	3.812E+103	3.812E+103	0.00	2.48	12421	127.53	76.41	97.40	1.27	423174646
03	1244369	6	1E+104	0.333	1.19	4.4047E+103	4.4047E+103	0.00	2.63	13173	127.53	76.41	103.29	1.35	423174646
A1	172002	6	1E+104	0.167	1.35	2.9615E+103	2.9615E+103	0.00	2.33	6984	49.04	76.41	142.41	1.86	40386575
A2	155573	6	1E+104	0.250	1.26	3.812E+103	3.812E+103	0.00	2.48	7453	49.04	76.41	151.98	1.99	40386575
A3	141740	6	1E+104	0.333	1.19	4.4047E+103	4.4047E+103	0.00	2.63	7904	49.04	76.41	161.17	2.11	40386575
A4	409493	6	1E+104	0.167	1.35	2.9615E+103	2.9615E+103	0.00	2.33	6984	65.79	76.41	106.15	1.39	82663170
A5	375537	6	1E+104	0.250	1.26	3.812E+103	3.812E+103	0.00	2.48	7453	65.79	76.41	113.28	1.48	82663170
A6	346048	6	1E+104	0.333	1.19	4.4047E+103	4.4047E+103	0.00	2.63	7904	65.79	76.41	120.13	1.57	82663170
A7	1032536	6	1E+104	0.167	1.35	2.9615E+103	2.9615E+103	0.00	2.33	6984	91.77	76.41	76.10	1.00	192918360
A8	968521	6	1E+104	0.250	1.26	3.812E+103	3.812E+103	0.00	2.48	7453	91.77	76.41	81.21	1.06	192918360
A9	909947	6	1E+104	0.333	1.19	4.4047E+103	4.4047E+103	0.00	2.63	7904	91.77	76.41	86.13	1.13	192918360
A10	1937028	6	1E+104	0.167	1.35	2.9615E+103	2.9615E+103	0.00	2.33	6984	118.66	76.41	58.85	0.77	341841936
A11	1852086	6	1E+104	0.250	1.26	3.812E+103	3.812E+103	0.00	2.48	7453	118.66	76.41	62.81	0.82	341841936
A12	1771294	6	1E+104	0.333	1.19	4.4047E+103	4.4047E+103	0.00	2.63	7904	118.66	76.41	66.61	0.87	341841936
01-NL	1649141	6	1E+104	0.167	1.35	2.9615E+103	2.9615E+103	0.00	2.33	11639	127.53	76.41	91.27	1.19	423174646
02-NL	1519941	6	1E+104	0.250	1.26	3.812E+103	3.812E+103	0.00	2.48	12421	127.53	76.41	97.40	1.27	423174646
03-NL	1405168	6	1E+104	0.333	1.19	4.4047E+103	4.4047E+103	0.00	2.63	13173	127.53	76.41	103.29	1.35	423174646
A1-NL	190076	6	1E+104	0.167	1.35	2.9615E+103	2.9615E+103	0.00	2.33	6984	49.04	76.41	142.41	1.86	40386575
A2-NL	170842	6	1E+104	0.250	1.26	3.812E+103	3.812E+103	0.00	2.48	7453	49.04	76.41	151.98	1.99	40386575
A3-NL	154800	6	1E+104	0.333	1.19	4.4047E+103	4.4047E+103	0.00	2.63	7904	49.04	76.41	161.17	2.11	40386575
A4-NL	462835	6	1E+104	0.167	1.35	2.9615E+103	2.9615E+103	0.00	2.33	6984	65.79	76.41	106.15	1.39	82663170
A5-NL	421980	6	1E+104	0.250	1.26	3.812E+103	3.812E+103	0.00	2.48	7453	65.79	76.41	113.28	1.48	82663170
A6-NL	386702	6	1E+104	0.333	1.19	4.4047E+103	4.4047E+103	0.00	2.63	7904	65.79	76.41	120.13	1.57	82663170
A7-NL	1180162	6	1E+104	0.167	1.35	2.9615E+103	2.9615E+103	0.00	2.33	6984	91.77	76.41	76.10	1.00	192918360
A8-NL	1105774	6	1E+104	0.250	1.26	3.812E+103	3.812E+103	0.00	2.48	7453	91.77	76.41	81.21	1.06	192918360
A9-NL	1036770	6	1E+104	0.333	1.19	4.4047E+103	4.4047E+103	0.00	2.63	7904	91.77	76.41	86.13	1.13	192918360
A10-NL	2190255	6	1E+104	0.167	1.35	2.9615E+103	2.9615E+103	0.00	2.33	6984	118.66	76.41	58.85	0.77	341841936
A11-NL	2101455	6	1E+104	0.250	1.26	3.812E+103	3.812E+103	0.00	2.48	7453	118.66	76.41	62.81	0.82	341841936
A12-NL	2014564	6	1E+104	0.333	1.19	4.4047E+103	4.4047E+103	0.00	2.63	7904	118.66	76.41	66.61	0.87	341841936
01-V	746778	6	1E+104	0.167	1.35	2.9615E+103	2.9615E+103	0.00	2.33	11639	127.53	76.41	91.27	1.19	423174646
02-V	699288	6	1E+104	0.250	1.26	3.812E+103	3.812E+103	0.00	2.48	12421	127.53	76.41	97.40	1.27	423174646
03-V	657544	6	1E+104	0.333	1.19	4.4047E+103	4.4047E+103	0.00	2.63	13173	127.53	76.41	103.29	1.35	423174646
A1-V	96373	6	1E+104	0.167	1.35	2.9615E+103	2.9615E+103	0.00	2.33	6984	49.04	76.41	142.41	1.86	40386575
A2-V	89173	6	1E+104	0.250	1.26	3.812E+103	3.812E+103	0.00	2.48	7453	49.04	76.41	151.98	1.99	40386575
A3-V	82952	6	1E+104	0.333	1.19	4.4047E+103	4.4047E+103	0.00	2.63	7904	49.04	76.41	161.17	2.11	40386575
A4-V	214920	6	1E+104	0.167	1.35	2.9615E+103	2.9615E+103	0.00	2.33	6984	65.79	76.41	106.15	1.39	82663170
A5-V	200468	6	1E+104	0.250	1.26	3.812E+103	3.812E+103	0.00	2.48	7453	65.79	76.41	113.28	1.48	82663170
A6-V	187834	6	1E+104	0.333	1.19	4.4047E+103	4.4047E+103	0.00	2.63	7904	65.79	76.41	120.13	1.57	82663170
A7-V	529866	6	1E+104	0.167	1.35	2.9615E+103	2.9615E+103	0.00	2.33	6984	91.77	76.41	76.10	1.00	192918360
A8-V	498794	6	1E+104	0.250	1.26	3.812E+103	3.812E+103	0.00	2.48	7453	91.77	76.41	81.21	1.06	192918360
A9-V	471276	6	1E+104	0.333	1.19	4.4047E+103	4.4047E+103	0.00	2.63	7904	91.77	76.41	86.13	1.13	192918360
A10-V	1022414	6	1E+104	0.167	1.35	2.9615E+103	2.9615E+103	0.00	2.33	6984	118.66	76.41	58.85	0.77	341841936
A11-V	970046	6	1E+104	0.250	1.26	3.812E+103	3.812E+103	0.00	2.48	7453	118.66	76.41	62.81	0.82	341841936
A12-V	923161	6	1E+104	0.333	1.19	4.4047E+103	4.4047E+103	0.00	2.63	7904	118.66	76.41	66.61	0.87	341841936
01-H	1328401	6	1E+104	0.167	1.35	2.9615E+103	2.9615E+103	0.00	2.33	11639	127.53	76.41	91.27	1.19	423174646
02-H	1177007	6	1E+104	0.250	1.26	3.812E+103	3.812E+103	0.00	2.48	12421	127.53	76.41	97.40	1.27	423174646
03-H	1045783	6	1E+104	0.333	1.19	4.4047E+103	4.4047E+103	0.00	2.63	13173	127.53	76.41	103.29	1.35	423174646
A1-H	142718	6	1E+104	0.167	1.35	2.9615E+103	2.9615E+103	0.00	2.33	6984	49.04	76.41	142.41	1.86	40386575
A2-H	116654	6	1E+104	0.250	1.26	3.812E+103	3.812E+103	0.00	2.48	7453	49.04	76.41	151.98	1.99	40386575
A3-H	95285	6	1E+104	0.333	1.19	4.4047E+103	4.4047E+103	0.00	2.63	7904	49.04	76.41	161.17	2.11	40386575
A4-H	373130	6	1E+104	0.167	1.35	2.9615E+103	2.9615E+103	0.00	2.33	6984	65.79	76.41	106.15	1.39	82663170
A5-H	326399	6	1E+104	0.250	1.26	3.812E+103	3.812E+103	0.00	2.48	7453	65.79	76.41	113.28	1.48	82663170
A6-H	286672	6	1E+104	0.333	1.19	4.4047E+103	4.4047E+103	0.00	2.63	7904	65.79	76.41	120.13	1.57	82663170
A7-H	991244	6	1E+104	0.167	1.35	2.9615E+103	2.9615E+103	0.00	2.33	6984	91.77	76.41	76.10	1.00	192918360
A8-H	910711	6	1E+104	0.250	1.26	3.812E+103	3.812E+103	0.00	2.48	7453	91.77	76.41	81.21	1.06	192918360
A9-H	838053	6	1E+104	0.333	1.19	4.4047E+103	4.4047E+103	0.00	2.63	7904	91.77	76.41	86.13	1.13	192918360
A10-H	1893858	6	1E+104	0.167	1.35	2.9615E+103	2.9615E+103	0.00	2.33	6984	118.66	76.41	58.85	0.77	341841936
A11-H	1789709	6	1E+104	0.250	1.26	3.812E+103	3.812E+103	0.00	2.48	7453	118.66	76.41	62.81	0.82	341841936
A12-H	1691406	6	1E+104	0.333	1.19	4.4047E+103	4.4047E+103	0.00	2.63	7904	118.66	76.41	66.61	0.87	341841936
01-VH	694424	6	1E+104	0.167	1.35	2.9615E+103	2.9615E+103	0.00	2.33	11639	127.53	76.41	91.27	1.19	423174646
02-VH	625908	6	1E+104	0.250	1.26	3.812E+103	3.812E+103	0.00	2.48	12421	127.53	76.41	97.40	1.27	423174646
03-VH	565757	6	1E+104	0.333	1.19	4.4047E+103	4.4047E+103	0.00	2.63	13173	127.53	76.41	103.29	1.35	423174646
A1-VH	81317	6	1E+104	0.167	1.35	2.9615E+103	2.9615E+103	0.00	2.33	6984	49.04	76.41	142.41	1.86	40386575
A2-VH	68367	6	1E+104	0.250	1.26	3.812E+103	3.812E+103	0.00	2.48	7453	49.04	76.41	151.98	1.99	40386575
A3-VH	57255	6	1E+104	0.333	1.19	4.4047E+103	4.4047E+103	0.00	2.63	7904	49.04	76.41	161.17	2.11	40386575
A4-VH	198327	6	1E+104	0.167	1.35	2.9615E+103	2.9615E+103	0.00	2.33	6984	65.79	76.41	106.15	1.39	82663170
A5-VH	177311	6	1E+104	0.250	1.26	3.812E+103	3.812E+103	0.00	2.48	7453	65.79	76.41	113.28	1.48	82663170
A6-VH	158981	6	1E+104	0.333	1.19	4.4047E+103	4.4047E+103	0.00	2.63	7904	65.79	76.41	120.13	1.57	82663170
A7-VH	512184	6	1E+104	0.167	1.35	2.9615E+103	2.9615E+103	0.00	2.33	6984	91.77	76.41	76.10	1.00	192918360
A8-VH	473838	6	1E+104	0.250	1.26	3.812E+103	3.812E+103	0.00	2.48	7453	91.77	76.41	81.21	1.06	192918360
A9-VH	439863	6	1E+104	0.333	1.19	4.4047E+103	4.4047E+103	0.00	2.63	7904	91.77	76.41	86.13	1.13	192918360
A10-VH	1003154	6	1E+104	0.167	1.35	2.9615E+103	2.9615E+103	0.00	2.33	6984	118.66	76.41	58.85	0.77	341841936
A11-VH	942610	6	1E+104	0.250	1.26	3.812E+103	3.812E+103	0.00	2.48	7453	118.66	76.41	62.81	0.82	341841936
A12-VH	888329	6	1E+104	0.333	1.19	4.4047E+103	4.4047E+103	0.00	2.63	7904	118.66	76.41	66.61	0.87	341841936
01-NLH	1503290	6	1E+104	0.167	1.35	2.9615E+103	2.9615E+103	0.00	2.33	11639	127.53	76.41	91.27	1.19	423174646
02-NLH	1323252	6	1E+104	0.250	1.26	3.812E+103	3.812E+103	0.00	2.48	12421	127.53	76.41	97.40	1.27	423174646
03-NLH	1168495	6	1E+104	0.333	1.19	4.4047E+103	4.4047E+103	0.00	2.63	13173	127.53	76.41	103.29	1.35	423174646
A1-NLH	156775	6	1E+104	0.167	1.35	2.9615E+103	2.9615E+103	0.00	2.33	6984	49.04	76.41	142.41	1.86	40386575
A2-NLH	127166	6	1E+104	0.250	1.26	3.812E+103	3.812E+103	0.00	2.48	7453	49.04	76.41	151.98	1.99	40386575
A3-NLH	103220	6	1E+104	0.333	1.19	4.4047E+103	4.4047E+103	0.00	2.63	7904	49.04	76.41	161.17	2.11	40386575
A4-NLH	419285	6	1E+104	0.167	1.35	2.9615E+103	2.9615E+103	0.00	2.33	6984	65.79	76.41	106.15	1.39	82663170
A5-NLH	364021	6	1E+104	0.250	1.26	3.812E+103	3.812E+103	0.00	2.48	7453	65.79	76.41	113.28	1.48	82663170
A6-NLH	317598	6	1E+104	0.333	1.19	4.4047E+103	4.4047E+103	0.00	2.63	7904	65.79	76.41	120.13	1.57	82663170
A7-NLH	1128783	6	1E+104	0.167	1.35	2.9615E+103	2.9615E+103	0.00	2.33	6984	91.77	76.41	76.10	1.00	192918360
A8-NLH	1034175	6	1E+104	0.250	1.26	3.812E+103	3.812E+103	0.00	2.48	7453	91.77	76.41	81.21	1.06	192918360
A9-NLH	948346	6	1E+104	0.333	1.19	4.4047E+103	4.4047E+103	0.00	2.63	7904	91.77	76.41	86.13	1.13	192918360
A10-NLH	2137754	6	1E+104	0.167	1.35	2.9615E+103	2.9615E+103	0.00	2.33	6984	118.66	76.41	58.85	0.77	341841936
A11-NLH	2024961	6	1E+104	0.250	1.26	3.812E+103	3.812E+103	0.00	2.48	7453	118.66	76.41	62.81	0.82	341841936
A12-NLH	1916063	6	1E+104	0.333	1.19	4.4047E+103	4.4047E+103	0.00	2.63	7904	118.66	76.41	66.61	0.87	341841936

NEN 6771 with Nomogram

	$A*f_{yd}$			$\alpha_k*(\lambda_{rel}-\lambda_0)*M_{Rk}/N_{Rk}$		M_{Rk}/γ_{M0}	N_{Rk}/γ_{M0}	π^2EI/L_{cr}^2	N_{cr}/F_{ult}			factor*N_{Ed}	$\varphi_0 x \alpha_h x \alpha_m$		$(2*\varphi N_{Ed}+(Q/F)*\varphi NEd+H)*h*C_m/2$	$N_{Ed}/N_{Rd}+(n/n-1)*F_{tot}*e^*/M_{Rd}$
	N_{Rk}	α_k	λ_0	e^*	γ_{M0}	M_{Rd}	N_{Rd}	N_{cr}	n	N_{Ed}	factor	F_{tot}	φ	φN_{Ed}	M_{Ed}	SOLVE FOR = 1
	N	[-]	[-]	mm	[-]	Nmm	N	N	[-]	N	[-]	N	[-]	N	Nmm	[-]
01	3772585	0.34	0.20	37.93	1	423174646	3772585	2644346	1.83	1447584	1.5	2171376	0.00365	5285.8	35679349	1.00
02	3772585	0.34	0.20	40.99	1	423174646	3772585	2321877	1.73	1339919	1.5	2009879	0.00365	4892.7	33025676	1.00
03	3772585	0.34	0.20	43.93	1	423174646	3772585	2064550	1.66	1244369	1.5	1866553	0.00365	4543.8	30670603	1.00
A1	855550	0.34	0.20	26.70	1	40386575	855550	246298	1.43	172002	1.5	258003	0.00408	702.2	2843893	1.00
A2	855550	0.34	0.20	28.71	1	40386575	855550	216263	1.39	155573	1.5	233360	0.00408	635.1	2572259	1.00
A3	855550	0.34	0.20	30.64	1	40386575	855550	192295	1.36	141740	1.5	212610	0.00408	578.7	2343535	1.00
A4	1307820	0.34	0.20	25.56	1	82663170	1307820	677645	1.65	409493	1.5	614240	0.00408	1671.7	6770585	1.00
A5	1307820	0.34	0.20	27.56	1	82663170	1307820	595008	1.58	375537	1.5	563305	0.00408	1533.1	6209149	1.00
A6	1307820	0.34	0.20	29.49	1	82663170	1307820	529065	1.53	346048	1.5	519072	0.00408	1412.7	5721580	1.00
A7	2185380	0.34	0.20	23.89	1	192918360	2185380	2203124	2.13	1032536	1.5	1548804	0.00408	4215.3	17072009	1.00
A8	2185380	0.34	0.20	25.90	1	192918360	2185380	1934460	2.00	968521	1.5	1452782	0.00408	3954.0	16013583	1.00
A9	2185380	0.34	0.20	27.83	1	192918360	2185380	1720069	1.89	909947	1.5	1364920	0.00408	3714.8	15045109	1.00
A10	3277360	0.34	0.20	20.22	1	341841936	3277360	5524428	2.85	1937028	1.5	2905543	0.00408	7907.9	32026937	1.00
A11	3277360	0.34	0.20	22.06	1	341841936	3277360	4850741	2.62	1852086	1.5	2778129	0.00408	7561.1	30622495	1.00
A12	3277360	0.34	0.20	23.82	1	341841936	3277360	4313148	2.44	1771294	1.5	2656941	0.00408	7231.3	29286678	1.00
01-NL	3772585	0.34	0.20	37.93	1	423174646	3772585	2644346	1.60	1649141	1.0	1649141	0.00365	6021.8	27098147	1.00
02-NL	3772585	0.34	0.20	40.99	1	423174646	3772585	2321877	1.53	1519941	1.0	1519941	0.00365	5550.0	24975179	1.00
03-NL	3772585	0.34	0.20	43.93	1	423174646	3772585	2064550	1.47	1405168	1.0	1405168	0.00365	5130.9	23089268	1.00
A1-NL	855550	0.34	0.20	26.70	1	40386575	855550	246298	1.30	190076	1.0	190076	0.00408	776.0	2095154	1.00
A2-NL	855550	0.34	0.20	28.71	1	40386575	855550	216263	1.27	170842	1.0	170842	0.00408	697.5	1883137	1.00
A3-NL	855550	0.34	0.20	30.64	1	40386575	855550	192295	1.24	154800	1.0	154800	0.00408	632.0	1706316	1.00
A4-NL	1307820	0.34	0.20	25.56	1	82663170	1307820	677645	1.46	462835	1.0	462835	0.00408	1889.5	5101694	1.00
A5-NL	1307820	0.34	0.20	27.56	1	82663170	1307820	595008	1.41	421980	1.0	421980	0.00408	1722.7	4651357	1.00
A6-NL	1307820	0.34	0.20	29.49	1	82663170	1307820	529065	1.37	386702	1.0	386702	0.00408	1578.7	4262504	1.00
A7-NL	2185380	0.34	0.20	23.89	1	192918360	2185380	2203124	1.87	1180162	1.0	1180162	0.00408	4818.0	13008577	1.00
A8-NL	2185380	0.34	0.20	25.90	1	192918360	2185380	1934460	1.75	1105774	1.0	1105774	0.00408	4514.3	12188615	1.00
A9-NL	2185380	0.34	0.20	27.83	1	192918360	2185380	1720069	1.66	1036770	1.0	1036770	0.00408	4232.6	11428008	1.00
A10-NL	3277360	0.34	0.20	20.22	1	341841936	3277360	5524428	2.52	2190255	1.0	2190255	0.00408	8941.7	24142536	1.00
A11-NL	3277360	0.34	0.20	22.06	1	341841936	3277360	4850741	2.31	2101455	1.0	2101455	0.00408	8579.2	23163711	1.00
A12-NL	3277360	0.34	0.20	23.82	1	341841936	3277360	4313148	2.14	2014564	1.0	2014564	0.00408	8224.4	22205942	1.00
01-V	3772585	0.34	0.20	37.93	1	423174646	3772585	2644346	3.54	746778	6	4480667	0.00365	2726.8	73624876	1.00
02-V	3772585	0.34	0.20	40.99	1	423174646	3772585	2321877	3.32	699288	6	4195730	0.00365	2553.4	68942872	1.00
03-V	3772585	0.34	0.20	43.93	1	423174646	3772585	2064550	3.14	657544	6	3945265	0.00365	2401.0	64827323	1.00
A1-V	855550	0.34	0.20	26.70	1	40386575	855550	246298	2.56	96373	6	578239	0.00408	393.4	6373759	1.00
A2-V	855550	0.34	0.20	28.71	1	40386575	855550	216263	2.43	89173	6	535037	0.00408	364.0	5897553	1.00
A3-V	855550	0.34	0.20	30.64	1	40386575	855550	192295	2.32	82952	6	497713	0.00408	338.7	5486142	1.00
A4-V	1307820	0.34	0.20	25.56	1	82663170	1307820	677645	3.15	214920	6	1289518	0.00408	877.4	14213970	1.00
A5-V	1307820	0.34	0.20	27.56	1	82663170	1307820	595008	2.97	200468	6	1202807	0.00408	818.4	13258183	1.00
A6-V	1307820	0.34	0.20	29.49	1	82663170	1307820	529065	2.82	187834	6	1127004	0.00408	766.8	12422635	1.00
A7-V	2185380	0.34	0.20	23.89	1	192918360	2185380	2203124	4.16	529866	6	3179198	0.00408	2163.2	35043355	1.00
A8-V	2185380	0.34	0.20	25.90	1	192918360	2185380	1934460	3.88	498794	6	2992764	0.00408	2036.3	32988352	1.00
A9-V	2185380	0.34	0.20	27.83	1	192918360	2185380	1720069	3.65	471276	6	2827656	0.00408	1924.0	31168410	1.00
A10-V	3277360	0.34	0.20	20.22	1	341841936	3277360	5524428	5.40	1022414	6	6134486	0.00408	4174.0	67618623	1.00
A11-V	3277360	0.34	0.20	22.06	1	341841936	3277360	4850741	5.00	970046	6	5820278	0.00408	3960.2	64155201	1.00
A12-V	3277360	0.34	0.20	23.82	1	341841936	3277360	4313148	4.67	923161	6	5538966	0.00408	3768.8	61054382	1.00
01-H	3772585	0.34	0.20	37.93	1	423174646	3772585	2644346	1.99	1328401	1.5	1992602	0.00365	4850.6	60866789	1.00
02-H	3772585	0.34	0.20	40.99	1	423174646	3772585	2321877	1.97	1177007	1.5	1765511	0.00365	4297.8	71197806	1.00
03-H	3772585	0.34	0.20	43.93	1	423174646	3772585	2064550	1.97	1045783	1.5	1568674	0.00365	3818.7	82025946	1.00
A1-H	855550	0.34	0.20	26.70	1	40386575	855550	246298	1.73	142718	1.5	214077	0.00408	582.6	8434706	1.00
A2-H	855550	0.34	0.20	28.71	1	40386575	855550	216263	1.85	116654	1.5	174980	0.00408	476.2	11041257	1.00
A3-H	855550	0.34	0.20	30.64	1	40386575	855550	192295	2.02	95285	1.5	142927	0.00408	389.0	13725446	1.00
A4-H	1307820	0.34	0.20	25.56	1	82663170	1307820	677645	1.82	373130	1.5	559695	0.00408	1523.3	12244350	1.00
A5-H	1307820	0.34	0.20	27.56	1	82663170	1307820	595008	1.82	326399	1.5	489598	0.00408	1332.5	14509198	1.00
A6-H	1307820	0.34	0.20	29.49	1	82663170	1307820	529065	1.85	286672	1.5	430009	0.00408	1170.3	16889859	1.00
A7-H	2185380	0.34	0.20	23.89	1	192918360	2185380	2203124	2.22	991244	1.5	1486865	0.00408	4046.7	22464277	1.00
A8-H	2185380	0.34	0.20	25.90	1	192918360	2185380	1934460	2.12	910711	1.5	1366067	0.00408	3718.0	24170255	1.00
A9-H	2185380	0.34	0.20	27.83	1	192918360	2185380	1720069	2.05	838053	1.5	1257080	0.00408	3421.3	26006421	1.00
A10-H	3277360	0.34	0.20	20.22	1	341841936	3277360	5524428	2.92	1893858	1.5	2840787	0.00408	7731.6	37388150	1.00
A11-H	3277360	0.34	0.20	22.06	1	341841936	3277360	4850741	2.71	1789709	1.5	2684564	0.00408	7306.5	38703652	1.00
A12-H	3277360	0.34	0.20	23.82	1	341841936	3277360	4313148	2.55	1691406	1.5	2537109	0.00408	6905.1	40115797	1.00
01-VH	3772585	0.34	0.20	37.93	1	423174646	3772585	2644346	3.81	694424	6.0	4166545	0.00365	2535.7	96588313	1.00
02-VH	3772585	0.34	0.20	40.99	1	423174646	3772585	2321877	3.71	625908	6.0	3755445	0.00365	2285.5	103895762	1.00
03-VH	3772585	0.34	0.20	43.93	1	423174646	3772585	2064550	3.65	565757	6.0	3394541	0.00365	2065.9	112028005	1.00
A1-VH	855550	0.34	0.20	26.70	1	40386575	855550	246298	3.03	81317	6.0	487900	0.00408	332.0	11452977	1.00
A2-VH	855550	0.34	0.20	28.71	1	40386575	855550	216263	3.16	68367	6.0	410202	0.00408	279.1	13634038	1.00
A3-VH	855550	0.34	0.20	30.64	1	40386575	855550	192295	3.36	57255	6.0	343529	0.00408	233.7	15936614	1.00
A4-VH	1307820	0.34	0.20	25.56	1	82663170	1307820	677645	3.42	198327	6.0	1189961	0.00408	809.7	19191591	1.00
A5-VH	1307820	0.34	0.20	27.56	1	82663170	1307820	595008	3.36	177311	6.0	1063867	0.00408	723.9	20839191	1.00
A6-VH	1307820	0.34	0.20	29.49	1	82663170	1307820	529065	3.33	158981	6.0	953883	0.00408	649.0	22664374	1.00
A7-VH	2185380	0.34	0.20	23.89	1	192918360	2185380	2203124	4.30	512184	6.0	3073105	0.00408	2091.0	39948922	1.00
A8-VH	2185380	0.34	0.20	25.90	1	192918360	2185380	1934460	4.08	473838	6.0	2843030	0.00408	1934.4	40450374	1.00
A9-VH	2185380	0.34	0.20	27.83	1	192918360	2185380	1720069	3.91	439863	6.0	2639176	0.00408	1795.7	41240852	1.00
A10-VH	3277360	0.34	0.20	20.22	1	341841936	3277360	5524428	5.51	1003154	6.0	6018921	0.00408	4095.4	72419787	1.00
A11-VH	3277360	0.34	0.20	22.06	1	341841936	3277360	4850741	5.15	942610	6.0	5655658	0.00408	3848.2	71453145	1.00
A12-VH	3277360	0.34	0.20	23.82	1	341841936	3277360	4313148	4.86	888329	6.0	5329971	0.00408	3626.6	70900696	1.00
01-NLH	3772585	0.34	0.20	37.93	1	423174646	3772585	2644346	1.76	1503290	1.0	1503290	0.00365	5489.2	52826583	1.00
02-NLH	3772585	0.34	0.20	40.99	1	423174646	3772585	2321877	1.75	1323252	1.0	1323252	0.00365	4831.8	63930747	1.00
03-NLH	3772585	0.34	0.20	43.93	1	423174646	3772585	2064550	1.77	1168495	1.0	1168495	0.00365	4266.7	75450327	1.00
A1-NLH	855550	0.34	0.20	26.70	1	40386575	855550	246298	1.57	156775	1.0	156775	0.00408	640.0	7803089	1.00
A2-NLH	855550	0.34	0.20	28.71	1	40386575	855550	216263	1.70	127166	1.0	127166	0.00408	519.2	10514213	1.00
A3-NLH	855550	0.34	0.20	30.64	1	40386575	855550	192295	1.86	103220	1.0	103220	0.00408	421.4	13287764	1.00
A4-NLH	1307820	0.34	0.20	25.56	1	82663170	1307820	677645	1.62	419285	1.0	419285	0.00408	1711.7	10696650	1.00
A5-NLH	1307820	0.34	0.20	27.56	1	82663170	1307820	595008	1.63	364021	1.0	364021	0.00408	1486.1	13124997	1.00
A6-NLH	1307820	0.34	0.20	29.49	1	82663170	1307820	529065	1.67	317598	1.0	317598	0.00408	1296.6	15650788	1.00
A7-NLH	2185380	0.34	0.20	23.89	1	192918360	2185380	2203124	1.95	1128783	1.0	1128783	0.00408	4608.2	18517239	1.00
A8-NLH	2185380	0.34	0.20	25.90	1	192918360	2185380	1934460	1.87	1034175	1.0	1034175	0.00408	4222.0	20511900	1.00
A9-NLH	2185380	0.34	0.20	27.83	1	192918360	2185380	1720069	1.81	948346	1.0	948346	0.00408	3871.6	22603333	1.00
A10-NLH	3277360	0.34	0.20	20.22	1	341841936	3277360	5524428	2.58	2137754	1.0	2137754	0.00408	8727.3	29638833	1.00
A11-NLH	3277360	0.34	0.20	22.06	1	341841936	3277360	4850741	2.40	2024961	1.0	2024961	0.00408	8266.9	31433041	1.00
A12-NLH	3277360	0.34	0.20	23.82	1	341841936	3277360	4313148	2.25	1916063	1.0	1916063	0.00408	7822.3	33270199	1.00

Modified EC1993-1-1- with Nomogram

	variable for solve function		W_l*f_{yd}	$A*f_{yd}$			$(EI_c/L_c)/(\mu(EI_b/L_b)$		$C_A*C_B*\lambda^2*\sin(\lambda)$	$(C_A+C_B)*\lambda*\cos(\lambda)+\sin(\lambda)$	eq1-eq2=0	π/λ (K_0)	$\pi/\lambda*h$	π^2EI/L_{cr}^2	$\bar{\lambda} = \sqrt{(F_{Rk}/F_{cr})}$
	F_{ult}	α	M_{Rk}	N_{Rk}	μ	C_A	C_B	λ	eq1	eq2	SOLVE FOR = 0, λ	nomogram	L_{cr}	N_{cr}	$\bar{\lambda}$
	N	[-]	Nmm	N	[-]	[-]	[-]	[-]	[-]	[-]	[-]	[-]	mm	N	[-]
01	1447584	0.34	423174646	3772585	6	1E+104	0.167	1.35	2.9615E+103	2.9615E+103	0.00	2.33	11639	2644346	1.19
02	1339919	0.34	423174646	3772585	6	1E+104	0.250	1.26	3.812E+103	3.812E+103	0.00	2.48	12421	2321877	1.27
03	1244369	0.34	423174646	3772585	6	1E+104	0.333	1.19	4.4047E+103	4.4047E+103	0.00	2.63	13173	2064550	1.35
A1	172002	0.34	40386575	855550	6	1E+104	0.167	1.35	2.9615E+103	2.9615E+103	0.00	2.33	6984	246298	1.86
A2	155573	0.34	40386575	855550	6	1E+104	0.250	1.26	3.812E+103	3.812E+103	0.00	2.48	7453	216263	1.99
A3	141740	0.34	40386575	855550	6	1E+104	0.333	1.19	4.4047E+103	4.4047E+103	0.00	2.63	7904	192295	2.11
A4	409493	0.34	82663170	1307820	6	1E+104	0.167	1.35	2.9615E+103	2.9615E+103	0.00	2.33	6984	677645	1.39
A5	375537	0.34	82663170	1307820	6	1E+104	0.250	1.26	3.812E+103	3.812E+103	0.00	2.48	7453	595008	1.48
A6	346048	0.34	82663170	1307820	6	1E+104	0.333	1.19	4.4047E+103	4.4047E+103	0.00	2.63	7904	529065	1.57
A7	1032536	0.34	192918360	2185380	6	1E+104	0.167	1.35	2.9615E+103	2.9615E+103	0.00	2.33	6984	2203124	1.00
A8	968521	0.34	192918360	2185380	6	1E+104	0.250	1.26	3.812E+103	3.812E+103	0.00	2.48	7453	1934460	1.06
A9	909947	0.34	192918360	2185380	6	1E+104	0.333	1.19	4.4047E+103	4.4047E+103	0.00	2.63	7904	1720069	1.13
A10	1937028	0.34	341841936	3277360	6	1E+104	0.167	1.35	2.9615E+103	2.9615E+103	0.00	2.33	6984	5524428	0.77
A11	1852086	0.34	341841936	3277360	6	1E+104	0.250	1.26	3.812E+103	3.812E+103	0.00	2.48	7453	4850741	0.82
A12	1771294	0.34	341841936	3277360	6	1E+104	0.333	1.19	4.4047E+103	4.4047E+103	0.00	2.63	7904	4313148	0.87
01-NL	1649141	0.34	423174646	3772585	6	1E+104	0.167	1.35	2.9615E+103	2.9615E+103	0.00	2.33	11639	2644346	1.19
02-NL	1519941	0.34	423174646	3772585	6	1E+104	0.250	1.26	3.812E+103	3.812E+103	0.00	2.48	12421	2321877	1.27
03-NL	1405168	0.34	423174646	3772585	6	1E+104	0.333	1.19	4.4047E+103	4.4047E+103	0.00	2.63	13173	2064550	1.35
A1-NL	190076	0.34	40386575	855550	6	1E+104	0.167	1.35	2.9615E+103	2.9615E+103	0.00	2.33	6984	246298	1.86
A2-NL	170842	0.34	40386575	855550	6	1E+104	0.250	1.26	3.812E+103	3.812E+103	0.00	2.48	7453	216263	1.99
A3-NL	154800	0.34	40386575	855550	6	1E+104	0.333	1.19	4.4047E+103	4.4047E+103	0.00	2.63	7904	192295	2.11
A4-NL	462835	0.34	82663170	1307820	6	1E+104	0.167	1.35	2.9615E+103	2.9615E+103	0.00	2.33	6984	677645	1.39
A5-NL	421980	0.34	82663170	1307820	6	1E+104	0.250	1.26	3.812E+103	3.812E+103	0.00	2.48	7453	595008	1.48
A6-NL	386702	0.34	82663170	1307820	6	1E+104	0.333	1.19	4.4047E+103	4.4047E+103	0.00	2.63	7904	529065	1.57
A7-NL	1180162	0.34	192918360	2185380	6	1E+104	0.167	1.35	2.9615E+103	2.9615E+103	0.00	2.33	6984	2203124	1.00
A8-NL	1105774	0.34	192918360	2185380	6	1E+104	0.250	1.26	3.812E+103	3.812E+103	0.00	2.48	7453	1934460	1.06
A9-NL	1036770	0.34	192918360	2185380	6	1E+104	0.333	1.19	4.4047E+103	4.4047E+103	0.00	2.63	7904	1720069	1.13
A10-NL	2190255	0.34	341841936	3277360	6	1E+104	0.167	1.35	2.9615E+103	2.9615E+103	0.00	2.33	6984	5524428	0.77
A11-NL	2101455	0.34	341841936	3277360	6	1E+104	0.250	1.26	3.812E+103	3.812E+103	0.00	2.48	7453	4850741	0.82
A12-NL	2014564	0.34	341841936	3277360	6	1E+104	0.333	1.19	4.4047E+103	4.4047E+103	0.00	2.63	7904	4313148	0.87
01-V	746778	0.34	423174646	3772585	6	1E+104	0.167	1.35	2.9615E+103	2.9615E+103	0.00	2.33	11639	2644346	1.19
02-V	699288	0.34	423174646	3772585	6	1E+104	0.250	1.26	3.812E+103	3.812E+103	0.00	2.48	12421	2321877	1.27
03-V	657544	0.34	423174646	3772585	6	1E+104	0.333	1.19	4.4047E+103	4.4047E+103	0.00	2.63	13173	2064550	1.35
A1-V	96373	0.34	40386575	855550	6	1E+104	0.167	1.35	2.9615E+103	2.9615E+103	0.00	2.33	6984	246298	1.86
A2-V	89173	0.34	40386575	855550	6	1E+104	0.250	1.26	3.812E+103	3.812E+103	0.00	2.48	7453	216263	1.99
A3-V	82952	0.34	40386575	855550	6	1E+104	0.333	1.19	4.4047E+103	4.4047E+103	0.00	2.63	7904	192295	2.11
A4-V	214920	0.34	82663170	1307820	6	1E+104	0.167	1.35	2.9615E+103	2.9615E+103	0.00	2.33	6984	677645	1.39
A5-V	200468	0.34	82663170	1307820	6	1E+104	0.250	1.26	3.812E+103	3.812E+103	0.00	2.48	7453	595008	1.48
A6-V	187834	0.34	82663170	1307820	6	1E+104	0.333	1.19	4.4047E+103	4.4047E+103	0.00	2.63	7904	529065	1.57
A7-V	529866	0.34	192918360	2185380	6	1E+104	0.167	1.35	2.9615E+103	2.9615E+103	0.00	2.33	6984	2203124	1.00
A8-V	498794	0.34	192918360	2185380	6	1E+104	0.250	1.26	3.812E+103	3.812E+103	0.00	2.48	7453	1934460	1.06
A9-V	471276	0.34	192918360	2185380	6	1E+104	0.333	1.19	4.4047E+103	4.4047E+103	0.00	2.63	7904	1720069	1.13
A10-V	1022414	0.34	341841936	3277360	6	1E+104	0.167	1.35	2.9615E+103	2.9615E+103	0.00	2.33	6984	5524428	0.77
A11-V	970046	0.34	341841936	3277360	6	1E+104	0.250	1.26	3.812E+103	3.812E+103	0.00	2.48	7453	4850741	0.82
A12-V	923161	0.34	341841936	3277360	6	1E+104	0.333	1.19	4.4047E+103	4.4047E+103	0.00	2.63	7904	4313148	0.87
01-H	1328401	0.34	423174646	3772585	6	1E+104	0.167	1.35	2.9615E+103	2.9615E+103	0.00	2.33	11639	2644346	1.19
02-H	1177007	0.34	423174646	3772585	6	1E+104	0.250	1.26	3.812E+103	3.812E+103	0.00	2.48	12421	2321877	1.27
03-H	1045783	0.34	423174646	3772585	6	1E+104	0.333	1.19	4.4047E+103	4.4047E+103	0.00	2.63	13173	2064550	1.35
A1-H	142718	0.34	40386575	855550	6	1E+104	0.167	1.35	2.9615E+103	2.9615E+103	0.00	2.33	6984	246298	1.86
A2-H	116654	0.34	40386575	855550	6	1E+104	0.250	1.26	3.812E+103	3.812E+103	0.00	2.48	7453	216263	1.99
A3-H	95285	0.34	40386575	855550	6	1E+104	0.333	1.19	4.4047E+103	4.4047E+103	0.00	2.63	7904	192295	2.11
A4-H	373130	0.34	82663170	1307820	6	1E+104	0.167	1.35	2.9615E+103	2.9615E+103	0.00	2.33	6984	677645	1.39
A5-H	326399	0.34	82663170	1307820	6	1E+104	0.250	1.26	3.812E+103	3.812E+103	0.00	2.48	7453	595008	1.48
A6-H	286672	0.34	82663170	1307820	6	1E+104	0.333	1.19	4.4047E+103	4.4047E+103	0.00	2.63	7904	529065	1.57
A7-H	991244	0.34	192918360	2185380	6	1E+104	0.167	1.35	2.9615E+103	2.9615E+103	0.00	2.33	6984	2203124	1.00
A8-H	910711	0.34	192918360	2185380	6	1E+104	0.250	1.26	3.812E+103	3.812E+103	0.00	2.48	7453	1934460	1.06
A9-H	838053	0.34	192918360	2185380	6	1E+104	0.333	1.19	4.4047E+103	4.4047E+103	0.00	2.63	7904	1720069	1.13
A10-H	1893858	0.34	341841936	3277360	6	1E+104	0.167	1.35	2.9615E+103	2.9615E+103	0.00	2.33	6984	5524428	0.77
A11-H	1789709	0.34	341841936	3277360	6	1E+104	0.250	1.26	3.812E+103	3.812E+103	0.00	2.48	7453	4850741	0.82
A12-H	1691406	0.34	341841936	3277360	6	1E+104	0.333	1.19	4.4047E+103	4.4047E+103	0.00	2.63	7904	4313148	0.87
01-VH	694424	0.34	423174646	3772585	6	1E+104	0.167	1.35	2.9615E+103	2.9615E+103	0.00	2.33	11639	2644346	1.19
02-VH	625908	0.34	423174646	3772585	6	1E+104	0.250	1.26	3.812E+103	3.812E+103	0.00	2.48	12421	2321877	1.27
03-VH	565757	0.34	423174646	3772585	6	1E+104	0.333	1.19	4.4047E+103	4.4047E+103	0.00	2.63	13173	2064550	1.35
A1-VH	81317	0.34	40386575	855550	6	1E+104	0.167	1.35	2.9615E+103	2.9615E+103	0.00	2.33	6984	246298	1.86
A2-VH	68367	0.34	40386575	855550	6	1E+104	0.250	1.26	3.812E+103	3.812E+103	0.00	2.48	7453	216263	1.99
A3-VH	57255	0.34	40386575	855550	6	1E+104	0.333	1.19	4.4047E+103	4.4047E+103	0.00	2.63	7904	192295	2.11
A4-VH	198327	0.34	82663170	1307820	6	1E+104	0.167	1.35	2.9615E+103	2.9615E+103	0.00	2.33	6984	677645	1.39
A5-VH	177311	0.34	82663170	1307820	6	1E+104	0.250	1.26	3.812E+103	3.812E+103	0.00	2.48	7453	595008	1.48
A6-VH	158981	0.34	82663170	1307820	6	1E+104	0.333	1.19	4.4047E+103	4.4047E+103	0.00	2.63	7904	529065	1.57
A7-VH	512184	0.34	192918360	2185380	6	1E+104	0.167	1.35	2.9615E+103	2.9615E+103	0.00	2.33	6984	2203124	1.00
A8-VH	473838	0.34	192918360	2185380	6	1E+104	0.250	1.26	3.812E+103	3.812E+103	0.00	2.48	7453	1934460	1.06
A9-VH	439863	0.34	192918360	2185380	6	1E+104	0.333	1.19	4.4047E+103	4.4047E+103	0.00	2.63	7904	1720069	1.13
A10-VH	1003154	0.34	341841936	3277360	6	1E+104	0.167	1.35	2.9615E+103	2.9615E+103	0.00	2.33	6984	5524428	0.77
A11-VH	942610	0.34	341841936	3277360	6	1E+104	0.250	1.26	3.812E+103	3.812E+103	0.00	2.48	7453	4850741	0.82
A12-VH	888329	0.34	341841936	3277360	6	1E+104	0.333	1.19	4.4047E+103	4.4047E+103	0.00	2.63	7904	4313148	0.87
01-NLH	1503290	0.34	423174646	3772585	6	1E+104	0.167	1.35	2.9615E+103	2.9615E+103	0.00	2.33	11639	2644346	1.19
02-NLH	1323252	0.34	423174646	3772585	6	1E+104	0.250	1.26	3.812E+103	3.812E+103	0.00	2.48	12421	2321877	1.27
03-NLH	1168495	0.34	423174646	3772585	6	1E+104	0.333	1.19	4.4047E+103	4.4047E+103	0.00	2.63	13173	2064550	1.35
A1-NLH	156775	0.34	40386575	855550	6	1E+104	0.167	1.35	2.9615E+103	2.9615E+103	0.00	2.33	6984	246298	1.86
A2-NLH	127166	0.34	40386575	855550	6	1E+104	0.250	1.26	3.812E+103	3.812E+103	0.00	2.48	7453	216263	1.99
A3-NLH	103220	0.34	40386575	855550	6	1E+104	0.333	1.19	4.4047E+103	4.4047E+103	0.00	2.63	7904	192295	2.11
A4-NLH	419285	0.34	82663170	1307820	6	1E+104	0.167	1.35	2.9615E+103	2.9615E+103	0.00	2.33	6984	677645	1.39
A5-NLH	364021	0.34	82663170	1307820	6	1E+104	0.250	1.26	3.812E+103	3.812E+103	0.00	2.48	7453	595008	1.48
A6-NLH	317598	0.34	82663170	1307820	6	1E+104	0.333	1.19	4.4047E+103	4.4047E+103	0.00	2.63	7904	529065	1.57
A7-NLH	1128783	0.34	192918360	2185380	6	1E+104	0.167	1.35	2.9615E+103	2.9615E+103	0.00	2.33	6984	2203124	1.00
A8-NLH	1034175	0.34	192918360	2185380	6	1E+104	0.250	1.26	3.812E+103	3.812E+103	0.00	2.48	7453	1934460	1.06
A9-NLH	948346	0.34	192918360	2185380	6	1E+104	0.333	1.19	4.4047E+103	4.4047E+103	0.00	2.63	7904	1720069	1.13
A10-NLH	2137754	0.34	341841936	3277360	6	1E+104	0.167	1.35	2.9615E+103	2.9615E+103	0.00	2.33	6984	5524428	0.77
A11-NLH	2024961	0.34	341841936	3277360	6	1E+104	0.250	1.26	3.812E+103	3.812E+103	0.00	2.48	7453	4850741	0.82
A12-NLH	1916063	0.34	341841936	3277360	6	1E+104	0.333	1.19	4.4047E+103	4.4047E+103	0.00	2.63	7904	4313148	0.87

Modified EC1993-1-1- with Nomogram

	$\Phi = 0.5(1+\alpha*(\lambda-0.2)+\lambda^2)$	$\chi = 1/(\Phi+\sqrt{(\Phi^2-\lambda^2)})$		M_{Rk}/γ_{M0}	N_{Rk}/γ_{M0}	$1/(1-((F_{ult}/F_{Rd})*\chi*\lambda\hat{}2))$			factor*N_{Ed}			$F_{ult}*h*3/2*C_m$	$F/N_{Rd}+(n/n-1)*F_{tot}*e^*/M_{Rd}$
	Φ	χ	γ_{M0}	M_{Rd}	N_{Rd}	k	N_{Ed}	factor	F_{lean}	φF	c_m	M_{Ed}	SOLVE FOR = 1, F_{ult}
	[-]	[-]	[-]	Nmm	N	[-]	N	[-]	N	N	[-]	N	[-]
01	1.38	0.48	1.0	423174646	3772585	1.36	1447584	0.5	723792	5285.8	0.9	39643722	1.00
02	1.50	0.44	1.0	423174646	3772585	1.34	1339919	0.5	669960	4892.7	0.9	36695195	1.00
03	1.61	0.40	1.0	423174646	3772585	1.32	1244369	0.5	622184	4543.8	0.9	34078448	1.00
A1	2.52	0.24	1.0	40386575	855550	1.20	172002	0.5	86001	702.2	0.9	3159881	1.00
A2	2.78	0.21	1.0	40386575	855550	1.18	155573	0.5	77787	635.1	0.9	2858066	1.00
A3	3.05	0.19	1.0	40386575	855550	1.16	141740	0.5	70870	578.7	0.9	2603928	1.00
A4	1.67	0.39	1.0	82663170	1307820	1.30	409493	0.5	204747	1671.7	0.9	7522872	1.00
A5	1.82	0.35	1.0	82663170	1307820	1.28	375537	0.5	187768	1533.1	0.9	6899055	1.00
A6	1.97	0.32	1.0	82663170	1307820	1.26	346048	0.5	173024	1412.7	0.9	6357311	1.00
A7	1.13	0.60	1.0	192918360	2185380	1.39	1032536	0.5	516268	4215.3	0.9	18968898	1.00
A8	1.21	0.56	1.0	192918360	2185380	1.39	968521	0.5	484261	3954.0	0.9	17792870	1.00
A9	1.29	0.52	1.0	192918360	2185380	1.38	909947	0.5	454973	3714.8	0.9	16716788	1.00
A10	0.89	0.74	1.0	341841936	3277360	1.35	1937028	0.5	968514	7907.9	0.9	35585486	1.00
A11	0.94	0.71	1.0	341841936	3277360	1.37	1852086	0.5	926043	7561.1	0.9	34024995	1.00
A12	0.99	0.68	1.0	341841936	3277360	1.39	1771294	0.5	885647	7231.3	0.9	32540753	1.00
01-NL	1.38	0.48	1.0	423174646	3772585	1.43	1649141	0.0	0	6021.8	0.9	30109052	1.00
02-NL	1.50	0.44	1.0	423174646	3772585	1.40	1519941	0.0	0	5550.0	0.9	27750199	1.00
03-NL	1.61	0.40	1.0	423174646	3772585	1.38	1405168	0.0	0	5130.9	0.9	25654742	1.00
A1-NL	2.52	0.24	1.0	40386575	855550	1.22	190076	0.0	0	776.0	0.9	2327948	1.00
A2-NL	2.78	0.21	1.0	40386575	855550	1.20	170842	0.0	0	697.5	0.9	2092375	1.00
A3-NL	3.05	0.19	1.0	40386575	855550	1.18	154800	0.0	0	632.0	0.9	1895906	1.00
A4-NL	1.67	0.39	1.0	82663170	1307820	1.36	462835	0.0	0	1889.5	0.9	5668549	1.00
A5-NL	1.82	0.35	1.0	82663170	1307820	1.33	421980	0.0	0	1722.7	0.9	5168175	1.00
A6-NL	1.97	0.32	1.0	82663170	1307820	1.30	386702	0.0	0	1578.7	0.9	4736115	1.00
A7-NL	1.13	0.60	1.0	192918360	2185380	1.47	1180162	0.0	0	4818.0	0.9	14453974	1.00
A8-NL	1.21	0.56	1.0	192918360	2185380	1.47	1105774	0.0	0	4514.3	0.9	13542905	1.00
A9-NL	1.29	0.52	1.0	192918360	2185380	1.46	1036770	0.0	0	4232.6	0.9	12697786	1.00
A10-NL	0.89	0.74	1.0	341841936	3277360	1.42	2190255	0.0	0	8941.7	0.9	26825040	1.00
A11-NL	0.94	0.71	1.0	341841936	3277360	1.44	2101455	0.0	0	8579.2	0.9	25737457	1.00
A12-NL	0.99	0.68	1.0	341841936	3277360	1.46	2014564	0.0	0	8224.4	0.9	24673269	1.00
01-V	1.38	0.48	1.0	423174646	3772585	1.16	746778	5.0	3733889	2726.8	0.9	81805417	1.00
02-V	1.50	0.44	1.0	423174646	3772585	1.15	699288	5.0	3496441	2553.4	0.9	76603191	1.00
03-V	1.61	0.40	1.0	423174646	3772585	1.15	657544	5.0	3287721	2401.0	0.9	72030359	1.00
A1-V	2.52	0.24	1.0	40386575	855550	1.10	96373	5.0	481866	393.4	0.9	7081955	1.00
A2-V	2.78	0.21	1.0	40386575	855550	1.10	89173	5.0	445864	364.0	0.9	6552837	1.00
A3-V	3.05	0.19	1.0	40386575	855550	1.09	82952	5.0	414761	338.7	0.9	6095713	1.00
A4-V	1.67	0.39	1.0	82663170	1307820	1.14	214920	5.0	1074598	877.4	0.9	15793300	1.00
A5-V	1.82	0.35	1.0	82663170	1307820	1.13	200468	5.0	1002339	818.4	0.9	14731314	1.00
A6-V	1.97	0.32	1.0	82663170	1307820	1.13	187834	5.0	939170	766.8	0.9	13802928	1.00
A7-V	1.13	0.60	1.0	192918360	2185380	1.17	529866	5.0	2649331	2163.2	0.9	38937061	1.00
A8-V	1.21	0.56	1.0	192918360	2185380	1.17	498794	5.0	2493970	2036.3	0.9	36653724	1.00
A9-V	1.29	0.52	1.0	192918360	2185380	1.17	471276	5.0	2356380	1924.0	0.9	34631566	1.00
A10-V	0.89	0.74	1.0	341841936	3277360	1.16	1022414	5.0	5112072	4174.0	0.9	75131803	1.00
A11-V	0.94	0.71	1.0	341841936	3277360	1.17	970046	5.0	4850232	3960.2	0.9	71283556	1.00
A12-V	0.99	0.68	1.0	341841936	3277360	1.17	923161	5.0	4615805	3768.8	0.9	67838203	1.00
01-H	1.38	0.48	1.0	423174646	3772585	1.32	1328401	0.5	664201	4850.6	0.9	67629765	1.00
02-H	1.50	0.44	1.0	423174646	3772585	1.29	1177007	0.5	588504	4297.8	0.9	79108673	1.00
03-H	1.61	0.40	1.0	423174646	3772585	1.26	1045783	0.5	522891	3818.7	0.9	91139940	1.00
A1-H	2.52	0.24	1.0	40386575	855550	1.16	142718	0.5	71359	582.6	0.9	9371895	1.00
A2-H	2.78	0.21	1.0	40386575	855550	1.13	116654	0.5	58327	476.2	0.9	12268063	1.00
A3-H	3.05	0.19	1.0	40386575	855550	1.10	95285	0.5	47642	389.0	0.9	15250495	1.00
A4-H	1.67	0.39	1.0	82663170	1307820	1.27	373130	0.5	186565	1523.3	0.9	13604834	1.00
A5-H	1.82	0.35	1.0	82663170	1307820	1.24	326399	0.5	163199	1332.5	0.9	16121332	1.00
A6-H	1.97	0.32	1.0	82663170	1307820	1.21	286672	0.5	143336	1170.3	0.9	18766510	1.00
A7-H	1.13	0.60	1.0	192918360	2185380	1.37	991244	0.5	495622	4046.7	0.9	24960307	1.00
A8-H	1.21	0.56	1.0	192918360	2185380	1.36	910711	0.5	455356	3718.0	0.9	26855838	1.00
A9-H	1.29	0.52	1.0	192918360	2185380	1.34	838053	0.5	419027	3421.3	0.9	28896023	1.00
A10-H	0.89	0.74	1.0	341841936	3277360	1.34	1893858	0.5	946929	7731.6	0.9	41542389	1.00
A11-H	0.94	0.71	1.0	341841936	3277360	1.36	1789709	0.5	894855	7306.5	0.9	43004058	1.00
A12-H	0.99	0.68	1.0	341841936	3277360	1.36	1691406	0.5	845703	6905.1	0.9	44573108	1.00
01-VH	1.38	0.48	1.0	423174646	3772585	1.14	694424	5.0	3472120	2535.7	0.9	107320348	1.00
02-VH	1.50	0.44	1.0	423174646	3772585	1.13	625908	5.0	3129538	2285.5	0.9	115439736	1.00
03-VH	1.61	0.40	1.0	423174646	3772585	1.12	565757	5.0	2828784	2065.9	0.9	124475561	1.00
A1-VH	2.52	0.24	1.0	40386575	855550	1.08	81317	5.0	406583	332.0	0.9	12725530	1.00
A2-VH	2.78	0.21	1.0	40386575	855550	1.07	68367	5.0	341835	279.1	0.9	15148931	1.00
A3-VH	3.05	0.19	1.0	40386575	855550	1.06	57255	5.0	286274	233.7	0.9	17707349	1.00
A4-VH	1.67	0.39	1.0	82663170	1307820	1.13	198327	5.0	991634	809.7	0.9	21323990	1.00
A5-VH	1.82	0.35	1.0	82663170	1307820	1.12	177311	5.0	886556	723.9	0.9	23154657	1.00
A6-VH	1.97	0.32	1.0	82663170	1307820	1.11	158981	5.0	794903	649.0	0.9	25182638	1.00
A7-VH	1.13	0.60	1.0	192918360	2185380	1.16	512184	5.0	2560921	2091.0	0.9	44387691	1.00
A8-VH	1.21	0.56	1.0	192918360	2185380	1.16	473838	5.0	2369191	1934.4	0.9	44944860	1.00
A9-VH	1.29	0.52	1.0	192918360	2185380	1.15	439863	5.0	2199313	1795.7	0.9	45823169	1.00
A10-VH	0.89	0.74	1.0	341841936	3277360	1.16	1003154	5.0	5015768	4095.4	0.9	80466431	1.00
A11-VH	0.94	0.71	1.0	341841936	3277360	1.16	942610	5.0	4713048	3848.2	0.9	79392383	1.00
A12-VH	0.99	0.68	1.0	341841936	3277360	1.16	888329	5.0	4441643	3626.6	0.9	78778551	1.00
01-NLH	1.38	0.48	1.0	423174646	3772585	1.38	1503290	0.0	0	5489.2	0.9	58696203	1.00
02-NLH	1.50	0.44	1.0	423174646	3772585	1.33	1323252	0.0	0	4831.8	0.9	71034163	1.00
03-NLH	1.61	0.40	1.0	423174646	3772585	1.30	1168495	0.0	0	4266.7	0.9	83833697	1.00
A1-NLH	2.52	0.24	1.0	40386575	855550	1.18	156775	0.0	0	640.0	0.9	8670099	1.00
A2-NLH	2.78	0.21	1.0	40386575	855550	1.14	127166	0.0	0	519.2	0.9	11682459	1.00
A3-NLH	3.05	0.19	1.0	40386575	855550	1.11	103220	0.0	0	421.4	0.9	14764182	1.00
A4-NLH	1.67	0.39	1.0	82663170	1307820	1.31	419285	0.0	0	1711.7	0.9	11885167	1.00
A5-NLH	1.82	0.35	1.0	82663170	1307820	1.27	364021	0.0	0	1486.1	0.9	14583330	1.00
A6-NLH	1.97	0.32	1.0	82663170	1307820	1.23	317598	0.0	0	1296.6	0.9	17389764	1.00
A7-NLH	1.13	0.60	1.0	192918360	2185380	1.44	1128783	0.0	0	4608.2	0.9	20574710	1.00
A8-NLH	1.21	0.56	1.0	192918360	2185380	1.42	1034175	0.0	0	4222.0	0.9	22791000	1.00
A9-NLH	1.29	0.52	1.0	192918360	2185380	1.40	948346	0.0	0	3871.6	0.9	25114814	1.00
A10-NLH	0.89	0.74	1.0	341841936	3277360	1.40	2137754	0.0	0	8727.3	0.9	32932037	1.00
A11-NLH	0.94	0.71	1.0	341841936	3277360	1.42	2024961	0.0	0	8266.9	0.9	34925601	1.00
A12-NLH	0.99	0.68	1.0	341841936	3277360	1.43	1916063	0.0	0	7822.3	0.9	36966888	1.00

	Current EC1993-1-1 with LBA															
	variable for solve function		W_i*f_{yd}	$A*f_{yd}$	LBA	$\bar{\lambda} = \sqrt{(N_{Rk}/N_{cr})}$	$\Phi = 0.5(1+\alpha*(\lambda-0.2)+\lambda^2)$	$\chi = 1/(\Phi+\sqrt{(\Phi^2-\lambda^2)})$		M_{Rk}/γ_{M0}	N_{Rk}/γ_{M0}	$1/(1-((F_{ult}/N_{Rd})*\chi*\lambda^2))$			
	N_{ult}	α	M_{Rk}	N_{Rk}	N_{cr}	$\bar{\lambda}$	Φ	χ	γ_{M0}	M_{Rd}	N_{Rd}	k	N_{Ed}	φF	c_m
	N	[-]	Nmm	N	N	[-]	[-]	[-]	[-]	Nmm	N	[-]	N	N	[-]
01	1230615	0.34	423174646	3772585	1789800	1.45	1.77	0.36	1.0	423174646	3772585	1.33	1230615	4493.6	0.9
02	1123588	0.34	423174646	3772585	1576800	1.55	1.93	0.33	1.0	423174646	3772585	1.30	1123588	4102.8	0.9
03	1028403	0.34	423174646	3772585	1401000	1.64	2.09	0.30	1.0	423174646	3772585	1.28	1028403	3755.2	0.9
A1	135630	0.34	40386575	855550	168970	2.25	3.38	0.17	1.0	40386575	855550	1.16	135630	553.7	0.9
A2	121045	0.34	40386575	855550	147850	2.41	3.77	0.15	1.0	40386575	855550	1.14	121045	494.2	0.9
A3	108978	0.34	40386575	855550	130990	2.56	4.17	0.13	1.0	40386575	855550	1.13	108978	444.9	0.9
A4	338450	0.34	82663170	1307820	461940	1.68	2.17	0.28	1.0	82663170	1307820	1.26	338450	1381.7	0.9
A5	305986	0.34	82663170	1307820	405600	1.80	2.38	0.25	1.0	82663170	1307820	1.24	305986	1249.2	0.9
A6	278058	0.34	82663170	1307820	359850	1.91	2.61	0.23	1.0	82663170	1307820	1.21	278058	1135.2	0.9
A7	910477	0.34	192918360	2185380	1471200	1.22	1.42	0.47	1.0	192918360	2185380	1.41	910477	3717.0	0.9
A8	843895	0.34	192918360	2185380	1302500	1.30	1.53	0.43	1.0	192918360	2185380	1.39	843895	3445.2	0.9
A9	781612	0.34	192918360	2185380	1160100	1.37	1.64	0.39	1.0	192918360	2185380	1.36	781612	3190.9	0.9
A10	1789986	0.34	341841936	3277360	3582200	0.96	1.09	0.62	1.0	341841936	3277360	1.45	1789986	7307.6	0.9
A11	1702045	0.34	341841936	3277360	3206500	1.01	1.15	0.59	1.0	341841936	3277360	1.46	1702045	6948.6	0.9
A12	1611243	0.34	341841936	3277360	2871200	1.07	1.22	0.55	1.0	341841936	3277360	1.45	1611243	6577.9	0.9
01-NL	1632663	0.34	423174646	3772585	2601000	1.20	1.40	0.48	1.0	423174646	3772585	1.43	1632663	5961.6	0.9
02-NL	1514411	0.34	423174646	3772585	2308900	1.28	1.50	0.44	1.0	423174646	3772585	1.40	1514411	5529.8	0.9
03-NL	1404397	0.34	423174646	3772585	2062900	1.35	1.61	0.40	1.0	423174646	3772585	1.38	1404397	5128.1	0.9
A1-NL	189527	0.34	40386575	855550	245420	1.87	2.53	0.24	1.0	40386575	855550	1.22	189527	773.7	0.9
A2-NL	170978	0.34	40386575	855550	216470	1.99	2.78	0.21	1.0	40386575	855550	1.20	170978	698.0	0.9
A3-NL	155179	0.34	40386575	855550	192850	2.11	3.04	0.19	1.0	40386575	855550	1.18	155179	633.5	0.9
A4-NL	459740	0.34	82663170	1307820	671120	1.40	1.68	0.38	1.0	82663170	1307820	1.36	459740	1876.9	0.9
A5-NL	421397	0.34	82663170	1307820	593880	1.48	1.82	0.35	1.0	82663170	1307820	1.33	421397	1720.3	0.9
A6-NL	387120	0.34	82663170	1307820	529820	1.57	1.97	0.32	1.0	82663170	1307820	1.30	387120	1580.4	0.9
A7-NL	1163564	0.34	192918360	2185380	2139200	1.01	1.15	0.59	1.0	192918360	2185380	1.47	1163564	4750.2	0.9
A8-NL	1097722	0.34	192918360	2185380	1907900	1.07	1.22	0.55	1.0	192918360	2185380	1.47	1097722	4481.4	0.9
A9-NL	1032774	0.34	192918360	2185380	1708500	1.13	1.30	0.52	1.0	192918360	2185380	1.45	1032774	4216.3	0.9
A10-NL	2151840	0.34	341841936	3277360	5214800	0.79	0.92	0.73	1.0	341841936	3277360	1.43	2151840	8784.9	0.9
A11-NL	2078624	0.34	341841936	3277360	4699400	0.84	0.96	0.70	1.0	341841936	3277360	1.45	2078624	8485.9	0.9
A12-NL	1999644	0.34	341841936	3277360	4230400	0.88	1.00	0.67	1.0	341841936	3277360	1.47	1999644	8163.5	0.9
01-V	375672	0.34	423174646	3772585	467540	2.84	4.98	0.11	1.0	423174646	3772585	1.10	375672	1371.8	0.9
02-V	334114	0.34	423174646	3772585	407140	3.04	5.62	0.10	1.0	423174646	3772585	1.09	334114	1220.0	0.9
03-V	299573	0.34	423174646	3772585	358790	3.24	6.27	0.09	1.0	423174646	3772585	1.08	299573	1093.9	0.9
A1-V	38348	0.34	40386575	855550	44217.4	4.40	10.89	0.05	1.0	40386575	855550	1.04	38348	156.6	0.9
A2-V	33631	0.34	40386575	855550	38232.7	4.73	12.46	0.04	1.0	40386575	855550	1.04	33631	137.3	0.9
A3-V	29890	0.34	40386575	855550	33597.7	5.05	14.06	0.04	1.0	40386575	855550	1.03	29890	122.0	0.9
A4-V	99844	0.34	82663170	1307820	120780	3.29	6.44	0.08	1.0	82663170	1307820	1.07	99844	407.6	0.9
A5-V	88269	0.34	82663170	1307820	104800	3.53	7.31	0.07	1.0	82663170	1307820	1.07	88269	360.4	0.9
A6-V	78855	0.34	82663170	1307820	92220.2	3.77	8.20	0.06	1.0	82663170	1307820	1.06	78855	321.9	0.9
A7-V	294507	0.34	192918360	2185380	383710	2.39	3.72	0.15	1.0	192918360	2185380	1.13	294507	1202.3	0.9
A8-V	264333	0.34	192918360	2185380	335900	2.55	4.15	0.13	1.0	192918360	2185380	1.12	264333	1079.1	0.9
A9-V	238436	0.34	192918360	2185380	296720	2.71	4.61	0.12	1.0	192918360	2185380	1.11	238436	973.4	0.9
A10-V	652575	0.34	341841936	3277360	931330	1.88	2.54	0.23	1.0	341841936	3277360	1.20	652575	2664.1	0.9
A11-V	596523	0.34	341841936	3277360	824800	1.99	2.79	0.21	1.0	341841936	3277360	1.18	596523	2435.3	0.9
A12-V	544789	0.34	341841936	3277360	732480	2.12	3.06	0.19	1.0	341841936	3277360	1.16	544789	2224.1	0.9
01-H	1127668	0.34	423174646	3772585	1789800	1.45	1.77	0.36	1.0	423174646	3772585	1.29	1127668	4117.7	0.9
02-H	985941	0.34	423174646	3772585	1576800	1.55	1.93	0.33	1.0	423174646	3772585	1.26	985941	3600.1	0.9
03-H	864076	0.34	423174646	3772585	1401000	1.64	2.09	0.30	1.0	423174646	3772585	1.22	864076	3155.2	0.9
A1-H	112814	0.34	40386575	855550	168970	2.25	3.38	0.17	1.0	40386575	855550	1.13	112814	460.6	0.9
A2-H	91124	0.34	40386575	855550	147850	2.41	3.77	0.15	1.0	40386575	855550	1.10	91124	372.0	0.9
A3-H	73663	0.34	40386575	855550	130990	2.56	4.17	0.13	1.0	40386575	855550	1.08	73663	300.7	0.9
A4-H	308382	0.34	82663170	1307820	461940	1.68	2.17	0.28	1.0	82663170	1307820	1.23	308382	1259.0	0.9
A5-H	266138	0.34	82663170	1307820	405600	1.80	2.38	0.25	1.0	82663170	1307820	1.20	266138	1086.5	0.9
A6-H	230738	0.34	82663170	1307820	359850	1.91	2.61	0.23	1.0	82663170	1307820	1.17	230738	942.0	0.9
A7-H	872399	0.34	192918360	2185380	1471200	1.22	1.42	0.47	1.0	192918360	2185380	1.38	872399	3561.6	0.9
A8-H	791806	0.34	192918360	2185380	1302500	1.30	1.53	0.43	1.0	192918360	2185380	1.35	791806	3232.5	0.9
A9-H	718382	0.34	192918360	2185380	1160100	1.37	1.64	0.39	1.0	192918360	2185380	1.32	718382	2932.8	0.9
A10-H	1746629	0.34	341841936	3277360	3582200	0.96	1.09	0.62	1.0	341841936	3277360	1.44	1746629	7130.6	0.9
A11-H	1640260	0.34	341841936	3277360	3206500	1.01	1.15	0.59	1.0	341841936	3277360	1.43	1640260	6696.3	0.9
A12-H	1533582	0.34	341841936	3277360	2871200	1.07	1.22	0.55	1.0	341841936	3277360	1.42	1533582	6260.8	0.9
01-VH	348701	0.34	423174646	3772585	467540	2.84	4.98	0.11	1.0	423174646	3772585	1.09	348701	1273.3	0.9
02-VH	298492	0.34	423174646	3772585	407140	3.04	5.62	0.10	1.0	423174646	3772585	1.08	298492	1089.9	0.9
03-VH	257347	0.34	423174646	3772585	358790	3.24	6.27	0.09	1.0	423174646	3772585	1.07	257347	939.7	0.9
A1-VH	32384	0.34	40386575	855550	44217.4	4.40	10.89	0.05	1.0	40386575	855550	1.04	32384	132.2	0.9
A2-VH	25836	0.34	40386575	855550	38232.7	4.73	12.46	0.04	1.0	40386575	855550	1.03	25836	105.5	0.9
A3-VH	20700	0.34	40386575	855550	33597.7	5.05	14.06	0.04	1.0	40386575	855550	1.02	20700	84.5	0.9
A4-VH	92053	0.34	82663170	1307820	120780	3.29	6.44	0.08	1.0	82663170	1307820	1.07	92053	375.8	0.9
A5-VH	78023	0.34	82663170	1307820	104800	3.53	7.31	0.07	1.0	82663170	1307820	1.06	78023	318.5	0.9
A6-VH	66736	0.34	82663170	1307820	92220.2	3.77	8.20	0.06	1.0	82663170	1307820	1.05	66736	272.4	0.9
A7-VH	284204	0.34	192918360	2185380	383710	2.39	3.72	0.15	1.0	192918360	2185380	1.13	284204	1160.3	0.9
A8-VH	250609	0.34	192918360	2185380	335900	2.55	4.15	0.13	1.0	192918360	2185380	1.11	250609	1023.1	0.9
A9-VH	222084	0.34	192918360	2185380	296720	2.71	4.61	0.12	1.0	192918360	2185380	1.10	222084	906.7	0.9
A10-VH	639142	0.34	341841936	3277360	931330	1.88	2.54	0.23	1.0	341841936	3277360	1.19	639142	2609.3	0.9
A11-VH	578295	0.34	341841936	3277360	824800	1.99	2.79	0.21	1.0	341841936	3277360	1.17	578295	2360.9	0.9
A12-VH	522819	0.34	341841936	3277360	732480	2.12	3.06	0.19	1.0	341841936	3277360	1.16	522819	2134.4	0.9
01-NLH	1488434	0.34	423174646	3772585	2601000	1.20	1.40	0.48	1.0	423174646	3772585	1.37	1488434	5435.0	0.9
02-NLH	1318531	0.34	423174646	3772585	2308900	1.28	1.50	0.44	1.0	423174646	3772585	1.33	1318531	4814.6	0.9
03-NLH	1167871	0.34	423174646	3772585	2062900	1.35	1.61	0.40	1.0	423174646	3772585	1.30	1167871	4264.5	0.9
A1-NLH	156334	0.34	40386575	855550	245420	1.87	2.53	0.24	1.0	40386575	855550	1.18	156334	638.2	0.9
A2-NLH	127264	0.34	40386575	855550	216470	1.99	2.78	0.21	1.0	40386575	855550	1.14	127264	519.6	0.9
A3-NLH	103462	0.34	40386575	855550	192850	2.11	3.04	0.19	1.0	40386575	855550	1.11	103462	422.4	0.9
A4-NLH	416524	0.34	82663170	1307820	671120	1.40	1.68	0.38	1.0	82663170	1307820	1.31	416524	1700.5	0.9
A5-NLH	363530	0.34	82663170	1307820	593880	1.48	1.82	0.35	1.0	82663170	1307820	1.27	363530	1484.1	0.9
A6-NLH	317931	0.34	82663170	1307820	529820	1.57	1.97	0.32	1.0	82663170	1307820	1.24	317931	1297.9	0.9
A7-NLH	1112886	0.34	192918360	2185380	2139200	1.01	1.15	0.59	1.0	192918360	2185380	1.44	1112886	4543.3	0.9
A8-NLH	1026665	0.34	192918360	2185380	1907900	1.07	1.22	0.55	1.0	192918360	2185380	1.42	1026665	4191.3	0.9
A9-NLH	944720	0.34	192918360	2185380	1708500	1.13	1.30	0.52	1.0	192918360	2185380	1.40	944720	3856.8	0.9
A10-NLH	2099855	0.34	341841936	3277360	5214800	0.79	0.92	0.73	1.0	341841936	3277360	1.42	2099855	8572.6	0.9
A11-NLH	2002690	0.34	341841936	3277360	4699400	0.84	0.96	0.70	1.0	341841936	3277360	1.43	2002690	8175.9	0.9
A12-NLH	1901710	0.34	341841936	3277360	4230400	0.88	1.00	0.67	1.0	341841936	3277360	1.43	1901710	7763.7	0.9

Current EC1993-1-1 with Nomogram

	$(2*\varphi N_{Ed}+(Q/F)*\varphi NEd+H)*h*C_m/2$	$N_{Ed}/N_{Rd}+(n/n-1)*F_{tot}*e^*/M_{Rd}$	variable for solve function										eq1-eq2=0	
	M_{Ed}	SOLVE FOR = 1, F_{ult}	N_{ult}	α	M_{Rk}	F_{Rk}	μ	C_A	C_B	λ	eq1	eq2	SOLVE FOR = 0	nomogram
	Nmm	[-]		[-]	Nmm	N								
01	33701784	1.00	1580631	0.34	423174646	3772585	6	1E+104	0.167	1.35	2.9615E+103	2.9615E+103	0.00	2.33
02	30770727	1.00	1462127	0.34	423174646	3772585	6	1E+104	0.250	1.26	3.812E+103	3.812E+103	0.00	2.48
03	28163972	1.00	1356185	0.34	423174646	3772585	6	1E+104	0.333	1.19	4.4047E+103	4.4047E+103	0.00	2.63
A1	2491688	1.00	184341	0.34	40386575	855550	6	1E+104	0.167	1.35	2.9615E+103	2.9615E+103	0.00	2.33
A2	2223734	1.00	166262	0.34	40386575	855550	6	1E+104	0.250	1.26	3.812E+103	3.812E+103	0.00	2.48
A3	2002061	1.00	151080	0.34	40386575	855550	6	1E+104	0.333	1.19	4.4047E+103	4.4047E+103	0.00	2.63
A4	6217720	1.00	444948	0.34	82663170	1307820	6	1E+104	0.167	1.35	2.9615E+103	2.9615E+103	0.00	2.33
A5	5621322	1.00	407273	0.34	82663170	1307820	6	1E+104	0.250	1.26	3.812E+103	3.812E+103	0.00	2.48
A6	5108256	1.00	374491	0.34	82663170	1307820	6	1E+104	0.333	1.19	4.4047E+103	4.4047E+103	0.00	2.63
A7	16726526	1.00	1127622	0.34	192918360	2185380	6	1E+104	0.167	1.35	2.9615E+103	2.9615E+103	0.00	2.33
A8	15503340	1.00	1059474	0.34	192918360	2185380	6	1E+104	0.250	1.26	3.812E+103	3.812E+103	0.00	2.48
A9	14359121	1.00	996091	0.34	192918360	2185380	6	1E+104	0.333	1.19	4.4047E+103	4.4047E+103	0.00	2.63
A10	32884137	1.00	2091391	0.34	341841936	3277360	6	1E+104	0.167	1.35	2.9615E+103	2.9615E+103	0.00	2.33
A11	31268571	1.00	2008789	0.34	341841936	3277360	6	1E+104	0.250	1.26	3.812E+103	3.812E+103	0.00	2.48
A12	29600426	1.00	1928205	0.34	341841936	3277360	6	1E+104	0.333	1.19	4.4047E+103	4.4047E+103	0.00	2.63
01-NL	29808215	1.00	1649141	0.34	423174646	3772585	6	1E+104	0.167	1.35	2.9615E+103	2.9615E+103	0.00	2.33
02-NL	27649228	1.00	1519941	0.34	423174646	3772585	6	1E+104	0.250	1.26	3.812E+103	3.812E+103	0.00	2.48
03-NL	25640657	1.00	1405168	0.34	423174646	3772585	6	1E+104	0.333	1.19	4.4047E+103	4.4047E+103	0.00	2.63
A1-NL	2321225	1.00	190076	0.34	40386575	855550	6	1E+104	0.167	1.35	2.9615E+103	2.9615E+103	0.00	2.33
A2-NL	2094039	1.00	170842	0.34	40386575	855550	6	1E+104	0.250	1.26	3.812E+103	3.812E+103	0.00	2.48
A3-NL	1900542	1.00	154800	0.34	40386575	855550	6	1E+104	0.333	1.19	4.4047E+103	4.4047E+103	0.00	2.63
A4-NL	5630636	1.00	462835	0.34	82663170	1307820	6	1E+104	0.167	1.35	2.9615E+103	2.9615E+103	0.00	2.33
A5-NL	5161033	1.00	421980	0.34	82663170	1307820	6	1E+104	0.250	1.26	3.812E+103	3.812E+103	0.00	2.48
A6-NL	4741232	1.00	386702	0.34	82663170	1307820	6	1E+104	0.333	1.19	4.4047E+103	4.4047E+103	0.00	2.63
A7-NL	14250686	1.00	1180162	0.34	192918360	2185380	6	1E+104	0.167	1.35	2.9615E+103	2.9615E+103	0.00	2.33
A8-NL	13444295	1.00	1105774	0.34	192918360	2185380	6	1E+104	0.250	1.26	3.812E+103	3.812E+103	0.00	2.48
A9-NL	12648842	1.00	1036770	0.34	192918360	2185380	6	1E+104	0.333	1.19	4.4047E+103	4.4047E+103	0.00	2.63
A10-NL	26354556	1.00	2190255	0.34	341841936	3277360	6	1E+104	0.167	1.35	2.9615E+103	2.9615E+103	0.00	2.33
A11-NL	25457840	1.00	2101455	0.34	341841936	3277360	6	1E+104	0.250	1.26	3.812E+103	3.812E+103	0.00	2.48
A12-NL	24490539	1.00	2014564	0.34	341841936	3277360	6	1E+104	0.333	1.19	4.4047E+103	4.4047E+103	0.00	2.63
01-V	41152797	1.00	1179849	0.34	423174646	3772585	6	1E+104	0.167	1.35	2.9615E+103	2.9615E+103	0.00	2.33
02-V	36600322	1.00	1112924	0.34	423174646	3772585	6	1E+104	0.250	1.26	3.812E+103	3.812E+103	0.00	2.48
03-V	32816555	1.00	1051253	0.34	423174646	3772585	6	1E+104	0.333	1.19	4.4047E+103	4.4047E+103	0.00	2.63
A1-V	2818005	1.00	146344	0.34	40386575	855550	6	1E+104	0.167	1.35	2.9615E+103	2.9615E+103	0.00	2.33
A2-V	2471377	1.00	134913	0.34	40386575	855550	6	1E+104	0.250	1.26	3.812E+103	3.812E+103	0.00	2.48
A3-V	2196429	1.00	124901	0.34	40386575	855550	6	1E+104	0.333	1.19	4.4047E+103	4.4047E+103	0.00	2.63
A4-V	7337019	1.00	336746	0.34	82663170	1307820	6	1E+104	0.167	1.35	2.9615E+103	2.9615E+103	0.00	2.33
A5-V	6486391	1.00	315071	0.34	82663170	1307820	6	1E+104	0.250	1.26	3.812E+103	3.812E+103	0.00	2.48
A6-V	5794627	1.00	295459	0.34	82663170	1307820	6	1E+104	0.333	1.19	4.4047E+103	4.4047E+103	0.00	2.63
A7-V	21641745	1.00	829250	0.34	192918360	2185380	6	1E+104	0.167	1.35	2.9615E+103	2.9615E+103	0.00	2.33
A8-V	19424415	1.00	790807	0.34	192918360	2185380	6	1E+104	0.250	1.26	3.812E+103	3.812E+103	0.00	2.48
A9-V	17521429	1.00	754548	0.34	192918360	2185380	6	1E+104	0.333	1.19	4.4047E+103	4.4047E+103	0.00	2.63
A10-V	47954266	1.00	1528214	0.34	341841936	3277360	6	1E+104	0.167	1.35	2.9615E+103	2.9615E+103	0.00	2.33
A11-V	43835315	1.00	1478728	0.34	341841936	3277360	6	1E+104	0.250	1.26	3.812E+103	3.812E+103	0.00	2.48
A12-V	40033644	1.00	1430805	0.34	341841936	3277360	6	1E+104	0.333	1.19	4.4047E+103	4.4047E+103	0.00	2.63
01-H	62132464	1.00	1444403	0.34	423174646	3772585	6	1E+104	0.167	1.35	2.9615E+103	2.9615E+103	0.00	2.33
02-H	73876098	1.00	1276880	0.34	423174646	3772585	6	1E+104	0.250	1.26	3.812E+103	3.812E+103	0.00	2.48
03-H	86163689	1.00	1131676	0.34	423174646	3772585	6	1E+104	0.333	1.19	4.4047E+103	4.4047E+103	0.00	2.63
A1-H	8822519	1.00	152348	0.34	40386575	855550	6	1E+104	0.167	1.35	2.9615E+103	2.9615E+103	0.00	2.33
A2-H	11799057	1.00	124042	0.34	40386575	855550	6	1E+104	0.250	1.26	3.812E+103	3.812E+103	0.00	2.48
A3-H	14853282	1.00	100983	0.34	40386575	855550	6	1E+104	0.333	1.19	4.4047E+103	4.4047E+103	0.00	2.63
A4-H	12415344	1.00	403930	0.34	82663170	1307820	6	1E+104	0.167	1.35	2.9615E+103	2.9615E+103	0.00	2.33
A5-H	15014262	1.00	352230	0.34	82663170	1307820	6	1E+104	0.250	1.26	3.812E+103	3.812E+103	0.00	2.48
A6-H	17738920	1.00	308418	0.34	82663170	1307820	6	1E+104	0.333	1.19	4.4047E+103	4.4047E+103	0.00	2.63
A7-H	22776986	1.00	1080089	0.34	192918360	2185380	6	1E+104	0.167	1.35	2.9615E+103	2.9615E+103	0.00	2.33
A8-H	24671400	1.00	992853	0.34	192918360	2185380	6	1E+104	0.250	1.26	3.812E+103	3.812E+103	0.00	2.48
A9-H	26697518	1.00	913327	0.34	192918360	2185380	6	1E+104	0.333	1.19	4.4047E+103	4.4047E+103	0.00	2.63
A10-H	38837628	1.00	2042745	0.34	341841936	3277360	6	1E+104	0.167	1.35	2.9615E+103	2.9615E+103	0.00	2.33
A11-H	40258498	1.00	1937877	0.34	341841936	3277360	6	1E+104	0.250	1.26	3.812E+103	3.812E+103	0.00	2.48
A12-H	41673699	1.00	1836760	0.34	341841936	3277360	6	1E+104	0.333	1.19	4.4047E+103	4.4047E+103	0.00	2.63
01-VH	69448275	1.00	1089831	0.34	423174646	3772585	6	1E+104	0.167	1.35	2.9615E+103	2.9615E+103	0.00	2.33
02-VH	79573164	1.00	986082	0.34	423174646	3772585	6	1E+104	0.250	1.26	3.812E+103	3.812E+103	0.00	2.48
03-VH	90690997	1.00	892381	0.34	423174646	3772585	6	1E+104	0.333	1.19	4.4047E+103	4.4047E+103	0.00	2.63
A1-VH	9129730	1.00	122287	0.34	40386575	855550	6	1E+104	0.167	1.35	2.9615E+103	2.9615E+103	0.00	2.33
A2-VH	12023539	1.00	102025	0.34	40386575	855550	6	1E+104	0.250	1.26	3.812E+103	3.812E+103	0.00	2.48
A3-VH	15021114	1.00	84742	0.34	40386575	855550	6	1E+104	0.333	1.19	4.4047E+103	4.4047E+103	0.00	2.63
A4-VH	13514502	1.00	308710	0.34	82663170	1307820	6	1E+104	0.167	1.35	2.9615E+103	2.9615E+103	0.00	2.33
A5-VH	15858523	1.00	275969	0.34	82663170	1307820	6	1E+104	0.250	1.26	3.812E+103	3.812E+103	0.00	2.48
A6-VH	18404063	1.00	246914	0.34	82663170	1307820	6	1E+104	0.333	1.19	4.4047E+103	4.4047E+103	0.00	2.63
A7-VH	27634679	1.00	798970	0.34	192918360	2185380	6	1E+104	0.167	1.35	2.9615E+103	2.9615E+103	0.00	2.33
A8-VH	28540891	1.00	747382	0.34	192918360	2185380	6	1E+104	0.250	1.26	3.812E+103	3.812E+103	0.00	2.48
A9-VH	29819803	1.00	699267	0.34	192918360	2185380	6	1E+104	0.333	1.19	4.4047E+103	4.4047E+103	0.00	2.63
A10-VH	53717169	1.00	1497127	0.34	341841936	3277360	6	1E+104	0.167	1.35	2.9615E+103	2.9615E+103	0.00	2.33
A11-VH	52620859	1.00	1433246	0.34	341841936	3277360	6	1E+104	0.250	1.26	3.812E+103	3.812E+103	0.00	2.48
A12-VH	51919186	1.00	1371751	0.34	341841936	3277360	6	1E+104	0.333	1.19	4.4047E+103	4.4047E+103	0.00	2.63
01-NLH	58424967	1.00	1503290	0.34	423174646	3772585	6	1E+104	0.167	1.35	2.9615E+103	2.9615E+103	0.00	2.33
02-NLH	70947978	1.00	1323252	0.34	423174646	3772585	6	1E+104	0.250	1.26	3.812E+103	3.812E+103	0.00	2.48
03-NLH	83822311	1.00	1168495	0.34	423174646	3772585	6	1E+104	0.333	1.19	4.4047E+103	4.4047E+103	0.00	2.63
A1-NLH	8664696	1.00	156775	0.34	40386575	855550	6	1E+104	0.167	1.35	2.9615E+103	2.9615E+103	0.00	2.33
A2-NLH	11683655	1.00	127166	0.34	40386575	855550	6	1E+104	0.250	1.26	3.812E+103	3.812E+103	0.00	2.48
A3-NLH	14767143	1.00	103220	0.34	40386575	855550	6	1E+104	0.333	1.19	4.4047E+103	4.4047E+103	0.00	2.63
A4-NLH	11851361	1.00	419285	0.34	82663170	1307820	6	1E+104	0.167	1.35	2.9615E+103	2.9615E+103	0.00	2.33
A5-NLH	14577315	1.00	364021	0.34	82663170	1307820	6	1E+104	0.250	1.26	3.812E+103	3.812E+103	0.00	2.48
A6-NLH	17393839	1.00	317598	0.34	82663170	1307820	6	1E+104	0.333	1.19	4.4047E+103	4.4047E+103	0.00	2.63
A7-NLH	20380012	1.00	1128783	0.34	192918360	2185380	6	1E+104	0.167	1.35	2.9615E+103	2.9615E+103	0.00	2.33
A8-NLH	22699023	1.00	1034175	0.34	192918360	2185380	6	1E+104	0.250	1.26	3.812E+103	3.812E+103	0.00	2.48
A9-NLH	25070405	1.00	948346	0.34	192918360	2185380	6	1E+104	0.333	1.19	4.4047E+103	4.4047E+103	0.00	2.63
A10-NLH	32467869	1.00	2137754	0.34	341841936	3277360	6	1E+104	0.167	1.35	2.9615E+103	2.9615E+103	0.00	2.33
A11-NLH	34652845	1.00	2024961	0.34	341841936	3277360	6	1E+104	0.250	1.26	3.812E+103	3.812E+103	0.00	2.48
A12-NLH	36791098	1.00	1916063	0.34	341841936	3277360	6	1E+104	0.333	1.19	4.4047E+103	4.4047E+103	0.00	2.63

Current EC1993-1-1 with Nomogram

													$(2*\varphi N_{Ed}+(Q/F)*\varphi NEd+H)*h*C_m/2$	$N_{Ed}/N_{Rd}+(n/n-1)*F_{tot}*e^*/M_{Rd}$
	$L_{cr,nen} = \pi*\sqrt{(EI/\alpha_{cr}*F)}$	F_{cr}	$\bar{\lambda} = \sqrt{(F_{Rk}/F_{cr})}$	$\Phi = 0.5(1+\alpha*(\lambda-0.2)+\lambda^2)$	$\chi = 1/(\Phi+\sqrt{(\Phi^2-\lambda^2)})$	γ_{M1}	M_{Rd}	N_{Rd}	k	φN_{Ed}	c_m	M_{Ed}	SOLVE FOR = 1
	mm	N	[-]	[-]	[-]	[-]								
01	11639	2644346	1.19	1.38	0.48	1.0	423174646	3772585	1.40	5771.6	0.9	43287374	1.00	-
02	12421	2321877	1.27	1.50	0.44	1.0	423174646	3772585	1.38	5338.9	0.9	40041989	1.00	-
03	13173	2064550	1.35	1.61	0.40	1.0	423174646	3772585	1.36	4952.1	0.9	37140663	1.00	-
A1	6984	246298	1.86	2.52	0.24	1.0	40386575	855550	1.22	752.6	0.9	3386560	1.00	-
A2	7453	216263	1.99	2.78	0.21	1.0	40386575	855550	1.19	678.8	0.9	3054436	1.00	-
A3	7904	192295	2.11	3.05	0.19	1.0	40386575	855550	1.18	616.8	0.9	2775511	1.00	-
A4	6984	677645	1.39	1.67	0.39	1.0	82663170	1307820	1.34	1816.5	0.9	8174223	1.00	-
A5	7453	595008	1.48	1.82	0.35	1.0	82663170	1307820	1.31	1662.7	0.9	7482089	1.00	-
A6	7904	529065	1.57	1.97	0.32	1.0	82663170	1307820	1.29	1528.9	0.9	6879843	1.00	-
A7	6984	2203124	1.00	1.13	0.60	1.0	192918360	2185380	1.44	4603.5	0.9	20715736	1.00	-
A8	7453	1934460	1.06	1.21	0.56	1.0	192918360	2185380	1.44	4325.3	0.9	19463783	1.00	-
A9	7904	1720069	1.13	1.29	0.52	1.0	192918360	2185380	1.43	4066.5	0.9	18299363	1.00	-
A10	6984	5524428	0.77	0.89	0.74	1.0	341841936	3277360	1.39	8538.1	0.9	38421298	1.00	-
A11	7453	4850741	0.82	0.94	0.71	1.0	341841936	3277360	1.42	8200.8	0.9	36903819	1.00	-
A12	7904	4313148	0.87	0.99	0.68	1.0	341841936	3277360	1.44	7871.9	0.9	35423383	1.00	-
01-NL	11639	2644346	1.19	1.38	0.48	1.0	423174646	3772585	1.43	6021.8	0.9	30109052	1.00	-
02-NL	12421	2321877	1.27	1.50	0.44	1.0	423174646	3772585	1.40	5550.0	0.9	27750199	1.00	-
03-NL	13173	2064550	1.35	1.61	0.40	1.0	423174646	3772585	1.38	5130.9	0.9	25654742	1.00	-
A1-NL	6984	246298	1.86	2.52	0.24	1.0	40386575	855550	1.22	776.0	0.9	2327948	1.00	-
A2-NL	7453	216263	1.99	2.78	0.21	1.0	40386575	855550	1.20	697.5	0.9	2092375	1.00	-
A3-NL	7904	192295	2.11	3.05	0.19	1.0	40386575	855550	1.18	632.0	0.9	1895906	1.00	-
A4-NL	6984	677645	1.39	1.67	0.39	1.0	82663170	1307820	1.36	1889.5	0.9	5668549	1.00	-
A5-NL	7453	595008	1.48	1.82	0.35	1.0	82663170	1307820	1.33	1722.7	0.9	5168175	1.00	-
A6-NL	7904	529065	1.57	1.97	0.32	1.0	82663170	1307820	1.30	1578.7	0.9	4736115	1.00	-
A7-NL	6984	2203124	1.00	1.13	0.60	1.0	192918360	2185380	1.47	4818.0	0.9	14453974	1.00	-
A8-NL	7453	1934460	1.06	1.21	0.56	1.0	192918360	2185380	1.47	4514.3	0.9	13542905	1.00	-
A9-NL	7904	1720069	1.13	1.29	0.52	1.0	192918360	2185380	1.46	4232.6	0.9	12697786	1.00	-
A10-NL	6984	5524428	0.77	0.89	0.74	1.0	341841936	3277360	1.42	8941.7	0.9	26825040	1.00	-
A11-NL	7453	4850741	0.82	0.94	0.71	1.0	341841936	3277360	1.44	8579.2	0.9	25737457	1.00	-
A12-NL	7904	4313148	0.87	0.99	0.68	1.0	341841936	3277360	1.46	8224.4	0.9	24673269	1.00	-
01-V	11639	2644346	1.19	1.38	0.48	1.0	423174646	3772585	1.27	4308.2	0.9	129245986	1.00	-
02-V	12421	2321877	1.27	1.50	0.44	1.0	423174646	3772585	1.27	4063.8	0.9	121914727	1.00	-
03-V	13173	2064550	1.35	1.61	0.40	1.0	423174646	3772585	1.26	3838.6	0.9	115158975	1.00	-
A1-V	6984	246298	1.86	2.52	0.24	1.0	40386575	855550	1.16	597.4	0.9	10754010	1.00	-
A2-V	7453	216263	1.99	2.78	0.21	1.0	40386575	855550	1.15	550.8	0.9	9914007	1.00	-
A3-V	7904	192295	2.11	3.05	0.19	1.0	40386575	855550	1.14	509.9	0.9	9178323	1.00	-
A4-V	6984	677645	1.39	1.67	0.39	1.0	82663170	1307820	1.24	1374.8	0.9	24745695	1.00	-
A5-V	7453	595008	1.48	1.82	0.35	1.0	82663170	1307820	1.23	1286.3	0.9	23152859	1.00	-
A6-V	7904	529065	1.57	1.97	0.32	1.0	82663170	1307820	1.22	1206.2	0.9	21711726	1.00	-
A7-V	6984	2203124	1.00	1.13	0.60	1.0	192918360	2185380	1.29	3385.4	0.9	60937212	1.00	-
A8-V	7453	1934460	1.06	1.21	0.56	1.0	192918360	2185380	1.30	3228.5	0.9	58112207	1.00	-
A9-V	7904	1720069	1.13	1.29	0.52	1.0	192918360	2185380	1.29	3080.4	0.9	55447755	1.00	-
A10-V	6984	5524428	0.77	0.89	0.74	1.0	341841936	3277360	1.26	6238.9	0.9	112300337	1.00	-
A11-V	7453	4850741	0.82	0.94	0.71	1.0	341841936	3277360	1.28	6036.9	0.9	108663839	1.00	-
A12-V	7904	4313148	0.87	0.99	0.68	1.0	341841936	3277360	1.29	5841.2	0.9	105142283	1.00	-
01-H	11639	2644346	1.19	1.38	0.48	1.0	423174646	3772585	1.36	5274.2	0.9	70806604	1.00	-
02-H	12421	2321877	1.27	1.50	0.44	1.0	423174646	3772585	1.32	4662.5	0.9	81843810	1.00	-
03-H	13173	2064550	1.35	1.61	0.40	1.0	423174646	3772585	1.28	4132.3	0.9	93492235	1.00	-
A1-H	6984	246298	1.86	2.52	0.24	1.0	40386575	855550	1.17	622.0	0.9	9548817	1.00	-
A2-H	7453	216263	1.99	2.78	0.21	1.0	40386575	855550	1.14	506.4	0.9	12403802	1.00	-
A3-H	7904	192295	2.11	3.05	0.19	1.0	40386575	855550	1.11	412.3	0.9	15355172	1.00	-
A4-H	6984	677645	1.39	1.67	0.39	1.0	82663170	1307820	1.30	1649.0	0.9	14170672	1.00	-
A5-H	7453	595008	1.48	1.82	0.35	1.0	82663170	1307820	1.26	1438.0	0.9	16595873	1.00	-
A6-H	7904	529065	1.57	1.97	0.32	1.0	82663170	1307820	1.23	1259.1	0.9	19166009	1.00	-
A7-H	6984	2203124	1.00	1.13	0.60	1.0	192918360	2185380	1.42	4409.4	0.9	26592501	1.00	-
A8-H	7453	1934460	1.06	1.21	0.56	1.0	192918360	2185380	1.40	4053.3	0.9	28364876	1.00	-
A9-H	7904	1720069	1.13	1.29	0.52	1.0	192918360	2185380	1.38	3728.6	0.9	30278881	1.00	-
A10-H	6984	5524428	0.77	0.89	0.74	1.0	341841936	3277360	1.38	8339.5	0.9	44277630	1.00	-
A11-H	7453	4850741	0.82	0.94	0.71	1.0	341841936	3277360	1.40	7911.3	0.9	45726074	1.00	-
A12-H	7904	4313148	0.87	0.99	0.68	1.0	341841936	3277360	1.41	7498.5	0.9	47243435	1.00	-
01-VH	11639	2644346	1.19	1.38	0.48	1.0	423174646	3772585	1.25	3979.5	0.9	150635046	1.00	-
02-VH	12421	2321877	1.27	1.50	0.44	1.0	423174646	3772585	1.23	3600.7	0.9	154894874	1.00	-
03-VH	13173	2064550	1.35	1.61	0.40	1.0	423174646	3772585	1.21	3258.5	0.9	160255408	1.00	-
A1-VH	6984	246298	1.86	2.52	0.24	1.0	40386575	855550	1.13	499.2	0.9	15736246	1.00	-
A2-VH	7453	216263	1.99	2.78	0.21	1.0	40386575	855550	1.11	416.5	0.9	17622305	1.00	-
A3-VH	7904	192295	2.11	3.05	0.19	1.0	40386575	855550	1.09	346.0	0.9	19727233	1.00	-
A4-VH	6984	677645	1.39	1.67	0.39	1.0	82663170	1307820	1.21	1260.3	0.9	29435438	1.00	-
A5-VH	7453	595008	1.48	1.82	0.35	1.0	82663170	1307820	1.19	1126.6	0.9	30404509	1.00	-
A6-VH	7904	529065	1.57	1.97	0.32	1.0	82663170	1307820	1.17	1008.0	0.9	31644368	1.00	-
A7-VH	6984	2203124	1.00	1.13	0.60	1.0	192918360	2185380	1.28	3261.8	0.9	65462101	1.00	-
A8-VH	7453	1934460	1.06	1.21	0.56	1.0	192918360	2185380	1.27	3051.2	0.9	65046146	1.00	-
A9-VH	7904	1720069	1.13	1.29	0.52	1.0	192918360	2185380	1.27	2854.7	0.9	64885451	1.00	-
A10-VH	6984	5524428	0.77	0.89	0.74	1.0	341841936	3277360	1.25	6112.0	0.9	116765935	1.00	-
A11-VH	7453	4850741	0.82	0.94	0.71	1.0	341841936	3277360	1.27	5851.2	0.9	115446615	1.00	-
A12-VH	7904	4313148	0.87	0.99	0.68	1.0	341841936	3277360	1.28	5600.1	0.9	114302698	1.00	-
01-NLH	11639	2644346	1.19	1.38	0.48	1.0	423174646	3772585	1.38	5489.2	0.9	58696203	1.00	-
02-NLH	12421	2321877	1.27	1.50	0.44	1.0	423174646	3772585	1.33	4831.8	0.9	71034163	1.00	-
03-NLH	13173	2064550	1.35	1.61	0.40	1.0	423174646	3772585	1.30	4266.7	0.9	83833697	1.00	-
A1-NLH	6984	246298	1.86	2.52	0.24	1.0	40386575	855550	1.18	640.0	0.9	8670099	1.00	-
A2-NLH	7453	216263	1.99	2.78	0.21	1.0	40386575	855550	1.14	519.2	0.9	11682459	1.00	-
A3-NLH	7904	192295	2.11	3.05	0.19	1.0	40386575	855550	1.11	421.4	0.9	14764182	1.00	-
A4-NLH	6984	677645	1.39	1.67	0.39	1.0	82663170	1307820	1.31	1711.7	0.9	11885167	1.00	-
A5-NLH	7453	595008	1.48	1.82	0.35	1.0	82663170	1307820	1.27	1486.1	0.9	14583330	1.00	-
A6-NLH	7904	529065	1.57	1.97	0.32	1.0	82663170	1307820	1.23	1296.6	0.9	17389764	1.00	-
A7-NLH	6984	2203124	1.00	1.13	0.60	1.0	192918360	2185380	1.44	4608.2	0.9	20574710	1.00	-
A8-NLH	7453	1934460	1.06	1.21	0.56	1.0	192918360	2185380	1.42	4222.0	0.9	22791000	1.00	-
A9-NLH	7904	1720069	1.13	1.29	0.52	1.0	192918360	2185380	1.40	3871.6	0.9	25114814	1.00	-
A10-NLH	6984	5524428	0.77	0.89	0.74	1.0	341841936	3277360	1.40	8727.3	0.9	32932037	1.00	-
A11-NLH	7453	4850741	0.82	0.94	0.71	1.0	341841936	3277360	1.42	8266.9	0.9	34925601	1.00	-
A12-NLH	7904	4313148	0.87	0.99	0.68	1.0	341841936	3277360	1.43	7822.3	0.9	36966888	1.00	-

Current EC1993-1-1 with Yura

	variable for solve function		W_i*f_{yd}	$A*f_{yd}$	$K_0*\sqrt{((\sum F+\sum Q)/\sum F)}$	K*h	π^2EI/L_{cr}^2	$\bar{\lambda} = \sqrt{(F_{Rk}/F_{cr})}$	$\Phi = 0.5(1+\alpha*(\lambda-0.2)+\lambda^2)$	$\chi = 1/(\Phi+\sqrt{(\Phi^2-\lambda^2)})$		M_{Rk}/γ_{M0}	N_{Rk}/γ_{M0}
	F_{ult}	α	M_{Rk}	N_{Rk}	K	L_{cr}	N_{cr}	$\bar{\lambda}$	Φ	χ	γ_{M0}	M_{Rd}	N_{Rd}
	N	[-]	Nmm	N	[-]	mm	N	[-]	[-]	[-]	[-]	Nmm	N
01	1217580	0.34	423174646	3772585	2.85	14255	1762898	1.46	1.78	0.36	1.0	423174646	3772585
02	1108386	0.34	423174646	3772585	3.04	15213	1547918	1.56	1.95	0.32	1.0	423174646	3772585
03	1014549	0.34	423174646	3772585	3.23	16133	1376367	1.66	2.12	0.29	1.0	423174646	3772585
A1	132386	0.34	40386575	855550	2.85	8553	164199	2.28	3.46	0.17	1.0	40386575	855550
A2	118447	0.34	40386575	855550	3.04	9128	144175	2.44	3.85	0.15	1.0	40386575	855550
A3	106942	0.34	40386575	855550	3.23	9680	128197	2.58	4.24	0.13	1.0	40386575	855550
A4	332739	0.34	82663170	1307820	2.85	8553	451763	1.70	2.20	0.28	1.0	82663170	1307820
A5	300648	0.34	82663170	1307820	3.04	9128	396672	1.82	2.42	0.25	1.0	82663170	1307820
A6	273569	0.34	82663170	1307820	3.23	9680	352710	1.93	2.65	0.22	1.0	82663170	1307820
A7	909562	0.34	192918360	2185380	2.85	8553	1468749	1.22	1.42	0.47	1.0	192918360	2185380
A8	838508	0.34	192918360	2185380	3.04	9128	1289640	1.30	1.53	0.43	1.0	192918360	2185380
A9	775450	0.34	192918360	2185380	3.23	9680	1146713	1.38	1.65	0.39	1.0	192918360	2185380
A10	1811409	0.34	341841936	3277360	2.85	8553	3682952	0.94	1.07	0.63	1.0	341841936	3277360
A11	1708904	0.34	341841936	3277360	3.04	9128	3233827	1.01	1.14	0.59	1.0	341841936	3277360
A12	1612470	0.34	341841936	3277360	3.23	9680	2875432	1.07	1.22	0.55	1.0	341841936	3277360
01-NL	1649141	0.34	423174646	3772585	2.33	11639	2644346	1.19	1.38	0.48	1.0	423174646	3772585
02-NL	1519941	0.34	423174646	3772585	2.48	12421	2321877	1.27	1.50	0.44	1.0	423174646	3772585
03-NL	1405168	0.34	423174646	3772585	2.63	13173	2064550	1.35	1.61	0.40	1.0	423174646	3772585
A1-NL	190076	0.34	40386575	855550	2.33	6984	246298	1.86	2.52	0.24	1.0	40386575	855550
A2-NL	170842	0.34	40386575	855550	2.48	7453	216263	1.99	2.78	0.21	1.0	40386575	855550
A3-NL	154800	0.34	40386575	855550	2.63	7904	192295	2.11	3.05	0.19	1.0	40386575	855550
A4-NL	462835	0.34	82663170	1307820	2.33	6984	677645	1.39	1.67	0.39	1.0	82663170	1307820
A5-NL	421980	0.34	82663170	1307820	2.48	7453	595008	1.48	1.82	0.35	1.0	82663170	1307820
A6-NL	386702	0.34	82663170	1307820	2.63	7904	529065	1.57	1.97	0.32	1.0	82663170	1307820
A7-NL	1180162	0.34	192918360	2185380	2.33	6984	2203124	1.00	1.13	0.60	1.0	192918360	2185380
A8-NL	1105774	0.34	192918360	2185380	2.48	7453	1934460	1.06	1.21	0.56	1.0	192918360	2185380
A9-NL	1036770	0.34	192918360	2185380	2.63	7904	1720069	1.13	1.29	0.52	1.0	192918360	2185380
A10-NL	2190255	0.34	341841936	3277360	2.33	6984	5524428	0.77	0.89	0.74	1.0	341841936	3277360
A11-NL	2101455	0.34	341841936	3277360	2.48	7453	4850741	0.82	0.94	0.71	1.0	341841936	3277360
A12-NL	2014564	0.34	341841936	3277360	2.63	7904	4313148	0.87	0.99	0.68	1.0	341841936	3277360
01-V	357434	0.34	423174646	3772585	5.70	28511	440724	2.93	5.24	0.10	1.0	423174646	3772585
02-V	319852	0.34	423174646	3772585	6.09	30426	386979	3.12	5.87	0.09	1.0	423174646	3772585
03-V	288839	0.34	423174646	3772585	6.45	32267	344092	3.31	6.51	0.08	1.0	423174646	3772585
A1-V	35867	0.34	40386575	855550	5.70	17106	41050	4.57	11.66	0.04	1.0	40386575	855550
A2-V	31874	0.34	40386575	855550	6.09	18256	36044	4.87	13.16	0.04	1.0	40386575	855550
A3-V	28622	0.34	40386575	855550	6.45	19360	32049	5.17	14.69	0.04	1.0	40386575	855550
A4-V	94218	0.34	82663170	1307820	5.70	17106	112941	3.40	6.83	0.08	1.0	82663170	1307820
A5-V	84088	0.34	82663170	1307820	6.09	18256	99168	3.63	7.68	0.07	1.0	82663170	1307820
A6-V	75771	0.34	82663170	1307820	6.45	19360	88178	3.85	8.54	0.06	1.0	82663170	1307820
A7-V	284251	0.34	192918360	2185380	5.70	17106	367187	2.44	3.86	0.15	1.0	192918360	2185380
A8-V	255538	0.34	192918360	2185380	6.09	18256	322410	2.60	4.30	0.13	1.0	192918360	2185380
A9-V	231623	0.34	192918360	2185380	6.45	19360	286678	2.76	4.75	0.12	1.0	192918360	2185380
A10-V	647169	0.34	341841936	3277360	5.70	17106	920738	1.89	2.57	0.23	1.0	341841936	3277360
A11-V	587585	0.34	341841936	3277360	6.09	18256	808457	2.01	2.84	0.21	1.0	341841936	3277360
A12-V	536894	0.34	341841936	3277360	6.45	19360	718858	2.14	3.11	0.19	1.0	341841936	3277360
01-H	1115881	0.34	423174646	3772585	2.85	14255	1762898	1.46	1.78	0.36	1.0	423174646	3772585
02-H	972863	0.34	423174646	3772585	3.04	15213	1547918	1.56	1.95	0.32	1.0	423174646	3772585
03-H	852730	0.34	423174646	3772585	3.23	16133	1376367	1.66	2.12	0.29	1.0	423174646	3772585
A1-H	110165	0.34	40386575	855550	2.85	8553	164199	2.28	3.46	0.17	1.0	40386575	855550
A2-H	89218	0.34	40386575	855550	3.04	9128	144175	2.44	3.85	0.15	1.0	40386575	855550
A3-H	72328	0.34	40386575	855550	3.23	9680	128197	2.58	4.24	0.13	1.0	40386575	855550
A4-H	303249	0.34	82663170	1307820	2.85	8553	451763	1.70	2.20	0.28	1.0	82663170	1307820
A5-H	261584	0.34	82663170	1307820	3.04	9128	396672	1.82	2.42	0.25	1.0	82663170	1307820
A6-H	227101	0.34	82663170	1307820	3.23	9680	352710	1.93	2.65	0.22	1.0	82663170	1307820
A7-H	871526	0.34	192918360	2185380	2.85	8553	1468749	1.22	1.42	0.47	1.0	192918360	2185380
A8-H	786796	0.34	192918360	2185380	3.04	9128	1289640	1.30	1.53	0.43	1.0	192918360	2185380
A9-H	712792	0.34	192918360	2185380	3.23	9680	1146713	1.38	1.65	0.39	1.0	192918360	2185380
A10-H	1767596	0.34	341841936	3277360	2.85	8553	3682952	0.94	1.07	0.63	1.0	341841936	3277360
A11-H	1646879	0.34	341841936	3277360	3.04	9128	3233827	1.01	1.14	0.59	1.0	341841936	3277360
A12-H	1534749	0.34	341841936	3277360	3.23	9680	2875432	1.07	1.22	0.55	1.0	341841936	3277360
01-VH	331854	0.34	423174646	3772585	5.70	28511	440724	2.93	5.24	0.10	1.0	423174646	3772585
02-VH	285835	0.34	423174646	3772585	6.09	30426	386979	3.12	5.87	0.09	1.0	423174646	3772585
03-VH	248201	0.34	423174646	3772585	6.45	32267	344092	3.31	6.51	0.08	1.0	423174646	3772585
A1-VH	30300	0.34	40386575	855550	5.70	17106	41050	4.57	11.66	0.04	1.0	40386575	855550
A2-VH	24495	0.34	40386575	855550	6.09	18256	36044	4.87	13.16	0.04	1.0	40386575	855550
A3-VH	19829	0.34	40386575	855550	6.45	19360	32049	5.17	14.69	0.04	1.0	40386575	855550
A4-VH	86887	0.34	82663170	1307820	5.70	17106	112941	3.40	6.83	0.08	1.0	82663170	1307820
A5-VH	74349	0.34	82663170	1307820	6.09	18256	99168	3.63	7.68	0.07	1.0	82663170	1307820
A6-VH	64144	0.34	82663170	1307820	6.45	19360	88178	3.85	8.54	0.06	1.0	82663170	1307820
A7-VH	274337	0.34	192918360	2185380	5.70	17106	367187	2.44	3.86	0.15	1.0	192918360	2185380
A8-VH	242305	0.34	192918360	2185380	6.09	18256	322410	2.60	4.30	0.13	1.0	192918360	2185380
A9-VH	215770	0.34	192918360	2185380	6.45	19360	286678	2.76	4.75	0.12	1.0	192918360	2185380
A10-VH	633859	0.34	341841936	3277360	5.70	17106	920738	1.89	2.57	0.23	1.0	341841936	3277360
A11-VH	569656	0.34	341841936	3277360	6.09	18256	808457	2.01	2.84	0.21	1.0	341841936	3277360
A12-VH	515273	0.34	341841936	3277360	6.45	19360	718858	2.14	3.11	0.19	1.0	341841936	3277360
01-NLH	1503290	0.34	423174646	3772585	2.33	11639	2644346	1.19	1.38	0.48	1.0	423174646	3772585
02-NLH	1323252	0.34	423174646	3772585	2.48	12421	2321877	1.27	1.50	0.44	1.0	423174646	3772585
03-NLH	1168495	0.34	423174646	3772585	2.63	13173	2064550	1.35	1.61	0.40	1.0	423174646	3772585
A1-NLH	156775	0.34	40386575	855550	2.33	6984	246298	1.86	2.52	0.24	1.0	40386575	855550
A2-NLH	127166	0.34	40386575	855550	2.48	7453	216263	1.99	2.78	0.21	1.0	40386575	855550
A3-NLH	103220	0.34	40386575	855550	2.63	7904	192295	2.11	3.05	0.19	1.0	40386575	855550
A4-NLH	419285	0.34	82663170	1307820	2.33	6984	677645	1.39	1.67	0.39	1.0	82663170	1307820
A5-NLH	364021	0.34	82663170	1307820	2.48	7453	595008	1.48	1.82	0.35	1.0	82663170	1307820
A6-NLH	317598	0.34	82663170	1307820	2.63	7904	529065	1.57	1.97	0.32	1.0	82663170	1307820
A7-NLH	1128783	0.34	192918360	2185380	2.33	6984	2203124	1.00	1.13	0.60	1.0	192918360	2185380
A8-NLH	1034175	0.34	192918360	2185380	2.48	7453	1934460	1.06	1.21	0.56	1.0	192918360	2185380
A9-NLH	948346	0.34	192918360	2185380	2.63	7904	1720069	1.13	1.29	0.52	1.0	192918360	2185380
A10-NLH	2137754	0.34	341841936	3277360	2.33	6984	5524428	0.77	0.89	0.74	1.0	341841936	3277360
A11-NLH	2024961	0.34	341841936	3277360	2.48	7453	4850741	0.82	0.94	0.71	1.0	341841936	3277360
A12-NLH	1916063	0.34	341841936	3277360	2.63	7904	4313148	0.87	0.99	0.68	1.0	341841936	3277360

	Current EC1993-1-1 with Yura						Current EC1993-1-1 with L.F. Geschwindner							
	$1/(1-((F_{ult}/F_{Rd})*\chi*\lambda^2))$			$(2*\varphi N_{Ed}+(Q/F)*\varphi NEd+H)*h*C_m/2$	$F/F_{Rd}+(n/n-1)*F_{tot}*e'/M_{Rd}$		variable for solve function		W_i*f_{yd}	$A*f_{yd}$		$(EI_c/L_c)/((EI_b/L_b)$		eq=0
	k	φF	c_m	M_{Ed}	SOLVE FOR = 1, F_{ult}		F_{ult}	α	M_{Rk}	N_{Rk}	G_A	G_B	K	SOLVE FOR = 0, K
	[-]	N	[-]	Nmm	[-]		N	[-]	Nmm	N	[-]	[-]	[-]	[-]
01	1.33	4446.0	0.9	33344800	1.00	-	1383838	0.34	423174646	3772585	1E+104	0.500	2.59	0.00
02	1.30	4047.3	0.9	30354405	1.00	-	1311735	0.34	423174646	3772585	1E+104	0.750	2.70	0.00
03	1.27	3704.6	0.9	27784570	1.00	-	1245353	0.34	423174646	3772585	1E+104	1.000	2.81	0.00
A1	1.15	540.5	0.9	2432081	1.00	-	154962	0.34	40386575	855550	1E+104	0.500	2.59	0.00
A2	1.14	483.6	0.9	2176016	1.00	-	144950	0.34	40386575	855550	1E+104	0.750	2.70	0.00
A3	1.12	436.6	0.9	1964652	1.00	-	136036	0.34	40386575	855550	1E+104	1.000	2.81	0.00
A4	1.26	1358.4	0.9	6112805	1.00	-	382971	0.34	82663170	1307820	1E+104	0.500	2.59	0.00
A5	1.23	1227.4	0.9	5523264	1.00	-	360968	0.34	82663170	1307820	1E+104	0.750	2.70	0.00
A6	1.21	1116.8	0.9	5025782	1.00	-	341009	0.34	82663170	1307820	1E+104	1.000	2.81	0.00
A7	1.41	3713.3	0.9	16709717	1.00	-	1012864	0.34	192918360	2185380	1E+104	0.500	2.59	0.00
A8	1.38	3423.2	0.9	15404369	1.00	-	968789	0.34	192918360	2185380	1E+104	0.750	2.70	0.00
A9	1.36	3165.8	0.9	14245930	1.00	-	927230	0.34	192918360	2185380	1E+104	1.000	2.81	0.00
A10	1.45	7395.0	0.9	33277717	1.00	-	1949912	0.34	341841936	3277360	1E+104	0.500	2.59	0.00
A11	1.46	6976.6	0.9	31394570	1.00	-	1892245	0.34	341841936	3277360	1E+104	0.750	2.70	0.00
A12	1.45	6582.9	0.9	29622974	1.00	-	1835943	0.34	341841936	3277360	1E+104	1.000	2.81	0.00
01-NL	1.43	6021.8	0.9	30109052	1.00	-	1792646	0.34	423174646	3772585	1E+104	0.500	2.17	0.00
02-NL	1.40	5550.0	0.9	27750199	1.00	-	1719189	0.34	423174646	3772585	1E+104	0.750	2.25	0.00
03-NL	1.38	5130.9	0.9	25654742	1.00	-	1649141	0.34	423174646	3772585	1E+104	1.000	2.33	0.00
A1-NL	1.22	776.0	0.9	2327948	1.00	-	213212	0.34	40386575	855550	1E+104	0.500	2.17	0.00
A2-NL	1.20	697.5	0.9	2092375	1.00	-	201113	0.34	40386575	855550	1E+104	0.750	2.25	0.00
A3-NL	1.18	632.0	0.9	1895906	1.00	-	190076	0.34	40386575	855550	1E+104	1.000	2.33	0.00
A4-NL	1.36	1889.5	0.9	5668549	1.00	-	509822	0.34	82663170	1307820	1E+104	0.500	2.17	0.00
A5-NL	1.33	1722.7	0.9	5168175	1.00	-	485546	0.34	82663170	1307820	1E+104	0.750	2.25	0.00
A6-NL	1.30	1578.7	0.9	4736115	1.00	-	462835	0.34	82663170	1307820	1E+104	1.000	2.33	0.00
A7-NL	1.47	4818.0	0.9	14453974	1.00	-	1258887	0.34	192918360	2185380	1E+104	0.500	2.17	0.00
A8-NL	1.47	4514.3	0.9	13542905	1.00	-	1219086	0.34	192918360	2185380	1E+104	0.750	2.25	0.00
A9-NL	1.46	4232.6	0.9	12697786	1.00	-	1180162	0.34	192918360	2185380	1E+104	1.000	2.33	0.00
A10-NL	1.42	8941.7	0.9	26825040	1.00	-	2279637	0.34	341841936	3277360	1E+104	0.500	2.17	0.00
A11-NL	1.44	8579.2	0.9	25737457	1.00	-	2234978	0.34	341841936	3277360	1E+104	0.750	2.25	0.00
A12-NL	1.46	8224.4	0.9	24673269	1.00	-	2190255	0.34	341841936	3277360	1E+104	1.000	2.33	0.00
01-V	1.09	1305.2	0.9	39154958	1.00	-	441385	0.34	423174646	3772585	1E+104	0.500	5.02	0.00
02-V	1.08	1167.9	0.9	35038056	1.00	-	409532	0.34	423174646	3772585	1E+104	0.750	5.26	0.00
03-V	1.07	1054.7	0.9	31640741	1.00	-	381882	0.34	423174646	3772585	1E+104	1.000	5.48	0.00
A1-V	1.04	146.4	0.9	2635688	1.00	-	45008	0.34	40386575	855550	1E+104	0.500	5.02	0.00
A2-V	1.04	130.1	0.9	2342255	1.00	-	41502	0.34	40386575	855550	1E+104	0.750	5.26	0.00
A3-V	1.03	116.8	0.9	2103263	1.00	-	38497	0.34	40386575	855550	1E+104	1.000	5.48	0.00
A4-V	1.07	384.6	0.9	6923574	1.00	-	117067	0.34	82663170	1307820	1E+104	0.500	5.02	0.00
A5-V	1.06	343.3	0.9	6179157	1.00	-	108360	0.34	82663170	1307820	1E+104	0.750	5.26	0.00
A6-V	1.06	309.3	0.9	5568023	1.00	-	100840	0.34	82663170	1307820	1E+104	1.000	5.48	0.00
A7-V	1.13	1160.5	0.9	20888104	1.00	-	347283	0.34	192918360	2185380	1E+104	0.500	5.02	0.00
A8-V	1.11	1043.2	0.9	18778161	1.00	-	323551	0.34	192918360	2185380	1E+104	0.750	5.26	0.00
A9-V	1.10	945.6	0.9	17020716	1.00	-	302768	0.34	192918360	2185380	1E+104	1.000	5.48	0.00
A10-V	1.20	2642.1	0.9	47557019	1.00	-	773006	0.34	341841936	3277360	1E+104	0.500	5.02	0.00
A11-V	1.18	2398.8	0.9	43178475	1.00	-	726435	0.34	341841936	3277360	1E+104	0.750	5.26	0.00
A12-V	1.16	2191.9	0.9	39453518	1.00	-	684848	0.34	341841936	3277360	1E+104	1.000	5.48	0.00
01-H	1.29	4074.6	0.9	61809662	1.00	-	1266206	0.34	423174646	3772585	1E+104	0.500	2.59	0.00
02-H	1.25	3552.4	0.9	73517957	1.00	-	1147619	0.34	423174646	3772585	1E+104	0.750	2.70	0.00
03-H	1.22	3113.7	0.9	85852972	1.00	-	1041287	0.34	423174646	3772585	1E+104	1.000	2.81	0.00
A1-H	1.12	449.7	0.9	8773864	1.00	-	128552	0.34	40386575	855550	1E+104	0.500	2.59	0.00
A2-H	1.10	364.2	0.9	11764033	1.00	-	108588	0.34	40386575	855550	1E+104	0.750	2.70	0.00
A3-H	1.08	295.3	0.9	14828755	1.00	-	91280	0.34	40386575	855550	1E+104	1.000	2.81	0.00
A4-H	1.23	1238.0	0.9	12321046	1.00	-	348355	0.34	82663170	1307820	1E+104	0.500	2.59	0.00
A5-H	1.20	1067.9	0.9	14930604	1.00	-	312932	0.34	82663170	1307820	1E+104	0.750	2.70	0.00
A6-H	1.17	927.1	0.9	17672105	1.00	-	281528	0.34	82663170	1307820	1E+104	1.000	2.81	0.00
A7-H	1.38	3558.0	0.9	22760958	1.00	-	970140	0.34	192918360	2185380	1E+104	0.500	2.59	0.00
A8-H	1.35	3212.1	0.9	24579361	1.00	-	908095	0.34	192918360	2185380	1E+104	0.750	2.70	0.00
A9-H	1.32	2910.0	0.9	26594829	1.00	-	850600	0.34	192918360	2185380	1E+104	1.000	2.81	0.00
A10-H	1.44	7216.2	0.9	39222815	1.00	-	1903425	0.34	341841936	3277360	1E+104	0.500	2.59	0.00
A11-H	1.43	6723.4	0.9	40380103	1.00	-	1824380	0.34	341841936	3277360	1E+104	0.750	2.70	0.00
A12-H	1.42	6265.6	0.9	41695135	1.00	-	1748063	0.34	341841936	3277360	1E+104	1.000	2.81	0.00
01-VH	1.09	1211.8	0.9	67602732	1.00	-	409350	0.34	423174646	3772585	1E+104	0.500	5.02	0.00
02-VH	1.07	1043.7	0.9	78186650	1.00	-	365324	0.34	423174646	3772585	1E+104	0.750	5.26	0.00
03-VH	1.06	906.3	0.9	89689083	1.00	-	327330	0.34	423174646	3772585	1E+104	1.000	5.48	0.00
A1-VH	1.03	123.7	0.9	8976565	1.00	-	37972	0.34	40386575	855550	1E+104	0.500	5.02	0.00
A2-VH	1.03	100.0	0.9	11925039	1.00	-	31829	0.34	40386575	855550	1E+104	0.750	5.26	0.00
A3-VH	1.02	81.0	0.9	14957138	1.00	-	26595	0.34	40386575	855550	1E+104	1.000	5.48	0.00
A4-VH	1.06	354.7	0.9	13134898	1.00	-	107853	0.34	82663170	1307820	1E+104	0.500	5.02	0.00
A5-VH	1.05	303.5	0.9	15588490	1.00	-	95658	0.34	82663170	1307820	1E+104	0.750	5.26	0.00
A6-VH	1.05	261.9	0.9	18213614	1.00	-	85176	0.34	82663170	1307820	1E+104	1.000	5.48	0.00
A7-VH	1.12	1120.0	0.9	26909536	1.00	-	334963	0.34	192918360	2185380	1E+104	0.500	5.02	0.00
A8-VH	1.11	989.2	0.9	27930717	1.00	-	306475	0.34	192918360	2185380	1E+104	0.750	5.26	0.00
A9-VH	1.10	880.9	0.9	29355825	1.00	-	281622	0.34	192918360	2185380	1E+104	1.000	5.48	0.00
A10-VH	1.19	2587.7	0.9	53328899	1.00	-	756838	0.34	341841936	3277360	1E+104	0.500	5.02	0.00
A11-VH	1.17	2325.6	0.9	51986032	1.00	-	703813	0.34	341841936	3277360	1E+104	0.750	5.26	0.00
A12-VH	1.15	2103.6	0.9	51364661	1.00	-	656618	0.34	341841936	3277360	1E+104	1.000	5.48	0.00
01-NLH	1.38	5489.2	0.9	58696203	1.00	-	1632935	0.34	423174646	3772585	1E+104	0.500	2.17	0.00
02-NLH	1.33	4831.8	0.9	71034163	1.00	-	1493692	0.34	423174646	3772585	1E+104	0.750	2.25	0.00
03-NLH	1.30	4266.7	0.9	83833697	1.00	-	1365992	0.34	423174646	3772585	1E+104	1.000	2.33	0.00
A1-NLH	1.18	640.0	0.9	8670099	1.00	-	175322	0.34	40386575	855550	1E+104	0.500	2.17	0.00
A2-NLH	1.14	519.2	0.9	11682459	1.00	-	148811	0.34	40386575	855550	1E+104	0.750	2.25	0.00
A3-NLH	1.11	421.4	0.9	14764182	1.00	-	125588	0.34	40386575	855550	1E+104	1.000	2.33	0.00
A4-NLH	1.31	1711.7	0.9	11885167	1.00	-	461185	0.34	82663170	1307820	1E+104	0.500	2.17	0.00
A5-NLH	1.27	1486.1	0.9	14583330	1.00	-	417516	0.34	82663170	1307820	1E+104	0.750	2.25	0.00
A6-NLH	1.23	1296.6	0.9	17389764	1.00	-	378070	0.34	82663170	1307820	1E+104	1.000	2.33	0.00
A7-NLH	1.44	4608.2	0.9	20574710	1.00	-	1204388	0.34	192918360	2185380	1E+104	0.500	2.17	0.00
A8-NLH	1.42	4222.0	0.9	22791000	1.00	-	1140298	0.34	192918360	2185380	1E+104	0.750	2.25	0.00
A9-NLH	1.40	3871.6	0.9	25114814	1.00	-	1079105	0.34	192918360	2185380	1E+104	1.000	2.33	0.00
A10-NLH	1.40	8727.3	0.9	32932037	1.00	-	2226146	0.34	341841936	3277360	1E+104	0.500	2.17	0.00
A11-NLH	1.42	8266.9	0.9	34925601	1.00	-	2155746	0.34	341841936	3277360	1E+104	0.750	2.25	0.00
A12-NLH	1.43	7822.3	0.9	36966888	1.00	-	2086130	0.34	341841936	3277360	1E+104	1.000	2.33	0.00

Current EC1993-1-1 with L.F. Geschwindner

	K*h	$\pi^2 EI/L_{cr}^2$	$\bar{\lambda} = \sqrt{(F_{Rk}/F_{cr})}$	$\Phi = 0.5(1+\alpha*(\lambda-0.2)+\lambda^2)$	$\chi = 1/(\Phi+\sqrt{('\Phi^2-\lambda^2)})$		M_{Rk}/γ_{M0}	N_{Rk}/γ_{M0}	$1/(1-((F_{ult}/F_{Rd})*\chi*\lambda^2))$			$(2*\varphi N_{Ed}+(Q/F)*\varphi NEd+H)*h*C_m/2$	$F/N_{Rd}+(n/n-1)*F_{tot}*e^*/M_{Rd}$
	L_{cr}	N_{cr}	$\bar{\lambda}$	Φ	χ	γ_{M0}	M_{Rd}	N_{Rd}	k	φF	c_m	M_{Ed}	SOLVE FOR = 1, F_{ult}
	mm	N	[-]	[-]	[-]	[-]	Nmm	N	[-]	N	[-]	Nmm	[-]
01	12971	2129248	1.33	1.58	0.41	1.0	423174646	3772585	1.37	5053.1	0.9	37897973	1.00
02	13506	1963878	1.39	1.66	0.39	1.0	423174646	3772585	1.35	4789.8	0.9	35923344	1.00
03	14028	1820560	1.44	1.75	0.37	1.0	423174646	3772585	1.33	4547.4	0.9	34105407	1.00
A1	7783	198321	2.08	2.98	0.20	1.0	40386575	855550	1.18	632.6	0.9	2846832	1.00
A2	8104	182918	2.16	3.17	0.18	1.0	40386575	855550	1.17	591.8	0.9	2662910	1.00
A3	8417	169570	2.25	3.37	0.17	1.0	40386575	855550	1.16	555.4	0.9	2499141	1.00
A4	7783	545645	1.55	1.93	0.33	1.0	82663170	1307820	1.30	1563.5	0.9	7035631	1.00
A5	8104	503267	1.61	2.04	0.30	1.0	82663170	1307820	1.28	1473.6	0.9	6631408	1.00
A6	8417	466540	1.67	2.15	0.29	1.0	82663170	1307820	1.26	1392.2	0.9	6264743	1.00
A7	7783	1773972	1.11	1.27	0.53	1.0	192918360	2185380	1.43	4135.0	0.9	18607498	1.00
A8	8104	1636195	1.16	1.33	0.50	1.0	192918360	2185380	1.42	3955.1	0.9	17797791	1.00
A9	8417	1516791	1.20	1.39	0.48	1.0	192918360	2185380	1.41	3785.4	0.9	17034296	1.00
A10	7783	4448311	0.86	0.98	0.69	1.0	341841936	3277360	1.43	7960.5	0.9	35822176	1.00
A11	8104	4102830	0.89	1.02	0.67	1.0	341841936	3277360	1.44	7725.1	0.9	34762758	1.00
A12	8417	3803418	0.93	1.05	0.64	1.0	341841936	3277360	1.45	7495.2	0.9	33728435	1.00
01-NL	10829	3054758	1.11	1.27	0.53	1.0	423174646	3772585	1.45	6545.8	0.9	32729081	1.00
02-NL	11238	2836863	1.15	1.33	0.50	1.0	423174646	3772585	1.44	6277.6	0.9	31387951	1.00
03-NL	11639	2644346	1.19	1.38	0.48	1.0	423174646	3772585	1.43	6021.8	0.9	30109052	1.00
A1-NL	6498	284524	1.73	2.26	0.27	1.0	40386575	855550	1.25	870.4	0.9	2611307	1.00
A2-NL	6743	264229	1.80	2.39	0.25	1.0	40386575	855550	1.24	821.0	0.9	2463116	1.00
A3-NL	6984	246298	1.86	2.52	0.24	1.0	40386575	855550	1.22	776.0	0.9	2327948	1.00
A4-NL	6498	782817	1.29	1.52	0.43	1.0	82663170	1307820	1.39	2081.3	0.9	6244025	1.00
A5-NL	6743	726979	1.34	1.59	0.41	1.0	82663170	1307820	1.37	1982.2	0.9	5946704	1.00
A6-NL	6984	677645	1.39	1.67	0.39	1.0	82663170	1307820	1.36	1889.5	0.9	5668549	1.00
A7-NL	6498	2545056	0.93	1.05	0.64	1.0	192918360	2185380	1.47	5139.4	0.9	15418154	1.00
A8-NL	6743	2363518	0.96	1.09	0.62	1.0	192918360	2185380	1.47	4976.9	0.9	14930688	1.00
A9-NL	6984	2203124	1.00	1.13	0.60	1.0	192918360	2185380	1.47	4818.0	0.9	14453974	1.00
A10-NL	6498	6381837	0.72	0.84	0.77	1.0	341841936	3277360	1.38	9306.6	0.9	27919739	1.00
A11-NL	6743	5926623	0.74	0.87	0.76	1.0	341841936	3277360	1.40	9124.3	0.9	27372774	1.00
A12-NL	6984	5524428	0.77	0.89	0.74	1.0	341841936	3277360	1.42	8941.7	0.9	26825040	1.00
01-V	25104	568433	2.58	4.22	0.13	1.0	423174646	3772585	1.11	1611.7	0.9	48351267	1.00
02-V	26281	518666	2.70	4.56	0.12	1.0	423174646	3772585	1.11	1495.4	0.9	44861964	1.00
03-V	27411	476785	2.81	4.90	0.11	1.0	423174646	3772585	1.10	1394.4	0.9	41833129	1.00
A1-V	15063	52945	4.02	9.23	0.06	1.0	40386575	855550	1.05	183.7	0.9	3307366	1.00
A2-V	15769	48309	4.21	10.04	0.05	1.0	40386575	855550	1.05	169.4	0.9	3049768	1.00
A3-V	16447	44408	4.39	10.84	0.05	1.0	40386575	855550	1.04	157.2	0.9	2828919	1.00
A4-V	15063	145668	3.00	5.46	0.10	1.0	82663170	1307820	1.09	477.9	0.9	8602625	1.00
A5-V	15769	132914	3.14	5.92	0.09	1.0	82663170	1307820	1.08	442.4	0.9	7962822	1.00
A6-V	16447	122182	3.27	6.37	0.08	1.0	82663170	1307820	1.07	411.7	0.9	7410185	1.00
A7-V	15063	473587	2.15	3.14	0.18	1.0	192918360	2185380	1.16	1417.8	0.9	25520020	1.00
A8-V	15769	432124	2.25	3.38	0.17	1.0	192918360	2185380	1.15	1320.9	0.9	23776063	1.00
A9-V	16447	397231	2.35	3.62	0.16	1.0	192918360	2185380	1.14	1236.0	0.9	22248784	1.00
A10-V	15063	1187540	1.66	2.13	0.29	1.0	341841936	3277360	1.23	3155.8	0.9	56804112	1.00
A11-V	15769	1083568	1.74	2.27	0.27	1.0	341841936	3277360	1.22	2965.7	0.9	53381844	1.00
A12-V	16447	996074	1.81	2.42	0.25	1.0	341841936	3277360	1.21	2795.9	0.9	50325811	1.00
01-H	12971	2129248	1.33	1.58	0.41	1.0	423174646	3772585	1.32	4623.5	0.9	65926482	1.00
02-H	13506	1963878	1.39	1.66	0.39	1.0	423174646	3772585	1.29	4190.5	0.9	78303828	1.00
03-H	14028	1820560	1.44	1.75	0.37	1.0	423174646	3772585	1.26	3802.2	0.9	91016819	1.00
A1-H	7783	198321	2.08	2.98	0.20	1.0	40386575	855550	1.15	524.8	0.9	9111644	1.00
A2-H	8104	182918	2.16	3.17	0.18	1.0	40386575	855550	1.12	443.3	0.9	12119885	1.00
A3-H	8417	169570	2.25	3.37	0.17	1.0	40386575	855550	1.10	372.6	0.9	15176917	1.00
A4-H	7783	545645	1.55	1.93	0.33	1.0	82663170	1307820	1.26	1422.2	0.9	13149684	1.00
A5-H	8104	503267	1.61	2.04	0.30	1.0	82663170	1307820	1.23	1277.5	0.9	15873933	1.00
A6-H	8417	466540	1.67	2.15	0.29	1.0	82663170	1307820	1.21	1149.3	0.9	18672002	1.00
A7-H	7783	1773972	1.11	1.27	0.53	1.0	192918360	2185380	1.41	3960.6	0.9	24572608	1.00
A8-H	8104	1636195	1.16	1.33	0.50	1.0	192918360	2185380	1.39	3707.3	0.9	26807779	1.00
A9-H	8417	1516791	1.20	1.39	0.48	1.0	192918360	2185380	1.37	3472.6	0.9	29126514	1.00
A10-H	7783	4448311	0.86	0.98	0.69	1.0	341841936	3277360	1.42	7770.7	0.9	41718144	1.00
A11-H	8104	4102830	0.89	1.02	0.67	1.0	341841936	3277360	1.42	7448.0	0.9	43640998	1.00
A12-H	8417	3803418	0.93	1.05	0.64	1.0	341841936	3277360	1.42	7136.4	0.9	45613964	1.00
01-VH	25104	568433	2.58	4.22	0.13	1.0	423174646	3772585	1.11	1494.7	0.9	76092083	1.00
02-VH	26281	518666	2.70	4.56	0.12	1.0	423174646	3772585	1.09	1334.0	0.9	86894268	1.00
03-VH	27411	476785	2.81	4.90	0.11	1.0	423174646	3772585	1.08	1195.2	0.9	98357213	1.00
A1-VH	15063	52945	4.02	9.23	0.06	1.0	40386575	855550	1.04	155.0	0.9	9540362	1.00
A2-VH	15769	48309	4.21	10.04	0.05	1.0	40386575	855550	1.04	129.9	0.9	12463924	1.00
A3-VH	16447	44408	4.39	10.84	0.05	1.0	40386575	855550	1.03	108.6	0.9	15454291	1.00
A4-VH	15063	145668	3.00	5.46	0.10	1.0	82663170	1307820	1.08	440.3	0.9	14675535	1.00
A5-VH	15769	132914	3.14	5.92	0.09	1.0	82663170	1307820	1.07	390.5	0.9	17154365	1.00
A6-VH	16447	122182	3.27	6.37	0.08	1.0	82663170	1307820	1.06	347.7	0.9	19759150	1.00
A7-VH	15063	473587	2.15	3.14	0.18	1.0	192918360	2185380	1.15	1367.5	0.9	31364632	1.00
A8-VH	15769	432124	2.25	3.38	0.17	1.0	192918360	2185380	1.14	1251.2	0.9	32646240	1.00
A9-VH	16447	397231	2.35	3.62	0.16	1.0	192918360	2185380	1.13	1149.7	0.9	34194934	1.00
A10-VH	15063	1187540	1.66	2.13	0.29	1.0	341841936	3277360	1.23	3089.8	0.9	62366034	1.00
A11-VH	15769	1083568	1.74	2.27	0.27	1.0	341841936	3277360	1.21	2873.3	0.9	61844515	1.00
A12-VH	16447	996074	1.81	2.42	0.25	1.0	341841936	3277360	1.20	2680.6	0.9	61751335	1.00
01-NLH	10829	3054758	1.11	1.27	0.53	1.0	423174646	3772585	1.39	5962.6	0.9	61063181	1.00
02-NLH	11238	2836863	1.15	1.33	0.50	1.0	423174646	3772585	1.36	5454.2	0.9	74145953	1.00
03-NLH	11639	2644346	1.19	1.38	0.48	1.0	423174646	3772585	1.33	4987.9	0.9	87439488	1.00
A1-NLH	6498	284524	1.73	2.26	0.27	1.0	40386575	855550	1.20	715.7	0.9	8897249	1.00
A2-NLH	6743	264229	1.80	2.39	0.25	1.0	40386575	855550	1.17	607.5	0.9	11947556	1.00
A3-NLH	6984	246298	1.86	2.52	0.24	1.0	40386575	855550	1.14	512.7	0.9	15038129	1.00
A4-NLH	6498	782817	1.29	1.52	0.43	1.0	82663170	1307820	1.34	1882.8	0.9	12398340	1.00
A5-NLH	6743	726979	1.34	1.59	0.41	1.0	82663170	1307820	1.31	1704.5	0.9	15238503	1.00
A6-NLH	6984	677645	1.39	1.67	0.39	1.0	82663170	1307820	1.27	1543.5	0.9	18130395	1.00
A7-NLH	6498	2545056	0.93	1.05	0.64	1.0	192918360	2185380	1.44	4916.9	0.9	21500682	1.00
A8-NLH	6743	2363518	0.96	1.09	0.62	1.0	192918360	2185380	1.43	4655.2	0.9	24090737	1.00
A9-NLH	6984	2203124	1.00	1.13	0.60	1.0	192918360	2185380	1.42	4405.4	0.9	26716283	1.00
A10-NLH	6498	6381837	0.72	0.84	0.77	1.0	341841936	3277360	1.37	9088.2	0.9	34014611	1.00
A11-NLH	6743	5926623	0.74	0.87	0.76	1.0	341841936	3277360	1.38	8800.8	0.9	36527393	1.00
A12-NLH	6984	5524428	0.77	0.89	0.74	1.0	341841936	3277360	1.39	8516.6	0.9	39049775	1.00

NEN 6771 with Nomogram

	variable for solve function			$(EI_c/L_c)/(\mu(EI_b/L_b)$		$C_A*C_B*\lambda^2*\sin(\lambda)$	$(C_A+C_B)*\lambda*\cos(\lambda)+\sin(\lambda)$	eq1-eq2=0	π/λ (K_0)	$\pi/\lambda*h$	$\sqrt{(I/A)}$	$\pi*\sqrt{(E/f_{yd})}$	L_{cr}/i	λ/λ_e	W_i*f_{yd}
	F_{ult}	μ	C_A	C_B	λ	eq1	eq2	SOLVE FOR = 0, λ	nomogram	L_{cr}	i	λ_e	λ	λ_{rel}	M_{Rk}
	N	[-]	[-]	[-]	[-]	[-]	[-]	[-]	[-]	mm	mm	mm	mm	[-]	Nmm
B01	2633298	6	0	0.167	2.72	0	1.43047E-09	0.00	1.157	5783	127.53	76.41	45.34	0.59	423174646.4
B02	2555024	6	0	0.250	2.57	0	1.55102E-10	0.00	1.222	6111	127.53	76.41	47.92	0.63	423174646.4
B03	2487218	6	0	0.333	2.46	0	-7.36087E-11	0.00	1.279	6397	127.53	76.41	50.16	0.66	423174646.4
B1	428014	6	0	0.167	2.72	0	1.43047E-09	0.00	1.157	3470	49.04	76.41	70.75	0.93	40386575
B2	405255	6	0	0.250	2.57	0	1.55102E-10	0.00	1.222	3667	49.04	76.41	74.77	0.98	40386575
B3	386321	6	0	0.333	2.46	0	-7.36086E-11	0.00	1.279	3838	49.04	76.41	78.26	1.02	40386575
B4	831361	6	0	0.167	2.72	0	1.43047E-09	0.00	1.157	3470	65.79	76.41	52.74	0.69	82663170
B5	800801	6	0	0.250	2.57	0	1.55102E-10	0.00	1.222	3667	65.79	76.41	55.73	0.73	82663170
B6	774584	6	0	0.333	2.46	0	-7.36086E-11	0.00	1.279	3838	65.79	76.41	58.34	0.76	82663170
B7	1660176	6	0	0.167	2.72	0	1.43047E-09	0.00	1.157	3470	91.77	76.41	37.81	0.49	192918360
B8	1621783	6	0	0.250	2.57	0	1.55102E-10	0.00	1.222	3667	91.77	76.41	39.96	0.52	192918360
B9	1588324	6	0	0.333	2.46	0	-7.36086E-11	0.00	1.279	3838	91.77	76.41	41.82	0.55	192918360
B10	2710193	6	0	0.167	2.72	0	1.43047E-09	0.00	1.157	3470	118.66	76.41	29.24	0.38	341841936.4
B11	2664910	6	0	0.250	2.57	0	1.55102E-10	0.00	1.222	3667	118.66	76.41	30.90	0.40	341841936.4
B12	2625295	6	0	0.333	2.46	0	-7.36086E-11	0.00	1.279	3838	118.66	76.41	32.34	0.42	341841936.4

NEN 6771 with Nomogram

	$A*f_{yd}$			$\alpha_k*(\lambda_{rel}-\lambda_0)*M_{Rk}/N_{Rk}$		M_{Rk}/γ_{M0}	N_{Rk}/γ_{M0}	π^2EI/L_{cr}^2	N_{cr}/F_{ult}			factor*N_{Ed}	$\varphi_0 x \alpha_h x \alpha_m$		boundary factor	$F_{ult}*h*3/2*C_m*bf$	$F/N_{Rd}+(n/n-1)*F_{tot}*e^*/M_{Rd}$
	N_{Rk}	α_k	λ_0	e^*	γ_{M0}	M_{Rd}	N_{Rd}	N_{cr}	n	N_{Ed}	factor	F_{tot}	φ	φF	bf	M_{Ed}	SOLVE FOR = 1, F_{ult}
	N	[-]	[-]	mm	[-]	Nmm	N	N	[-]	N	[-]	N	[-]	N	[-]	Nmm	[-]
B01	3772585	0.34	0.20	15.00	1	423174646.4	3772585	10713839	4.07	2633297.8	1.5	3949946.7	0.00365	9615.4	0.57	37121854.4	1.00
B02	3772585	0.34	0.20	16.29	1	423174646.4	3772585	9592917	3.75	2555024.3	1.5	3832536.5	0.00365	9329.6	0.60	37769970.2	1.00
B03	3772585	0.34	0.20	17.41	1	423174646.4	3772585	8755266	3.52	2487218.4	1.5	3730827.5	0.00365	9082.0	0.62	38278389.6	1.00
B1	855550	0.34	0.20	11.65	1	40386575	855550	997902	2.33	428014.4	1.5	642021.6	0.00408	1747.4	0.57	4045405.5	1.00
B2	855550	0.34	0.20	12.50	1	40386575	855550	893498	2.20	405254.6	1.5	607881.9	0.00408	1654.4	0.60	4019646.2	1.00
B3	855550	0.34	0.20	13.23	1	40386575	855550	815478	2.11	386320.9	1.5	579481.4	0.00408	1577.1	0.62	3990595.9	1.00
B4	1307820	0.34	0.20	10.53	1	82663170	1307820	2745547	3.30	831361.2	1.5	1247041.7	0.00408	3394.0	0.57	7860015.6	1.00
B5	1307820	0.34	0.20	11.38	1	82663170	1307820	2458297	3.07	800800.7	1.5	1201201.1	0.00408	3269.3	0.60	7941965.7	1.00
B6	1307820	0.34	0.20	12.11	1	82663170	1307820	2243640	2.90	774583.6	1.5	1161875.4	0.00408	3162.2	0.62	7998745.2	1.00
B7	2185380	0.34	0.20	8.85	1	192918360	2185380	8926181	5.38	1660176.0	1.5	2490264.0	0.00408	6777.6	0.57	15705900.1	1.00
B8	2185380	0.34	0.20	9.69	1	192918360	2185380	7992290	4.93	1621783.0	1.5	2432674.6	0.00408	6620.9	0.60	16079614.2	1.00
B9	2185380	0.34	0.20	10.43	1	192918360	2185380	7294405	4.59	1588323.9	1.5	2382485.8	0.00408	6484.3	0.62	16390987.4	1.00
B10	3277360	0.34	0.20	6.48	1	341841936.4	3277360	22382783	8.26	2710193.2	1.5	4065289.8	0.00408	11064.3	0.57	25661869.8	1.00
B11	3277360	0.34	0.20	7.25	1	341841936.4	3277360	20041011	7.52	2664910.0	1.5	3997365.0	0.00408	10879.4	0.60	26411995.9	1.00
B12	3277360	0.34	0.20	7.92	1	341841936.4	3277360	18291036	6.97	2625294.6	1.5	3937941.8	0.00408	10717.7	0.62	27067495.0	1.00

Modified EC1993-1-1 with Nomogram

	variable for solve function		W_i*f_{yd}	$A*f_{yd}$			$(EI_c/L_c)/(\mu(EI_b/L_b)$		$C_A*C_B*\lambda^{2}*\sin(\lambda)$	$(C_A+C_B)*\lambda*\cos(\lambda)+\sin(\lambda)$	eq1-eq2=0	π/λ (K_0)	$\pi/\lambda*h$	$\pi^2EI/L_{cr}^{\ 2}$	$\bar{\lambda} = \sqrt{(F_{Rk}/F_{cr})}$	$\Phi = 0.5(1+\alpha*(\lambda-0.2)+\lambda^2)$
	F_{ult}	α	M_{Rk}	N_{Rk}	μ	C_A	C_B	λ	eq1	eq2	SOLVE FOR = 0, λ	nomogram	L_{cr}	N_{cr}	$\bar{\lambda}$	Φ
	N	[-]	Nmm	N	[-]	[-]	[-]	[-]	[-]	[-]	[-]	[-]	mm	N	[-]	[-]
B01	2633298	0.34	423174646	3772585	6	0	0.167	2.72	0	1.43047E-09	0.00	1.16	5783	10713839	0.59	0.74
B02	2555024	0.34	423174646	3772585	6	0	0.250	2.57	0	1.55102E-10	0.00	1.22	6111	9592917	0.63	0.77
B03	2487218	0.34	423174646	3772585	6	0	0.333	2.46	0	-7.36087E-11	0.00	1.28	6397	8755266	0.66	0.79
B1	428014	0.34	40386575	855550	6	0	0.167	2.72	0	1.43047E-09	0.00	1.16	3470	997902	0.93	1.05
B2	405255	0.34	40386575	855550	6	0	0.250	2.57	0	1.55102E-10	0.00	1.22	3667	893498	0.98	1.11
B3	386321	0.34	40386575	855550	6	0	0.333	2.46	0	-7.36086E-11	0.00	1.28	3838	815478	1.02	1.16
B4	831361	0.34	82663170	1307820	6	0	0.167	2.72	0	1.43047E-09	0.00	1.16	3470	2745547	0.69	0.82
B5	800801	0.34	82663170	1307820	6	0	0.250	2.57	0	1.55102E-10	0.00	1.22	3667	2458297	0.73	0.86
B6	774584	0.34	82663170	1307820	6	0	0.333	2.46	0	-7.36086E-11	0.00	1.28	3838	2243640	0.76	0.89
B7	1660176	0.34	192918360	2185380	6	0	0.167	2.72	0	1.43047E-09	0.00	1.16	3470	8926181	0.49	0.67
B8	1621783	0.34	192918360	2185380	6	0	0.250	2.57	0	1.55102E-10	0.00	1.22	3667	7992290	0.52	0.69
B9	1588324	0.34	192918360	2185380	6	0	0.333	2.46	0	-7.36086E-11	0.00	1.28	3838	7294405	0.55	0.71
B10	2710193	0.34	341841936	3277360	6	0	0.167	2.72	0	1.43047E-09	0.00	1.16	3470	22382783	0.38	0.60
B11	2664910	0.34	341841936	3277360	6	0	0.250	2.57	0	1.55102E-10	0.00	1.22	3667	20041011	0.40	0.62
B12	2625295	0.34	341841936	3277360	6	0	0.333	2.46	0	-7.36086E-11	0.00	1.28	3838	18291036	0.42	0.63

Modified EC1993-1-1 with Nomogram

	$\chi = 1/(\Phi+\sqrt{('\Phi^2-\lambda^2)})$		M_{Rk}/γ_{M0}	N_{Rk}/γ_{M0}	$1/(1-((F_{ult}/F_{Rd})*\chi*\lambda\text{^}2))$			factor*N_{Ed}			boundary factor	$F_{ult}*h*3/2*C_m*bf$	$F/N_{Rd}+(n/n-1)*F_{tot}*e^*/M_{Rd}$
	χ	γ_{M0}	M_{Rd}	N_{Rd}	k	N_{Ed}	factor	F_{lean}	φF	c_m	bf	M_{Ed}	SOLVE FOR = 1, F_{ult}
	[-]	[-]	Nmm	N	[-]	N	[-]	N	N	[-]	[-]	N	[-]
B01	0.84	1.0	423174646	3772585	1.26	2633298	0.5	1316649	9615.4	0.9	0.57	41246505	1.00
B02	0.82	1.0	423174646	3772585	1.28	2555024	0.5	1277512	9329.6	0.9	0.60	41966633	1.00
B03	0.81	1.0	423174646	3772585	1.30	2487218	0.5	1243609	9082.0	0.9	0.62	42531544	1.00
B1	0.64	1.0	40386575	855550	1.38	428014	0.5	214007	1747.4	0.9	0.57	4494895	1.00
B2	0.61	1.0	40386575	855550	1.38	405255	0.5	202627	1654.4	0.9	0.60	4466274	1.00
B3	0.58	1.0	40386575	855550	1.38	386321	0.5	193160	1577.1	0.9	0.62	4433995	1.00
B4	0.79	1.0	82663170	1307820	1.31	831361	0.5	415681	3394.0	0.9	0.57	8733351	1.00
B5	0.77	1.0	82663170	1307820	1.33	800801	0.5	400400	3269.3	0.9	0.60	8824406	1.00
B6	0.75	1.0	82663170	1307820	1.35	774584	0.5	387292	3162.2	0.9	0.62	8887495	1.00
B7	0.89	1.0	192918360	2185380	1.20	1660176	0.5	830088	6777.6	0.9	0.57	17451000	1.00
B8	0.87	1.0	192918360	2185380	1.22	1621783	0.5	810892	6620.9	0.9	0.60	17866238	1.00
B9	0.86	1.0	192918360	2185380	1.23	1588324	0.5	794162	6484.3	0.9	0.62	18212208	1.00
B10	0.93	1.0	341841936	3277360	1.13	2710193	0.5	1355097	11064.3	0.9	0.57	28513189	1.00
B11	0.92	1.0	341841936	3277360	1.14	2664910	0.5	1332455	10879.4	0.9	0.60	29346662	1.00
B12	0.92	1.0	341841936	3277360	1.15	2625295	0.5	1312647	10717.7	0.9	0.62	30074995	1.00

Current EC1993-1-1 with LBA

	variable for solve function		W_i*f_{yd}	$A*f_{yd}$	LBA	$\bar{\lambda} = \sqrt{(N_{Rk}/N_{cr})}$	$\Phi = 0.5(1+\alpha*(\lambda-0.2)+\lambda^2)$	$\chi = 1/(\Phi+\sqrt{('\Phi^2-\lambda^2)})$		M_{Rk}/γ_{M0}	N_{Rk}/γ_{M0}	$1/(1-((F_{ult}/F_{Rd})*\chi*\lambda\text{^}2))$	
	F_{ult}	α	M_{Rk}	N_{Rk}	N_{cr}	$\bar{\lambda}$	Φ	χ	γ_{M0}	M_{Rd}	N_{Rd}	k	N_{Ed}
	N	[-]	Nmm	N	N	[-]	[-]	[-]	[-]	Nmm	N	[-]	N
B01	2548750	0.34	423174646	3772585	7045600	0.73	0.86	0.77	1.0	423174646	3772585	1.38	2548750
B02	2466145	0.34	423174646	3772585	6384900	0.77	0.89	0.74	1.0	423174646	3772585	1.40	2466145
B03	2391908	0.34	423174646	3772585	5866100	0.80	0.92	0.72	1.0	423174646	3772585	1.42	2391908
B1	389233	0.34	40386575	855550	681020	1.12	1.28	0.52	1.0	40386575	855550	1.43	389233
B2	364768	0.34	40386575	855550	612360	1.18	1.37	0.49	1.0	40386575	855550	1.41	364768
B3	344642	0.34	40386575	855550	560490	1.24	1.44	0.46	1.0	40386575	855550	1.39	344642
B4	793760	0.34	82663170	1307820	1839900	0.84	0.96	0.70	1.0	82663170	1307820	1.43	793760
B5	760224	0.34	82663170	1307820	1660900	0.89	1.01	0.67	1.0	82663170	1307820	1.44	760224
B6	730945	0.34	82663170	1307820	1523000	0.93	1.05	0.64	1.0	82663170	1307820	1.45	730945
B7	1620582	0.34	192918360	2185380	5707400	0.62	0.76	0.83	1.0	192918360	2185380	1.31	1620582
B8	1583023	0.34	192918360	2185380	5201300	0.65	0.79	0.81	1.0	192918360	2185380	1.33	1583023
B9	1548404	0.34	192918360	2185380	4793100	0.68	0.81	0.80	1.0	192918360	2185380	1.35	1548404
B10	2648310	0.34	341841936	3277360	13435000	0.49	0.67	0.89	1.0	341841936	3277360	1.21	2648310
B11	2609889	0.34	341841936	3277360	12391000	0.51	0.69	0.88	1.0	341841936	3277360	1.23	2609889
B12	2573134	0.34	341841936	3277360	11493000	0.53	0.70	0.87	1.0	341841936	3277360	1.24	2573134

Current EC1993-1-1 with LBA

				$F_{ult}*h*3/2*C_m*bf$	$F/N_{Rd}+(n/n-1)*F_{tot}*e^*/M_{Rd}$	
	φF	c_m	bound. Fact.	M_{Ed}	SOLVE FOR = 1, F_{ult}	
	N	[-]	[-]	Nmm	[-]	
B01	9306.7	0.9	0.57	39922190	1.00	-
B02	9005.1	0.9	0.60	40506779	1.00	-
B03	8734.0	0.9	0.62	40901729	1.00	-
B1	1589.0	0.9	0.57	4087625	1.00	-
B2	1489.2	0.9	0.60	4020078	1.00	-
B3	1407.0	0.9	0.62	3955629	1.00	-
B4	3240.5	0.9	0.57	8338353	1.00	-
B5	3103.6	0.9	0.60	8377274	1.00	-
B6	2984.1	0.9	0.62	8386784	1.00	-
B7	6616.0	0.9	0.57	17034811	1.00	-
B8	6462.7	0.9	0.60	17439238	1.00	-
B9	6321.3	0.9	0.62	17754476	1.00	-
B10	10811.7	0.9	0.57	27862137	1.00	-
B11	10654.8	0.9	0.60	28740758	1.00	-
B12	10504.8	0.9	0.62	29477447	1.00	-

Current EC1993-1-1 with Nomogram

variable for solve function		W_i*f_{yd}	$A*f_{yd}$			$(EI_c/L_c)/(\mu(EI_b/L_b)$		$C_A*C_B*\lambda^2*\sin(\lambda)$	$(C_A+C_B)*\lambda*\cos(\lambda)+\sin(\lambda)$	eq1-eq2=0
F_{ult}	α	M_{Rk}	N_{Rk}	μ	C_A	C_B	λ	eq1	eq2	SOLVE FOR = 0, λ
N	[-]	Nmm	N	[-]	[-]	[-]	[-]	[-]	[-]	[-]
2792657	0.34	423174646	3772585	6	0	0.167	2.72	0	1.43047E-09	0.00
2720617	0.34	423174646	3772585	6	0	0.250	2.57	0	1.55102E-10	0.00
2657147	0.34	423174646	3772585	6	0	0.333	2.46	0	-7.36087E-11	0.00
465503	0.34	40386575	855550	6	0	0.167	2.72	0	1.43047E-09	0.00
441378	0.34	40386575	855550	6	0	0.250	2.57	0	1.55102E-10	0.00
421063	0.34	40386575	855550	6	0	0.333	2.46	0	-7.36086E-11	0.00
890810	0.34	82663170	1307820	6	0	0.167	2.72	0	1.43047E-09	0.00
861220	0.34	82663170	1307820	6	0	0.250	2.57	0	1.55102E-10	0.00
835388	0.34	82663170	1307820	6	0	0.333	2.46	0	-7.36086E-11	0.00
1737822	0.34	192918360	2185380	6	0	0.167	2.72	0	1.43047E-09	0.00
1704263	0.34	192918360	2185380	6	0	0.250	2.57	0	1.55102E-10	0.00
1674586	0.34	192918360	2185380	6	0	0.333	2.46	0	-7.36086E-11	0.00
2790069	0.34	341841936	3277360	6	0	0.167	2.72	0	1.43047E-09	0.00
2752452	0.34	341841936	3277360	6	0	0.250	2.57	0	1.55102E-10	0.00
2719155	0.34	341841936	3277360	6	0	0.333	2.46	0	-7.36086E-11	0.00

Current EC1993-1-1 with Nomogram

π/λ (K_0)	$\pi/\lambda*h$	π^2EI/L_{cr}^2	$\bar{\lambda} = \sqrt{(F_{Rk}/F_{cr})}$	$\Phi = 0.5(1+\alpha*(\lambda-0.2)+\lambda^2)$	$\chi = 1/(\Phi+\sqrt{('\Phi^2-\lambda^2)})$		M_{Rk}/γ_{M0}	N_{Rk}/γ_{M0}	$1/(1-((F_{ult}/F_{Rd})*\chi*\lambda\text{^}2))$			boundary factor	$F_{ult}*h*3/2*C_m*bf$	$F/N_{Rd}+(n/n-1)*F_{tot}*e^*/M_{Rd}$
nomogram	l_{cr}	N_{cr}	$\bar{\lambda}$	Φ	χ	γ_{M0}	M_{Rd}	N_{Rd}	k	φF	c_m	bf	M_{Ed}	SOLVE FOR = 1, F_{ult}
[-]	mm	N	[-]	[-]	[-]	[-]	Nmm	N	[-]	N	[-]	[-]	N	[-]
1	5783	10713839	0.59	0.74	0.84	1.0	423174646	3772585	1.28	10197.3	0.9	0.57	43742617	1.00
1	6111	9592917	0.63	0.77	0.82	1.0	423174646	3772585	1.30	9934.3	0.9	0.60	44686523	1.00
1	6397	8755266	0.66	0.79	0.81	1.0	423174646	3772585	1.32	9702.5	0.9	0.62	45437329	1.00
1	3470	997902	0.93	1.05	0.64	1.0	40386575	855550	1.43	1900.4	0.9	0.57	4888586	1.00
1	3667	893498	0.98	1.11	0.61	1.0	40386575	855550	1.43	1801.9	0.9	0.60	4864384	1.00
1	3838	815478	1.02	1.16	0.58	1.0	40386575	855550	1.43	1719.0	0.9	0.62	4832753	1.00
1	3470	2745547	0.69	0.82	0.79	1.0	82663170	1307820	1.34	3636.7	0.9	0.57	9357856	1.00
1	3667	2458297	0.73	0.86	0.77	1.0	82663170	1307820	1.37	3515.9	0.9	0.60	9490190	1.00
1	3838	2243640	0.76	0.89	0.75	1.0	82663170	1307820	1.39	3410.5	0.9	0.62	9585154	1.00
1	3470	8926181	0.49	0.67	0.89	1.0	192918360	2185380	1.21	7094.6	0.9	0.57	18267180	1.00
1	3667	7992290	0.52	0.69	0.87	1.0	192918360	2185380	1.23	6957.6	0.9	0.60	18774872	1.00
1	3838	7294405	0.55	0.71	0.86	1.0	192918360	2185380	1.25	6836.5	0.9	0.62	19201313	1.00
1	3470	22382783	0.38	0.60	0.93	1.0	341841936	3277360	1.13	11390.4	0.9	0.57	29353536	1.00
1	3667	20041011	0.40	0.62	0.92	1.0	341841936	3277360	1.15	11236.8	0.9	0.60	30310702	1.00
1	3838	18291036	0.42	0.63	0.92	1.0	341841936	3277360	1.16	11100.9	0.9	0.62	31150241	1.00

Current EC1993-1-1 with Yura

	variable for solve function		W_i*f_{yd}	$A*f_{yd}$	$K_0*\sqrt{((\sum F+\sum Q)/\sum F)}$	K*h	π^2EI/L_{cr}^2	$\bar{\lambda} = \sqrt{(F_{Rk}/F_{cr})}$	$\Phi = 0.5(1+\alpha*(\lambda-0.2)+\lambda^2)$	$\chi = 1/(\Phi+\sqrt{('\Phi^2-\lambda^2)})$		M_{Rk}/γ_{M0}	N_{Rk}/γ_{M0}
	F_{ult}	α	M_{Rk}	N_{Rk}	K	L_{cr}	N_{cr}	$\bar{\lambda}$	Φ	χ	γ_{M0}	M_{Rd}	N_{Rd}
	N	[-]	Nmm	N	[-]	mm	N	[-]	[-]	[-]	[-]	Nmm	N
B01	-	2557988	0.34	423174646	3772585	1.42	7082	7142559	0.73	0.85	0.77	1.0	423174646	3772585
B02	-	2467319	0.34	423174646	3772585	1.50	7484	6395278	0.77	0.89	0.74	1.0	423174646	3772585
B03	-	2388101	0.34	423174646	3772585	1.57	7834	5836844	0.80	0.93	0.72	1.0	423174646	3772585
B1	-	384324	0.34	40386575	855550	1.42	4249	665268	1.13	1.30	0.52	1.0	40386575	855550
B2	-	358989	0.34	40386575	855550	1.50	4491	595665	1.20	1.39	0.48	1.0	40386575	855550
B3	-	338333	0.34	40386575	855550	1.57	4701	543652	1.25	1.47	0.45	1.0	40386575	855550
B4	-	792324	0.34	82663170	1307820	1.42	4249	1830365	0.85	0.97	0.70	1.0	82663170	1307820
B5	-	756346	0.34	82663170	1307820	1.50	4491	1638865	0.89	1.02	0.67	1.0	82663170	1307820
B6	-	725518	0.34	82663170	1307820	1.57	4701	1495760	0.94	1.06	0.64	1.0	82663170	1307820
B7	-	1633349	0.34	192918360	2185380	1.42	4249	5950787	0.61	0.75	0.83	1.0	192918360	2185380
B8	-	1590961	0.34	192918360	2185380	1.50	4491	5328193	0.64	0.78	0.82	1.0	192918360	2185380
B9	-	1553473	0.34	192918360	2185380	1.57	4701	4862937	0.67	0.80	0.80	1.0	192918360	2185380
B10	-	2681907	0.34	341841936	3277360	1.42	4249	14921855	0.47	0.66	0.90	1.0	341841936	3277360
B11	-	2635722	0.34	341841936	3277360	1.50	4491	13360674	0.50	0.67	0.89	1.0	341841936	3277360
B12	-	2594702	0.34	341841936	3277360	1.57	4701	12194024	0.52	0.69	0.88	1.0	341841936	3277360

Current EC1993-1-1 with Yura

$1/(1-((F_{ult}/F_{Rd})*\chi*\lambda\text{^}2))$			boundary factor	$F_{ult}*h*3/2*C_m*bf$	$F/F_{Rd}+(n/n-1)*F_{tot}*e^*/M_{Rd}$	
k	φF	c_m	bf	M_{Ed}	SOLVE FOR = 1, F_{ult}	
[-]	N	[-]	[-]	Nmm	[-]	
1.38	9340.5	0.9	0.57	40066899	1.00	-
1.40	9009.4	0.9	0.60	40526056	1.00	-
1.42	8720.1	0.9	0.62	40836626	1.00	-
1.42	1569.0	0.9	0.57	4036069	1.00	-
1.41	1465.6	0.9	0.60	3956388	1.00	-
1.39	1381.2	0.9	0.62	3883213	1.00	-
1.43	3234.6	0.9	0.57	8323270	1.00	-
1.44	3087.8	0.9	0.60	8334540	1.00	-
1.45	2961.9	0.9	0.62	8324523	1.00	-
1.30	6668.1	0.9	0.57	17169005	1.00	-
1.32	6495.1	0.9	0.60	17526686	1.00	-
1.34	6342.0	0.9	0.62	17812599	1.00	-
1.19	10948.8	0.9	0.57	28215602	1.00	-
1.21	10760.3	0.9	0.60	29025242	1.00	-
1.23	10592.8	0.9	0.62	29724534	1.00	-

Current EC1993-1-1 with L.F. Geschwindner

variable for solve function		W_i*f_{yd}	$A*f_{yd}$			$(EI_c/L_c)/((EI_b/L_b)$		eq=0
F_{ult}	α	M_{Rk}	N_{Rk}	G_A	G_B		K	SOLVE FOR = 0, K
N	[-]	Nmm	N	[-]	[-]		[-]	[-]
2672444	0.34	423174646	3772585	0	0.50		1.29	0.00
2613902	0.34	423174646	3772585	0	0.75		1.34	0.00
2560279	0.34	423174646	3772585	0	1.00		1.39	0.00
421976	0.34	40386575	855550	0	0.50		1.29	0.00
404442	0.34	40386575	855550	0	0.75		1.34	0.00
388944	0.34	40386575	855550	0	1.00		1.39	0.00
839939	0.34	82663170	1307820	0	0.50		1.29	0.00
816453	0.34	82663170	1307820	0	0.75		1.34	0.00
795126	0.34	82663170	1307820	0	1.00		1.39	0.00
1684351	0.34	192918360	2185380	0	0.50		1.29	0.00
1656704	0.34	192918360	2185380	0	0.75		1.34	0.00
1631281	0.34	192918360	2185380	0	1.00		1.39	0.00
2734348	0.34	341841936	3277360	0	0.50		1.29	0.00
2703132	0.34	341841936	3277360	0	0.75		1.34	0.00
2674400	0.34	341841936	3277360	0	1.00		1.39	0.00

	Current EC1993-1-1 with L.F. Geschwindner														
	$K*h$	$\pi^2 EI/L_{cr}^2$	$\bar{\lambda} = \sqrt{(F_{Rk}/F_{cr})}$	$\Phi = 0.5(1+\alpha*(\lambda-0.2)+\lambda^2)$	$\chi = 1/(\Phi+\sqrt{(\Phi^2-\lambda^2)})$		M_{Rk}/γ_{M0}	N_{Rk}/γ_{M0}	$1/(1-((F_{ult}/F_{Rd})*\chi*\lambda\wedge 2))$			boundary factor	$F_{ult}*h*3/2*C_m*bf$	$F/N_{Rd}+(n/n-1)*F_{tot}*e^*/M_{Rd}$
	L_{cr}	N_{cr}	$\bar{\lambda}$	Φ	χ	γ_{M0}	M_{Rd}	N_{Rd}	k	φF	c_m	bf	M_{Ed}	SOLVE FOR = 1, F_{ult}
	mm	N	[-]	[-]	[-]	[-]	Nmm	N	[-]	N	[-]	[-]	Nmm	[-]
B01	6466	8568908	0.66	0.80	0.80	1.0	423174646	3772585	1.33	9758.4	0.9	0.57	41859676	1.00
B02	6707	7964255	0.69	0.82	0.79	1.0	423174646	3772585	1.35	9544.6	0.9	0.60	42933701	1.00
B03	6930	7459693	0.71	0.84	0.78	1.0	423174646	3772585	1.36	9348.8	0.9	0.62	43780879	1.00
B1	3880	798120	1.04	1.18	0.57	1.0	40386575	855550	1.44	1722.7	0.9	0.57	4431478	1.00
B2	4024	741802	1.07	1.23	0.55	1.0	40386575	855550	1.43	1651.1	0.9	0.60	4457319	1.00
B3	4158	694806	1.11	1.27	0.53	1.0	40386575	855550	1.42	1587.9	0.9	0.62	4464104	1.00
B4	3880	2195883	0.77	0.89	0.74	1.0	82663170	1307820	1.40	3429.0	0.9	0.57	8823463	1.00
B5	4024	2040934	0.80	0.92	0.72	1.0	82663170	1307820	1.41	3333.2	0.9	0.60	8996890	1.00
B6	4158	1911634	0.83	0.95	0.71	1.0	82663170	1307820	1.42	3246.1	0.9	0.62	9123195	1.00
B7	3880	7139142	0.55	0.71	0.86	1.0	192918360	2185380	1.25	6876.3	0.9	0.57	17705118	1.00
B8	4024	6635379	0.57	0.73	0.85	1.0	192918360	2185380	1.27	6763.5	0.9	0.60	18250937	1.00
B9	4158	6215006	0.59	0.74	0.84	1.0	192918360	2185380	1.28	6659.7	0.9	0.62	18704773	1.00
B10	3880	17901706	0.43	0.63	0.91	1.0	341841936	3277360	1.16	11162.9	0.9	0.57	28767318	1.00
B11	4024	16638499	0.44	0.64	0.91	1.0	341841936	3277360	1.17	11035.5	0.9	0.60	29767570	1.00
B12	4158	15584394	0.46	0.65	0.90	1.0	341841936	3277360	1.18	10918.2	0.9	0.62	30637541	1.00

APPENDIX D – SCRIPT

The scripts below are the parametric scripts for all frame configurations with a leaning column, frames A, A-V, A-H, A-VH, and B. The input is generated from an Excel sheet, as given in Appendix B. For each analysis type (GMNIA IV, GMNIA III, and LBA), a different script is used.

```
# -*- coding: mbcs -*-
from part import *
from material import *
from section import *
from assembly import *
from step import *
from interaction import *
from load import *
from mesh import *
from optimization import *
from job import *
from sketch import *
from visualization import *
from connectorBehavior import *
from caeModules import *
import os
import sys
import csv
import odbAccess
import math
import numpy as np
import xlsxwriter

session.journalOptions.setValues(replayGeometry=COORDINATE, recoverGeometry=COORDINATE)
# ======================setting up================================

input_file=open('C:/Users/20174572/Google Drive/Wim Broeks/TUe/2. Master/Afstuderen/4. FE Modelling/4. Parametric/INPUT.txt')

for line in input_file:
    extracted_line = line
    extracted_list = extracted_line.split()
    if "id" not in extracted_line:
        id = extracted_list[0]
        E = float(extracted_list[1])
        pois = float(extracted_list[2])
        F = float(extracted_list[3])
        Q = float(extracted_list[4])
        H = float(extracted_list[5])
        fy = float(extracted_list[6])
        fu = float(extracted_list[7])
        strain = float(extracted_list[8])
        h = float(extracted_list[9])
        b1 = float(extracted_list[10])
        b2 = float(extracted_list[11])
        P1h = float(extracted_list[16])
        P1b = float(extracted_list[17])
        P1tw = float(extracted_list[18])
        P1tf = float(extracted_list[19])
        P2h = float(extracted_list[27])
        P2b = float(extracted_list[28])
        P2tw = float(extracted_list[29])
        P2tf = float(extracted_list[30])
        P4h = float(extracted_list[38])
        P4b = float(extracted_list[39])
        P4tw = float(extracted_list[40])
        P4tf = float(extracted_list[41])
        P5h = float(extracted_list[49])
        P5b = float(extracted_list[50])
        P5tw = float(extracted_list[51])
        P5tf = float(extracted_list[52])
        joint = float(extracted_list[59])
        condition = float(extracted_list[60])
        ma1 = float(extracted_list[62])
        mb1 = float(extracted_list[63])
        mc1 = float(extracted_list[64])
        rs1 = float(extracted_list[65])
        ma2 = float(extracted_list[66])
        mb2 = float(extracted_list[67])
        mc2 = float(extracted_list[68])
        rs2 = float(extracted_list[69])
        ma4 = float(extracted_list[70])
        mb4 = float(extracted_list[71])
        mc4 = float(extracted_list[72])
        rs4 = float(extracted_list[73])
        ma5 = float(extracted_list[74])
        mb5 = float(extracted_list[75])
        mc5 = float(extracted_list[76])
        rs5 = float(extracted_list[77])

        mode1 = extracted_list[80]
        mode2 = extracted_list[81]
        mode3 = extracted_list[82]
        A1 = float(extracted_list[126])
        A2 = float(extracted_list[127])
        A3 = float(extracted_list[128])
```

```
86
87          #mesh
88          P1sy = ma1
89          P1sx = mb1
90          P1sz = mc1
91
92          P2sy = mb2
93          P2sx = ma2
94          P2sz = mc2
95
96          P3sx = mb1
97          P3sz = mc1
98
99          P4sy = ma4
100         P4sx = mb4
101         P4sz = mc4
102
103         P5sy = mb5
104         P5sx = ma5
105         P5sz = mc5
106
107         P6sx = mb4
108         P6sz = mc4
109
110         # ======================setting up================================
111         Filename='Frame-'+id
112         Loadpath='F:\\Graduation project Wim\\parametric study\\plot\\{0}'.format(Filename)
113         if not os.path.exists(Loadpath):
114             os.makedirs(Loadpath)
115         os.chdir(Loadpath)
116
117         Mymodel=mdb.Model(name='GMNIA_IV-frame-'+id)
118         Myassembly=Mymodel.rootAssembly
119
120         #part 1 - stabilizing columns
121         Mymodel.ConstrainedSketch(name='__sweep__', sheetSize=200.0)
122         Mysketchs=Mymodel.sketches['__sweep__']
123         Mysketchs.Line(point1=(0.0, 0.0), point2=(0.0, h+P2h/2))
124         Mysketchs.geometry.findAt((0.0, h/2))
125         Mysketchs.VerticalConstraint(addUndoState= False, entity=Mysketchs.geometry.findAt((0.0, h/2), ))
126         Mymodel.ConstrainedSketch(name='__profile__', sheetSize=200.0, transform=(1.0, 0.0, 0.0, 0.0, 0.0,
            1.0, -0.0, -1.0, -0.0, 0.0, 0.0, 0.0))
127         Mysketchp=Mymodel.sketches['__profile__']
128         Mysketchp.ConstructionLine(point1=(-100.0, 0.0), point2=(100.0, 0.0))
129         Mysketchp.ConstructionLine(point1=(0.0, -100.0), point2=(0.0, 100.0))
130         Mysketchp.Line(point1=(-(P1h/2), (P1b/2)), point2=(-(P1h/2), -(P1b/2)))
131         Mysketchp.VerticalConstraint(addUndoState=False, entity=Mysketchp.geometry[4])
132         Mysketchp.Line(point1=((P1h/2), (P1b/2)), point2=((P1h/2), -(P1b/2)))
133         Mysketchp.VerticalConstraint(addUndoState=False, entity=Mysketchp.geometry[5])
134         Mysketchp.Line(point1=(-(P1h/2), 0.0), point2=((P1h/2), 0.0))
135         Mysketchp.HorizontalConstraint(addUndoState=False, entity=Mysketchp.geometry[6])
136         Mymodel.Part(dimensionality=THREE_D, name='Part-1', type=DEFORMABLE_BODY)
137         Mypart1=Mymodel.parts['Part-1']
138         Mypart1.BaseShellSweep(path=Mysketchs, sketch=Mysketchp)
139
140         Mypart1.DatumPlaneByPrincipalPlane(offset=(h-(P2h/2)), principalPlane=XZPLANE)
141         Mypart1.DatumPlaneByPrincipalPlane(offset=(h+(P2h/2)), principalPlane=XZPLANE)
142         Mypart1.DatumPlaneByPrincipalPlane(offset=(h), principalPlane=XZPLANE)
143
144         #part 2 - stabilizing beam
145         Mymodel.ConstrainedSketch(name='__sweep__', sheetSize=200.0)
146         Mysketchs=Mymodel.sketches['__sweep__']
147         Mysketchs.Line(point1=(P1h/2, h), point2=((b1-P1h/2), h))
148         Mysketchs.HorizontalConstraint(addUndoState=False, entity=Mysketchs.geometry[2])
149         Mymodel.ConstrainedSketch(name='__profile__', sheetSize=200.0, transform=(0.0, -1.0, 0.0, -0.0, 0.0,
            1.0, -1.0, -0.0, -0.0, 0, h, 0.0))
150         Mysketchp=Mymodel.sketches['__profile__']
151         Mysketchp.ConstructionLine(point1=(-100.0, 0.0), point2=(100.0, 0.0))
152         Mysketchp.ConstructionLine(point1=(0.0, -100.0), point2=(0.0, 100.0))
153         Mysketchp.Line(point1=(-(P2h/2), (P2b/2)), point2=(-(P2h/2), -(P2b/2)))
154         Mysketchp.VerticalConstraint(addUndoState=False, entity=Mysketchp.geometry[4])
155         Mysketchp.Line(point1=((P2h/2), (P2b/2)), point2=((P2h/2), -(P2b/2)))
156         Mysketchp.VerticalConstraint(addUndoState=False, entity=Mysketchp.geometry[5])
157         Mysketchp.Line(point1=(-(P2h/2), 0.0), point2=((P2h/2), 0.0))
158         Mysketchp.HorizontalConstraint(addUndoState=False, entity=Mysketchp.geometry[6])
159         Mymodel.Part(dimensionality=THREE_D, name='Part-2', type=DEFORMABLE_BODY)
160         Mypart2=Mymodel.parts['Part-2']
161         Mypart2.BaseShellSweep(path=Mysketchs, sketch=Mysketchp)
162
163         #part 3a - stiffeners stabilizing column
164         Mymodel.ConstrainedSketch(name='__profile__', sheetSize=200.0)
165         Mysketchp=Mymodel.sketches['__profile__']
166         Mysketchp.Line(point1=(0.0, 0.0), point2=(P1h, 0.0))
167         Mysketchp.geometry.findAt((P1h/2, 0.0))
168         Mysketchp.HorizontalConstraint(addUndoState=False, entity=Mysketchp.geometry.findAt((P1h/2, 0.0), ))
169         Mymodel.Part(dimensionality=THREE_D, name='Part-3a', type=DEFORMABLE_BODY)
```

```
170         Mypart3a=Mymodel.parts['Part-3a']
171         Mypart3a.BaseShellExtrude(depth=P1b, sketch=Mysketchp)
172         Mypart3a.DatumPlaneByPrincipalPlane(offset=(P1b/2), principalPlane=XYPLANE)
173
174         #part 3b - stiffeners stabilizing column
175         Mymodel.ConstrainedSketch(name='__profile__', sheetSize=200.0)
176         Mysketchp=Mymodel.sketches['__profile__']
177         Mysketchp.Line(point1=(0.0, 0.0), point2=(P1h, 0.0))
178         Mysketchp.geometry.findAt((P1h/2, 0.0))
179         Mysketchp.HorizontalConstraint(addUndoState=False, entity=Mysketchp.geometry.findAt((P1h/2, 0.0), ))
180         Mymodel.Part(dimensionality=THREE_D, name='Part-3b', type=DEFORMABLE_BODY)
181         Mypart3b=Mymodel.parts['Part-3b']
182         Mypart3b.BaseShellExtrude(depth=P1b, sketch=Mysketchp)
183         Mypart3b.DatumPlaneByPrincipalPlane(offset=(P1b/2), principalPlane=XYPLANE)
184
185         #part 4 - leaning column
186         Mymodel.ConstrainedSketch(name='__sweep__', sheetSize=200.0)
187         Mysketchs=Mymodel.sketches['__sweep__']
188         Mysketchs.Line(point1=(b1+b2, 0.0), point2=(b1+b2, h+P5h/2))
189         Mymodel.ConstrainedSketch(name='__profile__', sheetSize=200.0, transform=(1.0, 0.0, 0.0, 0.0, 0.0,
            1.0, -0.0, -1.0, -0.0, b1+b2, 0.0, 0.0))
190         Mysketchp=Mymodel.sketches['__profile__']
191         Mysketchp.ConstructionLine(point1=(-100.0, 0.0), point2=(100.0, 0.0))
192         Mysketchp.ConstructionLine(point1=(0.0, -100.0), point2=(0.0, 100.0))
193         Mysketchp.Line(point1=(-P4h/2, P4b/2), point2=(-P4h/2, -P4b/2))
194         Mysketchp.Line(point1=(P4h/2, P4b/2), point2=(P4h/2, -P4b/2))
195         Mysketchp.Line(point1=(-P4h/2, 0.0), point2=(P4h/2, 0.0))
196         Mymodel.Part(dimensionality=THREE_D, name='Part-4', type=DEFORMABLE_BODY)
197         Mypart4=Mymodel.parts['Part-4']
198         Mypart4.BaseShellSweep(path=Mysketchs, sketch=Mysketchp)
199
200         Mypart4.DatumPlaneByPrincipalPlane(offset=h-P5h/2, principalPlane=XZPLANE)
201         Mypart4.DatumPlaneByPrincipalPlane(offset=h+P5h/2, principalPlane=XZPLANE)
202         Mypart4.DatumPlaneByPrincipalPlane(offset=(h), principalPlane=XZPLANE)
203
204         #part 5 - leaning beam
205         Mymodel.ConstrainedSketch(name='__sweep__', sheetSize=200.0)
206         Mysketchs=Mymodel.sketches['__sweep__']
207         Mysketchs.Line(point1=(b1+P1h/2, h), point2=(b1+b2-P4h/2, h))
208         Mymodel.ConstrainedSketch(name='__profile__', sheetSize=200.0, transform=(0.0, -1.0, 0.0, -0.0, 0.0,
            1.0, -1.0, -0.0, -0.0, b1, h, 0.0))
209         Mysketchp=Mymodel.sketches['__profile__']
210         Mysketchp.ConstructionLine(point1=(-100.0, 0.0), point2=(100.0, 0.0))
211         Mysketchp.ConstructionLine(point1=(0.0, -100.0), point2=(0.0, 100.0))
212         Mysketchp.Line(point1=(-P5h/2, P5b/2), point2=(-P5h/2, -P5b/2))
213         Mysketchp.Line(point1=(P5h/2, P5b/2), point2=(P5h/2, -P5b/2))
214         Mysketchp.Line(point1=(-P5h/2, 0.0), point2=(P5h/2, 0.0))
215         Mymodel.Part(dimensionality=THREE_D, name='Part-5', type=DEFORMABLE_BODY)
216         Mypart5=Mymodel.parts['Part-5']
217         Mypart5.BaseShellSweep(path=Mysketchs, sketch=Mysketchp)
218
219         if (joint ==1):
220         #part 6a - stiffeners leaning column
221             Mymodel.ConstrainedSketch(name='__profile__', sheetSize=200.0)
222             Mysketchp=Mymodel.sketches['__profile__']
223             Mysketchp.Line(point1=(0.0, 0.0), point2=(P4h, 0.0))
224             Mysketchp.geometry.findAt((P4h/2, 0.0))
225             Mysketchp.HorizontalConstraint(addUndoState=False, entity=Mysketchp.geometry.findAt((P4h/2, 0.0),
                ))
226             Mymodel.Part(dimensionality=THREE_D, name='Part-6a', type=DEFORMABLE_BODY)
227             Mypart6a=Mymodel.parts['Part-6a']
228             Mypart6a.BaseShellExtrude(depth=P4b, sketch=Mysketchp)
229             Mypart6a.DatumPlaneByPrincipalPlane(offset=(P4b/2), principalPlane=XYPLANE)
230
231         elif (joint ==2):
232         #part 6a - stiffeners leaning column
233             Mymodel.ConstrainedSketch(name='__profile__', sheetSize=200.0)
234             Mysketchp=Mymodel.sketches['__profile__']
235             Mysketchp.Line(point1=(0.0, 0.0), point2=(P4h, 0.0))
236             Mysketchp.geometry.findAt((P4h/2, 0.0))
237             Mysketchp.HorizontalConstraint(addUndoState=False, entity=Mysketchp.geometry.findAt((P4h/2, 0.0),
                ))
238             Mymodel.Part(dimensionality=THREE_D, name='Part-6a', type=DEFORMABLE_BODY)
239             Mypart6a=Mymodel.parts['Part-6a']
240             Mypart6a.BaseShellExtrude(depth=P4b, sketch=Mysketchp)
241             Mypart6a.DatumPlaneByPrincipalPlane(offset=(P4b/2), principalPlane=XYPLANE)
242         #part 6b - stiffeners leaning column
243             Mymodel.ConstrainedSketch(name='__profile__', sheetSize=200.0)
244             Mysketchp=Mymodel.sketches['__profile__']
245             Mysketchp.Line(point1=(0.0, 0.0), point2=(P4h, 0.0))
246             Mysketchp.geometry.findAt((P4h/2, 0.0))
247             Mysketchp.HorizontalConstraint(addUndoState=False, entity=Mysketchp.geometry.findAt((P4h/2, 0.0),
                ))
248             Mymodel.Part(dimensionality=THREE_D, name='Part-6b', type=DEFORMABLE_BODY)
249             Mypart6b=Mymodel.parts['Part-6b']
250             Mypart6b.BaseShellExtrude(depth=P4b, sketch=Mysketchp)
```

```
            Mypart6b.DatumPlaneByPrincipalPlane(offset=(P4b/2), principalPlane=XYPLANE)

        #assembly
        Myassembly.DatumCsysByDefault(CARTESIAN)
        Myassembly.Instance(dependent=ON, name='Part-1-1', part=Mypart1)
        Myassembly.Instance(dependent=ON, name='Part-2-1', part=Mypart2)
        Myassembly.Instance(dependent=ON, name='Part-1-2', part=Mypart1)
        Myassembly.translate(instanceList=('Part-1-2', ), vector=(b1, 0.0, 0.0))
        Myassembly.Instance(dependent=ON, name='Part-4-1', part=Mypart4)
        Myassembly.Instance(dependent=ON, name='Part-5-1', part=Mypart5)

        #partition
            #part 1
        Mypart1.PartitionFaceByDatumPlane(datumPlane=Mypart1.datums[2], faces=Mypart1.faces.findAt(((-P1h/2, h/4, P1b/4), ), ((-P1h/2, h/4, -P1b/4), ), ((P1h/2, h/4, P1b/4), ), ((P1h/2, h/4, -P1b/4), ), ((P1h/4, h/4, 0.0), ), ))
            #part 4
        Mypart4.PartitionFaceByDatumPlane(datumPlane=Mypart4.datums[2], faces=Mypart4.faces.findAt(((b1+b2-P4h/2, h/4, P4b/4), ), ((b1+b2-P4h/2, h/4, -P4b/4), ), ((b1+b2+P4h/2, h/4, P4b/4), ), ((b1+b2+P4h/2, h/4, -P4b/4), ), ((b1+b2, h/4, 0.0), ), ))

            #part 3a-1
        Mypart3a.PartitionFaceByDatumPlane(datumPlane=Mypart3a.datums[2], faces=Mypart3a.faces.findAt(((P1h/4, 0.0, P1b/4), )))
        Myassembly.Instance(dependent=ON, name='Part-3a-1', part=Mypart3a)
        Mymodel.Tie(adjust=ON, master=Region(edges=Myassembly.instances['Part-1-1'].edges.findAt(((-P1h/2, h+(P2h/2), P1b/4), ), (((P1h/2), h+(P2h/2), P1b/4), ), ((-(P1h/2), h+(P2h/2), -P1b/4), ), (((P1h/2), h+(P2h/2), -P1b/4), ),((0.0, h+(P2h/2), 0.0), ), )), name='Tie_A_a', positionToleranceMethod=COMPUTED, slave=Region(edges=Myassembly.instances['Part-3a-1'].edges.findAt(((0.0, 0.0, P1b/4), ), ((P1h, 0.0, P1b/4), ),((0.0, 0.0, P1b/4*3), ), ((P1h, 0.0, P1b/4*3), ), ((P1h/2, 0.0, P1b/2), ), )), thickness=ON, tieRotations=ON)
        Myassembly.translate(instanceList=('Part-3a-1', ), vector=((-P1h/2, h+(P2h/2), -(P1b/2))))

            #part 3b-1
        Mypart3b.PartitionFaceByDatumPlane(datumPlane=Mypart3b.datums[2], faces=Mypart3b.faces.findAt(((P1h/4, 0.0, P1b/4),  )))
        Myassembly.Instance(dependent=ON, name='Part-3b-1', part=Mypart3b)
        Mymodel.Tie(adjust=ON, master=Region(edges=Myassembly.instances['Part-1-1'].edges.findAt(((-(P1h/2), h-(P2h/2), P1b/4), ), (((P1h/2), h-(P2h/2), P1b/4), ), ((-(P1h/2), h-(P2h/2), -P1b/4), ), (((P1h/2), h-(P2h/2), -P1b/4), ), ((0.0, h-(P2h/2), 0.0), ), )), name='Tie_A_b', positionToleranceMethod=COMPUTED, slave=Region(edges=Myassembly.instances['Part-3b-1'].edges.findAt(((0.0, 0.0, P1b/4), ), ((P1h, 0.0, P1b/4), ), ((0.0, 0.0, P1b/4*3), ), ((P1h, 0.0, P1b/4*3), ), ((P1h/2, 0.0, P1b/2), ), )), thickness=ON, tieRotations=ON)
        Myassembly.translate(instanceList=('Part-3b-1', ), vector=(-P1h/2, (h-(P2h/2)), -(P1b/2)))

            #part 3a-2
        Myassembly.Instance(dependent=ON, name='Part-3a-2', part=Mypart3a)
        Mymodel.Tie(adjust=ON, master=Region(edges=Myassembly.instances['Part-1-2'].edges.findAt(((-(P1h/2)+b1, h+(P2h/2), P1b/4), ), (((P1h/2)+b1, h+(P2h/2), P1b/4), ), ((-(P1h/2)+b1, h+(P2h/2), -P1b/4), ), (((P1h/2)+b1, h+(P2h/2), -P1b/4), ), ((b1, h+(P2h/2), 0.0), ), )), name='Tie_B_a', positionToleranceMethod=COMPUTED, slave=Region(edges=Myassembly.instances['Part-3a-2'].edges.findAt(((0.0, 0.0, P1b/4), ), ((P1h, 0.0, P1b/4), ),((0.0, 0.0, P1b/4*3), ), ((P1h, 0.0, P1b/4*3), ), ((P1h/2, 0.0, P1b/2), ), )), thickness=ON, tieRotations=ON)
        Myassembly.translate(instanceList=('Part-3a-2', ), vector=(-P1h/2+b1, (h+(P2h/2)), -(P1b/2)))

            #part 3b-2
        Myassembly.Instance(dependent=ON, name='Part-3b-2', part=Mypart3b)
        Mymodel.Tie(adjust=ON, master=Region(edges=Myassembly.instances['Part-1-2'].edges.findAt(((-(P1h/2)+b1, h-(P2h/2), P1b/4), ), (((P1h/2)+b1, h-(P2h/2), P1b/4), ), ((-(P1h/2)+b1, h-(P2h/2), -P1b/4), ), (((P1h/2)+b1, h-(P2h/2), -P1b/4), ), ((b1, h-(P2h/2), 0.0), ), )), name='Tie_B_b', positionToleranceMethod=COMPUTED, slave=Region(edges=Myassembly.instances['Part-3b-2'].edges.findAt(((0.0, 0.0, P1b/4), ), ((P1h, 0.0, P1b/4), ),((0.0, 0.0, P1b/4*3), ), ((P1h, 0.0, P1b/4*3), ), ((P1h/2, 0.0, P1b/2), ), )), thickness=ON, tieRotations=ON)
        Myassembly.translate(instanceList=('Part-3b-2', ), vector=(-P1h/2+b1, (h-(P2h/2)), -(P1b/2)))

        if (joint ==1):
            #part 6-1
            Mypart6a.PartitionFaceByDatumPlane(datumPlane=Mypart6a.datums[2], faces=Mypart6a.faces.findAt(((P4h/4, 0.0, P4b/4), )))
            Myassembly.Instance(dependent=ON, name='Part-6a-1', part=Mypart6a)
            Mymodel.Tie(adjust=ON, master=Region(edges=Myassembly.instances['Part-4-1'].edges.findAt(((-(P4h/2)+b1+b2, h+(P5h/2), P4b/4), ), (((P4h/2)+b1+b2, h+(P5h/2), P4b/4), ), ((-(P4h/2)+b1+b2, h+(P5h/2), -P4b/4), ), (((P4h/2)+b1+b2, h+(P5h/2), -P4b/4), ), ((b1+b2, h+(P5h/2), 0.0), ), )), name='Tie_C_a', positionToleranceMethod=COMPUTED, slave=Region(edges=Myassembly.instances['Part-6a-1'].edges.findAt(((0.0, 0.0, P4b/4), ), ((P4h, 0.0, P4b/4), ), ((0.0, 0.0, P4b/4*3), ), ((P4h, 0.0, P4b/4*3), ), ((P4h/2, 0.0, P4b/2), ), )), thickness=ON, tieRotations=ON)
            Myassembly.translate(instanceList=('Part-6a-1', ), vector=(-P4h/2+b1+b2, (h+(P5h/2)), -(P4b/2)))

        elif (joint ==2):
            #part 6-1
            Mypart6a.PartitionFaceByDatumPlane(datumPlane=Mypart6a.datums[2], faces=Mypart6a.faces.findAt(((P4h/4, 0.0, P4b/4), )))
            Myassembly.Instance(dependent=ON, name='Part-6a-1', part=Mypart6a)
            Mymodel.Tie(adjust=ON, master=Region(edges=Myassembly.instances['Part-4-1'].edges.findAt(((-(P4h/2)+b1+b2, h+(P5h/2), P4b/4), ), (((P4h/2)+b1+b2, h+(P5h/2), P4b/4), ), ((-(P4h/2)+b1+b2, h+(P5h/2), -P4b/4), ), (((P4h/2)+b1+b2, h+(P5h/2), -P4b/4), ), ((b1+b2, h+(P5h/2), 0.0), ), )), name=
```

```
            'Tie_C_a', positionToleranceMethod=COMPUTED, slave=Region(edges=Myassembly.instances['Part-6a-1'
            ].edges.findAt(((0.0, 0.0, P4b/4), ), ((P4h, 0.0, P4b/4), ), ((0.0, 0.0, P4b/4*3), ), ((P4h, 0.0,
             P4b/4*3), ), ((P4h/2, 0.0, P4b/2), ), )), thickness=ON, tieRotations=ON)
301         Myassembly.translate(instanceList=('Part-6a-1', ), vector=(-P4h/2+b1+b2, (h+(P5h/2)), -(P4b/2)))
302         #part 6-2
303         Mypart6b.PartitionFaceByDatumPlane(datumPlane=Mypart6b.datums[2], faces=Mypart6b.faces.findAt(((
            P4h/4, 0.0, P4b/4), )))
304         Myassembly.Instance(dependent=ON, name='Part-6b-1', part=Mypart6b)
305         Mymodel.Tie(adjust=ON, master=Region(edges=Myassembly.instances['Part-4-1'].edges.findAt(((-(P4h/
            2)+b1+b2, h-(P5h/2), P4b/4), ), (((P4h/2)+b1+b2, h-(P5h/2), P4b/4), ), ((-(P4h/2)+b1+b2, h-(P5h/2
            ), -P4b/4), ), (((P4h/2)+b1+b2, h-(P5h/2), -P4b/4), ), ((b1+b2, h-(P5h/2), 0.0), ), )), name=
            'Tie_C_b', positionToleranceMethod=COMPUTED, slave=Region(edges=Myassembly.instances['Part-6b-1'
            ].edges.findAt(((0.0, 0.0, P4b/4), ), ((P4h, 0.0, P4b/4), ), ((0.0, 0.0, P4b/4*3), ), ((P4h, 0.0,
             P4b/4*3), ), ((P4h/2, 0.0, P4b/2), ), )), thickness=ON, tieRotations=ON)
306         Myassembly.translate(instanceList=('Part-6b-1', ), vector=(-P4h/2+b1+b2, (h-(P5h/2)), -(P4b/2)))

307
308
309     #interaction
310         #reference points
311     Myassembly.ReferencePoint(point=(0.0, h, 0.0))
312     Myassembly.ReferencePoint(point=(b1, h, 0.0))
313     Myassembly.ReferencePoint(point=(b1+b2, h, 0.0))
314         #part 1-1 with 2-1
315     Myassembly.translate(instanceList=('Part-2-1', ), vector=(0.0, 1000.0, 0.0))
316     Mymodel.Tie(adjust=ON, master=Region(faces=Myassembly.instances['Part-1-1'].faces.findAt(((P1h/2, h,
        P1b/4), ), ((P1h/2, h, -P1b/4), ), )), name='Constraint-7', positionToleranceMethod=COMPUTED, slave=
        Region(edges=Myassembly.instances['Part-2-1'].edges.findAt(((P1h/2, h+P2h/2+1000, P2b/4), ), ((P1h/2,
         h+P2h/2+1000, -P2b/4), ), ((P1h/2, h-P2h/2+1000, P2b/4), ), ((P1h/2, h-P2h/2+1000, -P2b/4), ), ((P1h
        /2, h+1000, 0.0), ), )), thickness=ON, tieRotations=ON)
317     Myassembly.translate(instanceList=('Part-2-1', ), vector=(0.0, -1000.0, 0.0))
318
319        #part 1-2 with 2-1
320     Myassembly.translate(instanceList=('Part-2-1', ), vector=(0.0, 1000.0, 0.0))
321     Mymodel.Tie(adjust=ON, master=Region(faces=Myassembly.instances['Part-1-2'].faces.findAt(((b1-P1h/2,
        h, P1b/4), ), ((b1-P1h/2, h, -P1b/4), ), )), name='Constraint-8', positionToleranceMethod=COMPUTED,
        slave=Region(edges=Myassembly.instances['Part-2-1'].edges.findAt(((b1-P1h/2, h-P2h/2+1000, -P1b/4),
        ), ((b1-P1h/2, h-P2h/2+1000, P1b/4), ), ((b1-P1h/2, h+1000, 0.0), ), ((b1-P1h/2, h+P2h/2+1000, P1b/4
        ), ), ((b1-P1h/2, h+P2h/2+1000, -P1b/4), ), )), thickness=ON, tieRotations=ON)
322     Myassembly.translate(instanceList=('Part-2-1', ), vector=(0.0, -1000.0, 0.0))
323
324         #part 1-2 with 5-1
325     Mypart5.PartitionEdgeByPoint(edge=Mypart5.edges.findAt((b1+P1h/2, h, 0.0), ), point=Mypart5.
        InterestingPoint(Mypart5.edges.findAt((b1+P1h/2, h, 0.0), ), MIDDLE))
326     Myassembly.translate(instanceList=('Part-5-1', ), vector=(0.0, 1000.0, 0.0))
327     Mymodel.Coupling(controlPoint=Region(vertices=Myassembly.instances['Part-5-1'].vertices.findAt(((b1+
        P1h/2, h+1000, 0.0), ))), couplingType=KINEMATIC, influenceRadius=WHOLE_SURFACE, localCsys=None, name
        ='Constraint-9', surface=Region(edges=Myassembly.instances['Part-5-1'].edges.findAt(((b1+P1h/2, h+P5h
        /2+1000, P5b/4), ), ((b1+P1h/2, h+P5h/2+1000, -P5b/4), ), ((b1+P1h/2, h-P5h/2+1000, P5b/4), ), ((b1+
        P1h/2, h-P5h/2+1000, -P5b/4), ), ((b1+P1h/2, h+P5h/4+1000, 0.0), ), ((b1+P1h/2, h-P5h/4+1000, 0.0),
        ), )), u1=ON, u2=ON, u3=ON, ur1=ON, ur2=ON, ur3=ON)
328     Mymodel.Tie(adjust=ON, master=Region(faces=Myassembly.instances['Part-1-2'].faces.findAt(((b1+P1h/2,
        h, P1b/4), ), ((b1+P1h/2, h, -P1b/4), ), )), name='Constraint-10', positionToleranceMethod=COMPUTED,
        slave=Region(vertices=Myassembly.instances['Part-5-1'].vertices.findAt(((b1+P1h/2, h+1000, 0.0), ))),
         thickness=ON, constraintRatio=10000.0, constraintRatioMethod=SPECIFIED, tieRotations=OFF)
329     Myassembly.translate(instanceList=('Part-5-1', ), vector=(0.0, -1000.0, 0.0))
330
331         #part 4-1 with 5-1
332     if (joint ==1):
333         Mypart5.PartitionEdgeByPoint(edge=Mypart5.edges.findAt((b1+b2-P4h/2, h, 0.0), ), point=Mypart5.
            InterestingPoint(Mypart5.edges.findAt((b1+b2-P4h/2, h, 0.0), ), MIDDLE))
334         Myassembly.translate(instanceList=('Part-5-1', ), vector=(0.0, 1000.0, 0.0))
335         Mymodel.Coupling(controlPoint=Region(vertices=Myassembly.instances['Part-5-1'].vertices.findAt(((
            b1+b2-P4h/2, h+1000, 0.0), ))), couplingType=KINEMATIC, influenceRadius=WHOLE_SURFACE, localCsys=
            None, name='Constraint-11', surface=Region(edges=Myassembly.instances['Part-5-1'].edges.findAt(((
            b1+b2-P4h/2, h+P5h/2+1000, P5b/4), ), ((b1+b2-P4h/2, h+P5h/2+1000, -P5b/4), ), ((b1+b2-P4h/2, h-
            P5h/2+1000, P5b/4), ), ((b1+b2-P4h/2, h-P5h/2+1000, -P5b/4), ), ((b1+b2-P4h/2, h+P5h/4+1000, 0.0
            ), ), ((b1+b2-P4h/2, h-P5h/4+1000, 0.0), ), )), u1=ON, u2=ON, u3=ON, ur1=ON, ur2=ON, ur3=ON)
336         Mymodel.Tie(adjust=ON, constraintRatio=10000.0, constraintRatioMethod=SPECIFIED, master=Region(
            faces=Myassembly.instances['Part-4-1'].faces.findAt(((b1+b2-P4h/2, h, P4b/4), ), ((b1+b2-P4h/2, h
            , -P4b/4), ), )), name='Constraint-12', positionToleranceMethod=COMPUTED, slave=Region(vertices=
            Myassembly.instances['Part-5-1'].vertices.findAt(((b1+b2-P4h/2, h+1000, 0.0), ))), thickness=ON,
            tieRotations=OFF)
337         Myassembly.translate(instanceList=('Part-5-1', ), vector=(0.0, -1000.0, 0.0))
338     elif (joint ==2):
339         Mymodel.Tie(adjust=ON, master=Region(faces=Myassembly.instances['Part-4-1'].faces.findAt(((b1+b2-
            P4h/2, h, P4b/4), ), ((b1+b2-P4h/2, h, -P4b/4), ), )), name='Constraint-11',
            positionToleranceMethod=COMPUTED, slave=Region(edges=Myassembly.instances['Part-5-1'].edges.
            findAt(((b1+b2-P4h/2, h+P5h/2, P5b/4), ), ((b1+b2-P4h/2, h+P5h/2, -P5b/4), ), ((b1+b2-P4h/2, h-
            P5h/2, P5b/4), ), ((b1+b2-P4h/2, h, 0.0), ),(( b1+b2-P4h/2, h-P5h/2, -P5b/4), ), )), thickness=ON
            , tieRotations=ON)
340
341     #coupling refference points
342     if (joint ==1):
343         Mymodel.Coupling(controlPoint=Region(referencePoints=(Myassembly.referencePoints[32], )),
            couplingType=KINEMATIC, influenceRadius=WHOLE_SURFACE, localCsys=None, name='Constraint-16',
```

```
            surface=Region(side1Faces=Myassembly.instances['Part-1-1'].faces.findAt(((P1h/4, h, 0.0), (0.0,
            0.0, 1.0)), ((-P1h/4, h, 0.0), (0.0, 0.0, 1.0)), ), u1=ON, u2=ON, u3=ON, ur1=ON, ur2=ON, ur3=ON)
344         Mymodel.Coupling(controlPoint=Region(referencePoints=(Myassembly.referencePoints[33], )),
            couplingType=KINEMATIC, influenceRadius=WHOLE_SURFACE, localCsys=None, name='Constraint-17',
            surface=Region(side1Faces=Myassembly.instances['Part-1-2'].faces.findAt(((b1+P1h/4, h, 0.0), (0.0
            , 0.0, 1.0)), ((b1-P1h/4, h, 0.0), (0.0, 0.0, 1.0)), ), u1=ON, u2=ON, u3=ON, ur1=ON, ur2=ON, ur3
            =ON)
345         Mymodel.Coupling(controlPoint=Region(referencePoints=(Myassembly.referencePoints[34], )),
            couplingType=KINEMATIC, influenceRadius=WHOLE_SURFACE, localCsys=None, name='Constraint-18',
            surface=Region(side1Faces=Myassembly.instances['Part-4-1'].faces.findAt(((b1+b2+P4h/4, h, 0.0), (
            0.0, 0.0, 1.0)), ((b1+b2-P4h/4, h, 0.0), (0.0, 0.0, 1.0)), ), u1=ON, u2=ON, u3=ON, ur1=ON, ur2=
            ON, ur3=ON)
346     elif (joint ==2):
347         Mymodel.Coupling(controlPoint=Region(referencePoints=(Myassembly.referencePoints[36], )),
            couplingType=KINEMATIC, influenceRadius=WHOLE_SURFACE, localCsys=None, name='Constraint-16',
            surface=Region(side1Faces=Myassembly.instances['Part-1-1'].faces.findAt(((P1h/4, h, 0.0), (0.0,
            0.0, 1.0)), ((-P1h/4, h, 0.0), (0.0, 0.0, 1.0)), ), u1=ON, u2=ON, u3=ON, ur1=ON, ur2=ON, ur3=ON)
348         Mymodel.Coupling(controlPoint=Region(referencePoints=(Myassembly.referencePoints[37], )),
            couplingType=KINEMATIC, influenceRadius=WHOLE_SURFACE, localCsys=None, name='Constraint-17',
            surface=Region(side1Faces=Myassembly.instances['Part-1-2'].faces.findAt(((b1+P1h/4, h, 0.0), (0.0
            , 0.0, 1.0)), ((b1-P1h/4, h, 0.0), (0.0, 0.0, 1.0)), ), u1=ON, u2=ON, u3=ON, ur1=ON, ur2=ON, ur3
            =ON)
349         Mymodel.Coupling(controlPoint=Region(referencePoints=(Myassembly.referencePoints[38], )),
            couplingType=KINEMATIC, influenceRadius=WHOLE_SURFACE, localCsys=None, name='Constraint-18',
            surface=Region(side1Faces=Myassembly.instances['Part-4-1'].faces.findAt(((b1+b2+P4h/4, h, 0.0), (
            0.0, 0.0, 1.0)), ((b1+b2-P4h/4, h, 0.0), (0.0, 0.0, 1.0)), ), u1=ON, u2=ON, u3=ON, ur1=ON, ur2=
            ON, ur3=ON)
350
351     #cross-sections
352         #part 1
353     Mymodel.HomogeneousShellSection(idealization=NO_IDEALIZATION, integrationRule=SIMPSON, material=
        'Steel', name='P1tf', numIntPts=5, poissonDefinition=DEFAULT, preIntegrate=OFF, temperature=GRADIENT,
         thickness=P1tf, thicknessField='', thicknessModulus=None, thicknessType=UNIFORM, useDensity=OFF)
354     Mymodel.HomogeneousShellSection(idealization=NO_IDEALIZATION, integrationRule=SIMPSON, material=
        'Steel', name='P1tw', numIntPts=5, poissonDefinition=DEFAULT, preIntegrate=OFF, temperature=GRADIENT,
         thickness=P1tw, thicknessField='', thicknessModulus=None, thicknessType=UNIFORM, useDensity=OFF)
355         #part 2
356     Mymodel.HomogeneousShellSection(idealization=NO_IDEALIZATION, integrationRule=SIMPSON, material=
        'Steel', name='P2tf', numIntPts=5, poissonDefinition=DEFAULT, preIntegrate=OFF, temperature=GRADIENT,
         thickness=P2tf, thicknessField='', thicknessModulus=None, thicknessType=UNIFORM, useDensity=OFF)
357     Mymodel.HomogeneousShellSection(idealization=NO_IDEALIZATION, integrationRule=SIMPSON, material=
        'Steel', name='P2tw', numIntPts=5, poissonDefinition=DEFAULT, preIntegrate=OFF, temperature=GRADIENT,
         thickness=P2tw, thicknessField='', thicknessModulus=None, thicknessType=UNIFORM, useDensity=OFF)
358         #part 4
359     Mymodel.HomogeneousShellSection(idealization=NO_IDEALIZATION, integrationRule=SIMPSON, material=
        'Steel leaning column', name='P4tf', numIntPts=5, poissonDefinition=DEFAULT, preIntegrate=OFF,
        temperature=GRADIENT, thickness=P4tf, thicknessField='', thicknessModulus=None, thicknessType=UNIFORM
        , useDensity=OFF)
360     Mymodel.HomogeneousShellSection(idealization=NO_IDEALIZATION, integrationRule=SIMPSON, material=
        'Steel leaning column', name='P4tw', numIntPts=5, poissonDefinition=DEFAULT, preIntegrate=OFF,
        temperature=GRADIENT, thickness=P4tw, thicknessField='', thicknessModulus=None, thicknessType=UNIFORM
        , useDensity=OFF)
361         #part 5
362     Mymodel.HomogeneousShellSection(idealization=NO_IDEALIZATION, integrationRule=SIMPSON, material=
        'Steel', name='P5tf', numIntPts=5, poissonDefinition=DEFAULT, preIntegrate=OFF, temperature=GRADIENT,
         thickness=P5tf, thicknessField='', thicknessModulus=None, thicknessType=UNIFORM, useDensity=OFF)
363     Mymodel.HomogeneousShellSection(idealization=NO_IDEALIZATION, integrationRule=SIMPSON, material=
        'Steel', name='P5tw', numIntPts=5, poissonDefinition=DEFAULT, preIntegrate=OFF, temperature=GRADIENT,
         thickness=P5tw, thicknessField='', thicknessModulus=None, thicknessType=UNIFORM, useDensity=OFF)
364
365     #section assignment
366         #part 1
367             #bottom flange
368     Mypart1.SectionAssignment(offset=0.0, offsetField='', offsetType=BOTTOM_SURFACE, region=Region(faces=
        Mypart1.faces.findAt(((P1h/2, h/4, -P1b/4), ), ((P1h/2, h, P1b/4), ), ((P1h/2, h, -P1b/4), ), ((P1h/2
        , h/4, P1b/4), ), )), sectionName='P1tf', thicknessAssignment=FROM_SECTION)
369             #top flange
370     Mypart1.SectionAssignment(offset=0.0, offsetField='', offsetType=TOP_SURFACE, region=Region(faces=
        Mypart1.faces.findAt(((-P1h/2, h/4, -P1b/4), ), ((-P1h/2, h, P1b/4), ), ((-P1h/2, h, -P1b/4), ), ((-
        P1h/2, h/4, P1b/4), ), )), sectionName='P1tf', thicknessAssignment=FROM_SECTION)
371             #web
372     Mypart1.SectionAssignment(offset=0.0, offsetField='', offsetType=MIDDLE_SURFACE, region=Region(faces=
        Mypart1.faces.findAt(((0.0, h/4, 0.0), ), ((0, h, 0.0), ), )), sectionName='P1tw',
        thicknessAssignment=FROM_SECTION)
373
374         #part 2
375             #bottom flange
376     Mypart2.SectionAssignment(offset=0.0, offsetField='', offsetType=BOTTOM_SURFACE, region=Region(faces=
        Mypart2.faces.findAt(((b1/2, h-(P2h/2), -P2b/4), ), ((b1/2, h-(P2h/2), P2b/4), ), )), sectionName=
        'P2tf', thicknessAssignment=FROM_SECTION)
377             #top flange
378     Mypart2.SectionAssignment(offset=0.0, offsetField='', offsetType=TOP_SURFACE, region=Region(faces=
        Mypart2.faces.findAt(((b1/2, h+(P2h/2), -P2b/4), ), ((b1/2, h+(P2h/2), P2b/4), ), )), sectionName=
        'P2tf', thicknessAssignment=FROM_SECTION)
379             #web
380     Mypart2.SectionAssignment(offset=0.0, offsetField='', offsetType=MIDDLE_SURFACE, region=Region(faces=
```

```
Mypart2.faces.findAt(((b1/2, h, 0.0), ))), sectionName='P2tw', thicknessAssignment=FROM_SECTION)

    #part 3a
Mypart3a.SectionAssignment(offset=0.0, offsetField='', offsetType=TOP_SURFACE, region=Region(faces=
Mypart3a.faces.getByBoundingBox(0.0, 0.0, 0.0, P1h, 0.0, P1b)), sectionName='P2tf',
thicknessAssignment=FROM_SECTION)
    #part 3b
Mypart3b.SectionAssignment(offset=0.0, offsetField='', offsetType=BOTTOM_SURFACE, region=Region(faces
=Mypart3b.faces.getByBoundingBox(0.0, 0.0, 0.0, P1h, 0.0, P1b)), sectionName='P2tf',
thicknessAssignment=FROM_SECTION)

    #part 4
        #bottom flange
Mypart4.SectionAssignment(offset=0.0, offsetField='', offsetType=BOTTOM_SURFACE, region=Region(faces=
Mypart4.faces.findAt(((b1+b2-P4h/2, h/4, -P4b/4), ), ((b1+b2-P4h/2, h, P4b/4), ), ((b1+b2-P4h/2, h/4,
 P4b/4), ), ((b1+b2-P4h/2, h, -P4b/4), ), )), sectionName='P4tf', thicknessAssignment=FROM_SECTION)

        #top flange
Mypart4.SectionAssignment(offset=0.0, offsetField='', offsetType=TOP_SURFACE, region=Region(faces=
Mypart4.faces.findAt(((b1+b2+P4h/2, h/4, -P4b/4), ), ((b1+b2+P4h/2, h/4, P4b/4), ), ((b1+b2+P4h/2, h,
 P4b/4), ), ((b1+b2+P4h/2, h, -P4b/4), ), )), sectionName='P4tf', thicknessAssignment=FROM_SECTION)

        #web
Mypart4.SectionAssignment(offset=0.0, offsetField='', offsetType=MIDDLE_SURFACE, region=Region(faces=
Mypart4.faces.findAt(((b1+b2, h, 0.0), ), ((b1+b2, h/4, 0.0), ), )), sectionName='P4tw',
thicknessAssignment=FROM_SECTION)

    #part 5
        #bottom flange
Mypart5.SectionAssignment(offset=0.0, offsetField='', offsetType=BOTTOM_SURFACE, region=Region(faces=
Mypart5.faces.findAt(((b1+b2/2, h-P5h/2, P5b/4), ), ((b1+b2/2, h-P5h/2, -P5b/4), ), )), sectionName=
'P5tf', thicknessAssignment=FROM_SECTION)
        #top flange
Mypart5.SectionAssignment(offset=0.0, offsetField='', offsetType=TOP_SURFACE, region=Region(faces=
Mypart5.faces.findAt(((b1+b2/2, h+P5h/2, P5b/4), ), ((b1+b2/2, h+P5h/2, -P5b/4), ), )), sectionName=
'P5tf', thicknessAssignment=FROM_SECTION)
        #web
Mypart5.SectionAssignment(offset=0.0, offsetField='', offsetType=MIDDLE_SURFACE, region=Region(faces=
Mypart5.faces.findAt(((b1+b2/2, h, 0.0), ))), sectionName='P5tw', thicknessAssignment=FROM_SECTION)

if (joint==1):
    #part 6a
    Mypart6a.SectionAssignment(offset=0.0, offsetField='', offsetType=TOP_SURFACE, region=Region(
    faces=Mypart6a.faces.getByBoundingBox(0.0, 0.0, 0.0, P4h, 0.0, P4b)), sectionName='P5tf',
    thicknessAssignment=FROM_SECTION)
elif (joint ==2):
    #part 6a
    Mypart6a.SectionAssignment(offset=0.0, offsetField='', offsetType=TOP_SURFACE, region=Region(
    faces=Mypart6a.faces.getByBoundingBox(0.0, 0.0, 0.0, P4h, 0.0, P4b)), sectionName='P5tf',
    thicknessAssignment=FROM_SECTION)
    #part 6b
    Mypart6b.SectionAssignment(offset=0.0, offsetField='', offsetType=BOTTOM_SURFACE, region=Region(
    faces=Mypart6b.faces.getByBoundingBox(0.0, 0.0, 0.0, P4h, 0.0, P4b)), sectionName='P5tf',
    thicknessAssignment=FROM_SECTION)

#material
Mymodel.Material(name='Steel')
Mymodel.materials['Steel'].Elastic(table=((E, pois), ))
Mymodel.materials['Steel'].Plastic(table=((fy, 0.0), (fu, strain)))
Mymodel.Material(name='Steel leaning column')
Mymodel.materials['Steel leaning column'].Elastic(table=(((Q/F)*E, pois), ))
Mymodel.materials['Steel leaning column'].Plastic(table=(((Q/F)*fy, 0.0), ((Q/F)*fu, strain)))

#geometry partition adjustment
        #part 1
Mypart1.PartitionEdgeByPoint(edge=Mypart1.edges.findAt((0.0, 0.0, 0.0), ), point=Mypart1.
InterestingPoint(Mypart1.edges.findAt((0.0, 0.0, 0.0), ), MIDDLE))

        #part 4
Mypart4.PartitionEdgeByPoint(edge=Mypart4.edges.findAt((b1+b2, 0.0, 0.0), ), point=Mypart4.
InterestingPoint(Mypart4.edges.findAt((b1+b2, 0.0, 0.0), ), MIDDLE))

#sets
        #set 1
if (joint ==1):
    Myassembly.Set(name='top_nodes', referencePoints=(Myassembly.referencePoints[32], Myassembly.
    referencePoints[33], Myassembly.referencePoints[34]))
elif (joint==2):
    Myassembly.Set(name='top_nodes', referencePoints=(Myassembly.referencePoints[36], Myassembly.
    referencePoints[37], Myassembly.referencePoints[38]))
        #set 2
Myassembly.Set(name='bottom_nodes', vertices=Myassembly.instances['Part-1-1'].vertices.findAt(((0.0,
0.0, 0.0), ), )+Myassembly.instances['Part-1-2'].vertices.findAt(((b1, 0.0, 0.0), ), )+Myassembly.
instances['Part-4-1'].vertices.findAt(((b1+b2, 0.0, 0.0), ), ))

#interactions and couplings
```

```
            #coupling column A
        Mymodel.Coupling(controlPoint=Region(vertices=Myassembly.instances['Part-1-1'].vertices.findAt(((0.0,
         0.0, 0.0), ))), couplingType=KINEMATIC, influenceRadius=WHOLE_SURFACE, localCsys=None, name=
        'Constraint-13', surface=Region(edges=Myassembly.instances['Part-1-1'].edges.findAt(((-P1h/2, 0.0, -
        P1b/4), ), ((P1h/2, 0.0, -P1b/4), ), ((P1h/2, 0.0, P1b/4), ), ((-P1h/2, 0.0, P1b/4), ), ((-P1h/4, 0.0
        , 0.0), ), ((P1h/4, 0.0, 0.0), ), )), u1=ON, u2=ON, u3=ON, ur1=ON, ur2=ON, ur3=ON)
            #coupling column B
        Mymodel.Coupling(controlPoint=Region(vertices=Myassembly.instances['Part-1-2'].vertices.findAt(((b1,
        0.0, 0.0), ))), couplingType=KINEMATIC, influenceRadius=WHOLE_SURFACE, localCsys=None, name=
        'Constraint-14', surface=Region(edges=Myassembly.instances['Part-1-2'].edges.findAt(((b1-P1h/2, 0.0,
        -P1b/4), ), ((b1+P1h/2, 0.0, -P1b/4), ), ((b1+P1h/2, 0.0, P1b/4), ), ((b1-P1h/2, 0.0, P1b/4), ), ((b1
        -P1h/4, 0.0, 0.0), ), ((b1+P1h/4, 0.0, 0.0), ), )), u1=ON, u2=ON, u3=ON, ur1=ON, ur2=ON, ur3=ON)
            #coupling column C
        Mymodel.Coupling(controlPoint=Region(vertices=Myassembly.instances['Part-4-1'].vertices.findAt(((b1+
        b2, 0.0, 0.0), ))), couplingType=KINEMATIC, influenceRadius=WHOLE_SURFACE, localCsys=None, name=
        'Constraint-15', surface=Region(edges=Myassembly.instances['Part-4-1'].edges.findAt(((b1+b2-P4h/2,
        0.0, -P4b/4), ), ((b1+b2+P4h/2, 0.0, -P4b/4), ), ((b1+b2+P4h/2, 0.0, P4b/4), ), ((b1+b2-P4h/2, 0.0,
        P4b/4), ), ((b1+b2-P4h/4, 0.0, 0.0), ), ((b1+b2+P4h/4, 0.0, 0.0), ), )), u1=ON, u2=ON, u3=ON, ur1=ON,
         ur2=ON, ur3=ON)

        #boundary condition
            #stabilizing frame
        if (condition == 1):
            Mymodel.PinnedBC(createStepName='Initial', localCsys=None, name='BC-1', region=Region(vertices=
            Myassembly.instances['Part-1-1'].vertices.findAt(((0.0, 0.0, 0.0), ), )+Myassembly.instances[
            'Part-1-2'].vertices.findAt(((b1, 0.0, 0.0), ), )))
        elif (condition ==2):
            Mymodel.EncastreBC(createStepName='Initial', localCsys=None, name='BC-1', region=Region(vertices=
            Myassembly.instances['Part-1-1'].vertices.findAt(((0.0, 0.0, 0.0), ), )+Myassembly.instances[
            'Part-1-2'].vertices.findAt(((b1, 0.0, 0.0), ), )))
            #leaning column
        Mymodel.PinnedBC(createStepName='Initial', localCsys=None, name='BC-2', region=Region(vertices=
        Myassembly.instances['Part-4-1'].vertices.findAt(((b1+b2, 0.0, 0.0), ))))
            #Z-direction
        Mymodel.DisplacementBC(amplitude=UNSET, createStepName='Initial', distributionType=UNIFORM, fieldName
        ='', localCsys=None, name='BC-3', region=Region(faces=Myassembly.instances['Part-1-1'].faces.findAt
        (((P1h/4, h, 0.0), (0.0, 0.0, 1.0)), ((-P1h/4, h, 0.0), (0.0, 0.0, 1.0)), ((0.0, h/4, 0.0), (0.0, 0.0
        , 1.0)), )+Myassembly.instances['Part-2-1'].faces.findAt(((b1/2, h, 0.0), (0.0, 0.0, 1.0)), )+
        Myassembly.instances['Part-1-2'].faces.findAt(((b1+P1h/4, h, 0.0), (0.0, 0.0, 1.0)), ((b1-P1h/4, h,
        0.0), (0.0, 0.0, 1.0)), ((b1, h/4, 0.0), (0.0, 0.0, 1.0)), )+Myassembly.instances['Part-5-1'].faces.
        findAt(((b1+b2/2, h, 0.0), (0.0, 0.0, 1.0)), )+Myassembly.instances['Part-4-1'].faces.findAt(((b1+b2+
        P4h/4, h, 0.0), (0.0, 0.0, 1.0)), ((b1+b2-P4h/4, h, 0.0), (0.0, 0.0, 1.0)), ((b1+b2, h/4, 0.0), (0.0,
         0.0, 1.0)), )), u1=UNSET, u2=UNSET, u3=SET, ur1=UNSET, ur2=UNSET, ur3=UNSET)

        #loads
        if (H ==0):
            Mymodel.StaticRiksStep(initialArcInc=0.1, maxNumInc=200, maxArcInc=22, minArcInc=1e-20, name=
            'Step-1', nlgeom=ON, previous='Initial', totalArcLength=20.0)

                #vertical load
            if (joint ==1):
                Mymodel.ConcentratedForce(cf2=-F, createStepName='Step-1', distributionType=UNIFORM, field=''
                , localCsys=None, name='VERT_F', region=Region(referencePoints=(Myassembly.referencePoints[32
                ], Myassembly.referencePoints[33], )))
                Mymodel.ConcentratedForce(cf2=-Q, createStepName='Step-1', distributionType=UNIFORM, field=''
                , localCsys=None, name='VERT_Q', region=Region(referencePoints=(Myassembly.referencePoints[34
                ], )))
            elif (joint==2):
                Mymodel.ConcentratedForce(cf2=-F, createStepName='Step-1', distributionType=UNIFORM, field=''
                , localCsys=None, name='VERT_F', region=Region(referencePoints=(Myassembly.referencePoints[36
                ], Myassembly.referencePoints[37], )))
                Mymodel.ConcentratedForce(cf2=-Q, createStepName='Step-1', distributionType=UNIFORM, field=''
                , localCsys=None, name='VERT_Q', region=Region(referencePoints=(Myassembly.referencePoints[38
                ], )))

        else:
            Mymodel.StaticStep(name='Step-1', previous='Initial')
            Mymodel.steps['Step-1'].setValues(nlgeom=ON)
            Mymodel.steps['Step-1'].setValues(minInc=1e-12)
            Mymodel.StaticRiksStep(initialArcInc=0.1, maxNumInc=200, maxArcInc=22, minArcInc=1e-20, name=
            'Step-2', nlgeom=ON, previous='Step-1', totalArcLength=20.0)
                #horizontal load
            Mymodel.ConcentratedForce(cf1=-H, createStepName='Step-1', distributionType=UNIFORM, field='',
            localCsys=None, name='HOR_H', region=Region(referencePoints=(Myassembly.referencePoints[34], )))
                #vertical load
            if (joint ==1):
                Mymodel.ConcentratedForce(cf2=-F, createStepName='Step-2', distributionType=UNIFORM, field=''
                , localCsys=None, name='VERT_F', region=Region(referencePoints=(Myassembly.referencePoints[32
                ], Myassembly.referencePoints[33], )))
                Mymodel.ConcentratedForce(cf2=-Q, createStepName='Step-2', distributionType=UNIFORM, field=''
                , localCsys=None, name='VERT_Q', region=Region(referencePoints=(Myassembly.referencePoints[34
                ], )))
            elif (joint==2):
                Mymodel.ConcentratedForce(cf2=-F, createStepName='Step-2', distributionType=UNIFORM, field=''
                , localCsys=None, name='VERT_F', region=Region(referencePoints=(Myassembly.referencePoints[36
                ], Myassembly.referencePoints[37], )))
```

```
                Mymodel.ConcentratedForce(cf2=-Q, createStepName='Step-2', distributionType=UNIFORM, field=''
                , localCsys=None, name='VERT_Q', region=Region(referencePoints=(Myassembly.referencePoints[38
                ], )))

        #mesh
            #part 1
                #y-direction
                    #top
            Mypart1.seedEdgeBySize(constraint=FINER, deviationFactor=0.1, edges=Mypart1.edges.findAt(((-P1h/2, h,
             0.0), ), ((-P1h/2, h, P1b/2), ), ((P1h/2, h, 0.0), ), ((-P1h/2, h, -P1b/2), ), ((P1h/2, h, P1b/2),
            ), ((P1h/2, h, -P1b/2), ), ), size=P2sy)
                    #bottom
            Mypart1.seedEdgeBySize(constraint=FINER, deviationFactor=0.1, edges=Mypart1.edges.findAt(((-P1h/2, h/
            4, 0.0), ), ((-P1h/2, h/4, -P1b/2), ), ((P1h/2, h/4, 0.0), ), ((P1h/2, h/4, -P1b/2), ), ((P1h/2, h/4,
             P1b/2), ), ((-P1h/2, h/4, P1b/2), ), ), size=P1sy)
                #x-direction
            Mypart1.seedEdgeBySize(constraint=FINER, deviationFactor=0.1, edges=Mypart1.edges.findAt(((-P1h/4, h-
            P2h/2, 0.0), ), ((P1h/4, h+P2h/2, 0.0), ), ((-P1h/4, 0.0, 0.0), ), ((P1h/4, 0.0, 0.0), ), ), size=
            P1sx)
                #z-direction
            Mypart1.seedEdgeBySize(constraint=FINER, deviationFactor=0.1, edges=Mypart1.edges.findAt(((-P1h/2, h-
            P2h/2, -P1b/4), ), ((-P1h/2, 0.0, -P1b/4), ), ((-P1h/2, h-P2h/2, P1b/4), ), ((-P1h/2, h+P2h/2, P1b/4
            ), ), ((P1h/2, h-P2h/2, -P1b/4), ), ((P1h/2, 0.0, -P1b/4), ), ((P1h/2, h-P2h/2, P1b/4), ), ((P1h/2,
            0.0, P1b/4), ), ((-P1h/2, 0.0, P1b/4), ), ((-P1h/2, h+P2h/2, -P1b/4), ), ((P1h/2, h+P2h/2, P1b/4), ),
             ((P1h/2, h+P2h/2, -P1b/4), ), ), size=P1sz)
                #mesh settings
            Mypart1.setMeshControls(elemShape=QUAD_DOMINATED, regions=Mypart1.faces.getByBoundingBox(-P1h/2, 0.0,
             -P1b/2, P1h/2, h+P2h/2, P1b/2), technique=FREE)
            Mypart1.setElementType(elemTypes=(ElemType(elemCode=S4, elemLibrary=STANDARD, secondOrderAccuracy=OFF
            ), ElemType(elemCode=S3, elemLibrary=STANDARD)), regions=(Mypart1.faces.getByBoundingBox(-P1h/2, 0.0,
             -P1b/2, P1h/2, h+P2h/2, P1b/2), ))
            Mypart1.generateMesh()
                #part 2
                    #y-direction
            Mypart2.seedEdgeBySize(constraint=FINER, deviationFactor=0.1, edges=Mypart2.edges.findAt(((b1-P1h/2,
            h, 0.0), ), ((P1h/2, h, 0.0), ), ), size=P2sy)
                    #x-direction
            Mypart2.seedEdgeBySize(constraint=FINER, deviationFactor=0.1, edges=Mypart2.edges.findAt(((b1/4, h+
            P2h/2, 0.0), ), ((b1/4, h+P2h/2, P2b/2), ), ((b1/4, h+P2h/2, -P2b/2), ), ((b1/4, h-P2h/2, 0.0), ), ((
            b1/4, h-P2h/2, P2b/2), ), ((b1/4, h-P2h/2, -P2b/2), ), ), size=P2sx)
                    #z-direction
            Mypart2.seedEdgeBySize(constraint=FINER, deviationFactor=0.1, edges=Mypart2.edges.findAt(((b1-P1h/2,
            h+P2h/2, P2b/4), ), ((P1h/2, h+P2h/2, P2b/4), ), ((P1h/2, h+P2h/2, -P2b/4), ), ((b1-P1h/2, h+P2h/2, -
            P2b/4), ), ((b1-P1h/2, h-P2h/2, P2b/4), ), ((P1h/2, h-P2h/2, P2b/4), ), ((P1h/2, h-P2h/2, -P2b/4), ),
             ((b1-P1h/2, h-P2h/2, -P2b/4), ), ((b1-P1h/2, h+P2h/2, P2b/8), ), ((P1h/2, h+P2h/2, P2b/8), ), ((P1h/
            2, h+P2h/2, -P2b/8), ), ((b1-P1h/2, h+P2h/2, -P2b/8), ), ((b1-P1h/2, h-P2h/2, P2b/8), ), ((P1h/2, h-
            P2h/2, P2b/8), ), ((P1h/2, h-P2h/2, -P2b/8), ), ((b1-P1h/2, h-P2h/2, -P2b/8), ), ), size=P2sz)
                    #mesh settings
            Mypart2.setMeshControls(elemShape=QUAD_DOMINATED, regions=Mypart2.faces.getByBoundingBox(P1h/2, h-P2h
            /2, -P2b/2, b1-P1h/2, h+P2h/2, P2b/2), technique=FREE)
            Mypart2.setElementType(elemTypes=(ElemType(elemCode=S4, elemLibrary=STANDARD, secondOrderAccuracy=OFF
            ), ElemType(elemCode=S3, elemLibrary=STANDARD)), regions=(Mypart2.faces.getByBoundingBox(P1h/2, h-P2h
            /2, -P2b/2, b1-P1h/2, h+P2h/2, P2b/2), ))
            Mypart2.generateMesh()

                #part 3a
                    #y-direction

                    #x-direction
            Mypart3a.seedEdgeBySize(constraint=FINER, deviationFactor=0.1, edges=Mypart3a.edges.findAt(((P1h/4,
            0.0, P1b), ), ((P1h/4, 0.0, 0.0), ), ((P1h/4, 0.0, P1b/2), ), ), minSizeFactor=0.1, size=P3sx)
                    #z-direction
            Mypart3a.seedEdgeBySize(constraint=FINER, deviationFactor=0.1, edges=Mypart3a.edges.findAt(((0.0, 0.0
            , P1b/4), ), ((0.0, 0.0, P1b/4*3), ), ((P1h, 0.0, P1b/4), ), ((P1h, 0.0, P1b/4*3), ), ),
            minSizeFactor=0.1, size=P3sz)
                    #mesh settings
            Mypart3a.setMeshControls(elemShape=QUAD_DOMINATED, regions=Mypart3a.faces.getByBoundingBox(0.0, 0.0,
            0.0, P1h, 0.0, P1b), technique=FREE)
            Mypart3a.setElementType(elemTypes=(ElemType(elemCode=S4, elemLibrary=STANDARD, secondOrderAccuracy=
            OFF), ElemType(elemCode=S3, elemLibrary=STANDARD)), regions=(Mypart3a.faces.getByBoundingBox(0.0, 0.0
            , 0.0, P1h, 0.0, P1b), ))
            Mypart3a.generateMesh()

                #part 3b
                    #y-direction

                    #x-direction
            Mypart3b.seedEdgeBySize(constraint=FINER, deviationFactor=0.1, edges=Mypart3b.edges.findAt(((P1h/4,
            0.0, P1b), ), ((P1h/4, 0.0, 0.0), ), ((P1h/4, 0.0, P1b/2), ), ), minSizeFactor=0.1, size=P3sx)
                    #z-direction
            Mypart3b.seedEdgeBySize(constraint=FINER, deviationFactor=0.1, edges=Mypart3b.edges.findAt(((0.0, 0.0
            , P1b/4), ), ((0.0, 0.0, P1b/4*3), ), ((P1h, 0.0, P1b/4), ), ((P1h, 0.0, P1b/4*3), ), ),
            minSizeFactor=0.1, size=P3sz)
                    #mesh settings
            Mypart3b.setMeshControls(elemShape=QUAD_DOMINATED, regions=Mypart3b.faces.getByBoundingBox(0.0, 0.0,
            0.0, P1h, 0.0, P1b), technique=FREE)
```

```
530         Mypart3b.setElementType(elemTypes=(ElemType(elemCode=S4, elemLibrary=STANDARD, secondOrderAccuracy=
            OFF), ElemType(elemCode=S3, elemLibrary=STANDARD)), regions=(Mypart3b.faces.getByBoundingBox(0.0, 0.0
            , 0.0, P1h, 0.0, P1b), ))
531         Mypart3b.generateMesh()
532
533             #part 4
534                 #y-direction
535                     #top
536         Mypart4.seedEdgeBySize(constraint=FINER, deviationFactor=0.1, edges=Mypart4.edges.findAt(((b1+b2-P4h/
            2, h, 0.0), ), ((b1+b2-P4h/2, h, P4b/2), ), ((b1+b2+P4h/2, h, 0.0), ), ((b1+b2-P4h/2, h, -P4b/2), ),
            ((b1+b2+P4h/2, h, P4b/2), ), ((b1+b2+P4h/2, h, -P4b/2), ), ),size=P5sy)
537                     #bottom
538         Mypart4.seedEdgeBySize(constraint=FINER, deviationFactor=0.1, edges=Mypart4.edges.findAt(((b1+b2-P4h/
            2, h/4, 0.0), ), ((b1+b2-P4h/2, h/4, -P4b/2), ), ((b1+b2+P4h/2, h/4, 0.0), ), ((b1+b2+P4h/2, h/4, -
            P4b/2), ), ((b1+b2+P4h/2, h/4, P4b/2), ), ((b1+b2-P4h/2, h/4, P4b/2), ), ),size=P4sy)
539                 #x-direction
540         Mypart4.seedEdgeBySize(constraint=FINER, deviationFactor=0.1, edges=Mypart4.edges.findAt(((b1+b2-P4h/
            4, h-P5h/2, 0.0), ), ((b1+b2+P4h/4, h+P5h/2, 0.0), ), ((b1+b2-P4h/4, 0.0, 0.0), ), ((b1+b2+P4h/4, 0.0
            , 0.0), ), ), size=P4sx)
541                 #z-direction
542         Mypart4.seedEdgeBySize(constraint=FINER, deviationFactor=0.1, edges=Mypart4.edges.findAt(((b1+b2-P4h/
            2, h-P5h/2, -P4b/4), ), ((b1+b2-P4h/2, 0.0, -P4b/4), ), ((b1+b2-P4h/2, h-P5h/2, P4b/4), ), ((b1+b2-
            P4h/2, h+P5h/2, P4b/4), ), ((b1+b2+P4h/2, h-P5h/2, -P4b/4), ), ((b1+b2+P4h/2, 0.0, -P4b/4), ), ((b1+
            b2+P4h/2, h-P5h/2, P4b/4), ), ((b1+b2+P4h/2, 0.0, P4b/4), ), ((b1+b2-P4h/2, 0.0, P4b/4), ), ((b1+b2-
            P4h/2, h+P5h/2, -P4b/4), ), ((b1+b2+P4h/2, h+P5h/2, P4b/4), ), ((b1+b2+P4h/2, h+P5h/2, -P4b/4), ), ),
             size=P4sz)
543                 #mesh settings
544         Mypart4.setMeshControls(elemShape=QUAD_DOMINATED, regions=Mypart4.faces.getByBoundingBox(b1+b2-P4h/2,
             0.0, -P4b/2, b1+b2+P4h/2, h+P5h/2, P4b/2), technique=FREE)
545         Mypart4.setElementType(elemTypes=(ElemType(elemCode=S4, elemLibrary=STANDARD, secondOrderAccuracy=OFF
            ), ElemType(elemCode=S3, elemLibrary=STANDARD)), regions=(Mypart4.faces.getByBoundingBox(b1+b2-P4h/2,
             0.0, -P4b/2, b1+b2+P4h/2, h+P5h/2, P4b/2), ))
546         Mypart4.generateMesh()
547
548             #part 5
549         if (joint ==1):
550                 #y-direction
551             Mypart5.seedEdgeBySize(constraint=FINER, deviationFactor=0.1, edges=Mypart5.edges.findAt(((b1+b2-
                P4h/2, h+P5h/4, 0.0), ),((b1+b2-P4h/2, h-P5h/4, 0.0), ), ((b1+P1h/2, h+P5h/4, 0.0), ), ((b1+P1h/2
                , h-P5h/4, 0.0), ), ), size=P5sy)
552                 #x-direction
553             Mypart5.seedEdgeBySize(constraint=FINER, deviationFactor=0.1, edges=Mypart5.edges.findAt(((b1+b2/
                4, h+P5h/2, 0.0), ), ((b1+b2/4, h+P5h/2, P5b/2), ), ((b1+b2/4, h+P5h/2, -P5b/2), ), ((b1+b2/4, h-
                P5h/2, 0.0), ), ((b1+b2/4, h-P5h/2, P5b/2), ), ((b1+b2/4, h-P5h/2, -P5b/2), ), ), size=P5sx)
554                 #z-direction
555             Mypart5.seedEdgeBySize(constraint=FINER, deviationFactor=0.1, edges=Mypart5.edges.findAt(((b1+b2-
                P4h/2, h+P5h/2, P5b/4), ), ((b1+P1h/2, h+P5h/2, P5b/4), ), ((b1+P1h/2, h+P5h/2, -P5b/4), ), ((b1+
                b2-P4h/2, h+P5h/2, -P5b/4), ), ((b1+b2-P4h/2, h-P5h/2, P5b/4), ), ((b1+P1h/2, h-P5h/2, P5b/4), ),
                 ((b1+P1h/2, h-P5h/2, -P5b/4), ), ((b1+b2-P4h/2, h-P5h/2, -P5b/4), ), ((b1+b2-P4h/2, h+P5h/2, P5b
                /8), ), ((b1+P1h/2, h+P5h/2, P5b/8), ), ((b1+P1h/2, h+P5h/2, -P5b/8), ), ((b1+b2-P4h/2, h+P5h/2,
                -P5b/8), ), ((b1+b2-P4h/2, h-P5h/2, P5b/8), ), ((b1+P1h/2, h-P5h/2, P5b/8), ), ((b1+P1h/2, h-P5h/
                2, -P5b/8), ), ((b1+b2-P4h/2, h-P5h/2, -P5b/8), ), ), size=P5sz)
556                 #mesh settings
557             Mypart5.setMeshControls(elemShape=QUAD_DOMINATED, regions=Mypart5.faces.getByBoundingBox(b1+P1h/2
                , h-P5h/2, -P5b/2, b1+b2-P4h/2, h+P5h/2, P5b/2), technique=FREE)
558             Mypart5.setElementType(elemTypes=(ElemType(elemCode=S4, elemLibrary=STANDARD, secondOrderAccuracy
                =OFF), ElemType(elemCode=S3, elemLibrary=STANDARD)), regions=(Mypart5.faces.getByBoundingBox(b1+
                P1h/2, h-P5h/2, -P5b/2, b1+b2-P4h/2, h+P5h/2, P5b/2), ))
559             Mypart5.generateMesh()
560
561         if (joint ==2):
562                 #y-direction
563             Mypart5.seedEdgeBySize(constraint=FINER, deviationFactor=0.1, edges=Mypart5.edges.findAt(((b1+b2-
                P4h/2, h, 0.0), ), ((b1+P1h/2, h+P5h/4, 0.0), ), ((b1+P1h/2, h-P5h/4, 0.0), ), ), size=P5sy)
564                 #x-direction
565             Mypart5.seedEdgeBySize(constraint=FINER, deviationFactor=0.1, edges=Mypart5.edges.findAt(((b1+b2/
                4, h+P5h/2, 0.0), ), ((b1+b2/4, h+P5h/2, P5b/2), ), ((b1+b2/4, h+P5h/2, -P5b/2), ), ((b1+b2/4, h-
                P5h/2, 0.0), ), ((b1+b2/4, h-P5h/2, P5b/2), ), ((b1+b2/4, h-P5h/2, -P5b/2), ), ), size=P5sx)
566                 #z-direction
567             Mypart5.seedEdgeBySize(constraint=FINER, deviationFactor=0.1, edges=Mypart5.edges.findAt(((b1+b2-
                P4h/2, h+P5h/2, P5b/4), ), ((b1+P1h/2, h+P5h/2, P5b/4), ), ((b1+P1h/2, h+P5h/2, -P5b/4), ), ((b1+
                b2-P4h/2, h+P5h/2, -P5b/4), ), ((b1+b2-P4h/2, h-P5h/2, P5b/4), ), ((b1+P1h/2, h-P5h/2, P5b/4), ),
                 ((b1+P1h/2, h-P5h/2, -P5b/4), ), ((b1+b2-P4h/2, h-P5h/2, -P5b/4), ), ((b1+b2-P4h/2, h+P5h/2, P5b
                /8), ), ((b1+P1h/2, h+P5h/2, P5b/8), ), ((b1+P1h/2, h+P5h/2, -P5b/8), ), ((b1+b2-P4h/2, h+P5h/2,
                -P5b/8), ), ((b1+b2-P4h/2, h-P5h/2, P5b/8), ), ((b1+P1h/2, h-P5h/2, P5b/8), ), ((b1+P1h/2, h-P5h/
                2, -P5b/8), ), ((b1+b2-P4h/2, h-P5h/2, -P5b/8), ), ), size=P5sz)
568                 #mesh settings
569             Mypart5.setMeshControls(elemShape=QUAD_DOMINATED, regions=Mypart5.faces.getByBoundingBox(b1+P1h/2
                , h-P5h/2, -P5b/2, b1+b2-P4h/2, h+P5h/2, P5b/2), technique=FREE)
570             Mypart5.setElementType(elemTypes=(ElemType(elemCode=S4, elemLibrary=STANDARD, secondOrderAccuracy
                =OFF), ElemType(elemCode=S3, elemLibrary=STANDARD)), regions=(Mypart5.faces.getByBoundingBox(b1+
                P1h/2, h-P5h/2, -P5b/2, b1+b2-P4h/2, h+P5h/2, P5b/2), ))
571             Mypart5.generateMesh()
572
573
574         if (joint ==1):
```

```
575             #part 6a
576                     #y-direction
577
578                     #x-direction
579             Mypart6a.seedEdgeBySize(constraint=FINER, deviationFactor=0.1, edges=Mypart6a.edges.findAt(((P4h/
                4, 0.0, P4b), ), ((P4h/4, 0.0, 0.0), ), ((P4h/4, 0.0, P4b/2), ), ), size=P6sx)
580                     #z-direction
581             Mypart6a.seedEdgeBySize(constraint=FINER, deviationFactor=0.1, edges=Mypart6a.edges.findAt(((0.0,
                 0.0, P4b/4), ), ((0.0, 0.0, P4b/4*3), ), ((P4h, 0.0, P4b/4), ), ((P4h, 0.0, P4b/4*3), ), ), size
                =P6sz)
582                     #mesh settings
583             Mypart6a.setMeshControls(elemShape=QUAD_DOMINATED, regions=Mypart6a.faces.getByBoundingBox(0.0,
                0.0, 0.0, P4h, 0.0, P4b), technique=FREE)
584             Mypart6a.setElementType(elemTypes=(ElemType(elemCode=S4, elemLibrary=STANDARD,
                secondOrderAccuracy=OFF), ElemType(elemCode=S3, elemLibrary=STANDARD)), regions=(Mypart6a.faces.
                getByBoundingBox(0.0, 0.0, 0.0, P4h, 0.0, P4b), ))
585             Mypart6a.generateMesh()
586         elif (joint ==2):
587             #part 6a
588                     #y-direction
589
590                     #x-direction
591             Mypart6a.seedEdgeBySize(constraint=FINER, deviationFactor=0.1, edges=Mypart6a.edges.findAt(((P4h/
                4, 0.0, P4b), ), ((P4h/4, 0.0, 0.0), ), ((P4h/4, 0.0, P4b/2), ), ), size=P6sx)
592                     #z-direction
593             Mypart6a.seedEdgeBySize(constraint=FINER, deviationFactor=0.1, edges=Mypart6a.edges.findAt(((0.0,
                 0.0, P4b/4), ), ((0.0, 0.0, P4b/4*3), ), ((P4h, 0.0, P4b/4), ), ((P4h, 0.0, P4b/4*3), ), ), size
                =P6sz)
594                     #mesh settings
595             Mypart6a.setMeshControls(elemShape=QUAD_DOMINATED, regions=Mypart6a.faces.getByBoundingBox(0.0,
                0.0, 0.0, P4h, 0.0, P4b), technique=FREE)
596             Mypart6a.setElementType(elemTypes=(ElemType(elemCode=S4, elemLibrary=STANDARD,
                secondOrderAccuracy=OFF), ElemType(elemCode=S3, elemLibrary=STANDARD)), regions=(Mypart6a.faces.
                getByBoundingBox(0.0, 0.0, 0.0, P4h, 0.0, P4b), ))
597             Mypart6a.generateMesh()
598
599             #part 6b
600                     #y-direction
601
602                     #x-direction
603             Mypart6b.seedEdgeBySize(constraint=FINER, deviationFactor=0.1, edges=Mypart6b.edges.findAt(((P4h/
                4, 0.0, P4b), ), ((P4h/4, 0.0, 0.0), ), ((P4h/4, 0.0, P4b/2), ), ), size=P6sx)
604                     #z-direction
605             Mypart6b.seedEdgeBySize(constraint=FINER, deviationFactor=0.1, edges=Mypart6b.edges.findAt(((0.0,
                 0.0, P4b/4), ), ((0.0, 0.0, P4b/4*3), ), ((P4h, 0.0, P4b/4), ), ((P4h, 0.0, P4b/4*3), ), ), size
                =P6sz)
606                     #mesh settings
607             Mypart6b.setMeshControls(elemShape=QUAD_DOMINATED, regions=Mypart6b.faces.getByBoundingBox(0.0,
                0.0, 0.0, P4h, 0.0, P4b), technique=FREE)
608             Mypart6b.setElementType(elemTypes=(ElemType(elemCode=S4, elemLibrary=STANDARD,
                secondOrderAccuracy=OFF), ElemType(elemCode=S3, elemLibrary=STANDARD)), regions=(Mypart6b.faces.
                getByBoundingBox(0.0, 0.0, 0.0, P4h, 0.0, P4b), ))
609             Mypart6b.generateMesh()
610
611         #element set
612
613         ##############################################error##############################
614         Myassembly.Set(elements=Myassembly.instances['Part-1-1'].elements[0:348]+Myassembly.instances[
            'Part-2-1'].elements[0:312]+Myassembly.instances['Part-1-2'].elements[0:348]+Myassembly.instances[
            'Part-3a-1'].elements[0:16]+Myassembly.instances['Part-3b-1'].elements[0:16]+Myassembly.instances[
            'Part-3b-1'].elements[0:16]+Myassembly.instances['Part-3b-2'].elements[0:16],name='Set-11')
615         Myassembly.Set(elements=Myassembly.instances['Part-1-2'].elements[283:284], name='Set-11')
616         ##############################################error##############################
617
618         #node set
619         Myassembly.Set(name='LE', nodes=Myassembly.instances['Part-1-1'].nodes[337:338])
620             #flanges
621         for lnf in [1, 2, 3, 4, 5, 6]:
622         #lnf = 6
623             Myassembly.Set(elements=
624                 Myassembly.instances['Part-1-1'].elements.getByBoundingBox(-P1h/2, 0.0, -(lnf*P1sz)-1, -P1h/2
                    , h+P2h/2, -((lnf-1)*P1sz)+1)+Myassembly.instances['Part-1-1'].elements.getByBoundingBox(P1h/
                    2, 0.0, -(lnf*P1sz)-1, P1h/2, h+P2h/2, -((lnf-1)*P1sz)+1)+Myassembly.instances['Part-1-1'].
                    elements.getByBoundingBox(-P1h/2, 0.0, (lnf-1)*P1sz-1, -P1h/2, h+P2h/2, (lnf)*P1sz+1)+
                    Myassembly.instances['Part-1-1'].elements.getByBoundingBox(P1h/2, 0.0, (lnf-1)*P1sz-1, P1h/2,
                     h+P2h/2, lnf*P1sz+1)
625                 +Myassembly.instances['Part-1-2'].elements.getByBoundingBox(b1-P1h/2, 0.0, -(lnf*P1sz)-1, b1-
                    P1h/2, h+P2h/2, -(lnf-1)*P1sz+1)+Myassembly.instances['Part-1-2'].elements.getByBoundingBox(
                    b1+P1h/2, 0.0, -(lnf*P1sz)-1, b1+P1h/2, h+P2h/2, -(lnf-1)*P1sz+1)+Myassembly.instances[
                    'Part-1-2'].elements.getByBoundingBox(b1-P1h/2, 0.0, (lnf-1)*P1sz-1, b1-P1h/2, h+P2h/2, (lnf*
                    P1sz)+1)+Myassembly.instances['Part-1-2'].elements.getByBoundingBox(b1+P1h/2, 0.0, (lnf-1)*
                    P1sz-1, b1+P1h/2, h+P2h/2, (lnf*P1sz)+1)
626                 , name='stress_P1F_'+'{0}'.format(lnf))
627             Myassembly.Set(elements=
628                 Myassembly.instances['Part-2-1'].elements.getByBoundingBox(P1h/2, h+P2h/2, -lnf*P2sz-1, b1-
                    P1h/2, h+P2h/2, -(lnf-1)*P2sz+1)+Myassembly.instances['Part-2-1'].elements.getByBoundingBox(
```

```
                    P1h/2, h-P2h/2, (lnf-1)*P2sz-1, b1-P1h/2, h-P2h/2, lnf*P2sz+1)+Myassembly.instances[
                    'Part-2-1'].elements.getByBoundingBox(P1h/2, h-P2h/2, -lnf*P2sz-1, b1-P1h/2, h-P2h/2, -(lnf-1
                    )*P2sz+1)+Myassembly.instances['Part-2-1'].elements.getByBoundingBox(P1h/2, h+P2h/2, (lnf-1)*
                    P2sz-1, b1-P1h/2, h+P2h/2, lnf*P2sz+1)
629                 , name='stress_P2F_'+'{0}'.format(lnf))
630             Myassembly.Set(elements=
631                 Myassembly.instances['Part-4-1'].elements.getByBoundingBox(b1+b2-P4h/2, 0.0, -lnf*P4sz-1, b1+
                    b2-P4h/2, h+P5h/2, -(lnf-1)*P4sz+1)+Myassembly.instances['Part-4-1'].elements.
                    getByBoundingBox(b1+b2+P4h/2, 0.0, -lnf*P4sz-1, b1+b2+P4h/2, h+P5h/2, -(lnf-1)*P4sz+1)+
                    Myassembly.instances['Part-4-1'].elements.getByBoundingBox(b1+b2-P4h/2, 0.0, (lnf-1)*P4sz-1,
                    b1+b2-P4h/2, h+P5h/2, lnf*P4sz+1)+Myassembly.instances['Part-4-1'].elements.getByBoundingBox(
                    b1+b2+P4h/2, 0.0, (lnf-1)*P4sz-1, b1+b2+P4h/2, h+P5h/2, lnf*P4sz+1)
632                 , name='stress_P4F_'+'{0}'.format(lnf))
633             Myassembly.Set(elements=
634                 Myassembly.instances['Part-5-1'].elements.getByBoundingBox(b1+P1h/2, h+P5h/2, -lnf*P5sz-1, b1
                    +b2-P4h/2, h+P5h/2, -(lnf-1)*P5sz+1)+Myassembly.instances['Part-5-1'].elements.
                    getByBoundingBox(b1+P1h/2, h-P5h/2, (lnf-1)*P5sz-1, b1+b2-P4h/2, h-P5h/2, lnf*P5sz+1)+
                    Myassembly.instances['Part-5-1'].elements.getByBoundingBox(b1+P1h/2, h-P5h/2, -lnf*P5sz-1, b1
                    +b2-P4h/2, h-P5h/2, -(lnf-1)*P5sz+1)+Myassembly.instances['Part-5-1'].elements.
                    getByBoundingBox(b1+P1h/2, h+P5h/2, (lnf-1)*P5sz-1, b1+b2-P4h/2, h+P5h/2, lnf*P5sz+1)
635                 , name='stress_P5F_'+'{0}'.format(lnf))
636
637             #web
638         for lnw in [1, 2, 3, 4]:
639             Myassembly.Set(elements=
640                 Myassembly.instances['Part-1-1'].elements.getByBoundingBox(-lnw*P1sx-1, 0.0, 0.0, -(lnw-1)*
                    P1sx+1, h+P2h/2, 0.0)+Myassembly.instances['Part-1-1'].elements.getByBoundingBox((lnw-1)*P1sx
                    -1, 0.0, 0.0, lnw*P1sx+1, h+P2h/2, 0.0)
641                 +Myassembly.instances['Part-1-2'].elements.getByBoundingBox(b1-lnw*P1sx, 0.0, 0.0, b1-(lnw-1
                    )*P1sx, h+P2h/2, 0.0)+Myassembly.instances['Part-1-2'].elements.getByBoundingBox(b1+(lnw-1)*
                    P1sx, 0.0, 0.0, b1+lnw*P1sx, h+P2h/2, 0.0)
642                 , name='stress_P1W_'+'{0}'.format(lnw))
643             Myassembly.Set(elements=
644                 Myassembly.instances['Part-2-1'].elements.getByBoundingBox(P1h/2, h+(lnw-1)*P2sy, 0.0, b1-P1h
                    /2, h+lnw*P2sy, 0.0)+Myassembly.instances['Part-2-1'].elements.getByBoundingBox(P1h/2, h-lnw*
                    P2sy, 0.0, b1-P1h/2, h-(lnw-1)*P2sy, 0.0)
645                 , name='stress_P2W_'+'{0}'.format(lnw))
646             Myassembly.Set(elements=
647                 Myassembly.instances['Part-4-1'].elements.getByBoundingBox(b1+b2-lnw*P4sx, 0.0, 0.0, b1+b2-(
                    lnw-1)*P4sx, h+P5h/2, 0.0)+Myassembly.instances['Part-4-1'].elements.getByBoundingBox(b1+b2+(
                    lnw-1)*P4sx, 0.0, 0.0, b1+b2+lnw*P4sx, h+P5h/2, 0.0)
648                 , name='stress_P4W_'+'{0}'.format(lnw))
649             Myassembly.Set(elements=
650                 Myassembly.instances['Part-5-1'].elements.getByBoundingBox(b1+P1h/2, h+(lnw-1)*P5sy, 0.0, b1+
                    b2-P4h/2, h+lnw*P5sy, 0.0)+Myassembly.instances['Part-5-1'].elements.getByBoundingBox(b1+P1h/
                    2, h-lnw*P5sy, 0.0, b1+b2-P4h/2, h-(lnw-1)*P5sy, 0.0)
651                 , name='stress_P5W_'+'{0}'.format(lnw))
652
653             #total
654         if (joint ==1):
655             Myassembly.Set(name='frame_node', nodes=
656                 Myassembly.instances['Part-1-1'].nodes.getByBoundingBox(-P1h/2, 0.0, -P1b/2, P1h/2, h+P2h/2,
                    P1b/2)+
657                 Myassembly.instances['Part-2-1'].nodes.getByBoundingBox(P1h/2, h-P2h/2, -P2b/2, b1-P1h/2, h+
                    P2h/2, P2b/2)+
658                 Myassembly.instances['Part-1-2'].nodes.getByBoundingBox(b1-P1h/2, 0.0, -P1b/2, b1+P1h/2, h+
                    P2h/2, P1b/2)+
659                 Myassembly.instances['Part-3a-1'].nodes.getByBoundingBox(-P1h/2, h+P2h/2, -P1b/2, P1h/2, h+
                    P2h/2, P1b/2)+
660                 Myassembly.instances['Part-3b-1'].nodes.getByBoundingBox(-P1h/2, h-P2h/2, -P1b/2, P1h/2, h-
                    P2h/2, P1b/2)+
661                 Myassembly.instances['Part-3a-2'].nodes.getByBoundingBox(b1-P1h/2, h+P2h/2, -P1b/2, b1+P1h/2,
                     h+P2h/2, P1b/2)+
662                 Myassembly.instances['Part-3b-2'].nodes.getByBoundingBox(b1-P1h/2, h-P2h/2, -P1b/2, b1+P1h/2,
                     h-P2h/2, P1b/2)+
663                 Myassembly.instances['Part-4-1'].nodes.getByBoundingBox(b1+b2-P4h/2, 0.0, -P4b/2, b1+b2+P4h/2
                    , h+P5h/2, P4b/2)+
664                 Myassembly.instances['Part-5-1'].nodes.getByBoundingBox(b1+P1h/2, h-P5h/2, -P5b/2, b1+b2-P4h/
                    2, h+P5h/2, P5b/2)+
665                 Myassembly.instances['Part-6a-1'].nodes.getByBoundingBox(b1+b2-P4h/2, h+P5h/2, -P4b/2, b1+b2+
                    P4h/2, h+P5h/2, P4b/2))
666
667         elif (joint==2):
668             Myassembly.Set(name='frame_node', nodes=
669                 Myassembly.instances['Part-1-1'].nodes.getByBoundingBox(-P1h/2, 0.0, -P1b/2, P1h/2, h+P2h/2,
                    P1b/2)+
670                 Myassembly.instances['Part-2-1'].nodes.getByBoundingBox(P1h/2, h-P2h/2, -P2b/2, b1-P1h/2, h+
                    P2h/2, P2b/2)+
671                 Myassembly.instances['Part-1-2'].nodes.getByBoundingBox(b1-P1h/2, 0.0, -P1b/2, b1+P1h/2, h+
                    P2h/2, P1b/2)+
672                 Myassembly.instances['Part-3a-1'].nodes.getByBoundingBox(-P1h/2, h+P2h/2, -P1b/2, P1h/2, h+
                    P2h/2, P1b/2)+
673                 Myassembly.instances['Part-3b-1'].nodes.getByBoundingBox(-P1h/2, h-P2h/2, -P1b/2, P1h/2, h-
                    P2h/2, P1b/2)+
674                 Myassembly.instances['Part-3a-2'].nodes.getByBoundingBox(b1-P1h/2, h+P2h/2, -P1b/2, b1+P1h/2,
                     h+P2h/2, P1b/2)+
```

```
                    Myassembly.instances['Part-3b-2'].nodes.getByBoundingBox(b1-P1h/2, h-P2h/2, -P1b/2, b1+P1h/2,
                     h-P2h/2, P1b/2)+
                    Myassembly.instances['Part-4-1'].nodes.getByBoundingBox(b1+b2-P4h/2, 0.0, -P4b/2, b1+b2+P4h/2
                    , h+P5h/2, P4b/2)+
                    Myassembly.instances['Part-5-1'].nodes.getByBoundingBox(b1+P1h/2, h-P5h/2, -P5b/2, b1+b2-P4h/
                    2, h+P5h/2, P5b/2)+
                    Myassembly.instances['Part-6a-1'].nodes.getByBoundingBox(b1+b2-P4h/2, h+P5h/2, -P4b/2, b1+b2+
                    P4h/2, h+P5h/2, P4b/2)+
                    Myassembly.instances['Part-6b-1'].nodes.getByBoundingBox(b1+b2-P4h/2, h-P5h/2, -P4b/2, b1+b2+
                    P4h/2, h-P5h/2, P4b/2))

            #field output request
            Mymodel.fieldOutputRequests['F-Output-1'].setValues(variables=('S', 'E', 'PE', 'PEEQ', 'PEMAG', 'LE',
             'U', 'RF', 'CF', 'CSTRESS', 'CDISP'))

            #history Output Requests and applying the imperfection
            if (H ==0):
                del Mymodel.historyOutputRequests['H-Output-1']
                Mymodel.HistoryOutputRequest(createStepName='Step-1', name='U1', rebar=EXCLUDE, region=Myassembly
                .sets['top_nodes'], sectionPoints=DEFAULT, variables=('U1', ))
                Mymodel.HistoryOutputRequest(createStepName='Step-1', name='RF2', rebar=EXCLUDE, region=
                Myassembly.sets['bottom_nodes'], sectionPoints=DEFAULT, variables=('RF2', ))
                    #Load applied
                Mymodel.HistoryOutputRequest(createStepName='Step-1', name='CF2', rebar=EXCLUDE, region=
                Myassembly.sets['top_nodes'], sectionPoints=DEFAULT, variables=('CF2', ))
                    #Strain
                Mymodel.HistoryOutputRequest(createStepName='Step-1', name='LE', rebar=EXCLUDE, region=Myassembly
                .sets['LE'], sectionPoints=DEFAULT, variables=('LE11', 'LE22', 'LE33', 'LE12', 'LE13', 'LE23',
                'LEP'))

                Mymodel.keywordBlock.synchVersions(storeNodesAndElements=False)
                sentence = 348
                if (A2 == 0):
                    Mymodel.keywordBlock.insert(sentence, "\n*IMPERFECTION, FILE=LBA-job-"+'{0}'.format(id)+",
                    STEP=1, NSET=frame_node\n"+'{0}'.format(mode1)+", "+'{0}'.format(A1))
                elif (A3 == 0):
                    Mymodel.keywordBlock.insert(sentence, "\n*IMPERFECTION, FILE=LBA-job-"+'{0}'.format(id)+",
                    STEP=1, NSET=frame_node\n"+'{0}'.format(mode1)+", "+'{0}'.format(A1)+"\n"+'{0}'.format(mode2
                    )+", "+'{0}'.format(A2))
                else:
                    Mymodel.keywordBlock.insert(sentence, "\n*IMPERFECTION, FILE=LBA-job-"+'{0}'.format(id)+",
                    STEP=1, NSET=frame_node\n"+'{0}'.format(mode1)+", "+'{0}'.format(A1)+"\n"+'{0}'.format(mode2
                    )+", "+'{0}'.format(A2)+"\n"+'{0}'.format(mode3)+", "+'{0}'.format(A3))
            else:
                Mymodel.HistoryOutputRequest(createStepName='Step-2', name='U1', rebar=EXCLUDE, region=Myassembly
                .sets['top_nodes'], sectionPoints=DEFAULT, variables=('U1', ))
                Mymodel.HistoryOutputRequest(createStepName='Step-2', name='RF2', rebar=EXCLUDE, region=
                Myassembly.sets['bottom_nodes'], sectionPoints=DEFAULT, variables=('RF2', ))
                    #Load applied
                Mymodel.HistoryOutputRequest(createStepName='Step-2', name='CF2', rebar=EXCLUDE, region=
                Myassembly.sets['top_nodes'], sectionPoints=DEFAULT, variables=('CF2', ))
                    #Strain
                Mymodel.HistoryOutputRequest(createStepName='Step-2', name='LE', rebar=EXCLUDE, region=Myassembly
                .sets['LE'], sectionPoints=DEFAULT, variables=('LE11', 'LE22', 'LE33', 'LE12', 'LE13', 'LE23',
                'LEP'))

                Mymodel.keywordBlock.synchVersions(storeNodesAndElements=False)
                sentence = 349
                if (A2 == 0):
                    Mymodel.keywordBlock.insert(sentence, "\n*IMPERFECTION, FILE=LBA-job-"+'{0}'.format(id)+",
                    STEP=1, NSET=frame_node\n"+'{0}'.format(mode1)+", "+'{0}'.format(A1))
                elif (A3 == 0):
                    Mymodel.keywordBlock.insert(sentence, "\n*IMPERFECTION, FILE=LBA-job-"+'{0}'.format(id)+",
                    STEP=1, NSET=frame_node\n"+'{0}'.format(mode1)+", "+'{0}'.format(A1)+"\n"+'{0}'.format(mode2
                    )+", "+'{0}'.format(A2))
                else:
                    Mymodel.keywordBlock.insert(sentence, "\n*IMPERFECTION, FILE=LBA-job-"+'{0}'.format(id)+",
                    STEP=1, NSET=frame_node\n"+'{0}'.format(mode1)+", "+'{0}'.format(A1)+"\n"+'{0}'.format(mode2
                    )+", "+'{0}'.format(A2)+"\n"+'{0}'.format(mode3)+", "+'{0}'.format(A3))

            #applying residual stresses
            for lnf in [1, 2, 3]:
                residual_stress = ((fy/6*5)-(fy/3*(lnf-1)))*rs1
                Mymodel.keywordBlock.insert(sentence+lnf, '\n*INITIAL CONDITIONS, TYPE=STRESS\nstress_P1F_'+'{0}'
                .format(lnf)+', '+'{0}'.format(residual_stress))
            for lnf in [4, 5, 6]:
                residual_stress = (-(fy/6)-(fy/3*(lnf-4)))*rs1
                Mymodel.keywordBlock.insert(sentence+lnf, '\n*INITIAL CONDITIONS, TYPE=STRESS\nstress_P1F_'+'{0}'
                .format(lnf)+', '+'{0}'.format(residual_stress))
            for lnf in [1, 2, 3]:
                residual_stress = ((fy/6*5)-(fy/3*(lnf-1)))*rs2
                Mymodel.keywordBlock.insert(sentence+6+lnf, '\n*INITIAL CONDITIONS, TYPE=STRESS\nstress_P2F_'+
                '{0}'.format(lnf)+', '+'{0}'.format(residual_stress))
            for lnf in [4, 5, 6]:
                residual_stress = (-(fy/6)-(fy/3*(lnf-4)))*rs2
                Mymodel.keywordBlock.insert(sentence+6+lnf, '\n*INITIAL CONDITIONS, TYPE=STRESS\nstress_P2F_'+
```

```
            '{0}'.format(lnf)+', '+'{0}'.format(residual_stress))
        for lnf in [1, 2, 3]:
            residual_stress = ((fy/6*5)-(fy/3*(lnf-1)))*rs4
            Mymodel.keywordBlock.insert(sentence+12+lnf, '\n*INITIAL CONDITIONS, TYPE=STRESS\nstress_P4F_'+
            '{0}'.format(lnf)+', '+'{0}'.format(residual_stress))
        for lnf in [4, 5, 6]:
            residual_stress = (-(fy/6)-(fy/3*(lnf-4)))*rs4
            Mymodel.keywordBlock.insert(sentence+12+lnf, '\n*INITIAL CONDITIONS, TYPE=STRESS\nstress_P4F_'+
            '{0}'.format(lnf)+', '+'{0}'.format(residual_stress))
        for lnf in [1, 2, 3]:
            residual_stress = ((fy/6*5)-(fy/3*(lnf-1)))*rs5
            Mymodel.keywordBlock.insert(sentence+18+lnf, '\n*INITIAL CONDITIONS, TYPE=STRESS\nstress_P5F_'+
            '{0}'.format(lnf)+', '+'{0}'.format(residual_stress))
        for lnf in [4, 5, 6]:
            residual_stress = (-(fy/6)-(fy/3*(lnf-4)))*rs5
            Mymodel.keywordBlock.insert(sentence+18+lnf, '\n*INITIAL CONDITIONS, TYPE=STRESS\nstress_P5F_'+
            '{0}'.format(lnf)+', '+'{0}'.format(residual_stress))

        for lnf in [1, 2]:
            residual_stress = (-(fy/4*3)+(fy/2*(lnf-1)))*rs1
            Mymodel.keywordBlock.insert(sentence+24+lnf, '\n*INITIAL CONDITIONS, TYPE=STRESS\nstress_P1W_'+
            '{0}'.format(lnf)+', '+'{0}'.format(residual_stress))
        for lnf in [3, 4]:
            residual_stress = ((fy/4)+(fy/2*(lnf-3)))*rs1
            Mymodel.keywordBlock.insert(sentence+24+lnf, '\n*INITIAL CONDITIONS, TYPE=STRESS\nstress_P1W_'+
            '{0}'.format(lnf)+', '+'{0}'.format(residual_stress))
        for lnf in [1, 2]:
            residual_stress = (-(fy/4*3)+(fy/2*(lnf-1)))*rs2
            Mymodel.keywordBlock.insert(sentence+28+lnf, '\n*INITIAL CONDITIONS, TYPE=STRESS\nstress_P2W_'+
            '{0}'.format(lnf)+', '+'{0}'.format(residual_stress))
        for lnf in [3, 4]:
            residual_stress = ((fy/4)+(fy/2*(lnf-3)))*rs2
            Mymodel.keywordBlock.insert(sentence+28+lnf, '\n*INITIAL CONDITIONS, TYPE=STRESS\nstress_P2W_'+
            '{0}'.format(lnf)+', '+'{0}'.format(residual_stress))
        for lnf in [1, 2]:
            residual_stress = (-(fy/4*3)+(fy/2*(lnf-1)))*rs4
            Mymodel.keywordBlock.insert(sentence+32+lnf, '\n*INITIAL CONDITIONS, TYPE=STRESS\nstress_P4W_'+
            '{0}'.format(lnf)+', '+'{0}'.format(residual_stress))
        for lnf in [3, 4]:
            residual_stress = ((fy/4)+(fy/2*(lnf-3)))*rs4
            Mymodel.keywordBlock.insert(sentence+32+lnf, '\n*INITIAL CONDITIONS, TYPE=STRESS\nstress_P4W_'+
            '{0}'.format(lnf)+', '+'{0}'.format(residual_stress))
        for lnf in [1, 2]:
            residual_stress = (-(fy/4*3)+(fy/2*(lnf-1)))*rs5
            Mymodel.keywordBlock.insert(sentence+36+lnf, '\n*INITIAL CONDITIONS, TYPE=STRESS\nstress_P5W_'+
            '{0}'.format(lnf)+', '+'{0}'.format(residual_stress))
        for lnf in [3, 4]:
            residual_stress = ((fy/4)+(fy/2*(lnf-3)))*rs5
            Mymodel.keywordBlock.insert(sentence+36+lnf, '\n*INITIAL CONDITIONS, TYPE=STRESS\nstress_P5W_'+
            '{0}'.format(lnf)+', '+'{0}'.format(residual_stress))

        #job
        mdb.Job(atTime=None, contactPrint=OFF, description='', echoPrint=OFF, explicitPrecision=SINGLE,
        getMemoryFromAnalysis=True, historyPrint=OFF, memory=90, memoryUnits=PERCENTAGE, model=
        'GMNIA_IV-frame-'+id, modelPrint=OFF, multiprocessingMode=DEFAULT, name='GMNIA_IV-job-'+id,
        nodalOutputPrecision=SINGLE, numCpus=1, numGPUs=0, queue=None, resultsFormat=ODB, scratch='', type=
        ANALYSIS, userSubroutine='', waitHours=0, waitMinutes=0)

        mdb.jobs['GMNIA_IV-job-'+id].submit(consistencyChecking=OFF)
        mdb.jobs['GMNIA_IV-job-'+id].waitForCompletion()

        #Create ODB output
        if (H== 0):
            RF_A, RF_B, RF_C, U1_A, U1_B, U1_C, CF_A, CF_B, CF_C, = ([] for i in range (9))

            Directory_odb = '{0}'.format(Loadpath)+'/'+'GMNIA_IV-job-'+id+'.odb'
            open_odb = session.openOdb(name=Directory_odb)
            odb = session.odbs[Directory_odb]
            session.viewports['Viewport: 1'].setValues(displayedObject=open_odb)
            frames = open_odb.steps['Step-1'].frames
            numFrames = len(frames)

            #Reaction Force
            xy_RF_A = session.XYDataFromHistory(name='XY-RF_A', odb=odb, outputVariableName='Reaction force:
            RF2 PI: PART-1-1 Node 19', steps=('Step-1', ), )
            RF_A = [abs(x[1]*10**(-3)) for x in xy_RF_A]
            Max_RF_A = max(RF_A)

            xy_RF_B = session.XYDataFromHistory(name='XY-RF_B', odb=odb, outputVariableName='Reaction force:
            RF2 PI: PART-1-2 Node 19', steps=('Step-1', ), )
            RF_B = [abs(x[1]*10**(-3)) for x in xy_RF_B]
            Max_RF_B = max(RF_B)

            xy_RF_C = session.XYDataFromHistory(name='XY-RF_C', odb=odb, outputVariableName='Reaction force:
            RF2 PI: PART-4-1 Node 19', steps=('Step-1', ), )
            RF_C = [abs(x[1]*10**(-3)) for x in xy_RF_C]
```

```
            Max_RF_C = max(RF_C)

            #Displacement
            xy_U1_A = session.XYDataFromHistory(name='XY_U', odb=odb, outputVariableName='Spatial
            displacement: U1 PI: rootAssembly Node 1 in NSET TOP_NODES', steps=('Step-1', ), )
            U1_A = [abs(x[1]*-1) for x in xy_U1_A]

            xy_U1_B = session.XYDataFromHistory(name='XY_U', odb=odb, outputVariableName='Spatial
            displacement: U1 PI: rootAssembly Node 2 in NSET TOP_NODES', steps=('Step-1', ), )
            U1_B = [abs(x[1]*-1) for x in xy_U1_A]

            xy_U1_C = session.XYDataFromHistory(name='XY_U', odb=odb, outputVariableName='Spatial
            displacement: U1 PI: rootAssembly Node 3 in NSET TOP_NODES', steps=('Step-1', ), )
            U1_C = [abs(x[1]*-1) for x in xy_U1_A]

            #Applied Force
            xy_CF_A = session.XYDataFromHistory(name='XY-CF_A', odb=odb, outputVariableName='Point loads:
            CF2 PI: rootAssembly Node 1 in NSET TOP_NODES', steps=('Step-1', ), )
            CF_A = [abs(x[1]*10**(-3)) for x in xy_CF_A]
            Max_CF_A = max(CF_A)

            xy_CF_B = session.XYDataFromHistory(name='XY-CF_B', odb=odb, outputVariableName='Point loads:
            CF2 PI: rootAssembly Node 2 in NSET TOP_NODES', steps=('Step-1', ), )
            CF_B = [abs(x[1]*10**(-3)) for x in xy_CF_B]
            Max_CF_B = max(CF_B)

            xy_CF_C = session.XYDataFromHistory(name='XY-CF_C', odb=odb, outputVariableName='Point loads:
            CF2 PI: rootAssembly Node 3 in NSET TOP_NODES', steps=('Step-1', ), )
            CF_C = [abs(x[1]*10**(-3)) for x in xy_CF_C]
            Max_CF_C = max(CF_C)

            #CREATE EXCEL VALUES
            INC=range(0, numFrames)

            workbook = xlsxwriter.Workbook('GMNIA_IV-'+'{0}.xlsx'.format(Filename))
            worksheet1 = workbook.add_worksheet('ABAQUSDATA')

            #Write general data
            bold = workbook.add_format({'bold': 1})
            headings1 = ['','{0}'.format(Filename)]
            headings2 = ['INC','U1_A','RF_A','CF_A','U1_B','RF_B','CF_B','U1_C','RF_C','CF_C']
            headings3 = ['(-)','(mm)','(kN)','(kN)','(mm)','(kN)','(kN)','(mm)','(kN)','(kN)']
            headings4 = ['','',Max_RF_A,Max_CF_A,'',Max_RF_B,Max_CF_B,'',Max_RF_C,Max_CF_C]
            worksheet1.write_row('A1', headings1, bold)
            worksheet1.write_row('A2', headings2, bold)
            worksheet1.write_row('A3', headings3)
            worksheet1.write_column(3, 0, INC)
            worksheet1.write_column(3, 1, U1_A)
            worksheet1.write_column(3, 2, RF_A)
            worksheet1.write_column(3, 3, CF_A)
            worksheet1.write_column(3, 4, U1_B)
            worksheet1.write_column(3, 5, RF_B)
            worksheet1.write_column(3, 6, CF_B)
            worksheet1.write_column(3, 7, U1_C)
            worksheet1.write_column(3, 8, RF_C)
            worksheet1.write_column(3, 9, CF_C)
            worksheet1.write_row('A205', headings4, bold)

            workbook.close()

        else:
            RF_A, RF_B, RF_C, U1_A, U1_B, U1_C, CF_A, CF_B, CF_C, = ([] for i in range (9))

            Directory_odb = '{0}'.format(Loadpath)+'/'+'GMNIA_IV-job-'+id+'.odb'
            open_odb = session.openOdb(name=Directory_odb)
            odb = session.odbs[Directory_odb]
            session.viewports['Viewport: 1'].setValues(displayedObject=open_odb)
            frames = open_odb.steps['Step-2'].frames
            numFrames = len(frames)

            #Reaction Force
            xy_RF_A = session.XYDataFromHistory(name='XY-RF_A', odb=odb, outputVariableName='Reaction force:
            RF2 PI: PART-1-1 Node 19', steps=('Step-2', ), )
            RF_A = [abs(x[1]*10**(-3)) for x in xy_RF_A]
            Max_RF_A = max(RF_A)

            xy_RF_B = session.XYDataFromHistory(name='XY-RF_B', odb=odb, outputVariableName='Reaction force:
            RF2 PI: PART-1-2 Node 19', steps=('Step-2', ), )
            RF_B = [abs(x[1]*10**(-3)) for x in xy_RF_B]
            Max_RF_B = max(RF_B)

            xy_RF_C = session.XYDataFromHistory(name='XY-RF_C', odb=odb, outputVariableName='Reaction force:
            RF2 PI: PART-4-1 Node 19', steps=('Step-2', ), )
            RF_C = [abs(x[1]*10**(-3)) for x in xy_RF_C]
            Max_RF_C = max(RF_C)
```

```
875             #Displacement
876             xy_U1_A = session.XYDataFromHistory(name='XY_U', odb=odb, outputVariableName='Spatial
                displacement: U1 PI: rootAssembly Node 1 in NSET TOP_NODES', steps=('Step-2', ), )
877             U1_A = [abs(x[1]*-1) for x in xy_U1_A]
878
879             xy_U1_B = session.XYDataFromHistory(name='XY_U', odb=odb, outputVariableName='Spatial
                displacement: U1 PI: rootAssembly Node 2 in NSET TOP_NODES', steps=('Step-2', ), )
880             U1_B = [abs(x[1]*-1) for x in xy_U1_A]
881
882             xy_U1_C = session.XYDataFromHistory(name='XY_U', odb=odb, outputVariableName='Spatial
                displacement: U1 PI: rootAssembly Node 3 in NSET TOP_NODES', steps=('Step-2', ), )
883             U1_C = [abs(x[1]*-1) for x in xy_U1_A]
884
885             #Applied Force
886             xy_CF_A = session.XYDataFromHistory(name='XY-CF_A', odb=odb, outputVariableName='Point loads:
                CF2 PI: rootAssembly Node 1 in NSET TOP_NODES', steps=('Step-2', ), )
887             CF_A = [abs(x[1]*10**(-3)) for x in xy_CF_A]
888             Max_CF_A = max(CF_A)
889
890             xy_CF_B = session.XYDataFromHistory(name='XY-CF_B', odb=odb, outputVariableName='Point loads:
                CF2 PI: rootAssembly Node 2 in NSET TOP_NODES', steps=('Step-2', ), )
891             CF_B = [abs(x[1]*10**(-3)) for x in xy_CF_B]
892             Max_CF_B = max(CF_B)
893
894             xy_CF_C = session.XYDataFromHistory(name='XY-CF_C', odb=odb, outputVariableName='Point loads:
                CF2 PI: rootAssembly Node 3 in NSET TOP_NODES', steps=('Step-2', ), )
895             CF_C = [abs(x[1]*10**(-3)) for x in xy_CF_C]
896             Max_CF_C = max(CF_C)
897
898             #CREATE EXCEL VALUES
899             INC=range(0, numFrames)
900
901             workbook = xlsxwriter.Workbook('GMNIA_IV-'+'{0}.xlsx'.format(Filename))
902             worksheet1 = workbook.add_worksheet('ABAQUSDATA')
903
904             #Write general data
905             bold = workbook.add_format({'bold': 1})
906             headings1 = ['','{0}'.format(Filename)]
907             headings2 = ['INC','U1_A','RF_A','CF_A','U1_B','RF_B','CF_B','U1_C','RF_C','CF_C']
908             headings3 = ['(-)','(mm)','(kN)','(kN)','(mm)','(kN)','(kN)','(mm)','(kN)','(kN)']
909             headings4 = ['','',Max_RF_A,Max_CF_A,'',Max_RF_B,Max_CF_B,'',Max_RF_C,Max_CF_C]
910             worksheet1.write_row('A1', headings1, bold)
911             worksheet1.write_row('A2', headings2, bold)
912             worksheet1.write_row('A3', headings3)
913             worksheet1.write_column(3, 0, INC)
914             worksheet1.write_column(3, 1, U1_A)
915             worksheet1.write_column(3, 2, RF_A)
916             worksheet1.write_column(3, 3, CF_A)
917             worksheet1.write_column(3, 4, U1_B)
918             worksheet1.write_column(3, 5, RF_B)
919             worksheet1.write_column(3, 6, CF_B)
920             worksheet1.write_column(3, 7, U1_C)
921             worksheet1.write_column(3, 8, RF_C)
922             worksheet1.write_column(3, 9, CF_C)
923             worksheet1.write_row('A205', headings4, bold)
924
925             workbook.close()
926
```

```
#GMNIA III is the exact script as GMNIA IV, only the scale factor for the eigenmode and the amount of
eigenmodes is different. The corresponding lines that differ are given below:

        e = float(extracted_list[118])

            Mymodel.keywordBlock.synchVersions(storeNodesAndElements=False)
            sentence = 348
            Mymodel.keywordBlock.insert(sentence, "\n*IMPERFECTION, FILE=LBA-job-"+'{0}'.format(id)+",
            STEP=1, NSET=frame_node\n1, "+'{0}'.format(e))
```

```
# -*- coding: mbcs -*-
from part import *
from material import *
from section import *
from assembly import *
from step import *
from interaction import *
from load import *
from mesh import *
from optimization import *
from job import *
from sketch import *
from visualization import *
from connectorBehavior import *
from caeModules import *
import os
import sys
import csv
import odbAccess
import math
import numpy as np
import xlsxwriter

session.journalOptions.setValues(replayGeometry=COORDINATE, recoverGeometry=COORDINATE)
# ======================setting up================================

input_file=open('C:/Users/20174572/Google Drive/Wim Broeks/TUe/2. Master/Afstuderen/4. FE Modelling/4. Parametric/INPUT.txt')

for line in input_file:
    extracted_line = line
    extracted_list = extracted_line.split()
    if "id" not in extracted_line:
        id = extracted_list[0]
        E = float(extracted_list[1])
        pois = float(extracted_list[2])
        F = float(extracted_list[3])
        Q = float(extracted_list[4])
        H = float(extracted_list[5])
        fy = float(extracted_list[6])
        fu = float(extracted_list[7])
        strain = float(extracted_list[8])
        h = float(extracted_list[9])
        b1 = float(extracted_list[10])
        b2 = float(extracted_list[11])
        P1h = float(extracted_list[16])
        P1b = float(extracted_list[17])
        P1tw = float(extracted_list[18])
        P1tf = float(extracted_list[19])
        P2h = float(extracted_list[27])
        P2b = float(extracted_list[28])
        P2tw = float(extracted_list[29])
        P2tf = float(extracted_list[30])
        P4h = float(extracted_list[38])
        P4b = float(extracted_list[39])
        P4tw = float(extracted_list[40])
        P4tf = float(extracted_list[41])
        P5h = float(extracted_list[49])
        P5b = float(extracted_list[50])
        P5tw = float(extracted_list[51])
        P5tf = float(extracted_list[52])
        joint = float(extracted_list[59])
        condition = float(extracted_list[60])
        ma1 = float(extracted_list[62])
        mb1 = float(extracted_list[63])
        mc1 = float(extracted_list[64])
        rs1 = float(extracted_list[65])
        ma2 = float(extracted_list[66])
        mb2 = float(extracted_list[67])
        mc2 = float(extracted_list[68])
        rs2 = float(extracted_list[69])
        ma4 = float(extracted_list[70])
        mb4 = float(extracted_list[71])
        mc4 = float(extracted_list[72])
        rs4 = float(extracted_list[73])
        ma5 = float(extracted_list[74])
        mb5 = float(extracted_list[75])
        mc5 = float(extracted_list[76])
        rs5 = float(extracted_list[77])

        #mesh
        P1sy = ma1
        P1sx = mb1
        P1sz = mc1

        P2sy = mb2
```

```
        P2sx = ma2
        P2sz = mc2

        P3sx = mb1
        P3sz = mc1

        P4sy = ma4
        P4sx = mb4
        P4sz = mc4

        P5sy = mb5
        P5sx = ma5
        P5sz = mc5

        P6sx = mb4
        P6sz = mc4
        # ======================setting up================================
        Filename='Frame-'+id
        Loadpath='F:\\Graduation project Wim\\parametric study\\plot\\{0}'.format(Filename)
        if not os.path.exists(Loadpath):
            os.makedirs(Loadpath)
        os.chdir(Loadpath)

        Mymodel=mdb.Model(name='LBA-frame-'+id)
        Myassembly=Mymodel.rootAssembly

        #part 1 - stabilizing columns
        Mymodel.ConstrainedSketch(name='__sweep__', sheetSize=200.0)
        Mysketchs=Mymodel.sketches['__sweep__']
        Mysketchs.Line(point1=(0.0, 0.0), point2=(0.0, h+P2h/2))
        Mysketchs.geometry.findAt((0.0, h/2))
        Mysketchs.VerticalConstraint(addUndoState= False, entity=Mysketchs.geometry.findAt((0.0, h/2), ))
        Mymodel.ConstrainedSketch(name='__profile__', sheetSize=200.0, transform=(1.0, 0.0, 0.0, 0.0, 0.0,
        1.0, -0.0, -1.0, -0.0, 0.0, 0.0, 0.0))
        Mysketchp=Mymodel.sketches['__profile__']
        Mysketchp.ConstructionLine(point1=(-100.0, 0.0), point2=(100.0, 0.0))
        Mysketchp.ConstructionLine(point1=(0.0, -100.0), point2=(0.0, 100.0))
        Mysketchp.Line(point1=(-(P1h/2), (P1b/2)), point2=(-(P1h/2), -(P1b/2)))
        Mysketchp.VerticalConstraint(addUndoState=False, entity=Mysketchp.geometry[4])
        Mysketchp.Line(point1=((P1h/2), (P1b/2)), point2=((P1h/2), -(P1b/2)))
        Mysketchp.VerticalConstraint(addUndoState=False, entity=Mysketchp.geometry[5])
        Mysketchp.Line(point1=(-(P1h/2), 0.0), point2=((P1h/2), 0.0))
        Mysketchp.HorizontalConstraint(addUndoState=False, entity=Mysketchp.geometry[6])
        Mymodel.Part(dimensionality=THREE_D, name='Part-1', type=DEFORMABLE_BODY)
        Mypart1=Mymodel.parts['Part-1']
        Mypart1.BaseShellSweep(path=Mysketchs, sketch=Mysketchp)

        Mypart1.DatumPlaneByPrincipalPlane(offset=(h-(P2h/2)), principalPlane=XZPLANE)
        Mypart1.DatumPlaneByPrincipalPlane(offset=(h+(P2h/2)), principalPlane=XZPLANE)
        Mypart1.DatumPlaneByPrincipalPlane(offset=(h), principalPlane=XZPLANE)

        #part 2 - stabilizing beam
        Mymodel.ConstrainedSketch(name='__sweep__', sheetSize=200.0)
        Mysketchs=Mymodel.sketches['__sweep__']
        Mysketchs.Line(point1=(P1h/2, h), point2=((b1-P1h/2), h))
        Mysketchs.HorizontalConstraint(addUndoState=False, entity=Mysketchs.geometry[2])
        Mymodel.ConstrainedSketch(name='__profile__', sheetSize=200.0, transform=(0.0, -1.0, 0.0, -0.0, 0.0,
        1.0, -1.0, -0.0, -0.0, 0, h, 0.0))
        Mysketchp=Mymodel.sketches['__profile__']
        Mysketchp.ConstructionLine(point1=(-100.0, 0.0), point2=(100.0, 0.0))
        Mysketchp.ConstructionLine(point1=(0.0, -100.0), point2=(0.0, 100.0))
        Mysketchp.Line(point1=(-(P2h/2), (P2b/2)), point2=(-(P2h/2), -(P2b/2)))
        Mysketchp.VerticalConstraint(addUndoState=False, entity=Mysketchp.geometry[4])
        Mysketchp.Line(point1=((P2h/2), (P2b/2)), point2=((P2h/2), -(P2b/2)))
        Mysketchp.VerticalConstraint(addUndoState=False, entity=Mysketchp.geometry[5])
        Mysketchp.Line(point1=(-(P2h/2), 0.0), point2=((P2h/2), 0.0))
        Mysketchp.HorizontalConstraint(addUndoState=False, entity=Mysketchp.geometry[6])
        Mymodel.Part(dimensionality=THREE_D, name='Part-2', type=DEFORMABLE_BODY)
        Mypart2=Mymodel.parts['Part-2']
        Mypart2.BaseShellSweep(path=Mysketchs, sketch=Mysketchp)

        #part 3a - stiffeners stabilizing column
        Mymodel.ConstrainedSketch(name='__profile__', sheetSize=200.0)
        Mysketchp=Mymodel.sketches['__profile__']
        Mysketchp.Line(point1=(0.0, 0.0), point2=(P1h, 0.0))
        Mysketchp.geometry.findAt((P1h/2, 0.0))
        Mysketchp.HorizontalConstraint(addUndoState=False, entity=Mysketchp.geometry.findAt((P1h/2, 0.0), ))
        Mymodel.Part(dimensionality=THREE_D, name='Part-3a', type=DEFORMABLE_BODY)
        Mypart3a=Mymodel.parts['Part-3a']
        Mypart3a.BaseShellExtrude(depth=P1b, sketch=Mysketchp)
        Mypart3a.DatumPlaneByPrincipalPlane(offset=(P1b/2), principalPlane=XYPLANE)

        #part 3b - stiffeners stabilizing column
        Mymodel.ConstrainedSketch(name='__profile__', sheetSize=200.0)
        Mysketchp=Mymodel.sketches['__profile__']
        Mysketchp.Line(point1=(0.0, 0.0), point2=(P1h, 0.0))
```

```
        Mysketchp.geometry.findAt((P1h/2, 0.0))
        Mysketchp.HorizontalConstraint(addUndoState=False, entity=Mysketchp.geometry.findAt((P1h/2, 0.0), ))
        Mymodel.Part(dimensionality=THREE_D, name='Part-3b', type=DEFORMABLE_BODY)
        Mypart3b=Mymodel.parts['Part-3b']
        Mypart3b.BaseShellExtrude(depth=P1b, sketch=Mysketchp)
        Mypart3b.DatumPlaneByPrincipalPlane(offset=(P1b/2), principalPlane=XYPLANE)

        #part 4 - leaning column
        Mymodel.ConstrainedSketch(name='__sweep__', sheetSize=200.0)
        Mysketchs=Mymodel.sketches['__sweep__']
        Mysketchs.Line(point1=(b1+b2, 0.0), point2=(b1+b2, h+P5h/2))
        Mymodel.ConstrainedSketch(name='__profile__', sheetSize=200.0, transform=(1.0, 0.0, 0.0, 0.0, 0.0,
        1.0, -0.0, -1.0, -0.0, b1+b2, 0.0, 0.0))
        Mysketchp=Mymodel.sketches['__profile__']
        Mysketchp.ConstructionLine(point1=(-100.0, 0.0), point2=(100.0, 0.0))
        Mysketchp.ConstructionLine(point1=(0.0, -100.0), point2=(0.0, 100.0))
        Mysketchp.Line(point1=(-P4h/2, P4b/2), point2=(-P4h/2, -P4b/2))
        Mysketchp.Line(point1=(P4h/2, P4b/2), point2=(P4h/2, -P4b/2))
        Mysketchp.Line(point1=(-P4h/2, 0.0), point2=(P4h/2, 0.0))
        Mymodel.Part(dimensionality=THREE_D, name='Part-4', type=DEFORMABLE_BODY)
        Mypart4=Mymodel.parts['Part-4']
        Mypart4.BaseShellSweep(path=Mysketchs, sketch=Mysketchp)

        Mypart4.DatumPlaneByPrincipalPlane(offset=h-P5h/2, principalPlane=XZPLANE)
        Mypart4.DatumPlaneByPrincipalPlane(offset=h+P5h/2, principalPlane=XZPLANE)
        Mypart4.DatumPlaneByPrincipalPlane(offset=(h), principalPlane=XZPLANE)

        #part 5 - leaning beam
        Mymodel.ConstrainedSketch(name='__sweep__', sheetSize=200.0)
        Mysketchs=Mymodel.sketches['__sweep__']
        Mysketchs.Line(point1=(b1+P1h/2, h), point2=(b1+b2-P4h/2, h))
        Mymodel.ConstrainedSketch(name='__profile__', sheetSize=200.0, transform=(0.0, -1.0, 0.0, -0.0, 0.0,
        1.0, -1.0, -0.0, -0.0, b1, h, 0.0))
        Mysketchp=Mymodel.sketches['__profile__']
        Mysketchp.ConstructionLine(point1=(-100.0, 0.0), point2=(100.0, 0.0))
        Mysketchp.ConstructionLine(point1=(0.0, -100.0), point2=(0.0, 100.0))
        Mysketchp.Line(point1=(-P5h/2, P5b/2), point2=(-P5h/2, -P5b/2))
        Mysketchp.Line(point1=(P5h/2, P5b/2), point2=(P5h/2, -P5b/2))
        Mysketchp.Line(point1=(-P5h/2, 0.0), point2=(P5h/2, 0.0))
        Mymodel.Part(dimensionality=THREE_D, name='Part-5', type=DEFORMABLE_BODY)
        Mypart5=Mymodel.parts['Part-5']
        Mypart5.BaseShellSweep(path=Mysketchs, sketch=Mysketchp)

        if (joint ==1):
        #part 6a - stiffeners leaning column
            Mymodel.ConstrainedSketch(name='__profile__', sheetSize=200.0)
            Mysketchp=Mymodel.sketches['__profile__']
            Mysketchp.Line(point1=(0.0, 0.0), point2=(P4h, 0.0))
            Mysketchp.geometry.findAt((P4h/2, 0.0))
            Mysketchp.HorizontalConstraint(addUndoState=False, entity=Mysketchp.geometry.findAt((P4h/2, 0.0),
             ))
            Mymodel.Part(dimensionality=THREE_D, name='Part-6a', type=DEFORMABLE_BODY)
            Mypart6a=Mymodel.parts['Part-6a']
            Mypart6a.BaseShellExtrude(depth=P4b, sketch=Mysketchp)
            Mypart6a.DatumPlaneByPrincipalPlane(offset=(P4b/2), principalPlane=XYPLANE)
        elif (joint ==2):
        #part 6a - stiffeners leaning column
            Mymodel.ConstrainedSketch(name='__profile__', sheetSize=200.0)
            Mysketchp=Mymodel.sketches['__profile__']
            Mysketchp.Line(point1=(0.0, 0.0), point2=(P4h, 0.0))
            Mysketchp.geometry.findAt((P4h/2, 0.0))
            Mysketchp.HorizontalConstraint(addUndoState=False, entity=Mysketchp.geometry.findAt((P4h/2, 0.0),
             ))
            Mymodel.Part(dimensionality=THREE_D, name='Part-6a', type=DEFORMABLE_BODY)
            Mypart6a=Mymodel.parts['Part-6a']
            Mypart6a.BaseShellExtrude(depth=P4b, sketch=Mysketchp)
            Mypart6a.DatumPlaneByPrincipalPlane(offset=(P4b/2), principalPlane=XYPLANE)
        #part 6b - stiffeners leaning column
            Mymodel.ConstrainedSketch(name='__profile__', sheetSize=200.0)
            Mysketchp=Mymodel.sketches['__profile__']
            Mysketchp.Line(point1=(0.0, 0.0), point2=(P4h, 0.0))
            Mysketchp.geometry.findAt((P4h/2, 0.0))
            Mysketchp.HorizontalConstraint(addUndoState=False, entity=Mysketchp.geometry.findAt((P4h/2, 0.0),
             ))
            Mymodel.Part(dimensionality=THREE_D, name='Part-6b', type=DEFORMABLE_BODY)
            Mypart6b=Mymodel.parts['Part-6b']
            Mypart6b.BaseShellExtrude(depth=P4b, sketch=Mysketchp)
            Mypart6b.DatumPlaneByPrincipalPlane(offset=(P4b/2), principalPlane=XYPLANE)

        #assembly
        Myassembly.DatumCsysByDefault(CARTESIAN)
        Myassembly.Instance(dependent=ON, name='Part-1-1', part=Mypart1)
        Myassembly.Instance(dependent=ON, name='Part-2-1', part=Mypart2)
        Myassembly.Instance(dependent=ON, name='Part-1-2', part=Mypart1)
        Myassembly.translate(instanceList=('Part-1-2', ), vector=(b1, 0.0, 0.0))
        Myassembly.Instance(dependent=ON, name='Part-4-1', part=Mypart4)
```

```
        Myassembly.Instance(dependent=ON, name='Part-5-1', part=Mypart5)

        #partition
            #part 1
        Mypart1.PartitionFaceByDatumPlane(datumPlane=Mypart1.datums[2], faces=Mypart1.faces.findAt(((-P1h/2, h/4, P1b/4), ), ((-P1h/2, h/4, -P1b/4), ), ((P1h/2, h/4, P1b/4), ), ((P1h/2, h/4, -P1b/4), ), ((P1h/4, h/4, 0.0), ), ))
            #part 4
        Mypart4.PartitionFaceByDatumPlane(datumPlane=Mypart4.datums[2], faces=Mypart4.faces.findAt(((b1+b2-P4h/2, h/4, P4b/4), ), ((b1+b2-P4h/2, h/4, -P4b/4), ), ((b1+b2+P4h/2, h/4, P4b/4), ), ((b1+b2+P4h/2, h/4, -P4b/4), ), ((b1+b2, h/4, 0.0), ), ))

            #part 3a-1
        Mypart3a.PartitionFaceByDatumPlane(datumPlane=Mypart3a.datums[2], faces=Mypart3a.faces.findAt(((P1h/4, 0.0, P1b/4), )))
        Myassembly.Instance(dependent=ON, name='Part-3a-1', part=Mypart3a)
        Mymodel.Tie(adjust=ON, master=Region(edges=Myassembly.instances['Part-1-1'].edges.findAt(((-P1h/2, h+(P2h/2), P1b/4), ), (((P1h/2), h+(P2h/2), P1b/4), ), ((-(P1h/2), h+(P2h/2), -P1b/4), ), (((P1h/2), h+(P2h/2), -P1b/4), ),((0.0, h+(P2h/2), 0.0), ), )), name='Tie_A_a', positionToleranceMethod=COMPUTED, slave=Region(edges=Myassembly.instances['Part-3a-1'].edges.findAt(((0.0, 0.0, P1b/4), ), ((P1h, 0.0, P1b/4), ),((0.0, 0.0, P1b/4*3), ), ((P1h, 0.0, P1b/4*3), ), ((P1h/2, 0.0, P1b/2), ), )), thickness=ON, tieRotations=ON)
        Myassembly.translate(instanceList=('Part-3a-1', ), vector=((-P1h/2, h+(P2h/2), -(P1b/2))))

            #part 3b-1
        Mypart3b.PartitionFaceByDatumPlane(datumPlane=Mypart3b.datums[2], faces=Mypart3b.faces.findAt(((P1h/4, 0.0, P1b/4),  )))
        Myassembly.Instance(dependent=ON, name='Part-3b-1', part=Mypart3b)
        Mymodel.Tie(adjust=ON, master=Region(edges=Myassembly.instances['Part-1-1'].edges.findAt(((-(P1h/2), h-(P2h/2), P1b/4), ), (((P1h/2), h-(P2h/2), P1b/4), ), ((-(P1h/2), h-(P2h/2), -P1b/4), ), (((P1h/2), h-(P2h/2), -P1b/4), ), ((0.0, h-(P2h/2), 0.0), ), )), name='Tie_A_b', positionToleranceMethod=COMPUTED, slave=Region(edges=Myassembly.instances['Part-3b-1'].edges.findAt(((0.0, 0.0, P1b/4), ), ((P1h, 0.0, P1b/4), ), ((0.0, 0.0, P1b/4*3), ), ((P1h, 0.0, P1b/4*3), ), ((P1h/2, 0.0, P1b/2), ), )), thickness=ON, tieRotations=ON)
        Myassembly.translate(instanceList=('Part-3b-1', ), vector=(-P1h/2, (h-(P2h/2)), -(P1b/2)))

            #part 3a-2
        Myassembly.Instance(dependent=ON, name='Part-3a-2', part=Mypart3a)
        Mymodel.Tie(adjust=ON, master=Region(edges=Myassembly.instances['Part-1-2'].edges.findAt(((-(P1h/2)+b1, h+(P2h/2), P1b/4), ), (((P1h/2)+b1, h+(P2h/2), P1b/4), ), ((-(P1h/2)+b1, h+(P2h/2), -P1b/4), ), (((P1h/2)+b1, h+(P2h/2), -P1b/4), ), ((b1, h+(P2h/2), 0.0), ), )), name='Tie_B_a', positionToleranceMethod=COMPUTED, slave=Region(edges=Myassembly.instances['Part-3a-2'].edges.findAt(((0.0, 0.0, P1b/4), ), ((P1h, 0.0, P1b/4), ),((0.0, 0.0, P1b/4*3), ), ((P1h, 0.0, P1b/4*3), ), ((P1h/2, 0.0, P1b/2), ), )), thickness=ON, tieRotations=ON)
        Myassembly.translate(instanceList=('Part-3a-2', ), vector=(-P1h/2+b1, (h+(P2h/2)), -(P1b/2)))

            #part 3b-2
        Myassembly.Instance(dependent=ON, name='Part-3b-2', part=Mypart3b)
        Mymodel.Tie(adjust=ON, master=Region(edges=Myassembly.instances['Part-1-2'].edges.findAt(((-(P1h/2)+b1, h-(P2h/2), P1b/4), ), (((P1h/2)+b1, h-(P2h/2), P1b/4), ), ((-(P1h/2)+b1, h-(P2h/2), -P1b/4), ), (((P1h/2)+b1, h-(P2h/2), -P1b/4), ), ((b1, h-(P2h/2), 0.0), ), )), name='Tie_B_b', positionToleranceMethod=COMPUTED, slave=Region(edges=Myassembly.instances['Part-3b-2'].edges.findAt(((0.0, 0.0, P1b/4), ), ((P1h, 0.0, P1b/4), ),((0.0, 0.0, P1b/4*3), ), ((P1h, 0.0, P1b/4*3), ), ((P1h/2, 0.0, P1b/2), ), )), thickness=ON, tieRotations=ON)
        Myassembly.translate(instanceList=('Part-3b-2', ), vector=(-P1h/2+b1, (h-(P2h/2)), -(P1b/2)))

        if (joint ==1):
            #part 6-1
            Mypart6a.PartitionFaceByDatumPlane(datumPlane=Mypart6a.datums[2], faces=Mypart6a.faces.findAt(((P4h/4, 0.0, P4b/4), )))
            Myassembly.Instance(dependent=ON, name='Part-6a-1', part=Mypart6a)
            Mymodel.Tie(adjust=ON, master=Region(edges=Myassembly.instances['Part-4-1'].edges.findAt(((-(P4h/2)+b1+b2, h+(P5h/2), P4b/4), ), (((P4h/2)+b1+b2, h+(P5h/2), P4b/4), ), ((-(P4h/2)+b1+b2, h+(P5h/2), -P4b/4), ), (((P4h/2)+b1+b2, h+(P5h/2), -P4b/4), ), ((b1+b2, h+(P5h/2), 0.0), ), )), name='Tie_C_a', positionToleranceMethod=COMPUTED, slave=Region(edges=Myassembly.instances['Part-6a-1'].edges.findAt(((0.0, 0.0, P4b/4), ), ((P4h, 0.0, P4b/4), ), ((0.0, 0.0, P4b/4*3), ), ((P4h, 0.0, P4b/4*3), ), ((P4h/2, 0.0, P4b/2), ), )), thickness=ON, tieRotations=ON)
            Myassembly.translate(instanceList=('Part-6a-1', ), vector=(-P4h/2+b1+b2, (h+(P5h/2)), -(P4b/2)))

        elif (joint ==2):
            #part 6-1
            Mypart6a.PartitionFaceByDatumPlane(datumPlane=Mypart6a.datums[2], faces=Mypart6a.faces.findAt(((P4h/4, 0.0, P4b/4), )))
            Myassembly.Instance(dependent=ON, name='Part-6a-1', part=Mypart6a)
            Mymodel.Tie(adjust=ON, master=Region(edges=Myassembly.instances['Part-4-1'].edges.findAt(((-(P4h/2)+b1+b2, h+(P5h/2), P4b/4), ), (((P4h/2)+b1+b2, h+(P5h/2), P4b/4), ), ((-(P4h/2)+b1+b2, h+(P5h/2), -P4b/4), ), (((P4h/2)+b1+b2, h+(P5h/2), -P4b/4), ), ((b1+b2, h+(P5h/2), 0.0), ), )), name='Tie_C_a', positionToleranceMethod=COMPUTED, slave=Region(edges=Myassembly.instances['Part-6a-1'].edges.findAt(((0.0, 0.0, P4b/4), ), ((P4h, 0.0, P4b/4), ), ((0.0, 0.0, P4b/4*3), ), ((P4h, 0.0, P4b/4*3), ), ((P4h/2, 0.0, P4b/2), ), )), thickness=ON, tieRotations=ON)
            Myassembly.translate(instanceList=('Part-6a-1', ), vector=(-P4h/2+b1+b2, (h+(P5h/2)), -(P4b/2)))
            #part 6-2
            Mypart6b.PartitionFaceByDatumPlane(datumPlane=Mypart6b.datums[2], faces=Mypart6b.faces.findAt(((P4h/4, 0.0, P4b/4), )))
            Myassembly.Instance(dependent=ON, name='Part-6b-1', part=Mypart6b)
            Mymodel.Tie(adjust=ON, master=Region(edges=Myassembly.instances['Part-4-1'].edges.findAt(((-(P4h/
```

```
            2)+b1+b2, h-(P5h/2), P4b/4), ), (((P4h/2)+b1+b2, h-(P5h/2), P4b/4), ), ((-(P4h/2)+b1+b2, h-(P5h/2
            ), -P4b/4), ), (((P4h/2)+b1+b2, h-(P5h/2), -P4b/4), ), ((b1+b2, h-(P5h/2), 0.0), ), )), name=
            'Tie_C_b', positionToleranceMethod=COMPUTED, slave=Region(edges=Myassembly.instances['Part-6b-1'
            ].edges.findAt(((0.0, 0.0, P4b/4), ), ((P4h, 0.0, P4b/4), ), ((0.0, 0.0, P4b/4*3), ), ((P4h, 0.0,
             P4b/4*3), ), ((P4h/2, 0.0, P4b/2), ), )), thickness=ON, tieRotations=ON)
297         Myassembly.translate(instanceList=('Part-6b-1', ), vector=(-P4h/2+b1+b2, (h-(P5h/2)), -(P4b/2)))

298
299     #interaction
300         #reference points
301     Myassembly.ReferencePoint(point=(0.0, h, 0.0))
302     Myassembly.ReferencePoint(point=(b1, h, 0.0))
303     Myassembly.ReferencePoint(point=(b1+b2, h, 0.0))
304         #part 1-1 with 2-1
305     Myassembly.translate(instanceList=('Part-2-1', ), vector=(0.0, 1000.0, 0.0))
306     Mymodel.Tie(adjust=ON, master=Region(faces=Myassembly.instances['Part-1-1'].faces.findAt(((P1h/2, h,
        P1b/4), ), ((P1h/2, h, -P1b/4), ), )), name='Constraint-7', positionToleranceMethod=COMPUTED, slave=
        Region(edges=Myassembly.instances['Part-2-1'].edges.findAt(((P1h/2, h+P2h/2+1000, P2b/4), ), ((P1h/2,
         h+P2h/2+1000, -P2b/4), ), ((P1h/2, h-P2h/2+1000, P2b/4), ), ((P1h/2, h-P2h/2+1000, -P2b/4), ), ((P1h
        /2, h+1000, 0.0), ), )), thickness=ON, tieRotations=ON)
307     Myassembly.translate(instanceList=('Part-2-1', ), vector=(0.0, -1000.0, 0.0))
308
309        #part 1-2 with 2-1
310     Myassembly.translate(instanceList=('Part-2-1', ), vector=(0.0, 1000.0, 0.0))
311     Mymodel.Tie(adjust=ON, master=Region(faces=Myassembly.instances['Part-1-2'].faces.findAt(((b1-P1h/2,
        h, P1b/4), ), ((b1-P1h/2, h, -P1b/4), ), )), name='Constraint-8', positionToleranceMethod=COMPUTED,
        slave=Region(edges=Myassembly.instances['Part-2-1'].edges.findAt(((b1-P1h/2, h-P2h/2+1000, -P1b/4),
        ), ((b1-P1h/2, h-P2h/2+1000, P1b/4), ), ((b1-P1h/2, h+1000, 0.0), ), ((b1-P1h/2, h+P2h/2+1000, P1b/4
        ), ), ((b1-P1h/2, h+P2h/2+1000, -P1b/4), ), )), thickness=ON, tieRotations=ON)
312     Myassembly.translate(instanceList=('Part-2-1', ), vector=(0.0, -1000.0, 0.0))
313
314         #part 1-2 with 5-1
315     Mypart5.PartitionEdgeByPoint(edge=Mypart5.edges.findAt((b1+P1h/2, h, 0.0), ), point=Mypart5.
        InterestingPoint(Mypart5.edges.findAt((b1+P1h/2, h, 0.0), ), MIDDLE))
316     Myassembly.translate(instanceList=('Part-5-1', ), vector=(0.0, 1000.0, 0.0))
317     Mymodel.Coupling(controlPoint=Region(vertices=Myassembly.instances['Part-5-1'].vertices.findAt(((b1+
        P1h/2, h+1000, 0.0), ))), couplingType=KINEMATIC, influenceRadius=WHOLE_SURFACE, localCsys=None, name
        ='Constraint-9', surface=Region(edges=Myassembly.instances['Part-5-1'].edges.findAt(((b1+P1h/2, h+P5h
        /2+1000, P5b/4), ), ((b1+P1h/2, h+P5h/2+1000, -P5b/4), ), ((b1+P1h/2, h-P5h/2+1000, P5b/4), ), ((b1+
        P1h/2, h-P5h/2+1000, -P5b/4), ), ((b1+P1h/2, h+P5h/4+1000, 0.0), ), ((b1+P1h/2, h-P5h/4+1000, 0.0),
        ), )), u1=ON, u2=ON, u3=ON, ur1=ON, ur2=ON, ur3=ON)
318     Mymodel.Tie(adjust=ON, master=Region(faces=Myassembly.instances['Part-1-2'].faces.findAt(((b1+P1h/2,
        h, P1b/4), ), ((b1+P1h/2, h, -P1b/4), ), )), name='Constraint-10', positionToleranceMethod=COMPUTED,
        slave=Region(vertices=Myassembly.instances['Part-5-1'].vertices.findAt(((b1+P1h/2, h+1000, 0.0), ))),
         thickness=ON, constraintRatio=10000.0, constraintRatioMethod=SPECIFIED, tieRotations=OFF)
319     Myassembly.translate(instanceList=('Part-5-1', ), vector=(0.0, -1000.0, 0.0))
320
321         #part 4-1 with 5-1
322     if (joint ==1):
323         Mypart5.PartitionEdgeByPoint(edge=Mypart5.edges.findAt((b1+b2-P4h/2, h, 0.0), ), point=Mypart5.
            InterestingPoint(Mypart5.edges.findAt((b1+b2-P4h/2, h, 0.0), ), MIDDLE))
324         Myassembly.translate(instanceList=('Part-5-1', ), vector=(0.0, 1000.0, 0.0))
325         Mymodel.Coupling(controlPoint=Region(vertices=Myassembly.instances['Part-5-1'].vertices.findAt(((
            b1+b2-P4h/2, h+1000, 0.0), ))), couplingType=KINEMATIC, influenceRadius=WHOLE_SURFACE, localCsys=
            None, name='Constraint-11', surface=Region(edges=Myassembly.instances['Part-5-1'].edges.findAt(((
            b1+b2-P4h/2, h+P5h/2+1000, P5b/4), ), ((b1+b2-P4h/2, h+P5h/2+1000, -P5b/4), ), ((b1+b2-P4h/2, h-
            P5h/2+1000, P5b/4), ), ((b1+b2-P4h/2, h-P5h/2+1000, -P5b/4), ), ((b1+b2-P4h/2, h+P5h/4+1000, 0.0
            ), ), ((b1+b2-P4h/2, h-P5h/4+1000, 0.0), ), )), u1=ON, u2=ON, u3=ON, ur1=ON, ur2=ON, ur3=ON)
326         Mymodel.Tie(adjust=ON, constraintRatio=10000.0, constraintRatioMethod=SPECIFIED, master=Region(
            faces=Myassembly.instances['Part-4-1'].faces.findAt(((b1+b2-P4h/2, h, P4b/4), ), ((b1+b2-P4h/2, h
            , -P4b/4), ), )), name='Constraint-12', positionToleranceMethod=COMPUTED, slave=Region(vertices=
            Myassembly.instances['Part-5-1'].vertices.findAt(((b1+b2-P4h/2, h+1000, 0.0), ))), thickness=ON,
            tieRotations=OFF)
327         Myassembly.translate(instanceList=('Part-5-1', ), vector=(0.0, -1000.0, 0.0))
328     elif (joint ==2):
329         Mymodel.Tie(adjust=ON, master=Region(faces=Myassembly.instances['Part-4-1'].faces.findAt(((b1+b2-
            P4h/2, h, P4b/4), ), ((b1+b2-P4h/2, h, -P4b/4), ), )), name='Constraint-11',
            positionToleranceMethod=COMPUTED, slave=Region(edges=Myassembly.instances['Part-5-1'].edges.
            findAt(((b1+b2-P4h/2, h+P5h/2, P5b/4), ), ((b1+b2-P4h/2, h+P5h/2, -P5b/4), ), ((b1+b2-P4h/2, h-
            P5h/2, P5b/4), ), ((b1+b2-P4h/2, h, 0.0), ),(( b1+b2-P4h/2, h-P5h/2, -P5b/4), ), )), thickness=ON
            , tieRotations=ON)
330
331     #coupling refference points
332     if (joint ==1):
333         Mymodel.Coupling(controlPoint=Region(referencePoints=(Myassembly.referencePoints[32], )),
            couplingType=KINEMATIC, influenceRadius=WHOLE_SURFACE, localCsys=None, name='Constraint-16',
            surface=Region(side1Faces=Myassembly.instances['Part-1-1'].faces.findAt(((P1h/4, h, 0.0), (0.0,
            0.0, 1.0)), ((-P1h/4, h, 0.0), (0.0, 0.0, 1.0)), )), u1=ON, u2=ON, u3=ON, ur1=ON, ur2=ON, ur3=ON)
334         Mymodel.Coupling(controlPoint=Region(referencePoints=(Myassembly.referencePoints[33], )),
            couplingType=KINEMATIC, influenceRadius=WHOLE_SURFACE, localCsys=None, name='Constraint-17',
            surface=Region(side1Faces=Myassembly.instances['Part-1-2'].faces.findAt(((b1+P1h/4, h, 0.0), (0.0
            , 0.0, 1.0)), ((b1-P1h/4, h, 0.0), (0.0, 0.0, 1.0)), )), u1=ON, u2=ON, u3=ON, ur1=ON, ur2=ON, ur3
            =ON)
335         Mymodel.Coupling(controlPoint=Region(referencePoints=(Myassembly.referencePoints[34], )),
            couplingType=KINEMATIC, influenceRadius=WHOLE_SURFACE, localCsys=None, name='Constraint-18',
            surface=Region(side1Faces=Myassembly.instances['Part-4-1'].faces.findAt(((b1+b2+P4h/4, h, 0.0), (
```

```
            0.0, 0.0, 1.0)), ((b1+b2-P4h/4, h, 0.0), (0.0, 0.0, 1.0)), )), u1=ON, u2=ON, u3=ON, ur1=ON, ur2=
            ON, ur3=ON)
        elif (joint ==2):
            Mymodel.Coupling(controlPoint=Region(referencePoints=(Myassembly.referencePoints[36], )),
            couplingType=KINEMATIC, influenceRadius=WHOLE_SURFACE, localCsys=None, name='Constraint-16',
            surface=Region(side1Faces=Myassembly.instances['Part-1-1'].faces.findAt(((P1h/4, h, 0.0), (0.0,
            0.0, 1.0)), ((-P1h/4, h, 0.0), (0.0, 0.0, 1.0)), )), u1=ON, u2=ON, u3=ON, ur1=ON, ur2=ON, ur3=ON)
            Mymodel.Coupling(controlPoint=Region(referencePoints=(Myassembly.referencePoints[37], )),
            couplingType=KINEMATIC, influenceRadius=WHOLE_SURFACE, localCsys=None, name='Constraint-17',
            surface=Region(side1Faces=Myassembly.instances['Part-1-2'].faces.findAt(((b1+P1h/4, h, 0.0), (0.0
            , 0.0, 1.0)), ((b1-P1h/4, h, 0.0), (0.0, 0.0, 1.0)), )), u1=ON, u2=ON, u3=ON, ur1=ON, ur2=ON, ur3
            =ON)
            Mymodel.Coupling(controlPoint=Region(referencePoints=(Myassembly.referencePoints[38], )),
            couplingType=KINEMATIC, influenceRadius=WHOLE_SURFACE, localCsys=None, name='Constraint-18',
            surface=Region(side1Faces=Myassembly.instances['Part-4-1'].faces.findAt(((b1+b2+P4h/4, h, 0.0), (
            0.0, 0.0, 1.0)), ((b1+b2-P4h/4, h, 0.0), (0.0, 0.0, 1.0)), )), u1=ON, u2=ON, u3=ON, ur1=ON, ur2=
            ON, ur3=ON)

        #cross-sections
            #part 1
        Mymodel.HomogeneousShellSection(idealization=NO_IDEALIZATION, integrationRule=SIMPSON, material=
        'Steel', name='P1tf', numIntPts=5, poissonDefinition=DEFAULT, preIntegrate=OFF, temperature=GRADIENT,
         thickness=P1tf, thicknessField='', thicknessModulus=None, thicknessType=UNIFORM, useDensity=OFF)
        Mymodel.HomogeneousShellSection(idealization=NO_IDEALIZATION, integrationRule=SIMPSON, material=
        'Steel', name='P1tw', numIntPts=5, poissonDefinition=DEFAULT, preIntegrate=OFF, temperature=GRADIENT,
         thickness=P1tw, thicknessField='', thicknessModulus=None, thicknessType=UNIFORM, useDensity=OFF)
            #part 2
        Mymodel.HomogeneousShellSection(idealization=NO_IDEALIZATION, integrationRule=SIMPSON, material=
        'Steel', name='P2tf', numIntPts=5, poissonDefinition=DEFAULT, preIntegrate=OFF, temperature=GRADIENT,
         thickness=P2tf, thicknessField='', thicknessModulus=None, thicknessType=UNIFORM, useDensity=OFF)
        Mymodel.HomogeneousShellSection(idealization=NO_IDEALIZATION, integrationRule=SIMPSON, material=
        'Steel', name='P2tw', numIntPts=5, poissonDefinition=DEFAULT, preIntegrate=OFF, temperature=GRADIENT,
         thickness=P2tw, thicknessField='', thicknessModulus=None, thicknessType=UNIFORM, useDensity=OFF)
            #part 4
        Mymodel.HomogeneousShellSection(idealization=NO_IDEALIZATION, integrationRule=SIMPSON, material=
        'Steel leaning column', name='P4tf', numIntPts=5, poissonDefinition=DEFAULT, preIntegrate=OFF,
        temperature=GRADIENT, thickness=P4tf, thicknessField='', thicknessModulus=None, thicknessType=UNIFORM
        , useDensity=OFF)
        Mymodel.HomogeneousShellSection(idealization=NO_IDEALIZATION, integrationRule=SIMPSON, material=
        'Steel leaning column', name='P4tw', numIntPts=5, poissonDefinition=DEFAULT, preIntegrate=OFF,
        temperature=GRADIENT, thickness=P4tw, thicknessField='', thicknessModulus=None, thicknessType=UNIFORM
        , useDensity=OFF)
            #part 5
        Mymodel.HomogeneousShellSection(idealization=NO_IDEALIZATION, integrationRule=SIMPSON, material=
        'Steel', name='P5tf', numIntPts=5, poissonDefinition=DEFAULT, preIntegrate=OFF, temperature=GRADIENT,
         thickness=P5tf, thicknessField='', thicknessModulus=None, thicknessType=UNIFORM, useDensity=OFF)
        Mymodel.HomogeneousShellSection(idealization=NO_IDEALIZATION, integrationRule=SIMPSON, material=
        'Steel', name='P5tw', numIntPts=5, poissonDefinition=DEFAULT, preIntegrate=OFF, temperature=GRADIENT,
         thickness=P5tw, thicknessField='', thicknessModulus=None, thicknessType=UNIFORM, useDensity=OFF)

        #section assignment
            #part 1
                #bottom flange
        Mypart1.SectionAssignment(offset=0.0, offsetField='', offsetType=BOTTOM_SURFACE, region=Region(faces=
        Mypart1.faces.findAt(((P1h/2, h/4, -P1b/4), ), ((P1h/2, h, P1b/4), ), ((P1h/2, h, -P1b/4), ), ((P1h/2
        , h/4, P1b/4), ), )), sectionName='P1tf', thicknessAssignment=FROM_SECTION)
                #top flange
        Mypart1.SectionAssignment(offset=0.0, offsetField='', offsetType=TOP_SURFACE, region=Region(faces=
        Mypart1.faces.findAt(((-P1h/2, h/4, -P1b/4), ), ((-P1h/2, h, P1b/4), ), ((-P1h/2, h, -P1b/4), ), ((-
        P1h/2, h/4, P1b/4), ), )), sectionName='P1tf', thicknessAssignment=FROM_SECTION)
                #web
        Mypart1.SectionAssignment(offset=0.0, offsetField='', offsetType=MIDDLE_SURFACE, region=Region(faces=
        Mypart1.faces.findAt(((0.0, h/4, 0.0), ), ((0, h, 0.0), ), )), sectionName='P1tw',
        thicknessAssignment=FROM_SECTION)

            #part 2
                #bottom flange
        Mypart2.SectionAssignment(offset=0.0, offsetField='', offsetType=BOTTOM_SURFACE, region=Region(faces=
        Mypart2.faces.findAt(((b1/2, h-(P2h/2), -P2b/4), ), ((b1/2, h-(P2h/2), P2b/4), ), )), sectionName=
        'P2tf', thicknessAssignment=FROM_SECTION)
                #top flange
        Mypart2.SectionAssignment(offset=0.0, offsetField='', offsetType=TOP_SURFACE, region=Region(faces=
        Mypart2.faces.findAt(((b1/2, h+(P2h/2), -P2b/4), ), ((b1/2, h+(P2h/2), P2b/4), ), )), sectionName=
        'P2tf', thicknessAssignment=FROM_SECTION)
                #web
        Mypart2.SectionAssignment(offset=0.0, offsetField='', offsetType=MIDDLE_SURFACE, region=Region(faces=
        Mypart2.faces.findAt(((b1/2, h, 0.0), ))), sectionName='P2tw', thicknessAssignment=FROM_SECTION)

            #part 3a
        Mypart3a.SectionAssignment(offset=0.0, offsetField='', offsetType=TOP_SURFACE, region=Region(faces=
        Mypart3a.faces.getByBoundingBox(0.0, 0.0, 0.0, P1h, 0.0, P1b)), sectionName='P2tf',
        thicknessAssignment=FROM_SECTION)
            #part 3b
        Mypart3b.SectionAssignment(offset=0.0, offsetField='', offsetType=BOTTOM_SURFACE, region=Region(faces
        =Mypart3b.faces.getByBoundingBox(0.0, 0.0, 0.0, P1h, 0.0, P1b)), sectionName='P2tf',
        thicknessAssignment=FROM_SECTION)
```

```
376
377             #part 4
378                 #bottom flange
379         Mypart4.SectionAssignment(offset=0.0, offsetField='', offsetType=BOTTOM_SURFACE, region=Region(faces=
            Mypart4.faces.findAt(((b1+b2-P4h/2, h/4, -P4b/4), ), ((b1+b2-P4h/2, h, P4b/4), ), ((b1+b2-P4h/2, h/4,
             P4b/4), ), ((b1+b2-P4h/2, h, -P4b/4), ), )), sectionName='P4tf', thicknessAssignment=FROM_SECTION)
380                 #top flange
381         Mypart4.SectionAssignment(offset=0.0, offsetField='', offsetType=TOP_SURFACE, region=Region(faces=
            Mypart4.faces.findAt(((b1+b2+P4h/2, h/4, -P4b/4), ), ((b1+b2+P4h/2, h/4, P4b/4), ), ((b1+b2+P4h/2, h,
             P4b/4), ), ((b1+b2+P4h/2, h, -P4b/4), ), )), sectionName='P4tf', thicknessAssignment=FROM_SECTION)
382                 #web
383         Mypart4.SectionAssignment(offset=0.0, offsetField='', offsetType=MIDDLE_SURFACE, region=Region(faces=
            Mypart4.faces.findAt(((b1+b2, h, 0.0), ), ((b1+b2, h/4, 0.0), ), )), sectionName='P4tw',
            thicknessAssignment=FROM_SECTION)
384
385             #part 5
386                 #bottom flange
387         Mypart5.SectionAssignment(offset=0.0, offsetField='', offsetType=BOTTOM_SURFACE, region=Region(faces=
            Mypart5.faces.findAt(((b1+b2/2, h-P5h/2, P5b/4), ), ((b1+b2/2, h-P5h/2, -P5b/4), ), )), sectionName=
            'P5tf', thicknessAssignment=FROM_SECTION)
388                 #top flange
389         Mypart5.SectionAssignment(offset=0.0, offsetField='', offsetType=TOP_SURFACE, region=Region(faces=
            Mypart5.faces.findAt(((b1+b2/2, h+P5h/2, P5b/4), ), ((b1+b2/2, h+P5h/2, -P5b/4), ), )), sectionName=
            'P5tf', thicknessAssignment=FROM_SECTION)
390                 #web
391         Mypart5.SectionAssignment(offset=0.0, offsetField='', offsetType=MIDDLE_SURFACE, region=Region(faces=
            Mypart5.faces.findAt(((b1+b2/2, h, 0.0), ))), sectionName='P5tw', thicknessAssignment=FROM_SECTION)
392
393             #part 6a
394         if (joint==1):
395             #part 6a
396             Mypart6a.SectionAssignment(offset=0.0, offsetField='', offsetType=TOP_SURFACE, region=Region(
                faces=Mypart6a.faces.getByBoundingBox(0.0, 0.0, 0.0, P4h, 0.0, P4b)), sectionName='P5tf',
                thicknessAssignment=FROM_SECTION)
397         elif (joint ==2):
398             #part 6a
399             Mypart6a.SectionAssignment(offset=0.0, offsetField='', offsetType=TOP_SURFACE, region=Region(
                faces=Mypart6a.faces.getByBoundingBox(0.0, 0.0, 0.0, P4h, 0.0, P4b)), sectionName='P5tf',
                thicknessAssignment=FROM_SECTION)
400             #part 6b
401             Mypart6b.SectionAssignment(offset=0.0, offsetField='', offsetType=BOTTOM_SURFACE, region=Region(
                faces=Mypart6b.faces.getByBoundingBox(0.0, 0.0, 0.0, P4h, 0.0, P4b)), sectionName='P5tf',
                thicknessAssignment=FROM_SECTION)
402
403         #material
404         Mymodel.Material(name='Steel')
405         Mymodel.materials['Steel'].Elastic(table=((E, pois), ))
406         Mymodel.Material(name='Steel leaning column')
407         Mymodel.materials['Steel leaning column'].Elastic(table=(((Q/F)*E, pois), ))
408
409         #geometry partition adjustment
410                 #part 1
411         Mypart1.PartitionEdgeByPoint(edge=Mypart1.edges.findAt((0.0, 0.0, 0.0), ), point=Mypart1.
            InterestingPoint(Mypart1.edges.findAt((0.0, 0.0, 0.0), ), MIDDLE))
412
413                 #part 4
414         Mypart4.PartitionEdgeByPoint(edge=Mypart4.edges.findAt((b1+b2, 0.0, 0.0), ), point=Mypart4.
            InterestingPoint(Mypart4.edges.findAt((b1+b2, 0.0, 0.0), ), MIDDLE))
415
416         #sets
417             #set 1
418         if (joint ==1):
419             Myassembly.Set(name='top_nodes', referencePoints=(Myassembly.referencePoints[32], Myassembly.
                referencePoints[33], Myassembly.referencePoints[34]))
420         elif (joint==2):
421             Myassembly.Set(name='top_nodes', referencePoints=(Myassembly.referencePoints[36], Myassembly.
                referencePoints[37], Myassembly.referencePoints[38]))
422             #set 2
423         Myassembly.Set(name='bottom_nodes', vertices=Myassembly.instances['Part-1-1'].vertices.findAt(((0.0,
            0.0, 0.0), ), )+Myassembly.instances['Part-1-2'].vertices.findAt(((b1, 0.0, 0.0), ), )+Myassembly.
            instances['Part-4-1'].vertices.findAt(((b1+b2, 0.0, 0.0), ), ))
424
425         #interactions and couplings
426             #coupling column A
427         Mymodel.Coupling(controlPoint=Region(vertices=Myassembly.instances['Part-1-1'].vertices.findAt(((0.0,
             0.0, 0.0), ))), couplingType=KINEMATIC, influenceRadius=WHOLE_SURFACE, localCsys=None, name=
            'Constraint-13', surface=Region(edges=Myassembly.instances['Part-1-1'].edges.findAt(((-P1h/2, 0.0, -
            P1b/4), ), ((P1h/2, 0.0, -P1b/4), ), ((P1h/2, 0.0, P1b/4), ), ((-P1h/2, 0.0, P1b/4), ), ((-P1h/4, 0.0
            , 0.0), ), ((P1h/4, 0.0, 0.0), ), )), u1=ON, u2=ON, u3=ON, ur1=ON, ur2=ON, ur3=ON)
428             #coupling column B
429         Mymodel.Coupling(controlPoint=Region(vertices=Myassembly.instances['Part-1-2'].vertices.findAt(((b1,
            0.0, 0.0), ))), couplingType=KINEMATIC, influenceRadius=WHOLE_SURFACE, localCsys=None, name=
            'Constraint-14', surface=Region(edges=Myassembly.instances['Part-1-2'].edges.findAt(((b1-P1h/2, 0.0,
            -P1b/4), ), ((b1+P1h/2, 0.0, -P1b/4), ), ((b1+P1h/2, 0.0, P1b/4), ), ((b1-P1h/2, 0.0, P1b/4), ), ((b1
```

```
-P1h/4, 0.0, 0.0), ), ((b1+P1h/4, 0.0, 0.0), ), )), u1=ON, u2=ON, u3=ON, ur1=ON, ur2=ON, ur3=ON)
    #coupling column C
Mymodel.Coupling(controlPoint=Region(vertices=Myassembly.instances['Part-4-1'].vertices.findAt(((b1+
b2, 0.0, 0.0), ))), couplingType=KINEMATIC, influenceRadius=WHOLE_SURFACE, localCsys=None, name=
'Constraint-15', surface=Region(edges=Myassembly.instances['Part-4-1'].edges.findAt(((b1+b2-P4h/2,
0.0, -P4b/4), ), ((b1+b2+P4h/2, 0.0, -P4b/4), ), ((b1+b2+P4h/2, 0.0, P4b/4), ), ((b1+b2-P4h/2, 0.0,
P4b/4), ), ((b1+b2-P4h/4, 0.0, 0.0), ), ((b1+b2+P4h/4, 0.0, 0.0), ), )), u1=ON, u2=ON, u3=ON, ur1=ON,
 ur2=ON, ur3=ON)

#boundary condition
    #stabilizing frame
if (condition == 1):
    Mymodel.PinnedBC(createStepName='Initial', localCsys=None, name='BC-1', region=Region(vertices=
    Myassembly.instances['Part-1-1'].vertices.findAt(((0.0, 0.0, 0.0), ), )+Myassembly.instances[
    'Part-1-2'].vertices.findAt(((b1, 0.0, 0.0), ), )))
elif (condition ==2):
    Mymodel.EncastreBC(createStepName='Initial', localCsys=None, name='BC-1', region=Region(vertices=
    Myassembly.instances['Part-1-1'].vertices.findAt(((0.0, 0.0, 0.0), ), )+Myassembly.instances[
    'Part-1-2'].vertices.findAt(((b1, 0.0, 0.0), ), )))
    #leaning column
Mymodel.PinnedBC(createStepName='Initial', localCsys=None, name='BC-2', region=Region(vertices=
Myassembly.instances['Part-4-1'].vertices.findAt(((b1+b2, 0.0, 0.0), ))))
    #Z-direction
Mymodel.DisplacementBC(amplitude=UNSET, createStepName='Initial', distributionType=UNIFORM, fieldName
='', localCsys=None, name='BC-3', region=Region(faces=Myassembly.instances['Part-1-1'].faces.findAt
(((P1h/4, h, 0.0), (0.0, 0.0, 1.0)), ((-P1h/4, h, 0.0), (0.0, 0.0, 1.0)), ((0.0, h/4, 0.0), (0.0, 0.0
, 1.0)), )+Myassembly.instances['Part-2-1'].faces.findAt(((b1/2, h, 0.0), (0.0, 0.0, 1.0)), )+
Myassembly.instances['Part-1-2'].faces.findAt(((b1+P1h/4, h, 0.0), (0.0, 0.0, 1.0)), ((b1-P1h/4, h,
0.0), (0.0, 0.0, 1.0)), ((b1, h/4, 0.0), (0.0, 0.0, 1.0)), )+Myassembly.instances['Part-5-1'].faces.
findAt(((b1+b2/2, h, 0.0), (0.0, 0.0, 1.0)), )+Myassembly.instances['Part-4-1'].faces.findAt(((b1+b2+
P4h/4, h, 0.0), (0.0, 0.0, 1.0)), ((b1+b2-P4h/4, h, 0.0), (0.0, 0.0, 1.0)), ((b1+b2, h/4, 0.0), (0.0,
 0.0, 1.0)), )), u1=UNSET, u2=UNSET, u3=SET, ur1=UNSET, ur2=UNSET, ur3=UNSET)

#step
Mymodel.BuckleStep(maxIterations=2000, name='Step-1', numEigen=350, previous='Initial', vectors=600)

#vertical load
if (joint ==1):
    Mymodel.ConcentratedForce(cf2=-F, createStepName='Step-1', distributionType=UNIFORM, field='',
    localCsys=None, name='VERT_F', region=Region(referencePoints=(Myassembly.referencePoints[32],
    Myassembly.referencePoints[33], )))
    Mymodel.ConcentratedForce(cf2=-Q, createStepName='Step-1', distributionType=UNIFORM, field='',
    localCsys=None, name='VERT_Q', region=Region(referencePoints=(Myassembly.referencePoints[34], )))
elif (joint==2):
    Mymodel.ConcentratedForce(cf2=-F, createStepName='Step-1', distributionType=UNIFORM, field='',
    localCsys=None, name='VERT_F', region=Region(referencePoints=(Myassembly.referencePoints[36],
    Myassembly.referencePoints[37], )))
    Mymodel.ConcentratedForce(cf2=-Q, createStepName='Step-1', distributionType=UNIFORM, field='',
    localCsys=None, name='VERT_Q', region=Region(referencePoints=(Myassembly.referencePoints[38], )))


#mesh
    #part 1
        #y-direction
            #top
Mypart1.seedEdgeBySize(constraint=FINER, deviationFactor=0.1, edges=Mypart1.edges.findAt(((-P1h/2, h,
 0.0), ), ((-P1h/2, h, P1b/2), ), ((P1h/2, h, 0.0), ), ((-P1h/2, h, -P1b/2), ), ((P1h/2, h, P1b/2),
), ((P1h/2, h, -P1b/2), ), ), size=P2sy)
            #bottom
Mypart1.seedEdgeBySize(constraint=FINER, deviationFactor=0.1, edges=Mypart1.edges.findAt(((-P1h/2, h/
4, 0.0), ), ((-P1h/2, h/4, -P1b/2), ), ((P1h/2, h/4, 0.0), ), ((P1h/2, h/4, -P1b/2), ), ((P1h/2, h/4,
 P1b/2), ), ((-P1h/2, h/4, P1b/2), ), ), size=P1sy)
        #x-direction
Mypart1.seedEdgeBySize(constraint=FINER, deviationFactor=0.1, edges=Mypart1.edges.findAt(((-P1h/4, h-
P2h/2, 0.0), ), ((P1h/4, h+P2h/2, 0.0), ), ((-P1h/4, 0.0, 0.0), ), ((P1h/4, 0.0, 0.0), ), ), size=
P1sx)
        #z-direction
Mypart1.seedEdgeBySize(constraint=FINER, deviationFactor=0.1, edges=Mypart1.edges.findAt(((-P1h/2, h-
P2h/2, -P1b/4), ), ((-P1h/2, 0.0, -P1b/4), ), ((-P1h/2, h-P2h/2, P1b/4), ), ((-P1h/2, h+P2h/2, P1b/4
), ), ((P1h/2, h-P2h/2, -P1b/4), ), ((P1h/2, 0.0, -P1b/4), ), ((P1h/2, h-P2h/2, P1b/4), ), ((P1h/2,
0.0, P1b/4), ), ((-P1h/2, 0.0, P1b/4), ), ((-P1h/2, h+P2h/2, -P1b/4), ), ((P1h/2, h+P2h/2, P1b/4), ),
 ((P1h/2, h+P2h/2, -P1b/4), ), ), size=P1sz)
        #mesh settings
Mypart1.setMeshControls(elemShape=QUAD_DOMINATED, regions=Mypart1.faces.getByBoundingBox(-P1h/2, 0.0,
 -P1b/2, P1h/2, h+P2h/2, P1b/2), technique=FREE)
Mypart1.setElementType(elemTypes=(ElemType(elemCode=S4, elemLibrary=STANDARD, secondOrderAccuracy=OFF
), ElemType(elemCode=S3, elemLibrary=STANDARD)), regions=(Mypart1.faces.getByBoundingBox(-P1h/2, 0.0,
 -P1b/2, P1h/2, h+P2h/2, P1b/2), ))
Mypart1.generateMesh()
    #part 2
        #y-direction
Mypart2.seedEdgeBySize(constraint=FINER, deviationFactor=0.1, edges=Mypart2.edges.findAt(((b1-P1h/2,
h, 0.0), ), ((P1h/2, h, 0.0), ), ), size=P2sy)
        #x-direction
Mypart2.seedEdgeBySize(constraint=FINER, deviationFactor=0.1, edges=Mypart2.edges.findAt(((b1/4, h+
P2h/2, 0.0), ), ((b1/4, h+P2h/2, P2b/2), ), ((b1/4, h+P2h/2, -P2b/2), ), ((b1/4, h-P2h/2, 0.0), ), ((
```

```
        b1/4, h-P2h/2, P2b/2), ), ((b1/4, h-P2h/2, -P2b/2), ), ), size=P2sx)
475             #z-direction
476     Mypart2.seedEdgeBySize(constraint=FINER, deviationFactor=0.1, edges=Mypart2.edges.findAt(((b1-P1h/2,
        h+P2h/2, P2b/4), ), ((P1h/2, h+P2h/2, P2b/4), ), ((P1h/2, h+P2h/2, -P2b/4), ), ((b1-P1h/2, h+P2h/2, -
        P2b/4), ), ((b1-P1h/2, h-P2h/2, P2b/4), ), ((P1h/2, h-P2h/2, P2b/4), ), ((P1h/2, h-P2h/2, -P2b/4), ),
         ((b1-P1h/2, h-P2h/2, -P2b/4), ), ((b1-P1h/2, h+P2h/2, P2b/8), ), ((P1h/2, h+P2h/2, P2b/8), ), ((P1h/
        2, h+P2h/2, -P2b/8), ), ((b1-P1h/2, h+P2h/2, -P2b/8), ), ((b1-P1h/2, h-P2h/2, P2b/8), ), ((P1h/2, h-
        P2h/2, P2b/8), ), ((P1h/2, h-P2h/2, -P2b/8), ), ((b1-P1h/2, h-P2h/2, -P2b/8), ), ), size=P2sz)
477             #mesh settings
478     Mypart2.setMeshControls(elemShape=QUAD_DOMINATED, regions=Mypart2.faces.getByBoundingBox(P1h/2, h-P2h
        /2, -P2b/2, b1-P1h/2, h+P2h/2, P2b/2), technique=FREE)
479     Mypart2.setElementType(elemTypes=(ElemType(elemCode=S4, elemLibrary=STANDARD, secondOrderAccuracy=OFF
        ), ElemType(elemCode=S3, elemLibrary=STANDARD)), regions=(Mypart2.faces.getByBoundingBox(P1h/2, h-P2h
        /2, -P2b/2, b1-P1h/2, h+P2h/2, P2b/2), ))
480     Mypart2.generateMesh()
481
482         #part 3a
483             #y-direction
484
485             #x-direction
486     Mypart3a.seedEdgeBySize(constraint=FINER, deviationFactor=0.1, edges=Mypart3a.edges.findAt(((P1h/4,
        0.0, P1b), ), ((P1h/4, 0.0, 0.0), ), ((P1h/4, 0.0, P1b/2), ), ), minSizeFactor=0.1, size=P3sx)
487             #z-direction
488     Mypart3a.seedEdgeBySize(constraint=FINER, deviationFactor=0.1, edges=Mypart3a.edges.findAt(((0.0, 0.0
        , P1b/4), ), ((0.0, 0.0, P1b/4*3), ), ((P1h, 0.0, P1b/4), ), ((P1h, 0.0, P1b/4*3), ), ),
        minSizeFactor=0.1, size=P3sz)
489             #mesh settings
490     Mypart3a.setMeshControls(elemShape=QUAD_DOMINATED, regions=Mypart3a.faces.getByBoundingBox(0.0, 0.0,
        0.0, P1h, 0.0, P1b), technique=FREE)
491     Mypart3a.setElementType(elemTypes=(ElemType(elemCode=S4, elemLibrary=STANDARD, secondOrderAccuracy=
        OFF), ElemType(elemCode=S3, elemLibrary=STANDARD)), regions=(Mypart3a.faces.getByBoundingBox(0.0, 0.0
        , 0.0, P1h, 0.0, P1b), ))
492     Mypart3a.generateMesh()
493
494         #part 3b
495             #y-direction
496
497             #x-direction
498     Mypart3b.seedEdgeBySize(constraint=FINER, deviationFactor=0.1, edges=Mypart3b.edges.findAt(((P1h/4,
        0.0, P1b), ), ((P1h/4, 0.0, 0.0), ), ((P1h/4, 0.0, P1b/2), ), ), minSizeFactor=0.1, size=P3sx)
499             #z-direction
500     Mypart3b.seedEdgeBySize(constraint=FINER, deviationFactor=0.1, edges=Mypart3b.edges.findAt(((0.0, 0.0
        , P1b/4), ), ((0.0, 0.0, P1b/4*3), ), ((P1h, 0.0, P1b/4), ), ((P1h, 0.0, P1b/4*3), ), ),
        minSizeFactor=0.1, size=P3sz)
501             #mesh settings
502     Mypart3b.setMeshControls(elemShape=QUAD_DOMINATED, regions=Mypart3b.faces.getByBoundingBox(0.0, 0.0,
        0.0, P1h, 0.0, P1b), technique=FREE)
503     Mypart3b.setElementType(elemTypes=(ElemType(elemCode=S4, elemLibrary=STANDARD, secondOrderAccuracy=
        OFF), ElemType(elemCode=S3, elemLibrary=STANDARD)), regions=(Mypart3b.faces.getByBoundingBox(0.0, 0.0
        , 0.0, P1h, 0.0, P1b), ))
504     Mypart3b.generateMesh()
505
506         #part 4
507             #y-direction
508                 #top
509     Mypart4.seedEdgeBySize(constraint=FINER, deviationFactor=0.1, edges=Mypart4.edges.findAt(((b1+b2-P4h/
        2, h, 0.0), ), ((b1+b2-P4h/2, h, P4b/2), ), ((b1+b2+P4h/2, h, 0.0), ), ((b1+b2-P4h/2, h, -P4b/2), ),
        ((b1+b2+P4h/2, h, P4b/2), ), ((b1+b2+P4h/2, h, -P4b/2), ), ),size=P5sy)
510                 #bottom
511     Mypart4.seedEdgeBySize(constraint=FINER, deviationFactor=0.1, edges=Mypart4.edges.findAt(((b1+b2-P4h/
        2, h/4, 0.0), ), ((b1+b2-P4h/2, h/4, -P4b/2), ), ((b1+b2+P4h/2, h/4, 0.0), ), ((b1+b2+P4h/2, h/4, -
        P4b/2), ), ((b1+b2+P4h/2, h/4, P4b/2), ), ((b1+b2-P4h/2, h/4, P4b/2), ), ),size=P4sy)
512             #x-direction
513     Mypart4.seedEdgeBySize(constraint=FINER, deviationFactor=0.1, edges=Mypart4.edges.findAt(((b1+b2-P4h/
        4, h-P5h/2, 0.0), ), ((b1+b2+P4h/4, h+P5h/2, 0.0), ), ((b1+b2-P4h/4, 0.0, 0.0), ), ((b1+b2+P4h/4, 0.0
        , 0.0), ), ), size=P4sx)
514             #z-direction
515     Mypart4.seedEdgeBySize(constraint=FINER, deviationFactor=0.1, edges=Mypart4.edges.findAt(((b1+b2-P4h/
        2, h-P5h/2, -P4b/4), ), ((b1+b2-P4h/2, 0.0, -P4b/4), ), ((b1+b2-P4h/2, h-P5h/2, P4b/4), ), ((b1+b2-
        P4h/2, h+P5h/2, P4b/4), ), ((b1+b2+P4h/2, h-P5h/2, -P4b/4), ), ((b1+b2+P4h/2, 0.0, -P4b/4), ), ((b1+
        b2+P4h/2, h-P5h/2, P4b/4), ), ((b1+b2+P4h/2, 0.0, P4b/4), ), ((b1+b2-P4h/2, 0.0, P4b/4), ), ((b1+b2-
        P4h/2, h+P5h/2, -P4b/4), ), ((b1+b2+P4h/2, h+P5h/2, P4b/4), ), ((b1+b2+P4h/2, h+P5h/2, -P4b/4), ), ),
         size=P4sz)
516             #mesh settings
517     Mypart4.setMeshControls(elemShape=QUAD_DOMINATED, regions=Mypart4.faces.getByBoundingBox(b1+b2-P4h/2,
         0.0, -P4b/2, b1+b2+P4h/2, h+P5h/2, P4b/2), technique=FREE)
518     Mypart4.setElementType(elemTypes=(ElemType(elemCode=S4, elemLibrary=STANDARD, secondOrderAccuracy=OFF
        ), ElemType(elemCode=S3, elemLibrary=STANDARD)), regions=(Mypart4.faces.getByBoundingBox(b1+b2-P4h/2,
         0.0, -P4b/2, b1+b2+P4h/2, h+P5h/2, P4b/2), ))
519     Mypart4.generateMesh()
520
521         #part 5
522     if (joint ==1):
523             #y-direction
524         Mypart5.seedEdgeBySize(constraint=FINER, deviationFactor=0.1, edges=Mypart5.edges.findAt(((b1+b2-
        P4h/2, h+P5h/4, 0.0), ),((b1+b2-P4h/2, h-P5h/4, 0.0), ), ((b1+P1h/2, h+P5h/4, 0.0), ), ((b1+P1h/2
```

```
                , h-P5h/4, 0.0), ), ), size=P5sy)
525                 #x-direction
526             Mypart5.seedEdgeBySize(constraint=FINER, deviationFactor=0.1, edges=Mypart5.edges.findAt(((b1+b2/
                4, h+P5h/2, 0.0), ), ((b1+b2/4, h+P5h/2, P5b/2), ), ((b1+b2/4, h+P5h/2, -P5b/2), ), ((b1+b2/4, h-
                P5h/2, 0.0), ), ((b1+b2/4, h-P5h/2, P5b/2), ), ((b1+b2/4, h-P5h/2, -P5b/2), ), ), size=P5sx)
527                 #z-direction
528             Mypart5.seedEdgeBySize(constraint=FINER, deviationFactor=0.1, edges=Mypart5.edges.findAt(((b1+b2-
                P4h/2, h+P5h/2, P5b/4), ), ((b1+P1h/2, h+P5h/2, P5b/4), ), ((b1+P1h/2, h+P5h/2, -P5b/4), ), ((b1+
                b2-P4h/2, h+P5h/2, -P5b/4), ), ((b1+b2-P4h/2, h-P5h/2, P5b/4), ), ((b1+P1h/2, h-P5h/2, P5b/4), ),
                 ((b1+P1h/2, h-P5h/2, -P5b/4), ), ((b1+b2-P4h/2, h-P5h/2, -P5b/4), ), ((b1+b2-P4h/2, h+P5h/2, P5b
                /8), ), ((b1+P1h/2, h+P5h/2, P5b/8), ), ((b1+P1h/2, h+P5h/2, -P5b/8), ), ((b1+b2-P4h/2, h+P5h/2,
                -P5b/8), ), ((b1+b2-P4h/2, h-P5h/2, P5b/8), ), ((b1+P1h/2, h-P5h/2, P5b/8), ), ((b1+P1h/2, h-P5h/
                2, -P5b/8), ), ((b1+b2-P4h/2, h-P5h/2, -P5b/8), ), ), size=P5sz)
529                 #mesh settings
530             Mypart5.setMeshControls(elemShape=QUAD_DOMINATED, regions=Mypart5.faces.getByBoundingBox(b1+P1h/2
                , h-P5h/2, -P5b/2, b1+b2-P4h/2, h+P5h/2, P5b/2), technique=FREE)
531             Mypart5.setElementType(elemTypes=(ElemType(elemCode=S4, elemLibrary=STANDARD, secondOrderAccuracy
                =OFF), ElemType(elemCode=S3, elemLibrary=STANDARD)), regions=(Mypart5.faces.getByBoundingBox(b1+
                P1h/2, h-P5h/2, -P5b/2, b1+b2-P4h/2, h+P5h/2, P5b/2), ))
532             Mypart5.generateMesh()
533
534         if (joint ==2):
535                 #y-direction
536             Mypart5.seedEdgeBySize(constraint=FINER, deviationFactor=0.1, edges=Mypart5.edges.findAt(((b1+b2-
                P4h/2, h, 0.0), ), ((b1+P1h/2, h+P5h/4, 0.0), ), ((b1+P1h/2, h-P5h/4, 0.0), ), ), size=P5sy)
537                 #x-direction
538             Mypart5.seedEdgeBySize(constraint=FINER, deviationFactor=0.1, edges=Mypart5.edges.findAt(((b1+b2/
                4, h+P5h/2, 0.0), ), ((b1+b2/4, h+P5h/2, P5b/2), ), ((b1+b2/4, h+P5h/2, -P5b/2), ), ((b1+b2/4, h-
                P5h/2, 0.0), ), ((b1+b2/4, h-P5h/2, P5b/2), ), ((b1+b2/4, h-P5h/2, -P5b/2), ), ), size=P5sx)
539                 #z-direction
540             Mypart5.seedEdgeBySize(constraint=FINER, deviationFactor=0.1, edges=Mypart5.edges.findAt(((b1+b2-
                P4h/2, h+P5h/2, P5b/4), ), ((b1+P1h/2, h+P5h/2, P5b/4), ), ((b1+P1h/2, h+P5h/2, -P5b/4), ), ((b1+
                b2-P4h/2, h+P5h/2, -P5b/4), ), ((b1+b2-P4h/2, h-P5h/2, P5b/4), ), ((b1+P1h/2, h-P5h/2, P5b/4), ),
                 ((b1+P1h/2, h-P5h/2, -P5b/4), ), ((b1+b2-P4h/2, h-P5h/2, -P5b/4), ), ((b1+b2-P4h/2, h+P5h/2, P5b
                /8), ), ((b1+P1h/2, h+P5h/2, P5b/8), ), ((b1+P1h/2, h+P5h/2, -P5b/8), ), ((b1+b2-P4h/2, h+P5h/2,
                -P5b/8), ), ((b1+b2-P4h/2, h-P5h/2, P5b/8), ), ((b1+P1h/2, h-P5h/2, P5b/8), ), ((b1+P1h/2, h-P5h/
                2, -P5b/8), ), ((b1+b2-P4h/2, h-P5h/2, -P5b/8), ), ), size=P5sz)
541                 #mesh settings
542             Mypart5.setMeshControls(elemShape=QUAD_DOMINATED, regions=Mypart5.faces.getByBoundingBox(b1+P1h/2
                , h-P5h/2, -P5b/2, b1+b2-P4h/2, h+P5h/2, P5b/2), technique=FREE)
543             Mypart5.setElementType(elemTypes=(ElemType(elemCode=S4, elemLibrary=STANDARD, secondOrderAccuracy
                =OFF), ElemType(elemCode=S3, elemLibrary=STANDARD)), regions=(Mypart5.faces.getByBoundingBox(b1+
                P1h/2, h-P5h/2, -P5b/2, b1+b2-P4h/2, h+P5h/2, P5b/2), ))
544             Mypart5.generateMesh()
545
546         if (joint ==1):
547             #part 6a
548                 #y-direction
549
550                 #x-direction
551             Mypart6a.seedEdgeBySize(constraint=FINER, deviationFactor=0.1, edges=Mypart6a.edges.findAt(((P4h/
                4, 0.0, P4b), ), ((P4h/4, 0.0, 0.0), ), ((P4h/4, 0.0, P4b/2), ), ), size=P6sx)
552                 #z-direction
553             Mypart6a.seedEdgeBySize(constraint=FINER, deviationFactor=0.1, edges=Mypart6a.edges.findAt(((0.0,
                 0.0, P4b/4), ), ((0.0, 0.0, P4b/4*3), ), ((P4h, 0.0, P4b/4), ), ((P4h, 0.0, P4b/4*3), ), ), size
                =P6sz)
554                 #mesh settings
555             Mypart6a.setMeshControls(elemShape=QUAD_DOMINATED, regions=Mypart6a.faces.getByBoundingBox(0.0,
                0.0, 0.0, P4h, 0.0, P4b), technique=FREE)
556             Mypart6a.setElementType(elemTypes=(ElemType(elemCode=S4, elemLibrary=STANDARD,
                secondOrderAccuracy=OFF), ElemType(elemCode=S3, elemLibrary=STANDARD)), regions=(Mypart6a.faces.
                getByBoundingBox(0.0, 0.0, 0.0, P4h, 0.0, P4b), ))
557             Mypart6a.generateMesh()
558         elif (joint ==2):
559             #part 6a
560                 #y-direction
561
562                 #x-direction
563             Mypart6a.seedEdgeBySize(constraint=FINER, deviationFactor=0.1, edges=Mypart6a.edges.findAt(((P4h/
                4, 0.0, P4b), ), ((P4h/4, 0.0, 0.0), ), ((P4h/4, 0.0, P4b/2), ), ), size=P6sx)
564                 #z-direction
565             Mypart6a.seedEdgeBySize(constraint=FINER, deviationFactor=0.1, edges=Mypart6a.edges.findAt(((0.0,
                 0.0, P4b/4), ), ((0.0, 0.0, P4b/4*3), ), ((P4h, 0.0, P4b/4), ), ((P4h, 0.0, P4b/4*3), ), ), size
                =P6sz)
566                 #mesh settings
567             Mypart6a.setMeshControls(elemShape=QUAD_DOMINATED, regions=Mypart6a.faces.getByBoundingBox(0.0,
                0.0, 0.0, P4h, 0.0, P4b), technique=FREE)
568             Mypart6a.setElementType(elemTypes=(ElemType(elemCode=S4, elemLibrary=STANDARD,
                secondOrderAccuracy=OFF), ElemType(elemCode=S3, elemLibrary=STANDARD)), regions=(Mypart6a.faces.
                getByBoundingBox(0.0, 0.0, 0.0, P4h, 0.0, P4b), ))
569             Mypart6a.generateMesh()
570
571             #part 6b
572                 #y-direction
573
574                 #x-direction
```

```
575             Mypart6b.seedEdgeBySize(constraint=FINER, deviationFactor=0.1, edges=Mypart6b.edges.findAt(((P4h/
                4, 0.0, P4b), ), ((P4h/4, 0.0, 0.0), ), ((P4h/4, 0.0, P4b/2), ), ), size=P6sx)
576                 #z-direction
577             Mypart6b.seedEdgeBySize(constraint=FINER, deviationFactor=0.1, edges=Mypart6b.edges.findAt(((0.0,
                 0.0, P4b/4), ), ((0.0, 0.0, P4b/4*3), ), ((P4h, 0.0, P4b/4), ), ((P4h, 0.0, P4b/4*3), ), ), size
                =P6sz)
578                 #mesh settings
579             Mypart6b.setMeshControls(elemShape=QUAD_DOMINATED, regions=Mypart6b.faces.getByBoundingBox(0.0,
                0.0, 0.0, P4h, 0.0, P4b), technique=FREE)
580             Mypart6b.setElementType(elemTypes=(ElemType(elemCode=S4, elemLibrary=STANDARD,
                secondOrderAccuracy=OFF), ElemType(elemCode=S3, elemLibrary=STANDARD)), regions=(Mypart6b.faces.
                getByBoundingBox(0.0, 0.0, 0.0, P4h, 0.0, P4b), ))
581             Mypart6b.generateMesh()
582
583         #imperfection
584         Mymodel.keywordBlock.synchVersions(storeNodesAndElements=False)
585         Mymodel.keywordBlock.replace(304, '\n*Output, field, variable=PRESELECT\n*NODE FILE\nU')
586
587         #job
588         mdb.Job(atTime=None, contactPrint=OFF, description='', echoPrint=OFF, explicitPrecision=SINGLE,
                getMemoryFromAnalysis=True, historyPrint=OFF, memory=90, memoryUnits=PERCENTAGE, model='LBA-frame-'+
                id, modelPrint=OFF, multiprocessingMode=DEFAULT, name='LBA-job-'+id,  nodalOutputPrecision=SINGLE,
                numCpus=1, numGPUs=0, queue=None, resultsFormat=ODB, scratch='', type=ANALYSIS, userSubroutine='',
                waitHours=0, waitMinutes=0)
589
590         mdb.jobs['LBA-job-'+id].submit(consistencyChecking=OFF)
591         mdb.jobs['LBA-job-'+id].waitForCompletion()
```